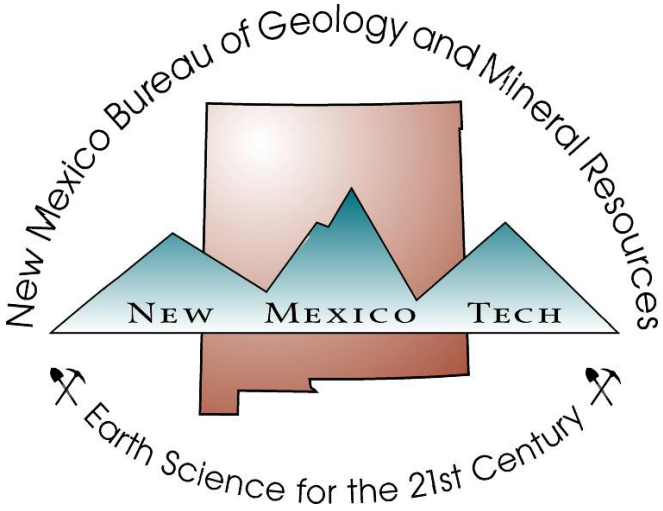

SPATIAL DISTRIBUTION OF FLUORIDE CONCENTRATION IN GOATHILL NORTH ROCK PILE, QUESTA MOLYBDENUM MINE, QUESTA, NEW MEXICO

BY

SHANNON F. WILLIAMS

New Mexico Bureau of Geology and Mineral Resources, New Mexico Tech
Socorro, New Mexico 87801

Open-file Report 534

November, 2010

University of Nevada, Reno

Spatial Distribution of Fluoride Concentration in Goathill North Rock Pile, Questa Molybdenum Mine, Questa, New Mexico

Submitted in partial fulfillment of the requirements
for the degree of Master of Science in Hydrology

by

Shannon F. Williams

Dr. Regina Tempel / Thesis Advisor

July, 2010

ABSTRACT

The New Mexico Bureau of Geology and Mineral Resources recently took part in an elaborate study called the Questa Rock Pile Weathering and Stability Project. The purpose of this project was to determine how and to what extent weathering affects the gravitational stability of the Questa mine rock piles over time periods on the order of 100s to 1000s of years. During the period of open pit mining (1969-1982) at Questa, several million tons of overburden rock was removed and deposited into rock piles on mountain slopes and into valleys. Since the emplacement of these rock piles, several minor slumps have occurred as well as a foundation failure at Goathill North (GHN) rock pile. This slide was halted and GHN made stable by removing material from the top and relocating it to the bottom forming a buttress. The regrading of GHN provided a rare opportunity to examine, sample, and develop a conceptual model of the undisturbed interior of a large mine rock pile in situ. During this process, several hundred parameters were measured, tested, and integrated. Specifically, this paper describes the techniques used to model the distribution of fluoride concentration within the rock pile.

Modeling was performed using the Geostatistical Analyst Extension in ESRI's ArcGIS (version 9.3.1) software. The models used were: Inverse Distance Weighting, Global Polynomial Interpolation, Local Polynomial Interpolation, and Radial Basis Functions. It was found that both Inverse Distance Weighting and Radial Basis Functions produced realistic models while Global Polynomial Interpolation and Local Polynomial Interpolation did not produce realistic models. Ultimately, however, the very nature of the fluoride distribution within the rock pile makes any model unrealistic. In the 30 years since the rock pile's emplacement, not enough weathering had occurred to preferentially relocate and concentrate fluoride. In the rock pile, fluoride is still randomly distributed and dependent on where loads of mined rock were dumped, rather than distributed by some physical process that can be effectively modeled.

INTRODUCTION

The purpose of this project is to examine the spatial distribution of fluoride concentrations in the Goathill North rock pile at the Questa Molybdenum Mine near Questa, New Mexico. The fluoride distribution will then be used to investigate spatial relationships with other elemental concentrations. This work expands on pioneering work of sampling and mapping the inside of a mine waste rock pile as highlighted by McLemore et al. (2009a).

Geologic, mineralogical, geochemical, geotechnical, and hydrologic characterization of mine rock piles with depth is important (Dawson, 1994; Shaw et al., 2002) to characterize pre-mining background conditions (Briggs et al., 2003), to characterize and predict stability and erosion (Dawson, 1994; URS Corporation, 2003), to predict acid-rock drainage (McLemore et al., 2004), to properly dispose of and manage mine overburden (Dawson, 1994), and to develop mine closure plans (URS Corporation, 2003; Wels et al., 2002). Most site characterizations of rock piles are based upon drilling of the rock piles (Robertson GeoConsultants, Inc. 2000a, b; URS Corporation, 2003), shallow surface test pits (URS Corporation, 2003), or composite surface sampling (Smith et al., 2000a, b; Munore and McLemore, 1999; Munroe et al., 2000; Briggs et al., 2003; Wildeman, 2003). Rarely do these methods of site characterization allow for

examination, mapping, and sampling of the undisturbed, interior of large rock piles in-situ. Examination of the interior of two mine rock piles during removal was described by Fines et al. (2003) and Tran et al. (2004) who revealed complex dipping layers within the rock piles. Other studies described mine rock piles using the techniques of drilling, surface test pits, and modeling.

It is with this lack of direct data that the New Mexico Bureau of Geology and Mineral Resources was granted a unique opportunity to sample and map rock pile material in-situ during the regrading of the Goathill North rock pile. This was accomplished through the construction of trenches dug into the rock pile as regrading progressed. Over the last six years, much of the data has been analyzed and published regarding clay mineralogy (Donahue et al., 2007), rock engineering properties (Viterbo et al., 2007), thermal imaging (Shannon, et al., 2005), near surface geophysics (van Dam, et al. 2005), microorganisms (Adams et al. 2007, and shear strength and deformational behavior (Fakhimi and Hosseinpour, 2008), among others. However, no studies have investigated the spatial relationships of chemical and mineralogical concentrations within and around the Goathill North rock pile. This project will fill that void.

BACKGROUND

The Questa Molybdenum Mine

Location and Climate

The Questa Molybdenum Mine is located in the Sangre de Cristo Mountains approximately five miles east of the town of Questa in Taos County, New Mexico, and is operated by Chevron Mining Inc. (Figure 1). The mine is located on south facing slopes and is bounded by the Red River to the south (approximate elevation 7,500 ft) and by mountain divides to the north (approximate elevation 10,750 ft). The region around Questa is semiarid with a 102-year precipitation average of approximately 21 inches. Average daily temperatures range from 38 degrees in the winter to 75 degrees in the summer with extreme averages ranging from 6 degrees to 94 degrees in the winter and summer respectively (WRCC, 2010a). Summers are usually hot during the day and cool at night. Heavy and localized rains caused by regional monsoons characterize the summer rainy season. The heavy rains often cause flash floods and mudflows, which have, in the past, blocked the highway. Fall is a period of warm days and cold nights with occasional snowfall. Winters are mild, and the roads are rarely blocked by snow. The heaviest snowfall occurs in the upper elevations. During the winter, there are many sunny days, and the ground is often bare in areas exposed to the sun. Snowfall averages 147.2 inches per year (WRCC, 2010b).

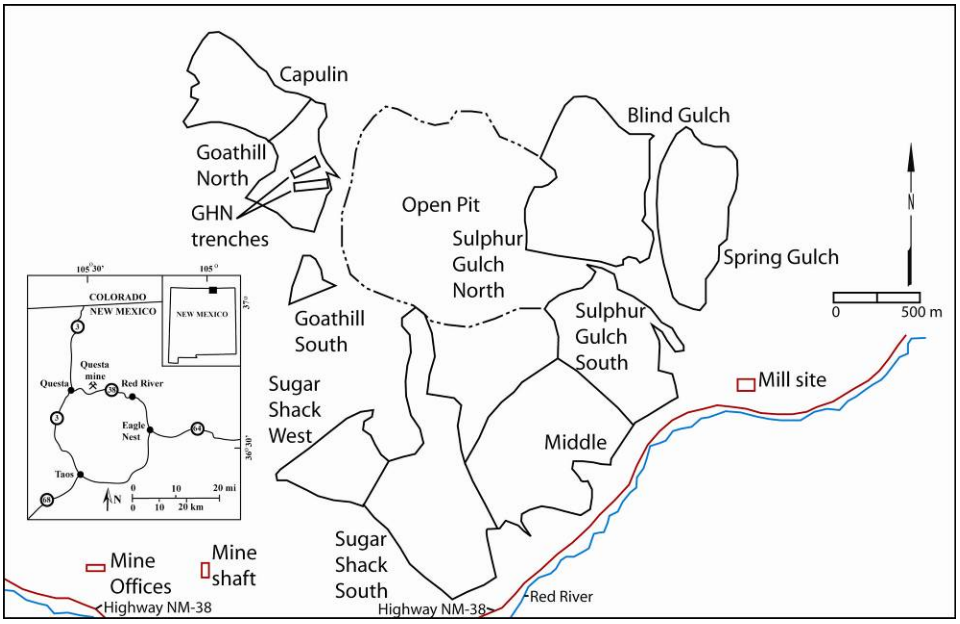

Figure 1. Figure showing the location of the Questa mine and the Questa rock piles and other mine features, including location of trenches constructed in GHN.

Geologic History

North central New Mexico has experienced many geologic events that have resulted in the complex geology studied today. The regional geology of the Questa-Red River area can be generally separated into five basic tectonic periods: Proterozoic, Paleozoic ancestral Rocky Mountains, Laramide orogeny, Rio Grand rift volcanism, and Quaternary Rio Grande rift fill (McLemore, 2009).

The Proterozoic basement rocks consist of metamorphosed sedimentary, volcanic, and volcaniclastic rocks that were intruded by a variety of plutonic rocks, which range in composition from mafic to felsic. These Proterozoic rocks have been subjected to amphibolite-grade regional metamorphism resulting in conspicuous foliation (McLemore, 2009). Proterozoic events created an underlying structural fabric that has controlled later structural and magmatic events (Graugh and Keller, 2004; Kelson et al., 2004). Regional northeast, north-south, and northwest trending structures are attributed to foliation and shear zones from the Proterozoic (Karlstrom and Humphreys, 1998).

The Uncompahgre-San Luis highlands and Sangre de Cristo uplift in the Tusas and Sangre de Cristo Mountains were created during the Paleozoic period of basin formation and uplift as part of the Ancestral Rocky Mountains. Most Paleozoic rocks are of clastic origin, though a recrystallized limestone and dolomite sequence is exposed as erosional outliers (Miller et al., 1963). Crustal shortening related to subduction of the Farallon plate during the Tertiary elevated the Sangre de Cristo Mountains. The Laramide orogeny reactivated Paleozoic structures that resulted in a series of thrust and high-angle reverse faults (Baltz and Myers, 1999; Cather, 1999).

The most significant rocks for the Questa mine are those related to Rio Grande rift volcanism, specifically those associated with the Latir volcanic field. The Latir volcanic field was emplaced

during the late Oligocene to early Miocene (Bauer and Kelson, 2004). Rocks associated with the Latir volcanic field consist of a series of mildly alkaline extrusive rocks ranging in composition from basalt to quartz-latite flows to high silica alkaline rhyolite tuffs that erupted from the Questa caldera 25.7 Ma ago. The Questa mine is located on the southern edge of the Questa caldera and Latir volcanic field. Later, the Latir volcanics were intruded by subvolcanic porphyries and granitic intrusions derived from a large buried batholith. These post-caldera intrusions are the apparent sources of the molybdenum deposits (McLemore, 2009).

Two classes of molybdenum deposits are recognized. The first type of molybdenum deposit is the porphyry-molybdenum deposit that is characterized by low fluorine content and usually forms in subduction zones related to arc-continent or continent-continent collisions. The second, type of molybdenum deposit is the Climax-type porphyry molybdenum deposit (Figure 2) which is characterized by anomalously high fluorine content and usually forms in rift zones (Sinclair, 1995). The molybdenum deposits located in the granitic intrusions show similarities to the Climax-type molybdenium deposits in that they are located in the Rio Grande rift valley, a cratonic rift zone, and they have a calc-alkaline composition and are high in fluorine and silica and notably depleted in yttrium, zirconium, and heavy rare earth elements (Johnson et al., 1989).

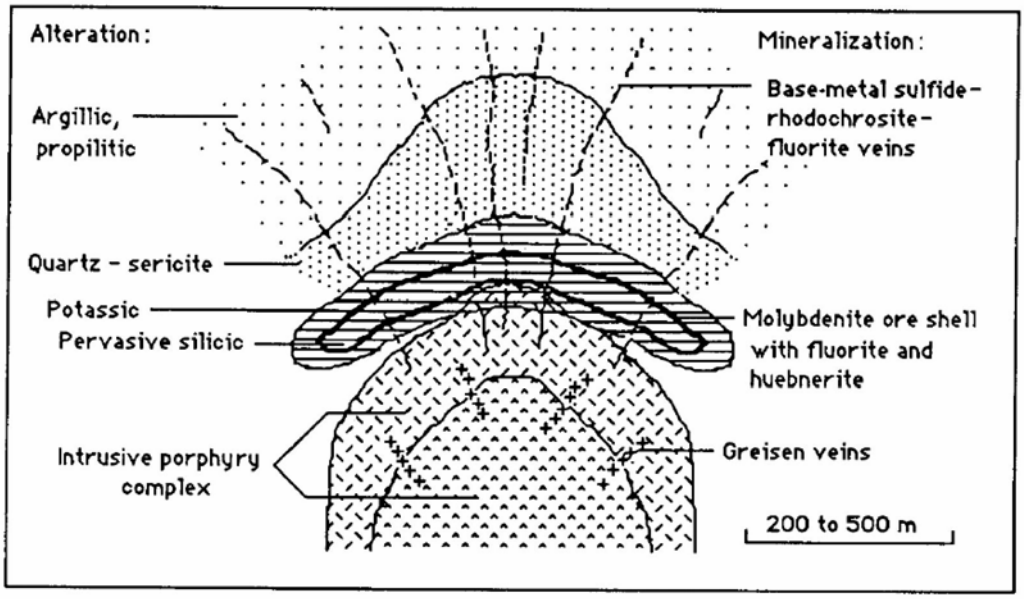

Figure 2. Schematic cross section of a Climax-type molybdenum deposit showing relationship of ore and alteration zoning to porphyry intrusions (Mutschler et al., 1981).

Furthermore, there are three morphological forms of porphyry molybdenum deposits that are recognized (Guilbert and Park, 1986; Ross et al., 2002; Rowe, 2005): 1) horizontal breccia body and veins (e.g., Questa, New Mexico), 2) vertical breccia pipe and veins (e.g., Victorio Mountains, New Mexico), and 3) stockwork veins without any breccia (e.g., Henderson, Colorado). Additionally, six types of hydrothermal alteration assemblages have been identified in the Questa and nearby Red River mining district (Molling, 1989; Meyer, 1991, McLemore, 2009):

1. early and late propylitic (consisting of chlorite, calcite, pyrite, albite, and epidote)

2. argillic (consisting of chlorite, calcite, epidote, quartz, and pyrite)
3. potassic (consisting of replacement by K-feldspar and potassium-bearing micas, with fluorite, quartz, and molybdenite)
4. quartz-sericite-pyrite (QSP), also is called phyllic, sericite and silicic
5. silicification (consisting of replacement by quartz)
6. post-mineral carbonate-fluorite and magnetite-hematite veining (occurring locally with anhydrite).

A more detailed description of alteration assemblages can be found in McLemore et al. (2008).

Mine History

Molybdenum was first discovered in the Questa district along the Red River around 1914 (Schilling, 1960, 1990), though it was originally misidentified as graphite. Mining began in 1918 using underground mining techniques and continued through 1958, producing 0.375 million tons of >4% MoS_2 (Schilling, 1960, 1990; McLemore et. al., 2009a). Exploration persisted from 1958 to 1964, when open-pit mining began. From 1965 through 1982, 81 million tons of ore at a grade of 0.191% MoS_2 was extracted from the open pit. In 1985, because of depletion of the open-pit reserves and new available technology, the mining operations returned to underground mining techniques (Molycorp, 2005) and continue to this day; though the mine was closed twice, from 1986 to 1989 and 1992 to 1995 because of poor market conditions. 21.11 million tons of 0.31% MoS2 was produced from 1983 to 2000 from the Goat Hill orebody. Today, mining continues on an adjacent D-orebody at grades between 0.3 to 0.5% (McLemore et. al., 2009a).

During the open pit mining days, the techniques used to recover the molybdenum ore produced 320 million tons of mined rock waste (Molycorp, 2005). Overburden, the material that covers a mineral bed that must be removed before the mineral can be removed in mining (Jackson, 1997), and mined rock was placed into nine rock piles (Fig. 3). Goathill North (GHN) rock pile is one of the nine rock piles and is being studied extensively by the New Mexico Bureau of Geology and Mineral Resources (NMBGMR). The rock pile is approximately 840 ft high with an overall slope of 22 degrees (Molycorp, 2005).

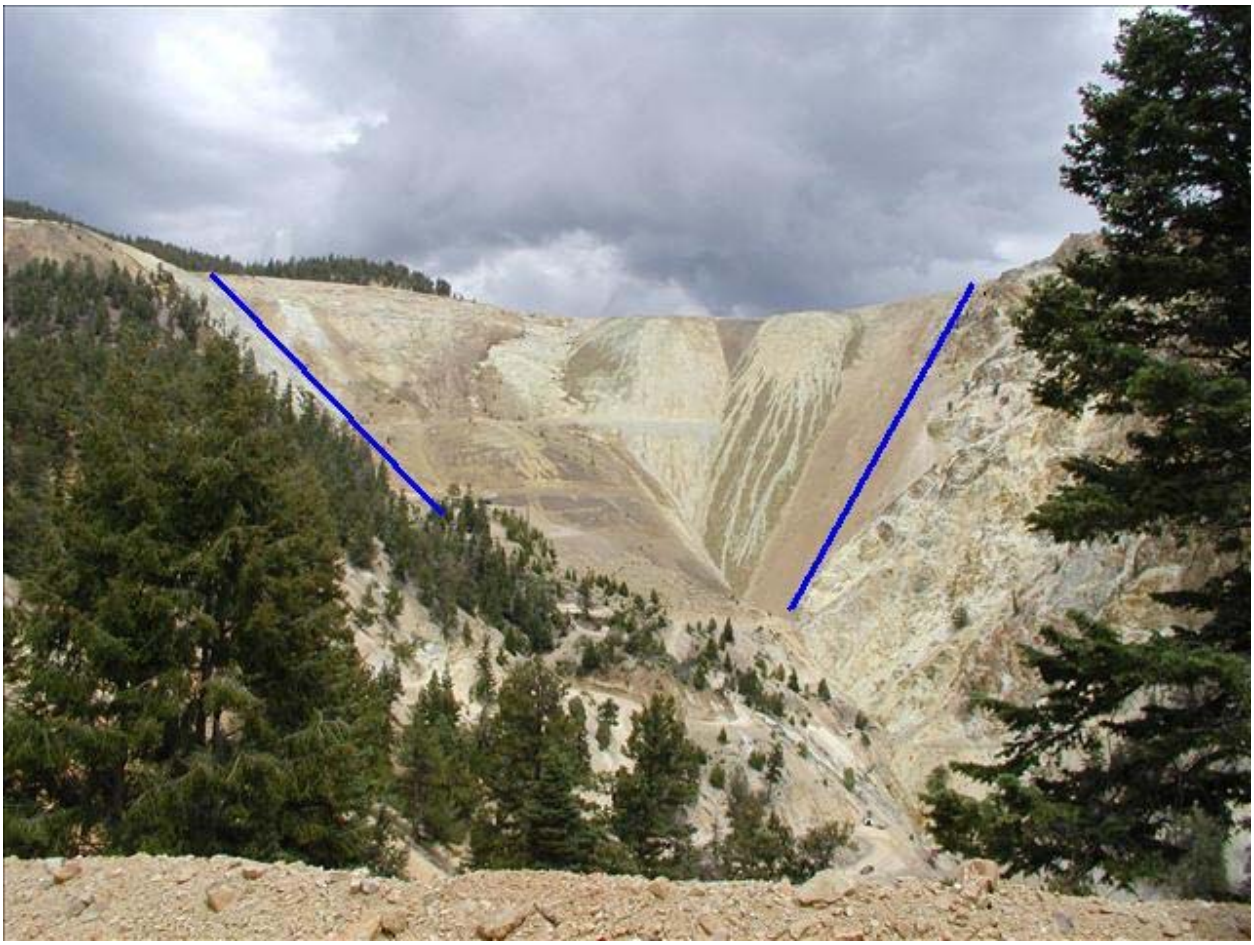

Figure 3. Goathill North rock pile, Outlined are the sides of Goathill Gulch before being filled in (photo by V.T. McLemore, 2004).

Questa Rock Pile Weathering and Stability Project (QRPWASP)

The Questa Rock Pile Weathering and Stability Project (QRPWASP) was a scientific research project, focusing on the earth sciences, hydrology, and geotechnical engineering. It was not a site-specific engineering or regulatory analysis of a specific rock pile. Rather, the purpose of the QRPWASP was/is to determine how and to what extent weathering affects the gravitational stability of the Questa mine rock piles over time periods on the orders of 100 and 1000 years. Many aspects of the mine have been studied since the project started in 2004, including, but not limited to, the structural, stratigraphic, physical, chemical, mineralogical, hydrological, and geotechnical characteristics, as well as the extent of weathering of the GHN rock pile (McLemore et. al., 2009a).

The New Mexico Bureau of Geology and Mineral Resources (NMBGMR) was the lead institution in characterizing the rock piles. During reclamation to address the stability of Goathill North rock pile, contractors removed portions of the rock pile from the top to the bottom (toe) of the pile, to form a buttress. During the pile movement, a team of scientists excavated trenches at different levels in the rock pile to facilitate sample collecting.

Logistically, contractors bulldozed the pile during the week (Figure 4), then, on Friday afternoons, the contractors would make a series of benches (Figure 5). Over the weekend, a team from the NMBGMR would conduct field tests and collect samples from these benches to take back to the laboratories for analysis. This was done over a period of several months during which thousands of samples were collected. The type of sampling described makes this project unique. By taking samples from varying depths of the rock pile, scientists are effectively looking into the rock pile itself. Hundreds of studies have been conducted on the outer portions of mine waste rock piles, but few studies have been performed on the interior of the rock pile. Looking at the inner portions of this rock pile will provide information on several aspects of its stability including water flow, airflow, and mineralization; all of which can be applied to the main question pertaining to weathering stability.

Figure 4. Bulldozers pushing mine rock from the top of Goathill North rock pile (photo by V.T. McLemore, 2004).

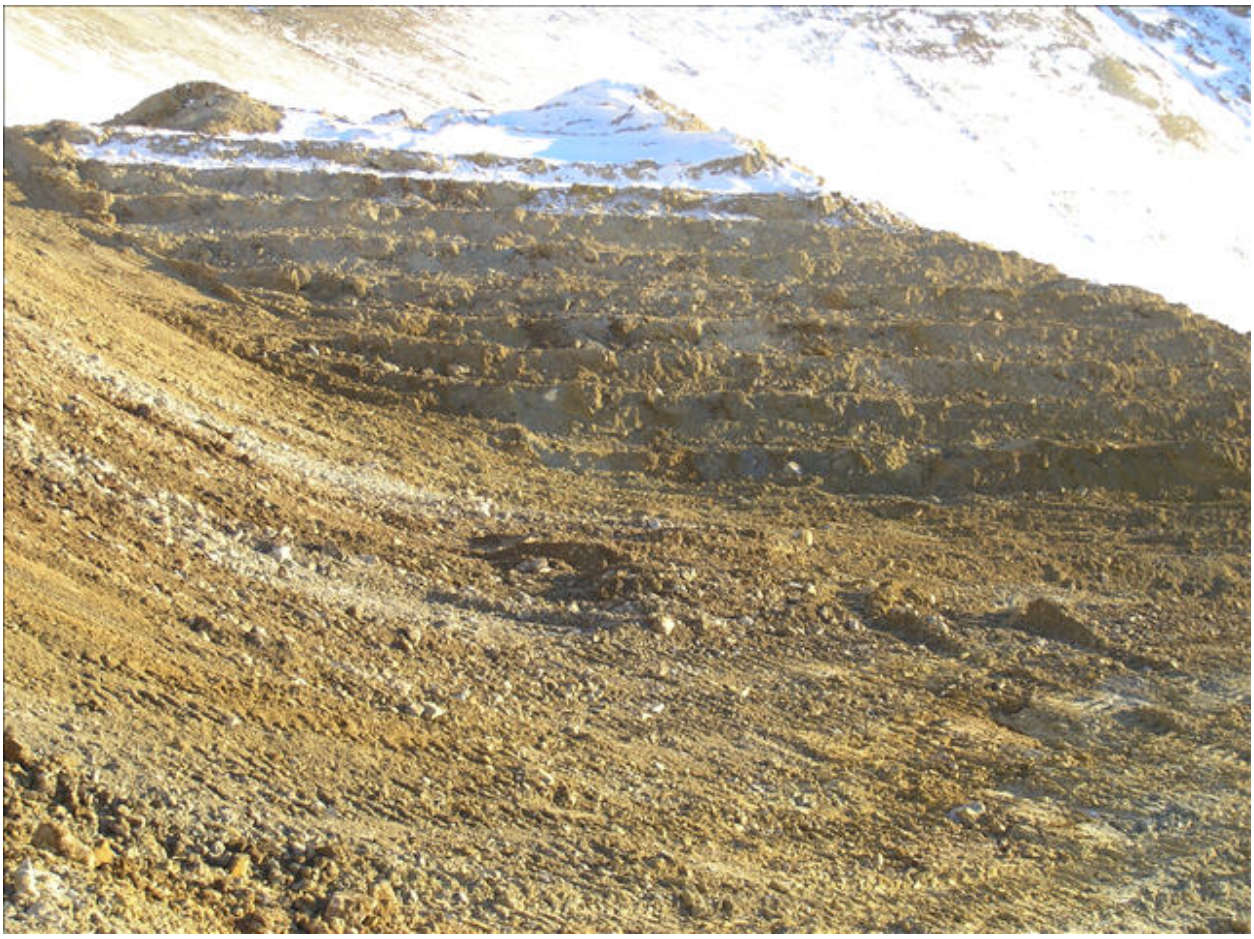

Figure 5. Benches created by bulldozers (photo by V.T. McLemore, 2004).

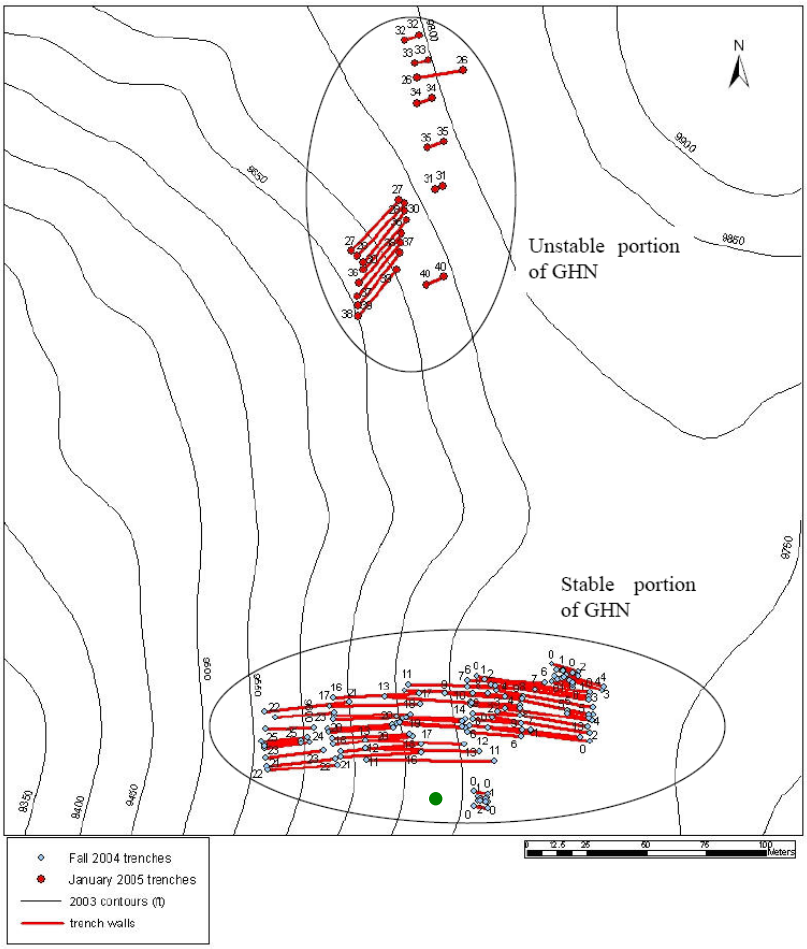

Figure 6. Map view of Goathill North rock pile. The green dot denotes the location of the borehole. The red lines represent each of the trench walls while the points at the end of the lines represent the corners of the trenches surveyed by mine staff using differential GPS. The trenches in the south are in the stable portion of the rock pile and were created in the Fall of 2004 for training purposes during re-grading. The trenchs in the north are in the unstable portion of the rock pile and were created in January of 2005. Because the area is/was unstable, the trenches here were much smaller to account for worker safety.

The reclamation of the Goathill North rock pile is only part of the major reclamation the mine site is undergoing. Presently, little vegetation exists on this rock pile. The long-term reclamation plan for the Questa Mine includes the development of a self-sustaining forest ecosystem at the mine site comparable to the surrounding region. The area will be reclaimed as a mixed conifer forest, deciduous woodland, and shrub ecosystem with a grass component. The establishment of these proposed vegetation types will create plant communities that will be suitable for ecological, recreational, and possibly economic development (LoVetere et al., 2004).

Molybdenum

Molybdenum is extracted from the Questa Mine in the form of the molybdenum sulfide ore called molybdenite (MoS_2), for which there are two main uses. The first use is as an alloy in

stainless steels and in alloy steels. Stainless steels are used in meeting the strength and corrosion-resistant requirements for equipment used in water distribution systems, food handling, chemical processing, homes, hospitals, and laboratories. Alloy steels are stronger and tougher than stainless steels and are needed to make automotive parts, construction equipment, and gas transmission pipes. The second major use of molybdenum is as an important material for the chemical and lubricant industries. Molybdenite, the molybdenum sulfide ore, has uses as catalysts, paint pigments, corrosion inhibitors, smoke and flame retardants, dry lubricant (molybdenum disulfide) on space vehicles and is resistant to high loads and temperatures. As a pure metal, molybdenum is used because of its high melting temperature of 4730 ^{o}F as filament supports in light bulbs, metal-working dies, and furnace parts (MII, 2005).

Fluoride

Fluorides are any organic and inorganic compounds that contain the element fluorine. Only inorganic fluorides are the focus of this study. In the environment, fluorides occur both naturally (e.g., rock weathering, volcanic emissions) and because of human activities (e.g., phosphate rock mining and use, aluminum manufacturing, drinking water fluoridation). Fluorides can be present: in air, as gases or particulates; in water, as fluoride ions or molecular compounds; in soils, typically as molecular compounds with calcium or aluminum; and in living organisms (Bégin, 2003).

Fluoride can have both a positive and a negative impact on humans. It is commonly used as a water additive to help prevent cavities, but at high intakes it can harm tooth development (dental fluorosis). Dental fluorosis is a condition that results from the intake of excessive amounts of fluoride during the period of tooth development, usually from birth to approximately 6–8 years of age. Mild dental fluorosis is usually characterized by the appearance of small white areas in the enamel; individuals with severe dental fluorosis have teeth that appear stained and pitted ("mottled") (Greenfacts, 2005).

The most serious effect of fluoride is its accumulation in bones from long-term excessive exposure, which can lead to skeletal fluorosis and bone fractures. The presence of fluoride in bones delays or inhibits bone hardening (mineralization), causing the bones to become brittle or less able to withstand pressure. The greater the amount of fluoride incorporated into bone, the more severe are the effects associated with skeletal fluorosis. In a pre-clinical phase of skeletal fluorosis, the patient may show no other symptoms than a slight increase in bone mass, detected radiographically. During the first and second clinical stages of skeletal fluorosis, the symptoms are: sporadic pain and stiffness of the joints, chronic joint pain, osteosclerosis of cancellous bone and calcification of ligaments. The third clinical phase is associated with crippling skeletal fluorosis, symptoms are: limited movement of the joints, skeletal deformities, intense calcification of ligaments, muscle wasting and neurological deficits. Other effects of skeletal fluorosis arise when high fluoride intakes overly stimulate bone formation, which can result in calcium deficiency, osteomalacia, and secondary hyperparathyroidism. The development of skeletal fluorosis depends on a number of factors, such as age, nutritional status, renal function and calcium intake, in addition to the extent and duration of exposure to fluoride. Skeletal fluorosis may be reversible to some degree (Greenfacts, 2005).

In nature, the most important fluoride minerals include fluorite (CaF_2), fluorapatite [$Ca_5(PO_4)_3F$], cryolite (Na_3AlF_6), and fluorophlogopite ($KMg_3AlSi_3O_{10}F_2$) (Elrashidi and Lindsay, 1986). The solubility of F^- in soil solution is variable and is affected by pH, speciation, adsorption and desorption reactions, and dissolution and precipitation reactions (Luther et al., 1996). It is these processes that then control the solubility, plant uptake, and mobility of F^- in the soil subsurface. Acidic conditions and low calcium carbonate content are favorable to F^- solubility and can therefore enhance both root uptake (Weinstein and Alscher-Herman, 1982) and migration to surface and ground water (Smith, 1983). Conversely, soils that contain significant amounts of calcium carbonate with alkaline conditions can fix F^- as insoluble calcium fluoride (CaF_2), and reduce its bioavailability and mobility (Reddy and Gloss., 1993). In soils, F^- can be found in four major fractions: (1) dissolved in soil solution; (2) sorbed to carbonates and Al, Fe, and Mn oxides and hydroxides; (3) solid phases, such as fluorite and fluorophlogopite; (4) associated with organic compounds (Selim, 2003), and (5) in other rock-forming minerals containing F.

It has been found that F^- in soil water will complex with Al and Fe, which can also affect plant uptake of F^-. Some studies suggest that at higher F^- concentrations and strong acidic conditions, the minerals AlF_3 and CaF_2 will precipitate while under strong alkaline conditions, the mineral $Ca_5(PO_4)_3F$ will precipitate. However, in slightly acidic and neutral soils with low Ca concentrations, F^- solubility is controlled by surface adsorption to Al and Fe oxides and hydroxides (Selim, 2003).

Because the Questa mine contains high amounts of naturally occurring fluoride as part of the mineralization process, it is important to understand its distribution and concentration and its possible effect on the residents of the neighboring town of Questa. The dissolution of fluoride from primary minerals can increase the concentration of dissolved fluoride in surface and groundwater, both of which are the main source for the town's drinking water. It is thus important to monitor fluoride concentration in the town's water supply because in high enough concentrations, fluoride can be a potential health hazard. I hypothesize that there is no preferential concentration of fluoride within the Goathill North rock pile.

METHODS

Sample Collection Preparation and Analysis

During the spring of 2006, several thousand samples were collected by a team of researchers led by Dr. Virginia McLemore of the New Mexico Bureau of Geology and Mineral Resources. Of these thousands of samples, approximately 200 were collected for analysis of fluoride. Samples were collected in a series of trenches that were excavated at the top half of Goathill North rock pile. Each trench consisted of four benches with heights varying from approximately three to four feet with the depth of a trench totaling about 15 ft. Samples were subsequently collected from each exposed bench wall. The samples included mine soil and mined rock at different weathering stages as indicated by differences in color and texture, as well as drill hole samples from various locations around the mine.

The samples collected underwent several analyses including: pH, Eh, conductivity, total dissolved solids, particle size, X-Ray fluorescence spectrometry, microprobe analysis, bulk density, mineralogy using XRD, stable isotopes, trace metals, iron, sulfur, fluoride, and geotechnical properties.

The analytical method (Appendix 1) to determine fluoride used in this study was taken from McQuaker and Gurney (1977) and adapted by Joanne Baker, a student coworker, and myself for use in the New Mexico Bureau of Geology and Mineral Resources Chemistry Laboratory. This method utilizes a high-temperature sodium hydroxide fusion followed by acidification to facilitate measurement with a fluoride electrode. Calculation of fluoride concentration in ppm from the milivolt value obtained from the fluoride electrode is done using a trendline analysis based on incremental measurements of known fluoride concentrations. Ideally, the standard fluoride concentration curve will follow the Nernst equation:

$$E_i = -S \log C_i + B$$

where C_i is the ugF yielding a millivolt potential of E_i; S is the Nernst slope (RT/F) which equals 58.5 mV at 22^{o}C, and B is a millivolt potential which is dependent on the ionic background (McQuaker and Gurney, 1977).

The actual standard operating procedure used can be found in Appendix 1.

Statistical Analysis

Only descriptive statistics were calculated for fluoride concentrations measured. Statistics were calculated in two groups, the first group was calculated for all fluoride samples and the second group was calculated for only GHN fluoride samples. The "All Samples" group consists of every sample collected at the Questa mine that was measured for fluoride; these samples have many different locations around the mine (see project database for locations). The "GHN Only" Sample group consists of only samples collected within the Goathill North rock pile that were tested for fluoride concentration. The Descriptive Statistics tool in Microsoft Excel was used to calculate: mean, standard error, median, mode, standard deviation, sample variance, kurtosis, skewness, range, minimum, maximum, sum, count, and 95% confidence level for both the All sample group and the GHN Only sample group. Finally, the Pearson product moment correlation coefficient and the r squared value were calculated for fluoride verses all other measured values individually for both groups with fluoride as the dependent value.

The Pearson coefficient, r, is a dimensionless index that ranges from -1.0 to 1.0 inclusive and reflects the extent of a linear relationship between two data sets. The equation to calculate the Pearson coefficient is:

$$r = \frac{\sum(x-\bar{x})(y-\bar{y})}{\sqrt{\sum(x-\bar{x})^2 \sum(y-\bar{y})^2}}$$

while the r squared, r^2, is the square of the Pearson coefficient and can be interpreted as the proportion of the variance in y attributable to the variance in x. For this study, fluoride is considered to be the x value. Following is a list of all the independent, or y values used.

1.SiO_2	17. FeOmeas	33. Ga	49. epidote	65. TotalClay
2.TiO_2	18. As	34. Cr	50. calcite	66. kaol
3.Al_2O_3	19. Ba	35. Co	51. pyrite	67. chlorite
4.Fe_2O_3T	20. Rb	36. La	52. FeMnOxide	68. illite
5.FeOT	21. Sr	37. Ce	53. goethite	69. smectite
6.MnO	22. Pb	38. Nd	54. hematite	70. MixLayer
7.MgO	23. Th	39. Sm	55. Gypsum	71. copiapite
8.CaO	24. U	40. Eu	56. AuthGyp	72. jarosite
9.Na2O	25. Zr	41. Gd	57. DetritGyp	73. sph
10. K_2O	26. Nb	42. Tb	58. molybdenit	74. rutile
11. P_2O_5	27. Y	43. Er	59. biotite	75. zircon
12. S	28. Sc	44. Yb	60. organics	76. rhodochros
13. SO_4	29. V	45. Lu	61. fluorite	77. vermiculite
14. C	30. Ni	46. Q	62. mag	78. Chalcopyr
15. Total	31. Cu	47. K	63. apatite	79. actinolite
16. Total S	32. Zn	48. P	64. hbld	80. pyroxene

More information about methods and analysis for each of these values can be found in the main study report by McLemore, et al. (2009a).

GIS Plotting

Determining the method for plotting sample points within the mine waste rock pile was actually one of the most challenging parts of this project. GIS software very easily plots points with x and y (easting and northing) coordinates, however, the rock pile samples were taken within relatively the same northing, but have different easting and elevation values. Several attempts were made to use ArcScene, ESRI's 3D plotting software but, unfortunately, none of the modeling tools work in conjunction with ArcScene. Finally, I found I was able to plot easting and elevation in ArcMap and simply not add any geographic datum information (Figure 7). Additionally, I obtained points created for an Excel plot that outline the original bedrock base of the mountain and the original outline of the mine waste rock pile before re-grading which then served as a physical boundary for my models after being converted to lines. So, while the sample points plotted in this manner can't be used in conjunction with other plots from other studies, I was able to plot the sample points in a cross-section view, which was one of the main objectives of this project.

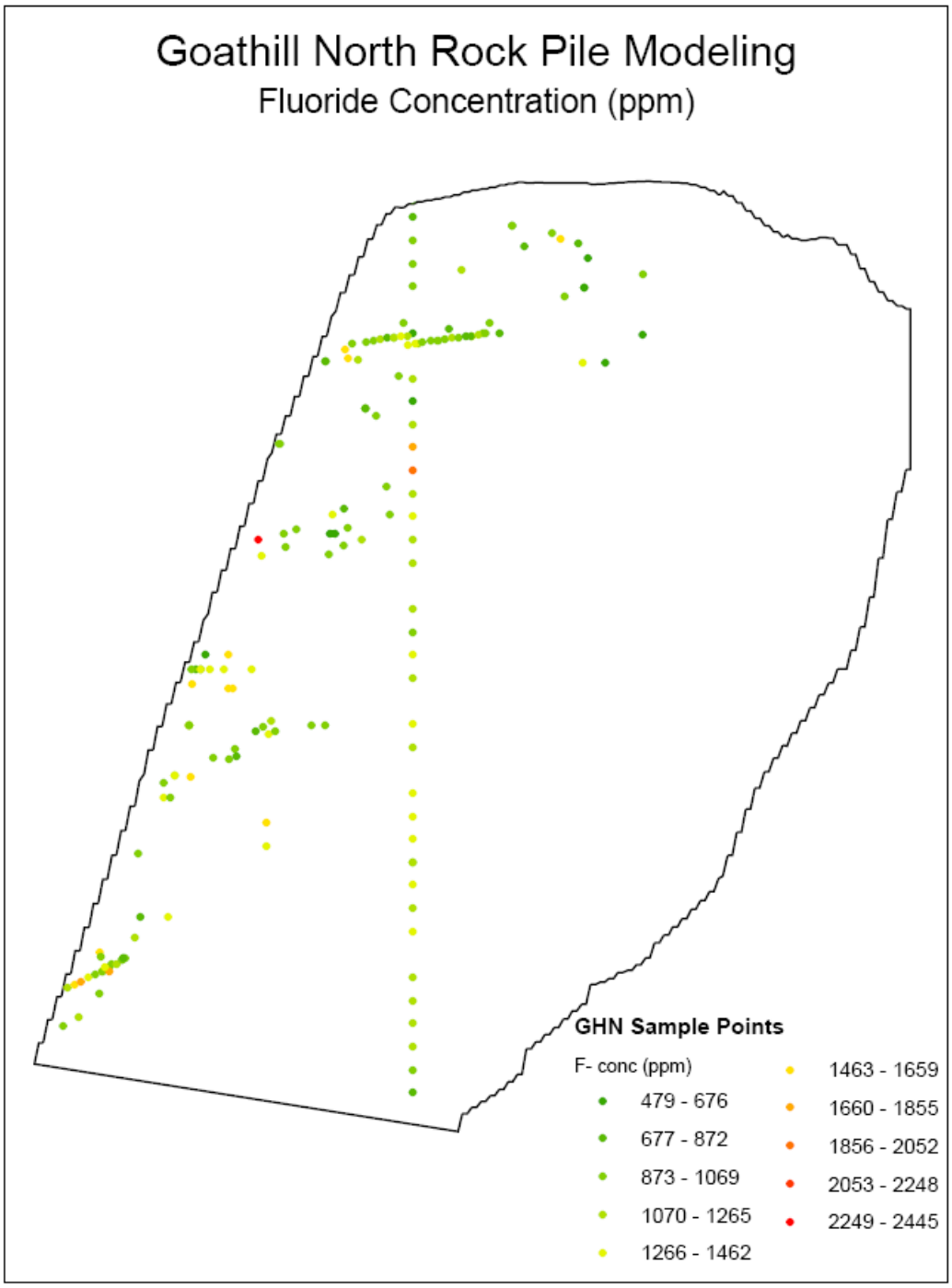

Figure 7. Cross-section plot of GHN Samples within the upper half of the GHN rock pile.

GIS Modeling

There are several modeling tools available for use in the ArcGIS (version 9.3.1) software package created by the Environmental Systems Research Institute (ESRI). This paper considers the models found in the Geostatistical Analyst Extension using the Geostatistical Wizard, specifically Inverse Distance Weighting, Global Polynomial Interpolation, Local Polynomial Interpolation, and Radial Basis Functions.

Inverse Distance Weighted (IDW) Interpolation

IDW interpolation explicitly implements the assumption that things that are close to one another are more alike than those that are farther apart (ESRI, 2010a). To predict a value for any unmeasured location, IDW will use the measured values surrounding the prediction location. Those measured values closest to the prediction location will have more influence on the predicted value than those farther away. Thus, IDW assumes that each measured point has a local influence that diminishes with distance. It weights the points closer to the prediction location greater than those farther away, hence the name inverse distance weighted.

Geostatistical Analyst calculates the optimal power value (p) by minimizing the root mean square prediction error (RMSPE). The RMSPE is the statistic that is calculated from cross-validation. In cross-validation, each measured point is removed and compared to the predicted value for that location. The RMSPE is a summary statistic quantifying the error of the prediction surface. Geostatistical Analyst evaluates several different powers for IDW to identify the power that produces the minimum RMSPE. The RMSPE is plotted for several different powers for the same dataset. A curve is fit to the points (a quadratic Local Polynomial equation), and from the curve the power that provides the smallest RMSPE is determined as the optimal power.

Weights are proportional to the inverse distance raised to the power value p. As a result, as the distance increases, the weights decrease rapidly. How fast the weights decrease is dependent on the value for p. If $p = 0$, there is no decrease with distance, and because each weight λi will be the same, the prediction will be the mean of all the measured values. As p increases, the weights for distant points decrease rapidly. If the p value is very high, only the immediate few surrounding points will influence the prediction. Geostatistical Analyst uses power functions greater than 1. A $p = 2$ is known as the inverse distance squared weighted interpolation.

This model assumes things that are close to one another are more alike than those farther away, as the locations get farther away, the measured values will have little relationship with the value of the prediction location. To speed calculations the model allows the operator to discount to zero the more distant points with little influence. As a result, it is common practice to limit the number of measured values that are used when predicting the unknown value for a location by specifying a search neighborhood. The specified shape of the neighborhood restricts how far and where to look for the measured values to be used in the prediction. Other neighborhood parameters restrict the locations that will be used within that shape.

The shape of the neighborhood is influenced by the input data and the surface being modeled. If there are no directional influences on the weighting of the data, it is best to consider points

equally in all directions. Therefore, the best shape to use to choose points in a neighborhood is a circle. However, if there is a directional influence on your data, such as a prevailing wind or slope angle, the shape of the neighborhood would be better represented by an ellipse with the major axis parallel to the wind or slope direction. The adjustment for this directional influence is justified because it is assumed that locations upwind or down slope from a prediction location are going to be more similar at remote distances than locations that are perpendicular to the wind or slope.

Once a neighborhood shape is specified, the model allows the user to restrict which locations within the shape should be used. The maximum and minimum number of locations to use can be defined, and the neighborhoods can be divided into sectors. If the neighborhood is divided into sectors, the maximum and minimum constraints will be applied to each sector. There are several different sectors configurations that can be used.

The points highlighted in the data view of the Searching Neighborhood dialog box identify the locations and the weights that will be used for predicting a location at the center of the ellipse. The neighborhood is contained within the displayed ellipse. The surface calculated using IDW depends on the selection of a power value (p) and the neighborhood search strategy. IDW is an exact interpolator, where the maximum and minimum values (see figure 8) in the interpolated surface can only occur at sample points. The output surface is sensitive to clustering and the presence of outliers. IDW assumes that the surface is being driven by the local variation, which can be captured through the neighborhood. (ESRI Help Manual)

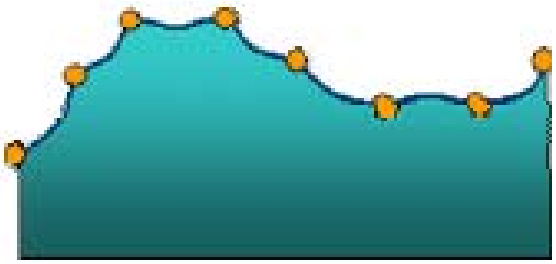

Figure 8. Example of how IDW might extrapolate between data points (ESRI, 2010a).

Global Polynomial Interpolation

Global Polynomial interpolation fits a smooth surface that is defined by a mathematical function (a polynomial) to the input sample points (ESRI, 2010b). The Global Polynomial surface changes gradually and captures coarse-scale patterns in the data. Conceptually, Global Polynomial interpolation is like taking a piece of paper and fitting it between a series of points.

Of course, a flat piece of paper will not accurately capture a landscape containing a valley. However, if the piece of paper is bent once, the fit is likely to be much better. Adding a term to the mathematical formula produces a similar result, a bend in the plane. A flat plane (no bend in the piece of paper) is a first-order polynomial (linear). Allowing for one bend is a second-order polynomial (quadratic), two bends a third-order (cubic), and so forth, up to 10 are allowed in Geostatistical Analyst.

Rarely will the piece of paper pass through the actual measured points, thus making Global Polynomial interpolation an inexact interpolator. Some points will be above the piece of paper and others will be below. However, by adding up how much higher each point is above the piece of paper and adding up how much lower each point is below the piece of paper, the two sums should be similar. The modeled surface is obtained by using a least squares regression fit. The resulting surface minimizes the squared differences among the raised values and the sheet of paper. The result from Global Polynomial interpolation is a smooth surface that represents gradual trends in the surface over the area of interest.

Global interpolation is appropriate for:

1. Fitting a surface to the sample points when the surface varies slowly from region to region over the area of interest (e.g., pollution over an industrial area).

2. Examining and/or removing the effects of long-range or global trends. In such circumstances the technique is often referred to as trend surface analysis.

Global Polynomial interpolation creates a slowly varying surface using low-order polynomials that possibly describe some physical process (e.g., pollution and wind direction). However, it should be noted that the more complex the polynomial, the more difficult it is to ascribe physical meaning to it. Furthermore, the calculated surfaces are highly susceptible to outliers (extremely high and low values), especially at the edges.

Local Polynomial Interpolation

While Global Polynomial interpolation fits a polynomial to the entire surface, Local Polynomial interpolation fits many polynomials, each within specified overlapping neighborhoods (ESRI, 2010c). The search neighborhood can be defined using the Search Neighborhood dialog box. The shape, maximum and minimum number of points to use, and the sector configuration can be specified. Alternatively, a slider can be used to define the width of the neighborhood in conjunction with a power parameter that will, based on distance, decrease the weights of the sample points within the neighborhood. Thus, Local Polynomial interpolation produces surfaces that account for more local variation.

A first-order Global Polynomial fits a single plane through the data; a second-order Global Polynomial fits a surface with a bend in it, allowing surfaces representing valleys; a third-order Global Polynomial allows for two bends; and so forth. However, when a surface has a different shape, such as a landscape that slopes, levels out, and then slopes again, a single Global Polynomial will not fit well. Multiple polynomial planes would be able to represent the surface more accurately.

Local Polynomial interpolation fits the specified order polynomial using all points only within the defined neighborhood. The neighborhoods overlap and the value used for each prediction is the value of the fitted polynomial at the center of the neighborhood. This process continues, centering on subsequent prediction locations, fitting Local Polynomials to predict the values. The model is optimized by iteratively cross-validating the output surfaces that are calculated

using different parameters. The optimal parameters are chosen to minimize the root-mean-square prediction error (RMSPE, similar to the selection of the power (p) value in IDW).

Global Polynomial interpolation is useful for creating smooth surfaces and identifying long-range trends in the dataset. However, in earth sciences the variable of interest usually has short-range variation in addition to long-range trend. When the dataset exhibits short-range variation, Local Polynomial interpolation maps can capture the short-range variation. Local Polynomial interpolation is sensitive to the neighborhood distance. For this reason, the Geostatistical Wizard allows the user to preview the surface before producing the output layer. As with IDW, you can define a model that accounts for anisotropy.

Radial Basis Functions

Radial Basis Function (RBF) methods are a series of exact interpolation techniques; that is, the surface must go through each measured sample value. There are five different basis functions (ESRI, 2010d):

1. Thin-plate spline
2. Spline with tension
3. Completely regularized spline
4. Multiquadric function
5. Inverse multiquadric function

Each basis function has a different shape and results in a slightly different interpolation surface. RBF methods are a form of artificial neural networks.

RBFs are conceptually similar to fitting a rubber membrane through the measured sample values while minimizing the total curvature of the surface. The selected basis function determines how the rubber membrane will fit between the values. Being exact interpolators, the RBF methods differ from the Global and Local Polynomial interpolators, which are both inexact interpolators that do not require the surface to pass through the measured points. When comparing an RBF to the IDW method, another exact interpolator, IDW will never predict values above the maximum measured value or below the minimum measured value as shown in Figure 9. However, the RBFs can predict values above the maximum and below the minimum measured values as in Figure 9. The optimal parameters are determined using cross validation in a similar manner as for IDW and Local Polynomial interpolation.

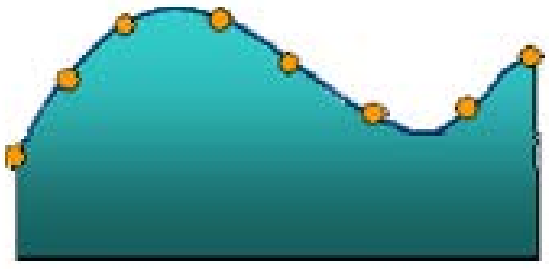

Figure 9. Example of how RBF might extrapolate between data points (ESRI, 2010b).

RBFs are used for calculating smooth surfaces from a large number of data points. The functions produce good results for gently varying surfaces such as elevation. The techniques are inappropriate when there are large changes in the surface values within a short horizontal distance and/or when you suspect the sample data is prone to error or uncertainty.

In Geostatistical Analyst, RBFs are formed over each data location. An RBF is a function that changes with distance from a location. For example, suppose the radial basis function is simply the distance from each location, so it forms an inverted cone over each location. Then, the weights w1, w2, w3, etc., are found by requiring that, when the prediction is moved to a location with a measured value, the data value is predicted exactly. This forms N equations in N unknowns and can be solved uniquely. Thus, the surface passes through the data values, making predictions exact. Each of the RBFs has a parameter that controls the "smoothness" of the surface. For all methods except inverse multiquadric, the higher the parameter value, the smoother the map; the opposite is true for inverse multiquadric.

DATA AND RESULTS

Statistics

Table 1a.

Descriptive Statistics for all F samples	(ppm)
Mean	1400.4
Standard Error	67.1
Median	1144
Mode	1032
Standard Deviation	1399.0
Sample Variance	1957251.3
Kurtosis	176.0
Skewness	11.5
Range	24338
Minimum	192
Maximum	24530
Sum	609188.5
Count	435
Largest(1)	24530
Smallest(1)	192
Confidence Level(95.0%)	131.8

Table 1b.

Descriptive Statistics for GHN F samples	(ppm)
Mean	1099.8
Standard Error	20.6
Median	1047
Mode	1032
Standard Deviation	290.2
Sample Variance	84190.3
Kurtosis	2.5
Skewness	0.9
Range	1966
Minimum	479
Maximum	2445
Sum	217768.5
Count	198
Largest(1)	2445
Smallest(1)	479
Confidence Level(95.0%)	40.7

Table 1a and 1b show the descriptive statistics for all samples tested for fluoride (Table 1a) and for all samples from GHN tested for fluoride (Table 1b). The large difference in values is caused by the maximum fluoride concentration value found in a sample outside of GHN that is an order of magnitude larger than the maximum fluoride concentration value found in GHN.

Table 2a.

All F samples		
Sample	**RSQ**	**count**
F	1	435
CaO	0.10	433
Gd	0.05	45
Cr	0.05	425
V	0.04	427
Co	0.03	59
sph	0.03	16
chlorite	0.03	430
FeOmeas	0.03	47

Table 2b.

GHN F samples		
Sample	**RSQ**	**count**
F	1	198
S	0.28	112
As	0.22	29
Yb	0.20	33
Gd	0.13	33
TotalClay	0.11	194
Co	0.10	28
K	0.10	195
illite	0.09	196

Tables 2a and 2b show the variables with the highest r squared values. A table of all the statistics calculated for all the measured values can be found in Appendix 2.

Correlation Graphs

Graphs were created using SigmaPlot to illustrate the lack of correlation between F and other measured values. Please note that for graphing purposes, the maximum value in the All Samples group was removed since it skewed the graphs such that other patterns were no longer discernable, though it was considered in all numerical calculations.

Figures 10a and 10b visually show the difference in r squared values for CaO for the All Sample group ($r^2 = 0.097$) verses the GHN Sample group ($r^2 = 9.8E\text{-}5$). SigmaPlots for all fluoride concentration vs all measured values for both groups can be found in Appendix 3.

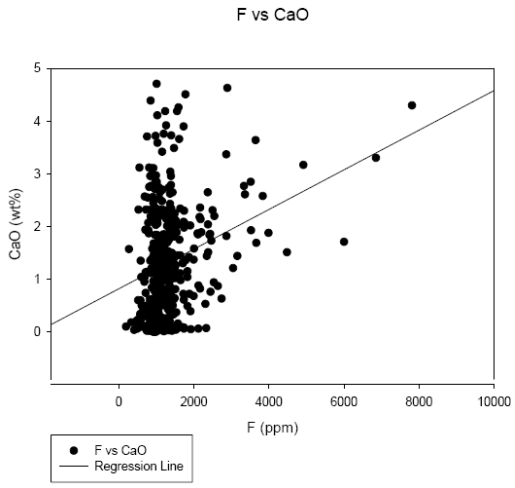

Figure 10a. F vs CaO for the All Sample group.

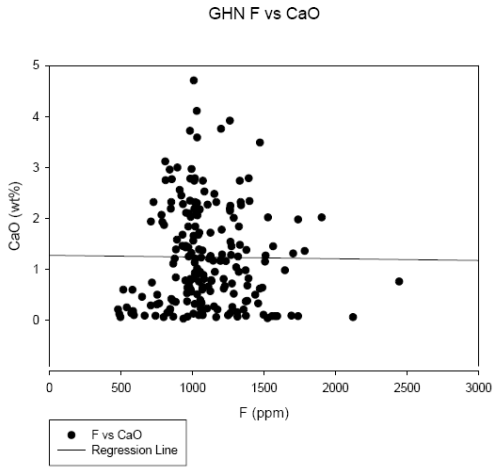

Figure 10b. F vs CaO for the GHN Samples group.

GIS Models

The following figures are examples of the results from each modeling method used. For plots of all the model iterations, please refer to Appendix 4.

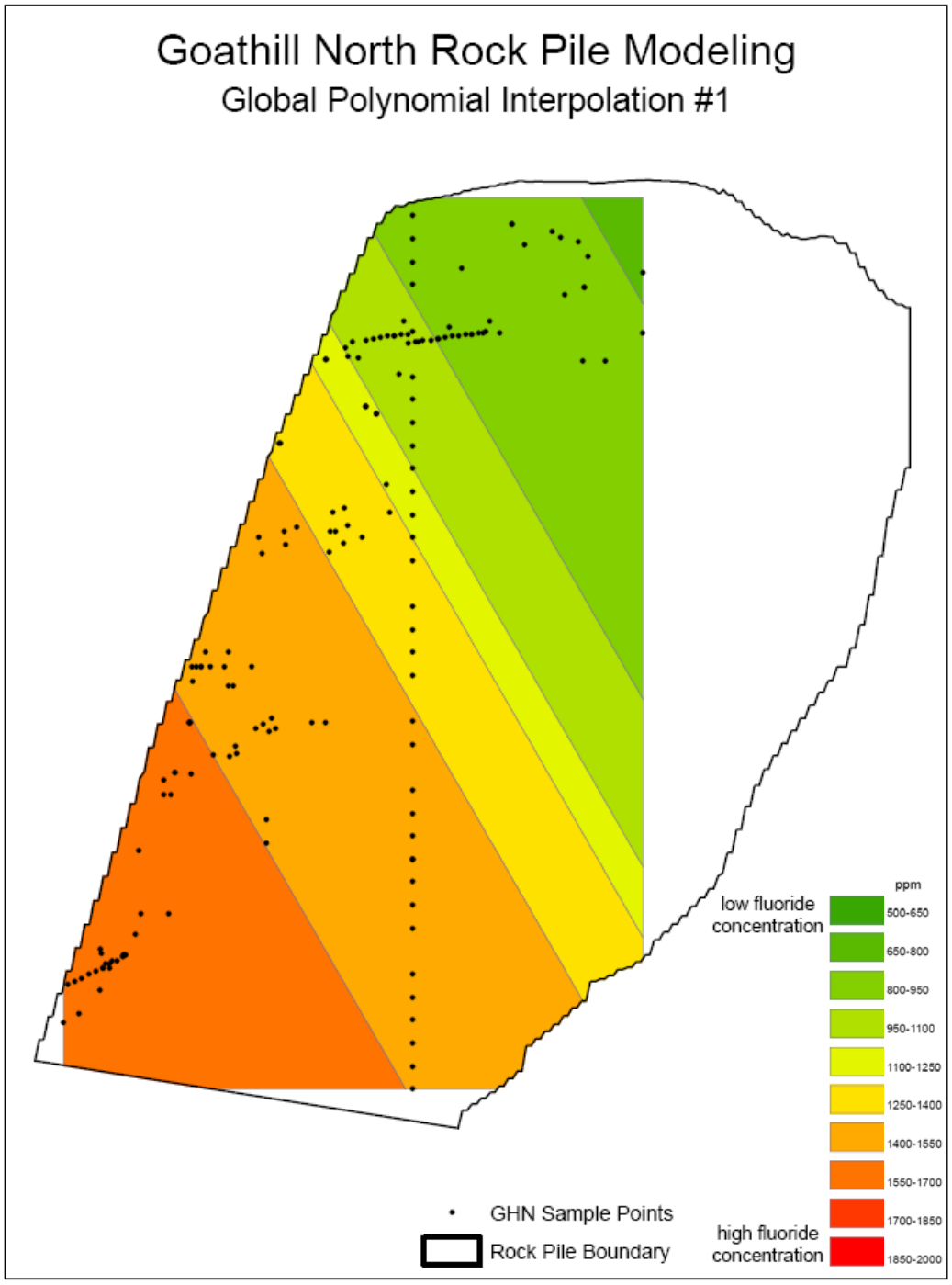

Figure 11.

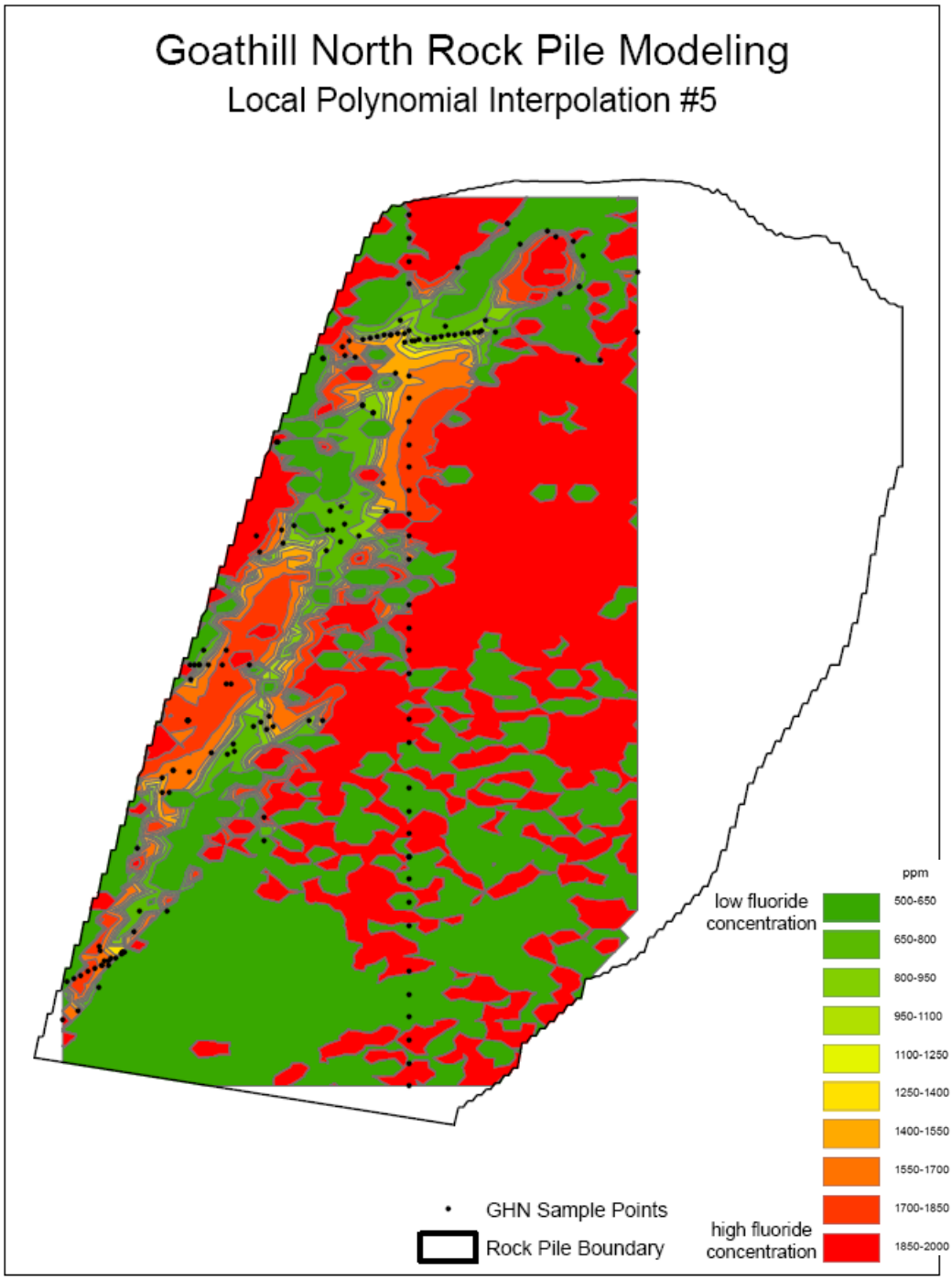
Goathill North Rock Pile Modeling
Local Polynomial Interpolation #5
ppm
low fluoride concentration
500-650
650-800
800-950
950-1100
1100-1250
1250-1400
1400-1550
1550-1700
1700-1850
1850-2000
high fluoride concentration
GHN Sample Points
Rock Pile Boundary

Figure 12.

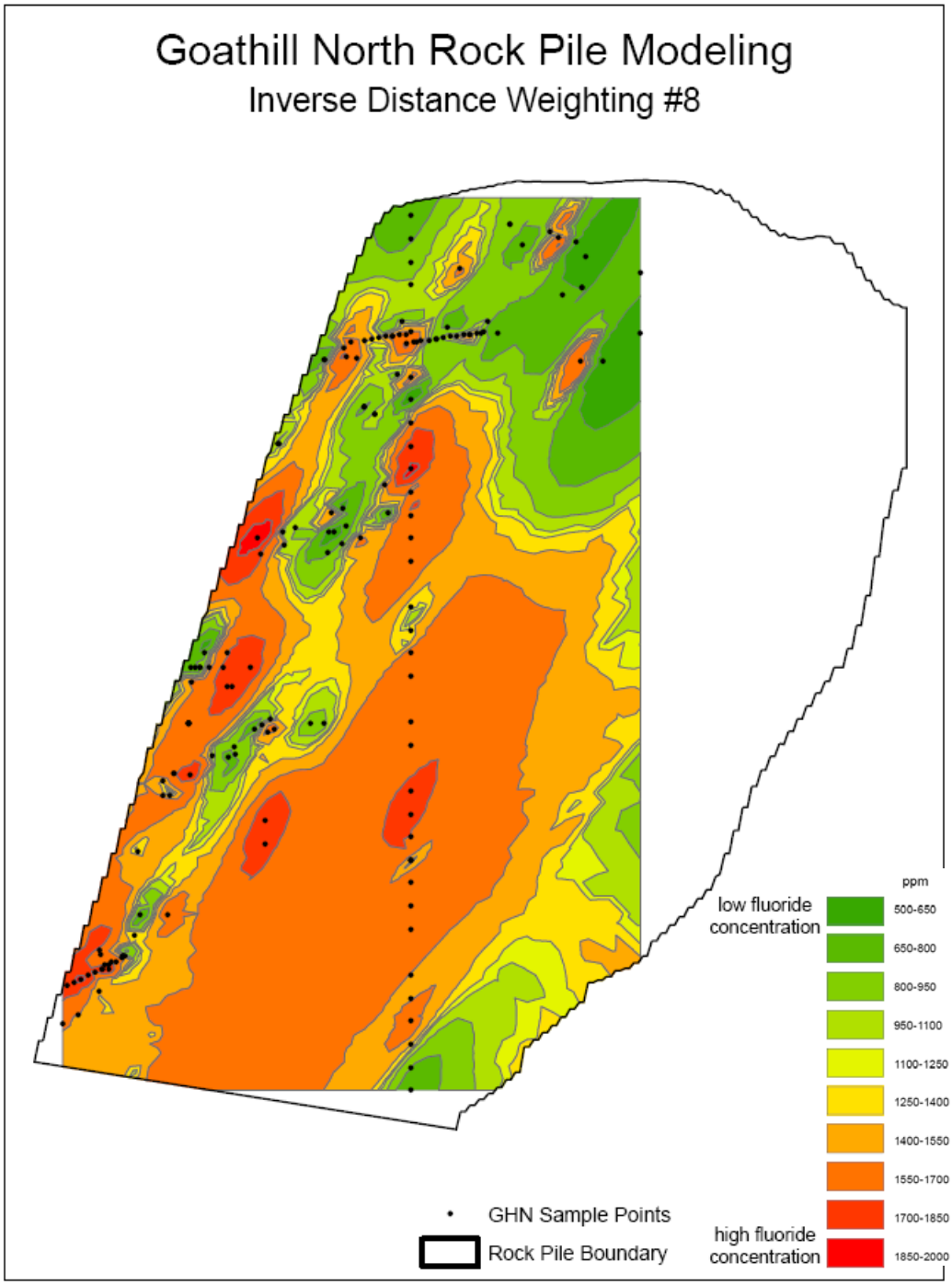
Goathill North Rock Pile Modeling
Inverse Distance Weighting #8
ppm
low fluoride concentration
500-650
650-800
800-950
950-1100
1100-1250
1250-1400
1400-1550
1550-1700
1700-1850
1850-2000
high fluoride concentration
GHN Sample Points
Rock Pile Boundary

Figure 13.

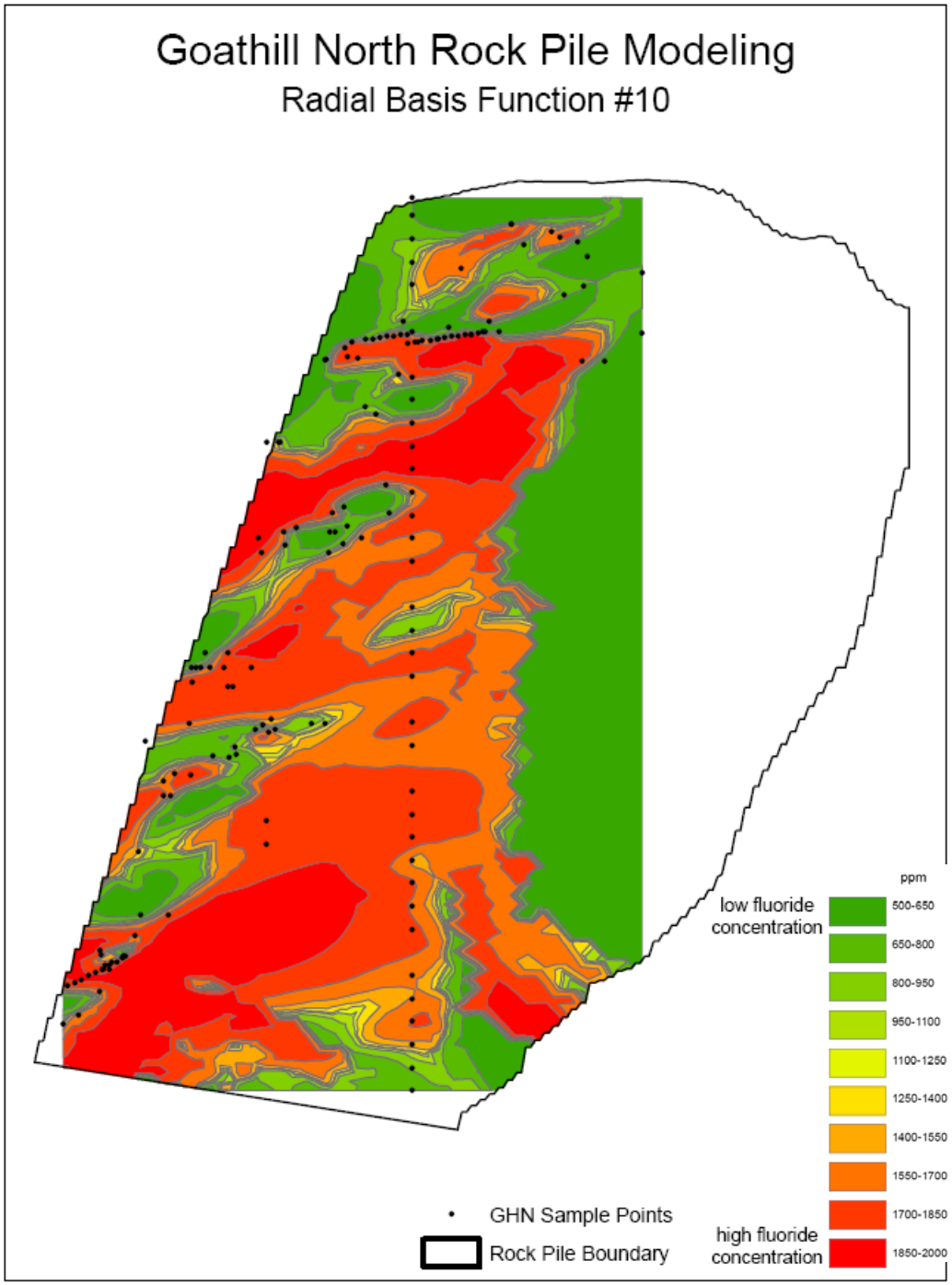
Goathill North Rock Pile Modeling
Radial Basis Function #10
ppm
low fluoride concentration
500-650
650-800
800-950
950-1100
1100-1250
1250-1400
1400-1550
1550-1700
1700-1850
1850-2000
high fluoride concentration
GHN Sample Points
Rock Pile Boundary

Figure 14.

Figures 15 and 16 are model runs using the same parameters as Figure 13 however the stable and unstable samples have been separated.

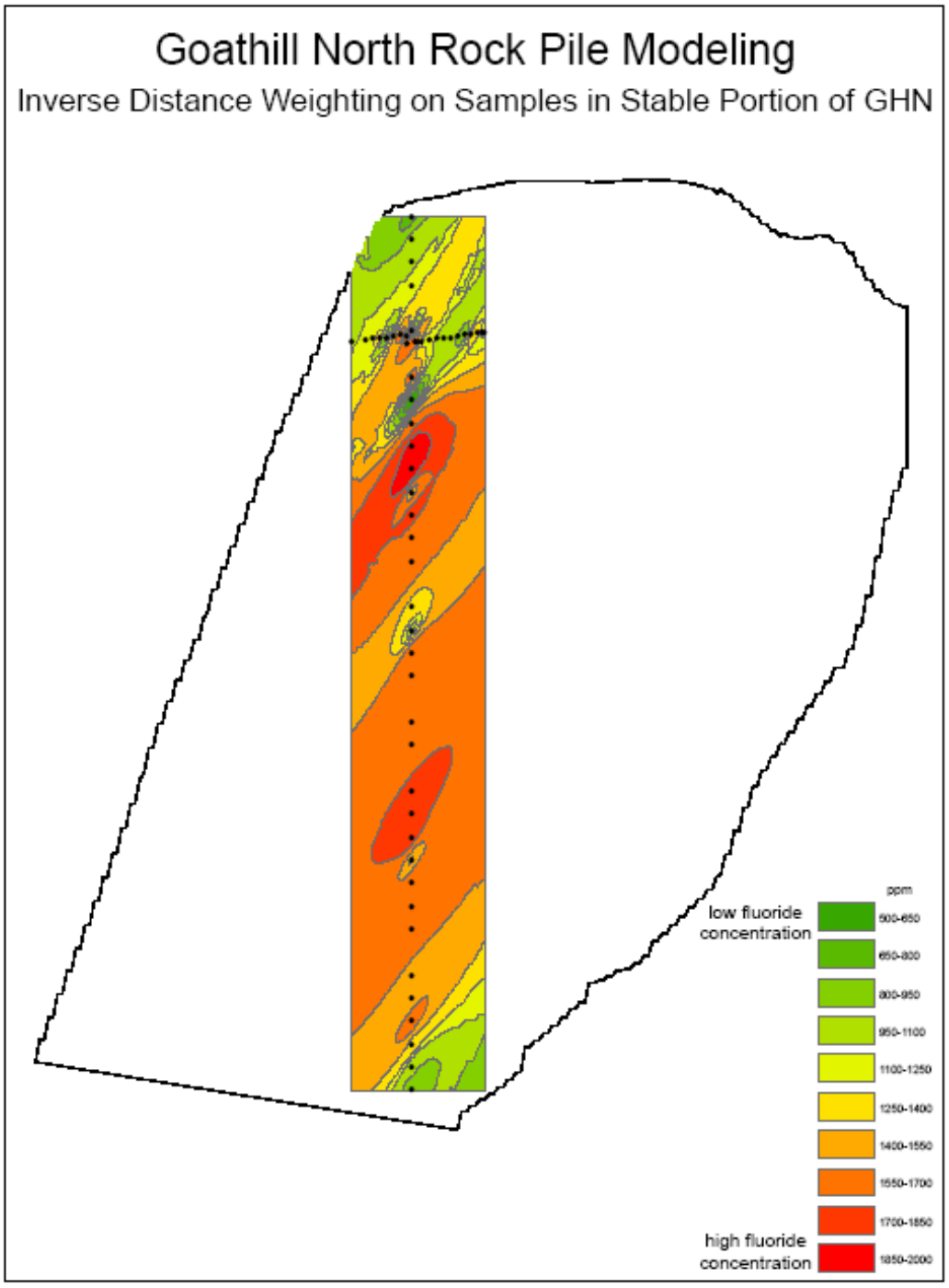

Figure 15.

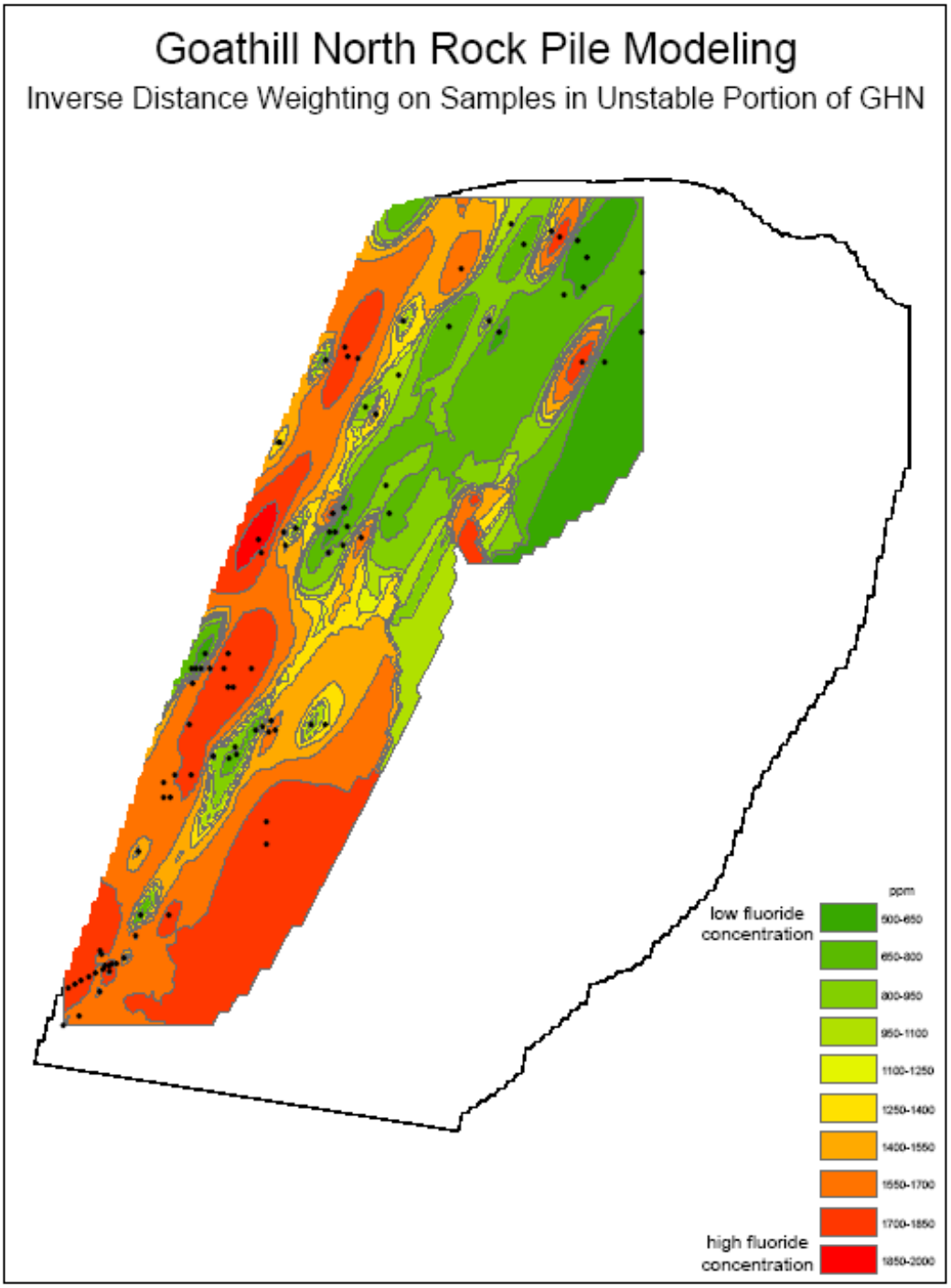
Goathill North Rock Pile Modeling
Inverse Distance Weighting on Samples in Unstable Portion of GHN
ppm
low fluoride concentration
500-650
650-800
800-950
950-1100
1100-1250
1250-1400
1400-1550
1550-1700
1700-1850
high fluoride concentration
1850-2000

Figure 16.

DISCUSSION

Interestingly, the maximum r squared values for both statistical groups do not coincide as much as expected (Table 2a and 2b). Of course, F will have an r squared value of 1 as there is no variation between the single value. The only other elements common to both groups' top 8 is Gadolinium (Gd) and Cobalt (Co) and are thus far an anomalous coincidence.

However, in the All Samples group, the second highest r squared value, occurs for CaO, which is understood and expected because Ca is the main constituent of the primary fluoride bearing minerals fluorite (CaF_2) and fluorapatite [$Ca_5(PO_4)_3F$]. Additionally, in the GHN Samples group, the highest r squared value occurs for S, which is also understood and expected. It is noteworthy that no r squared value occurs above 0.3, which in most applications, would not be considered to have any correlation.

With respect to the Global Polynomial Interpolation (Figure 11) and the Local Polynomial Interpolation (Figure 12), it was noticed immediately that neither of these models could be realistic. This was expected as the intended use for these models does not coincide with modeling fluoride concentration in rock. However, both the Inverse Distance Weighting (Figure 13) and the Radial Basis Function (Figure 14) produced realistic models. The models in Figures 15 and 16 are helpful in that the model area is limited to areas where data points exist.

As outlined in the fluoride analysis SOP, many steps were taken to ensure accurate, precise, and reproducible results. If an anomalous value was obtained, the sample would be re-run in a different batch. It was thus noticed that values from the same crushed sample could have a difference as great as 10%. Additionally, a (rough) hand contoured plot was created and during this exercise, it was particularly noted that within just a few meters fluoride concentration samples could have an order of magnitude of difference between them. This is believed to be caused by the nugget effect.

The nugget effect is an idea common to mining practices that implies there is no practical way of getting a completely homogoneous, representitive sample for one collection point, because one small nugget of a heavy mineral such as fluorite or gold could be found in one sample split and not the other. Even though I may split a 1-gram sub sample from the original sample, there's no guarantee it will be the same the second time I split another 1-gram sample because there's always the possibility in one of the two splits that I get a small fragment of, say, pure fluorite, that would not be found in the second split.

Currently, the fluoride data being obtained is only a small part of the entire Questa Rock Pile Weathering Stability Study. The reason determining fluoride concentration and distribution is necessary for this project is due to the high concentrations of fluorine associated with this Climax-type molybdenum deposit as discussed in the background section. Additionally, because the water that percolates through the rock pile and subsequently into groundwater is acidic, there is a greater potential for F^- mobility and thus a greater risk of groundwater contamination. Therefore, the knowledge of fluoride concentration and distribution is an essential aspect of the project because there is a significant possibility that fluoride treatment becomes a necessary portion of the mine remediation process.

With respect to concentrations, the Environmental Protection Agency (EPA) has a fluoride drinking water standard of 4.0 mg/L (4.0 ppm) (EPA, 2007). However, the study is finding fluoride on the order of thousands of mg/L in the mine waste samples. Fluoride occurs throughout the entire igneous and mineralized system so it is reasonable to believe that most of the fluoride measured occurs here. Additionally, the extremely high values (i.e. PIT-VCV-0024 at 24530 ppm) of fluoride likely occur from bits of fluorite that have been found using microprobe analysis (McLemore, et al., 2009b).

Both the Inverse Distance Weighting and Radial Basis Function models show zones of high concentration down the borehole and in a zone along the surface at the base of the pile. Ritter (2009) found that pyrite is also located in zones and that those zones produce acidic fluids. Since the models show fluoride is occurring in zones, and since acidic conditions are present, there is the possibility of mobile fluoride within the rock pile. It is worth noting, however, that Ritter (2009) also found the rock piles to be unsaturated and interpreted fluid flow likely to occur mainly in the gas phase. The zone of higher concentration on the surface at the toe of the pile may, in fact, be caused by preferential water movement. It would be reasonable to suggest that meteoric water traveled through the rock pile, dissolved fluoride bearing minerals and precipitated secondary fluoride minerals at the base. Additional work would need to be done to determine where the fluoride occurs, whether in primary or secondary minerals. Overall, however, the models suggest little to no preferential concentration of fluoride has occurred. This is a reasonable analysis since the Questa mine is located in a relatively arid region where the time since the rock pile's emplacement has not been great enough.

CONCLUSION

In summary, the purpose of the Questa Rock Pile Weathering Stability Study is to determine a long-term reclamation plan for the area around the Questa Molybdenum Mine. Of the many aspects of this project, this paper focused on the research regarding the total determination of fluoride in the mine rock waste samples. Fluoride in high concentrations (>4.0 ppm) can be hazardous to humans. Every sample analyzed thus far has contained some non-trivial amount (>300 ppm) of fluorine. These results are typical for the Climax-type Molybdenum deposit the Questa Mine is operating from.

It is important to be aware of the limitations of this study and these models. This study only analyzed solid rock; no waters or gasses were analyzed. Regarding the models, it is important to note that there is sample no control in the center of the rock pile, aside from the borehole, so any contours or high vs low concentration modeled is derived solely from models.

Finally, because no direct correlation was found between fluoride and other expected elements, like calcium, it is believed that fluoride may actually be environmentally available; however, it would be found in the aqueous phase rather than the rock and clay portions that this study measured. The next step would be to monitor fluid seepage from the bottom of the pile to determine the extent of fluoride availability. Further analysis is needed to determine the effect of fluoride concentrations on the groundwater supply and its migration to the town of Questa, New

Mexico at the base of the mine. Additionally, more research and analysis is required to determine the total effects of the Questa Mine on the environment.

ACKNOWLEDGEMENTS

I would like to thank Dr. Regina Tempel for taking the time and energy to be my adviser. I would also like to thank my committee members Dr. Lisa Stillings and Dr. Greg Pohll for giving me their time. Additionally, I am grateful to Dr. Virginia McLemore of the New Mexico Bureau of Geology and Mineral Resources for allowing me to use this data set I worked on as an undergraduate for my master's degree. Finally, I give many thanks to my husband, Spc. Daniel Williams who endured my tenure as a graduate student.

REFERENCES

Adams, R., Ahfeld, D., and Sengupta, A., 2007, Investigating the potential for ongoing pollution from an abandoned pyrite mine: Mine Water and the Environment, v. 26, p. 2-13.

Baltz, E. H. and Myers, D. A., 1999, Stratigraphic framework of upper Paleozoic rocks, southeastern Sangre de Cristo Mountains, New Mexico, with a section on speculations and implications for regional interpretation of Ancestral Rocky Mountains paleotectonics: New Mexico Bureau of Geology an dMineral Resources, Memoir 48, 272p.

Bauer, P. V. and Kelson, K. I., 2004, Cenozoic structural development of the Taos area, New Mexico: New Mexico Geological Society Guidebook 55, p. 129-146.

Bégin, L., and J. Fortin, 2003, Evaluation of an acid ammonium oxalate extraction to determine fluoride resident concentrations in soils: J Environ, Qual, Vol. 32, March-April, p662-673.

Briggs, P. H., Sutley, S. J., and Livo, K. E., 2003, Questa Baseline and Pre-mining Ground Water Investigation: 11. Geochemistry of composited material from alteration scars and mine-waste piles: U. S. Geological Survey Open-File Report 03-458, 17 p.

Cather, S. M., 1999, Implications of Jurassic, Cretaceous, and Proterozoic piercing lines for Laramide oblique-slip faulting in New Mexico and rotation of the Colorado Plateau: Geological Society of America, v. 111, p. 849-868.

City-Data.com, Questa, New Mexico, Retrieved November 5, 2005, from www.city-data.com.

Dawson, R. F., 1994, Mine waste geotechnics: University of Alberta, Edmonton, PhD thesis, 262 p.

Donahue, K. M., Dunbar, N. W., and McLemore, V. T., 2007, Origins of clay minerals in the Molycorp Mine Goathill North Rock pile, Questa NM: Society of Mining, Metallurgy and Exploration Annual Convention, Denver, February 2007, no. 07-100, 8 p.

Elrashidi, M. A. and W. L. Lindsay, 1985, Solubility relationships of fluorine minerals in soils: Soil Science Society of America Journal. Vol. 49, p1133.

Environmental Protection Agency, Retrieved December 9, 2007, Drinking Water Contaminants, www.epa.gov.

ESRI Help Manual, accessed January 3, 2010a, Geostatistical Analyst: How Inverse Distance Weighted (IDW) interpolation works, software help files.

ESRI Help Manual, accessed January 3, 2010b, Geostatistical Analyst: How Radial Basis Functions (RBF) work, software help files.

ESRI Help Manual, accessed January 3, 2010c, Geostatistical Analyst: How Local Polynomial interpolation works, software help files.

ESRI Help Manual, accessed January 3, 2010d, Geostatistical Analyst: How Global Polynomial interpolation works, software help files.

Fakhimi, A. and Hosseinpour, H., 2008, The role of oversize particles on the shear strength and deformational behavior of rock pile material, 42nd U.S. Rock Mechanics Symposium, June 29 – July 2, 2008, San Francisco, CA.

Fines, P., Wilson, G. W., Williams, D. J., Tran, A. B., and Miller, S., 2003, Field characterization of two full-scale waste rock piles: *in* ICARD 2003 – Proceedings from the 5th International Conference on Acid Rock Drainage: The Australasian Institute of Mining and Metallurgy, Melbourne, p. 903-909.

Grauch, V. J. S. and Keller, G. R., 2004, Gravity and aeromagnetic expression of tectonic and volcanic elements of the southern San Luis Basin, New Mexico and Colorado: New Mexico Geological Society Guidebook 55, p. 230-243.

Greenfacts.org – Facts on health and the environment, Scientific facts on fluoride, Retrieved November 7, 2005, from http://greenfacts.org.

Guilbert, J. M., and Park, C. F., Jr., 1986, The geology of ore deposits: W. H. Freeman and Company, New York, New York, 985 p.

Johnson, C. M., Czamanske, G. K., and Lipman, P. W., 1989, Geochemistry of intrusive rocks associated with the Latir volcanic field, New Mexico, and contrasts between evolution of plutonic and volcanic rocks: Contributions to Mineralogy and Petrology, v. 103, no. 1, p. 90-109.

Karlstrom, E. E., and Humphreys, E. D., 1998, Persistent influence of Proterozoic accretionary boundaries in the tectonic evolution of southwestern North America: Interaction of cratonic grain and mantle modification events: Rocky Mountain Geology, v. 33, p. 161-179.

Kelson, K. I., Bauer, P. W., Connell, S. D., Love, D. W., Rawling, C. G., and Mansell, M., Initial paleoseismic and hydrogeologic assessment of the southern Sangre de Cristo fault at the Taos Pueblo site, Taos County, New Mexico: New Mexico Geological Society Guidebook 55, p. 289-299.

LoVetere, S. H., Nordstrom, D. K., Maest, A. S., and Naus, C. A., 2004, Questa baseline and pre-mining ground-water quality investigation. 3. Historical ground-water quality for the Red River Valley, New Mexico: U. S. Geologic Survey, Water Investigations Report 03-4186, 238 p.

Luther, S. M. et al., 1996, Fluoride sorption and mineral stability in an Alberta soil interacting with phosphogypsum leachate: Canada Journal of Soil Science. Vol 76. p83.

McQuaker, N. R., and M. Gurney, 1977, Determination of total fluoride in soil and vegetation using an alkali fusion-selective ion electrode technique: Anal. Chem. Vol. 49, p53-56.

McLemore, V. T., 2009, Geologic Setting and Mining History of the Questa mine, Taos County, New Mexico: New Mexico Bureau of Geology and Mineral Resources, Open-file Report 515, 29 p.

McLemore, V. T., Ayakwah, G., Boakye, K., Campbell, A., Dickens, A., Donahue, K., Dunbar, N., Graf, G., Gutierrez, L., Heizler, L., Lynn, R., Lueth, V., Osantowski, E., Phillips, E., Shannon, H., Tachie-Menson, S., van Dam, R., Viterbo, V. C., Walsh, P., Wilson, G. W., and van Zyl, D., 2009a, Characterization of Goathill North rock pile, New Mexico: New Mexico Bureau of Geology and Mineral Resources, Open-file Report 523.

McLemore, V. T., Donahue, K., Dunbar, N., and Heizler, L., 2008, Characterization of physical and chemical weathering in the rock piles and evaluation of weathering indices for the Questa rock piles: unpublished report to Chevron, task 1.3, B1.1.

McLemore, V. T., Russell, C. C., Smth, K. S., and the Sampling and Monitoring Committee of the Acid Drainage Technology Initiative – Metals Mining Sector (ADTI – MMS), 2004, Sampling and Monitoring for Closure: Society of Mining, Exploration, and Metallurgy, SME Preprint No. 04-62, CD-ROM, 10 p.

McLemore, V., Sweeney, D., Dunbar, N., Heizler, L., and Phillips, E., 2009b, Determining quantitative mineralogy using a combination of petrographic techniques, whole rock chemistry, and MODAN: Society of Mining, Metallurgy and Exploration Annual Convention, preprint 09-20, 19 p.

Meyer, J. W., 1991, Volcanic, plutonic, tectonic and hydrothermal history of the southern Questa Caldera, New Mexico: University Microfilms, Ph.D. dissertation, 348 p.

Miller, J.P., Montgomery, A., and Sutherland, P. K., 1963, Geology of part of the southern Sangre de Cristo Mountains, New Mexico: New Mexico Bureau of Mines and Mineral Resources Memoir 11, 106 p.

Mineral Information Institute (MII), Retrieved November 25, 2005, from http://www.mii.org.

Molling, P. A., 1989, Applications of the reaction progress variable to hydrothermal alteration associated with the deposition of the Questa molybdenite deposit: Ph.D. dissertation, Johns Hopkins University, Baltimore, MD, 227 p.

Molycorp, Retrieved November 3, 2005, Molybdenum operations history, from www.molycorp.com.

Munroe, E. A. and McLemore, V. T., 1999, Waste rock pile characterization, heterogeneity and geochemical anomalies in the Hillsboro mining district, Sierra County, New Mexico: Journal of Geochemical Exploration, v. 66, p. 389-405.

Munroe, E. A., McLemore, V. T., and Dunbar, N. W., 2000, Mine waste rock pile geochemistry and mineralogy in southwestern New Mexico, USA, *in* ICARD 2000 – Proceedings from the 5th International Conference on Acid Rock Drainage: Society for Mining, Metallurgy, and Exploration, Inc., Littleton, Colorado, p. 1327-1336.

Mutschler, F. E., Wright, E. G., Ludington, S.D., and Abbott, J. T., 1981, Granitic molybdenite systems: Economic Geology, v. 76, p. 874-897.

National Atmospheric Deposition Program (NADP)/National Trends Network, Retrieved November 30, 2005, from http://nadp.sws.uiuc.edu.

Reddy, K. J. and S. P. Gloss, 1993, Geochemical speciation as related to the mobility of F, Mo, and Se in soil leachates: Applied Geochemistry. Vol. S2. p159.

Ritter, M., 2009, Fluid flow estimates in molybdenum mine rock piles using borehole temperature logs, Environmental & Engineering Geoscience, v. 15, no. 3, p. 175-195.

Robertson GeoConsultants, Inc., 2000a, Progress report: Results of phase 1 physical waste rock characterization, Questa, New Mexico: unpublished report to Molycorp, Inc., 052007/4, June.

Robertson GeoConsultants, Inc., 2000b, Interim mine site characterization study, Questa Mine, New Mexico: unpublished report to Molycorp, Inc., 052008/10, November.

Ross, P. S., Jebrak, M., and Walker, B. M., 2002, Discharge of hydrothermal fluids from a magma chamber and concomitant formation of a stratified brecia zone at the Questa porphyry molybdenum deposit, New Mexico: Economic Geology, v. 97, p. 1679-1699.

Rowe, A., 2005, Fluid evolution of the magmatic hydrothermal breccia of the Goat Hill orebody, Questa Climax-type porphyry molybdenum system, New Mexico – a fluid inclusion study: M.S. thesis, New Mexico Institute of Mining and Technology, Socorro, 134 p.

Schilling, J. H., 1960, Mineral resources of Taos County, New Mexico: New Mexico Bureau of Mines and Mineral Resources, Bulletin 71, 124 p.

Schilling, J. H., 1990, A history of the Questa molybdenum (moly) mines, Taos County, New Mexico: New Mexico Geological Society, Guidebook 41, p. 381-386.

Selim, H. M. and W. L. Kingery, 2003, Geochemical and Hydrological Reactivity of Heavy Metals in Soils: Lewis Publishers. p331-333.

Shannon, H., Sigda, J., van Dam, R., Hendrickx, J., and McLemore, V. T., 2005, Thermal Camera Imaging of Rock Piles at the Questa Molybdenum Mine, Questa, New Mexico: National Meeting of the American Society of Mining and Reclamation, Breckenridge, Colorado, June, CD-ROM.

Shaw, S., Wels, C., Robertson, A., and Lorinczi, G., 2002, Physical and geochemical characterization of mine rock piles at the Questa mine, New Mexico; *in* Tailings and Mine Waste '02: Proceedings of the Ninth International Conference on Tailings and Mine Waste: Fort Collins, Colorado, USA, 27-30 January, p. 447-458.

Sinclair, D. W., 1995, Prophyry Mo (climax-type): Ministry of Energy, Mines and Petroleum Resources, Retrieved November, 26, 2005, from http://www.em.gov.bc.ca.

Smith, F. A., 1983, Fluorides in everyday life: Fluorides: Effects on Vegetation, Animals and Humans, J.L. Shupe, et al, Eds., Paragon Press, Inc., Salt Lake City, UT, p7.

Smith, K. S., Briggs, P. H., Campbell, D. L., Castle, C. J., Desborough, G. A., Eppinger, R. G., III, Fitterman, D. V., Hageman, P. L., Leinz, R. W., Meeker, G. P., Stanton, M. R., Sutley, S. J., Swayze, G. A., and Yager, D. B., 2000a, Tools for the rapid screening and characterization of historical metal-mining waste dumps, *in* Proceedings of the 2000 Billings Land Reclamation Symposium, Billings, Montana, March 20-24, 2000: Bozeman, Montana State University, Reclamation Research Unit Publication No. 00-10 (CD-ROM), p. 435-442.

Smith, K. S., Ramsey, C. A., and Hageman, P. L., 2000b, Sampling strategy for rapid screening of mine-waste dumps on abandoned mine lands: in proceedings; *in* ICARD 2000 – Proceedings from the 5th International Conference on Acid Rock Drainage: Society for Mining, Metallurgy and Exploration, Inc., v. II, p. 1453-1461.

Tran, A. B., Miller, S., Williams, D. J., Fines, P., and Wilson, G. W., 2003, Geochemical and mineralogical characterization of two contrasting waste rock dumps – The INAP waste rock dump characterization project; *in* ICARD 2003 – Proceedings from the 5th International Conference on Acid Rock Drainage: The Australasian Institute of Mining and Metallurgy, Melbourne, p. 939-947.

URS Corporation, 2003, Mine rock pile erosion and stability evaluations, Questa mine: Unpublished Report to Molycorp, Inc. 4 volumes.

van Dam, R. L., Gutierrez, L. A., McLemore, V. T., Wilson, G. W., Hendrickx, J. M. H., and Walker, B. M., 2005, Near surface geophysics for the structural analysis of a mine rock pile, northern New Mexico: 2005 National Meeting of the American Society of Mining and Reclamation, Breckenridge, Colorado, June, CD-ROM.

Viterbo, V., McLemore, V., Donahue, K., Aimone-Martin, C., Fakhimi, A., and Sweeney, D., 2007, Effects of Chemistry, Mineralogy, Petrography and Alteration on Rock Engineering Properties of the Goathill North Rock Pile at the Molycorp Questa Mine, New Mexico:

Society of Mining, Metallurgy and Exploration Annual Convention, Denver, February 2007, no. 07-099, 8p.

Weinstein, L. H. and R. Alscher-Herman, 1982, Physiological responses of plants to fluorine: Effects of Gaseous Air Pollution in Agriculture and Horticulture, M. H. Unsworth and D. P. Ormrod, Eds, Butterworths, London, p139.

Wels, C., Loudon, S., and Fortin, S., 2002, Factors influencing net infiltration into mine rock piles at Questa Mine, New Mexico; *in* Tailings and Mine Waste '02: Proceedings of the Ninth International Conference on Tailings and Mine Waste: Fort Collins, Colorado, USA 27-30 January, p. 469-477.

Western Regional Climate Center (WRCC), 2010a, Period of Record General Climate Summery – Temperature, http://www.wrcc.dri.edu/cgi-bin/cliMAIN.pl?nm7323, accessed April 11, 2010.

Western Regional Climate Center (WRCC), 2010b, Period of Record General Climate Summery – Precipitation, http://www.wrcc.dri.edu/cgi-bin/cliMAIN.pl?nm7323, accessed April 11, 2010.

Wildeman, T. R., Ranville, J. F., Herron, J., and Robinson, R. H., 2003, Development of a simple scheme to determine the chemical toxicity of mine wastes, in Proceedings, 2003 National Meeting of the American Society of Mining and Reclamation and 9th Billings Land Reclamation Symposium, Billings, Montana, June 3-6, 2003: Lexington, Kentucky, American Society of Mining and Reclamation.

APPENDIX 1 – FLUORIDE SOP

STANDARD OPERATING PROCEDURE NO. 69
DETERMINATION OF TOTAL FLUORIDE AND FERROUS IRON IN SOLID SAMPLES

	REVISION LOG	
SOP 69v1	**Original SOP**	**Shannon Archer, Joann Baker, Stacy O'Neil, Bonnie Frey 11/10/05**
SOP 69v1	**Edits LMK**	**11/1105**
SOP 69v2	**Procedural updates by BAF**	**4/3/07**
SOP 69v2	**LMK made minor edits to content and formatting.** **Finalized by LMK for posting to Molycorp project website and to send to George Robinson for lab audit**	**4/4/07**

1.0 PURPOSE AND SCOPE

This Standard Operating Procedure (SOP) provides technical guidance and procedures for two analyses to be completed on the Questa Mine rock pile samples for the Rock Pile Stability Study: analysis of fluoride using a NaOH fusion – selective ion electrode technique, and analysis of ferrous iron using an acid digestion – potassium dichromate titration method. This SOP addresses equipment, sample preparation, laboratory and instrument procedures, personnel responsibilities and quality control. Topics applying to both methods, such as safety and quality control objectives, will be addressed in sections 1.0 through 6.0. Topics applying to individual methods will be discussed in a separate section for each method – Part I for Total Fluoride and Part II for Ferrous Iron..

2.0 RESPONSIBILITIES AND QUALIFICATIONS

The New Mexico Bureau of Geology and Mineral Resources Chemistry Laboratory Manager, under the direction of the Team Leader and Characterization Team, will have the overall responsibility for implementing this SOP. She will be responsible for assigning appropriate staff to implement this SOP and for ensuring that the procedures are followed accurately.

All personnel performing these procedures are required to have the appropriate health and safety training. In addition, all personnel are required to have a complete understanding of the procedures described within this SOP and to receive specific training regarding these procedures, if necessary.

All environmental staff and assay laboratory staff are responsible for reporting deviations from this SOP to the Team Leader.

3.0 DATA QUALITY OBJECTIVES

This SOP addresses the following objectives in the data quality objectives outlined in the "Geological and Hydrological Characterization work plan at the Molycorp Questa Mine, Taos County, New Mexico":

1. To provide principle investigator (PI) researchers with quality analytical laboratory data that have been verified and validated.
2. To provide PI researchers with analytical data that have appropriate detection limits and that have been conducted in accordance with acceptable procedures.
3. To provide PI researchers with confidence that the data have been generated and transferred to the centralized database utilizing the procedures outlined in the project SOPs.

4.0 RELATED STANDARD OPERATING PROCEDURES

The procedures for providing analyses by ICP-MS set forth in this SOP are intended for use with the following SOPs:

- SOP 1 Data management (including verification and validation)
- SOP 2 Sample management (including chain of custody)
- SOP 5 Sampling outcrops, rock piles, and drill core (solid)
- SOP 22 Analytical data validation
- SOP 36 Sample preservation, storage, shipping and custody

5.0 LABORATORY SAFETY

Several safety aspects must be observed by all laboratory personnel: the proper and safe handling of acids, especially hydrofluoric acid, and all other general safe laboratory practices detailed in New Mexico Tech's Laboratory Safety Manual.

Hydrofluoric acid are among the most dangerous chemicals used in the Chem Lab. Special precautions must be taken during their use. The most important and basic of these precautions are posted in the vicinity of the perchloric acid fume hood, which will be used for all procedures. Basic first aid (instruction posted near fume hood) should be administered if any personnel become exposed to these acids through skin contact, eye contact, inhalation, or ingestion.

6.0 QUALITY ASSURANCE/QUALITY CONTROL

Laboratory analytical balances should be calibrated every day using the autocal function.

Run a standard with every set of samples. Run a duplicate sample for every 10 samples. If the relative percent difference of the Standard Reference Materials at the beginning of a set is greater than 10%, the samples will be reanalyzed.

Part I. DETERMINATION OF TOTAL FLUORIDE

I.1 Materials List

- Fisherbrand 4" x 4" weighing paper
- 150-mL nickel crucibles
- Fisherbrand 5000-uL pipetter and polypropylene pipette tips
- Blue M Stabil-Therm Power-O-Matic 70 low-temperature (capacity to 150°C) oven
- Dessicator
- Thermolyne 46200 high-temperature muffle furnace (capacity to 600°C)
- Thermolyne Cimarec 1 4"x 4" hot plate
- Hydrion Paper Insta-check 0-13 pH paper
- Teflon stir rods
- Nalgene polypropylene 250-mL volumetric flasks
- Nalgene polypropylene 250-mL storage bottles
- Polystyrene 65-mm disposable funnels
- Whatman 4 filter paper
- Cole-Parmer fluoride ion electrode
- Oakton pH 2100 Series Benchtop Meter
- Plastic or Teflon 100-mL or 150-mL beakers
- Stir magnets
- VWR Scientific Products stir plate
- Small piece of Styrofoam for top of stir plate
- Lab notebook and indelible pen
- Fisherbrand 100-1000 uL pipetter and polypropylene pipette tips
- (2) 1-L Nalgene plastic storage bottles
- (2) 500-mL Nalgene plastic storage bottles
- Laboratory tape
- "Sharpie" or similar indelible marker pen
- Ohaus Voyager balance

I.2 Chemical List

- Water filtered by reverse osmosis to 18.4 MOhms (hereafter referred to as RO water)
- Granular sodium fluoride (NaF)
- Glacial acetic acid
- Sodium citrate dihydrate
- Sodium hydroxide (NaOH) pellets

- American Chemical Society (ACS) grade hydrochloric acid (HCl)

I.3 Reagents List

- *Stock Fluoride Solution (1000 ppm F).* Dissolve 2.210 g pre-dried reagent grade NaF in RO water and dilute to 1 liter. Store in a closed polyethylene container.

- *Total Ionic Strength Adjustment Buffer (TISAB).* To 300 mL of RO water add 58 mL of glacial acetic acid and 12.0 g of sodium citrate dihydrate. Stir to dissolve. Adjust the pH to 5.2 using 6 N NaOH. Cool and dilute with RO water to 1 liter. (Note: More than 100 mL of 6N NaOH will be needed. 6N NaOH is 24 g NaOH pellets per 100 mL of RO water.)

- *Sodium Hydroxide Solution*. Dissolve 670 g of NaOH pellets in RO water and dilute to 1 liter. Store in polyethylene container. (Note: It will take more than a full day to make this solution.)

- *Fluoride Storage Solution*. A 0.01 M fluoride solution made up from the stock fluoride solution with 1% TISAB.

I.4 PROCEDURES

I.4.1 Sample Preparation

1. Samples to be analyzed are received in powdered form following SOP 8 Solid Sample Preparation.

2. Preheat the low-temperature oven to 150°C.

3. Weigh 0.500 g of sample onto weighing paper.

4. Record the exact weight of sample in the lab notebook. See section 5.5 in this SOP (Documentation for Sample Preparation) for specific details.

5. Carefully transfer sample to a 150-mL nickel crucible. If doing several samples at a time, mark the sample number on the outside of the crucible using a Sharpie®.

6. Moisten the sample slightly with RO. Use a few drops to cover the sample – just enough to wet the bottom of the crucible. Do the same for blanks.

7. Add 6.0 mL of the NaOH solution to each crucible. Note: A series of blanks must also be prepared to use as a calibration solution. Prepare five (5) such blanks in the same manner as above but without sample. Only three (3) will be used in the end, but more are prepared in case of loss of blank during the procedure.

8. Place the crucibles in the low-temperature oven at 150°C for 1½ hours.

9. Wearing appropriate safety equipment, remove crucibles from the oven and place them in the desiccator. Samples should solidify within 10 minutes. If the samples do not solidify, place them back in the oven for at least another half hour before returning them to the desiccator to solidify

10. While waiting for the samples to solidify, turn on the high-temperature furnace and set the temperature to 300°C using the arrow buttons. (NOTE: The high-temperature furnace will burn off any sharpie marks on the crucible. On a piece of paper, note the location of each sample in the furnace. In a desiccator, mark and label the location with lab tape where each sample will later be moved to cool.)

11. Once samples have solidified and the target temperature has been reached, wear protective gloves and place them in the high-temperature furnace.

12. Allow high-temperature furnace to return to 300°C.

13. Once the furnace has reached 300°C, start program 7 and fuse the samples at 600°C for 30 minutes. Once the program has ended, allow the furnace temperature to reach 400°C before removing the samples.

14. Wearing appropriate safety equipment, remove the samples from the furnace and place them on their labeled locations in the desiccator. The samples should crystallize quickly. Allow the samples to cool to room temperature.

15. Once the samples have cooled, rewrite the sample numbers on the crucibles with a Sharpie and add 10 mL of RO water to each crucible.

16. Under a fume hood, heat the samples slightly using small hot plates set to a medium heat. Heat until there is no solid left. NOTE: The remaining steps will produce HF acid and will require appropriate safety equipment.

17. Under the fume hood, add 7 mL of ACS grade HCl using the 5000-uL pipetter. (NOTE: Adding concentrated HCl to concentrated NaOH is a violent reaction that creates HF. Add the acid dropwise, or as slowly as possible, while continually stirring using a Teflon stir rod. From this step on, only plastic or Teflon labware should be used as the HF will etch anything made of glass.)

18. After 7 mL of HCl has been added, test the solution pH using pH paper. The desired pH is between 8 and 9. If this pH is not attained, add 100 uL or less of HCl at a time until the desired pH is reached. Samples will turn to a baby-food consistency and blanks will remain liquid. (NOTE: Blanks are difficult to acidify as their pH changes rapidly. If a blank is over-acidified, discard and use one of the spares until three (3) blanks have the desired pH.)

19. Transfer samples to a polypropylene 250-mL volumetric flask using filter stands and polystyrene disposable funnels. Dilute to volume with RO water.

20. Once filled to volume, filter through a dry Whatman No. 4 or 40 filter paper into a 250-mL polypropylene bottle. Write the sample name, crucible number, and date on each bottle with a Sharpie marker. NOTE: Do not moisten filter paper before filtration. Leave the filters to dry overnight and dispose of in a trash container specified for fluorine waste.

21. If blanks have been done during this run, combine all three into one polypropylene container large enough to hold 750 mL.

I.4.2 Sample Analysis

1. Construct a table like the one described in section 5.5 in this SOP (Documentation for Sample Analysis) in the lab notebook.

2. Soak the fluoride probe in the Fluoride Storage Solution for at least half an hour before analysis.

3. Using a graduated cylinder, measure out 25 mL of TISAB solution into a plastic or Teflon beaker.

4. Rinse a different graduated cylinder with RO water. Place 10-15 mL of the blank solution in the graduated cylinder. Swirl the sample around the graduated cylinder making sure the sample touches the entire inner surface of the graduated cylinder. Discard this amount of sample in an appropriate fluorine waste container.

5. In the rinsed graduated cylinder, measure out 25 mL of blank sample solution into the same beaker as the TISAB solution.

6. Place beaker on a small stir plate. (NOTE: A small piece of Styrofoam must be placed between the top of the plate and the sample beaker to help absorb the heat created by the stir plate. This heat could cause errors in measurements.)

7. Place a stir magnet in the bottom of the beaker and begin stirring the solution slowly. Once the solution has begun stirring, adjust the stir plate setting to 1 or 2.

8. Rinse the fluoride probe with RO into a waste container and gently place the probe in the beaker. Do not allow the stir magnet to bump the probe. Also, make sure the probe is a few centimeters away from the edges of the beaker as the plastic or Teflon may interfere and cause an inaccurate reading.

9. Wait about 5 minutes for the fluoride meter to stabilize before recording the mV value in the lab notebook.

10. Using the 100-1000uL pipetter (blue), add 100uL of 10ppm fluoride solution.

11. Wait about 5minutes for the meter to stabilize and record the new value.

12. Continue to add 100uL of 10ppm fluoride solution and record the values until 5-ug fluoride have been added.

13. Begin adding 100uL of 100 ppm fluoride solution and record the values until you reach one measurement below 50 mV. (This usually occurs around 145-165 ug fluoride.) Note that the meter will stabilize faster once more fluoride has been added requiring only a couple of minutes of waiting for the meter to stabilize.

14. Once a reading below 50mV has been reached, carefully remove the probe from the beaker and rinse with RO water. Remove the stir magnet and rinse with RO water. Dispose the solution in the beaker into an appropriate fluoride waste container.

15. Repeat steps 2-7 for each sample.

16. Rinse the fluoride probe with RO into a waste container and gently place the probe in the beaker. Do not allow the stir magnet to bump the probe. Also, make sure the probe is a few centimeters away from the edges of the beaker as the plastic or Teflon may interfere and cause an inaccurate reading.

17. Wait about 5 minutes for the fluorine meter to stabilize. Record the mV value.

18. Remove the probe and stir magnet and rinse both with RO water.

19. Repeat steps 15-19 for all samples.

20. Dispose of the analyzed sample in an appropriate fluorine waste container.

I.4.3 Data Analysis

The following directions describe how final fluoride concentrations are to be calculated in Microsoft Excel. Figures 2 and 3 provide visual instruction for the setup of these calculations.

1. Create columns labeled **ugF**, **log (ugF)**, and **mV**. Enter the data from the lab book into the appropriate columns. Calculate log (ugF).

2. Make two plots of log (ugF) vs. mV as x and y coordinates respectively in an XY scatter plot. The first plot will be for all log (ugF) values. The second plot will be for log (ugF) values of ugF greater than 15.

3. For each plot, create a trendline and display the associated trandline equation and R-squared value. Ideally the equation should follow the Nernst equation:

$$E_i = -S \log C_i + B$$

where C_i is the ugF yielding a millivolt potential of E_i; S is the Nernst slope (RT/F) which equals 58.5 mV at 22°C, and B is a millivolt potential which is dependent on the ionic background (McQuaker, p. 54).

4. Below the ugF/mV table, create another table with the following headings: **sample name**, **weight**, **mV**, **mL in probe**, **x=log(ugF)**, **ug in the 25mL**, **ppm F**, **mg/L in soln**, **given ppm**, **% difference**, **User name or initials (prep)**, **User name or initials(analysis)**.

5. Enter information from the fluoride lab book under the headings of **sample name**, **weight**, **mV**, and **mL in probe**.

6. Using the equation from the log (ugF) vs. mV plots, solve for x and enter this equation under the **x=log (ugF)** heading. Use this calculation for all mV readings taken on samples.

7. Under the **ug in the 25mL** heading, take the antilog of the value from the previous step.

8. Under the **ppmF** heading, multiply the value from the previous step by 10 and divide by the sample weight.

9. Under the **mg/L in soln** heading, divide the value from the ug in the 25mL cell by 25. Note, the 25 is from the **mL in probe** column, which should be the same for all the samples. In the rare cases where sample dilutions are required, this cell will be provide the dilution multiplier.

10. Under the **given ppm** heading, type the certified value provided for all Standard Reference Materials.

11. Under the **% difference** heading, enter a formula to calculate percent different between the measured value of each Standard Reference Material and its certified value. (= 100 * (difference between measured and certified values) / (average of measured and certified values)

12. Under the **User (prep)** heading, record the initials of the person who prepared the sample, and under the **User (analysis)** heading, record the initials of the person who analyzed the sample.

I.5 CALCULATIONS

Calculations are to be done as described in the Data Analysis portion of the Procedure (Section 5.3) in an Excel spreadsheet. No other calculations are necessary.

I.6 DOCUMENTATION

I.6.1 Chain of Custody

Chain of custody forms must be used in accordance with SOP 2.

I.6.2 Sample Preparation

At the top of the page, record the date, the worker's initials, and the title "Determination of Total Fluoride". Under the title line, create three columns: **crucible**, **sample ID**, and **weight**. Under the crucible column, number the crucibles being used beginning with the number 1. Next to this crucible number, under the sample ID column, list the samples that are to be placed in the respective crucible. Record the weight (g) of the amount of sample placed in the crucible under the weight column.

I.6.3 Sample Analysis

At the top of the page, record the date, the worker's initials, and the title "Determination of Total Fluoride". On the left hand side of the page, make two columns **ugF** and **mV**. Under the **ugF** column, record each volume ugF added. The amounts should be 0, 1, 2, 3, 4, 5, 15, 25, 35, 45 … until the last addition is completed. Under the **mV** column, record the electrode potentional measured by the fluoride meter from steps 9, 12, and 13 of the Sample Analysis Procedure. Leaving a small amount of space, make two more columns with the headings **Sample ID** and **mV**. Record the Sample ID and the mV reading obtained in step 17 of the Sample Analysis Procedure.

I.6.4 Data Analysis

Refer to section 5.1 Data Analysis Procedure and Figures 1-3.

I.6.5 Data Reporting

Data will be reported to the Project Manager in two columns, one with the sample name, the other with the concentration of fluoride (mg/kg) measured.

I.7 LIMITATIONS/INTERFERENCES

For samples with greater than 3000 ppm fluoride, a more accurate measurement is obtained with a 1:5 dilution of the sample as well as a 1:5 dilution of the calibration standard. Only plastic or Teflon labware can be used with fluoride, therefore class A volumetrics were not available for dilutions. Only eight samples could be run at a time because of oven space limitations, therefore, several days worth of samples were analyzed during one calibration.

Alkaline conditions are required during the filtering process to insure the removal of interfering cations. At this alkaline state, possible interfering cations like aluminum and iron are preferentially removed as insoluble oxides. Filtering during alkaline conditions removes these cations from hundreds of ppm to <0.05ppm (McQuaker).

Part I FIGURES

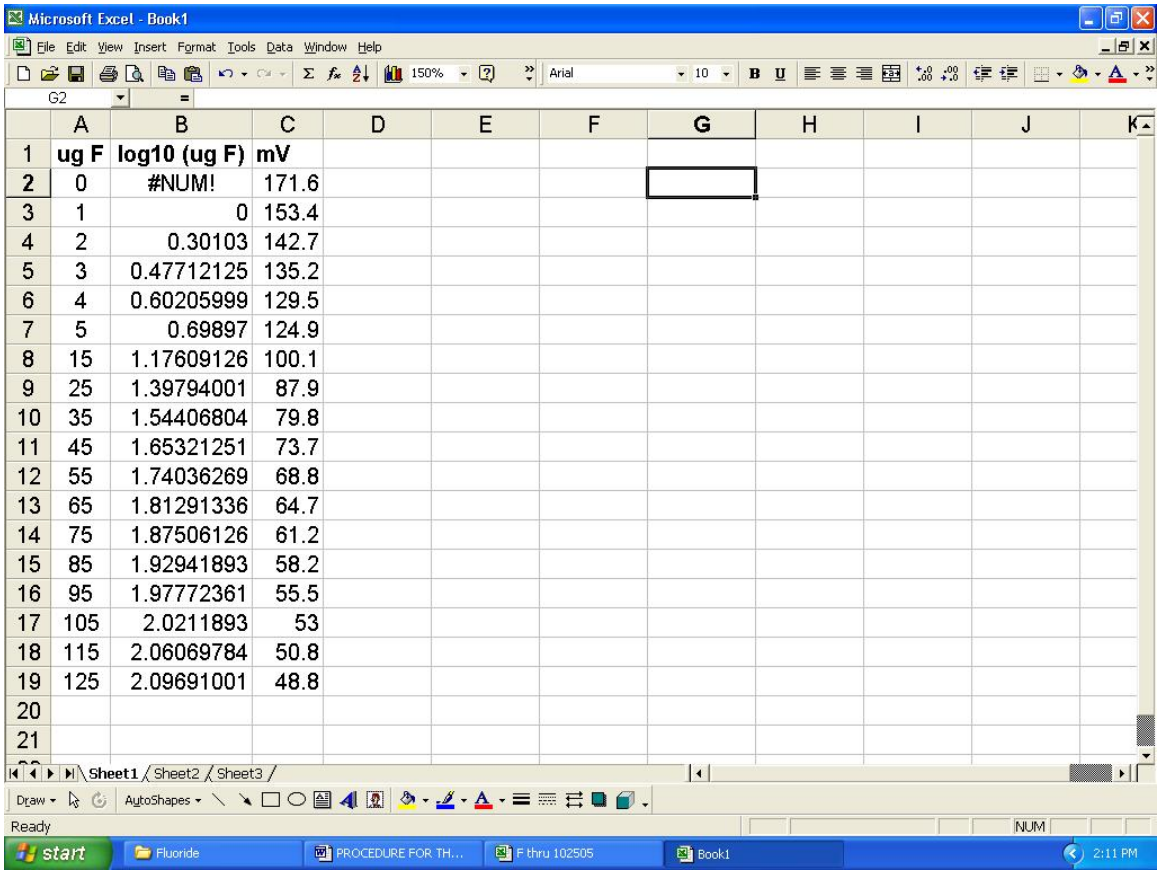

	A	B	C
1	ug F	log10 (ug F)	mV
2	0	#NUM!	171.6
3	1	0	153.4
4	2	0.30103	142.7
5	3	0.47712125	135.2
6	4	0.60205999	129.5
7	5	0.69897	124.9
8	15	1.17609126	100.1
9	25	1.39794001	87.9
10	35	1.54406804	79.8
11	45	1.65321251	73.7
12	55	1.74036269	68.8
13	65	1.81291336	64.7
14	75	1.87506126	61.2
15	85	1.92941893	58.2
16	95	1.97772361	55.5
17	105	2.0211893	53
18	115	2.06069784	50.8
19	125	2.09691001	48.8
20			
21			

Figure 1 – Example data analysis spreadsheet for calibration curve.

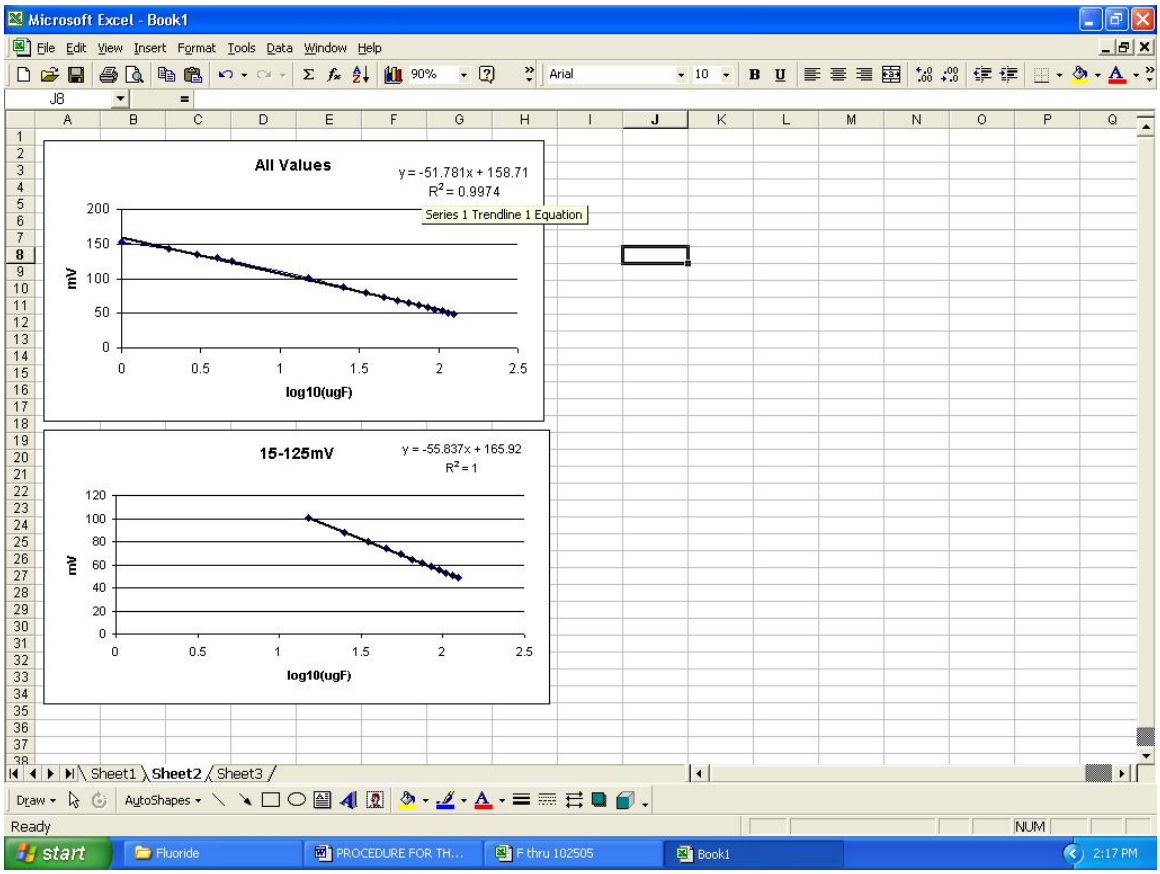

Figure 2 – Example charts for determining the calibration curve.

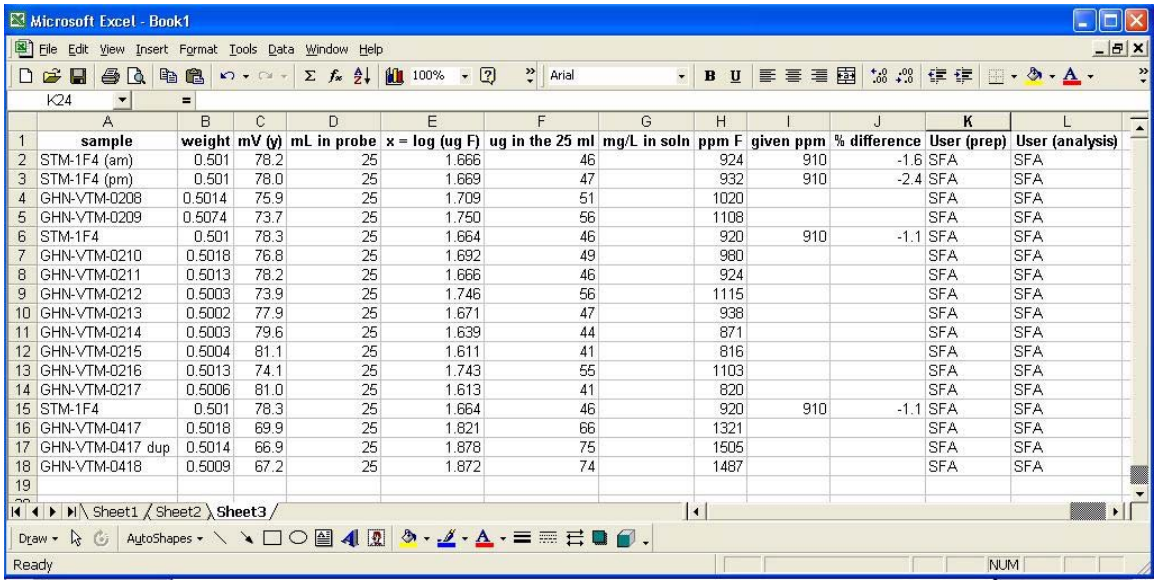

	A	B	C	D	E	F	G	H	I	J	K	L
1	sample	weight	mV (y)	mL in probe	x = log (ug F)	ug in the 25 ml	mg/L in soln	ppm F	given ppm	% difference	User (prep)	User (analysis)
2	STM-1F4 (am)	0.501	78.2	25	1.666	46		924	910	-1.6	SFA	SFA
3	STM-1F4 (pm)	0.501	78.0	25	1.669	47		932	910	-2.4	SFA	SFA
4	GHN-VTM-0208	0.5014	75.9	25	1.709	51		1020			SFA	SFA
5	GHN-VTM-0209	0.5074	73.7	25	1.750	56		1108			SFA	SFA
6	STM-1F4	0.501	78.3	25	1.664	46		920	910	-1.1	SFA	SFA
7	GHN-VTM-0210	0.5018	76.8	25	1.692	49		980			SFA	SFA
8	GHN-VTM-0211	0.5013	78.2	25	1.666	46		924			SFA	SFA
9	GHN-VTM-0212	0.5003	73.9	25	1.746	56		1115			SFA	SFA
10	GHN-VTM-0213	0.5002	77.9	25	1.671	47		938			SFA	SFA
11	GHN-VTM-0214	0.5003	79.6	25	1.639	44		871			SFA	SFA
12	GHN-VTM-0215	0.5004	81.1	25	1.611	41		816			SFA	SFA
13	GHN-VTM-0216	0.5013	74.1	25	1.743	55		1103			SFA	SFA
14	GHN-VTM-0217	0.5006	81.0	25	1.613	41		820			SFA	SFA
15	STM-1F4	0.501	78.3	25	1.664	46		920	910	-1.1	SFA	SFA
16	GHN-VTM-0417	0.5018	69.9	25	1.821	66		1321			SFA	SFA
17	GHN-VTM-0417 dup	0.5014	66.9	25	1.878	75		1505			SFA	SFA
18	GHN-VTM-0418	0.5009	67.2	25	1.872	74		1487			SFA	SFA
19												

Figure 3 – Example of data analysis spreadsheet.

Part I REFERENCES

McQuaker, Neil R., Gurney, Mary. Determination of total fluoride in soil and vegetation using an alkali fusion-selective ion electrode technique. Analytical Chemistry, Vol. 49, No. 1, January 1977, pp. 53-56.

Cole-Parmer Laboratory Fluoride Ion Electrode Instruction Manual, Cole-Parmer catalog number 27502-19.

Part II. DETERMINATION OF FERROUS IRON

A solution of potassium dichromate ($K_2Cr_2O_7$) complexes with ferrous iron as it is released from a sample by heating with sulfuric acid and hydrofluoric acid in a water bath. A solution to indicate excess $K_2Cr_2O_7$ is added and titrated with an Fe^{2+} solution to determine the excess $K_2Cr_2O_7$, which in turn is used to determine ferrous iron in the sample.

II.1 MATERIALS LIST

- 25 ml glass pipette
- Plastic graduated cylinder (for H_2SO_4)
- Hot plate
- Teflon® beakers and lids, including one to monitor the temperature of the solutions.
- Two burettes (for Fe^{2+} solution and $K_2Cr_2O_7$ solution)
- Dropper (for indicator)
- 5 ml pipetter and tips (for HF and H_3PO_4)
- Parafilm®
- Magnetic stirrers and plate, including Teflon® stirrers

II.2 REAGENTS LIST (all made up from ACS grade chemicals):

- Standard $K_2Cr_2O_7$ (potassium dichromate) solution: 2.730g standard grade $K_2Cr_2O_7$/ 1L H_2O (RO) made up in a 1000ml glass volumetric flask. $K_2Cr_2O_7$ must be dried overnight in low temperature oven.
- Fe^{2+} solution: 24g of $Fe(NH_4)_2(SO_4)_2 \cdot 6H_2O$ (Ferrous ammonium sulfate), 10 ml concentrated H_2SO_4, brought to 1L with H_2O in a 1000-ml glass volumetric flask. The $Fe(NH_4)_2(SO_4)_2 \cdot 6H_2O$ should not be dried in a drying oven or it will oxidize to Fe^{3+}.
- Indicator solution: 0.2% solution of sodium diphenylamine sulfonate in H_2O made up in a 250-ml glass volumetric flask.

- Ferric sulfate powder dried overnight in low temperature oven.
- 1:3 H_2SO_4 made up in 1 L bottle with 333 ml H_2SO_4 brought to volume in a 1-L bottle. Make solution up slowly, because the solution will heat up quickly and create a safety hazard.
- Concentrated HF
- 85% H_3PO_4

II.3 PROCEDURES

- II.3.1 Sample preparation:
  - Transfer 25ml of standard $K_2Cr_2O_7$ into each Teflon beaker with a glass pipette.
  - Add 25ml of 1:3 H_2SO_4 to each beaker with a graduated cylinder.
  - Add 0.050g of ferric sulfate to the blank and other samples in which Fe is expected to be near the detection limit to prevent the $Cr_2O_7^{2-}$ from reacting with HF. Refer to total Fe data provided by the Project Manager.
  - Add each sample and record the weight. The sample must pass through 100-mesh sieve and therefore should be the ground samples described in SOP 36. The amount of sample added depends on the amount of total iron in the sample to provide an excess of $K_2Cr_2O_7$ for titration. The following guidelines will help make this determination.
    - The weight of the sample must be $\leq$ (0.111g)/(wt% Fe_2O_3T)
    - The weight of the sample must be $\leq$ (0.10g)/(wt% FeOT)
  - Under a fume hood using HF protective gear, add 5 ml HF and stir with a stream of water with an RO bottle. The amount of RO can vary, as long as it is stirred and does not exceed 12 ml.
  - Cover the beakers with the Teflon watch glasses and then cover with Parafilm. A second option is to use 60-mL Teflon vials with screw-top lids.
  - Set beakers or vials in a water bath under a fume hood and heat them between 65^{o}-70^{o}C overnight. Use a separate beaker with water to monitor the temperature.

- II.3.2 Titration (The following steps must be done under a fume hood in HF protective clothing)
  - Remove the beakers from the water bath and let cool to room temperature.
  - Take off lids; rinse lids and sides of beakers with RO to make sure all sample remains in bottom of the beakers for titration.
  - Add magnetic stirrers and place on a stir plate.
  - Add 5 ml 85% H_3PO_4 (with 5 ml pipetter) and a few drops of indicator solution. If the solution does not turn purple, there was too much Fe^{2+} in the original sample for the volume of $K_2Cr_2O_7$ used. The digestion process must be repeated for that sample with less sample used.

- Titrate the sample solution with the Fe^{2+} solution until the sample solution turns green. Record the volume.
- Back-titrate the sample solution with $K_2Cr_2O_7$ until it turns grey-green, and then add drop by drop until the solution remains purple for 30 seconds. Add this volume to the total volume of $K_2Cr_2O_7$.

II.4 DOCUMENTATION AND CALCULATIONS

II.4.1 Chain of Custody

Chain of custody forms must be used in accordance with SOP 2.

II.4.2 Sample Lab Book and spreadsheet calculations

All measurements will be kept in a sample laboratory book. These measurements and their associated sample names will be transferred to a spreadsheet where the following calculations will be completed:

- (Volume $K_2Cr_2O_7$)/(Volume Fe^{2+} solution) = relative strength (R)
  - This calculation is made with the blank solution; it standardizes the Fe^{2+} while considering any effects on the $K_2Cr_2O_7$ during digestion.
- (Volume Fe^{2+} solution)(R) = Volume excess $K_2Cr_2O_7$
- [(Volume $K_2Cr_2O_7$ - Volume excess $K_2Cr_2O_7$)(0.0040)]/(sample weight) x 100%=% FeO in sample

II.4.3 Data Reporting

Data will be reported to the Project Manager in two columns, one with the sample name, the other with the concentration of fluoride (mg/kg) measured.

II.5 INTERFERENCES

Sulfide minerals will interfere with ferrous iron measurements. S(II) will reduce some of the Fe(III) resulting in a high Fe(II) measurement. Pyrite will not decompose except in bomb or sealed tube, resulting in a low value for FeO and a high value for Fe2O3. Corrections will be calculated for pyrite sulfides using sulfide / sulfate measurements provided by the Project Manager. Oxidation by Mn^{3+} can also cause an interference.

Part II REFERENCES

Reichen, L., and Fahey, J. An Improved Method of the Determination of FeO in Rocks and Minerals including Garnet, Geological Survey Bulletin 1144-B. United States Government Printing Office, Washington, D.C.: 1962.

Potts, P.J., A Handbook of Silicate Rock Analysis. Chapman and Hall, New York, N.Y.: 1987.

APPENDIX 2 – TABLES OF STATISTICS

Sample	UTMeast	UTMnorth	elevation	DistEdge	depth	F	SiO2	TiO2	Al2O3	Fe2O3T	FeOT	MnO
	ft NAD27Z13	ft NAD27Z13	ft NAD27Z13	ft	ft	ppm	wt %	wt %	wt %	wt %	wt %	wt %
BCS-VWL-0004	466549	4065237	10340			917	65.95	0.54	15.35	3.96	3.6	0.069
CAP-MLJ-0001	453402	4062833				795	76.65	0.22	11.86	2.87		0.04
ESS-VWL-0001	460951	4062976	9120			841	71.27	1.31	13.44	3.56		0.02
GHN-ACT-0001	453709.9	4062158	9765.4		0	840	75.4	0.17	12	1.969	1.79	0.022
GHN-ACT-0002	453709.9	4062158	9761.4		-4	823	76.52	0.16	11.83	1.694	1.54	0.024
GHN-ACT-0003	453709.9	4062158	9756.4		-9	962	75.39	0.16	11.36	2.013	1.83	0.38
GHN-ACT-0004	453709.9	4062158	9751.4		-14	987	72.12	0.21	11.65	2.882	2.62	0.042
GHN-ACT-0005	453709.9	4062158	9746.4		-19	1032	69.58	0.44	12.75	4.367	3.97	0.576
GHN-ACT-0006	453709.9	4062158	9736.4		-29	584	74	0.22	11.89	2.508	2.28	0.068
GHN-ACT-0007	453709.9	4062158	9726.4		-39	1261	64.12	0.66	14.16	5.81	5.29	0.576
GHN-ACT-0008	453709.9	4062158	9721.4		-44	496	73.96	0.14	12.71	1.914	1.74	0.022
GHN-ACT-0009	453709.9	4062158	9716.4		-49	1233	63.05	0.69	14.43	6.26	5.6	0.488
GHN-ACT-0010	453709.9	4062158	9711.4		-54	1704	63.71	0.71	14.54	5.544	5.04	0.418
GHN-ACT-0011	453709.9	4062158	9706.4		-59	1903	64.48	0.65	14.09	5	4.54	0.338
GHN-ACT-0012	453709.9	4062158	9701.4		-64	1105	63.98	0.7	14.4	4.972	4.52	0.278
GHN-ACT-0013	453709.9	4062158	9696.4		-69	1398	63.68	0.72	14.63	4.84	4.4	0.275
GHN-ACT-0014	453709.9	4062158	9691.4		-74	1151.5	63.27	0.74	14.59	4.917	4.47	0.343
GHN-ACT-0015	453709.9	4062158	9686.4		-79	1261	63.75	0.67	15.05	4.653	4.23	0.269
GHN-ACT-0016	453709.9	4062158	9676.4		-89	1069	67.96	0.46	13.66	3.861	3.51	0.195
GHN-ACT-0017	453709.9	4062158	9671.4		-94	970	68.51	0.47	13.73	3.597	3.27	0.178
GHN-ACT-0018	453709.9	4062158	9666.4		-99	1278	76.14	0.17	11.31	1.859	1.69	0.031
GHN-ACT-0019	453709.9	4062158	9661.4		-104	1217.5	69.52	0.39	13.07	3.113	2.83	0.06
GHN-ACT-0020	453709.9	4062158	9651.4		-114	1313.5	74.98	0.28	12.86	1.727	1.57	0.038
GHN-ACT-0021	453709.9	4062158	9646.4		-119	1165	74.73	0.2	11.61	2.134	1.94	0.023
GHN-ACT-0022	453709.9	4062158	9636.4		-129	1357	69.43	0.29	12.21	2.937	2.67	0.047
GHN-ACT-0023	453709.9	4062158	9631.4		-134	1382	67.95	0.41	13.03	3.487	3.17	0.088
GHN-ACT-0024	453709.9	4062158	9626.4		-139	1383	68.64	0.44	13.25	3.443	3.13	0.137
GHN-ACT-0025	453709.9	4062158	9621.4		-144	1045	65.73	0.57	14.85	4.158	3.78	0.2
GHN-ACT-0026	453709.9	4062158	9621.4		-144	1060	65.08	0.56	14.93	4.378	3.98	0.223
GHN-ACT-0027	453709.9	4062158	9621.4		-144	1115	65.44	0.54	14.47	4.158	3.78	0.192
GHN-ACT-0028	453709.9	4062158	9616.4		-149	1272	63.22	0.6	15.27	4.719	4.29	0.252
GHN-ACT-0029	453709.9	4062158	9611.4		-154	1203	62.91	0.66	15.26	5.038	4.58	0.207
GHN-ACT-0030	453709.9	4062158	9606.4		-159	1288	63.8	0.65	15.31	4.697	4.27	0.264
GHN-ACT-0031	453709.9	4062158	9596.4		-169	1150	72.15	0.3	12.41	2.772	2.52	0.133
GHN-ACT-0032	453709.9	4062158	9591.4		-174	1102	73.88	0.24	11.81	2.442	2.22	0.094
GHN-ACT-0033	453709.9	4062158	9586.4		-179	1264	70.21	0.62	15.08	2.43	2.19	0.039
GHN-ACT-0034	453709.9	4062158	9581.4		-184	1071	64.15	0.61	15.62	4.763	4.33	0.018
GHN-ACT-0035	453709.9	4062158	9576.4		-189	965	62.16	0.61	15.7	5.41	4.92	0.015
GHN-ACT-0036	453709.9	4062158	9571.4		-194	865	64.03	0.57	15.49	5.126	4.66	0.021
GHN-EHP-0001	453688	4062313	9651.2	2		985	67.14	0.47	13.71	3.62	3.29	0.11
GHN-EHP-0002	453691	4062315	9651.2			1015	74.45	0.25	12.27	2.046	1.86	0.061
GHN-EHP-0003	453678.4	4062415	9712.1			1062	65.03	0.443	12.61	4.74	4.31	0.041
GHN-EHP-0004	453680.9	4062416	9712.1			1044	63.29	0.555	13.58	3.41	3.1	0.37
GHN-EHP-0007	453681.2	4062416	9712.1			982	58.15	0.624	17.43	6.237	5.67	0.166
GHN-HRS-0001	453746.7	4062150	9729.8	2		1392.5	63.62	0.75	14.28	5.53	5.03	0.36
GHN-HRS-0002	453751.6	4062148	9729.8	19		572	76.94	0.16	11.57	2.03	1.85	0.07
GHN-HRS-0088	453663	4062329	9663.1	21.5		708	75.65	0.16	12.12	2.25	2.04	0.06
GHN-HRS-0089	453664	4062331	9663.1	28		488	77.07	0.16	11.96	1.76	1.6	0.02
GHN-HRS-0090	453666	406233	9663.1	38		1312	72.33	0.36	13.32	3.417	3.106	0.04
GHN-HRS-0091	453664	4062331	9663.1	29		1373	72.43	0.47	14.82	2.101	1.91	0.02
GHN-HRS-0092	453675	4062343	9663.1	84		1458.5	63.78	0.64	15.08	4.598	2.68	0.07
GHN-HRS-0094	453662	4062328	9663.1	17		882	73.4	0.21	11.86	2.49	2.27	0.04
GHN-HRS-0095	453692	40623532	9692.7	3		647	63.6	0.66	14.67	4.741	4.31	0.061
GHN-HRS-0096	453693.1	4062354	9692.7	7		665	65.77	0.64	14.87	2.827	2.57	0.033
GHN-JRM-0001	453642.2	4062137	9602	61		1646	61.64	0.53	13.65	5.24	4.76	0.08
GHN-JRM-0002	453642.4	4062137	9601	61.5		1047	61.04	0.84	14.36	7.586	6.896	0.36
GHN-JRM-0006	453642.1	4062130	9592.9	60		1040	61.41	0.74	14.86	5.986	5.442	0.426
GHN-JRM-0008	453637.6	4062123	9587.6	59.5		1144	62.558	0.74	14.73	6.937	6.306	0.377
GHN-JRM-0009	453634.2	406123	9585.8	48		1016	70.872	0.37	11.96	3.793	3.448	0.183
GHN-JRM-0022	453649.8	4062138	9605.1	86		1262	62.14	0.62	14.6	5.433	4.939	0.59
GHN-JRM-0027	453644.7	4062115	9599.3	80		1015	61.68	0.651	14.18	5.346	4.86	0.53
GHN-JRM-0037	453665	4062334	9666.5	37.5		540	75.715	0.15	11.6	1.93	1.755	0.028
GHN-JRM-0038	453670	4062340	9666.5	64		1496	68.797	0.42	13.43	4.573	4.157	0.056
GHN-JRM-0039	453671	4062334	9659	59		1592	66.64	0.6	15.1	2.58	2.34	0.02
GHN-JRM-0040	453670	406233	9659	55		1576	70.26	0.5	14.75	3.212	2.92	0.011
GHN-JRM-0047	453669	4062335	9663.1	50		1288	66.84	0.55	14.69	4.706	4.278	0.078
GHN-KMD-0013	453711.1	4062142	9734.113	52		1193	63.68	0.6	14.59	6.23		0.07
GHN-KMD-0014	453717.8	4062145	9737.2	33		809	61.05	0.82	14.79	5.1		0.22
GHN-KMD-0015	453722.7	4062142	9735.76	90		1376	63.83	0.7	14.36	5.72		0.37
GHN-KMD-0016	453725.1	4062141	9736.107	98		993	61.88	0.79	14.44	5.51		0.31
GHN-KMD-0017	453695.9	4062143	9730.946	2		1507	61.34	0.61	14.37	6.03		0.08
GHN-KMD-0018	453698.1	4062143	9730.53	10		1217	70.45	0.36	12.95	3.48		0.22
GHN-KMD-0019	453726.6	4062144	9738.55	63		1032	61.78	0.81	14.94	5.35		0.32
GHN-KMD-0026	453728.7	4062141	9736.127	110		753	69.83	0.32	12.81	3.86	3.52	0.15
GHN-KMD-0027	453707.9	4062148	9738.5	10		991	68.03	0.43	12.93	4.57	4.15	0.21
GHN-KMD-0028	453706.9	4062142	9726.8	3		1005	62.36	0.574	14.28	4.796	4.36	0.269

Sample	UTMeast	UTMnorth	elevation	DistEdge	depth	F	SiO2	TiO2	Al2O3	Fe2O3T	FeOT	MnO
	ft NAD27Z13	ft NAD27Z13	ft NAD27Z13	ft	ft	ppm	wt %	wt %	wt %	wt %	wt %	wt %
GHN-KMD-0048	453691.8	4062132	9688.4	52		1016	63.11	0.75	14.72	5.55	5.047	0.45
GHN-KMD-0050	453704.2	4062145	9702.8	84		984	62.5	0.74	14.74	5.423	4.93	0.43
GHN-KMD-0051	453695.1	4062146	9698.023	54		709	67.83	0.59	14.44	4.32		0.29
GHN-KMD-0052	453692.6	4062146	9697	46		1336	61.82	0.6	14.16	5.34	4.85	0.37
GHN-KMD-0053	453684.7	4062146	9693.727	20		961	70.62	0.33	12.82	3.73		0.3
GHN-KMD-0054	453682	4062146	9692.6	11		1013	62.74	0.73	14.19	5.21	4.74	0.24
GHN-KMD-0055	453676.5	4062147	9691.3	-7		2445	71.86	0.27	12.19	3.49	3.17	0.06
GHN-KMD-0056	453704.9	4062140	9696.936	97		875	68.34	0.59	14.53	4.31		0.22
GHN-KMD-0057	453695.8	4062140	9694	67		910	62.67	0.71	14.99	5.192	4.72	0.349
GHN-KMD-0062	453682.4	4062141	9689.8	23		1032	67.01	0.49	13.66	5.27	4.79	0.442
GHN-KMD-0063	453677.2	4062141	9688.1	6		1318	64.27	0.62	13.64	5.91	5.377	0.166
GHN-KMD-0064	453694.9	4062132	9690.1	57		977	68.4	0.42	13.51	4.54	4.125	0.22
GHN-KMD-0065	453698.9	4062132	9691.493	70		1206	66.82	0.66	14.69	6.12		0.52
GHN-KMD-0071	453678.7	4062138	9649.177	97		1269	67.81	0.49	14.77	3.85		0.13
GHN-KMD-0072	453671.4	4062137	9646	73		975	63.63	0.65	14.26	5.25	4.77	0.4
GHN-KMD-0073	453666.7	4062137	9644.116	58		933	62.63	0.72	14.38	5.14		0.34
GHN-KMD-0074	453680.2	4062138	9649.825	102		1007	65.16	0.71	14.68	5.7		0.33
GHN-KMD-0077	453670.2	4062134	9643.7	71		883	68.84	0.37	13.93	4.004	3.64	0.114
GHN-KMD-0078	453671.7	4062134	9644.4	76		863	70	0.43	13.14	3.597	3.27	0.113
GHN-KMD-0079	453679.3	4062138	9651.936	99		1126	67.58	0.55	14.22	4.56		0.23
GHN-KMD-0080	453677.5	4062138	9650.7			982	64.18	0.68	14.57	5.193	4.721	0.375
GHN-KMD-0081	453675.9	4062137	9650	88		865	66.8	0.43	14.17	3.82	3.47	0.13
GHN-KMD-0082	453656	4062127	9635.3	42		1330	60.3	0.74	14.32	5.31	4.83	0.64
GHN-KMD-0088	453657.4	4062127	9635.4	36		1015	64.35	0.49	14.19	4.19	3.81	0.16
GHN-KMD-0092	453661.9	4062134	9640	44		1563	63.51	0.49	14.93	4.268	3.88	0.223
GHN-KMD-0095	453656	4062119	9638.6	15		1066	75.4	0.16	11.65	1.727	1.57	0.025
GHN-KMD-0096	453658.4	4062119	9640.3	23		1069	72.29	0.23	11.91	2.31	2.1	0.037
GHN-KMD-0097	453658.4	4062119	9640.3			1371	67.2	0.37	12.99	3.245	2.95	0.12
GHN-KMD-0100	453631	4062132	9632	58		1047	67.74	0.48	13.19	4.708	4.28	0.311
GHN-LFG-0001	453253	4062510	9020			1130	67.64	0.63	15.63	1.6467	1.497	0.012
GHN-LFG-0002	453253	4062510	9020			1052	67.659	0.64	15.14	0.869	0.79	0.01
GHN-LFG-0003	453309	4062040	9044			1524	77.45	0.17	11.48	1.59	1.44	0.01
GHN-LFG-0004	453309	4062040	9044			1248	66.54	0.49	13.21	4.2306	3.846	0.0246
GHN-LFG-0005	453309	4062040	9044			1044	72.97	0.52	13.36	1.5334	1.394	0.0212
GHN-LFG-0006	453309	4062040	9044			1006	70.36	0.53	13.35	2.96	2.692	0.026
GHN-LFG-0018	453747	4062150	9746	12		1053.5	69.216	0.36	13.7	4.313	3.921	0.102
GHN-LFG-0020	453747	4062150	9746	12		580	72.489	0.28	12.49	4.044	3.676	0.143
GHN-LFG-0037	453742.8	4062149	9744.2	0		884	61.32	0.5	13.88	5.1	4.64	0.29
GHN-LFG-0041	453759.7	4062147	9736	45.6		479	75.454	0.16	12.02	2.42	2.2	0.091
GHN-LFG-0060	453720.5	4062141	9749.9	90		1197	64.64	0.583	13.49	4.664	4.24	0.109
GHN-LFG-0085	453731.4	4062143	9759.678	47		1024	62.66	0.69	14.68	6.13		0.28
GHN-LFG-0086	453731.4	4062143	9759.7	47		987	60.4	0.67	14.25	6.09	5.5	0.3
GHN-LFG-0087	453741.9	4062142	9756.667	82		1471	61.03	0.78	14.74	5.17		0.58
GHN-LFG-0088	453734.1	4062140	9755.044	44		840	61.25	0.77	14.44	5.04		0.3
GHN-LFG-0089	453747.8	4062138	9752.4	90		516	70.71	0.307	13.21	3.09	2.81	0.054
GHN-LFG-0090	453740.1	4062141	9758.012	76		1031	60.36	0.77	14.7	6.52		0.46
GHN-LFG-0091	453759.8	4062135	9749.166	130		950	62.44	0.59	14.64	4.66	4.24	0.051
GHN-RDL-0002	453791	4062312	9853			1692	71	0.63	14.27	1.3	1.17	0.02
GHN-RDL-0003	453791	4062312	9853			2122	71.84	0.64	15.09	0.67	0.61	0.02
GHN-RDL-0004	453791	4062312	9853			1555	73.15	0.52	13.22	1.133	1.03	0.01
GHN-SAW-0003	45682.1	4062297	9615.2			936	80.93	0.15	11.21	0.645	0.586	0.018
GHN-SAW-0004	453657	4062290	9609.6	33		1275.5	62.629	0.57	14.32	5.437	4.943	0.052
GHN-SAW-0005	453651	4062282	9609.6	-3		741	75.337	0.17	11.85	2.945	2.677	0.046
GHN-SAW-0200	453650.5	4062394	9623.4	12		1018	61.044	0.58	14.78	5.201	4.728	0.204
GHN-SAW-0201	453647	4062394	9648.2	9		852	69.8	0.26	12.266	4.303	3.912	0.058
GHN-STM-0001	453586	4062104	9526			1391	71.09	0.47	13.03	3.63		0.09
GHN-STM-0002	453589	4062110	9537			843	75.91	0.18	12.06	1.64		0.03
GHN-STM-0003	453506	4062188	9516			798	75.97	0.19	12.05	2.07		0.02
GHN-STM-0004	453582	4062213	9489			851	68.83	0.29	12.04	3.17		0.1
GHN-STM-0005	453517	4062293	9460			590	75.43	0.15	11.63	2.15		0.06
GHN-VTM-0003	453361	4062050	9119			1738	69.53	0.73	14.54	2.618	2.38	0.025
GHN-VTM-0109	453745.8	4062141	9755.9	95		716	69.88	0.373	12.7	3.487	3.17	0.178
GHN-VTM-0194	453695.3	4062143	9732.86	0		1511	61.99	0.55	13.18	5.09	4.81	0.13
GHN-VTM-0195	453696.8	4062143	9734.1	5		971	62.5	0.6	13.42	5.66	5.1	0.23
GHN-VTM-0197	453699.8	4062143	9734.51	15		1048	61.22	0.71	14.47	5.43	4.91	0.37
GHN-VTM-0198	453701.4	4062143	9734.726	20		1031	66.79	0.43	13.39	4.5	4.09	0.28
GHN-VTM-0199	453702.9	4062142	9734.943	25		1076	67.28	0.43	13.37	4.74	4.31	0.28
GHN-VTM-0200	453704.4	4062142	9735.16	30		767	71.77	0.28	14.04	3.18	2.72	0.15
GHN-VTM-0201	453708.8	4062145	9735.478	6		1110	64.84	0.44	13.72	4.9	4.45	0.2
GHN-VTM-0202	453705.9	4062142	9735.376	35		973	65.92	0.51	13.3	5.29	4.64	0.24
GHN-VTM-0203	453705.9	4062142	9735.376	35		1156	66.12	0.49	13.21	5.28	4.7	0.37
GHN-VTM-0204	453707.4	4062142	9735.593	40		1305	60.17	0.72	14.77	6.72	6.11	0.59
GHN-VTM-0205	453708.9	4062142	9733.81	45		1438	62.2	0.67	14.25	7.3	6.49	0.38
GHN-VTM-0206	453710.5	4062142	9734.026	50		1323	62.13	0.71	14.64	6.82	6.18	0.85
GHN-VTM-0207	453712	4062142	9734.243	55		964	65.97	0.55	13.84	5.36	4.79	0.57
GHN-VTM-0208	453713.8	4062142	9734.503	61		1012	67.14	0.72	14.56	5.19		0.29

Sample	UTMeast	UTMnorth	elevation	DistEdge	depth	F	SiO2	TiO2	Al2O3	Fe2O3T	FeOT	MnO
	ft NAD27Z13	ft NAD27Z13	ft NAD27Z13	ft	ft	ppm	wt %	wt %	wt %	wt %	wt %	wt %
GHN-VTM-0209	453715.3	4062141	9734.72	66		1025	64.37	0.72	14.41	5.53	4.9	0.43
GHN-VTM-0210	453715.4	4062142	9734.72	66		955	64.4	0.7	14.26	5.18	4.6	0.45
GHN-VTM-0211	453716.9	4062142	9734.937	71		894	62.37	0.73	14.65	5.15	4.56	0.37
GHN-VTM-0212	453718.4	4062142	9735.153	76		1072	63.65	0.73	14.56	5.36	4.86	0.47
GHN-VTM-0213	453719.9	4062142	9735.37	81		921.5	62.95	0.73	14.66	5.3	4.82	0.47
GHN-VTM-0214	453721.4	4062142	9735.587	86		854.5	62.57	0.8	15.24	5.66	5.16	0.41
GHN-VTM-0215	453722.6	4062141	9735.76	90		783	63.84	0.73	14.46	5.55	5.11	0.57
GHN-VTM-0216	453724.2	4062141	9735.977	95		1083	62.94	0.74	14.52	5.32	4.85	0.44
GHN-VTM-0217	453725.7	4062141	9736.2	100		992	69.51	0.41	12.92	4.07	3.67	0.16
GHN-VTM-0417	453635.2	4062133	9594.087	50		1226	71.65	0.31	12.06	3.79		0.06
GHN-VTM-0418	453636.7	4062133	9594.828	55		1488	70.52	0.37	13.02	3.43		0.05
GHN-VTM-0419	453638.1	4062133	9595.568	60		1784	63.51	0.54	14.14	6.24		0.09
GHN-VTM-0420	453639.7	4062133	9596.309	65		1331	57.48	0.83	14.43	9.72		0.51
GHN-VTM-0421	453641.2	4062133	9597.05	70		951	62.88	0.73	14.26	6.24		0.34
GHN-VTM-0422	453642.7	4062133	9597.79	75		1080	66.22	0.49	13.32	4.895	4.45	0.31
GHN-VTM-0423	453642.8	4062133	9597.79	75		1006	67.645	0.51	13.34	4.79		0.25
GHN-VTM-0424	453644.2	4062133	9598.531	80		1061	70.37	0.29	12.52	4.01		0.16
GHN-VTM-0425	453644.2	4062133	9597.531	80		1738	62.15	0.59	15.19	5.14		0.32
GHN-VTM-0426	453645.8	4062133	9599.272	85		1265	61.43	0.74	14.85	5.86		0.78
GHN-VTM-0450	453647.7	4062115	9600.673	90		930	63.45	0.77	14.62	6.38		0.36
GHN-VTM-0451	453647.1	4062115	9600.402	88		1019	61.69	0.74	14.62	5.15		0.41
GHN-VTM-0452	453647.2	4062115	9600.457	88.4		929	63.39	0.65	14.13	5.34		0.28
GHN-VTM-0453	453643.3	4062115	9598.7	75.4		1339	59.8	0.71	14.49	6.18	5.47	0.46
GHN-VTM-0454	453647.1	4062115	9600.402	88		953	64.87	0.48	15.32	4.11		0.19
GHN-VTM-0455	453647.3	4062115	9600.511	88.8		789	67.69	0.56	13.73	4		0.17
GHN-VTM-0500	453702	4062402	9718.4	3		1050	62.08	0.56	15.45	4.97		0.3
GHN-VTM-0501	453702	4062402	9718.4	3		1056	62.91	0.63	15.48	5.506		0.05
GHN-VTM-0502	453699.7	4062401	9720	12		848	62.12	0.51	13.52	4.08		0.04
GHN-VTM-0503	453699.7	4062401	9720	12		1166	58.87	0.56	16.55	4.34		0.38
GHN-VTM-0504	453699.7	4062401	9720	12		811.5	61.18	0.59	15.8	5.2		0.16
GHN-VTM-0506	453691.1	4062401	9730	46		891	60.26	0.58	14.91	5.28	4.64	0.04
GHN-VTM-0507	453691	4062400	9730	46		801	62.83	0.55	14.3	4.09	3.72	0.04
GHN-VTM-0508	453687.5	4062400	9740	60		727	55.32	0.59	15.18	5.61	5.1	0.07
GHN-VTM-0509	453687.5	4062400	9740	60		1034	58.67	0.62	15.79	4.04		0.05
GHN-VTM-0510	453687.5	4062400	9740	60		1372	55.29	0.57	17.8	5.661		0.06
GHN-VTM-0598	453661.5	4062434	9651.2	10	-6	1174	76.435	0.23	12.4	1.94		0.05
GHN-VTM-0599	453661.5	4062434	9651.2	10	-10	1264	59.87	0.56	15.65	4.873	4.43	0.186
GHN-VTM-0602	453661.5	4062434	9651.2	10	-8.4	1527	55.65	0.55	16.5	5.89	5.35	0.24
GHN-VTM-0603	453661.5	4062434	9651.2	10	-7.5	1132	61.31	0.68	15.99	5.33	4.74	0.1
GHN-VTM-0604	453661.5	4062434	9651.2	10	-12	982	61.375	0.56	16.04	4.67	4.24	0.18
GHN-VTM-0605	453662.2	4062392	9660.1	10		1470	66.59	0.61	14.77	4.91		0.12
GHN-VTM-0606	453648	4062394	9648.2	14		751	71.25	0.35	12.09	3.63	3.27	0.06
GHN-VTM-0607	453646.9	4062393	9648.2	9		1124	68.88	0.5	14.32	4.05		0.16
GHN-VTM-0610	453649.5	4062391	9647.4			1125	66.93	0.345	12.76	3.047	2.77	0.101
GHN-VTM-0611	453650.1	4062391	9647.4	13.5		1324	65.3	0.51	14.59	2.94		0.09
GHN-VTM-0612	453650.1	4062391	9647.4	13.5		1199	58.55	0.44	13.7	2.58	2.25	0.25
GHN-VTM-0613	453650.1	4062391	9647.4	13.5		1008.5	53.49	0.52	14.44	4.49		0.17
GHN-VTM-0614	453652	4062391	9647.4	6		1029	63.72	0.71	18.09	4.14		0.05
GHN-VTM-0624	453650	4062394	9647.4	14		1068	62.55	0.68	15.68	4.93		0.08
GHR-VWL-0004	453071	4061257	8966			1533	58.53	0.68	16.41	8.4		0.11
GHR-VWL-0007	453071	4061293	8966			1381	63.97	0.6	14.25	9.27		0.11
GMG-PIT-0001	454471.6	4061702	9046		-42	1608	53.65	0.97	20.96	5.45		0.05
GMG-PIT-0006	454497.6	4062318	8724		-159	1290	73.32	0.24	12.07	0.36	0.33	0.056
GMG-PIT-0007	455597.5	4062318	8721		-162	1033	73.76	0.26	12.73	0.847	0.77	0.04
GMG-PIT-0009	454039.9	4062035	9485.5		-11.5	601	68.27	0.45	14.85	2.9	2.08	0.023
GMG-PIT-0010	454039.8	4062034	9459.5		-137.5	1397	58.33	0.63	14.2	6.45		0.08
GMG-PIT-0011	454039.8	4062034	9459.5		-137.5	3047	66.3	0.85	13.81	5		0.05
GMG-PIT-0014	454039.8	4062034	9297.5		-299.5	1910	65.82	0.53	15.72	6.71		0.01
GMG-PIT-0015	454039.8	4062034	9269.5		-327.5	2101	65.28	0.57	15.11	3.78		0.05
HAS-GJG-0001						967	62.93	0.171	10.65	13.41	12.19	0.003
HAS-GJG-0002	459094	4062929	9099			1198	77.03	0.166	11.68	1.705	1.55	0.002
HAS-GJG-0004						749	66.47	0.734	14.81	3.553	3.23	0.023
HAS-GJG-0005						839	66.58	0.618	15.51	3.696	3.36	0.094
HAS-GJG-0006					0	923	49.79	1.002	13.46	8.052	7.32	0.125
HAS-GJG-0007					1	1237	46.86	0.84	12.39	9.339	8.49	0.084
HAS-GJG-0008					10	850	47.31	0.938	12.43	7.975	7.25	0.124
HAS-GJG-0009	459288	40627957	8880		17	1350	59.18	1.048	21.37	1.232	1.12	0.009
HAS-GJG-0010	459288	40627957	8880		22	1642	66.89	0.778	14.32	2.002	1.82	0.049
MID-AAF-0002	454395	4060694	9441		-2	1184	63.01	0.517	13.67	5.005	4.55	0.039
MID-AAF-0003	454395	4060694	9441			1219	65.35	0.458	13.57	3.24	2.95	0.045
MID-GJG-4001						1503	62.61	0.55	14.1	5.73	5.21	0.12
MID-GMG-0014	454862	4060591	9287		-2	1727	57.61	0.77	13.47	5.01	4.55	0.065
MID-GMG-0015	454862	4060591	9279		-10	1411	70.2	0.36	13.16	2.18	1.98	0.057
MID-GMG-0016	454862	4060591	9277		-12	9286	62.04	0.65	13.82	3.98	3.62	0.097
MID-GMG-0017	545862	4060591	9256		-33	4919	61.45	0.78	13.52	5.36	4.87	0.154
MID-GMG-0018	454862	4060591	9205		-84	2180	65.7	0.51	13.38	3.795	3.45	0.078

Sample	UTMeast	UTMnorth	elevation	DistEdge	depth	F	SiO2	TiO2	Al2O3	Fe2O3T	FeOT	MnO
	ft NAD27Z13	ft NAD27Z13	ft NAD27Z13	ft	ft	ppm	wt %	wt %	wt %	wt %	wt %	wt %
MID-GMG-0019	45861.5	4060591	9137		-152	4483	64.81	0.49	13.82	2.464	2.24	0.028
MID-GMG-0020	454862	4060591	9107		-182	2384	60.79	0.8	15.42	5.69	3.46	0.06
MID-GMG-0021	454862	4060591	9071		-218	2532	63.42	0.74	16.17	4.95	4.5	0.041
MID-GMG-0022	454862	4060591	9047		-242	1832	64.27	0.57	14.76	5.929	5.39	0.052
MID-GMG-0023	454892	4060591	9015		-274	2640	59.75	0.61	13.88	8.954	8.14	0.045
MID-GMG-0024	454862	4060591	8999		-290	1251	62.7	0.55	14.99	5.39	4.9	0.086
MID-GMG-0025	454862	406591	8995		-294	966	65.93	0.3	14.1	5.51	5.01	0.119
MID-GMG-0026	454862	4060591	8993		-296	273	76.64	0.15	12	1.529	1.39	0.047
MID-KXB-0001	454399	4060698				1079	65.9	0.447	13.83	4.059	3.69	0.047
MID-KXB-0003	454349	4060874				1092	74.04	0.167	10.3	1.562	1.42	0.71
MID-VTM-4001						1491	59.99	0.57	14.26	5.6	5.09	0.14
MIN-AAF-0001	452374	4059911	7904			1284	73.34	0.391	12.82	3.014	2.74	0.021
MIN-AAF-0004	452374	4059912	7904			1258	71.85	0.376	13.14	3.19	2.9	0.018
MIN-AAF-0010	452366	4059925				1298	70.2	0.499	13.68	2.948	2.68	0.02
MIN-AAF-0013						1006	74.83	0.33	12.12	1.74	1.58	0.02
MIN-AAF-0015	452366	4059925				1056	74.47	0.407	12.36	1.782	1.62	0.018
MIN-GFA-0001	452331	4059891			2	1281	72.65	0.502	13.17	2.442	2.22	0.22
MIN-GFA-0003	452331	4059891			6.5	1045	70.88	0.46	12.98	3.586	3.26	0.39
MIN-GFA-0005	452331	4059891			8.5	1416	73.7	0.392	13.2	2.112	1.92	0.022
MIN-GFA-0006	452331	4059891			9	1116	70.03	0.506	12.97	4.191	3.81	0.036
MIN-GFA-0007					28	1448	73.95	0.409	12.92	2.266	2.06	0.02
MIN-GFA-0009	452331	405989			3	1737	74.7	0.397	12.5	2.585	2.35	0.02
MIN-SAN-0002	452369	4059919				1092	71.07	0.45	12.74	2.96	2.69	0.02
MIN-VTM-0002						1061						
MIN-VTM-0003	455648.3	4060960	8120		6	1477	67.02	0.47	14.55	3.091	2.81	0.043
MIN-VTM-0004						1639	65.16	0.542	13.29	4.026	3.66	0.079
MIN-VTM-0005						1372	63.58	0.459	12.57	3.113	2.83	0.09
MIN-VTM-0006						1464	67.04	0.509	12.72	3.146	2.86	0.029
MIN-VTM-0007						1882	66.84	0.565	13.5	4.389	3.99	0.039
MIN-VTM-0008						1735	68.01	0.535	13.43	3.718	3.38	0.065
MIN-VTM-0009						1396	65.27	0.536	13.14	4.455	4.05	0.05
MIN-VTM-0018	452871	4060366	8305		0	1708	59.62	0.83	15.12	7.16	6.45	0.2
MIN-VTM-0019	452871	4060366	8305		0	1433	58.84	0.91	15.19	6.996	6.36	0.198
MIN-VTM-0020	453817	4062418	9968		0	1149	62.3	0.64	15.5	5.43	4.89	0.15
MIN-VTM-0021	453817	4062418	9968			1330	62.35	0.62	16.37	5.918	5.38	0.07
PIT-KMD-0007	454583.4	4061682	9001		-42	3515	63.27	0.59	14.32	2.5		0.11
PIT-KMD-0008	454583.4	4061682	8901		-142	6004	63.96	0.61	14.69	3.92		0.07
PIT-KMD-0009	454583.4	4061682	8712		-331	2865	63.74	0.65	14.98	4.1		0.1
PIT-KXB-0101	454150	4062562	9570		0	1097	65.39	0.64	13.99	5.346	4.86	0.044
PIT-LFG-0001	454248	4061502	9444		0	1155	61.56	0.66	15.38	5.57		0.05
PIT-LFG-0003	454217	4061535	9462		0	1341	60.52	0.63	13.68	9.39		0.08
PIT-LFG-0005	454127	4061594	9523		0	1274	56.398	0.53	13.53	6.681	6.074	0.13
PIT-LFG-0007	453915.4	4061674	9620		0	1129	75.726	0.14	10.95	1.692	1.538	0.034
PIT-LFG-0009	453975	4061560	9617		0	686	74.531	0.15	11.81	2.1395	1.945	0.077
PIT-LFG-0013	453659	4061819	9947		0	1304	64.37	0.57	13.89	4.126	3.75	0.049
PIT-RDL-0001	453822	4061505	9912		0	848	74.92	0.15	11.33	2.33	2.1	0.02
PIT-RDL-0002	453822	4061505	9912		0	749	78.11	0.15	11.39	1.188	1.08	0.017
PIT-RDL-0003	453822	4061588	9916		0	1070	75.41	0.16	11.8	1.529	1.39	0.015
PIT-RDL-0004	453741	4061869	9894		0	1049	77.6	0.16	10.83	2.365	2.15	0.014
PIT-RDL-0005	453822	4061505	9912		0	793	75.35	0.16	11.33	2.211	2.01	0.02
PIT-RDL-0006	453822	4061588	9916			1036	75.97	0.15	11.49	1.507	1.37	0.02
PIT-RDL-0007	453822	4061588	9916			1201	74.68	0.14	11.34	2.53	2.3	0.03
PIT-VCV-0001	453678.2	4061879	9630		-320	1506	62.64	0.686	15.49	5.346	4.86	0.134
PIT-VCV-0002	453678.2	4061878	9625		-325	1326	68.37	0.352	13.16	4.235	3.85	0.123
PIT-VCV-0003	453086.6	4061207	8557		-315	1508	61.44	0.708	16.07	5.83	5.3	0.097
PIT-VCV-0004	453678.2	4061878	9901		-49	926	81.8	0.135	10.45	0.803	0.73	0.029
PIT-VCV-0005	453678.2	4061878	9911		-39	980	79.67	0.133	10.62	1.463	1.33	0.034
PIT-VCV-0006	453678.2	4061878	9918		-32	918						
PIT-VCV-0007	453678.2	4061878	9318		-632	1050	66	0.56	14.88	4.301	3.91	0.057
PIT-VCV-0008	453678.2	4061878	9315		-635	1094	68.84	0.443	12.56	3.806	3.46	0.14
PIT-VCV-0009	453678.2	4061878	9305		-645	1211	63.49	0.591	14.29	6.138	5.58	0.153
PIT-VCV-0010	453678.2	4061878	8819		-1131	1086	66.98	0.467	14.45	2.277	2.07	0.032
PIT-VCV-0011	453678.2	4061878	8827		-1123	1118	66.49	0.49	14.21	2.695	2.45	0.083
PIT-VCV-0012	453678.2	4061878	9490		-460	768	71.65	0.324	12.45	3.267	2.97	0.174
PIT-VCV-0013	453678.2	4061878	9479		-471	1086	73.97	0.278	11.81	2.2	2	0.123
PIT-VCV-0014	453678.2	4061878	9471		-479	920	73.3	0.3	12.35	2.398	2.18	0.133
PIT-VCV-0015	454185.6	4062158	8140		-1340	572	76.04	0.157	11.49	0.539	0.49	0.007
PIT-VCV-0016	454185.6	4062158	8346		-1134	3159	67.83	0.726	14.1	1.155	1.05	0.044
PIT-VCV-0017	45185.6	4062158	8175		-1305	2123	70.05	0.47	13.96	0.408	1.02	0.024
PIT-VCV-0018	454185.6	4062158	8182		-1298	1133	71.07	0.33	12.52	0.649	0.59	0.022
PIT-VCV-0019					-20	1100	61.11	0.709	18.55	3.08	2.8	0.025
PIT-VCV-0020					-39	1543	60.32	0.75	18.5	4.356	3.96	0.047
PIT-VCV-0021					-48	2893	52.11	0.858	13.48	5.874	5.34	0.101
PIT-VCV-0022					-57	1552	54.33	0.86	12.5	7.65	6.96	0.075
PIT-VCV-0023					-65	1776	51.62	0.838	11.98	8.734	7.94	0.048
PIT-VCV-0024					-506	24530	61.86	0.66	15.36	1.529	1.39	0.086

Sample	UTMeast	UTMnorth	elevation	DistEdge	depth	F	SiO2	TiO2	Al2O3	Fe2O3T	FeOT	MnO
	ft NAD27Z13	ft NAD27Z13	ft NAD27Z13	ft	ft	ppm	wt %	wt %	wt %	wt %	wt %	wt %
PIT-VCV-0025	454039.9	4062034	9276		-321	1995	68.135	0.509	13.49	4.73	4.3	0.078
PIT-VCV-0026	454039.9	4062035	9273			1832	65.79	0.532	13.6	5.599	5.09	0.033
PIT-VCV-0027	454039.9	4062035	9543			1720	64.85	0.548	15.73	4.51	4.1	0.019
PIT-VCV-0028	454039.9	4062035	7667			610	75.21	0.172	12.04	0.539	0.49	0.015
PIT-VCV-0029	454039.9	4062035	9076			1995	63.58	0.544	15.8	4.081	3.71	0.039
PIT-VCV-0030	454039.9	4062035	9067			1832	64.81	0.539	15.51	3.784	3.44	0.025
PIT-VTM-0001	453800	4061694				1322	65.63	0.738	15.41	5.005	4.55	0.185
PIT-VTM-0002	443841	4061908				691	62.18	0.554	14.84	5.984	5.44	0.139
PIT-VTM-0004	45403.9	4062034	9462			1367	63.422	0.61	14.76	5.5077	5.007	0.0576
PIT-VTM-0005	45403.9	4062035	9387			2740	68.969	0.45	14.16	5.124	4.658	0.071
PIT-VTM-0006	45367.2	4061878	9907			1287	79.57	0.15	11.36	0.96		0.05
PIT-VTM-0007	453678.2	4061878	9851			1573	74.85	0.16	12	3.75		0.08
PIT-VTM-0008	453678.2	4061878	9928			1323	78.18	0.18	11.88	0.68		0.04
PIT-VTM-0009	453867	4062310	9812			410	81.486	0.21	13.11	0.44	0.403	0.002
PIT-VTM-0010	454230	4061513	9456			1198	60.66	0.68	15.02	7		0.08
PIT-VTM-0600	454215	4061522	9476			771	65.12	0.62	14.89	5.445	4.95	0.098
PIT-VWL-0001	453652	4062088	9878			743	76.79	0.14	10.25	2.19		0.01
PIT-VWL-0007	453867	4062310	9812			1920	80.98	0.22	11.41	0.7		0
PIT-VWL-0009	454266	4062560	9580			954	39.03	0.47	7.15	37.06		0.01
QPS-AAF-0003	454144	4062571	9553			1291	63.06	0.592	14.53	4.796	4.36	0.054
QPS-AAF-0005	454144	4062571	9553			1164	61.85	0.599	14.31	4.84	4.4	0.049
QPS-AAF-0008	454138	4062528	9589			2328	62.48	0.677	14.09	4.565	4.15	0.038
QPS-AAF-0009	454138	4062528	9589			940	63.95	0.692	14.47	4.334	3.94	0.028
QPS-AAF-0022	454135	4062582				1395	64.34	0.626	14.57	4.785	4.35	0.034
QPS-SAN-0002	454146	4062551				1070	67.69	0.5	13.66	3.36	3.06	0.02
QPS-VTM-0001	454122	4062568				1065	63.62	0.61	14.26	4.58	4.16	0.04
QPS-VTM-4001						1158	62.3	0.61	14.36	4.98	4.53	0.05
ROC-KMD-0001						975	61.14	0.7	13.61	5.27	4.75	0.13
ROC-NWD-0001	462734	4065869	8458			192	76.94	0.14	12.31	0.979	0.898	0.002
ROC-NWD-0002						1172	60.55	0.82	16.78	6.424	5.84	0.065
ROC-NWD-0003	413742	4049489	6604			332	76.46	0.19	11.72	1.419	1.29	0.113
ROC-VTM-0032	466507	4055963	9404			551	58.69	0.66	16.11	5.99		0.1
ROC-VTM-0033	466507	4055963	9404			755	60.2	0.78	14.92	5.9		0.13
SCS-LFG-0001	459910	4064097	9432			1755	62.15	0.54	15.36	2.56		0.05
SCS-LFG-0002	459910	4064097	9432			1616	62.58	0.51	14.48	5.17		0.07
SCS-LFG-0003	459910	4064097	9432			1376	65.445	0.525	14.58	2.005		0.03
SCS-LFG-0004	459926	4064047	9429			2199	61.475	0.525	15.445	2.235		0.06
SCS-LFG-0005	459973	4063905	9433		8	1316	64.97	0.61	15.86	2.81		0.07
SCS-LFG-0006	459973	4063905	9433		6	1032	67.07	0.55	15.6	1.97		0.05
SCS-LFG-0007	459973	4063905	9433		4	976	65.27	0.51	15.13	3.2	2.97	0.06
SCS-LFG-0008	459973	4063905	9433		0	894	64.75	0.46	13.28	9	8.11	0.01
SGS-ESO-0101						3663	63.16	0.72	15.01	5.06	4.6	0.11
SGS-VTM-0024						2377	55.76	0.54	12.87	5.63	5.12	0.09
SGS-VTM-0026						2469	59.74	0.61	14.03	4.31	3.92	0.08
SGS-VTM-0605						2346	62.01	0.733	14.63	6.006	5.46	0.064
SPR-AAF-0001	455245	4062313				2151	62	0.78	14.42	5.5	5	0.11
SPR-AAF-0003	4062313	455245				2434	60.25	0.79	14.42	5.82	5.29	0.13
SPR-JWM-0002	455254	4062384	9319			2415	62.81	0.7	14.44	6.281	5.71	0.109
SPR-KMD-0001	455795	4062171	9043.4			2546	65.08	0.67	14.58	3.85		0.05
SPR-KMD-0002	455795	4062171	8998.4			3646	63.03	0.7	14.07	4.66		0.09
SPR-KMD-0003	455838	4062293				3523	71.33	0.45	13.94	2.1		0.09
SPR-OTH-0001						3336	63.68	0.57	13.75	3.97	3.61	0.12
SPR-OTH-0002						3838	64.09	0.57	13.72	3.78	2.14	0.12
SPR-SAN-0002	455255	4062285				2498	59.74	0.73	14.39	5.9	5.36	0.11
SPR-VTM-0001	455250	4062369	9308			6853	61.51	0.705	15.415	5.955		0.1
SPR-VTM-0002	455250	4062369	9308			1171	62.97	0.71	15.42	5.78		0.1
SPR-VTM-0005	455255	4062367	9320			2870	62.12	0.711	15.74	6.006	5.46	0.09
SPR-VTM-0010	455257	455257				2372	61.9	0.814	14.51	6.116	5.56	0.13
SPR-VTM-0012	4062735	454439				757	80.11	0.145	11.66	0.308	0.77	0.009
SPR-VTM-0014	4062735	454439				819	77.69	0.15	11.55	0.9	0.82	0.01
SPR-VTM-0017	4062735	454439				1202	76.17	0.293	12.85	1.397	1.27	0.015
SPR-VTM-0019	454440	4062735				895	76.81	0.14	11.53	1.31	1.19	0.01
SPR-VTM-0021	454440	4062735				1007	76.77	0.15	11.8	1.09	0.99	0.02
SSS-AAF-0001	454131	4060898				2112	59.44	0.64	14.29	6.34	5.76	0.06
SSS-EHP-0002					-9	3990	68.53	0.478	12.85	3.102	2.82	0.095
SSS-EHP-0003					-19	1866	70.14	0.374	12.7	2.981	2.71	0.67
SSS-EHP-0004					-29	3362	60.28	0.693	15.23	4.994	4.54	0.103
SSS-EHP-0023	454404	4060242	8547		-209	1441	62.285	0.525	14.415	4.655		0.115
SSS-EHP-0032					-289	1105	72.04	0.336	12.37	2.662	2.42	0.105
SSS-EHP-0033					-299	829	70.29	0.478	13.35	3.597	3.27	0.126
SSS-EHP-0034					-309	852	70.01	0.434	13.39	3.718	3.38	0.167
SSS-GMG-0009	454313	4060564	9288		-1	1013	61.11	0.48	13.77	4.686	4.26	0.029
SSS-GMG-0010	454313	4060564	9281		-8	1297	63.57	0.72	15.78	5.742	5.22	0.059
SSS-GMG-0011	454313	4060564	9274		-15	2169	57.71	0.95	14.81	8.283	7.53	0.197
SSS-GMG-0012	454313	4060564	9242		-47	1297	62.27	0.83	14.56	5.709	5.19	0.238
SSS-GMG-0013	454313	4060564	9213		-76	1123	63.17	0.66	14.76	5.995	5.45	0.1123

Sample	UTMeast	UTMnorth	elevation	DistEdge	depth	F	SiO2	TiO2	Al2O3	Fe2O3T	FeOT	MnO
	ft NAD27Z13	ft NAD27Z13	ft NAD27Z13	ft	ft	ppm	wt %	wt %	wt %	wt %	wt %	wt %
SSS-GMG-0014	454313	4060564	9145		-144	1354	69.9	0.41	13.86	4.169	3.79	0.083
SSS-GMG-0015	454313	4060564	9072		-217	988	68.84	0.39	12.97	3.883	3.53	0.137
SSS-GMG-0016	454313	4060564	9056		-233	997	67.86	0.45	13.41	3.806	3.46	0.137
SSS-KMD-0001	454181	4060503	9263			1077	64.65	0.6	14.68	4.97		0.07
SSS-KMD-0002						7814	61.34	0.65	13.43	5.49		0.19
SSS-VEV-0001	454286	4060187	8756			1007	49.479	0.79	11.43	22.759	20.69	0.017
SSS-VTM-0005	454404	4060242				1333	54.82	0.06	5.65	24.64	22.4	0.015
SSS-VTM-0600	454120	4060712				2165	67.31	0.526	14.75	4.444	4.04	0.132
SSW-AAF-0001	453672	4060616	9022			2006	60.28	0.78	14.9	6.54	5.95	0.11
SSW-AAF-0002	453672	4060617	9028			1338	61.99	0.577	14.08	5.456	4.96	0.097
SSW-AAF-0005	453699	4060554				1186	60.01	0.56	13.63	5.3	4.82	0.06
SSW-AAF-0007	4060551	453687				1346	64.77	0.57	13.76	4.58	4.16	0.05
SSW-AAF-1002	453672	4060617				1741	61.25	0.702	14.56	5.599	5.09	0.115
SSW-AAF-1005	453672	4060617	9022			1143	63.89	0.583	14.34	5.368	4.88	0.08
SSW-AAF-1009	453677	4060616				1434	62.28	0.579	13.71	4.862	4.42	0.064
SSW-GJG-4000						1569	58.94	0.65	14.27	6.16	5.6	0.1
SSW-KMD-0001	453872.1	4060686	9406.5			1365	61.04	0.66	14.89	6.53		0.09
SSW-SAN-0002	453682	4060534				1035	62.56	0.59	14.28	5.03	4.57	0.07
SSW-SAN-0006	453975	4060822				1358	65.71	0.47	13.16	3.7	3.36	0.06
SSW-VTM-0006						1640	57.6	0.55	13.33	6.53	5.94	0.09
SSW-VTM-0008						1317	58.68	0.56	13.53	5.76	5.24	0.07
SSW-VTM-0010						972	64.43	0.41	13.02	2.5	2.27	0.03
SSW-VTM-0012						1082	62.58	0.45	13.07	4.19	3.81	0.04
SSW-VTM-0013						1417	57.24	0.5	13.17	5.64	5.13	0.06
SSW-VTM-0015						1415	58.3	0.52	13.53	5.36	4.87	0.07
SSW-VTM-0016	453841	4060491				1339	62.24	0.679	14.9	5.995	5.45	0.105
SSW-VTM-0019	453841	4060491				1214	60.99	0.652	14.74	6.204	5.64	0.1
SSW-VTM-0023	453838	4060499				1455	61.46	0.627	14.62	6.061	5.51	0.086
SSW-VTM-0027	453832	4060592	9520			1122	62.29	0.647	14.59	5.874	5.34	0.103
SSW-VTM-0028	453832	406592	9520			1133	62.79	0.638	14.46	5.852	5.32	0.01
SSW-VTM-0030	453831	4060588	9520			1727	62.14	0.628	14.47	5.467	4.97	0.087
SSW-VTM-0032	453831	4060588	9520			1391	61.49	0.614	14.33	5.885	5.35	0.067
SSW-VTM-4001						1514	67.55	0.67	14.16	6.06	5.51	0.1
SWH-GJG-0001						548	60.87	0.741	12.39	8.965	8.15	0.032
SWH-GJG-0002	458665	4062587				1129	66.88	0.78	14.66	2.915	2.65	0.014
SWH-GJG-0003						829	66.59	0.601	15.79	3.894	3.54	0.054
SWH-GJG-0004						948	53.21	0.646	11.64	17.083	15.53	0.114
SWH-GJG-0005						1282	68.64	0.539	15.03	3.762	3.42	0.01
SWH-GJG-0006						740	68.63	0.539	15.03	3.8	3.418	0.01
SWH-GJG-0007						917	67.04	0.667	14.48	4.93	4.43	0.03
SWH-GJG-0008					0	526	62.52	0.402	12.69	3.883	3.53	0.035
SWH-GJG-0009					1.1	954	49.71	0.423	11.99	10.494	9.54	0.085
SWH-GJG-0010					1.3	1413	58.3	0.517	14.22	6.149	5.59	0.081
SWH-GJG-0011	458732	4062439			1.5	583	65.46	0.423	12.72	4.4	4	0.049
SWH-GJG-0012	458732	4062439			11.3	717	66.11	0.567	15.49	1.375	1.25	0.036
SWH-GJG-0013	458737	4062439			18.8	967	69.11	0.536	14.16	3.729	3.39	0.005
SWH-GJG-0014					28.9	2308	68.91	0.884	17.46	0.484	0.44	0.002
SWH-GJG-0015					37.1	1593	53.13	0.492	13.12	5.203	4.73	0.064
SWH-GJG-0019						1144	52.05	0.497	11.2	14.344	13.04	0.026
SWH-GJG-0020					0	1275	57.09	1.293	14.92	7.05	6.41	0.116
SWH-GJG-0021					3	1393	57.61	1.165	13.05	3.894	3.54	0.087
SWH-GJG-0022					5	1503	62.65	1.374	16.2	1.892	1.72	0.022
SWH-GJG-0023					7	1007	49.73	0.56	11.86	15.686	14.26	0.029
SWH-GJG-4000						685	64.4	0.59	14.46	2.27	2.06	0.02
SWH-VTM-4001						1148	61.44	0.55	14.19	2.54	2.31	0.05
average	496455.5362	4240568.686	9490.440128	#DIV/0!	-147.5395973	1400.433333	65.72377829	0.533713626	13.85471363	4.520990531	3.982076023	0.135322633
RSQ w/ F as x values	0.000155964	0.000192515	0.038851638	#DIV/0!	0.009532864	1	0.018592929	0.027500948	0.015768763	0.00036135	0.000379917	0.00273048
Pearson coeff of F	-0.012488537	-0.013874965	-0.197108188	#DIV/0!	-0.097636389	1	-0.136355891	0.165834097	0.125573734	-0.019009202	-0.019491459	-0.052253994
count	370	370	328	0	149	435	433	433	433	433	342	433

Sample	MgO	CaO	Na2O	K2O	P2O5	S	SO4	C	LOI	Total	TotalS	FeOmeas
	wt %	wt %	wt %	wt %	wt %	wt %	wt %	wt %	wt %	wt %	wt %	wt %
BCS-VWL-0004	1.44	1.57	3.56	3.65	0.251	0.39	0.08	0.37	4.64	101.82	0.47	
CAP-MLJ-0001	0.44	0.13	1.04	4.83	0.01	0.25	0.19	0.13	2.59	101.25	0.44	2.61
ESS-VWL-0001	0.45	0.16	0.17	4.7	0.06				4.98			
GHN-ACT-0001	0.37	0.19	1.25	5.03	0.041			0	2.71		0.13	
GHN-ACT-0002	0.34	0.15	1.02	5.18	0.32			0	2.73		0.173333	
GHN-ACT-0003	0.38	0.37	0.49	4.87	0.032				3.97		0.316666	
GHN-ACT-0004	0.56	0.6	0.6	4.82	0.058			0	4.83		0.433333	
GHN-ACT-0005	2.07	1.02	2.23	3.92	0.288			0	4.38		0.29	
GHN-ACT-0006	0.39	0.18	2.26	4.78	0.06			0	2.5		0.143333	
GHN-ACT-0007	2.07	3.92	2.23	3.92	0.288			0	4.38		0.116666	
GHN-ACT-0008	0.15	0.06	3.46	3.76	0.025			0	2.7		0.12	
GHN-ACT-0009	2.12	1.16	2.56	3.78	0.306			0	4.35		0.126666	
GHN-ACT-0010	2.1	1.31	2.9	3.78	0.308			0	4.25		0.14	
GHN-ACT-0011	2.02	2.02	3.34	3.58	0.289				3.62		0.076666	
GHN-ACT-0012	2.35	2.27	3.32	3.84	0.319				3.14		0.053333	
GHN-ACT-0013	2.46	2.34	3.25	3.56	0.319				3.43		0.05	
GHN-ACT-0014	2.42	2.48	3.42	3.47	0.318				3.38		0.036666	
GHN-ACT-0015	2.21	2.19	3.62	3.57	0.28				3.24		0.086666	
GHN-ACT-0016	1.39	1.37	3.09	3.72	0.198			0	3.14		0.166666	
GHN-ACT-0017	1.44	1.84	3.09	3.96	0.189				2.52		0.123333	
GHN-ACT-0018	0.4	0.26	1.89	4.51	0.048			0	2.56		0.136666	0.51
GHN-ACT-0019	1.07	0.62	1.29	4.06	0.138			0	4.46		0.346666	
GHN-ACT-0020	0.32	0.07	0.13	3.35	0.089			0	4.74		0.423333	
GHN-ACT-0021	0.37	0.06	0.24	4.2	0.05			0	4.55		0.37	0.96
GHN-ACT-0022	0.66	0.21	0.62	4.02	0.11			0	6.39		0.576666	
GHN-ACT-0023	1.05	0.38	0.95	4.21	0.144			0	5.96		0.46	
GHN-ACT-0024	1.2	0.68	1.53	4.07	0.159			0	4.76		0.35	
GHN-ACT-0025	1.49	1.39	2.98	3.79	0.241			0	3.47		0.17	
GHN-ACT-0026	1.39	1.23	2.78	3.77	0.234				3.93		0.176666	
GHN-ACT-0027	1.45	1.21	2.87	3.69	0.221			0	3.5		0.176666	
GHN-ACT-0028	1.59	1.45	2.77	3.48	0.259			0	4.74		0.243333	
GHN-ACT-0029	1.89	1.78	3.01	3.49	0.268				4.06		0.216666	
GHN-ACT-0030	1.76	2.01	3.25	3.42	0.268			0	3.75		0.17	
GHN-ACT-0031	0.74	0.27	0.99	4.41	0.098			0	4.24		0.283333	1.17
GHN-ACT-0032	0.61	0.23	0.69	4.54	0.075			0	3.77		0.246666	
GHN-ACT-0033	0.71	0.14	0.56	4.62	0.198			0	4.44		0.106666	
GHN-ACT-0034	0.91	0.1	0.14	4.15	0.215			0	6.53		0.03	
GHN-ACT-0035	0.86	0.07	0.13	4.24	0.209			0	6.37		0.07	
GHN-ACT-0036	1.2	0.07	1.14	3.31	0.143			0	6.7		0.046666	
GHN-EHP-0001	1.23	0.81	2.22	3.97	0.19	0.57	0.03	0.08	4.55	98.7	0.6	
GHN-EHP-0002	0.62	0.32	0.79	4.46	0.071	0.08	0.3	0.08	3.24	99.04	0.38	
GHN-EHP-0003	0.78	0.33	1.26	3.97	0.117	0.57	0.3	0.08	7.88	98.15	0.87	
GHN-EHP-0004	1.04	0.76	0.95	3.55	0.277				9.9			
GHN-EHP-0007	2.31	0.77	1.3	3.68	0.271				7.13		0.216666	
GHN-HRS-0001	2.66	2.79	3.1	3.22	0.33				3.39		0.063986	
GHN-HRS-0002	0.26	0.14	2.19	4.94	0.036				1.73		0.06232	
GHN-HRS-0088	0.35	0.29	1.96	4.98	0.04				2.39		0.165806	
GHN-HRS-0089	0.22	0.12	2.52	5.17	0.03				1.49		0.10155	
GHN-HRS-0090	0.66	0.16	0.86	3.91	0.136				4.36		0.322813	
GHN-HRS-0091	0.42	0.087	0.15	3.8	0.188				5.22		0.368453	
GHN-HRS-0092	0.96	0.33	0.66	4.08	0.3				6.61		0.488606	
GHN-HRS-0094	0.43	0.36	0.98	4.58	0.06				3.82		0.303296	
GHN-HRS-0095	1.38	0.46	2.56	3.61	0.325	0.04	0.6	0.39	6.37	99.47	0.64	
GHN-HRS-0096	0.81	0.09	3.18	3.84	0.111	0.03	0.99	0.08	5.43	98.7	1.02	
GHN-JRM-0001	1.28	0.98	1.87	3.91	0.19	2.01	1.12	0.07	8.81	101.38	3.13	
GHN-JRM-0002	2.566	1.72	2.82	3.33	0.402	0.14	0.34	0.06	4.66	100.22	0.48	
GHN-JRM-0006	2.237	1.676	3.006	3.456	0.34				4.55		0.214103	
GHN-JRM-0008	2.467	1.17	2.227	4.443	0.35				3.74		0.09745	
GHN-JRM-0009	1.224	0.93	0.62	2.705	0.18	1.3	0.55	0.07	5.42	100.18	1.85	
GHN-JRM-0022	2.35	2.149	2.528	3.588	0.285				4.6		0.17635	
GHN-JRM-0027	2.39	2.32	2.75	3.38	0.299				4.16		0.173333	
GHN-JRM-0037	0.254	0.252	1.726	5.677	0.03	0.21	0.24	0.05	2.48	100.34	0.45	
GHN-JRM-0038	0.724	0.108	0.398	4.198	0.165	1.12	0.54	0.06	5.63	100.22	1.66	
GHN-JRM-0039	0.5	0.08	0.15	3.65	0.23	0.43	0.58	0.08	6.28	96.92	1.01	
GHN-JRM-0040	0.37	0.08	0.1	3.69	0.19	2.08	0.47	0.05	5.85	101.61	2.55	
GHN-JRM-0047	0.99	0.52	0.86	3.77	0.25	0.68	0.52	0.07	5.99	100.51	1.2	
GHN-KMD-0013	1.46	1.17	2.42	3.68	0.23	0.06	0.23	0.05	4.81	99.28	0.29	
GHN-KMD-0014	2.74	3.12	3.31	4.65	0.29	0.01	0.01	0.17	2.34	98.62	0.02	
GHN-KMD-0015	2.05	1.38	2.49	4.07	0.25	0.05	0.17	0.16	3.7	99.3	0.22	
GHN-KMD-0016	2.83	2.97	3.36	3.12	0.29				3.42			
GHN-KMD-0017	1.51	1.15	2.5	3.49	0.23	1.68	1.22	0.03	7.4	101.64	2.9	
GHN-KMD-0018	1.23	0.81	1.29	4.81	0.08			0	4.2			
GHN-KMD-0019	3.14	3.59	3.48	2.92	0.26	0.04	0.05	0.24	4.3	101.22	0.09	2.19
GHN-KMD-0026	0.76	0.5	2.59	4.26	0.13	0.03	0.12	0.05	3.53	98.94	0.15	0.43
GHN-KMD-0027	1.05	0.56	2.03	4.15	0.19	0.01	0.18	0.07	4.48	98.89	0.19	
GHN-KMD-0028	1.82	1.56	2.51	3.64	0.251				5.49		0.4	

Sample	MgO	CaO	Na2O	K2O	P2O5	S	SO4	C	LOI	Total	TotalS	FeOmeas
	wt %	wt %	wt %	wt %	wt %	wt %	wt %	wt %	wt %	wt %	wt %	wt %
GHN-KMD-0048	2.64	2.79	3.57	3.28	0.34			0.13	3.43		0.050433	
GHN-KMD-0050	2.736	2.78	3.29	3.33	0.34			0.099	3.84		0.119553	
GHN-KMD-0051	1.8	1.94	3.22	3.96	0.16				2.72			2.55
GHN-KMD-0052	2.23	2.32	2.48	3.44	0.27	0.98	0.09	0.29	4.49	98.88	1.07	
GHN-KMD-0053	0.91	0.53	1.78	4.54	0.06	0.06	0.2	0.07	3.65	99.6	0.26	0.6
GHN-KMD-0054	2.33	2.19	2.7	3.64	0.32	0.25	0.23	0.05	4.2	99.02	0.48	
GHN-KMD-0055	0.63	0.76	0.38	3.88	0.1	1.97	0.46	0.06	5.04	101.15	2.43	
GHN-KMD-0056	1.64	1.21	3.21	3.8	0.16	0.1	0.08	0.04	3.09	101.32	0.18	1.69
GHN-KMD-0057	2.62	2.56	3.05	3.52	0.326	0.09	0.01	0.13	3.38	99.6	0.1	
GHN-KMD-0062	1.35	0.51	1.8	4.18	0.2	0.02	0.24	0.12	4.72	100.01	0.26	
GHN-KMD-0063	1.89	1.25	2	3.79	0.22	0.55	0.75	0.04	5.97	101.07	1.3	
GHN-KMD-0064	0.95	0.66	2.68	4.06	0.178			0	3.58		0.150736	
GHN-KMD-0065	2.15	1.29	2.76	3.73	0.2	0.05	0.06	0.03	3.59	102.67	0.11	1.6
GHN-KMD-0071	1.35	1.28	3.1	3.75	0.13	0.42	0.19	0.04	3.35	100.66	0.61	1.7
GHN-KMD-0072	2.25	2.1	3.09	3.57	0.29	0.05	0.01	0.1	3.6	99.25	0.06	
GHN-KMD-0073	2.65	2.28	3.33	3.37	0.26	0.14	0.1	0.14	3.17	98.65	0.24	2.23
GHN-KMD-0074	2.26	1.66	2.86	3.53	0.22	0.11	0.08	0.04	3.23	100.57	0.19	2.34
GHN-KMD-0077	0.85	0.84	3.02	3.96	0.165	0.05	0.12	0.04	3.4	99.7	0.17	
GHN-KMD-0078	1.08	0.38	2.92	3.93	0.173	0.22	0.2	0.04	3.31	99.53	0.42	
GHN-KMD-0079	1.49	1.26	2.8	3.82	0.16	0.15	0.17	0.05	3.21	100.25	0.32	1.62
GHN-KMD-0080	2.37	2.35	3.36	3.4	0.309	0.1	0.1	0.082	3.09	100.16	0.2	
GHN-KMD-0081	1.32	1.11	2.79	3.87	0.19	0.32	0.14	0.05	3.16	98.3	0.46	1.48
GHN-KMD-0082	2.74	2.74	3.46	3.05	0.34	0.03	0.25	0.12	4.6	98.64	0.28	
GHN-KMD-0088	1.51	1.13	2.92	3.8	0.21	0.55	0.41	0.04	5.14	99.09	0.96	2.54
GHN-KMD-0092	1.69	1.45	2.63	3.7	0.226	0.44	0.47	0.04	5.43	99.5	0.91	
GHN-KMD-0095	0.39	0.14	0.47	4.81	0.032	0.18	0.28	0.04	3.51	98.81	0.46	
GHN-KMD-0096	0.63	0.66	0.77	4.57	0.046	0.16	0.66	0.06	4.84	99.17	0.82	
GHN-KMD-0097	1	0.98	0.92	5.14	0.147	0.79	0.77	0.06	6.03	99.76	1.56	
GHN-KMD-0100	1.47	0.93	2.05	4.15	0.211	0.01	0.2	0.06	3.91	99.42	0.21	
GHN-LFG-0001	0.55	0.786	0.103	4.379	0.076	0.005	0.75	0.08	5.17	97.46	0.755	
GHN-LFG-0002	0.52	0.95	0.08	4.16	0.08	0	0.68	0.07	4.82	95.68	0.68	
GHN-LFG-0003	0.48	0.04	0.1	3.4	0.03	0.01	0.39	0.05	3.8	99	0.4	
GHN-LFG-0004	0.723	0.0967	0.053	3.34	0.14	0	1.18	0.04	7.73	97.8	1.18	
GHN-LFG-0005	0.516	0.1	0.0556	3.688	0.058	0.01	0.46	0.04	4.58	97.91	0.47	
GHN-LFG-0006	0.851	0.129	0.0687	3.88	0.117	0	0.71	0.06	5.87	98.91	0.71	
GHN-LFG-0018	0.781	0.397	2.335	4.352	0.161			0	3.94		0.213813	
GHN-LFG-0020	0.687	0.598	2.619	4.53	0.125			0	2.25		0.05414	
GHN-LFG-0037	1.87	1.39	2.05	3.57	0.24			0	5.5		0.28	
GHN-LFG-0041	0.244	0.212	2.579	4.915	0.044			0	1.92		0.085403	
GHN-LFG-0060	1.57	1.17	2.64	3.44	0.213				5.12		0.086666	
GHN-LFG-0085	2.48	2.08	2.62	3.56	0.24	0.04	0.24	0.04	4.94	100.68	0.28	
GHN-LFG-0086	2.37	2.03	2.53	3.46	0.31				5.32		0.43	
GHN-LFG-0087	2.91	3.49	3.25	3.27	0.26			0.149	3.73			
GHN-LFG-0088	2.77	2.96	3.31	3.41	0.27	0.05	0.05	0.23	6.03	100.88	0.1	
GHN-LFG-0089	0.52	0.6	3.07	4.3	0.121				2.39		0.08	
GHN-LFG-0090	2.55	2.3	3.32	3.37	0.29	0.57	0.31	0.13	4.13	99.78	0.88	
GHN-LFG-0091	1.52	0.78	2.94	3.65	0.179	1.47	0.96	0.05	6.87	100.8	2.43	
GHN-RDL-0002	0.64	0.09	0.11	4.24	0.07	0.01	0.19	0.31	4.29	97.17	0.2	
GHN-RDL-0003	0.76	0.06	0.04	4.41	0.03			0	3.14		0.04	
GHN-RDL-0004	0.53	0.08	0.07	3.96	0.06	0	0.14	0.18	3.32	96.37	0.14	
GHN-SAW-0003	0.307	0.032	0.0559	3.557	0.029	0.14	0.09	0.04	2.21	99.41	0.23	
GHN-SAW-0004	1.251	0.721	2.678	3.65	0.133	0.29	1.03	0.07	7.04	99.87	1.32	
GHN-SAW-0005	0.338	0.087	1.417	5.057	0.046	0.03	0.16	0.03	2.69	100.2	0.19	
GHN-SAW-0200	1.706	1.212	0.793	3.601	0.219	0.1	0.26	0.51	6.02	96.23	0.36	
GHN-SAW-0201	0.766	0.417	1.077	4.218	0.286	0.09	0.49	0.15	5.46	99.64	0.58	
GHN-STM-0001	1.09	0.82	1.64	3.72	0.11			0	4.3			
GHN-STM-0002	0.4	0.22	0.82	5.06	0	0.27	0.2	0.04	2.96	99.79	0.47	
GHN-STM-0003	0.38	0.06	1.38	5.21	0			0	2.72			
GHN-STM-0004	0.82	2.32	1.8	4.36	0.06				4.22			
GHN-STM-0005	0.28	0.1	1.9	5.05	0			0	2.06			
GHN-VTM-0003	1.08	0.08	1.04	4.03	0.222				4.49		0.28	
GHN-VTM-0109	1.05	0.74	2.07	4.69	0.146				2.96		0.413333	
GHN-VTM-0194	1.51	1.27	2.28	3.52	0.27	1.36	1.24	0.08	8.05	100.52	2.6	
GHN-VTM-0195	2.16	1.43	2.22	3.93	0.29	0	0.6	0.02	5.23	98.29	0.6	
GHN-VTM-0197	2.44	2.17	2.57	3.59	0.27	0.02	0.54	0.07	5.35	99.22	0.56	
GHN-VTM-0198	1.22	0.9	2.2	4.34	0.18	0.04	0.25	0.04	4.01	98.57	0.29	
GHN-VTM-0199	1.23	0.89	2.06	4.02	0.19	0.08	0.21	0.04	4.11	98.93	0.29	
GHN-VTM-0200	0.54	0.33	2.45	4.81	0.07	0.05	0.15	0.03	2.68	100.53	0.2	
GHN-VTM-0201	1.34	0.66	2.02	4.02	0.21	0.25	0.4	0.03	5.06	98.09	0.65	
GHN-VTM-0202	1.56	1.25	2.17	3.84	0.19	0.2	0.35	0.04	4.47	99.33	0.55	1.95
GHN-VTM-0203	1.42	0.95	1.82	4.31	0.19	0.13	0.33	0.03	4.43	99.08	0.46	
GHN-VTM-0204	2.28	1.04	2.33	3.54	0.34	0.02	0.31	0.03	5.47	98.33	0.33	1.36
GHN-VTM-0205	1.9	0.5	2.26	3.3	0.26	0.04	0.3	0.04	5.59	98.99	0.34	1.63
GHN-VTM-0206	2.13	0.95	2.86	3.33	0.29	0.05	0.14	0.03	4.88	99.81	0.19	0.77
GHN-VTM-0207	1.58	0.64	2.59	3.9	0.22	0.01	0.15	0.03	4.12	99.53	0.16	0.52
GHN-VTM-0208	2.48	2.74	3.52	3.68	0.25	0.02	0.18	0.04	2.87	103.68	0.2	1.91

Sample	MgO	CaO	Na2O	K2O	P2O5	S	SO4	C	LOI	Total	TotalS	FeOmeas
	wt %	wt %	wt %	wt %	wt %	wt %	wt %	wt %	wt %	wt %	wt %	wt %
GHN-VTM-0209	2.3	2.31	3.42	3.34	0.29	0.02	0.13	0.04	3.23	100.54	0.15	1.46
GHN-VTM-0210	2.14	2.11	3.32	3.54	0.27	0.05	0.11	0.03	3.3	99.86	0.16	
GHN-VTM-0211	2.6	3	3.48	3.27	0.3	0.02	0.12	0.13	3.54	99.73	0.14	1.37
GHN-VTM-0212	2.62	2.74	3.29	3.32	0.3	0.03	0.15	0.06	3.34	100.62	0.18	1.63
GHN-VTM-0213	2.45	2.45	3.18	3.57	0.3	0.01	0.12	0.12	3.7	100.01	0.13	1.34
GHN-VTM-0214	2.73	2.77	3.75	3.11	0.31	0.01	0.03	0.14	3.69	101.22	0.04	1.51
GHN-VTM-0215	2.39	2.07	3.2	3.29	0.29	0.02	0.06	0.06	3.6	100.13	0.08	1.27
GHN-VTM-0216	2.53	2.53	3.44	3.33	0.3	0.02	0.04	0.1	3.52	99.77	0.06	1.65
GHN-VTM-0217	0.94	1.32	2.43	4.32	0.16	0.05	0.04	0.06	2.52	98.91	0.09	0.75
GHN-VTM-0417	0.74	0.67	0.24	4.21	0.06			0	5.14		0.22	
GHN-VTM-0418	0.72	0.64	0.53	4.2	0.05			0	5.4		0.33	
GHN-VTM-0419	1.27	1.36	1.72	3.86	0.2				6.62		0.09	
GHN-VTM-0420	2.93	1.48	2.37	3.22	0.34			0	6.26		0.45	
GHN-VTM-0421	2.21	1.43	2.87	3.62	0.28				4.23		0.27	
GHN-VTM-0422	1.41	0.81	2.07	4.11	0.21			0	4.42		0.26	1.41
GHN-VTM-0423	1.6	0.82	2.14	4.44	0.27			0	3.65		0.23	1.68
GHN-VTM-0424	0.72	0.35	1.61	4.49	0.08			0	4.42		0.25	0.57
GHN-VTM-0425	2.03	1.98	2.73	3.51	0.19			0	5.16		0.35	
GHN-VTM-0426	2.39	1.54	3.17	3.32	0.3			0	4.94		0.24	1.16
GHN-VTM-0450	2.6	1.68	3.27	3.3	0.25	0.06	0.11	0.06	3.19	100.1	0.17	
GHN-VTM-0451	2.42	1.84	3.75	3.2	0.26	0.06	0.34	0.05	3.82	98.35	0.4	
GHN-VTM-0452	2.07	1.46	3.08	3.32	0.21	0.2	0.3	0.05	4.05	98.53	0.5	
GHN-VTM-0453	2.57	2.26	2.61	3.53	0.29	1.31	0.47	0.14	5.13	99.95	1.78	
GHN-VTM-0454	1.61	1.46	2.68	3.68	0.13	0.37	0.48	0.05	4.9	100.33	0.85	
GHN-VTM-0455	1.94	1.93	3.25	3.53	0.16	0.02	0.12	0.07	2.33	99.5	0.14	
GHN-VTM-0500	3.7	2.18	1.08	3.31	0.19	0.08	0.14	0.48	5.31	99.83	0.22	
GHN-VTM-0501	1.45	0.23	0.12	4.65	0.2	0	0.68	0.14	7.2	99.25	0.68	
GHN-VTM-0502	0.97	2.19	0.14	4.02	0.12	0.05	1.74	0.08	8.19	97.77	1.79	
GHN-VTM-0503	2.46	2.32	1.69	3.16	0.17	0	1.13	0.13	7.14	98.9	1.13	
GHN-VTM-0504	2.58	2.75	1.87	3.44	0.2				5.15		0.06	
GHN-VTM-0506	1.02	1.58	0.12	4.36	0.16	0	1.51	0.01	8.5	98.33	1.51	
GHN-VTM-0507	1.01	1.87	2.49	2.96	0.209	0.27	1.17	0.03	6.88	98.7	1.44	
GHN-VTM-0508	1.62	2.32	2.51	3	0.25	0.05	1.86	0.13	9.81	98.32	1.91	
GHN-VTM-0509	1.24	2.06	0.84	4.13	0.11	0.01	0.88	1.06	10.97	100.47	0.89	
GHN-VTM-0510	1.62	0.37	2.08	3.75	0.25			0	9.31		0.53	
GHN-VTM-0598	0.53	0.21	0.16	3.73	0.04			0.01	4.19		0.31	
GHN-VTM-0599	2.1	2.25	0.74	3.74	0.219	0.19	0.04	0.53	6.08	97.03	0.23	
GHN-VTM-0602	1.84	2.02	0.62	3.86	0.24	0	1.03	0.53	8.28	97.25	1.03	4.53
GHN-VTM-0603	1.75	0.77	0.93	3.64	0.15	0.01	0.63	0.89	8.37	100.55	0.64	4.81
GHN-VTM-0604	2.08	3.72	1.75	4.18	0.19	0.01	0.05	0.57	4.77	100.15	0.06	
GHN-VTM-0605	1.53	0.62	0.9	3.53	0.2				5.83		0.22	
GHN-VTM-0606	0.67	0.31	1.09	4.27	0.16	0.03	0.33	0.13	5.32	99.69	0.36	1.06
GHN-VTM-0607	1.21	0.57	1.45	3.81	0.14	0.23	0.39	0.07	5.25	101.03	0.62	1.64
GHN-VTM-0610	0.98	1.72	1.62	4.07	0.107	0.02	0.91	0.13	5.78	98.52	0.93	
GHN-VTM-0611	1.22	1.84	0.12	3.97	0.15	0.04	1.18	0.06	6.71	98.72	1.22	0.49
GHN-VTM-0612	1.6	3.76	1.37	3.72	0.12	0.13	1.82	0.16	7.67	95.87	1.95	1.02
GHN-VTM-0613	1.48	4.71	0.6	3.49	0.18	0.11	2.81	0.19	10.3	96.98	2.92	
GHN-VTM-0614	1.23	4.11	0.21	5.36	0.06	0	2.53	0.23	9.28	109.72	2.53	0.85
GHN-VTM-0624	1.56	0.6	0.77	3.61	0.21	0.03	0.58	0.62	8.36	100.26	0.61	4.34
GHR-VWL-0004	1.84	0.37	0.4	4.16	0.17			0	9.15			
GHR-VWL-0007	1.1	0.48	0.85	4.23	0.19	0.05	0.11	0.06	5.23	100.5	0.16	
GMG-PIT-0001	0.28	3.66	0.34	5.3	0.15				5.19			
GMG-PIT-0006	0.24	1.42	1.75	7.14	0.058				1.55		0.06	
GMG-PIT-0007	0.46	0.91	2.16	5.8	0.069				1.84		0.05	
GMG-PIT-0009	0.92	1.04	3.48	4.8	0.151				2.91		0.023333	
GMG-PIT-0010	3.49	3.73	1.37	2.55	0.19				5.73			
GMG-PIT-0011	3.46	1.21	2.8	3.07	0.28				3.09			
GMG-PIT-0014	0.94	0.39	0.38	4.92	0.11				5.08			
GMG-PIT-0015	1.43	1.87	0.91	4.75	0.11				4.54			
HAS-GJG-0001	0.16	0.01	0.64	3.51	0.062	0.1	0.42	0.04	7.01	99.12	0.52	
HAS-GJG-0002	0.17	0.03	0.54	4.02	0.035	0.07	0.08	0.06	3.31	98.9	0.15	
HAS-GJG-0004	1.46	0.36	2.95	3.36	0.301	0.03	0.31	0.04	4.27	98.67	0.34	
HAS-GJG-0005	1.33	1.35	3.15	3.85	0.271	0	0.03	0.1	4.27	100.85	0.03	
HAS-GJG-0006	5.68	3.11	0.63	4.02	0.568	2.55	1.7	0.03	11.35	102.07	4.25	
HAS-GJG-0007	4.7	4.19	0.74	2.44	0.66	3.33	2.68	0.02	15.63	103.9	6.01	
HAS-GJG-0008	5.29	4.39	0.45	2.54	0.439	0.25	2.98	0.05	13.58	98.75	3.23	
HAS-GJG-0009	0.61	1.07	0.11	5.96	0.166	0.17	0.97	0.01	6.33	98.23	1.14	
HAS-GJG-0010	2.29	1.11	0.07	4.04	0.161	0.09	0.89	0.02	6.27	98.98	0.98	
MID-AAF-0002	1.14	1.61	1.34	4.19	0.153	0.38	1.29	0.04	7.6	99.98	1.67	
MID-AAF-0003	1.23	1.31	0.92	4.51	0.083	0.25	1.1	0.04	7.11	99.22	1.35	
MID-GJG-4001	1.78	1.24	1.77	3.89	0.24	0.91	0.96	0.06	6.72	100.68	1.87	
MID-GMG-0014	3.26	3.9	3	3.41	0.37				7.69		0.723333	
MID-GMG-0015	0.89	1.49	2.48	5.05	0.13				3.46		0.26	
MID-GMG-0016	2.48	3.21	2.43	4.64	0.0315				3.97		0.146666	
MID-GMG-0017	4.22	3.17	3.28	2.75	0.351				4.7		0.08	
MID-GMG-0018	2.32	2.14	2.55	4.6	0.228				4.05		0.183333	

Sample	MgO	CaO	Na2O	K2O	P2O5	S	SO4	C	LOI	Total	TotalS	FeOmeas
	wt %	wt %	wt %	wt %	wt %	wt %	wt %	wt %	wt %	wt %	wt %	wt %
MID-GMG-0019	1.84	1.51	0.8	5.33	0.194				7.5		0.373333	
MID-GMG-0020	1.51	1.51	1.35	4.12	0.343				6.47		0.043333	
MID-GMG-0021	0.96	0.94	0.51	4.51	0.34				6.72		0.02	
MID-GMG-0022	1.54	1.04	1.62	4.21	0.26				5.4		0.033333	
MID-GMG-0023	0.206	0.87	2.27	4.2	0.286				6.76		0.136666	
MID-GMG-0024	1.61	1.84	2.63	3.72	0.241				5.6		0.093333	
MID-GMG-0025	2.04	2.71	3.46	2.49	0.105				3.28		0.153333	
MID-GMG-0026	3	1.57	4.34	1.54	0.033				1.75		0.053333	
MID-KXB-0001	1.64	1.09	2.27	4.74	0.193	0.32	0.48	0.04	4	99.06	0.8	
MID-KXB-0003	0.45	1.76	0.31	4.28	0.035	0.39	0.72	0.17	4.55	99.44	1.11	
MID-VTM-4001	1.84	2.25	2.18	3.49	0.24	0.86	0.73	0.04	6.22	98.41	1.59	
MIN-AAF-0001	0.66	0.1	0.39	4.29	0.114	0	0.38	0.23	4.27	100.02	0.38	
MIN-AAF-0004	0.62	0.09	0.45	4.39	0.12	0.01	0.43	0.26	4.71	99.65	0.44	
MIN-AAF-0010	0.67	0.06	0.42	4.51	0.098	0.06	0.62	0.39	4.58	98.76	0.68	
MIN-AAF-0013	0.5	0.04	0.53	4.28	0.07	0.01	0.23	0.07	3.2	97.97	0.24	
MIN-AAF-0015	0.59	0.04	0.56	4.3	0.066	0.03	0.22	0.04	3.07	97.95	0.25	
MIN-GFA-0001	0.79	0.1	0.62	4.31	0.102	0.05	0.21	0.02	3.46	98.65	0.26	
MIN-GFA-0003	1.23	0.71	1.07	3.53	0.179	0.09	0.07	0.03	2.91	98.11	0.16	
MIN-GFA-0005	0.68	0.02	0.46	4.19	0.092	0.05	0.25	0.01	3.68	98.86	0.3	
MIN-GFA-0006	1.27	0.56	1.65	3.41	0.187	0.05	0.17	0.08	3.95	99.06	0.22	
MIN-GFA-0007	0.67	0.05	0.58	4	0.112	0.02	0.28	0.04	3.8	99.12	0.3	
MIN-GFA-0009	0.6	0.06	0.57	4.03	0.129	0.03	0.23	0.03	3.42	99.3	0.26	
MIN-SAN-0002	0.64	0.1	0.69	4.23	0.12	0	0.54	0.3	4.68	98.54	0.54	
MIN-VTM-0002												
MIN-VTM-0003	1.01	1.4	2.51	4.91	0.164	0.03	0.21	0.04	4.3	99.75	0.24	
MIN-VTM-0004	1.48	1.45	1.79	4.1	0.221	0.12	0.69	0.14	5.13	98.22	0.81	
MIN-VTM-0005	0.99	3.04	1.88	4.07	0.162	0.05	1.63	0.19	7.26	99.08	1.68	
MIN-VTM-0006	1.18	1.81	1.5	4.12	0.183	0.02	1.03	0.05	5.64	98.98	1.05	
MIN-VTM-0007	1.42	0.72	1.55	4.12	0.234	0.01	0.42	0.08	4.99	98.88	0.43	
MIN-VTM-0008	1.35	0.61	1.87	4.24	0.203	0.07	0.19	0.44	4.43	99.16	0.26	
MIN-VTM-0009	1.44	1.36	1.62	4.02	0.219	0.01	0.77	0.04	5.93	98.86	0.78	
MIN-VTM-0018	4.77	1.3	3.1	2.54	0.37	0.03	0.03	0.07	5.14	100.28	0.06	
MIN-VTM-0019	5.2	2.65	3.33	2.89	0.42	0.06			2.65		0.06	
MIN-VTM-0020	1.46	0.53	0.95	3.7	0.32	0.04	0.04	0.78	7.14	98.98	0.08	
MIN-VTM-0021	1.67	0.41	0.15	3.98	0.28	0.03	0.02	0.19	5.53	97.59	0.05	
PIT-KMD-0007	2.39	2.85	3.26	5.76	0.18				2.44			
PIT-KMD-0008	1.79	1.71	3.89	2.89	0.04				4.17			
PIT-KMD-0009	2.39	3.37	3.35	4.06	0.24				3			
PIT-KXB-0101	1.34	0.6	1.81	3.52	0.314				6.58		0.45	
PIT-LFG-0001	2.67	3.42	2.64	3.26	0.2	0.57	0.07	0.27	3.34	99.66	0.64	
PIT-LFG-0003	1.99	1.48	1.76	3.45	0.19	0.72	1.34	0.07	7.16	102.46	2.06	
PIT-LFG-0005	1.72	2.307	1.017	3.553	0.377	0.14	1.66	0.05	10.2	98.29	1.8	
PIT-LFG-0007	0.491	0.72	0.152	4.381	0.026	0.08	0.62	0.03	4.29	99.33	0.7	
PIT-LFG-0009	0.38	1.033	2.008	4.965	0.033	0.75	0.05	0.25	2.75	100.93	0.8	
PIT-LFG-0013	1.187	0.44	1.905	3.797	0.102	0.54	1.23	0.05	8.29	100.55	1.77	
PIT-RDL-0001	0.35	0.05	0.25	5.2	0.04	0.02	0.19	0.15	3.48	98.48	0.21	
PIT-RDL-0002	0.29	0.06	0.39	5.86	0.024	0.06		0	1.81		0.05	
PIT-RDL-0003	0.4	0.07	0.14	5.34	0.032	0.01	0.21	0.05	3.58	98.75	0.22	
PIT-RDL-0004	0.37	0.03	0.07	3.26	0.034	1.64	0.12	0.02	3.29	99.8	1.76	
PIT-RDL-0005	0.32	0.08	0.21	5.22	0.04	0.01	0.2	0.14	2.97	98.26	0.21	
PIT-RDL-0006	0.38	0.07	0.23	5.54	0.03	0.01	0.18	0.06	2.75	98.39	0.19	
PIT-RDL-0007	0.48	0.04	0.11	4.57	0.03	1.06	0.43	0.04	4.11	99.59	1.49	
PIT-VCV-0001	0.9	1.02	2.62	4.75	0.337	4.43	0.05	0.15	4.91	103.46	4.48	
PIT-VCV-0002	0.75	1.32	0.9	5.3	0.134	3.13	0.05	0.29	4.05	102.16	3.18	
PIT-VCV-0003	1.34	0.81	3.42	3.92	0.342	4.46	0.06	0.07	5.09	103.66	4.52	
PIT-VCV-0004	0.33	0	0.07	3.46	0.023	0.02	0.01	0.02	1.99	99.14	0.03	
PIT-VCV-0005	0.36	0	0.07	3.48	0.021	0.02	0.23	0.02	4.77	100.89	0.25	
PIT-VCV-0006						0.03	0.13	0.05			0.16	
PIT-VCV-0007	0.85	1.04	1.28	5.61	0.19	2.37	0.06	0.16	4.21	101.57	2.43	
PIT-VCV-0008	0.79	2.29	0.38	4.45	0.162	2.16	0.04	0.67	4.76	101.49	2.2	
PIT-VCV-0009	1.3	1.37	1.75	4.11	0.225	3.3	0.06	0.26	4.9	101.94	3.36	
PIT-VCV-0010	1.16	1.12	2.4	6.16	0.187	1.55	0.05	0.23	3.46	100.52	1.6	
PIT-VCV-0011	1.29	1.52	2.12	5.24	0.179	1.88	0.05	0.3	4.38	100.93	1.93	
PIT-VCV-0012	0.64	1.14	0.2	5.19	0.107	1.53	0.03	0.36	3.79	100.85	1.56	
PIT-VCV-0013	0.55	1.57	0.08	4.05	0.083	1.06	0.04	0.37	3.47	99.65	1.1	
PIT-VCV-0014	0.58	0.96	0.12	4.73	0.088	1.08	0.04	0.29	3.22	99.59	1.12	
PIT-VCV-0015	0.19	0.34	1.91	6.45	0.031	0.34	0.02	0.06	1.09	98.66	0.36	
PIT-VCV-0016	1.22	1.44	1.79	6.98	0.247	0.13	0.03	0.24	2.47	98.4	0.16	
PIT-VCV-0017	0.71	0.88	0.99	7.25	0.159	0.46	0.04	0.14	2.48	98.02	0.5	
PIT-VCV-0018	0.57	1.04	1.41	6.78	0.116	0.53	0.02	0.22	2.24	97.52	0.55	
PIT-VCV-0019	0.17	2.65	0.31	3.68	0.279	0.55	1.4	0.03	7.03	99.57	1.95	
PIT-VCV-0020	0.33	1.89	0.49	5.26	0.296	1.44	0.1	0.05	5.55	99.38	1.54	
PIT-VCV-0021	4.16	4.63	2.18	3.9	0.375	1.95	2.28	0.05	8.36	100.31	4.23	
PIT-VCV-0022	3	4.19	3.28	2.77	0.399	4.66	1.85	0.05	8.95	104.56	6.51	
PIT-VCV-0023	1.46	4.51	2.33	3.06	0.421	6.33	2.04	0.06	10.83	104.26	8.37	
PIT-VCV-0024	0.73	5.22	0.21	5.39	0.534	1.01	0.13	0.1	3.81	96.63	1.14	

Sample	MgO	CaO	Na2O	K2O	P2O5	S	SO4	C	LOI	Total	TotalS	FeOmeas
	wt %	wt %	wt %	wt %	wt %	wt %	wt %	wt %	wt %	wt %	wt %	wt %
PIT-VCV-0025	1.08	0.68	0.18	4.94	0.199	3.39	0.19	0.12	4.86	102.58	3.58	
PIT-VCV-0026	1.24	0.49	0.27	5	0.173	4.06	0.18	0.05	5.53	102.55	4.24	
PIT-VCV-0027	1.37	0.72	1.6	4.99	0.242	2.67	0.05	0.1	4.3	101.7	2.72	
PIT-VCV-0028	0.15	0.5	2.81	5.91	0.032	0.23	0.04	0.12	0.91	98.68	0.27	
PIT-VCV-0029	1.54	1.37	1.67	5.6	0.24	2.44	0.06	0.25	4.32	101.53	2.5	
PIT-VCV-0030	1.5	1.15	1.34	5.02	0.246	2.48	0.04	0.2	4.99	101.63	2.52	
PIT-VTM-0001	2.13	1.02	3.67	1.92	0.218				3.33		0.033333	
PIT-VTM-0002	2.36	2.57	3.63	3.55	0.248				2.73		0.103333	
PIT-VTM-0004	2.861	2.624	2.325	2.676	0.262				4.69		0.039726	
PIT-VTM-0005	1.084	0.631	0.218	4.856	0.159				4.78		0.044536	
PIT-VTM-0006	0.43	0.04	0.12	4.65	0.01				2.15		0.08	
PIT-VTM-0007	0.56	0.16	0.17	3.86	0.03				3.71		0.06	
PIT-VTM-0008	0.31	0.03	0.2	6.49	0.02				1.7		0.056666	
PIT-VTM-0009	0.02132	0.037	0.046	0.597	0.06				4.5		0.047486	
PIT-VTM-0010	2.26	1.6	2.2	3.43	0.27				5.35		0.31	
PIT-VTM-0600	2.11	2.55	3.1	3.25	0.265	0.41	0.0001	0.19	3.18	101.23	0.4101	
PIT-VWL-0001	0.23	0.03	0.66	5.69	0				3.18			
PIT-VWL-0007	0.39	0.05	0.09	3.23	0.01	0.02			2.71			
PIT-VWL-0009	0.84	0.21	0.3	2.42	0.33	0.63		0	10.09			
QPS-AAF-0003	1.57	1.25	1.88	3.71	0.241	0.06	0.91	0.03	6.74	99.42	0.97	
QPS-AAF-0005	1.54	1.44	1.82	3.65	0.23	0.02	1.17	0.03	8.03	99.58	1.19	
QPS-AAF-0008	1.06	0.07	1.14	3.51	0.257	0.1	1.57	0.06	8.15	97.77	1.67	
QPS-AAF-0009	1.02	1.61	1.21	3.65	0.263	0.18	1.18	0.03	6.93	99.55	1.36	
QPS-AAF-0022	1.34	0.74	1.56	3.59	0.254	0.05	0.75	0.08	6.08	98.8	0.8	
QPS-SAN-0002	0.93	0.68	1.24	3.71	0.17	0	0.97	0.04	5.13	98.1	0.97	
QPS-VTM-0001	1.4	1	1.85	3.6	0.24	0.13	0.75	0.05	6.27	98.4	0.88	
QPS-VTM-4001	1.55	0.98	2.06	3.47	0.26	0.12	0.75	0.05	6.81	98.35	0.87	
ROC-KMD-0001	3.11	2.86	2.84	3.23	0.35	0.05	0.01	1.74	6.81	101.85	0.06	
ROC-NWD-0001	0.02	0.1	3.63	4.94	0.013	0	0.01	0.04	0.94	100.06	0.01	
ROC-NWD-0002	1.73	0.52	4.91	3.52	0.397	3.5	0.18	0.05	4.75	104.2	3.68	
ROC-NWD-0003	0.08	0.18	4.15	4.79	0.015	0.01	0	0.14	0.52	99.79	0.01	
ROC-VTM-0032	1.3	3.12	2.41	3.01	0.16	0	0	0	6.49	98.04	0	4.26
ROC-VTM-0033	2.1	3.71	3.48	3.68	0.3	0	0		4.37		0	
SCS-LFG-0001	2.6	2.06	1.1	3.09	0.14				9.59			0.78
SCS-LFG-0002	2.15	1.75	2.47	2.8	0.19	3.31	0.66	0.11	6.35	102.6	3.97	
SCS-LFG-0003	1.605	1.9	0.585	3.37	0.07	0.67	1.58	0.08	7.145	99.59	2.25	
SCS-LFG-0004	2.71	1.89	0.815	2.595	0.13	0.26	1.35	0.07	7.82	97.38	1.61	0.77
SCS-LFG-0005	2.58	1.53	0.85	4.11	0.14	0.93	1.13	0.04	5.59	101.22	2.06	1.07
SCS-LFG-0006	2.19	0.76	3.03	3.81	0.19	0.27	0.46	0.05	4.59	100.59	0.73	0.87
SCS-LFG-0007	2.06	0.49	3.81	3.79	0.24	1.71	0.12	0.05	4.29	100.73	1.83	
SCS-LFG-0008	0.46	0.25	0.15	3.92	0.19	7.36	0.36	0.05	7.44	107.68	7.72	
SGS-ESO-0101	2.44	1.69	3.15	4.54	0.328	0.27	0.46	0.05	2.91	99.9		
SGS-VTM-0024	1.72	2.04	1.29	4.14	0.2	0.27	2.48	0.02	12.22	99.27	2.75	
SGS-VTM-0026	1.61	1.73	1.02	4.58	0.17	0.22	1.66	0.03	8.69	98.48	1.88	
SGS-VTM-0605	1.65	1.44	2.43	4.61	0.391	0.74	0.58	0.02	4.23	99.53	1.32	
SPR-AAF-0001	3.69	2.18	3.38	2.77	0.33	0.29	0.12	0.04	2.96	98.57	0.41	
SPR-AAF-0003	3.31	1.86	3.2	3.04	0.35	0.29	0.27	0.05	4.24	98.02	0.56	
SPR-JWM-0002	3.6	1.84	4.19	2.57	0.301	1.11	0.04	0.13	3.1	101.22	1.15	
SPR-KMD-0001	2.53	2.2	2.09	4.84	0.19	1.13	0.06	0.61	2.5	100.38	1.19	
SPR-KMD-0002	3.38	3.64	2.62	3.54	0.24	0.75	0.05	0.52	2.79	100.08	0.8	
SPR-KMD-0003	0.94	1.93	2.67	5.2	0.09	0.46	0.03	0.28	1.13	100.64	0.49	
SPR-OTH-0001	2.17	2.77	2.49	4.45	0.26	0.78	0.08	0.44	3.83	99.36	0.86	
SPR-OTH-0002	2.09	2.58	2.41	4.3	0.24	0.9	0.09	0.34	3.66	98.89	0.99	
SPR-SAN-0002	2.96	2.31	2.79	3.5	0.38	0.18	0.46	0.05	4.22	97.72	0.64	
SPR-VTM-0001	2.51	3.305	4.7	3.175	0.25	0.51	0.03	0.28	1.66	100.11	0.54	
SPR-VTM-0002	2.5	2.7	5.05	2.88	0.25	0.09			0.9			
SPR-VTM-0005	2.69	1.82	4.72	3.21	0.345	0.33	0.04	0.06	2.04	99.92	0.37	
SPR-VTM-0010	3.81	2.65	3.54	2.72	0.341	0.44	0.03	0.28	3.1	100.38	0.47	
SPR-VTM-0012	0.23	0.02	0.14	3.48	0.035	0.15	0.11	0.03	2.64	99.07	0.26	
SPR-VTM-0014	0.27	0.02	0.36	4	0.03	0.09	0.11	0.03	2.44	97.65	0.2	
SPR-VTM-0017	0.51	0.01	0.14	4.23	0.028	0.46	0.21	0.03	3.23	99.57	0.67	
SPR-VTM-0019	0.37	0.01	0.16	4.14	0.03	0.14	0.12	0.02	2.77	97.56	0.26	
SPR-VTM-0021	0.37	0.01	0.11	4.29	0.03	0.13	0.11	0.01	2.71	97.6	0.24	
SSS-AAF-0001	2.28	1.85	1.33	3.67	0.27	0.28	0.83	0.02	6.79	98.09	1.11	
SSS-EHP-0002	1.56	1.88	2.17	4.65	0.19	0.94	0.11	0.21	3.02	99.78	1.05	
SSS-EHP-0003	0.71	1.42	1.74	5.33	0.138	1.33	0.15	0.19	3.14	101.01	1.48	
SSS-EHP-0004	1.69	2.61	1.73	4.59	0.329	1.38	0.67	0.17	5.45	99.92	2.05	
SSS-EHP-0023	1.27	1.035	0.875	3.92	0.15			0.18	9.955			
SSS-EHP-0032	0.9	0.71	1.39	4.68	0.109	0.48	0.21	0.1	3.23	99.32	0.69	
SSS-EHP-0033	1.19	0.62	2.24	4.18	0.169	0.08	0.07	0.03	2.79	99.21	0.15	
SSS-EHP-0034	1.2	0.53	2.26	4.26	0.169	0.15	0.08	0.04	3.04	99.45	0.23	
SSS-GMG-0009	1.53	2.85	2.37	3.81	0.196	0.72			8.13		0.6	
SSS-GMG-0010	1.17	1.7	2.52	3.49	0.315	0.209			4.85		0.063333	
SSS-GMG-0011	2.46	2.36	2.74	2.98	49	0.268			5.78		0.223333	
SSS-GMG-0012	2.68	2.28	2.43	3.94	0.363	0.084			4.27		0.07	
SSS-GMG-0013	1.95	1.82	3.04	4.06	0.285	0.187			3.9		0.053333	

Sample	MgO	CaO	Na2O	K2O	P2O5	S	SO4	C	LOI	Total	TotalS	FeOmeas
	wt %	wt %	wt %	wt %	wt %	wt %	wt %	wt %	wt %	wt %	wt %	wt %
SSS-GMG-0014	1.11	0.56	0.81	4.3	0.168	0.108			4.94		0.09	
SSS-GMG-0015	0.96	0.62	1.59	4.36	0.496				5.53		0.413333	
SSS-GMG-0016	1.23	1.09	2.1	4.28	0.196	0.408			4.69		0.34	
SSS-KMD-0001	1.96	2.32	2.82	3.71	0.17	1.1	0.43	0.26	3.88	101.62	1.53	
SSS-KMD-0002	2.69	4.3	2.86	3.67	0.22	0.78	0.57	0.32	2.31	98.82	1.35	
SSS-VEV-0001	0.6899	0.1467	1.713	3.005	0.222	0.86		0	8.47		0.443436	
SSS-VTM-0005	0.25	0.04	0.06	2.15	0.163	3			9.39		0.44	
SSS-VTM-0600	1.25	0.82	1.5	4.1	0.225	0.11	0.1	0.06	4.2	99.53	0.21	
SSW-AAF-0001	2.25	1.58	2.35	3.64	0.36	0.22	0.1	0.06	6.01	99.18	0.32	
SSW-AAF-0002	1.75	1.75	1.13	3.65	0.212	0.44	0.43	0.07	7.48	99.11	0.87	
SSW-AAF-0005	1.86	1.85	2.28	3.67	0.25	0.12	1.34	0.04	7.63	98.6	1.46	
SSW-AAF-0007	1.69	1.14	1.67	3.83	0.24	0.79	0.61	0.04	5.37	99.11	1.4	
SSW-AAF-1002	2.46	2.3	2.59	3.86	0.304	0.37			5.05		0.306666	
SSW-AAF-1005	1.47	1.58	1.54	3.63	0.242	0.65	0.78	0.02	5.79	99.96	1.43	
SSW-AAF-1009	1.83	1.99	1.93	3.9	0.233	0.5	1.19	0.03	6.9	100	1.69	
SSW-GJG-4000	2.25	2.03	2.28	3.34	0.29	0.24	0.91	0.04	7.25	98.75	1.15	
SSW-KMD-0001	2.53	2.43	2.57	3.81	0.21	1.56			3.08			
SSW-SAN-0002	1.79	1.29	2.38	3.78	0.25	0.2	1.26	0.03	5.44	98.95	1.46	
SSW-SAN-0006	0.93	0.87	0.9	4.03	0.12	0.05	1.45	0.03	6.84	98.32	1.5	
SSW-VTM-0006	1.87	2.34	1.79	3.68	0.25	1.39	1.41	0.06	9	99.89	2.8	
SSW-VTM-0008	1.83	2.03	1.86	3.7	0.26	0.29	1.51	0.04	8.73	98.85	1.8	
SSW-VTM-0010	0.85	1.22	1.52	4.66	0.07	0.18	1.45	0.05	8.24	98.63	1.63	
SSW-VTM-0012	0.96	1.28	1.87	4.43	0.08	0.64	0.19	0.03	8.14	97.95	0.83	
SSW-VTM-0013	1.64	2.2	2.34	3.89	0.23	0.42	1.81	0.04	9.6	98.78	2.23	
SSW-VTM-0015	1.95	2.15	2.62	3.79	0.25	0.41	1.61	0.04	8.53	99.13	2.02	
SSW-VTM-0016	2.01	1.98	2.5	3.61	0.303	0.88	0.27	0.14	4.6	100.21	1.15	
SSW-VTM-0019	2.04	1.85	2.48	3.66	0.295	0.98	0.58	0.07	5.48	100.12	1.56	
SSW-VTM-0023	1.86	1.88	1.91	3.69	0.276	1.36	0.55	0.08	5.87	100.33	1.91	
SSW-VTM-0027	2.26	1.45	1.52	3.69	0.272	0.35	0.71	0.04	5.84	99.64	1.06	
SSW-VTM-0028	2.2	1.33	1.67	3.63	0.268	0.47	0.66	0.03	5.58	99.59	1.13	
SSW-VTM-0030	1.78	2.09	1.88	3.66	0.263	0.64	0.71	0.07	5.8	99.68	1.35	
SSW-VTM-0032	1.75	1.92	1.58	3.69	0.256	0.61	0.93	0.06	6.71	99.89	1.54	
SSW-VTM-4001	2.25	2.12	2.21	3.44	0.32	0.3	1.21	0.04	8.36	108.79	1.51	
SWH-GJG-0001	1.8	0.16	3.19	2.58	0.272	0.26	0.96	0.05	7.59	99.86	1.22	
SWH-GJG-0002	2.07	0.06	1.02	3.27	0.193	0.05	0.64	0.01	6.4	98.96	0.69	
SWH-GJG-0003	1.92	0.5	2.84	3.69	0.294	0.01	0.02	0.02	3.03	99.25	0.03	
SWH-GJG-0004	1.2	0.48	2.06	3.46	0.373	0	0.83	0.05	8.23	99.38	0.83	
SWH-GJG-0005	0.95	0.11	3.51	2.79	0.176	0	0.22	0.15	3.43	99.32	0.22	
SWH-GJG-0006	0.952	0.109	3.505	2.787	0.176	0	0.12	0.02	3.43	99.11	0.12	
SWH-GJG-0007	1.23	0.34	1.22	3.5	0.233	0	0.2	0.4	5.32	99.59	0.2	
SWH-GJG-0008	1.02	2.32	2.72	4.36	0.213	0.32	1.49	0.03	7.64	99.64	1.81	
SWH-GJG-0009	1.79	2.73	2.23	2.82	0.671	0.59	2.59	0.05	13.98	100.15	3.18	
SWH-GJG-0010	2.43	1.5	0.95	3.21	0.365	1.76	1.33	0.05	10.08	100.94	3.09	
SWH-GJG-0011	1.08	1.35	2.99	3.87	0.206	0.09	1.05	0.02	5.72	99.43	1.14	
SWH-GJG-0012	1.61	1.13	2.94	2.96	0.048	0.4	0.75	0.02	5.47	98.91	1.15	
SWH-GJG-0013	0.24	0.96	0.1	3.06	0.185	2.34	0.66	0.01	5.47	100.57	3	
SWH-GJG-0014	0.23	0.53	0.86	3.43	0.316	0.15	0.45	0.02	4.58	98.31	0.6	
SWH-GJG-0015	2.35	4.26	1.26	2.35	0.394	0.08	3.41	0.02	13.9	100.03	3.49	
SWH-GJG-0019	1.63	0.5	0.99	3.04	0.815	0	1.71	0.06	12.08	98.94	1.71	
SWH-GJG-0020	4.12	1.23	3.54	2.57	0.5	2.33	0.43	0.01	6.76	101.96	2.76	
SWH-GJG-0021	3.5	2.96	1.93	2.25	0.202	0.41	1.78	0.04	9.51	98.39	2.19	
SWH-GJG-0022	1.92	2.05	0.35	4.04	0.095	0.68	1.39	0.04	6.12	98.82	2.07	
SWH-GJG-0023	1.62	0.87	0.83	2.8	0.791	0	2.11	0.1	12.67	99.66	2.11	
SWH-GJG-4000	1.6	0.95	2.88	2.88	0.14	0.14	1.06	0.03	6.9	98.32	1.2	
SWH-VTM-4001	1.92	1.7	2.88	2.76	0.1	0.14	1.74	0.04	8.29	98.34	1.88	
average	1.506293811	1.331818476	1.844072055	3.946099307	0.313650115	0.552464286	0.559007192	0.10283237	5.017898383	99.66324138	0.853240963	1.630851064
RSQ w/ F as x values	0.014582744	0.096694792	7.58732E-05	0.006941398	0.001222242	0.009086508	0.000853231	0.005108753	0.000628046	0.007815282	0.004143617	0.029176046
Pearson coeff of F	0.120759034	0.310957862	-0.008710522	0.083315053	0.034960572	0.095323178	-0.02921011	0.071475543	-0.025060845	-0.088404084	0.064370936	-0.170809969
count	433	433	433	433	433	308	292	346	433	290	407	47

Sample	As	Ba	Rb	Sr	Pb	Th	U	Zr	Nb	Y	Sc	V
	ppm	ppm	ppm	ppm	ppm	ppm	ppm	ppm	ppm	ppm	ppm	ppm
BCS-VWL-0004		1357	94	663	73	9	4	145	9	13	9	75
CAP-MLJ-0001	5	340	157	66	103	12	4	283	38	46	2	15
ESS-VWL-0001		1302	205	220	589.9	5.61	0	131	12	0		158
GHN-ACT-0001		196		72	62	12	3	287	31.9	50	1	14
GHN-ACT-0002		176	163	64	56	12	6	293	33.4	53	1	13
GHN-ACT-0003		172	159	60	78	10	5	289	33.4	50	0	12
GHN-ACT-0004		310	158	94	101	11	5	272	32.2	51	3	22
GHN-ACT-0005		713	124	245	93	12	5	236	25	39	4	53
GHN-ACT-0006		399	146	108	56	14	4	275	31.3	54	1	19
GHN-ACT-0007		1256	118	342	222	8	3	190	15.6	28	9	81
GHN-ACT-0008		241	112	54	55	15	7	293	35.4	53	0	7
GHN-ACT-0009		1448	101	375	168	8	3	185	14	23	8	81
GHN-ACT-0010		1297	98	423	133	8	3	187	14.8	78	8	78
GHN-ACT-0011		1039	91	464	96	9	3	197	17	36	8	79
GHN-ACT-0012		1237	93	555	85	9	2	187	14.6	24	8	83
GHN-ACT-0013		1236	92	576	111	8	1	180	13.5	19	9	84
GHN-ACT-0014		1193	88	610	82	9	2	177	12.4	22	9	82
GHN-ACT-0015		1232	86	561	89	11	1	178	12.6	27	9	76
GHN-ACT-0016		853	101	360	78	12	4	207	18.3	42	6	54
GHN-ACT-0017		928	104	415	60	12	3	207	19.3	37	6	50
GHN-ACT-0018		292	143	124	51	13	3	267	30.6	48.7	2	14
GHN-ACT-0019		702	132	168	81	12	3	209	21.8	34	6	52
GHN-ACT-0020		347	94	221	56	14	5	290	31.4	62	3	33
GHN-ACT-0021		236	130	67	85	15	5	300	33.3	62	2	18
GHN-ACT-0022		399	132	90	144	15	3	256	27.9	53	4	35
GHN-ACT-0023		625	143	113	165	10	5	232	23.7	40	6	52
GHN-ACT-0024		700	136	239	172	11	2	213	22.5	35	5	53
GHN-ACT-0025		1084	111	426	109	9	3	171	14.2	25	8	75
GHN-ACT-0026		1089	117	401	166	8	4	175	14.1	27	8	27
GHN-ACT-0027		1060	110	524	145	8	3	169	14.6	26	8	69
GHN-ACT-0028		1182	110	456	104	9	3	175	12.2	27	9	83
GHN-ACT-0029		1177	106	480	72	7	4	173	12.4	27	10	88
GHN-ACT-0030		1136	99	481	95	9	5	168	12.5	22	9	86
GHN-ACT-0031		431	144	109	204	11	3	264	28.7	53	4	33
GHN-ACT-0032		320	147	77	132	11	5	282	30.3	58	3	24
GHN-ACT-0033		988	144	528	48	13	4	215	20.7	37	9	100
GHN-ACT-0034		1196	132	502	49	14	3	179	10.4	18	9	18
GHN-ACT-0035		1278	131	763	27	12	6	157	8.6	54	11	96
GHN-ACT-0036		1323	101	172	22	10	3	160	9.1	35	9	87
GHN-EHP-0001		794.3	129.5	223	59.9	11.6	5	190.8	20.1	28.7	6.4	55
GHN-EHP-0002		363	145	88	74	16	6	270	31.7	55	2	23
GHN-EHP-0003	1.9	575	137	132	51	9	3	218	20	35	7	65
GHN-EHP-0004	6.5	714	101	172	49	12	5	210	18	30	10	71
GHN-EHP-0007	4	700	101	149	38	7	4	155	7.9	29	11	105
GHN-HRS-0001		1162	76.5	562	227	8.7	3.1	178	12.4	20	9.5	79
GHN-HRS-0002		237	155	82.7	48.1	13.2	6.8	286.3	33.3	57	1.4	10
GHN-HRS-0088		180.8	1543	79.1	43.1	13.7	5.1	299	34.1	52.8	2.1	10
GHN-HRS-0089		157.5	149.5	79	26	12.9	4.6	304	34.4	53	1.4	12
GHN-HRS-0090		505.5	132.5	113.3	143.7	12.3	5.7	262.3	25.7	47.7	4.5	47
GHN-HRS-0091		744.3	112.7	643.2	107.9	17.3	3.8	249.1	21.4	49.9	6.4	60
GHN-HRS-0092		1073	140.6	577.1	512.4	11.6	2.8	184.2	12.4	27.8	9.4	90
GHN-HRS-0094		284.3	150.5	102.9	80.7	13.4	5.7	290.7	32.1	58.8	2.5	21
GHN-HRS-0095		1385	82	644	36	9	4	181	10.4	15	9	78
GHN-HRS-0096		1644	86	6795	23	24	0	157	1	12	9	142
GHN-JRM-0001		832	134	136	153	11	5	163	16	25	9	74
GHN-JRM-0002		1222.8	92.5	512.4	130.7	7.3	1.1	173	11.8	18.5	10.8	106
GHN-JRM-0006		1218.9	90.3	472.1	157.2	7.8	4.3	177.5	12.6	28.1	9.8	86
GHN-JRM-0008		1307.8	124.9	461.8	111.3	9.7	4.4	183	12.1	25.2	9.3	95
GHN-JRM-0009		506.3	94.9	65.5	132.2	11.2	5.7	207.9	18.3	42.6	6.7	53
GHN-JRM-0022		1264.7	107.3	406.4	117.9	8.9	1.3	167.7	11.8	30	9.6	81
GHN-JRM-0027	1.9	1224	91	424	159	9	2	170	11.5	21	9	69
GHN-JRM-0037		171.4	155.7	63	42.5	12.3	4.7	301.2	33.9	60.6	1.1	9
GHN-JRM-0038		627.2	153.7	86.1	399	10.7	3.8	221.5	21.3	39.3	7.9	58
GHN-JRM-0039		1060	97	739	72	14	4	211	14	42	9	80
GHN-JRM-0040		594	106	829	56	15	4	235	20.2	85	8	63
GHN-JRM-0047		823.2	125.4	344	248.3	10.4	3.6	205.5	16.7	35.6	8.2	79
GHN-KMD-0013		1015	99	367	158.5	9.82	3.59	176	17	27.4		110
GHN-KMD-0014		1629	93	719	67	6.68	0.37	182	14	17.3		102
GHN-KMD-0015		1564	102	421	117.4	10.34	1.65	160	14	20.7		106
GHN-KMD-0016		1174	76	579	186.2	7.82	2.52	164	15	16.3		126
GHN-KMD-0017		1186	118	183	125.2	13.39	3.98	132	13	15.3	9.5	116
GHN-KMD-0018		712	149	197	154	10.45	4.31	240	32	38		51
GHN-KMD-0019		1065	73	668	154	8	3	182	13	17	10	91
GHN-KMD-0026		609	127	191	81	13	5	242	26	49	4	36
GHN-KMD-0027		726	130	221	103	13	4	238	24	40	5	42
GHN-KMD-0028		1154	105	358	91	9	4	183	13.9	27	8	71

Sample	As	Ba	Rb	Sr	Pb	Th	U	Zr	Nb	Y	Sc	V
	ppm	ppm	ppm	ppm	ppm	ppm	ppm	ppm	ppm	ppm	ppm	ppm
GHN-KMD-0048		1080.9	76.3	589.3	93.2	9.6	1.8	191.1	13	37.5	10.1	72
GHN-KMD-0050		1119.7	82.8	618.8	133.8	8.5	3	177.9	12.1	24.9	8.7	82
GHN-KMD-0051		963	99	436	150.5	9.02	3.22	204	23	33.5		80
GHN-KMD-0052		1217	106	386	99	9	4	170	12	20	8	76
GHN-KMD-0053		583	136	165	67.1	15.87	4.31	264	33	56.4		42
GHN-KMD-0054		1180	98	496	242	9	4	181	14	23	9	87
GHN-KMD-0055		237.9	127.4	50.5	101.7	14.8	4	255.4	26.2	50.5	3.9	37
GHN-KMD-0056		935	100	324	102	9.64	3.88	206	23	28.1		83
GHN-KMD-0057		1243	101	613	141	9	3	182	12.5	19	10	89
GHN-KMD-0062		833.1	128.5	221.6	117.6	10.3	3.8	24.8	22.1	45.5	5.3	54
GHN-KMD-0063		977.1	117.9	294.8	116.7	8.6	3.1	184.7	16	26.7	8.1	80
GHN-KMD-0064		770.9	121.8	229.8	84.5	11.3	3.4	210.7	21.3	41.6	5.3	51
GHN-KMD-0065		1124	99	376	121.8	9.9	2.91	194	20	35.6		87
GHN-KMD-0071		1102	101	399	132.2	9.61	5.66	185	19	33		73
GHN-KMD-0072		1036.9	89.6	475	89.6	10.9	2	198	16.5	35.5	8.3	67
GHN-KMD-0073		1338	88	549	175.9	7.45	1.47	151	13	15.3	9.7	106
GHN-KMD-0074		1180	88	412	112.9	8.79	3.47	180	18	25.7		92
GHN-KMD-0077		753	108	307	56	11	4	217	21.7	48	5	47
GHN-KMD-0078		660	109	215	68	11	4	230	24.2	38	4	43
GHN-KMD-0079		1027	109	305	52.4	12.81	2.62	215	22	30.7		75
GHN-KMD-0080		1084.8	82.3	554.8	73.8	9.6	2.3	193.7	14.3	37.3	8.2	66
GHN-KMD-0081		813.2	105	339	129	11	4.75	208	21	42.5	5.8	61
GHN-KMD-0082		1139	74	552	239	9	3	179	12	31	10	84
GHN-KMD-0088		1216	102	374	60	7	4	176	13	25.6	6	60
GHN-KMD-0092		1126	105	362	119	9	4	176	14	39	7	66
GHN-KMD-0095		179	157	52	109	10	6	288	34.2	57	1	13
GHN-KMD-0096		274	146	89	121	10	5	266	31	51	2	22
GHN-KMD-0097		686	156	119	276	14	3	207	25.5	29	4	37
GHN-KMD-0100		780	126	282	116	10	4	226	22.7	44	6	54
GHN-LFG-0001		879.3	103.9	34	17.7	12.9	3.7	252	27.5	19	6	56
GHN-LFG-0002		760	97	27	13.6	14	4	249.6	27.7	19.5	5.6	56
GHN-LFG-0003		77	108	26	15	15	6	285	3	79	2	9
GHN-LFG-0004		1927.1	104.4	36.9	25.7	15.1	4.6	235.3	26.1	19.3	3.9	42
GHN-LFG-0005		1604.8	95.3	34.2	9.1	15.8	3.8	239.5	28.5	18.9	4.4	44
GHN-LFG-0006		1107	100.7	33.7	27	15.1	4.3	263.3	29.1	15.8	4.6	44
GHN-LFG-0018		802.9	134.3	201.7	82.1	10.6	5.2	224.5	21.3	40.8	5.8	46
GHN-LFG-0020		480.1	133	198.9	43.2	11.2	4.5	266.1	28.1	58.2	4.2	32
GHN-LFG-0037	0.56	1066	121	286	53	7	4	172	12	25	8	68
GHN-LFG-0041		228.4	146.4	87.2	50.6	14	5.1	292.1	33.7	51	2.4	12
GHN-LFG-0060	3.1	1093	111	253	48	8	3	163	11.1	17	8	71
GHN-LFG-0085	1.5	1279										
GHN-LFG-0086		1176	107	414	347.5	7.6	2.7	175.4	11.8	17.4	9.2	81.6
GHN-LFG-0087		1165	78	627	191.7	7.52	3.41	157	15	49.1		117
GHN-LFG-0088		1161										
GHN-LFG-0089	0.6	707	119	286	82	12	6	239	24.1	44	4	38
GHN-LFG-0090		1203	85	458	339.6	7.47	2.45	145	14	14.4		123
GHN-LFG-0091		1212	114	351	64	8	3	169	10.9	13	9	86
GHN-RDL-0002		973	103	70	88	14	5	260	7	53	6	55
GHN-RDL-0003		2191	113	66	55	11	4	239	29	28	6	55
GHN-RDL-0004		715.5	100.2	60.8	44.6	12.6	3.4	240.7	29.1	27.8	4.1	43
GHN-SAW-0003		110.6	113.3	7.9	14	15.1	5.5	311.5	33	74.2	0.08	8
GHN-SAW-0004		899.1	121.1	236.2	135.8	9.1	3.9	161	12.4	14.6	8.9	90
GHN-SAW-0005		236.4	165.4	73.9	89.5	14.7	5.3	293.1	33.8	56.6	1.2	12
GHN-SAW-0200		1062.8	94.1	156.3	57.7	7.7	2.1	172.9	9.9	28.7	9.8	87
GHN-SAW-0201		491.7	144.2	126.8	97.1	10.9	5.4	288.2	25.6	39	3.6	40
GHN-STM-0001		1013	138	141	161.8	7.2	2.29	173	18	20.1		82
GHN-STM-0002		222	163	54	96.9	10.46	6.15	302	42	50.6		7
GHN-STM-0003		223	163	62	67.3	10.62	5.02	296	39	47.2		14
GHN-STM-0004		551	131	165	125.2	8.59	4.34	230	31	39		38
GHN-STM-0005		142	143	65	43.5	10.85	5.33	303	41	50		5
GHN-VTM-0003		838	133	77	64	11	5	195	24.8	34	8	79
GHN-VTM-0109		597	137	223	88	13	4	252	27.6	51	5	36
GHN-VTM-0194	6.6	778	112	161	93	12	4	149	12	17	9	77
GHN-VTM-0195	5	1030	112	401	115	10	3	202.5	16.6	25.5	7.5	70
GHN-VTM-0197	1.4	1057	98	411	79	8	3	184	14	30	9	75
GHN-VTM-0198	2.5	712	129	275	100	13	4	236	24	45	5	50
GHN-VTM-0199	4.7	853	128	246	145	13	3	216	21	43	6	55
GHN-VTM-0200	3	429	138	117	68	14	5	255	29	52	3	22
GHN-VTM-0201		953	126	229	85	11	5	198	18	37	6	61
GHN-VTM-0202	3.1	858	122	279	134	11	4	206	19	32	6	66
GHN-VTM-0203		927	144	221	163	12	2	205	18	31	6	31
GHN-VTM-0204	4.3	1245	111	351	198	12	4	175	13	24	9	82
GHN-VTM-0205	2.8	1031	107	259	236	10	5	178	15	28	7	81
GHN-VTM-0206	3	1125	100	380	115	10	3	184	13	30	10	82
GHN-VTM-0207	3.3	938	106	291	160	12	4	209	19	38	6	60
GHN-VTM-0208	0.6	1294										

Sample	As	Ba	Rb	Sr	Pb	Th	U	Zr	Nb	Y	Sc	V
	ppm	ppm	ppm	ppm	ppm	ppm	ppm	ppm	ppm	ppm	ppm	ppm
GHN-VTM-0209	0.7	1117	84	553	128	9	4	187	14	43	9	91
GHN-VTM-0210		1118	88	544	133	9	4	187	15	46	9	82
GHN-VTM-0211	1.6	1173	83	619	180	9	4	180	12	22	9	84
GHN-VTM-0212	2.1	1137	85	600	153	8	2	178	12	24	9	90
GHN-VTM-0213	2.6	1206	86	588	141	9	3	175	12	28	9	78
GHN-VTM-0214	1.7	1123	73	653	88	9	3	187	13	25	9	91
GHN-VTM-0215	1.5	1148	79	538	106	9	1	183	13	28	9	79
GHN-VTM-0216	1.8	1091	79	565	241	9	2	183	13	44	10	82
GHN-VTM-0217	1.3	705	127	278	60.5	11	5	234.5	24	44	5	48
GHN-VTM-0417		455	147	46	95	10	5	247	27.2	49	4	39
GHN-VTM-0418		625	144	63	132	10	4	221	22.3	37	5	51
GHN-VTM-0419		665	144	179	162	10	4	167	14.9	21	9	86
GHN-VTM-0420		1061	98	394	214	7	2	178	14.2	22	9	108
GHN-VTM-0421		1134	98	427	108	8	2	187	14.8	22	8	89
GHN-VTM-0422		771	125	261	104	10	4	227	22.8	50	6	59
GHN-VTM-0423		823	130	284	87	10	4	228	22.4	41	5	57
GHN-VTM-0424		557	144	134	144	11	4	252	27.7	58	3	31
GHN-VTM-0425		1158	97	416	309	9	2	171	13.5	35	8	79
GHN-VTM-0426		1160	84	460	113	7	1	172	12.4	39	9	77
GHN-VTM-0450		1229	81	456	103.9	7.97	1.43	381	16	19.7		115
GHN-VTM-0451		1229	75	468	209	7.18	3	169	16	28.7		99
GHN-VTM-0452		1169	83	404	125.6	9.25	1.97	168	16	28.9		109
GHN-VTM-0453		1333	96	393	108	8	3	173	12	51	8	76
GHN-VTM-0454		969	99	317	182.5	9.66	5.85	178	20	38.9		82
GHN-VTM-0455		934	93	466	70	8.48	4.47	223	23	45.2		77
GHN-VTM-0500		1117	90	181	9	6	2	145	8.1	34	10	82
GHN-VTM-0501		1208	119	77	20	5	3	162	8.1	13	10	92
GHN-VTM-0502		538	101	108	42	6	1	126	6.7	19	9	78
GHN-VTM-0503		915	80	161	10	4	2	139	7.1	24	10	80
GHN-VTM-0504		564	89	202	11	6	0	158	8.5	16	11	87
GHN-VTM-0506		1077	108	96	227	5	3	134	7	17	10	89
GHN-VTM-0507		1347	71	238	22	7	3	146	7.4	13	11	111
GHN-VTM-0508		2412	72	361	18	4	4	146	7	12	11	108
GHN-VTM-0509		1117	96	221	49	9	3	171	10	24	11	84
GHN-VTM-0510		2863	95	437	38	10	3	144	8.1	22	10	100
GHN-VTM-0598		199	117	34	204	11	5	295	32	60	2	26
GHN-VTM-0599		888	108	138	15.8	5.4	2	154.8	8.7	19	10	88
GHN-VTM-0602		881.6	106.5	138.4	58.7	5.4	3	135.1	7.3	30.5	12.2	100
GHN-VTM-0603		1008	98	150	56	7	2	180	10	26	12	94
GHN-VTM-0604		2960	102	438	16	7	1	147	8.8	15	11	84
GHN-VTM-0605		639	137	138	120	8	3	204	16.8	21	9	78
GHN-VTM-0606		426	143	110.5	106	12	6	303	26.5	41	4	39
GHN-VTM-0607		992	134	158	231	11	3	198	18	45.5	7	65
GHN-VTM-0610	1.4	853	105	101	27	11	5	216	24.3	47	5	45
GHN-VTM-0611		506	110	164	63	13	5	223	25.7	16	7	41
GHN-VTM-0612		770	87	165	37	12	6	195	22	31	4	36
GHN-VTM-0613		670	95	205	49	6	2	153	12	20	9	74
GHN-VTM-0614		1276	112	184	9	6	3	131	7	18	11	97
GHN-VTM-0624		797	87	101	63	7	3	168	10	26	9	85
GHR-VWL-0004		1200	160	363	205	3	17.91	0	118	5.1		128
GHR-VWL-0007		1076	157	260	77.4	12.77	2.44	186	17	18		100
GMG-PIT-0001		862	199	1004	13	6.76	0.3	222	16	28.3		189
GMG-PIT-0006		448	171	126	14	23	3	132	31	11	2	11
GMG-PIT-0007		503	161	115	17	24	6	153	27.7	13	2	15
GMG-PIT-0009		1083	145	271	21	15	6	218	25.6	16	5	35
GMG-PIT-0010		864	123	488	146.3	7.74	1.64	132	10	8.4		126
GMG-PIT-0011		268	169	186	31.6	7.11	2.39	168	14	17.3		116
GMG-PIT-0014		637	180	15	9.3	12.3	4.65	204	30	25		73
GMG-PIT-0015		1159	159	121	19	14.49	3.52	240	31	18.9		61
HAS-GJG-0001	3.1	180	98	40	26	11	2	254	29.6	55	2	18
HAS-GJG-0002	3.5	159	115	44	30	15	4	298	37	70	2	8
HAS-GJG-0004	2.6	1067	85	380	13	12	4	190	17.8	6	5	75
HAS-GJG-0005		1287	108	561	13	10	3	172	13.6	30	6	68
HAS-GJG-0006	8.9	2983	80	1106	24	7	2	161	21.4	19	16	153
HAS-GJG-0007	8.3	1730	53	364	23	10	3	138	17.2	12	15	136
HAS-GJG-0008	7.4	1863	73	434	40	6	2	149	20	14	15	141
HAS-GJG-0009	3.9	1136	188	66	19	8	2	232	14.5	10	7	105
HAS-GJG-0010	4.9	1257	126	128	28	8	2	168	13.5	15	10	116
MID-AAF-0002	3	1030	149	322	125	10	1	166	12.5	14	7	65
MID-AAF-0003	2.8	859	170	208	38	12	3	186	22	15	6	48
MID-GJG-4001	4.9	1031.7	137.1	289.4	45	8.6	3.3	171	13.7	19.5	7.9	80.2
MID-GMG-0014		1176	116	722	45	6	2	177	10.4	17	13	108
MID-GMG-0015		510	158	232	56	20	6	137	23.4	14	6	43
MID-GMG-0016	0.9	974	161	451	54	15	4	154	11.9	17	12	96
MID-GMG-0017	1.8	792	95	415	20	8	4	170	10.1	18	14	110
MID-GMG-0018		837	179	486	19	15	4	150	17.4	16	10	71

Sample	As	Ba	Rb	Sr	Pb	Th	U	Zr	Nb	Y	Sc	V
	ppm	ppm	ppm	ppm	ppm	ppm	ppm	ppm	ppm	ppm	ppm	ppm
MID-GMG-0019		811	182	245	40	13	5	182	19.5	16	7	60
MID-GMG-0020	0.5	1179	157	336	26	7	3	175	11.2	18	15	124
MID-GMG-0021		858	159	121	11	11	3	177	12.1	19	12	104
MID-GMG-0022	1.7	1001	149	190	9	9	3	165	10.7	16	9	81
MID-GMG-0023	1.6	1031	149	250	31	8	3	174	13.9	14	9	55
MID-GMG-0024	1.7	1168	123	379	29	9	2	152	9.6	14	10	81
MID-GMG-0025	1	779	73	287	17	4	2	102	9	15	13	90
MID-GMG-0026	0.6	442	44	207	8	7	4	1152	10.3	17	5	5
MID-KXB-0001		1408	141	345	55	10	4	180	14.8	17	7	63
MID-KXB-0003	1.7	209	143	64	32	10	5	243	30.8	52	2	19
MID-VTM-4001	2.6	1093	134.6	465.1	47.7	7.1	2.4	148.1	9.8	15.5	9.7	82.9
MIN-AAF-0001		591	149	92	93	13	3	229	25.4	36	4	46
MIN-AAF-0004		658	150	102	124	16	2	240	25.9	37	3	47
MIN-AAF-0010		900	146	89	75	11	4	231	22.1	31	6	69
MIN-AAF-0013	1.7	432	130.8	72.3	57.4	13.7	4.7	263.6	29.1	59.1	3.6	34.6
MIN-AAF-0015		705	135	90	43	12	4	222	25.4	38	4	45
MIN-GFA-0001	0.77	642	149	133	70	13	5	215	24	32	5	61
MIN-GFA-0003		822	104	280	32	8	6	172	16.9	23	6	62
MIN-GFA-0005	1.1	613	149	138	103	12	4.5	240.5	25.5	40	4	46
MIN-GFA-0006	1.8	871	104	265	51	8	4	189	16.2	21	7	73
MIN-GFA-0007		666	134	140	98	13	5	226	24.1	35	5	46
MIN-GFA-0009	3.4	591	137	145	47	11	5	213	24	33	5	44
MIN-SAN-0002		703	137.6	116	88.2	13.1	3.9	228.7	24.5	35	4.5	56.8
MIN-VTM-0002	1.4											
MIN-VTM-0003	1.8	1221	157	232	47	15	4	222	26.3	18	5	42
MIN-VTM-0004	2.8	857	142	285	70	13	4	173	18.9	21	9	72
MIN-VTM-0005	2.2	763	151	225	58	14	6	178	18.7	17	7	56
MIN-VTM-0006	0.52	888	131	277	31	11	3	183	18.3	21	7	68
MIN-VTM-0007	2.1	935	137	320	50	12	4	183	18.4	21	9	78
MIN-VTM-0008	1.4	856	141	270	44	11	3	181	19.3	20	7	69
MIN-VTM-0009	2.5	897	134	334	64	12	4	171	17.1	19	9	73
MIN-VTM-0018		1132	79	415	20	5.5	2	181	12	23	14	131
MIN-VTM-0019		1223	66	696	9	7	1	186	11.1	23	16	142
MIN-VTM-0020		1218	102	174	33	6	5	207	11	22	9	80
MIN-VTM-0021		947.7	112.4	65.2	96	6.4	2.7	162.9	8.3	18.3	10.7	88
PIT-KMD-0007		1333	186	496	44.2	7.52	0.97	176	11	17.2		116
PIT-KMD-0008		1404	130	282	46.1	5.29	1.79	228	15	22.5		161
PIT-KMD-0009		1237	121	637	26.3	6.97	1.77	145	14	15.5		102
PIT-KXB-0101		1021	107	476	55	9	4	166	13	17	9	85
PIT-LFG-0001		1219	109	713	30.9	7.6	2.31	142	11	15.7		121
PIT-LFG-0003		1007	125	397	132.5	7.73	1.54	117	10	9.5		122
PIT-LFG-0005		1234.4	126	470.9	32.6	5.5	1.9	139.4	8.9	7	7.7	78
PIT-LFG-0007		332.4	176.3	45.3	46.9	10.7	7.4	267.6	31.4	58.3	1.7	12
PIT-LFG-0009		143.5	148.9	68	27.5	13.9	4.9	288.5	34.6	69.5	0.4	7
PIT-LFG-0013		1038.6	123.1	152.4	97.9	8.5	4	166.2	14.1	19.6	9.3	84
PIT-RDL-0001		204	171	60	112	12	8	300.5	35	58	1	11
PIT-RDL-0002		216	191	56	21	9	6	310	35.9	59	1	7
PIT-RDL-0003		215	169	51	146	14	5	300	34.9	300	1	7
PIT-RDL-0004		56	107	7	469	13	6	271	30.1	61	1	19
PIT-RDL-0005		197.2	171.5	58.6	95.8	10	5.1	291.3	35.2	49.9	1.4	11
PIT-RDL-0006		210.9	173.6	52.5	73.7	10.6	4.7	303.1	35.4	58.4	1.8	6
PIT-RDL-0007		168.9	162.1	14.4	385	14.3	5.2	293.9	33.9	63.9	0.4	7
PIT-VCV-0001		1054	151	165	31	10	3	171	12.2	19	11	103
PIT-VCV-0002		886	173	105	22	12	3	268	27	58	6	52
PIT-VCV-0003		878	130	164	27	8	2	166	10.3	19	11	93
PIT-VCV-0004		75	123	6	107	15	6	309	34.5	70	1	9
PIT-VCV-0005		63	118	3	201	13	4	314	36.3	70	1	6
PIT-VCV-0006												
PIT-VCV-0007		1519	198	210	17	12	3	211	23.9	18	7	53
PIT-VCV-0008		943	173	138	157	11	5	176	20.5	13	5	46
PIT-VCV-0009		971	168	171	25	14	3	194	20.6	19	8	71
PIT-VCV-0010		1423	164	249	9	16	6	207	25.8	17	6	46
PIT-VCV-0011		1147	163	242	40	14	10	201	23.6	19	5	51
PIT-VCV-0012		744	188	97	16	18	3	161	24.9	15	3	27
PIT-VCV-0013		305	184	40	19	18	2	146	23.2	11	3	22
PIT-VCV-0014		746	174	75	11	18	3	148	23.7	13	3	23
PIT-VCV-0015		219	169	93	17	26	4	96	24	7	1	8
PIT-VCV-0016		873	2114	281	19	18	3	363	42.8	25	6	37
PIT-VCV-0017		551	206	169	18	25	3	222	32.4	19	4	33
PIT-VCV-0018		594	164	148	20	37	3	165	19.3	14	3	19
PIT-VCV-0019		751	155	852	7	8	2	155	8.9	16	19	144
PIT-VCV-0020		999	196	969	7	7	3	164	10.8	20	22	130
PIT-VCV-0021		868	165	489	6	8	3	166	10.3	20	15	135
PIT-VCV-0022		1253	108	543	5	7	3	158	10.6	18	14	123
PIT-VCV-0023		769	104	681	6	8	0	154	9.9	20	16	126
PIT-VCV-0024		543	259	98	164	9	1	117	5.4	14	11	83

Sample	As	Ba	Rb	Sr	Pb	Th	U	Zr	Nb	Y	Sc	V
	ppm	ppm	ppm	ppm	ppm	ppm	ppm	ppm	ppm	ppm	ppm	ppm
PIT-VCV-0025		578	206	49	82	9	2	220	24	16	7	53
PIT-VCV-0026		611	192	55	28	12	4	218	25.2	21	6	47
PIT-VCV-0027		1109	158	190	12	8	3	171	9.5	14	8	81
PIT-VCV-0028		204	154	91	16	28	7	111	27.6	7	2	9
PIT-VCV-0029		1294	191	208	8	8	2	170	9.7	17	10	78
PIT-VCV-0030		1262	160	211	20	9	2	172	9.5	16	7	85
PIT-VTM-0001		673	68	372	26	10	5	163	8.9	29	29	116
PIT-VTM-0002		1529	107	440	11	8	4	164	8.7	14	9	81
PIT-VTM-0004		881.5	124	495.8	21.1	7.2	3.7	151.3	9.6	16.1	9.8	90
PIT-VTM-0005		583.8	184	57.7	70.4	9.2	6.1	204.1	23	15.6	5.4	51
PIT-VTM-0006		197	164	10	58	12	4	316	36.6	66	2	8
PIT-VTM-0007		184	152	5	1446	14	9	293	32.2	65	1	12
PIT-VTM-0008		3.94	207	1	43	14	4	312	35	64	1	11
PIT-VTM-0009		363.2	8.5	195.5	46.2	10.1	1.1	292.2	29.7	16.5	1.9	23
PIT-VTM-0010		1250	123	502	52	8.45	2	144	11	13.5	11	118
PIT-VTM-0600		1180	119	650	21	9	3	145	9	13	11	92
PIT-VWL-0001		160	170	29	60.4	11.22	5.25	341	41	58.9		0
PIT-VWL-0007		852	114	61	7.9	10.89	4.87	288	45	72.2		9
PIT-VWL-0009		887	50	80	14.7	7.55	3.8	109	12	8.5		76
QPS-AAF-0003	3.1	1416	117	362	55	11	3	168	12.5	20	9	88
QPS-AAF-0005	3.7	1086	116	371	58	10	2	169	12.4	18	10	86
QPS-AAF-0008	3.8	1054	102	292	38	9	3	162	10.1	17	11	99
QPS-AAF-0009	3.8	933	103	380	40	9	3	170	11.5	18	10	97
QPS-AAF-0022	1.3	1137	108	349	73	9	4	186	13.3	20	3	93
QPS-SAN-0002		724	109	285	32.6	11.1	5.1	200	19.4	28.5	7.8	68.9
QPS-VTM-0001	3	1046	108.3	350.8	53.4	8.6	2.9	170.7	12.3	20.3	10	88.1
QPS-VTM-4001	3.2	1131.8	103.6	337.1	50.7	9.2	2.4	175.7	12.7	18.8	337.1	85.2
ROC-KMD-0001		1264	85	708	64	8	2	209	11	22	11	100
ROC-NWD-0001		17	142	7	32	18	7	407	39.8	56	1	
ROC-NWD-0002		939	125	268	9	7	3	175	10.1	14	13	109
ROC-NWD-0003		42	110	9	15	13	4	348	31.6	57	3	10
ROC-VTM-0032		992	82	594	33.8	7.67	1.31	194	12	27.7		101
ROC-VTM-0033		1298	87	707	31.7	7.05	3.42	218	14	24		130
SCS-LFG-0001		957	92	108	160	7	3	132	7	13	8.5	68
SCS-LFG-0002		958	88	212	111.3	7.51	2.28	119	8	12.3		94
SCS-LFG-0003		806	90	79	164	6.14	1.65	104	8	8.2		91
SCS-LFG-0004		720	79	67	37.3	9.7	2.9	166	11	14.1		74
SCS-LFG-0005		796	118	195.5	65	10	4	170	9	14	9	93
SCS-LFG-0006		1414	89	341	115	10	5	169	10	13	7	67
SCS-LFG-0007		1583.5	81	366	43	7.5	2	174	9.4	13	7	66
SCS-LFG-0008		1230	96	63	15	2	2	151	9	10	8	80
SGS-ESO-0101		1205	144	490	18	8	2	170	11.5	20	15	122
SGS-VTM-0024	0.89	910	167.1	179.6	562.7	7.7	3.6	148.8	8.5	10.3	10	76.5
SGS-VTM-0026	1	914	183	162.7	585.8	7.7	4.5	160.7	9.1	10.7	162.7	86.9
SGS-VTM-0605	0.93	117	157	404	28	10	2	161	11.9	17	15	134
SPR-AAF-0001	0.67	1040	88.8	629.8	14.3	7.4	4.4	173.8	11.4	19.9	12.8	107.4
SPR-AAF-0003	0.93	1037	99.9	580.2	15.2	7.3	3.9	175.3	11.5	20.5	13.4	114.5
SPR-JWM-0002		782	92	553	8	6	2	169	10.2	17	13	98
SPR-KMD-0001		861	158	410	23.6	7.8	2.24	194	18	22.1		122
SPR-KMD-0002		846	135	572	12	7.35	1.47	178	11	25.7		140
SPR-KMD-0003		744	157	418	119	12.3	1.94	129	27	14.8		62
SPR-OTH-0001		832	146	420	24	11	5	164	16	19	10	82
SPR-OTH-0002		813	147	553	48	13	4	173	17	20	9	78
SPR-SAN-0002		1075	112.6	725.2	20.7	8	3	166.5	10.9	20.5	13.8	122
SPR-VTM-0001		1261	93	579	20.1	11.4	2.785	180.5	12.5	23.8		120.5
SPR-VTM-0002		1220	70	817	21.7	8.14	2.08	183	13	21		130
SPR-VTM-0005	0.5	1117	108	615	12	12	3	173	11.1	22	13	108
SPR-VTM-0010	0.42	967	91	589	8	8	2	171	10.4	21	14	112
SPR-VTM-0012	0.85	139	99	29	29	15	6	280	34.4	63	1	11
SPR-VTM-0014	1	189	118.1	28.1	34.9	14.2	4.6	276.8	35.1	65.5	1	13
SPR-VTM-0017	3.5	329	143	23	32	14	5	259	29.7	55	4	34
SPR-VTM-0019	1.8	188	139.4	22.6	26.7	12.6	4.6	285.3	35.8	70.2	0.8	12.7
SPR-VTM-0021	0.62	203	141.9	23.3	29.7	12.6	5.4	285.6	36.1	67.3	0.9	12.7
SSS-AAF-0001	1.8	960	155.4	214.1	26.4	5.7	2.4	158.4	10.8	11.7	9.7	95.7
SSS-EHP-0002	1.9	630	154	224	46	15	3	146	22.9	16	7	60
SSS-EHP-0003		567	174	167	38	17	5	137	24.2	14	6	44
SSS-EHP-0004	4.9	955	170	533	34	9	3	159	13.8	19	13	118
SSS-EHP-0023		932										
SSS-EHP-0032	2.8	701	148	151	112	12	5	246	25.9	44	5	39
SSS-EHP-0033	3.5	837	126	250	75	9	3	213	21.3	34	5	62
SSS-EHP-0034	6.5	689	134	209	118	9	4	223	22	36	5	56
SSS-GMG-0009		1318	122	600	11	10	4	155	9.7	12	7	67
SSS-GMG-0010	4.8	1007	144	395	37	7	5	150	10.1	13	111	47
SSS-GMG-0011	22	1000	128	795	113	7	2	181	10.4	21	18	151
SSS-GMG-0012	2.6	1222	114	434	58	9	3	172	12	15	11	97
SSS-GMG-0013	2.2	1420	128	537	76	8	3	148	10.1	14	12	94

Sample	As	Ba	Rb	Sr	Pb	Th	U	Zr	Nb	Y	Sc	V
	ppm	ppm	ppm	ppm	ppm	ppm	ppm	ppm	ppm	ppm	ppm	ppm
SSS-GMG-0014	6.3	770	141	115	126	11	4	199	19.1	35	9	52
SSS-GMG-0015	2.9	612	138	154	114	11	4	225	22.4	37	6	37
SSS-GMG-0016	2.3	839	131	262	72	10	3	224	21.2	32	8	54
SSS-KMD-0001		1155	123	492	59.6	7.78	2.2	148	15	16.8		101
SSS-KMD-0002		977	142	477	91.6	9.97	1.78	171	14	21.3		116
SSS-VEV-0001		969.7	92.7	274.6	53.8	4.7	2	167.1	10.7	11.8	12.4	143
SSS-VTM-0005		104	70	12	226	4	3	138	15.9	23	0	25
SSS-VTM-0600	4.1	966	133	247	104	12	4	200	17.8	29	7	73
SSW-AAF-0001	1.8	1018	149	445	75	9	3	180	12	23	12	118
SSW-AAF-0002	4.1	973	137	356	48	7	2	159	11.9	17	9	88
SSW-AAF-0005	0.95	1089	129.1	433.6	45.4	10.5	3.8	155.9	10.6	13.8	8.4	79.5
SSW-AAF-0007	1.2	1148	130.9	301.9	33.3	9.6	2.4	161.4	11.1	15.3	9	80.3
SSW-AAF-1002		1074	154	474	115	8	4	172	11.1	21	11	102
SSW-AAF-1005	4.3	1005	136	276	29	8	3	155	11.3	16	11	92
SSW-AAF-1009	1.8	953	149	364	103	10	4	180	16.1	20	9	79
SSW-GJG-4000		1052	124.6	480.4	54.9	8	3.3	167.3	10	18.9	10	102.6
SSW-KMD-0001		1148	147	466	49	10.76	3.24	165	12	18.7		122
SSW-SAN-0002		1090	130.9	388.7	30.9	7.9	3.5	155.5	9.5	12.5	8.9	79.3
SSW-SAN-0006		777	146.1	189.1	70	8	3.6	191.4	16.9	28.2	6.8	66.6
SSW-VTM-0006	17	974	137.2	340.7	116.2	9.4	2.9	168.3	13	21.6	8.3	80.6
SSW-VTM-0008	1.8	951	140.6	339.9	131.6	9.8	3.1	163.1	12.9	18	8.9	82.4
SSW-VTM-0010	1	975	149.3	250.3	56.2	11.1	3.6	190.6	23.6	13	4.1	36
SSW-VTM-0012	1.9	1010	149.2	290.3	77.8	8.1	4.1	199	18.5	13.6	5.3	49.6
SSW-VTM-0013	1.9	1073	141.9	412.9	159.3	12.3	3.8	156.4	9.4	11.9	8.7	71.6
SSW-VTM-0015	1.6	1091	136.5	416.4	162.9	11.6	3.3	151.7	9.4	12.8	9.2	74.6
SSW-VTM-0016	2.9	1272	124	470	32	7	3	152	10.8	16	10	97
SSW-VTM-0019	5	1255	123	465		7	3	147	10.5	16	11	98
SSW-VTM-0023	3.5	1151	132	499	33	8	3	157	11.3	15	11	91
SSW-VTM-0027	2.2	1182	129	390	29	8	4	153	10.5	12	9	93
SSW-VTM-0028	4	1141	127	351	30	7	2	154	11.4	154	10	98
SSW-VTM-0030	4	1198	138	443	28	8	3	154	11.6	14	10	94
SSW-VTM-0032		1109	141	393	41	8	4	154	11.4	12	11	92
SSW-VTM-4001	2.2	1014.2	128.9	468.8	61.5	8.3	3.2	166.4	10.7	18.5	10.8	103.4
SWH-GJG-0001	2.1	2186	58	546	14	5	2	157	9	12	11	105
SWH-GJG-0002	4.9	1509	95	385	11	6	3	163	9.7	21	12	112
SWH-GJG-0003	5.1	1620	102	619	8	8	4	168	12.6	12	7	70
SWH-GJG-0004	2.6	1290	76	756	39	14	4	166	11.2	11	10	89
SWH-GJG-0005	10											
SWH-GJG-0006	7.1	1071	76	230	113	8	1	144	8.6	9	9	79
SWH-GJG-0007	10	1072	92	292	99	10	4	168	12.8	12	8	82
SWH-GJG-0008	7.3	883	113	372	16	11	3	165	22.5	8	4	38
SWH-GJG-0009	37	1306	70	578	31	5	0	107	6.2	8	7	75
SWH-GJG-0010	20	1037	128	275	45	6	4	132	8.3	9	9	78
SWH-GJG-0011	1.5	754	102	385	28	11	4	184	24.8	9	4	38
SWH-GJG-0012	1.5	695	87	531	49	8	1	136	7.8	17	10	84
SWH-GJG-0013	2.9	731	70	385	133	5	0	161	8.7	9	6	78
SWH-GJG-0014	1	1377	77	861	83	11	5	200	15.2	19	12	114
SWH-GJG-0015	7.8	1035	86	362	28	9	1	146	7.9	12	8	68
SWH-GJG-0019	18	799	82	437	38	7	2	127	7.7	8	7	86
SWH-GJG-0020	1.7	1615	50	437	17	5	3	220	25.7	16	15	175
SWH-GJG-0021	2.3	1624	60	317	44	5	2	188	22.3	13	14	121
SWH-GJG-0022	3.1	1417	96	161	40	6	2	223	27.3	20	17	154
SWH-GJG-0023	22	1434	66	410	58	7	3	142	10.7	11	9	91
SWH-GJG-4000	3.2	631	74	349.2	22.9	10.9	3.6	178.6	10.3	11.7	8.7	81.2
SWH-VTM-4001	2.1	1361	75.8	623.1	227.9	7.5	3	143.4	8	9.9	8.6	77.6
average	3.702246377	908.1591204	130.2487119	317.564486	86.04074941	10.26614486	3.541740654	198.785514	18.46098131	29.40233645	9.037813333	70.62880562
RSQ w/ F as x values	0.006681823	0.000273886	0.011845821	5.76815E-05	8.89055E-05	0.001061157	0.016864267	0.021968017	0.018716251	0.014600822	0.002435872	0.039270182
Pearson coeff of F	-0.081742418	0.016549496	0.10883851	0.007594833	0.00942897	-0.032575399	-0.129862491	-0.148216115	-0.13680735	-0.120833861	0.049354552	0.198167055
count	138	432	427	428	427	428	428	428	428	428	375	427

Sample	Ni	Cu	Zn	Ga	Cr	Co	La	Ce	Nd	Sm	Eu	Gd
	ppm	ppm	ppm	ppm	ppm	ppm	ppm	ppm	ppm	ppm	ppm	ppm
BCS-VWL-0004	20	65	92	19	39		35	59	28			
CAP-MLJ-0001	36	37	39	39	96		40	81	34.4	6.7	0.34	5.34
ESS-VWL-0001	0	25	10	8.2	92	57						
GHN-ACT-0001	7	24	48	24	11		40	76	31			
GHN-ACT-0002	8	17	65	24	10		35	79	38			
GHN-ACT-0003	6	19	68	25	7		45	82	37			
GHN-ACT-0004	10	22	75	23	14		60	110	39			
GHN-ACT-0005	29	53	177	22	41		53	96	41			
GHN-ACT-0006	11	39	111	24	13		37	84	40			
GHN-ACT-0007	44	120	750	21	61		56	105	50			
GHN-ACT-0008	9	215	214	26	5		39	107	51			
GHN-ACT-0009	58	126	1174	19	76		50	94	43			
GHN-ACT-0010	44	91	655	22	62		53	101	48			
GHN-ACT-0011	49	89	542	20	56		60	108	51			
GHN-ACT-0012	48	56	370	20	62		49	88	41			
GHN-ACT-0013	48	54	295	20	70		43	83	36			
GHN-ACT-0014	51	46	354	18	68		47	87	39			
GHN-ACT-0015	44	47	352	20	60		5	101	47			
GHN-ACT-0016	29	38	267	20	37		56	111	53			
GHN-ACT-0017	27	41	222	20	37		50	98	49			
GHN-ACT-0018	7	17	48	24	9		33	63	28			
GHN-ACT-0019	18	35	73	22	40		51	98	41			
GHN-ACT-0020	11	15	65	25	19		73	140	61			
GHN-ACT-0021	7	17	36	24	12		66	130	56			
GHN-ACT-0022	16	28	100	24	24		54	114	49			
GHN-ACT-0023	26	39	164	23	43		43	85	36			
GHN-ACT-0024	27	42	241	23	42		40	76	35			
GHN-ACT-0025	35	35	284	19	44		43	77	35			
GHN-ACT-0026	31	38	343	21	39		44	86	41			
GHN-ACT-0027	31	34	329	19	42		37	78	35			
GHN-ACT-0028	42	43	327	19	48		52	107	52			
GHN-ACT-0029	45	43	306	19	60		52	107	52			
GHN-ACT-0030	40	43	317	19	54		43	90	45			
GHN-ACT-0031	22	37	206	23	25		57	112	51			
GHN-ACT-0032	17	25	141	24	15		57	121	55			
GHN-ACT-0033	16	21	71	23	36		107	262	141			
GHN-ACT-0034	39	30	55	20	78		61	134	73			
GHN-ACT-0035	19	14	58	19	42		46	85	46			
GHN-ACT-0036	33	15	130	19	59		38	74	31			
GHN-EHP-0001	26.6	26.7	162	20.1	37		41.3	73.2	29			
GHN-EHP-0002	10	18	49	22	13		50	103	45.5	8.8	0.52	0.55
GHN-EHP-0003	7	25	57	24	27		61	124	43			
GHN-EHP-0004	19	231	210	19	58		52	97	43			
GHN-EHP-0007	42	58	321	20	50		37	77	34			
GHN-HRS-0001	47.6	43.6	361	18	67.5		44	84.1	37			
GHN-HRS-0002	5.8	16.7	86.5	24.3	8.4		46.9	105	36.8			
GHN-HRS-0088	7.2	12.9	67.2	25.9	8.5		31.4	65.9	24.4			
GHN-HRS-0089	5.8	8.9	50	24.6	6.5		25.4	51.1	21.3			
GHN-HRS-0090	8.6	26.6	67.1	23.7	28.3		66	126	52.1	9.8		7.01
GHN-HRS-0091	10.5	37.8	69.1	23.5	41		64.5	138	72.7			
GHN-HRS-0092	16.2	61.3	129.4	20.2	56		58.6	128	58.4			
GHN-HRS-0094	6.1	22.2	51.3	25.4	11.9		47.9	94.2	41.3			
GHN-HRS-0095	25	42	92	19	73		39	72	34			
GHN-HRS-0096	13	16	36	19	75		34	79	30			
GHN-JRM-0001	30	172	92	21	57		49	96	40.3	7.3	1.15	5.3
GHN-JRM-0002	49.3	87.6	294.8	21.3	86.9		45	102	46	8.2	1.54	5.88
GHN-JRM-0006	49.3	117.6	577.5	20.9	65.9		61	126	70.4	12.9	2.24	10.09
GHN-JRM-0008	45.6	128.4	365.6	18.5	65.9		61.8	103	48.3			
GHN-JRM-0009	27.5	99.3	252.1	16.6	48.2		42	93	47	9.1	0.94	6.46
GHN-JRM-0022	53.3	82.7	719.7	18.6	58.5		53.7	103	46.7			
GHN-JRM-0027	50	75	1095	18	56		40	82	35			
GHN-JRM-0037	4.5	14.3	54.7	24.1	5.6		38.8	81.8	33.1			
GHN-JRM-0038	16.5	93.3	123.4	23.9	43.3		55.3	115	51.7			
GHN-JRM-0039	12	23	40	21	53		56	121	62			
GHN-JRM-0040	24	55	54	24	45		69	148	81			
GHN-JRM-0047	23.1	60.6	143.2	21.1	54.3		65.4	128	55.9			
GHN-KMD-0013	21	133	486	37.3	92	50						
GHN-KMD-0014	39	19	438	34.4	111	46						
GHN-KMD-0015	25	95	387	31.7	116	39						
GHN-KMD-0016	49	59	451	35.1	88	39						
GHN-KMD-0017	4	92	109	21.2	86	32	52	98	14			
GHN-KMD-0018	0	105	502	39	76	58						
GHN-KMD-0019	59	54	320	20	81		42	83	36.9	6.5	1.72	5.13
GHN-KMD-0026	19	40	180	23	27		52	110	51			
GHN-KMD-0027	25	78	160	23	36		64	118	49			
GHN-KMD-0028	29	66	306	19	54		53	120	56			

Sample	Ni	Cu	Zn	Ga	Cr	Co	La	Ce	Nd	Sm	Eu	Gd
	ppm	ppm	ppm	ppm	ppm	ppm	ppm	ppm	ppm	ppm	ppm	ppm
GHN-KMD-0048	55.8	64.7	668.2	19.1	64		66.5	114	56.5			
GHN-KMD-0050	55.1	53.7	474.1	20.3	67.6		55.3	105	46.1			
GHN-KMD-0051	14	54	403	33.8	78	47						
GHN-KMD-0052	38	87	357	19	55		42	76	32			
GHN-KMD-0053	0	86	416	37.1	34	46						
GHN-KMD-0054	48	61	374	20	71		44	100	54			
GHN-KMD-0055	18	146.1	137.2	19	23.7		57.7	112	49.7			
GHN-KMD-0056	5	50	253	27.8	79	45						
GHN-KMD-0057	52	63	319	21	73		43	87	39			
GHN-KMD-0062	32.5	122.9	385.7	21.1	41.1		58.8	121	66			
GHN-KMD-0063	31.6	41.8	212.7	20.7	61.2		52.4	99	44.3			
GHN-KMD-0064	21.1	65.8	233.5	20.8	34.5		52.7	111	50.9			
GHN-KMD-0065	46	190	552	40.7	79	37						
GHN-KMD-0071	0	35	256	26.8	64	40						
GHN-KMD-0072	49.6	69.3	486.9	20.7	60.6		53.7	109	48.8			
GHN-KMD-0073	44	61	426	33.5	100	40	47	93	42.2	7.3	1.9	6.06
GHN-KMD-0074	22	135	378	32.2	92	50						
GHN-KMD-0077	22	37	201	23	35		70	134	64			
GHN-KMD-0078	22	31	161	21	36		51	99	41			
GHN-KMD-0079	2	67	256	28.2	61	45						
GHN-KMD-0080	47	60.3	520.8	21.4	57.6		62.1	121	59.5			
GHN-KMD-0081	25	43	238	25	48	30	64	143	69.9	13.9	1.37	11.67
GHN-KMD-0082	82	96	1117.5	20	74		63	114	50.7			
GHN-KMD-0088	31	40	221	20	47		41	102	53.8	10.2	1.07	8.09
GHN-KMD-0092	41	82	490	19	45		58	138	66			
GHN-KMD-0095	7	38	41	24	8		51	101	44.3	8.6	0.41	7.15
GHN-KMD-0096	11	30	53	24	16		56	113	13.1	9.6	0.41	7.26
GHN-KMD-0097	20	43	320	21	27		51	90	37			
GHN-KMD-0100	31	66	320	23	41		45	88	38			
GHN-LFG-0001	2.7	8.8	16.7	20	8.2		51.6	89.6	34.4			
GHN-LFG-0002	27.7	8.2	12.2	19.9	6		50	90	34			
GHN-LFG-0003	6	28	42	26	10		51	95	37			
GHN-LFG-0004	2.9	18.3	24.7	20.5	8.2		45.9	85.3	32.8			
GHN-LFG-0005	3.1	9.5	26.9	18.4	5.7		49	79.5	27.5			
GHN-LFG-0006	4.2	18.4	43	17.7	8.1		49.4	93.8	37.3			
GHN-LFG-0018	14	49.7	171.2	22.1	29.4		70.2	136	54.9			
GHN-LFG-0020	18.3	51.8	288.2	23.9	20.2		56.9	94.6	55.5			
GHN-LFG-0037	30	41	231	19	49		47	86	40			
GHN-LFG-0041	7.1	25.6	100.3	26.3	9		35.5	122	31.9			
GHN-LFG-0060	35	52	78	17	82		29	55	25			
GHN-LFG-0085												
GHN-LFG-0086	32	70.7	344.6	19.5	64		50.4	89.7	46			
GHN-LFG-0087	82	29	1320	73.6	108	39						
GHN-LFG-0088												
GHN-LFG-0089	4	31	65	21	19		71	138	57			
GHN-LFG-0090	39	101	789	49.6	96	47						
GHN-LFG-0091	29	23	45	19	74		46	85	31			
GHN-RDL-0002	7	9	55	88	24		24	46	19.2	3.9	0.65	2.68
GHN-RDL-0003	6.7	3	23.8	22.9	41		49.5	87.7	34.7			
GHN-RDL-0004	6.7	6	34.5	20	12.4		48.6	92	39.2			
GHN-SAW-0003	3.2	12.2	26.2	26.5	4.3		59.1	124	55.9			
GHN-SAW-0004	15.2	28.9	49.4	23.5	60.7		49.1	72	23.9			
GHN-SAW-0005	5.4	35.1	68.4	24.8	8.2		49	90.1	37.8			
GHN-SAW-0200	25.1	36	159.7	19.5	44.5		40.4	77.5	35			
GHN-SAW-0201	11.4	33.4	96.3	22.3	29.4		43	85.1	36.2			
GHN-STM-0001	0	27	104	20.2	86	76						
GHN-STM-0002	0	32	47	20.7	23	102						
GHN-STM-0003	0	27	36	20.6	30	105						
GHN-STM-0004	0	18	92	20.3	40	99						
GHN-STM-0005	0	12	75	21.8	43	62						
GHN-VTM-0003	12	20	19	25	143		50	89	39			
GHN-VTM-0109	18	36	202	23	29		53	113	50			
GHN-VTM-0194	25	56	108	20	52		51	95	40.2	6.6	1.26	5.18
GHN-VTM-0195	42	102	392	20	62		39	97	9.8	6.5	1.24	5.24
GHN-VTM-0197	50	102	515	20	61		46	104	59.1	11	1.99	9.27
GHN-VTM-0198	28	102	303	22	39		56	115	57.1	11.3	1.15	9.37
GHN-VTM-0199	29	91	350	21	42		53	114	53.6	10.6	1.29	8.82
GHN-VTM-0200	14	40	113	25	21		102	269	137.3	27.3	1.09	15.32
GHN-VTM-0201	23	95	245	22	44		87	163	76			
GHN-VTM-0202	32	76	288	21	47		51	110	50	9.7	1.16	7.67
GHN-VTM-0203	31	76	294	21	47		46	101	45			
GHN-VTM-0204	51	139	497	21	71		57	125	58	10.5	1.96	8.57
GHN-VTM-0205	38	173	392	20	62		50	112	54.1	10.7	1.59	8.75
GHN-VTM-0206	58	180	571	20	64		56	144	67.1	13	2.13	10.64
GHN-VTM-0207	40	116	449	22	48		54	130	59.3	11.5	1.64	9.41
GHN-VTM-0208							63	122	59	11	2.01	10

Sample	Ni	Cu	Zn	Ga	Cr	Co	La	Ce	Nd	Sm	Eu	Gd
	ppm	ppm	ppm	ppm	ppm	ppm	ppm	ppm	ppm	ppm	ppm	ppm
GHN-VTM-0209	59	127	724	21	62		73	140	66.4	13	2.29	13.29
GHN-VTM-0210	60	99	798	19	60		78	135	64			
GHN-VTM-0211	54	68	462	19	69		49	91	43.8	7.6	1.8	6.54
GHN-VTM-0212	63	112	700	20	71		47	93	41.2	41.2	1.79	6.56
GHN-VTM-0213	58	78	588	20	65		55	114	52.7	9.6	2.14	8.66
GHN-VTM-0214	61	71	468	21	73		51	107	51.5	9.2	2.97	7.93
GHN-VTM-0215	57	121	560	20	65		53	113	51.2	9.3	1.96	8.15
GHN-VTM-0216	67	183	1033	20	63		67	134	63.8	12.7	2.25	12.15
GHN-VTM-0217	25.5	34	184	22	34		46	103	46	9	1.01	7.56
GHN-VTM-0417	14	34	60	24	29		62	118	53			
GHN-VTM-0418	16	50	78	19	32		54	102	44			
GHN-VTM-0419	29	165	150	22	54		47	86	36			
GHN-VTM-0420	54	129	483	23	83		67	119	53			
GHN-VTM-0421	50	103	356	20	72		48	95	44			
GHN-VTM-0422	34	98	418	22	46		68	139	63			
GHN-VTM-0423	37	72	349	22	46		50	97	43			
GHN-VTM-0424	18	75	252	23	23		77	151	571			
GHN-VTM-0425	50	115	842	19	54		50	108	54			
GHN-VTM-0426	66	130	891	19	64		73	142	75			
GHN-VTM-0450	35	102	381	32.2	89	42						
GHN-VTM-0451	16	159	1066	62.2	87	84						
GHN-VTM-0452	0	80	500	37.6	80	75						
GHN-VTM-0453	72	156	1067	18	63		80	168	79			
GHN-VTM-0454	0	121	551	40.5	66	105						
GHN-VTM-0455	2	45	444	35.9	76	55						
GHN-VTM-0500	53	46	304	18	43		41	67	43			
GHN-VTM-0501	19	27	109	21	43		38	58	27			
GHN-VTM-0502	17	27	129	18	35		32	59	23			
GHN-VTM-0503	75	65	537	19	40		29	73	36			
GHN-VTM-0504	34	38	122	19	42		34	64	31			
GHN-VTM-0506	17	19	132	19	37		32	62	26			
GHN-VTM-0507	23	45	48	19	41		42	55	25			
GHN-VTM-0508	2	53	103	19	55		26	46.5	23			
GHN-VTM-0509	36	69	187	20	48		39	82	45			
GHN-VTM-0510	38	19	156	24	53		40	69	35			
GHN-VTM-0598	10	23	70	29	12		68	123	53			
GHN-VTM-0599	42	47	146	19	50.3		34.3	68	31.8			
GHN-VTM-0602	45.2	49.5	413	20.9	45.2		36.8	71.8	41.6			
GHN-VTM-0603	32	79	224	20	49		38	74	45			
GHN-VTM-0604	34	36	100	19	40		31	58	26			
GHN-VTM-0605	34	76	136	20	58		42	76	31			
GHN-VTM-0606	15	36	94	22	25		44	87	35			
GHN-VTM-0607	21	30	129	21	40		60	116	56			
GHN-VTM-0610	14	30	249	22	26		32	60	28			
GHN-VTM-0611	11	9	196	19	8		42	59	18			
GHN-VTM-0612	24	12	634	16	8		47	108	38			
GHN-VTM-0613	39	83	676	18	35	83	36	64	33			
GHN-VTM-0614	12	9	71	18	36		28	52	25			
GHN-VTM-0624	35	34	266	18	42		35	68	34			
GHR-VWL-0004	31	190	147	21.4	97	16						
GHR-VWL-0007	7	105	217	25.5	66	32						
GMG-PIT-0001	22	40	6	17.5	61	16						
GMG-PIT-0006	8	49	5	14	1		53	82	23			
GMG-PIT-0007	7	84	15	16	3		48	77	24			
GMG-PIT-0009	10	328	30	20	5		48	83	29			
GMG-PIT-0010	36	147	117	20.6	83	20						
GMG-PIT-0011	19	153	34	17.9	132	54						
GMG-PIT-0014	0	7	14	17.3	10	46						
GMG-PIT-0015	0	143	43	17.2	4	27						
HAS-GJG-0001	4	71	82	22	15		41	80	28			
HAS-GJG-0002	2	8	22	24	8		52	97	34			
HAS-GJG-0004	10	13	42	21	21		41	65	18			
HAS-GJG-0005	92	65	173	18	213		99	153	82			
HAS-GJG-0006	92	65	173	18	213		30	64	32			
HAS-GJG-0007	82	53	173	14	191		14	37	17			
HAS-GJG-0008	59	45	166	16	199		39	70	29			
HAS-GJG-0009	5	7	19	13	109		17	31	11			
HAS-GJG-0010	9	9	47	19	93		36	64	25			
MID-AAF-0002	14	84	54	20	43		30	65	27			
MID-AAF-0003	4	172	53	21	19		42	66	27			
MID-GJG-4001	24.8	103.2	50.6	20	57.7		42.6	80.1	33.2			
MID-GMG-0014	69	164	66	17	135		41	82	37			
MID-GMG-0015	19	70	73	18	31		39	75	22			
MID-GMG-0016	48	191	91	18	89		44	86	34			
MID-GMG-0017	76	42	99	19	155		45	89	40			
MID-GMG-0018	48	135	30	75			42	81	31			

Sample	Ni	Cu	Zn	Ga	Cr	Co	La	Ce	Nd	Sm	Eu	Gd
	ppm	ppm	ppm	ppm	ppm	ppm	ppm	ppm	ppm	ppm	ppm	ppm
MID-GMG-0019	29	137	33	16	34		43	79	28			
MID-GMG-0020	49	94	52	20	105		41	80	35			
MID-GMG-0021	29	126	69	20	75		47	88	38			
MID-GMG-0022	25	20	33	18	42		41	77	33			
MID-GMG-0023	17	36	42	18	41		35	70	28			
MID-GMG-0024	52	240	225	18	52		29	65	27			
MID-GMG-0025	20	53	133	15	10		13	28	15			
MID-GMG-0026	6	11	43	14	1		23	44	20			
MID-KXB-0001	16	82	45	19	35		28	61	25			
MID-KXB-0003	0	23	22	20	9		39	87	37			
MID-VTM-4001	28.1	173.2	78.5	18.2	56.3		41.3	76.5	32.2			
MIN-AAF-0001	0	18	20	22	24		54	102	40			
MIN-AAF-0004	0	23	21	23	25		49	92	39			
MIN-AAF-0010	2	20	19	23	62		50	94	39			
MIN-AAF-0013	0.3	13.8	15.9	21.9	21.4		42.4	82.6	36			
MIN-AAF-0015	2	17	14	19	32		48	97	38			
MIN-GFA-0001	5	24	25	20	42		47	95	41			
MIN-GFA-0003	14	37	68	17	43		29	57	25			
MIN-GFA-0005	1	17	21	22	27		50	98	41.5			
MIN-GFA-0006	12	45	50		53		34	63	24			
MIN-GFA-0007	1	19	21	21	29		46	98	41			
MIN-GFA-0009	1	26	23	19	30		46	91	37			
MIN-SAN-0002	2.6	24.9	19.2	21.6	31.1		53.4	107.2	42.6			
MIN-VTM-0002												
MIN-VTM-0003	10	512	71	20	6		55	94	30			
MIN-VTM-0004	17	94	46		64		41	80	33			
MIN-VTM-0005	11	83	53	16	37		32	61	26			
MIN-VTM-0006	9	57	25	17	45		39	71	28			
MIN-VTM-0007	13	74	33	18	56		43	80	32			
MIN-VTM-0008	15	72	46	20	56		40	66	27			
MIN-VTM-0009	15	82	45	18	56		49	82	28			
MIN-VTM-0018	87	111	132	20	134		44	84	42			
MIN-VTM-0019	80	35	127	20	151		43	85	40			
MIN-VTM-0020	57	44	159	18	67		43	84	37			
MIN-VTM-0021	62.3	29.2	256.8	20.4	78.1		26	56.5	28.4			
PIT-KMD-0007	12	295	67	16.6	89	31						
PIT-KMD-0008	100	175	119	20.6	401	34						
PIT-KMD-0009	0	23	67	17.8	76	60						
PIT-KXB-0101	34	48	74	21	79		30	61	26			
PIT-LFG-0001	36	93	49	17.4	102	24						
PIT-LFG-0003	17	71	57	17.3	67	17	31	59	24.7	4.1	1.06	3.31
PIT-LFG-0005	20.8	58.7	98	18.2	42.4		19.1	33.5	14.2			
PIT-LFG-0007	3.7	42.6	23.5	23.5	4.9		55.8	111	51.6			
PIT-LFG-0009	7	15	59.6	24.9	6.6		63.8	131	58			
PIT-LFG-0013	19	31.7	70.3	18.9	53.5		39.1	71.6	27.4			
PIT-RDL-0001	5.5	17	32.5	24	9.5		39	67	26.4	5	0.22	3.99
PIT-RDL-0002	7	7	19	25	6		40	85	38			
PIT-RDL-0003	7	10	18	26	7		48	85	36			
PIT-RDL-0004	10	34	584	24	8	34	70	141	70			
PIT-RDL-0005	8	15.2	30.2	26.7	6.7		33.8	66.6	26.3			
PIT-RDL-0006	6.8	8.9	15.6	27.3	7.8		57.6	117	52.2			
PIT-RDL-0007	9.6	68.4	301.4	25.5	6.9		59.3	127	55.6			
PIT-VCV-0001	10	20	41	21	44		38	78	34			
PIT-VCV-0002	10	12	34	24	21		64	124	54			
PIT-VCV-0003	10	6	62	20	44		48	94	40			
PIT-VCV-0004	1	6	16	25	4		65	135	56			
PIT-VCV-0005	1	8	18	24	4		68	138	58			
PIT-VCV-0006												
PIT-VCV-0007	18	9	43	16	28		42	76	27			
PIT-VCV-0008	17	39	101	17	16		35	69	23			
PIT-VCV-0009	9	5	78	17	41		41	77	29			
PIT-VCV-0010	14	112	13	16	18		49	88	33			
PIT-VCV-0011	14	462	46	18	23		47	78	28			
PIT-VCV-0012	7	41	57	16	6		41	66	20			
PIT-VCV-0013	5	66	40	17	3		39	60	18			
PIT-VCV-0014	5	3	35	17	5		41	66	19			
PIT-VCV-0015	3	59	9	14	2		39	53	10			
PIT-VCV-0016	9	71	21	20	8							
PIT-VCV-0017	8	167	17	16	6		71	117	37			
PIT-VCV-0018	8	55	16	14	4		65	100	27			
PIT-VCV-0019	10	18	2	18	50		38	83	37			
PIT-VCV-0020	19	18	4	19	74		38	82	35			
PIT-VCV-0021	82	58	19	16	161		48	87	39			
PIT-VCV-0022	106	40	15	15	171		40	85	39			
PIT-VCV-0023	26	27	7	15	170		38		36			
PIT-VCV-0024	24	70	247	19	53		45	68	23			

Sample	Ni	Cu	Zn	Ga	Cr	Co	La	Ce	Nd	Sm	Eu	Gd
	ppm	ppm	ppm	ppm	ppm	ppm	ppm	ppm	ppm	ppm	ppm	ppm
PIT-VCV-0025	21	201	237	17	19		36	61	24			
PIT-VCV-0026	17	34	47	18	23		39	74	27			
PIT-VCV-0027	27	20	19	20	39		39	75	31			
PIT-VCV-0028	0	68	11	14	2		38	48	8			
PIT-VCV-0029	25	39	14	19	39		43	76	31			
PIT-VCV-0030	24	118	18	16	37		39	74	30			
PIT-VTM-0001	52	32	174	17	128		46	96	49			
PIT-VTM-0002	38	131	85	16	73		39	67	27			
PIT-VTM-0004	36.8	69.5	52.8	19.8	71.5		36.3	62.7	25.9			
PIT-VTM-0005	20.1	17.5	116.7	15.9	8.8		41.3	63.3	24			
PIT-VTM-0006	6	7	24	26	4		78	157	68			
PIT-VTM-0007	11	339	2374	24	7		75	154	67			
PIT-VTM-0008	7	8	22	26	8		69	137	59			
PIT-VTM-0009	2.3	3.3	4.4	21.3	15.3		41.7	85.9	34.1			
PIT-VTM-0010	31	118	57	19	98	38	35	67	29.5	4.9	1.38	3.89
PIT-VTM-0600	42	164	49	19	72		34	63	27			
PIT-VWL-0001	0	12	10	18.8	11	72						
PIT-VWL-0007	0	3	27	22.5	27	81						
PIT-VWL-0009	0	364	48	13.3	91	52						
QPS-AAF-0003	20	44	82	21	63		36	67	28			
QPS-AAF-0005	17	43	73	20	61		33	65	27			
QPS-AAF-0008	10	45	30	19	66		33	66	27			
QPS-AAF-0009	11	29	29	19	68		37	67	29			
QPS-AAF-0022	14	49	58	21	73		40	73	31			
QPS-SAN-0002	7.8	33.7	33.7	22.8	48.3		41.1	79.4	31.4			
QPS-VTM-0001	17.1	45.1	66.5	19.8			34.6	65.4	26.5			
QPS-VTM-4001	21.4	43.2	79	20.1	72.2		33.3	59.9	27.6			
ROC-KMD-0001	75.5	58	173	20	126		41	82	37.5	6.4	1.63	5
ROC-NWD-0001	6	1	58	27	2		5	13	6			
ROC-NWD-0002	71	449	39	24	82		32	68	34			
ROC-NWD-0003	6	4	105	22	2		33	79	44			
ROC-VTM-0032	4	24	81	18.6	52	45						
ROC-VTM-0033	70	40	80	18.4	174	43	51	95	11.7	7.8	2.01	6.75
SCS-LFG-0001	8	68	121	20	23		36.5	64	26			
SCS-LFG-0002	0	141	357	31	27	25						
SCS-LFG-0003	0	53	81	17.3	38	171						
SCS-LFG-0004	0	47	77	19.6	66	88						
SCS-LFG-0005	15	14	44	21	46		45	74	32			
SCS-LFG-0006	17	12	62	19	45		33	61	24			
SCS-LFG-0007	28	19	56	20	43		28.5	57	24			
SCS-LFG-0008	11	13	17	23	46		23	41	17			
SGS-ESO-0101	35	178	47	18	77							
SGS-VTM-0024	14.2	167.4	181.5	19.8	63.4		32.4	67.2	23.6			
SGS-VTM-0026	13.8	145.4	74.3	20.8	76.4		33.6	61.9	23.6			
SGS-VTM-0605	27	91	31	17	74		43	78	31			
SPR-AAF-0001	63.8	91.2	61.1	17.9	115		38.1	71.8	33.2			
SPR-AAF-0003	63	114.5	60.8	19.4	119.8		41.2	84.7	37.1			
SPR-JWM-0002	80	165	44	21	101		41	79	33			
SPR-KMD-0001	6	178	32	15.6	75	34	42	81	34.8	5.8	1.49	4.88
SPR-KMD-0002	43	201	34	16.2	131	30	39	81	9.6	7.3	1.83	6.27
SPR-KMD-0003	0	131	121	18.6	61	59	47	81	8.1	4.5	0.94	3.73
SPR-OTH-0001	41	179	52	18	74		47	80	31			
SPR-OTH-0002	41	182	72	18	182		51	86	32			
SPR-SAN-0002	62.8	138.7	47.9	18.7	105.6		46.6	89.3	37.5			
SPR-VTM-0001	24.5	158	42	17.65	73.5	32.5						
SPR-VTM-0002	10	44	63	17.3	77	49						
SPR-VTM-0005	36	198	37	20	59		46	84	36			
SPR-VTM-0010	70	100	58	19	112		39	77	38			
SPR-VTM-0012	0	88	20	25	6		63	131	52			
SPR-VTM-0014	0	66.8	16.3	25.8	6.3		64.3	120.1	50.7			
SPR-VTM-0017	1	35	18	25	23		58	114	49			
SPR-VTM-0019	0	71.5	16.2	24.9	6.5		60.7	129.8	56.1			
SPR-VTM-0021	0	66.5	17	25.6	5.5		57.5	125.6	55.2			
SSS-AAF-0001	26.2	78.8	72	19.7	77.4		19.9	35.9	15.1			
SSS-EHP-0002	28	68	102	18	59		40	78	29			
SSS-EHP-0003	17	141	113	17	27			34	64	20		
SSS-EHP-0004	35	94	58	18	76		39	73	33			
SSS-EHP-0023												
SSS-EHP-0032	14	31	140	19	31		34	76	33			
SSS-EHP-0033	20	29	145	20	48		35	64	32			
SSS-EHP-0034	23	27	181	21	43		32	64	29			
SSS-GMG-0009	25	73	24	19	44		31	61	26			
SSS-GMG-0010	134	134	53	20	76		38	78	35			
SSS-GMG-0011	85	181	166	20	170		47	98	47			
SSS-GMG-0012	54	46	182	21	82		41	84	38			
SSS-GMG-0013	51	119	116	19	73		40	73	33			

Sample	Ni	Cu	Zn	Ga	Cr	Co	La	Ce	Nd	Sm	Eu	Gd
	ppm	ppm	ppm	ppm	ppm	ppm	ppm	ppm	ppm	ppm	ppm	ppm
SSS-GMG-0014	29	104	138	20	38		83	178	77			
SSS-GMG-0015	25	40	171	22	48		39	73	35			
SSS-GMG-0016	27	34	166	221	42		48	87	33			
SSS-KMD-0001	20	96	71	18.9	83	21	33	65	28.4	4.8	1.13	4.04
SSS-KMD-0002	21	119	291	26.9	127	39	41	79	34.9	6.5	1.45	5.2
SSS-VEV-0001	11.3	130.3	62.1	15.2	173.5		37.6	72.9	31.8			
SSS-VTM-0005	7	624	19	14	7		23	41	19			
SSS-VTM-0600	29	53	154	22	50		47	98	43			
SSW-AAF-0001	32	200	161	20	53		43	87	41			
SSW-AAF-0002	24	139	77	20	62		31	59	27			
SSW-AAF-0005	22.8	108.6	46.8	18.2	57.1		34.8	67.5	24.9			
SSW-AAF-0007	27.6	136.3	45.1	18.8	61.8		33.5	68	30.1			
SSW-AAF-1002	39	16	200	19	57		40	75	33			
SSW-AAF-1005	27	109	60	19	62		26	52	23			
SSW-AAF-1009	26	144	99	19	47		39	73	31			
SSW-GJG-4000	33.2	166.3	111.4	18.1	64.5		39.1	77.4	35			
SSW-KMD-0001	40	204	161	22.8		28	34	68	29.9	5	1.3	4.17
SSW-SAN-0002	31.3	110.4	50.8	18.7	66.7		31.4	58.1	24.5			
SSW-SAN-0006	10.3	44.5	61	20.5	47.2		32	66.2	27			
SSW-VTM-0006	26	304.7	109.3	19	52.6		44.2	79.2	35.1			
SSW-VTM-0008	24.3	141.2	99.1	18.2	57.8		40.6	70.8	28.7			
SSW-VTM-0010	4.1	169.6	31.9	18.2	7.9		39.2	69.1	22.6			
SSW-VTM-0012	5.8	118.9	27.3	18	22.6		35.7	60.4	20.1			
SSW-VTM-0013	15.9	114.9	77.3	18.3	48.9		35.6	66.5	26.1			
SSW-VTM-0015	22.1	134.3	85.6	17.2	54		33.5	63.9	26.3			
SSW-VTM-0016	48	141	70	20	94		42	74	32			
SSW-VTM-0019	46	190	62	20	89		37	73	34			
SSW-VTM-0023	38	129	53	19	77		37	69	28			
SSW-VTM-0027	29	85	74	19	72		29	56	23			
SSW-VTM-0028	31	93	68	18	75		27	54	23			
SSW-VTM-0030	36	130	44	19	72		34	66	29			
SSW-VTM-0032	28	112	42	20	67		29	56	23			
SSW-VTM-4001	33.3	178.5	91.7	18.9	63.7		42.9	8.2	34.6			
SWH-GJG-0001	4	17	31	18	38		24	57	16			
SWH-GJG-0002	4	12	18	18	40		50	93	42			
SWH-GJG-0003	30	11	89	21	34		38	82	37			
SWH-GJG-0004	43	116	137	17	135		23	39	18			
SWH-GJG-0005												
SWH-GJG-0006	6	40	42	18	40		28	55	21			
SWH-GJG-0007	18	32	62	19	48		41	75	30			
SWH-GJG-0008	11	9	38	15	14		18	32	12			
SWH-GJG-0009	10	9	29	15	30		20	40	16			
SWH-GJG-0010	18	11	52	18	29		17	32	14			
SWH-GJG-0011	11	7	46	17	12		13	24	7			
SWH-GJG-0012	7	24	22	18	24		34	61	28			
SWH-GJG-0013	26	19	10	17	44		24	46	19			
SWH-GJG-0014	5	27	15	24	93		44	87	36			
SWH-GJG-0015	10	19	51	16	65		35	64	25			
SWH-GJG-0019	10	27	26	16	65		30	57	22			
SWH-GJG-0020	66	128	101	20	98		18	42	22			
SWH-GJG-0021	37	20	82	20	84		18	36	19			
SWH-GJG-0022	13	11	28	22	101		48	101	45			
SWH-GJG-0023	10	17	32	15	84		32	63	24			
SWH-GJG-4000	4	15.4	15.9	19.6	60		41.1	76.8	29.3			
SWH-VTM-4001	4.7	11.7	41.3	17.1	37.2		22.8	49.8	18.7			
average	25.19883178	73.34042056	174.6196262	21.76443662	53.45341176	50.73728814	44.83910761	87.35380577	39.24057592	9.917391304	1.441363636	7.088444444
RSQ w/ F as x values	0.01108495	0.024885252	0.001319302	0.001793088	0.047452518	0.033458452	6.831E-06	0.002488675	0.002329248	0.02623673	0.00068912	0.053956988
Pearson coeff of F	0.10528509	0.157750599	-0.036322204	-0.042344875	0.217835988	-0.182916515	-0.002613618	-0.049886624	-0.048262281	-0.161977562	-0.026251086	-0.232286436
count	428	428	428	426	425	59	381	381	382	46	44	45

Sample	Tb	Er	Yb	Lu	Q	K	P	epidote	calcite	pyrite	FeMnOxide	goethite
	ppm	ppm	ppm	ppm	ppm	ppm	ppm	%	%	%	%	%
BCS-VWL-0004					26	21	24	0.01	1	0.7	3	
CAP-MLJ-0001			1.38	1.17	47	20	8	0.01	0.3	0.5		
ESS-VWL-0001					44	17	0.8	0.4	0.01	0.1	4	
GHN-ACT-0001					44	34	2	0.2		0.22	2	0.01
GHN-ACT-0002					47	25	8	0.01		0.83		
GHN-ACT-0003					49	23	3	1	0.1	0.4	2	
GHN-ACT-0004					46	23	4	3	0.01	0.9	3	
GHN-ACT-0005					37	26	12	3	0.1	1.07		0.04
GHN-ACT-0006					42	26	18	0.3		0.5	3	
GHN-ACT-0007					29	20	18	15	1	0.6	1	0.11
GHN-ACT-0008					39	20	29	0.01		2	2	
GHN-ACT-0009					32	17	21	3	0.1	0.5	3	0.06
GHN-ACT-0010					32	20	27	5	0.1	0.5	5	0.03
GHN-ACT-0011					28	19	28	8	0.1	0.1	3	0.1
GHN-ACT-0012					26	21	27	9	0.1	0.1	3	
GHN-ACT-0013					26	25	21	9	0.1	0.9	2	0.02
GHN-ACT-0014					26	19	28	10	0	0.9	2	0.1
GHN-ACT-0015					25	19	30	8	0	1	2	0.05
GHN-ACT-0016					32	26	20	4	0.3	0.9	2	
GHN-ACT-0017					31	29	19	7	0.3	0.9	1	
GHN-ACT-0018					45	32	8		0.6	0.9	1	
GHN-ACT-0019					40	24	5	2	1	2	2	
GHN-ACT-0020					51	11			0.2	2	0.1	
GHN-ACT-0021					49	23			0.1	0.7	2	
GHN-ACT-0022					45	22		0.3	0.1	0.7	2	
GHN-ACT-0023					40	17	8	0.9	0	1	4	0.01
GHN-ACT-0024					38	18	13	2	0	0.9	3	0.02
GHN-ACT-0025					28	18	25	5	0	1	3	0.05
GHN-ACT-0026					30	17	23	4	0	0.7	3	0.1
GHN-ACT-0027					30	17	24	4	0	1	3	0.03
GHN-ACT-0028					28	20	19	5	0	0.5	3	0.02
GHN-ACT-0029					26	21	20	7	0.1	0.7	3	
GHN-ACT-0030					26	22	22	8	0.1	0.7	2	0.1
GHN-ACT-0031					44	27	2	0.6	0	0	3	0.05
GHN-ACT-0032					48	20	5	0.6	0	0.3	3	0.06
GHN-ACT-0033					47	20	5	0.5	0	2	3	0.16
GHN-ACT-0034					35	11	0.7	0.01	0	5	6	0
GHN-ACT-0035					33	10	0.7	1	0	6	6	0
GHN-ACT-0036					34	7	9	0.01	0	5	6	0.05
GHN-EHP-0001					35	24	13	0.9		1	2	
GHN-EHP-0002			2.34	1.53	47	21	1		0.6	0.1	0.9	
GHN-EHP-0003					40	13	11	0.01	0.6	0	4	
GHN-EHP-0004					40	12	8	0.01	0.1		3	
GHN-EHP-0007					25	11	8	0.01	0.3	0	6	
GHN-HRS-0001					28	24	20	11	0.3	0.1	2	
GHN-HRS-0002					43	36	9		0.2	0.4	2	
GHN-HRS-0088					41	39	11	0.01	0	0.01	2	
GHN-HRS-0089					44	18	3	0.01	0	0.01	4	
GHN-HRS-0090			2.12	1.47	44	19	3	0.01	0	0.01	4	
GHN-HRS-0091					45	12		0.01	0	0	4	
GHN-HRS-0092					46	30	1	0.01	0	0.01	2	
GHN-HRS-0094					46	30	1	0.01	0	0.01	2	
GHN-HRS-0095					34	10	20	0.01	0	0.01	3	
GHN-HRS-0096					35	10	27	0.01	0	0.01		
GHN-JRM-0001			1.18	0.88	35	7	15	0.01	0.4	3	0.01	
GHN-JRM-0002			1.22	0.84	26	18	19	0.3	0.6	0.3	7	
GHN-JRM-0006			2.02	1.22	27	23	22	6	0	0.01		
GHN-JRM-0008					26	28	12	3	0	0.01	6	
GHN-JRM-0009			1.42	1.11	50	2	5	0.01	0.7	2	0.5	
GHN-JRM-0022					27	23	16	8	0.4		2	
GHN-JRM-0027					28	24	18	9	0	0.01	3	
GHN-JRM-0037					43	39	5	0.01	0.4	0.4	1	
GHN-JRM-0038					43	12	3	0.01	0.2	2	3	
GHN-JRM-0039					43	5	1	0.01		0.8	0.1	
GHN-JRM-0040					44	6	1	0.01		4	0.2	
GHN-JRM-0047					41	5	7	0.01	0.5	1	2	
GHN-KMD-0013					29	20	16	0.2	0.4	0.1	6	0.2
GHN-KMD-0014					19	37	19	9	1.4	0.2	1	
GHN-KMD-0015					30	20	15	0.1	1.4	0.1	5	0.1
GHN-KMD-0016					24	22	22	12	0.01	0.2	0.5	0.04
GHN-KMD-0017					32	3	21		0.1	3	0.6	
GHN-KMD-0018					39	25	4	0.4		0.4	1.7	0.1
GHN-KMD-0019			1.16	0.92	24	18	24	7	2	0.1	2	
GHN-KMD-0026					36	29	15	0.01	0.3	0.1	4	
GHN-KMD-0027					35	26	11	0.01	0.7	0.01	5	
GHN-KMD-0028												

Sample	Tb	Er	Yb	Lu	Q	K	P	epidote	calcite	pyrite	FeMnOxide	goethite
	ppm	ppm	ppm	ppm	ppm	ppm	ppm	%	%	%	%	%
GHN-KMD-0048					25	24	24	10	0.4	0.1	2	
GHN-KMD-0050					25	23	22	8	0.9	0.1	2	
GHN-KMD-0051					27	25	19	4	1.8	0.2	3	
GHN-KMD-0052					29	20	16	3	2.5	2	2	
GHN-KMD-0053					38	27	8	1	0.7	0.1	3	
GHN-KMD-0054					28	24	17	5	0.5	0.5	3	
GHN-KMD-0055					48	14		5	0.5	3	0.7	
GHN-KMD-0056					30	24	20	3	0.5	0.2	3	
GHN-KMD-0057					26	17	25	7	1	0.2	2	
GHN-KMD-0062					35	21	10		1	0.01	5	
GHN-KMD-0063					33	16	13	0.1	0.2	1	4	
GHN-KMD-0064					33	27	16	2	0.1	0.3	4	
GHN-KMD-0065					29	22	17	3	0.4	0.1	5	
GHN-KMD-0071					30	23	20	2	0.4	0.8	2	
GHN-KMD-0072					27	24	20	6	1	0.1	3	
GHN-KMD-0073			1.58	0.99	25	22	21	5	1	0.3	2	
GHN-KMD-0074					28	21	18	5	0.4	0.2	3	
GHN-KMD-0077					32	26	19	2	0.4	0.1	3.5	
GHN-KMD-0078					35	26	18		0.4	0.4	3	
GHN-KMD-0079					31	23	17	2	0.5	0.3	4	
GHN-KMD-0080					24	23	23	10	0.4	0.1	2	
GHN-KMD-0081			2.98	2.12	33	21	18	1	0.5	0.6	3	
GHN-KMD-0082					26	23	23	5	1	0.3	2	
GHN-KMD-0088			1.81	1.32	29	23	19	0.01	0.2	0.9	3	
GHN-KMD-0092					30	20	17		0.3	0.7	3	
GHN-KMD-0095			2.44	3.11	48	25			0	0.3	0.7	
GHN-KMD-0096			2.15	2.19	46	19	2	0.01	0.5	0.3	0.4	
GHN-KMD-0097					39	25	2	0.01	0.3	1	0.4	
GHN-KMD-0100					34	25	11		0.5	0.01	4	
GHN-LFG-0001					41	6			0.6	0.02	0.1	
GHN-LFG-0002					42	8			0.5		0.01	
GHN-LFG-0003					58	7			0.3		0.2	
GHN-LFG-0004					47	2	0.01	0.01	0.1		3	
GHN-LFG-0005					50	7	0.3		0.01	0.3	0.4	
GHN-LFG-0006					49	3			0.4	0.3	0.6	
GHN-LFG-0018					36	20	21	0.7	0		5	
GHN-LFG-0020					38	24	21	2	0		4	
GHN-LFG-0037					31	16	18	5	0.1	0.1	4	
GHN-LFG-0041					41	27	21	0.5	0.6	0.1	3	
GHN-LFG-0060												
GHN-LFG-0085					27	22	17	7	0.4	0.1	4	
GHN-LFG-0086					26	22	16	7	0.3	2	2	
GHN-LFG-0087					25	17	27	12	1		0.7	
GHN-LFG-0088					24	24	22	8	2	0.1	2	
GHN-LFG-0089					36	23	25	1	0.4	0	3	
GHN-LFG-0090					23	21	23	3	1.2	1	4	
GHN-LFG-0091					31	11	23	0.01	0.3	2	0.1	
GHN-RDL-0002			0.94	0.93	46	10		0.01	0.2	0.01	0.5	
GHN-RDL-0003					44	13		0.01		0.01	0.3	
GHN-RDL-0004					50	10	0.1	0.01	0.1	0.1	0.6	
GHN-SAW-0003					58	11		0.01	0.2	0.3	0.4	
GHN-SAW-0004					35	3	24	0.01	0.6	0.5	1	
GHN-SAW-0005					45	23	11	0.01	0.2	0.1	3	
GHN-SAW-0200					34	10	6	0.01	3	0.2	4	
GHN-SAW-0201					41	21	8	0.01	0.8	0.2	5	
GHN-STM-0001					43	16	14		0.01		3	
GHN-STM-0002					44	28			0.3	0.5	6	
GHN-STM-0003					45	26	11		0.01	0.01	2	
GHN-STM-0004					39	25	15	11	0.01	0.01	0.3	
GHN-STM-0005					44	27	15	0.01	0.01	0.01	2	
GHN-VTM-0003					40	13	8	0.01	0.3	0.01	3	
GHN-VTM-0109					38	25	17	2	0.01	0.01	3	
GHN-VTM-0194			1.05	0.92	31	22	14	2.6	0.6	2.3	2.7	
GHN-VTM-0195			1.42	1.08	31	20	14	0.5	0.2		4	0.1
GHN-VTM-0197			1.86	1.38	26	20	16	0.6	0.5	0.04	4	0.06
GHN-VTM-0198			2.29	1.75	33	29	12	2	0.4	0.1	4	0.09
GHN-VTM-0199			2.14	1.64	34	25	11	2	0.4	0.1	4	0.1
GHN-VTM-0200			2.61	1.92	28	34	27	0.01	0.2	0.1	0.7	
GHN-VTM-0201					33	21	12	1	0.3	0.5	3.5	0.1
GHN-VTM-0202			1.86	1.41	32	24	12	3.8	0.4	0.4	3.6	
GHN-VTM-0203					33	26	9		0.2	0.2	5	
GHN-VTM-0204			1.78	1.12	27	18	15		0.2		7	
GHN-VTM-0205			1.71	1.13	31	13	16	0.01	0.01	0.1	7	
GHN-VTM-0206			2.23	1.39	27	18	19		0.5	0.1	8	
GHN-VTM-0207			2.01	1.51	31	23	16		0.3		5	
GHN-VTM-0208			2.25	1.35	27	27	21	10	0.4		1	

Sample	Tb	Er	Yb	Lu	Q	K	P	epidote	calcite	pyrite	FeMnOxide	goethite
	ppm	ppm	ppm	ppm	ppm	ppm	ppm	%	%	%	%	%
GHN-VTM-0209			2.86	1.78	27	23	23	7	0.4		3	
GHN-VTM-0210					27	25	21	7	0.4	0.1	2	
GHN-VTM-0211			1.62	1.06	24	23	23	10	1		1	
GHN-VTM-0212			1.62	1.05	26	23	21	8	0.6	0.1	2	
GHN-VTM-0213			2.01	1.21	25	23	21	5	1	0.01	3	
GHN-VTM-0214			1.78	1.2	23	20	26	8	1		2	
GHN-VTM-0215			1.9	1.21	27	22	21	6	0.6		3	
GHN-VTM-0216			3	1.75	24	27	23	8	1		3	
GHN-VTM-0217			1.99	1.53	34	30	13	3	0.6	0.1	3	
GHN-VTM-0417					47	17	1	3	0.01	0.01	3	
GHN-VTM-0418					44	16	4	3	0.01	2	3	
GHN-VTM-0419					31	16	14	5	0.01	3	6	
GHN-VTM-0420					25	17	16	4	0.6	0.6	8	
GHN-VTM-0421					27	23	18	5	0.1	0.8	4	
GHN-VTM-0422					34	26	11	2	0.1		4	
GHN-VTM-0423					33	29	11	2	0.1		4	
GHN-VTM-0424					40	22	13	1	0.01	0.01	4	
GHN-VTM-0425					27	16	23	8	0.01	0.01	3	
GHN-VTM-0426					26	15	27	3	0.01	0.01	5	
GHN-VTM-0450					26	20	22	5	0.6	0.4	4	
GHN-VTM-0451					24	21	27	1	0.5	0.1	4	
GHN-VTM-0452					29	20	21	1	0.3	0.4	4	
GHN-VTM-0453					25	20	17	1	1	2	4	
GHN-VTM-0454					28	19	17	1	0.4	0.6	3	
GHN-VTM-0455					32	25	21	5	0.6	0.01	2	
GHN-VTM-0500					32	8	8	0.7	3	0.1	3	
GHN-VTM-0501					37	6	0.6	0.01	0.4		3	
GHN-VTM-0502					42	0	1	0.4	0.4	0.1	0.5	
GHN-VTM-0503					29	0.7	14	0.01	1		2	
GHN-VTM-0504					30	20	17				2	
GHN-VTM-0506					38	0.9	0.9	0.01		0.01	2	
GHN-VTM-0507					35	3	2	0.01	0.1	0.5	2	
GHN-VTM-0508					27	2	23	0.01	0.9	0.1	4	
GHN-VTM-0509					33	0.8	7	0.01	4	0.01	1	
GHN-VTM-0510					20	14	16	0.01	0.01	0.01	6	
GHN-VTM-0598					52	12	1	0.5	0.01	0.01	2	
GHN-VTM-0599					30	13	3	0.1	5	0.4	4	
GHN-VTM-0602					29	1	5	0.1	4	0.01	3	
GHN-VTM-0603					33	2	7	0	2	0.01	3	
GHN-VTM-0604					25	22	9	6	5	0.01	2	
GHN-VTM-0605					38	9	9	0.01	0.01	0.01	5	
GHN-VTM-0606					47	10	8	0.01	0.6	0.1	2	
GHN-VTM-0607					39	13	9	0.01	0.6	0.4	3	
GHN-VTM-0610					39	16	14	0.01	0.6	0.1	2	
GHN-VTM-0611					39	11	0.5	0.01	0.5	0.1	3	
GHN-VTM-0612					31	17	12	7	1	0.2	0.01	
GHN-VTM-0613					28	12	5	2	2	0.2	1	
GHN-VTM-0614					31	1	1	3	0.3		0.1	
GHN-VTM-0624					37		7	0.01	1	0.01	3	
GHR-VWL-0004					28	11	3	0.7			9	
GHR-VWL-0007					34	14	7	0.01	0.4	0.1	11	
GMG-PIT-0001					13	17	2	17			2	
GMG-PIT-0006					36	43	16	0.01		0.1	0.1	
GMG-PIT-0007					38	33	17	3		0.1	0.1	
GMG-PIT-0009					29	27	30	0.01		0.1	1	
GMG-PIT-0010					29	9	11	17		0.1		
GMG-PIT-0011					32	13	22	4		0.1	4	
GMG-PIT-0014					32	28	1	9		1	0.1	
GMG-PIT-0015					32	27	0.8	8	0.1	0.1	2	
HAS-GJG-0001					42	11	3	0.01	0.02	0.1	15	
HAS-GJG-0002					53	14	4	0.01	0.1	0.1	2	
HAS-GJG-0004					32	13	25	0.01	0.1	0.1	3	
HAS-GJG-0005					29	16	26	0.01	0.8	0.01	4	
HAS-GJG-0006					21	21	4			4	2	
HAS-GJG-0007					24	9	5			5	3	
HAS-GJG-0008					28	6	3			0.4		
HAS-GJG-0009					20	16		0.01	0.1	0.3	1	
HAS-GJG-0010					41	10		0.03		0.2	0.3	
MID-AAF-0002					35	10	9		0.2	0.6	4	
MID-AAF-0003					40	9	8	0.01	0.4	0.4	0.3	
MID-GJG-4001					32	12	12	3	0.5	2	1	
MID-GMG-0014					24	21	26	15	1	0.01	0.1	
MID-GMG-0015					36	27	20	5	0.8	0.01	0.7	
MID-GMG-0016					25	26	26	13	0.8	0.01	0.1	
MID-GMG-0017					27	16	26	13	0.8	0.01	1	
MID-GMG-0018					34	26	6	5	0.9	0.01	0.8	

Sample	Tb	Er	Yb	Lu	Q	K	P	epidote	calcite	pyrite	FeMnOxide	goethite
	ppm	ppm	ppm	ppm	ppm	ppm	ppm	%	%	%	%	%
MID-GMG-0019					34	26	6	5	0.9	0.01	0.8	
MID-GMG-0020					30	16	11	4	0.9	0.01	3	
MID-GMG-0021					32	14	4	1	0.9	0.01	1	
MID-GMG-0022					32	17	13	2	0.9	0.01	6	
MID-GMG-0023					27	19	19	1	0.7	0.01	11	
MID-GMG-0024					28	17	22	6	0.9	0.01	4	
MID-GMG-0025					31	12	29	10	0.8	0.01	3	
MID-GMG-0026					43	7	35	0.9	1	0.1	0.1	
MID-KXB-0001					33	22	19	0.01	0.2	0.6	0.1	
MID-KXB-0003					52	18	2	3	1	0.7	0.1	
MID-VTM-4001					28	18	15	0.01	0.3	1	5	
MIN-AAF-0001					47	15		0.01	0.1	0.01	2	
MIN-AAF-0004					43	22	0.01		1	0.01	3	
MIN-AAF-0010					44	12	0.6		1	0.1	0.7	
MIN-AAF-0013					50	14	4		0.01	0.01	1	
MIN-AAF-0015					48	14	4		0.01	0.01	1	
MIN-GFA-0001					45	18	0.6		0.2	0.1	2	
MIN-GFA-0003					43	16	5		0.5		3	
MIN-GFA-0005					43	12	9	0.7	0.04	0.2	2	
MIN-GFA-0006					40	17	10		0.4		4	
MIN-GFA-0007					48	14	1		0.2		1	
MIN-GFA-0009					48	16	0.7		0.1	0.1	2	
MIN-SAN-0002					45	13	2		0.1	0.01	1	
MIN-VTM-0002												
MIN-VTM-0003					30	24	20		0.7	0.09	3	
MIN-VTM-0004					36	18	11		1	0.2	2	
MIN-VTM-0005												
MIN-VTM-0006					40	17	8		0.3		2	
MIN-VTM-0007					37	18	9		0.6		3	
MIN-VTM-0008					38	18	11		1	0.1	2	
MIN-VTM-0009					37	18	9		0.2		3	
MIN-VTM-0018					24	9	26	2	0.6	0.1	5	
MIN-VTM-0019					22	13	27	7	0.8	0.1	3	
MIN-VTM-0020					33	10	8	0.01	1	0.1	6	
MIN-VTM-0021					32	11		0.01	1	0.1	6	
PIT-KMD-0007					22	33	29	4	0.01	0.1	0.5	
PIT-KMD-0008					28	15	34	8	0.01	0.1	2	
PIT-KMD-0009					24	24	27	14	0.01	0.5	0.1	
PIT-KXB-0101					36	13	15	0.8	0.01	0.1	6	
PIT-LFG-0001					26	19	18	8	0.6	1	1.6	
PIT-LFG-0003			0.81	0.57	28	18	10	4	0.5	1	7	
PIT-LFG-0005					35	1	9		0.2	0.3	4	
PIT-LFG-0007					54	14			0.2	0.1	0.3	
PIT-LFG-0009					42	34	8		2	1	0.9	
PIT-LFG-0013					39	0.6	17		0.3	0.9		
PIT-RDL-0001			1.34	1.23	47	30	0		0.7		2	
PIT-RDL-0002					46	40			0.1		1	
PIT-RDL-0003					50	22	0.3	0.01	0.1	0.1	0.9	
PIT-RDL-0004					57	10	0.2	0.01	0.1	3	0.2	
PIT-RDL-0005					45	29	0.9	0.01	0.7	0.01	2	
PIT-RDL-0006					48	24	1	0.01	0.3	0.01	1	
PIT-RDL-0007					52	17	0.2	0.01	0.2	2	0.6	
PIT-VCV-0001					25	30	15	0.01	1	7	0.01	
PIT-VCV-0002					37	33			2	5	0.01	
PIT-VCV-0003					23	17	29		0.5	7		
PIT-VCV-0004					59	16			0.1	0.01	1	
PIT-VCV-0005					58	12			0.1	0.01	1	
PIT-VCV-0006							7					
PIT-VCV-0007					30	35	2	0.2	1	4	0.8	
PIT-VCV-0008					41	17	2	0.9	5.3	3.7		
PIT-VCV-0009					31	17	14	1.5	2.1	5.6		
PIT-VCV-0010					28	32	19	0.01	2	3	0.01	
PIT-VCV-0011					30	35	9		2	3	0.01	
PIT-VCV-0012					48	18	1	0.01	0.8	3	1	
PIT-VCV-0013					55	10	0.2	0.01	3	2	0.4	
PIT-VCV-0014					48	19	0.2	0.01	2	2	0.7	
PIT-VCV-0015					41	37	15	0.01	0.5	0.6	0.01	
PIT-VCV-0016					29	38	14	0.01	2	0.0001	0.2	
PIT-VCV-0017					33	38	7	0.01	1	0.9	0.1	
PIT-VCV-0018					37	38	11	0.01	2	1	0.01	
PIT-VCV-0019					30		4	0.01	0.1	0.9	1	
PIT-VCV-0020					24	17	4	5	0.5	2	1	
PIT-VCV-0021					23	16	15	0.01	0.05	3	0.01	
PIT-VCV-0022					23	18	24	0.01	0.1	7	0.01	
PIT-VCV-0023					26	14	18	0.01	0.1	9	0.01	
PIT-VCV-0024					31	22	3	0.01	1	2	0.01	

Sample	Tb	Er	Yb	Lu	Q	K	P	epidote	calcite	pyrite	FeMnOxide	goethite
	ppm	ppm	ppm	ppm	ppm	ppm	ppm	%	%	%	%	%
PIT-VCV-0025					40	18	0.7	0.01	0.8	6	0.01	
PIT-VCV-0026					37	19	1	0.01	0.3	7	0.01	
PIT-VCV-0027					28	28	6	0.01	0.7	5	0.4	
PIT-VCV-0028					39	36	23	0.01	1	0.4	0.1	
PIT-VCV-0029					26	25	13	0.01	0.7	5	0.4	
PIT-VCV-0030					31	21	10	0.01	2	4	0.01	
PIT-VTM-0001					32	6	30	0.5	0.1	0.1	4	
PIT-VTM-0002					23	27	24	11	0.1	0.2	2	
PIT-VTM-0004					31	10	19	11	0.01	0.1	2	
PIT-VTM-0005					40	18	1	2	0.01	0.1	5	
PIT-VTM-0006					54	19	0.2	0.1	0.01	0.1	0.9	
PIT-VTM-0007					51	13	0.2	0.6	0.01	0.1	4	
PIT-VTM-0008					47	32	0.4	0.01	0.01	0.1	0.6	
PIT-VTM-0009					58		5	0.01	0.01	0.1	0.5	
PIT-VTM-0010			0.93	0.61	41	12	33	0.01	1	0.1	0.1	
PIT-VTM-0600					28	20	21	7	2	0.8	1	
PIT-VWL-0001												
PIT-VWL-0007					61	4	0.9					
PIT-VWL-0009					24	10	2	0.01			43	
QPS-AAF-0003					34	10	14		0.09	0.09	3	
QPS-AAF-0005					34	6	14	0.01	0.09		3	
QPS-AAF-0008					40	0.4	10		0.01	0.2	2	
QPS-AAF-0009					38	4	9	3	0.09	0.3	3	
QPS-AAF-0022					37	5	12		0.6	0.1	3	
QPS-SAN-0002					42	4	10		0.2		0.8	
QPS-VTM-0001					33	12	16	0.01	0.4	0.2	4	
QPS-VTM-4001					34	7	16		0.2	0.2	4	
ROC-KMD-0001			1.26	0.96	28	19	19		6	0.1	4	
ROC-NWD-0001					38	38	19		0.2	0.01	1	
ROC-NWD-0002					16	20	36		0.2	6	0.8	
ROC-NWD-0003					37	35	21		0.8	0.01	2	
ROC-VTM-0032					19	14	29	0.01	1		7	
ROC-VTM-0033			2.31	2.02	18	26	28		0.5		5	
SCS-LFG-0001					23				0.01	0.01	3	
SCS-LFG-0002					31	13	20	0.01	1	5	0.1	
SCS-LFG-0003					45	1	5	0.3	0.6	1	0.2	
SCS-LFG-0004					17				0.001	0.001	2	
SCS-LFG-0005					34	6	5	2	0.1		0.3	
SCS-LFG-0006					30	18	21		0.1	0.5	0.1	
SCS-LFG-0007					26	26	26		0.2	3		
SCS-LFG-0008					40	10	0.8		0.3	11	0.01	
SGS-ESO-0101					24	22	25	0.01	0.3	0.5	4	
SGS-VTM-0024					33	13	0.1	5	0.1	0.4	0.1	
SGS-VTM-0026					34	8	7		0.1	0.3	0.3	
SGS-VTM-0605					28	17	20	0.01	0.1	1	4	
SPR-AAF-0001					24	16	28	5	0.6	0.5	2	
SPR-AAF-0003					25	18	22	2	0.4	0.5	4	
SPR-JWM-0002					25	17	30	4	1	2	2	
SPR-KMD-0001			1.33	1.06	26	33	9	0.01	5	2	0.6	
SPR-KMD-0002			1.87	1.39	28	23	16	6	4	1	0.01	
SPR-KMD-0003			1.12	0.99	31	36	12	3	2.2	0.8	0.01	
SPR-OTH-0001					27	31	13	3	4	1	1	
SPR-OTH-0002					33	31	15		4	2	0.01	
SPR-SAN-0002					25	21	18	2	0.5	0.3	4	
SPR-VTM-0001					20	21	33		3	0.9	5	
SPR-VTM-0002					21	16	41	6	2	0.2	3	
SPR-VTM-0005					20	17	39	5	0.5	0.6	4	
SPR-VTM-0010					26	17	25	5	2	0.8	2	
SPR-VTM-0012					56	11	0.8	0.01	0.1	0.3	0.7	
SPR-VTM-0014					54	14	3		0.01	0.2	0.4	
SPR-VTM-0017					49	18			0.1	0.9	0.3	
SPR-VTM-0019					52	21			0.1	0.3	0.8	
SPR-VTM-0021					51	22			0.1	0.2	0.5	
SSS-AAF-0001					29	14	7		0.2	0.4	6	
SSS-EHP-0002					34	33	10	3	2	2	0.2	
SSS-EHP-0003					35	36	5	0.5	2	2	0.6	
SSS-EHP-0004					25	25	8		1	2	3	
SSS-EHP-0023												
SSS-EHP-0032					40	28	5		0.8	0.8	1	
SSS-EHP-0033					37	26	12		0.3	0.1	3	
SSS-EHP-0034					36	27	12		0.3	0.3	3	
SSS-GMG-0009								8	0.2	1	2	
SSS-GMG-0010					27	13	27	0.9	0.2	0.4	6	
SSS-GMG-0011					26	13	27	0.8	0.2	0.4	8	
SSS-GMG-0012					26	19	26	4	0.2	0.1	4	
SSS-GMG-0013					24	20	32	0.7	0.2	0.4	6	

Sample	Tb	Er	Yb	Lu	Q	K	P	epidote	calcite	pyrite	FeMnOxide	goethite
	ppm	ppm	ppm	ppm	ppm	ppm	ppm	%	%	%	%	%
SSS-GMG-0014					40	16	8	0.01	0.2	0.2	4	
SSS-GMG-0015					39	20	13	0.01	0.2	0.1	4	
SSS-GMG-0016					35	21	17	3	0.3	0.8	2	
SSS-KMD-0001			1.16	0.86	28	21	18	1	2	2	2	
SSS-KMD-0002			1.8	1.62	26	26	17	7	3	1	1	
SSS-VEV-0001					27	18	12	0.01	0		19	
SSS-VTM-0005					44	9	0.2	0.01	0.1	5	26	
SSS-VTM-0600					36	17	13		0.2	0.2	4	
SSW-AAF-0001					25	21	20	0	0.1	0.4	6	
SSW-AAF-0002					34	16	6	0.01	0.7	0.7	5	
SSW-AAF-0005					33	11	18		0.2	0.2	4	
SSW-AAF-0007					35	16	10		0.1	1	2	
SSW-AAF-1002					25	18	21	8	0.2	0.6	2	
SSW-AAF-1005					37	3	12			1	2	
SSW-AAF-1009					30	16	16	5	0.3	0.8	1	
SSW-GJG-4000					28	13	16		0.1	0.4	5	
SSW-KMD-0001			1.21	0.91	25	21	16		0.7	1	5	
SSW-SAN-0002					32	8	18	0.01	0.1	0.3	2	
SSW-SAN-0006					37	22	2	3	0.3	0.1	0.6	
SSW-VTM-0006					31	10	13	0.01	0.3	2	5	
SSW-VTM-0008					32	6	15		0.1	0.4	3	
SSW-VTM-0010					38	12	10		0.3	0.3	0.1	
SSW-VTM-0012					31	30	9	3	0.3	1	3	
SSW-VTM-0013					32	7	20	0.01	0.2	0.8	2	
SSW-VTM-0015					27	12	19	7	0.3	0.7	1	
SSW-VTM-0016					28	20	16	2	1	1	4	
SSW-VTM-0019					27	20	16	0.01	0.4	2	5	
SSW-VTM-0023					29	18	12	0.01	0.5	2	4	
SSW-VTM-0027					30	16	8	5	0.4	0.5	3	
SSW-VTM-0028					33	13	11	0.01		0.8	4	
SSW-VTM-0030					31	8	13	7	0.6	1	1	
SSW-VTM-0032					33	9	13	0.01	0.4	1	4	
SSW-VTM-4001					36	9	16			0.5	4	
SWH-GJG-0001					35	3	28	0.01	0.1	0.5	7	
SWH-GJG-0002					42	1	9	0.01	0.01	0.1	0.3	
SWH-GJG-0003					42	1	9	0.01	0.01	0.1	3	
SWH-GJG-0004					29	6	18	0.01	0.2	0.1	19	
SWH-GJG-0005					35	7	30	0.01	0.1	0.1	3	
SWH-GJG-0006					34	8	30	0.01	0.1	0.1	4	
SWH-GJG-0007					39	7	10	0.01	0.6	0.1	5	
SWH-GJG-0008					30	22	24	0.01		0.6	3	
SWH-GJG-0009					23	13	20			1	12	
SWH-GJG-0010					30	13	7			3	3	
SWH-GJG-0011					32	22	26			0.2		
SWH-GJG-0012					30	13	28			0.7		
SWH-GJG-0013					45	3	0.7	0.8	0.1	4	0.8	
SWH-GJG-0014					38	4	7	0.01	0.5	0.3		
SWH-GJG-0015					33	16						
SWH-GJG-0019					33	6	8	0.01	0.1	0.1	17	
SWH-GJG-0020					22	12	34			4		
SWH-GJG-0021					32	8	17			0.7		
SWH-GJG-0022					37	12				1		
SWH-GJG-0023					31	0.8	7	0.01	0.4	0.1	18	
SWH-GJG-4000					35	1	25		0.1	0.3	1	
SWH-VTM-4001					32	6	24		0.2	0.3	2	
average	#DIV/0!	#DIV/0!	1.774888889	1.320222222	34.42622951	17.9957346	13.82743719	2.615122699	0.600360614	0.86847039	2.877696078	0.066451613
RSQ w/ F as x values	#DIV/0!	#DIV/0!	0.019574888	0.000425423	0.020888973	0.002314076	7.2894E-05	0.009812038	0.022287107	0.003853447	0.006785943	0.010895156
Pearson coeff of F	#DIV/0!	#DIV/0!	-0.139910285	-0.020625784	-0.14453018	0.048104839	0.008537797	0.099055731	0.149288671	0.06207614	-0.082376837	0.104379864
count	0	0	45	45	427	422	398	326	391	385	408	31

Sample	hematite	Gypsum	AuthGyp	DetritGyp	molybdenit	biotite	organics	fluorite	mag	apatite	hbld	TotalClay
	%	%	%	%	%	%	%	%	%	%	%	%
BCS-VWL-0004		0.404	0.4	0.004		0.01	0.5			0.8		22
CAP-MLJ-0001										0.1		21
ESS-VWL-0001										0.1		32.9
GHN-ACT-0001	0.01	0.4				0.01				0.1	0	16.9
GHN-ACT-0002		0								0.4		17.8
GHN-ACT-0003		0.7		0.7		0.01		0.02		0.1	0	21
GHN-ACT-0004		0.7				1				0.2	0	21
GHN-ACT-0005	0.12	0.1								0.7		17
GHN-ACT-0006	0.04									0.1		10.8
GHN-ACT-0007	0.01	0								0.7		15
GHN-ACT-0008	0.09	0						0.02		0.01	1	8.2
GHN-ACT-0009	0.14	0								0.8		22
GHN-ACT-0010	0.21	0								0.9		8.5
GHN-ACT-0011	0.65	0.1				0.01				0.7		13
GHN-ACT-0012	0.4	0.01								0.8		10
GHN-ACT-0013	0.02	0.1								0.66		14
GHN-ACT-0014	0.11	0								0.8		14
GHN-ACT-0015	0.08	0.1								0.7		14
GHN-ACT-0016		0.1								0.5		14
GHN-ACT-0017		0.1								0.5		11
GHN-ACT-0018		0.01						0.01		0.01		12
GHN-ACT-0019		0.1								0.4		25
GHN-ACT-0020		0.1								0.1		35
GHN-ACT-0021		0.1						0.01		0.1		25
GHN-ACT-0022		0.1						0.02		0.3		29
GHN-ACT-0023		0.1						0.01		0.4		29
GHN-ACT-0024	0.05	0.1								0.4		25
GHN-ACT-0025	0.01	0.1			0.02					0.8		19
GHN-ACT-0026	0.1	0.1								0.6		22
GHN-ACT-0027		0.1								0.6		20
GHN-ACT-0028	0.02	0.1						0.07		0.7		24
GHN-ACT-0029	0.02	0.1								0.7		21
GHN-ACT-0030	0.06	0.1								0.7		18
GHN-ACT-0031		0						0.02		0.02		24
GHN-ACT-0032		0.1						0.01		0.2		24
GHN-ACT-0033	0.1	0	0.1							0.2		23
GHN-ACT-0034	0.36	0.1			35	11	0.7			0.3		42
GHN-ACT-0035	0.18	0.1								0.3		44
GHN-ACT-0036	0.13	0.1						0.02		0.2		39
GHN-EHP-0001		0.1								0.5		22
GHN-EHP-0002		0.6								0.1		27
GHN-EHP-0003		0.1								0.2		29
GHN-EHP-0004										0.7		35
GHN-EHP-0007										11		48
GHN-HRS-0001										0.8		14
GHN-HRS-0002								0.02		0.1		8.5
GHN-HRS-0088										0.1		6.4
GHN-HRS-0089										0.3		30
GHN-HRS-0090										0.3		30
GHN-HRS-0091										0.3		41
GHN-HRS-0092										0.1		20
GHN-HRS-0094										0.1		20
GHN-HRS-0095										0.4		32
GHN-HRS-0096										0.1		27
GHN-JRM-0001		1.2	1.1	0.1		0.01				0.2		33
GHN-JRM-0002		1.6	0.2	1.4					0.01	0.9		26
GHN-JRM-0006		0.1								0.8		21
GHN-JRM-0008										0.9		23
GHN-JRM-0009		0.8	0.7	0.1						0.5		36
GHN-JRM-0022		0.01								0.7		22
GHN-JRM-0027										0.7		16
GHN-JRM-0037		0.1								0		10.6
GHN-JRM-0038										0.01		36
GHN-JRM-0039										0.3		48
GHN-JRM-0040										0.3		43
GHN-JRM-0047		0.3								0.4		40
GHN-KMD-0013	0.3	1	0.4	0.6	0.01	0.01				0.6		26
GHN-KMD-0014	0.7	0.04	0.02	0.02	0.01	0.01				0.7		11
GHN-KMD-0015	0.06	0.7	0.5	0.2						0.6		26
GHN-KMD-0016	0.3	1	0.5	0.5						0.7		17
GHN-KMD-0017		1.5	0.5	1						0.4		33
GHN-KMD-0018	0.1	1.2	0.6	0.6				0.01		0.2		26
GHN-KMD-0019		0.24	0.16	0.08						0.6		21
GHN-KMD-0026		0.6	0.3	0.3						0.3		15
GHN-KMD-0027		0.6	0.3	0.3						0.5		21
GHN-KMD-0028												

Sample	hematite	Gypsum	AuthGyp	DetritGyp	molybdenit	biotite	organics	fluorite	mag	apatite	hbld	TotalClay
	%	%	%	%	%	%	%	%	%	%	%	%
GHN-KMD-0048										0.8		13
GHN-KMD-0050										0.8		18
GHN-KMD-0051		2	0.01	1.9						0.4		18
GHN-KMD-0052		0.4								0.7		24
GHN-KMD-0053		0.6	0.4	0.2				0.01		0.1		21
GHN-KMD-0054		1						0.01		0.8		20
GHN-KMD-0055		1						0.03		0.2		32
GHN-KMD-0056		0.41	0.4	0.01						0.4		19
GHN-KMD-0057									0.01	0.8		21
GHN-KMD-0062		0.1								0.2		26
GHN-KMD-0063		0								0.3		29
GHN-KMD-0064										0.4		17
GHN-KMD-0065		0.3	0.2	0.1		0.01				0.5		23
GHN-KMD-0071		0.8	0.4	0.4						0.3		20
GHN-KMD-0072										0.7		18
GHN-KMD-0073		0.4	0.1	0.3						0.5		23
GHN-KMD-0074		0.4	0.2	0.2						0.5		22
GHN-KMD-0077										0.4		16
GHN-KMD-0078										0.4		17
GHN-KMD-0079		0.8	0.5	0.3						0.4		21
GHN-KMD-0080										0.7		17
GHN-KMD-0081		0.7	0.3	0.4				0.2		0.5		21
GHN-KMD-0082		1.2	0.7	0.5		0.01				0.6		17
GHN-KMD-0088		1.8	1.7	0.1						0.2		22
GHN-KMD-0092										0.4		27
GHN-KMD-0095		0.2								0.01		25
GHN-KMD-0096		0.81	0.8	0.01		0.01				0.1		28
GHN-KMD-0097		0								0.2		28
GHN-KMD-0100										0.4		24
GHN-LFG-0001		0.9	0.9					0.007		0.2		47
GHN-LFG-0002		1	1					0.004		0.2		45
GHN-LFG-0003		0						0.02				32
GHN-LFG-0004		0.2		0.2				0.001		0.01		45
GHN-LFG-0005		0.2		0.2				0.01		0.2		40
GHN-LFG-0006		0.2		0.2				0.01		0.1		42
GHN-LFG-0018										0.4		11
GHN-LFG-0020										0.3		10
GHN-LFG-0037		0.1								0.6		25
GHN-LFG-0041		0.1								0.1		7.4
GHN-LFG-0060												
GHN-LFG-0085		0.2	0.1	0.1						0.6		22
GHN-LFG-0086		1.7	1	0.7						0.7		21
GHN-LFG-0087										0.6		16
GHN-LFG-0088		0.28	0.2	0.08						0.7		17
GHN-LFG-0089										0.3		11
GHN-LFG-0090		1.5	0.5	1						0.7		21
GHN-LFG-0091		1	2.1	3.9						0.3		27
GHN-RDL-0002								0.03		0.1		42
GHN-RDL-0003										0.1		42
GHN-RDL-0004										0.1		37
GHN-SAW-0003										0.01		29.8
GHN-SAW-0004										0.4		30
GHN-SAW-0005										0.01		16.7
GHN-SAW-0200										0.3		43
GHN-SAW-0201												23
GHN-STM-0001										0.3		24
GHN-STM-0002		0.2								0.01		20.5
GHN-STM-0003								0.02		0.01		15.8
GHN-STM-0004								0.01		0.2		10
GHN-STM-0005								0.02		0.01		11.8
GHN-VTM-0003		0.01								0.3		35
GHN-VTM-0109										0.4		15
GHN-VTM-0194		1.8	1.7	0.1						0.6		22
GHN-VTM-0195	0.2	1.6	0.5	1.1						0.7		26
GHN-VTM-0197	0.4	2.4	0.9	1.6						0.6		28
GHN-VTM-0198	0.2	0.2	0.14	0.06						0.4		19
GHN-VTM-0199	0.1	1	0.4	0.6						0.5		22
GHN-VTM-0200		0.42	0.4	0.02						0.1		10
GHN-VTM-0201	0.06	1	0.5	0.5						0.5		25
GHN-VTM-0202		1.602	0.002	1.6		0.9				0.5		20.7
GHN-VTM-0203		1.5	1	0.5						0.3		24
GHN-VTM-0204		1.4	0.4	1						0.5		31
GHN-VTM-0205		0.7	0.3	0.4		0.01				0.4		30
GHN-VTM-0206		0.7	0.3	0.4						0.7		26
GHN-VTM-0207		0.7	0.5	0.2						0.3		24
GHN-VTM-0208		0.21	0.2	0.01						0.6		13

Sample	hematite	Gypsum	AuthGyp	DetritGyp	molybdenit	biotite	organics	fluorite	mag	apatite	hbld	TotalClay
	%	%	%	%	%	%	%	%	%	%	%	%
GHN-VTM-0209		0.61	0.01	0.6		0.01				0.7		17
GHN-VTM-0210		0.2		0.2						0.7		16
GHN-VTM-0211		0.61	0.01	0.6						0.7		15
GHN-VTM-0212		0.7								0.7		18
GHN-VTM-0213		0.601	0.001	0.6						0.7		20
GHN-VTM-0214		0.1	0.01	0.7						0.7		18
GHN-VTM-0215		0.3	0.15	0.15						0.7		18
GHN-VTM-0216		0.202	0.002	0.2						0.7		13
GHN-VTM-0217		0.301	0.001	0.3						0.4		
GHN-VTM-0417										0.2		28
GHN-VTM-0418		1								0.1		30
GHN-VTM-0419		0.1								0.5		25
GHN-VTM-0420		1	0.5	0.5						0.8		27
GHN-VTM-0421		1.9	0.4	1.5						0.7		19
GHN-VTM-0422		1.9	0.4	1.5						0.5		20
GHN-VTM-0423		1.9	0.5	1.4						0.7		18
GHN-VTM-0424										0.2		20
GHN-VTM-0425										0.5		22
GHN-VTM-0426										0.7		22
GHN-VTM-0450						0.01				0.6		20
GHN-VTM-0451		1.3	1	0.3						0.6		20
GHN-VTM-0452		2.01	2	0.01		0.001				0.5		21
GHN-VTM-0453		2	1	1		1				0.4		26
GHN-VTM-0454		2.5	0.5	2						0.2		28
GHN-VTM-0455										0.4		13
GHN-VTM-0500		0.7								0.5		44
GHN-VTM-0501										0.3		49
GHN-VTM-0502		3								0.3		46
GHN-VTM-0503		3								0.3		47
GHN-VTM-0504										0.5		
GHN-VTM-0506		3	1	2						0.3		40
GHN-VTM-0507		3	1	1		0.001	1			0.4		31
GHN-VTM-0508		3	1	1		0.01				0.4		32.8
GHN-VTM-0509			0.01							0.3		49.8
GHN-VTM-0510		1	1	0.001						0.7		43
GHN-VTM-0598		0								0.1		32
GHN-VTM-0599		0.2		1						0.5		43
GHN-VTM-0602		1							0.01	0.01		53
GHN-VTM-0603		0.4								0.01		48
GHN-VTM-0604		0.2		1						0.5		30
GHN-VTM-0605		0								0.5		38
GHN-VTM-0606		1	0.4	0.6	0					0.2		28
GHN-VTM-0607		0.6								0.2		33
GHN-VTM-0610		2								0.2		25
GHN-VTM-0611		3	2	1		5				0.3		43
GHN-VTM-0612		3				1				0.3		27
GHN-VTM-0613		3	2	1						0.5		36
GHN-VTM-0614		6						0.01		0.2		51
GHN-VTM-0624		1.45	0.5	0.95		0.001				0.4		48
GHR-VWL-0004										0.4		47
GHR-VWL-0007		0.3								0.4		33
GMG-PIT-0001										0.4		46.8
GMG-PIT-0006										0.2		4
GMG-PIT-0007										0.2		8
GMG-PIT-0009										0.4		13
GMG-PIT-0010										0.5		32
GMG-PIT-0011										0.7		25
GMG-PIT-0014										0.3		28
GMG-PIT-0015										0.3		29
HAS-GJG-0001										0.1		27
HAS-GJG-0002										0.1		26.3
HAS-GJG-0004		0.4								0.4		25
HAS-GJG-0005		1								0.6		22
HAS-GJG-0006		8										41
HAS-GJG-0007		12										41
HAS-GJG-0008		15										48
HAS-GJG-0009		2								0.3		
HAS-GJG-0010		2								0.3		47
MID-AAF-0002		3								0.2		34
MID-AAF-0003		2								0.2		36
MID-GJG-4001		2								0.5		32
MID-GMG-0014										1		12
MID-GMG-0015										0.3		10
MID-GMG-0016										0.1		9
MID-GMG-0017										0.9		14
MID-GMG-0018										0.5		27

Sample	hematite	Gypsum	AuthGyp	DetritGyp	molybdenit	biotite	organics	fluorite	mag	apatite	hbld	TotalClay
	%	%	%	%	%	%	%	%	%	%	%	%
MID-GMG-0019										0.5		27
MID-GMG-0020										0.9		34
MID-GMG-0021										0.9		42
MID-GMG-0022										0.7		29
MID-GMG-0023										0.7		21
MID-GMG-0024										0.6		22
MID-GMG-0025										0.3		13
MID-GMG-0026										1		11
MID-KXB-0001		2								0.4		22
MID-KXB-0003		2								0.3		21
MID-VTM-4001		3								0.5		28
MIN-AAF-0001		0.1	0.1							0.1		34
MIN-AAF-0004		0.01								0.01		29
MIN-AAF-0010		0.1						0.002		0.1		37
MIN-AAF-0013		0.08								0.01		29
MIN-AAF-0015		0						0.2		0.1		31
MIN-GFA-0001		0.01						0.01		0.1		33
MIN-GFA-0003		0.3				0.01		0.01		0.6		31
MIN-GFA-0005		0.04						0.01		0.1		30
MIN-GFA-0006		0.8				0.01				0.1		28
MIN-GFA-0007		0.1						0.02		0.1		34
MIN-GFA-0009		0.1						0.02		0.1		31
MIN-SAN-0002		0.2								0.2		34
MIN-VTM-0002												
MIN-VTM-0003		1						0.3		0.7		19
MIN-VTM-0004		2								0.4		27
MIN-VTM-0005												
MIN-VTM-0006		3								0.3		27
MIN-VTM-0007		0.6								0.4		29
MIN-VTM-0008		0								0.3		27
MIN-VTM-0009		2								0.4		28
MIN-VTM-0018		0.1								0.9		32
MIN-VTM-0019		0.3								1		25
MIN-VTM-0020										0.4		42
MIN-VTM-0021		0								0.2		49
PIT-KMD-0007										1		9
PIT-KMD-0008										0.1		13
PIT-KMD-0009										0.6		8.4
PIT-KXB-0101										0.8		28
PIT-LFG-0001		0.301	0.001	0.3						0.5		25
PIT-LFG-0003		0.3	0.3							0.4		30
PIT-LFG-0005		4		4						0.6		42
PIT-LFG-0007		1		1				0.02				28
PIT-LFG-0009		0.2		0.2				0.02				8.4
PIT-LFG-0013		0.5		0.5						0.1		36
PIT-RDL-0001		0.1								0.01		18.7
PIT-RDL-0002										0.01		12.6
PIT-RDL-0003										0.1		26
PIT-RDL-0004		0.2								0.1		30
PIT-RDL-0005		0.103	0.1	0.003						0.01		21.7
PIT-RDL-0006		0.01	0.1									24
PIT-RDL-0007		0.08	0.08						0.01	0.01		26
PIT-VCV-0001		0.2	0.2							0.6		20
PIT-VCV-0002		0.2								0.3		22
PIT-VCV-0003		0.3								0.7		22.6
PIT-VCV-0004										0.01		24
PIT-VCV-0005		0								0.01		27
PIT-VCV-0006												
PIT-VCV-0007		0.3				0.01			0.01	0.5		26
PIT-VCV-0008		0				2			0.5	0.4		27.1
PIT-VCV-0009		0							1	0.5		26.8
PIT-VCV-0010		0.2		0.2		3			0.01	0.4		14.8
PIT-VCV-0011		0.2		0.2		5			0	0.6		19
PIT-VCV-0012		0.1		0.1					0.01	0.2		27.9
PIT-VCV-0013		0.2		0.2					0.0001	0.2		29
PIT-VCV-0014		0.2		0.2					1	0.01		30
PIT-VCV-0015		0.1		0.1		1			0.0001	0.1		5.6
PIT-VCV-0016		0.1		0.1		1			0.01	0.7		15
PIT-VCV-0017		0.2		0.2		2				0.4		19
PIT-VCV-0018		0.1		0.2					0.01	0.4		12
PIT-VCV-0019		4		4						0.4		57.4
PIT-VCV-0020		0.5		0.5		7				0.8		43.8
PIT-VCV-0021		7		7	0.03	0				0.7		32
PIT-VCV-0022		7				3				6		19
PIT-VCV-0023		9		9	0.01	0.01				7		23
PIT-VCV-0024		0.6		0.6						2		38

Sample	hematite	Gypsum	AuthGyp	DetritGyp	molybdenit	biotite	organics	fluorite	mag	apatite	hbld	TotalClay
	%	%	%	%	%	%	%	%	%	%	%	%
PIT-VCV-0025		0.3								0.4		33
PIT-VCV-0026		0.4		0.4						0.4		34
PIT-VCV-0027		0.2		0.2						0.5		31
PIT-VCV-0028		0.2		0.2		1				0.4		0.5
PIT-VCV-0029		0.3		0.2						0.5		28
PIT-VCV-0030										0.7		31
PIT-VTM-0001										0.5		26
PIT-VTM-0002										0.6		12
PIT-VTM-0004										0.7		26
PIT-VTM-0005								0.04		0.4		33
PIT-VTM-0006										0.1		25
PIT-VTM-0007										0.1		30
PIT-VTM-0008										0.1		18.8
PIT-VTM-0009										0.1		36.3
PIT-VTM-0010										1		10
PIT-VTM-0600		0.05	0.05						0.01	0.7		19
PIT-VWL-0001												14.5
PIT-VWL-0007												33
PIT-VWL-0009										0.5		19
QPS-AAF-0003		2								0.4		34
QPS-AAF-0005		2								0.4		36.9
QPS-AAF-0008		0								0.3		41.8
QPS-AAF-0009		3								0.4		39.9
QPS-AAF-0022		0.6								0.4		38
QPS-SAN-0002		1								0.2		38
QPS-VTM-0001		1	1.1	0.06						0.5		32
QPS-VTM-4001		1								0.4		35
ROC-KMD-0001		0.05								0.4		23
ROC-NWD-0001		0.05								0.01		0
ROC-NWD-0002		0.2								0.6		19
ROC-NWD-0003										0.01		0
ROC-VTM-0032		0.01	0.005	0.005		1				2		27.01
ROC-VTM-0033						1				1	14	6
SCS-LFG-0001		11	9	2		3						60
SCS-LFG-0002		2						0.2		0.4		27
SCS-LFG-0003		3						0.2		0.2		43
SCS-LFG-0004		8	7	1		13						60
SCS-LFG-0005		2.3	2	0.3						0.3		45
SCS-LFG-0006		1				6				0.3		26
SCS-LFG-0007		0.6						0.2		0.3		17.2
SCS-LFG-0008		0.1						0.2		0.3		35.4
SGS-ESO-0101		2								0.7		20
SGS-VTM-0024		3						0.02		0.2		37
SGS-VTM-0026		3						0.03		0.3		42
SGS-VTM-0605										0.8		25
SPR-AAF-0001		0.6		0.6						0.7		23
SPR-AAF-0003		1								0.8		25
SPR-JWM-0002		0.02	0.2			0.01		0.01		0.7		18
SPR-KMD-0001		0.26	0.2	0.06	0.01	0.01		0.03		0.01		23
SPR-KMD-0002		0.202	0.2	0.002	0.01			0.05		0.7		21
SPR-KMD-0003		0.14	0.14			0.01		0.05	0.01	0.3		14
SPR-OTH-0001		0.38	0.3	0.08		1		0.01	0.01	0.7		18
SPR-OTH-0002		0.44	0.4	0.04	0.01	0.01		0.01	0.01	1		13
SPR-SAN-0002		2								0.9		26
SPR-VTM-0001		0.101	0.1	0.001		0.01		0.1		2		14
SPR-VTM-0002										0.2		9
SPR-VTM-0005		0.2								0.9		13
SPR-VTM-0010		0.1								0.8		21
SPR-VTM-0012		0.04	0.04					0.01				30
SPR-VTM-0014										0.1		28.7
SPR-VTM-0017		0.02						0.02				31
SPR-VTM-0019		0.02		0.02								25
SPR-VTM-0021		0.02		0.02								26
SSS-AAF-0001		3								0.4		39
SSS-EHP-0002		0.5						0.05		0.5		17
SSS-EHP-0003		0.7						0.01		0.3		18
SSS-EHP-0004		3								0.7		31
SSS-EHP-0023												8
SSS-EHP-0032		0.5								0.2		22
SSS-EHP-0033		0.3								0.1		20
SSS-EHP-0034		0.4								0.3		21
SSS-GMG-0009										0.5		14
SSS-GMG-0010										0.9		25
SSS-GMG-0011										0.8		25
SSS-GMG-0012										0.9		20
SSS-GMG-0013										0.7		15

Sample	hematite	Gypsum	AuthGyp	DetritGyp	molybdenit	biotite	organics	fluorite	mag	apatite	hbld	TotalClay
	%	%	%	%	%	%	%	%	%	%	%	%
SSS-GMG-0014										0.4		31
SSS-GMG-0015										1		22
SSS-GMG-0016										0.5		19
SSS-KMD-0001		2.1	1.4	0.7		0.01				0.4		23
SSS-KMD-0002		2.6	2.3	0.3				0.14	0.01	0.6		15
SSS-VEV-0001										1		22.3
SSS-VTM-0005										0.2		15
SSS-VTM-0600		0								0.7		28
SSW-AAF-0001		0.51	0.5	0.01						0.9		25
SSW-AAF-0002		2								0.7		35
SSW-AAF-0005		0						0.01		0.3		29.4
SSW-AAF-0007		2								0.3		32
SSW-AAF-1002										0.7		19
SSW-AAF-1005		3		3						0.2		38
SSW-AAF-1009		3.5	3.5			0.01				0.5		25
SSW-GJG-4000		3								0.5		32
SSW-KMD-0001		3.6	3.2	0.4						0.4		27
SSW-SAN-0002		2				0.01				0.3		33
SSW-SAN-0006		1								0.3		28
SSW-VTM-0006		3								0.4		33
SSW-VTM-0008		3								0.3		35
SSW-VTM-0010		2						0.01		0.01		32
SSW-VTM-0012		0.9						0.005		0.2		21
SSW-VTM-0013		3								0.4		30
SSW-VTM-0015		3								0.6		24
SSW-VTM-0016		1								0.8		26
SSW-VTM-0019		3								0.5		27
SSW-VTM-0023		3								0.5		31
SSW-VTM-0027		2.3	1.4	0.9						0.6		33
SSW-VTM-0028		2								0.5		35
SSW-VTM-0030		3.1	2.6	0.5						0.7		31
SSW-VTM-0032		3								0.4		35
SSW-VTM-4001		3								0.4		30
SWH-GJG-0001										0.3		22
SWH-GJG-0002										0.2		44
SWH-GJG-0003		0.1								0.2		44
SWH-GJG-0004										0.5		23
SWH-GJG-0005										0.2		23
SWH-GJG-0006										0.2		23
SWH-GJG-0007										0.1		36
SWH-GJG-0008		4								0.4		20
SWH-GJG-0009		12										21
SWH-GJG-0010		7										38
SWH-GJG-0011		5										15
SWH-GJG-0012		4										23.6
SWH-GJG-0013		1								0.5		47.6
SWH-GJG-0014		0.5								0.6		53.7
SWH-GJG-0015		4										48
SWH-GJG-0019										1		32
SWH-GJG-0020		2										27
SWH-GJG-0021		9										34
SWH-GJG-0022		5										56
SWH-GJG-0023		0.4								2		37
SWH-GJG-4000		1.5								0.2		32
SWH-VTM-4001		3						0.01		0.1		31
average	0.1665625	1.291760656	0.772141414	0.724627119	#DIV/0!	1.375745098	0.733333333	0.044316667	#DIV/0!	0.490444444	3	26.16957845
RSQ w/ F as x values	0.014346014	2.10407E-05	0.018306069	1.02373E-06	#DIV/0!	0.001304815	0.279894308	0.022133742	#DIV/0!	0.017729977	0.046571539	0.001424925
Pearson coeff of F	0.119774846	0.004587013	0.135299923	-0.001011794	#DIV/0!	-0.03612222	-0.529050384	0.148774129	#DIV/0!	0.133153958	-0.2158044	0.037748179
count	32	305	99	118	0	51	3	60	0	405	5	427

Sample	kaol	chlorite	illite	smectite	MixLayer	copiapite	jarosite	sph	rutile	zircon
	%	%	%	%	%	%	%	%	%	%
BCS-VWL-0004	2	4	14	2	0		0.01		0.4	0.03
CAP-MLJ-0001	1	1	18	1			1		0.1	
ESS-VWL-0001	1	0.9	30	1					1	
GHN-ACT-0001	1	0.9	14	1	0	0.01	0.09		0.1	0.06
GHN-ACT-0002	1	0.8	15	1		0.01	0.03	0.03	0.1	0.03
GHN-ACT-0003	1	1	18	1		0.01	0.08	0.01	0.1	0.06
GHN-ACT-0004	1	1	18	1	0	0.02	0.08	0.03	0.1	0.06
GHN-ACT-0005	1	5	10	1	0	0.1	0.01	0.02	0.3	0.04
GHN-ACT-0006	1	0.8	8	1					0.1	
GHN-ACT-0007	1	5	8	1		0.02	0.01		0.3	0.04
GHN-ACT-0008	1	0.2	6	1		0.01	0.01	0.04	0.01	0.06
GHN-ACT-0009	1	5	15	1		0.12	0.01		0.5	0.03
GHN-ACT-0010	1	6	0.5	1		0.1	0.01		0.5	0.04
GHN-ACT-0011	1	5	6	1	0	0.02	0.02		0.6	0.04
GHN-ACT-0012	1	6	2	1	0	0.02	0.02		0.6	0.04
GHN-ACT-0013	1	6	6	1	0	0.02	0.04		0.7	0.03
GHN-ACT-0014	1	6	6	1		0.02	0.02		0.7	0.03
GHN-ACT-0015	1	6	6	1		0.02	0.02		0.6	0.03
GHN-ACT-0016	1	4	8	1	0	0.02	0.02		0.4	0.04
GHN-ACT-0017	1	4	5	1	0	0.1	0.02		0.4	0.04
GHN-ACT-0018	1	1	9	1	0	0.01	0.2		0.1	0.06
GHN-ACT-0019	1	3	20	1	0	0.01	0.06	0.04	0.3	0.04
GHN-ACT-0020	1	1	32	1	0	0.01	0.3	0.02	0.3	0.06
GHN-ACT-0021	1	1	22	1	0		0.5	0.02	0.1	0.06
GHN-ACT-0022	1	2	25	1		0.01	0.5	0.04	0.2	0.04
GHN-ACT-0023	1	3	24	1			0.33	0.08	0.3	0.04
GHN-ACT-0024	1	3	20	1		0.02	0.21	0.04	0.3	0.04
GHN-ACT-0025	1	4	13	1		0.01	0.01		0.5	0.03
GHN-ACT-0026	1	4	16	1		0.02	0.02		0.4	0.03
GHN-ACT-0027	1	1	14	4			0		0.4	0.03
GHN-ACT-0028	1	4	18	1		0.02	0.11		0.5	0.03
GHN-ACT-0029	1	5	14	1	0	0.02	0.02		0.6	0.03
GHN-ACT-0030	1	5	11	1		0.02	0.02		0.6	0.03
GHN-ACT-0031	1	2	20	1		0.02	0.19		0.2	0.06
GHN-ACT-0032	1	2	20	1		0.02	0.3		0.2	0.06
GHN-ACT-0033	1	1	20	1		0.01	0.2	0.06	0.1	0.06
GHN-ACT-0034	1	2	38	1		0.03	0.05	0.2	0.4	0.03
GHN-ACT-0035	1	2	40	1		0.01			0.4	0.03
GHN-ACT-0036	1	3	34	1		0.02	0.05		0.3	0.03
GHN-EHP-0001	1	3	17	1	0		0		0.4	0.04
GHN-EHP-0002	1	2	23	1	0		2		0.2	0.06
GHN-EHP-0003	1	2	25	1			2			
GHN-EHP-0004	1	3	30	1					0.5	
GHN-EHP-0007	1	6	40	1					0.4	
GHN-HRS-0001	1	7	5	1					0.7	0.03
GHN-HRS-0002	1	0.5	6	1					0.1	0.06
GHN-HRS-0088	1	0.4	4	1			0.06		0.1	
GHN-HRS-0089	1	1	27	1					0.2	0.06
GHN-HRS-0090	1	1	27	1					0.2	0.06
GHN-HRS-0091	1	1	38	1					0.4	
GHN-HRS-0092	1	1	17	1					0.1	
GHN-HRS-0094	1	1	17	1					0.1	
GHN-HRS-0095	1	4	26	1					0.6	
GHN-HRS-0096	1	2	23	1					0.7	
GHN-JRM-0001	1	3	27	2			4		0.4	0.03
GHN-JRM-0002	0	6	16	4			0.01		0.5	0.03
GHN-JRM-0006	1	6	13	1					0.6	
GHN-JRM-0008	1	6	15	1					0.5	
GHN-JRM-0009	1	3	31	1			1.9		0.4	0.04
GHN-JRM-0022	1	7	13	1			0		0.6	0.03
GHN-JRM-0027	1	6	8	1					0.6	
GHN-JRM-0037	1	0.6	8	1			1		0.1	
GHN-JRM-0038	1	2	32	1			1		0.3	
GHN-JRM-0039	1	2	44	1			1		0.7	0.04
GHN-JRM-0040	1	1	40	1			1		0.5	0.04
GHN-JRM-0047	1	2	36	1			2		0.5	0.04
GHN-KMD-0013	1	3	20	2		0.2	0.01	0.01	0.3	0.03
GHN-KMD-0014	1	7	1	2		0.2	0.01		0.8	0.03
GHN-KMD-0015	2	5	16	3		0.14	0.01		0.5	0.03
GHN-KMD-0016	1	7	4	5			0		0.7	0.03
GHN-KMD-0017	1	4	25	3		0.06	4	0.01	0.6	0.03
GHN-KMD-0018	1	3	19	3		0.06	1.4		0.3	0.04
GHN-KMD-0019	1	8	9	3			0		0.7	0.03
GHN-KMD-0026	1	2	10	2			0		0.1	0.04
GHN-KMD-0027	2	2	15	2	2		0.3		0.2	0.04
GHN-KMD-0028										

Sample	kaol	chlorite	illite	smectite	MixLayer	copiapite	jarosite	sph	rutile	zircon
	%	%	%	%	%	%	%	%	%	%
GHN-KMD-0048	1	7	4	1					0.7	0.04
GHN-KMD-0050	1	7	8	2					0.7	0.03
GHN-KMD-0051	2	4	8	4			0		0.5	0.04
GHN-KMD-0052	1	6	16	1			0		0.5	0.03
GHN-KMD-0053	2	2	15	2	0		0.5		0.2	0.06
GHN-KMD-0054	1	6	12	1			0.5		0.6	0.03
GHN-KMD-0055	1	2	28	1			1		0.3	0.04
GHN-KMD-0056	1	4	10	4			0		0.5	0.04
GHN-KMD-0057	1	7	11	2					0.6	0.03
GHN-KMD-0062	1	3	20	2	0		1		0.3	0.04
GHN-KMD-0063	2	5	20	2			1.6		0.5	0.03
GHN-KMD-0064	1	2	11	3					0.2	0.04
GHN-KMD-0065	2	5	14	2			0		0.4	0.04
GHN-KMD-0071	2	3	13	2			0		0.4	0.03
GHN-KMD-0072	1	6	8	3					0.5	
GHN-KMD-0073	4	7	8	4			0		0.5	0.03
GHN-KMD-0074	2	6	12	2			0		0.6	0.03
GHN-KMD-0077	1	2	11	2					0.2	0.04
GHN-KMD-0078	2	3	10	2					0.3	0.04
GHN-KMD-0079	1	4	13	3			0.01		0.4	0.04
GHN-KMD-0080	3	7	4	3					0.7	0.04
GHN-KMD-0081	1	3	14	3			0		0.3	0.04
GHN-KMD-0082	1	7	8	1			0		0.6	0.03
GHN-KMD-0088	2	4	14	2			0.1		0.4	0.03
GHN-KMD-0092	1	4	19	3					0.4	0.03
GHN-KMD-0095	2	1	20	2	0		1		0.1	0.06
GHN-KMD-0096	2	2	23	1			2.5		0.2	0.06
GHN-KMD-0097	1	3	23	1			2		0.4	0.04
GHN-KMD-0100	3	4	15	2					0.3	0.04
GHN-LFG-0001	1	1	44	1			3		0.6	0.04
GHN-LFG-0002	1	1	42	1			2		0.6	0.04
GHN-LFG-0003	0	1	30	1			2		0.2	0.04
GHN-LFG-0004	1	0	35	9			3		0.4	0.04
GHN-LFG-0005	1	1	37	1			2		0.5	0.04
GHN-LFG-0006	1	2	38	1			4		0.6	0.06
GHN-LFG-0018	1	2	7	1					0.2	
GHN-LFG-0020	1	1	7	1					0.1	
GHN-LFG-0037	1	5	18	1	1				0.4	0.03
GHN-LFG-0041	1	0.4	5	1	1				0.01	
GHN-LFG-0060										
GHN-LFG-0085	1	7	13	1			0		0.6	
GHN-LFG-0086	1	6	13	1			0		0.6	0.03
GHN-LFG-0087	1	8	6	1					0.5	0.04
GHN-LFG-0088	1	8	7	1			0		0.7	
GHN-LFG-0089	1	1	8	1					0.2	
GHN-LFG-0090	1	7	11	2			0		0.6	0.03
GHN-LFG-0091	1	4	21	1			0		0.6	
GHN-RDL-0002	1	2	38	1	1		1		0.7	6
GHN-RDL-0003	1	2	38	1					0.7	
GHN-RDL-0004	1	1	34	1			0.7		0.5	
GHN-SAW-0003	1	0.8	27	1	2				0.1	
GHN-SAW-0004	1	4	24	1			5		0.6	
GHN-SAW-0005	1	0.7	14	1	1		0.9		0.01	
GHN-SAW-0200	1	6	35	1	2		1		0.4	
GHN-SAW-0201	1	2	19	1	3		1		0.1	
GHN-STM-0001	1	3	19	1					0.4	0.03
GHN-STM-0002	2	0.5	17	1	0		0.8		0.01	0.06
GHN-STM-0003	1	0.8	13	1					0.1	6
GHN-STM-0004	1	2	6	1	4				0.3	0.04
GHN-STM-0005	1	0.8	9	1					0.1	0.06
GHN-VTM-0003	1	3	30	1					0.7	
GHN-VTM-0109	1	3	10	1					0.2	
GHN-VTM-0194	1	4	15	2		0	0.5		0.5	0.03
GHN-VTM-0195	2	5	16	3		0.1	1.4		0.4	0.04
GHN-VTM-0197	3	6	17	2		0.15	0.01		0.5	0.03
GHN-VTM-0198	1	3	13	2		0.02	0.01		0.3	0.04
GHN-VTM-0199	1	3	15	3		0	0		0.3	0.04
GHN-VTM-0200	1	1	4	4		0	0.03		0.2	0.04
GHN-VTM-0201	1	3	19	2		0.07	1		0.3	0.04
GHN-VTM-0202	0.9	4	13	2.8		0	0		0.4	0.04
GHN-VTM-0203	1	3	16	4		0	0		0.3	0.04
GHN-VTM-0204	1	6	21	3		0	0		0.5	0.03
GHN-VTM-0205	1	5	22	2		0	0.8		0.4	0.03
GHN-VTM-0206	2	5	17	2		0	0		0.4	0.04
GHN-VTM-0207	1	4	14	5		0	0		0.3	0.03
GHN-VTM-0208	1	6	3	3		0	0		0.7	

Sample	kaol	chlorite	illite	smectite	MixLayer	copiapite	jarosite	sph	rutile	zircon
	%	%	%	%	%	%	%	%	%	%
GHN-VTM-0209	2	6	7	2		0	0		0.6	0.03
GHN-VTM-0210	2	6	6	2		0	0		0.6	0.04
GHN-VTM-0211	1	7	5	2		0	0		0.7	0.03
GHN-VTM-0212	2	7	7	2		0	0		0.7	0.03
GHN-VTM-0213	2	6	10	2		0	0		0.6	0.03
GHN-VTM-0214	1	7	7	3		0	0		0.7	0.04
GHN-VTM-0215	1	6	8	3		0	0		0.7	0.03
GHN-VTM-0216	1	5	0	7		0	0		0.6	0.03
GHN-VTM-0217		2	8	5		0	0		0.3	0.04
GHN-VTM-0417	1	2	24	1					0.2	
GHN-VTM-0418	1	2	26	1			0		0.3	
GHN-VTM-0419	1	3	20	1			0		0.3	
GHN-VTM-0420	1	7	18	1			0		0.5	0.03
GHN-VTM-0421	1	6	11	1			0		0.6	0.04
GHN-VTM-0422	1	4	14	1			0		0.3	0.04
GHN-VTM-0423	1	4	12	1			0		0.3	0.04
GHN-VTM-0424	1	2	16	1					0.1	
GHN-VTM-0425	1	5	15	1					0.5	
GHN-VTM-0426	1	6	14	1					0.6	
GHN-VTM-0450	1	7	10	2					0.6	0.07
GHN-VTM-0451	2	6	10	2			0		0.6	0.03
GHN-VTM-0452	1	5	13	2	0		0		0.5	0.03
GHN-VTM-0453	1	7	17	1			0		0.6	0.03
GHN-VTM-0454	2	4	19	3			0		0.4	0.03
GHN-VTM-0455	1	5	6	1					0.5	0.04
GHN-VTM-0500	1	10	32	1					0.5	
GHN-VTM-0501	1	4	43	1			3		0.5	
GHN-VTM-0502	1	3	41	1	5		5		0.5	
GHN-VTM-0503	1	7	38	1	2		2		0.5	
GHN-VTM-0504		8	22						0.7	0.03
GHN-VTM-0506	1	3	35	1			5		0.5	
GHN-VTM-0507	1	3	26	1			3		0.5	
GHN-VTM-0508	0.9	0	31	0.9			3		0.4	
GHN-VTM-0509	0.9	4	44	0.9	1		0		0.6	
GHN-VTM-0510	1	4	37	1	7		0		0.3	
GHN-VTM-0598	1	1	29	1					0.1	
GHN-VTM-0599	1	5	36	1	0		0		0.4	0.03
GHN-VTM-0602	0	5	47	1	0		3		0.5	0.03
GHN-VTM-0603	1	5	41	1	0		3		0.5	0.03
GHN-VTM-0604	1	5	23	1	0		0		0.5	0.03
GHN-VTM-0605	1	4	32	1					0.4	
GHN-VTM-0606	1	2	24	1			3		0.3	
GHN-VTM-0607	1	3	27	2			1		0.4	0.04
GHN-VTM-0610	1	3	20	1					0.03	
GHN-VTM-0611	1	3	38	1			0		0.4	
GHN-VTM-0612	1	5	20	1	2		0		0.5	
GHN-VTM-0613	1	4	30	1			0		0.6	
GHN-VTM-0614	1	3	46	1	2		6		0.7	0.03
GHN-VTM-0624	1	4	42	1	4		3		0.6	
GHR-VWL-0004	1	4	41	1	1				0.3	
GHR-VWL-0007	1	2	29	1			0.2		0.1	
GMG-PIT-0001	1	0.8	44	1					1	0.4
GMG-PIT-0006	1	1	1	1					0.2	0.03
GMG-PIT-0007	1	1	5	1					0.3	0.03
GMG-PIT-0009	1	3	7	2					0.4	0.04
GMG-PIT-0010	1	10	18	3					0.7	
GMG-PIT-0011	4	9	11	1					0.7	0.03
GMG-PIT-0014	0	4	23	1					0.6	0.04
GMG-PIT-0015	1	4	23	1					0.5	0.04
HAS-GJG-0001	1	1	24	1			2		0.1	
HAS-GJG-0002	1	0.3	24	1			0.4		0.1	
HAS-GJG-0004	1	4	19	1						
HAS-GJG-0005	1	3	17	1					0.5	
HAS-GJG-0006	5	12	14	10	0		0			
HAS-GJG-0007	0	9	24	8	0		0			
HAS-GJG-0008	0	16	32	0	0		0			
HAS-GJG-0009	1	2	56		0		0		1	
HAS-GJG-0010	0	6	36	5	0		0		1	
MID-AAF-0002	0	3	28	3			1		0.3	0.03
MID-AAF-0003	1	4	30	1			4		0.5	
MID-GJG-4001	1	5	23	3			3		0.4	0.03
MID-GMG-0014	1	9	1	1					0.7	
MID-GMG-0015	1	2	6	1					0.3	
MID-GMG-0016	1	6	1	1					0.6	
MID-GMG-0017	1	11	1	1					0.8	
MID-GMG-0018	1	5	20	1					0.5	

Sample	kaol	chlorite	illite	smectite	MixLayer	copiapite	jarosite	sph	rutile	zircon
	%	%	%	%	%	%	%	%	%	%
MID-GMG-0019	1	5	20	1					0.5	
MID-GMG-0020	1	4	28	1					0.6	
MID-GMG-0021	1	2	38	1					0.5	
MID-GMG-0022	1	3	24	1					0.3	
MID-GMG-0023	1	1	18	1					0.1	
MID-GMG-0024	1	4	16	1					0.4	
MID-GMG-0025	1	5	6	1					0.2	
MID-GMG-0026	1	7	2	1					0.1	
MID-KXB-0001	1	4	16	1			0.8		0.5	
MID-KXB-0003	1	1	18	1			0.5		0.2	
MID-VTM-4001	1	5	21	1			0		0.4	0.01
MIN-AAF-0001	2	2	29	1			2		0.3	0.04
MIN-AAF-0004	2	1	25	1			2		0.2	0.04
MIN-AAF-0010	1	2	33	1			3		0.5	0.03
MIN-AAF-0013	2	1	25	1			1		0.3	0.06
MIN-AAF-0015	2	1	26	2			1		0.4	0.04
MIN-GFA-0001	2	2	28	1			1		0.5	0.04
MIN-GFA-0003	2	3	25	1			0.01		0.3	0.03
MIN-GFA-0005	0	3	25	2			0		0.3	0.05
MIN-GFA-0006	3	3	21	1					0.3	0.04
MIN-GFA-0007	2	2	29	1			1		0.4	0.04
MIN-GFA-0009	2	1	27	1			1		0.3	0.04
MIN-SAN-0002	3	2	28	1	0		3		0.4	0.04
MIN-VTM-0002										
MIN-VTM-0003	1	2	15	1			0		0.3	0.04
MIN-VTM-0004	1	4	21	1			2		0.5	
MIN-VTM-0005										
MIN-VTM-0006	1	3	22	1			2		0.5	
MIN-VTM-0007	1	4	23	1			2		0.5	
MIN-VTM-0008	1	4	21	1			2		0.5	
MIN-VTM-0009	1	4	22	1			2		0.4	
MIN-VTM-0018	1	13	17	1					0.6	0.03
MIN-VTM-0019	1	14	9	1					0.8	0.04
MIN-VTM-0020	1	4	36	1					0.4	0.04
MIN-VTM-0021	2	4	41	2			0.1		0.4	0.03
PIT-KMD-0007	1	6	1	1					0.6	
PIT-KMD-0008	1	5	6	1					0.6	
PIT-KMD-0009	1	6	0.4	1					0.7	
PIT-KXB-0101	1	3	23	1					0.4	
PIT-LFG-0001	1	7	16	1			0		0.6	0.03
PIT-LFG-0003	0	5	18	7			0		0.3	0.03
PIT-LFG-0005	0	5	36	1			4		0.4	0.03
PIT-LFG-0007	1	1	25	1			2		0.1	0.06
PIT-LFG-0009	5	0.4	2	1			0.03		0.1	0.06
PIT-LFG-0013	2	3	30	1			5.6		0.6	0.03
PIT-RDL-0001	1	0.7	16	1					0.1	0.06
PIT-RDL-0002	1	0.6	10	1					0.1	0.06
PIT-RDL-0003	1	1	23	1			1		0.1	
PIT-RDL-0004	1	1	27	1					0.2	
PIT-RDL-0005	3	0.7	16	2			1		0.1	0.04
PIT-RDL-0006	1	1	19	3			1		0.1	0.06
PIT-RDL-0007	0	1	24	1			0.9		0.1	0.06
PIT-VCV-0001	0	2	18	0	0		0		0.7	0.03
PIT-VCV-0002	0	2	20	0	0		0		0.4	0.06
PIT-VCV-0003	0.8	3	18	0.8			0		0.8	0.03
PIT-VCV-0004	1	1	21	1			0.06		0.1	0.06
PIT-VCV-0005	1	1	24	1			1		0.1	0.06
PIT-VCV-0006										
PIT-VCV-0007	1	2	22	1			0.01		0.6	0.04
PIT-VCV-0008	0.9	0.3	25	0.9			0.2		0.5	
PIT-VCV-0009	0.9	3	22	0.9			0.06		0.6	0.04
PIT-VCV-0010	0.9	3	10	0.9	0		0		0.5	0.04
PIT-VCV-0011	1	3	14	1	0		0		0.5	0.04
PIT-VCV-0012	1	2	24	0.9			0		0.3	0.03
PIT-VCV-0013	0	1	28	0	0		0		0.3	0.03
PIT-VCV-0014	1	2	26	1	0		0		0.3	0.03
PIT-VCV-0015	1	0.6	3	1			0		0.2	0.01
PIT-VCV-0016	1	3	10	1			0		0.8	0.07
PIT-VCV-0017	1	2	15	1			0		0.5	0.04
PIT-VCV-0018	1	1	9	1			0		0.3	0.03
PIT-VCV-0019	1	0.4	55	1			3		0.7	0.03
PIT-VCV-0020	1	0.8	41	1	0		0		0.8	0.03
PIT-VCV-0021	1	12	18	1			3		0.9	
PIT-VCV-0022	1	9	8	1			0.3		0.9	0.03
PIT-VCV-0023	1	4	17	1			1		1	0.02
PIT-VCV-0024	0	6	32	0			0		0.7	0.03

Sample	kaol	chlorite	illite	smectite	MixLayer	copiapite	jarosite	sph	rutile	zircon
	%	%	%	%	%	%	%	%	%	%
PIT-VCV-0025	1	2	29	1			0		0.5	0.04
PIT-VCV-0026	1	3	29	1			0		0.5	0.04
PIT-VCV-0027	1	4	25	1			0		0.6	0.03
PIT-VCV-0028	0	0.4	0.1	0			0		0.2	0.01
PIT-VCV-0029	1	4	22	1			0		0.6	0.03
PIT-VCV-0030	0	4	27	0			0		0.6	0.03
PIT-VTM-0001	1	6	18	1					0.6	0.03
PIT-VTM-0002	1	6	4	1					0.5	0.03
PIT-VTM-0004	1	8	16	1					0.6	
PIT-VTM-0005	1	2	29	1					0.2	0.04
PIT-VTM-0006	1	1	22	1					0.1	
PIT-VTM-0007	1	1	27	1					0.1	
PIT-VTM-0008	1	0.8	16	1					0.2	
PIT-VTM-0009	1	0.3	34	1					0.2	
PIT-VTM-0010	1	7	1	1					1	
PIT-VTM-0600	1	6	11	1			0		0.6	0.03
PIT-VWL-0001	1	0.5	12	1					0.1	
PIT-VWL-0007	1	1	30	1						
PIT-VWL-0009	1	2	15	1					0.5	
QPS-AAF-0003	1	4	28	1	0		3		0.5	0.03
QPS-AAF-0005	3	4	29	0.9			3		0.5	0.03
QPS-AAF-0008	0.9	3	37	0.9			4		0.6	
QPS-AAF-0009	2	3	34	0.9			3		0.6	0.03
QPS-AAF-0022	1	4	32	1			3		0.6	
QPS-SAN-0002	1	3	31	3	0		4		0.4	0.04
QPS-VTM-0001	1	3	25	3			0.3		0.4	0.03
QPS-VTM-4001	2	4	27	2		0.01	2		0.5	0.03
ROC-KMD-0001	1	8	13	1			0		0.6	
ROC-NWD-0001	0	0	0	0					0.1	0.07
ROC-NWD-0002	1	5	10	3			0.7		0.8	0.03
ROC-NWD-0003	0	0	0	0					0.1	0.07
ROC-VTM-0032	1	0.01	10	16			0		0.4	0.04
ROC-VTM-0033	1	0	4	1					0.4	0.04
SCS-LFG-0001	5	10	30	15			0			
SCS-LFG-0002	1	5	19	2	2		0.8		0.5	0.03
SCS-LFG-0003	1	4	37	1	2				0.6	0.03
SCS-LFG-0004	5	5	26	24	0		0			
SCS-LFG-0005	1	6	35	3	2		3		0.6	0.03
SCS-LFG-0006	1	5	19	1	9		1		0.6	0.03
SCS-LFG-0007	0.2	6	10	1			0		0.6	0.03
SCS-LFG-0008	1	0.4	33	1			0.4		0.5	0.03
SGS-ESO-0101	1	6	12	1					0.6	
SGS-VTM-0024	2	4	29	2			7		0.5	0.02
SGS-VTM-0026	2	5	33	2			5		0.6	
SGS-VTM-0605	1	4	19	1			1		0.6	
SPR-AAF-0001	1	10	9	3			0.01		0.7	0.03
SPR-AAF-0003	1	9	12	3			0		0.7	0.03
SPR-JWM-0002	1	9	5	3			0.01		0.6	0.03
SPR-KMD-0001	1	5	10	7			0.01		0.7	0.04
SPR-KMD-0002	1	9	10	1			0		0.7	0.03
SPR-KMD-0003	4	2	7	1			0		0.5	0.03
SPR-OTH-0001	1	6	10	1			0		0.6	0.03
SPR-OTH-0002	1	4	6	2			0		0.6	0.03
SPR-SAN-0002	1	8	14	3			0.03		0.6	
SPR-VTM-0001	1	6	6	1			0		0.5	0.03
SPR-VTM-0002	1	6	1	1					0.6	0.03
SPR-VTM-0005	1	7	4	1			0		0.6	
SPR-VTM-0010	1	10	9	1			0		0.7	
SPR-VTM-0012	2	0	26	2			0.6		0.1	0.06
SPR-VTM-0014	1	0.7	26	1			0.6		0.1	
SPR-VTM-0017	2	0	24	5			1		0.3	0.04
SPR-VTM-0019	2	0	20	3			0.6		0.1	0.06
SPR-VTM-0021	2	0	20	4			0		0.2	0.06
SSS-AAF-0001	3	6	27	3			0.6		0.4	0.03
SSS-EHP-0002	2	4	9	2			0		0.5	0.05
SSS-EHP-0003	3	2	11	2			0		0.4	0.3
SSS-EHP-0004	3	4	23	1			0		0.5	0.03
SSS-EHP-0023	1	1	3	3	2					
SSS-EHP-0032	2	2	16	2			0.6		0.3	
SSS-EHP-0033	1	3	14	2			0		0.3	
SSS-EHP-0034	1	3	14	3			0		0.3	
SSS-GMG-0009	1	4	8	1					0.5	
SSS-GMG-0010	1	3	20	1					0.5	
SSS-GMG-0011	1	3	20	1					0.5	
SSS-GMG-0012	1	7	11	1					0.7	
SSS-GMG-0013	1	5	8	1					0.4	

Sample	kaol	chlorite	illite	smectite	MixLayer	copiapite	jarosite	sph	rutile	zircon
	%	%	%	%	%	%	%	%	%	%
SSS-GMG-0014	1	3	26	1					0.2	
SSS-GMG-0015	1	2	18	1					0.2	
SSS-GMG-0016	1	3	14	1					0.4	
SSS-KMD-0001	1	5	15	2			0		0.5	0.03
SSS-KMD-0002	1	7	6	1			0	0.01	0.6	0.03
SSS-VEV-0001	1	0.3	20	1	2				0.1	
SSS-VTM-0005	1	1	12	1					0.1	
SSS-VTM-0600	7	2	18	1			0.6		0.4	0.04
SSW-AAF-0001	1	5	14	5			0.5			
SSW-AAF-0002	1	4	29	1					0.4	
SSW-AAF-0005	1	0.4	25	3			3		0.6	0.03
SSW-AAF-0007	1	4	23	4			2		0.4	0.03
SSW-AAF-1002	1	6	11	1					6	0.03
SSW-AAF-1005	1	3	32	2			4			
SSW-AAF-1009	2	5	16	2			2			
SSW-GJG-4000	1	6	23	2		0.01	1		0.5	0.03
SSW-KMD-0001	1	6	18	2			0		0.5	0.03
SSW-SAN-0002	1	5	23	4	0		4		0.5	0.03
SSW-SAN-0006	1	3	23	1	0		5		0.4	0.04
SSW-VTM-0006	1	5	25	2		0.01	0.3		0.4	0.03
SSW-VTM-0008	1	5	26	3		0.01	4		0.4	0.03
SSW-VTM-0010	2	2	25	3		0.01	5		0.4	0.04
SSW-VTM-0012	2	2	14	3		0.01	0		0.4	0.04
SSW-VTM-0013	1	4	24	1		0.01	5		0.4	0.03
SSW-VTM-0015	1	5	14	4		0.01	4		0.5	0.03
SSW-VTM-0016	1	5	19	1					0.8	
SSW-VTM-0019	1	5	20	1					0.5	
SSW-VTM-0023	1	5	24	1					0.5	
SSW-VTM-0027	2	6	23	2			0.7		0.5	0.03
SSW-VTM-0028	1	6	27	1			1		0.5	
SSW-VTM-0030	1	5	23	2			3.5		0.6	0.03
SSW-VTM-0032	1	5	28	1			1		0.5	
SSW-VTM-4001	1	6	22	1		0.01	2		0.4	0.03
SWH-GJG-0001	1	4	16	1					0.5	
SWH-GJG-0002	1	6	36	1			3		0.8	
SWH-GJG-0003	1	6	36	1					0.8	
SWH-GJG-0004	1	2	19	1			4		0.1	
SWH-GJG-0005	1	2	19	1			1		0.4	
SWH-GJG-0006	1	2	19	1			0.6		0.4	
SWH-GJG-0007	1	2	32	1					0.5	
SWH-GJG-0008	3	3	10	4			0.8		0.3	
SWH-GJG-0009	3	0	10	8	0		0			
SWH-GJG-0010	5	1	23	9			0			
SWH-GJG-0011	0	9	3	3			0			
SWH-GJG-0012	0	0.6	16	7	0		0			
SWH-GJG-0013	5	0.6	41	1	0		0.5		0.5	
SWH-GJG-0014	1	0.7	46	6	0				0.9	
SWH-GJG-0015	7	0	27	14	0					
SWH-GJG-0019	1	3	27	1			3		0.1	
SWH-GJG-0020	2	11	8	6	0					
SWH-GJG-0021	0	7	20	7	0					
SWH-GJG-0022	0	7	42	7	0					
SWH-GJG-0023	1	3	32	1			3		0.1	
SWH-GJG-4000	1	4	25	2		0.01	3.6		0.5	0.03
SWH-VTM-4001	1	5	22	3		0.01	2		0.4	0.03
average	1.210981308	3.761418605	19.47906977	1.79135514	0.810810811	0.028028169	0.940730897	0.04125	0.446512195	0.084569288
RSQ w/ F as x values	0.000818515	0.032217026	1.39899E-05	0.001548365	0.014676736	0.000988711	0.002497272	0.032308736	0.020851476	9.87058E-05
Pearson coeff of F	-0.028609696	0.179491018	0.003740305	-0.039349269	-0.121147581	0.031443777	-0.049972711	-0.179746311	0.144400402	-0.009935079
count	428	430	430	428	74	71	301	16	410	267

APPENDIX 3 – CORRELATION PLOTS

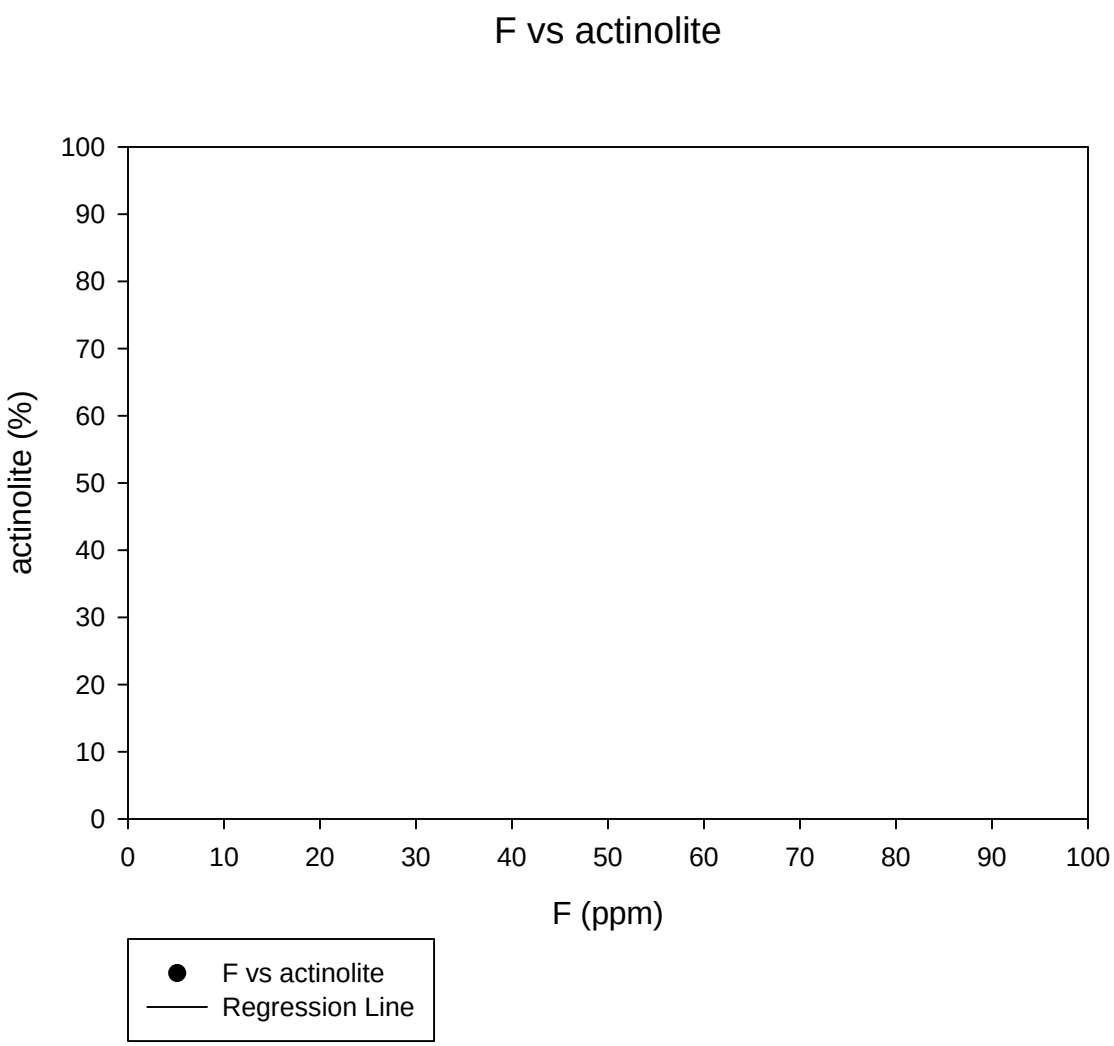
F vs actinolite
actinolite (%)
100
90
80
70
60
50
40
30
20
10
0
0
10
20
30
40
50
60
70
80
90
100
F (ppm)
F vs actinolite
Regression Line

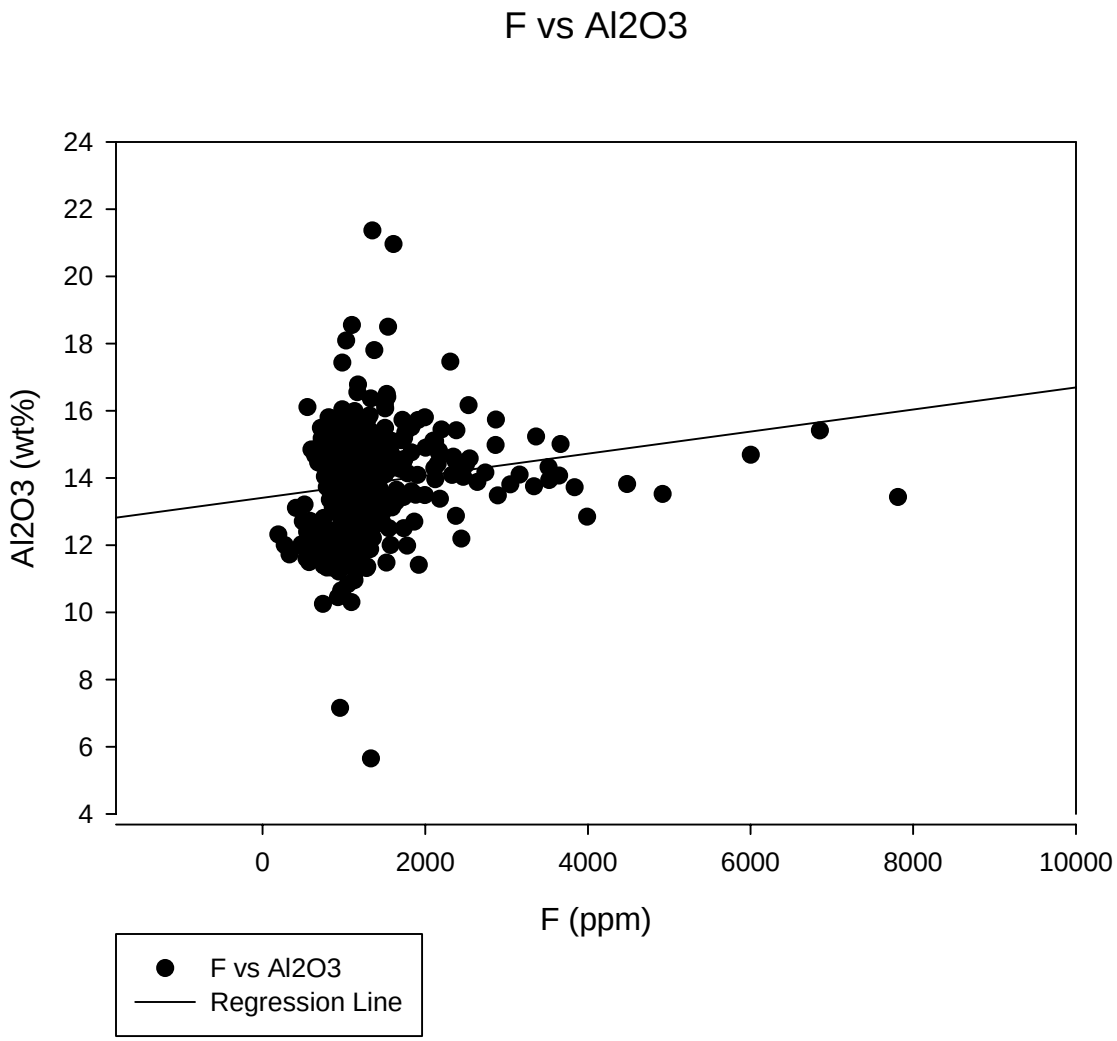
F vs Al2O3
Al2O3 (wt%)
24
22
20
18
16
14
12
10
8
6
4
0
2000
4000
6000
8000
10000
F (ppm)
F vs Al2O3
Regression Line

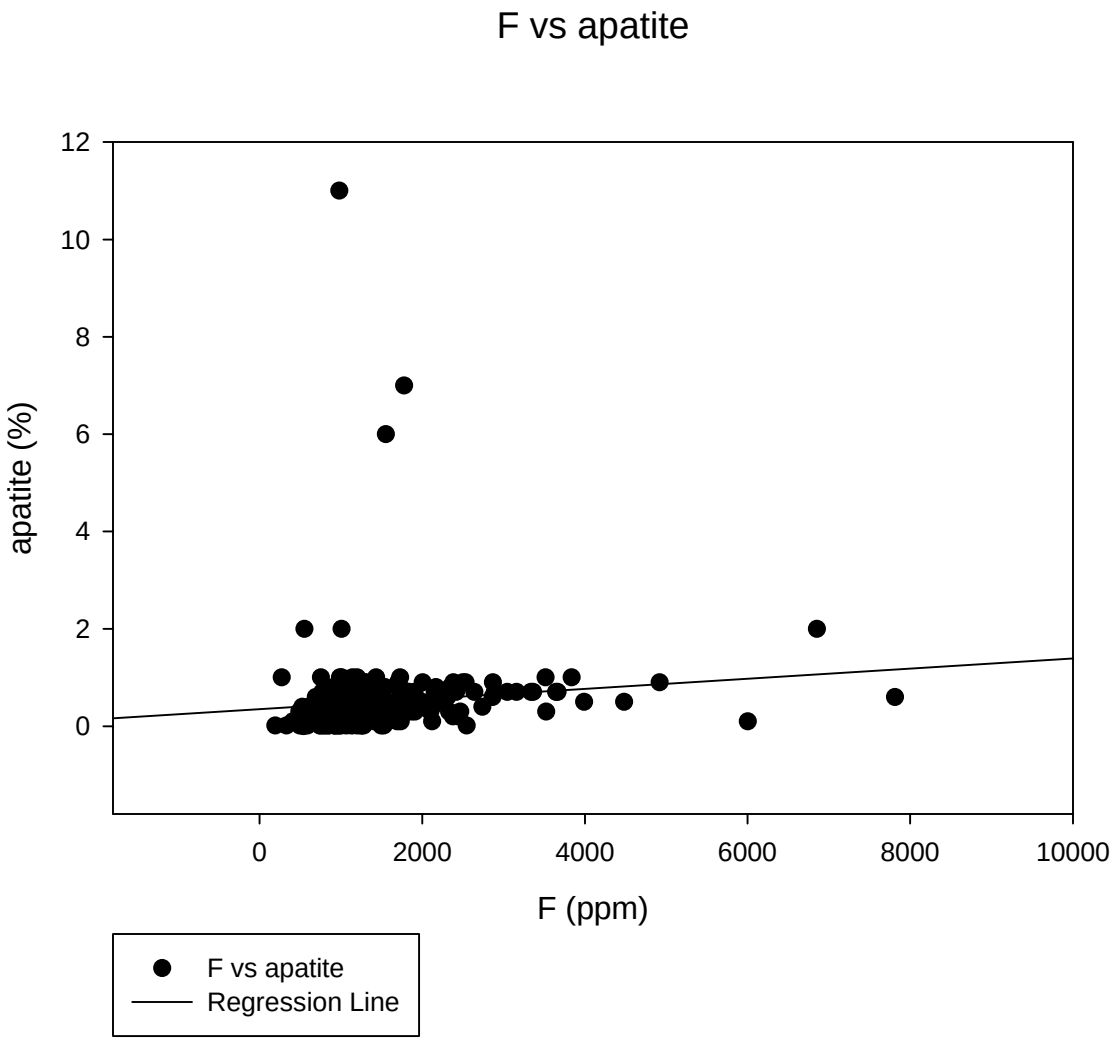
F vs apatite
12
10
8
6
4
2
0
apatite (%)
0
2000
4000
6000
8000
10000
F (ppm)
F vs apatite
Regression Line

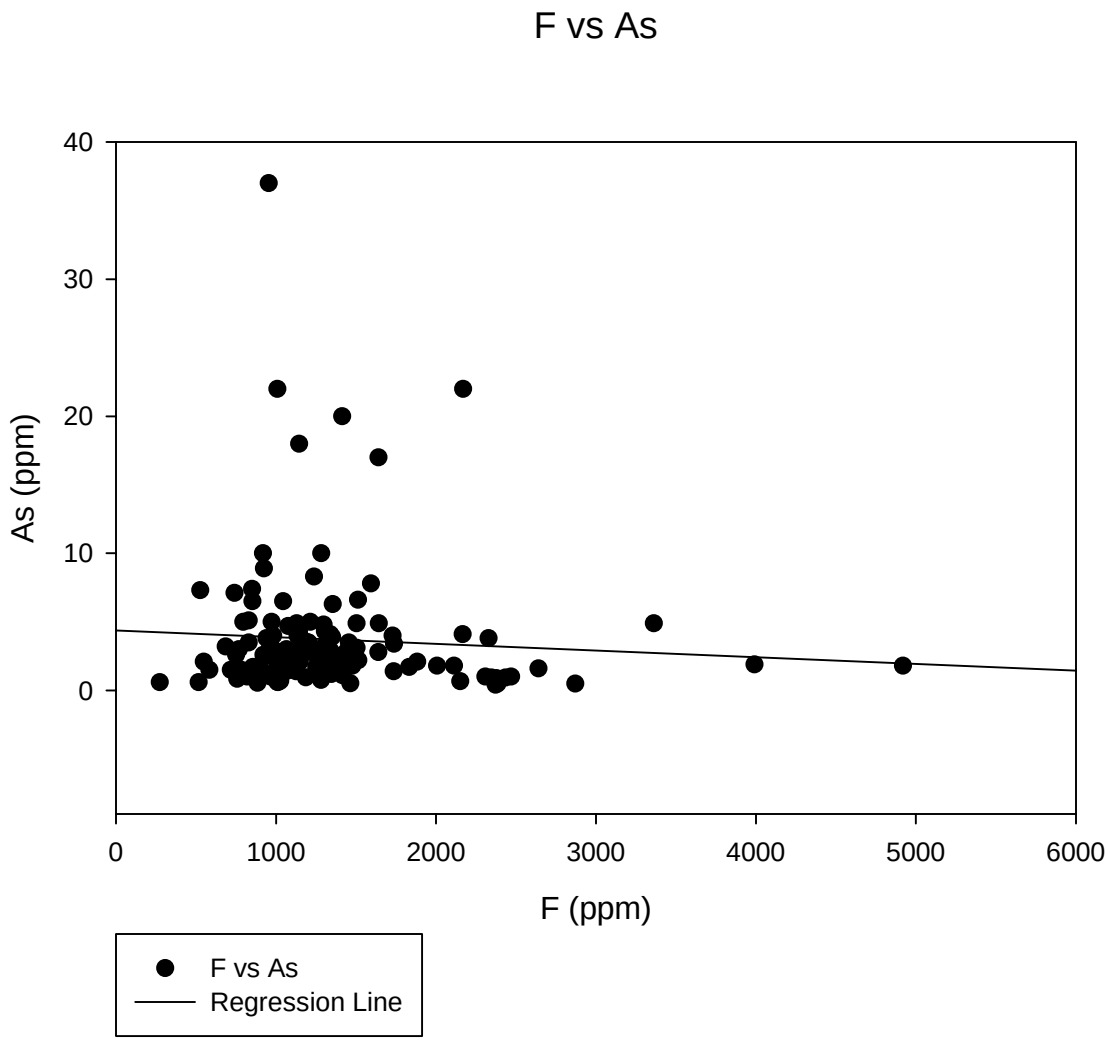
F vs As
40
30
20
10
0
As (ppm)
0
1000
2000
3000
4000
5000
6000
F (ppm)
F vs As
Regression Line

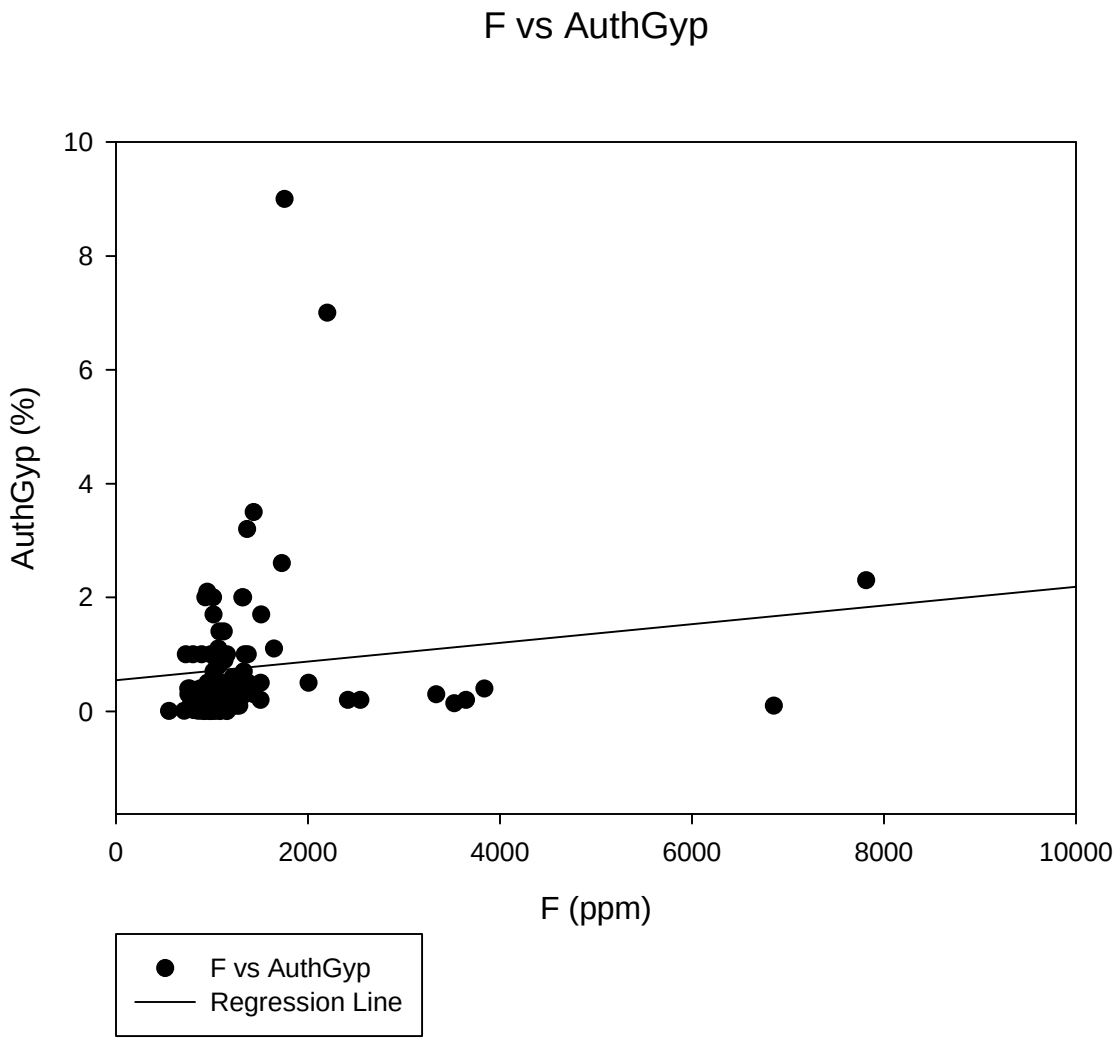
F vs AuthGyp
AuthGyp (%)
10
8
6
4
2
0
0
2000
4000
6000
8000
10000
F (ppm)
F vs AuthGyp
Regression Line

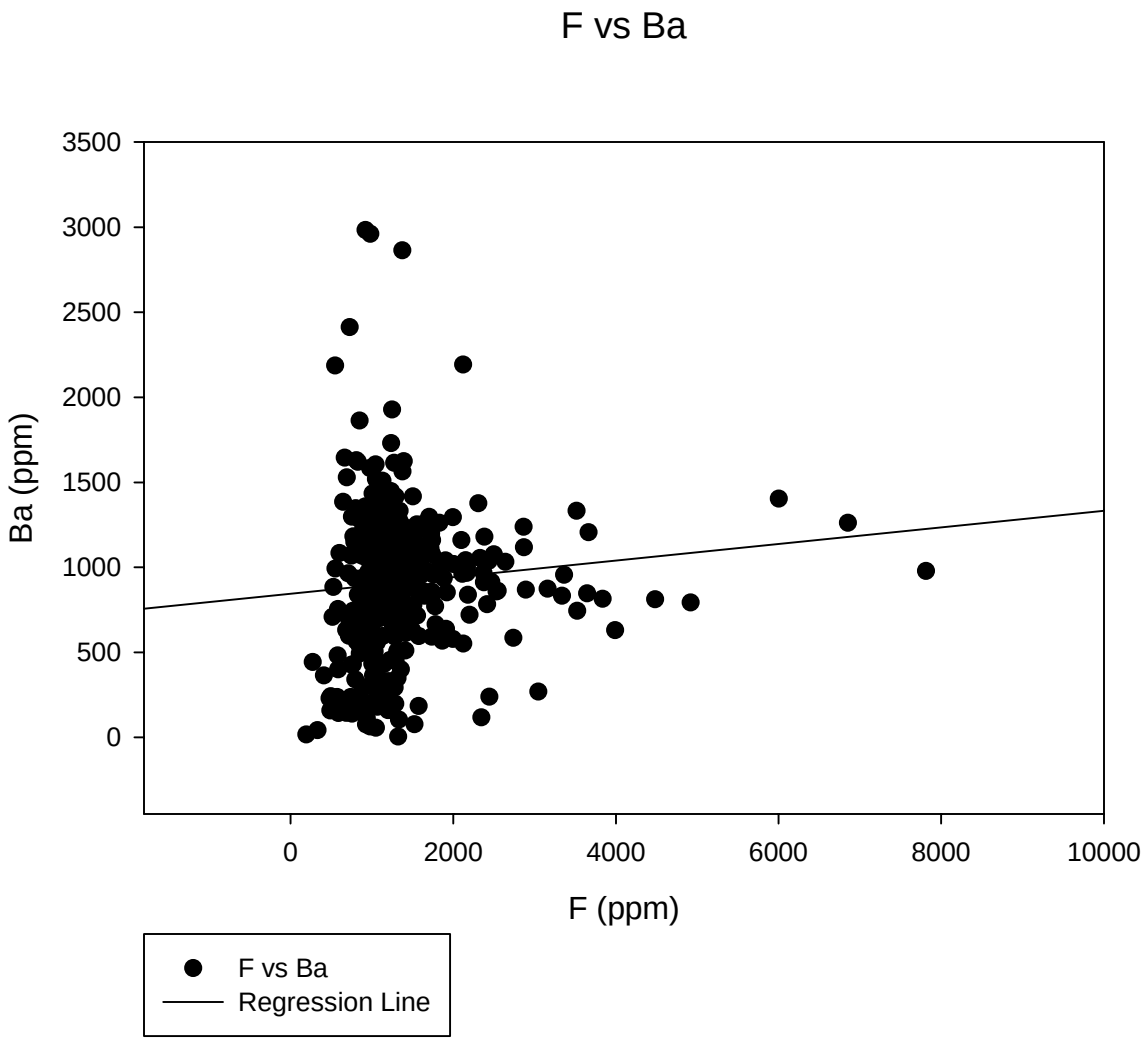
F vs Ba
3500
3000
2500
2000
1500
1000
500
0
Ba (ppm)
0
2000
4000
6000
8000
10000
F (ppm)
F vs Ba
Regression Line

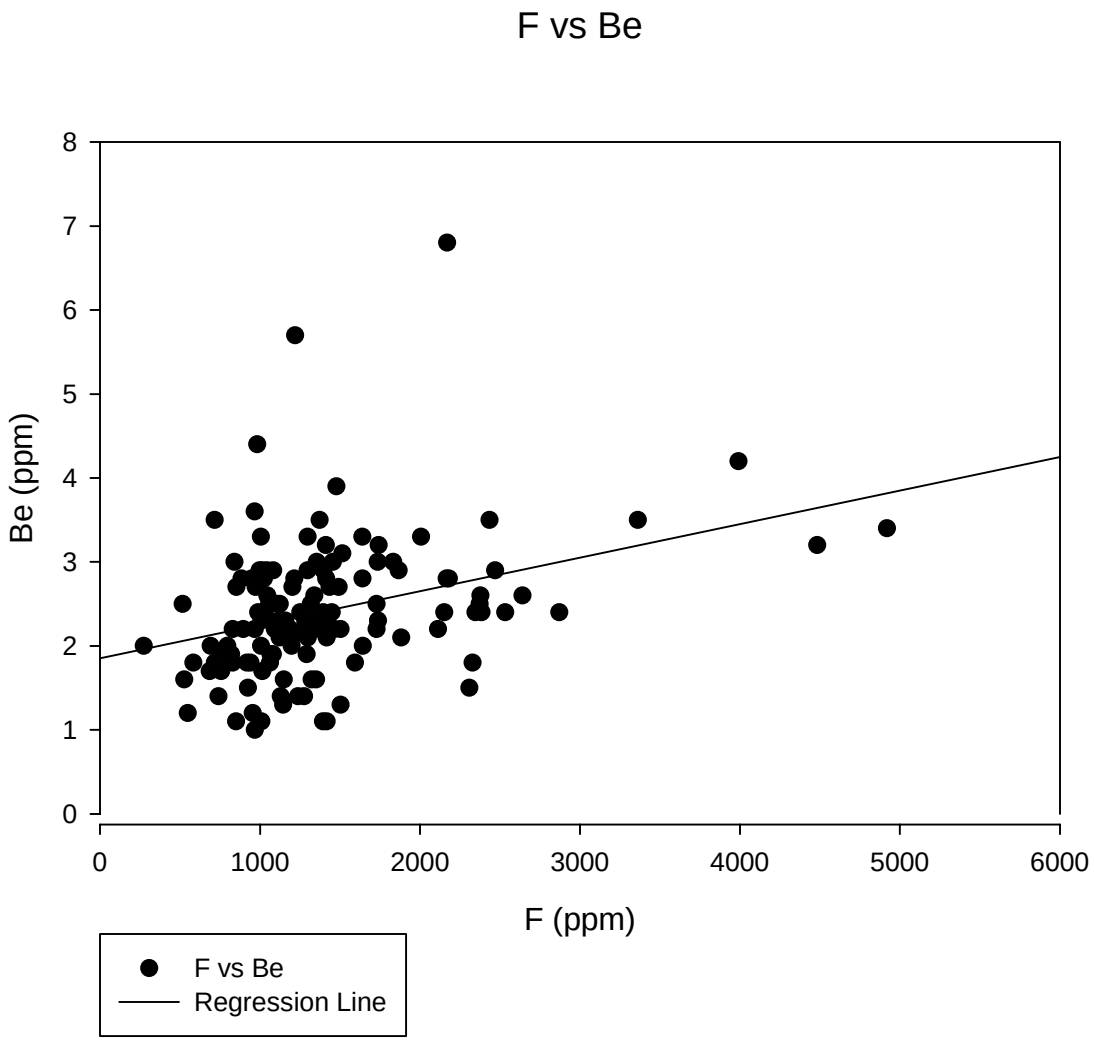
F vs Be
Be (ppm)
F (ppm)
0
1
2
3
4
5
6
7
8
0
1000
2000
3000
4000
5000
6000
F vs Be
Regression Line

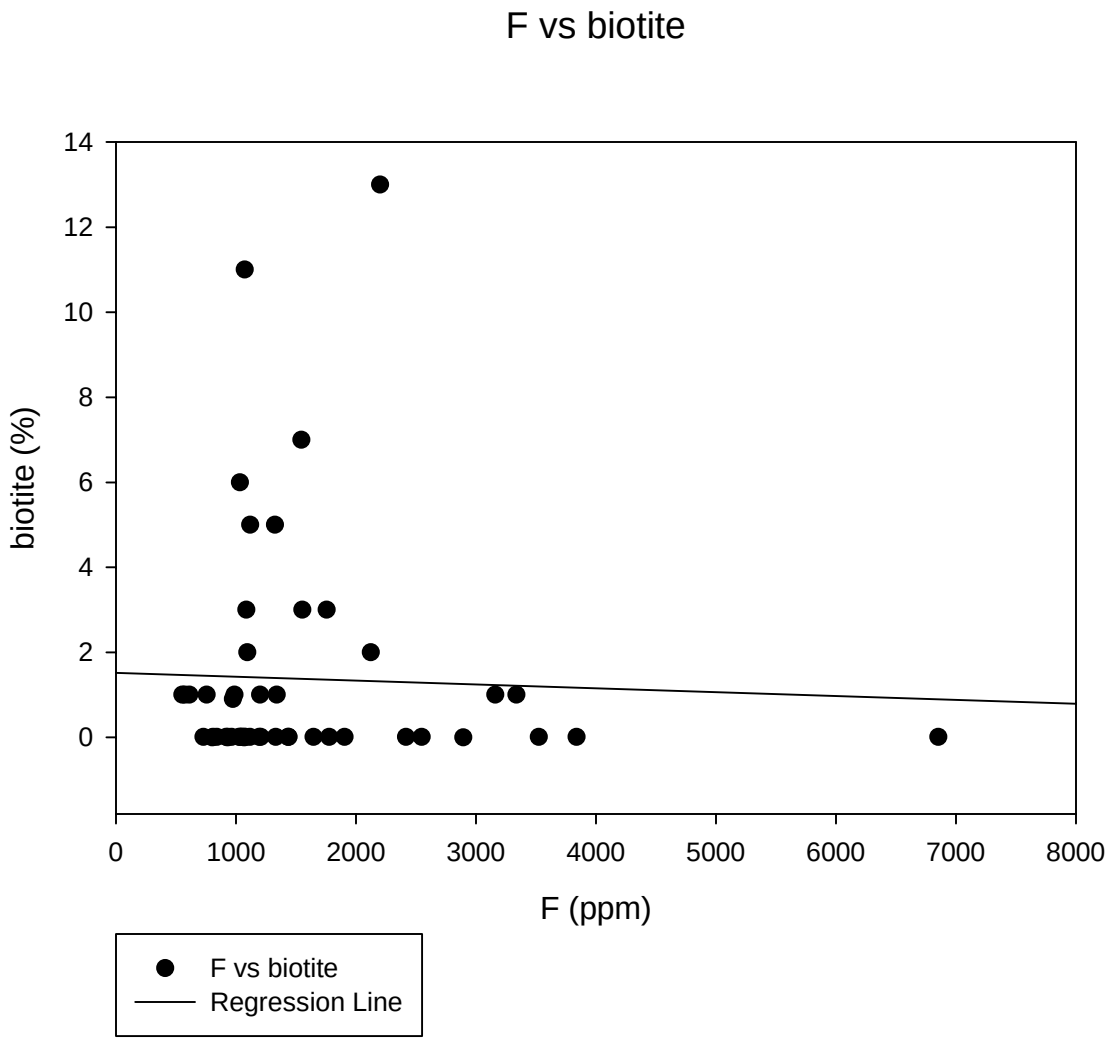
F vs biotite
biotite (%)
14
12
10
8
6
4
2
0
0
1000
2000
3000
4000
5000
6000
7000
8000
F (ppm)
F vs biotite
Regression Line

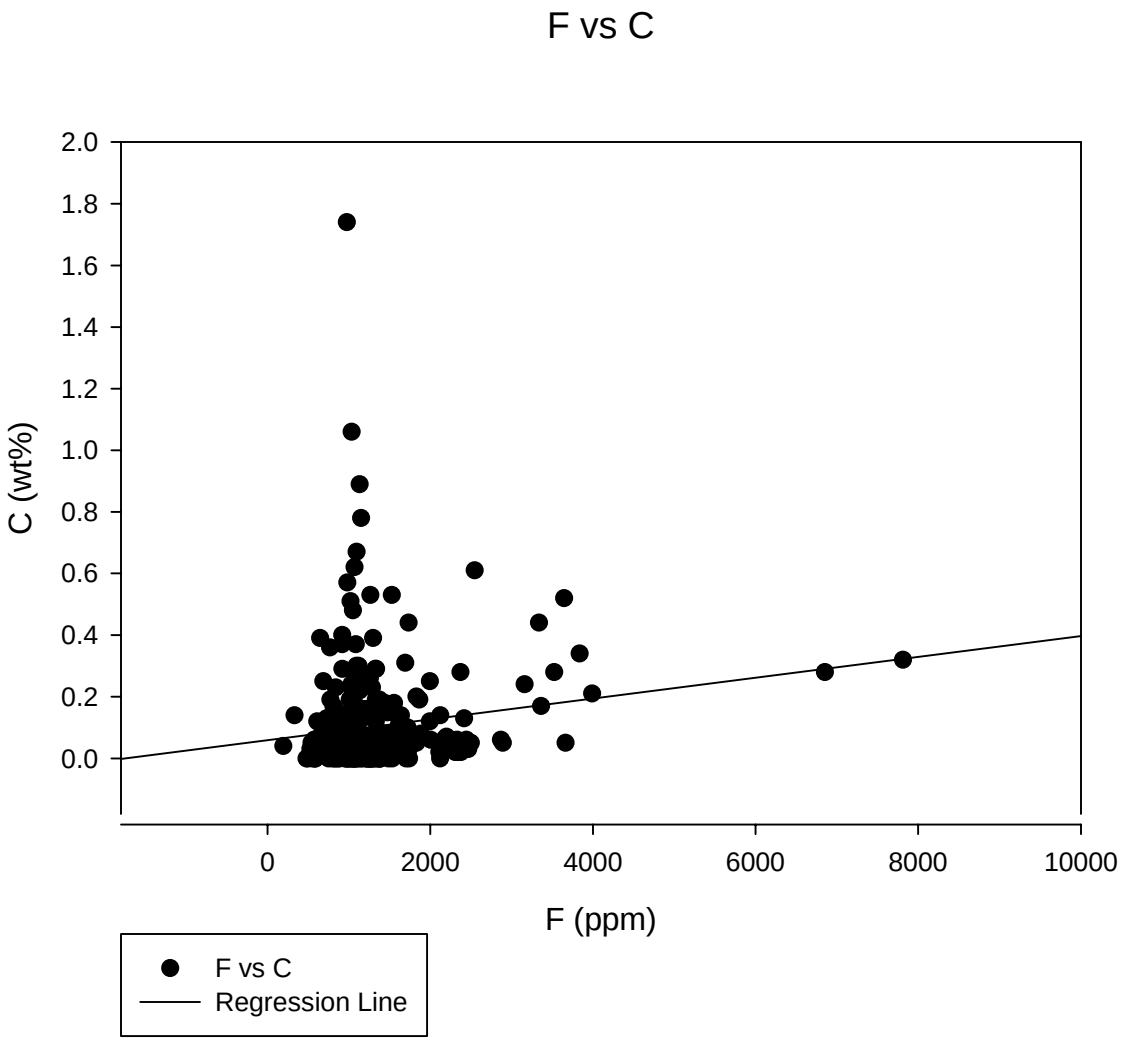
F vs C
2.0
1.8
1.6
1.4
1.2
1.0
0.8
0.6
0.4
0.2
0.0
C (wt%)
0
2000
4000
6000
8000
10000
F (ppm)
F vs C
Regression Line

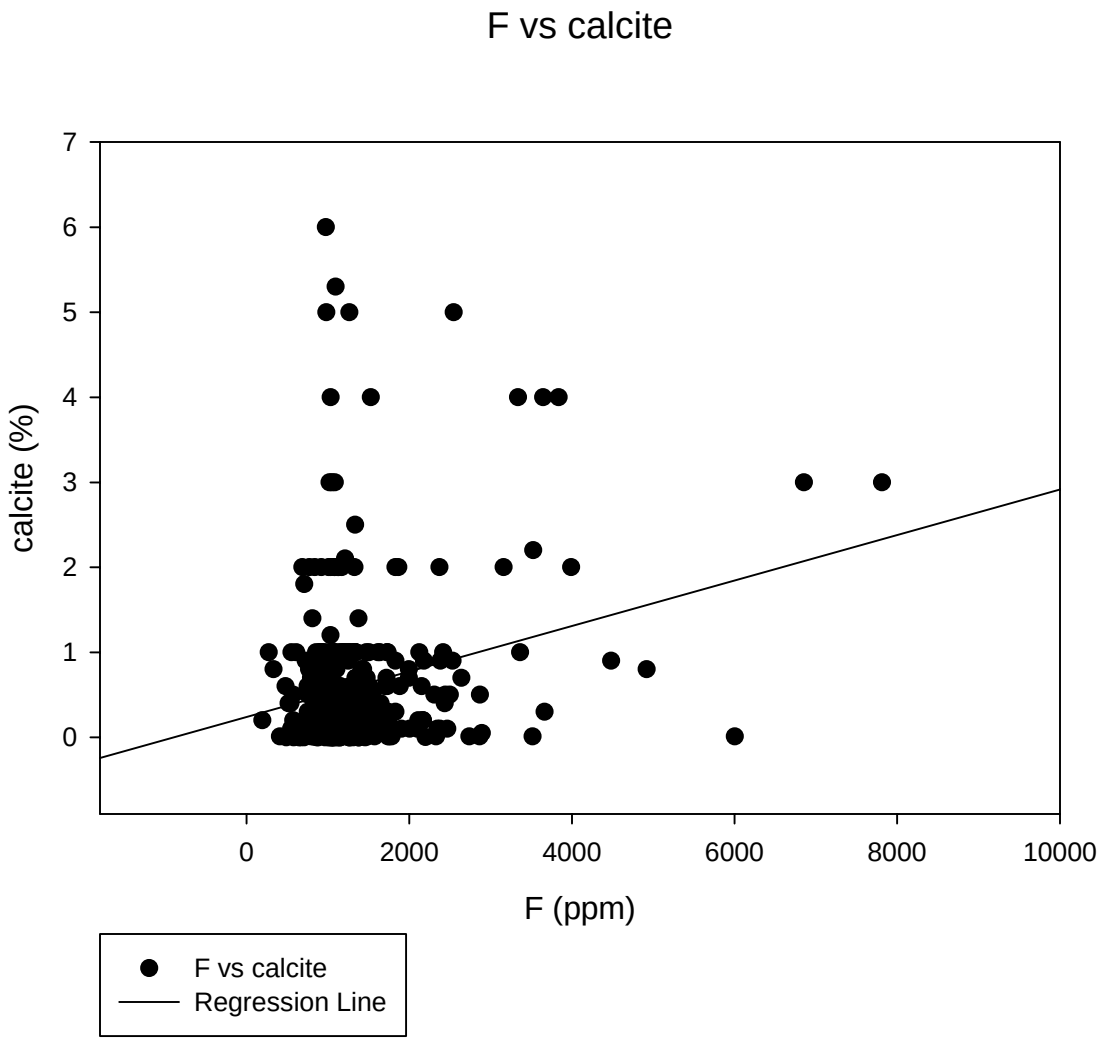
F vs calcite
calcite (%)
7
6
5
4
3
2
1
0
0
2000
4000
6000
8000
10000
F (ppm)
F vs calcite
Regression Line

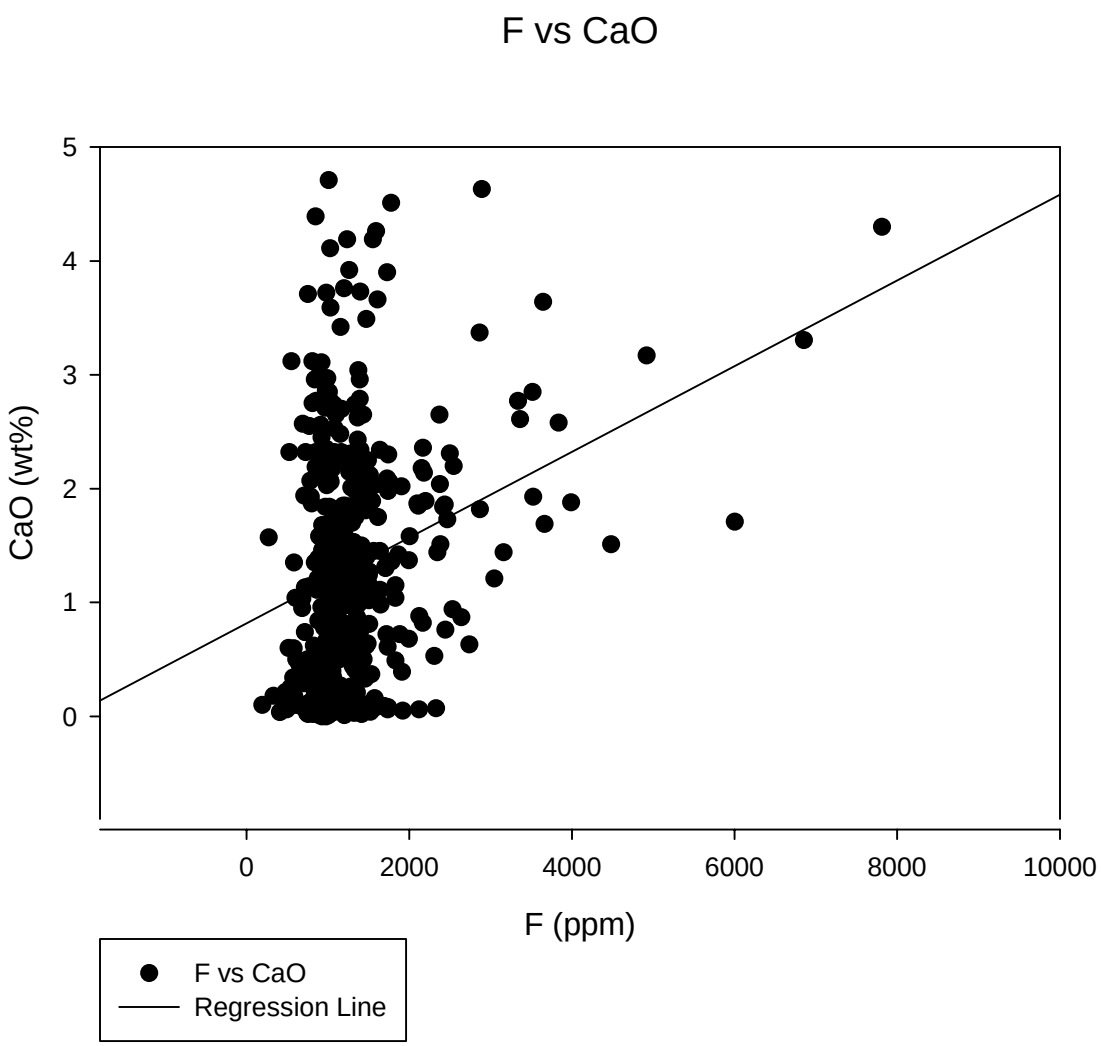
F vs CaO
CaO (wt%)
5
4
3
2
1
0
0
2000
4000
6000
8000
10000
F (ppm)
F vs CaO
Regression Line

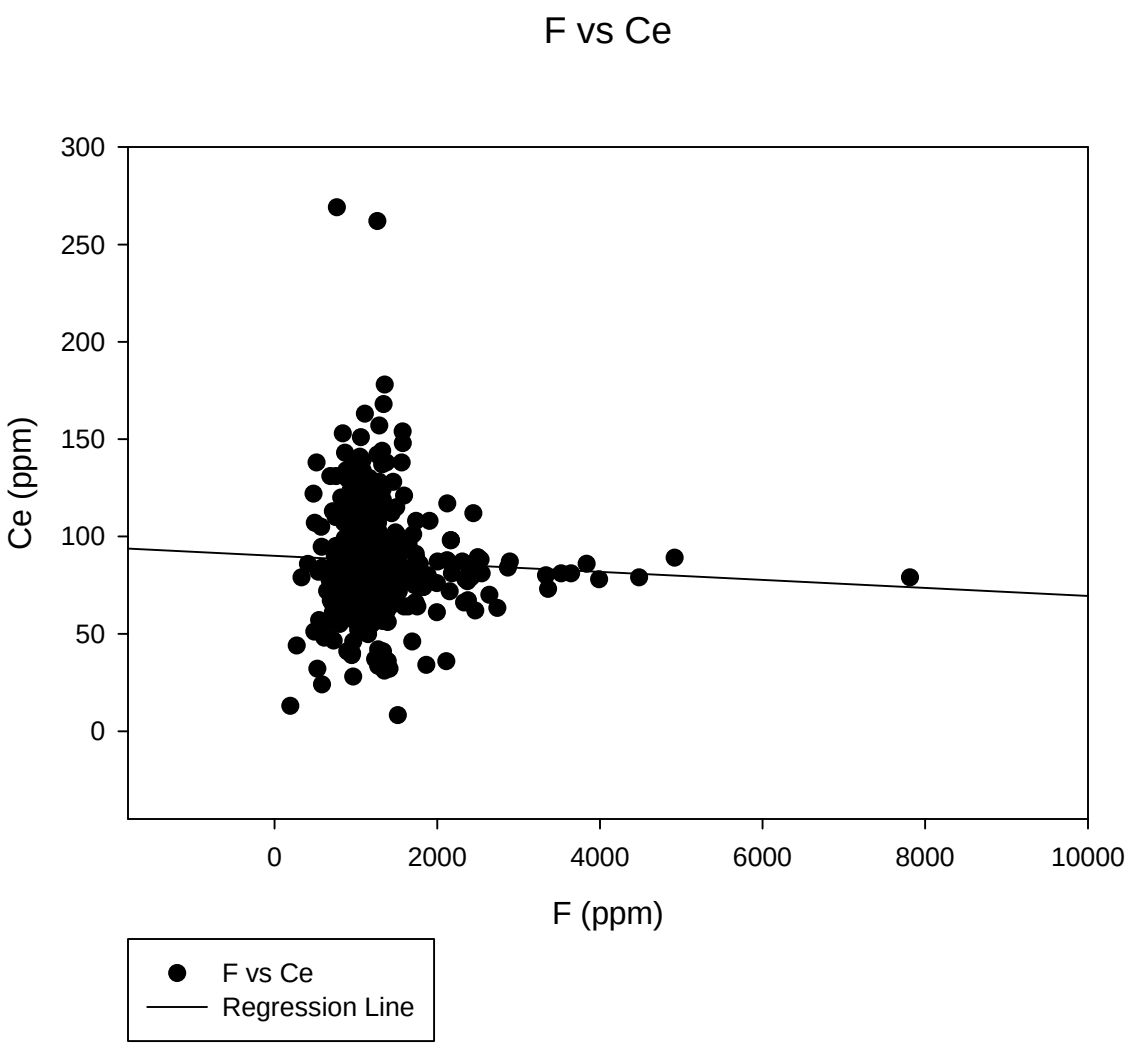
F vs Ce
300
250
200
150
100
50
0
Ce (ppm)
0
2000
4000
6000
8000
10000
F (ppm)
F vs Ce
Regression Line

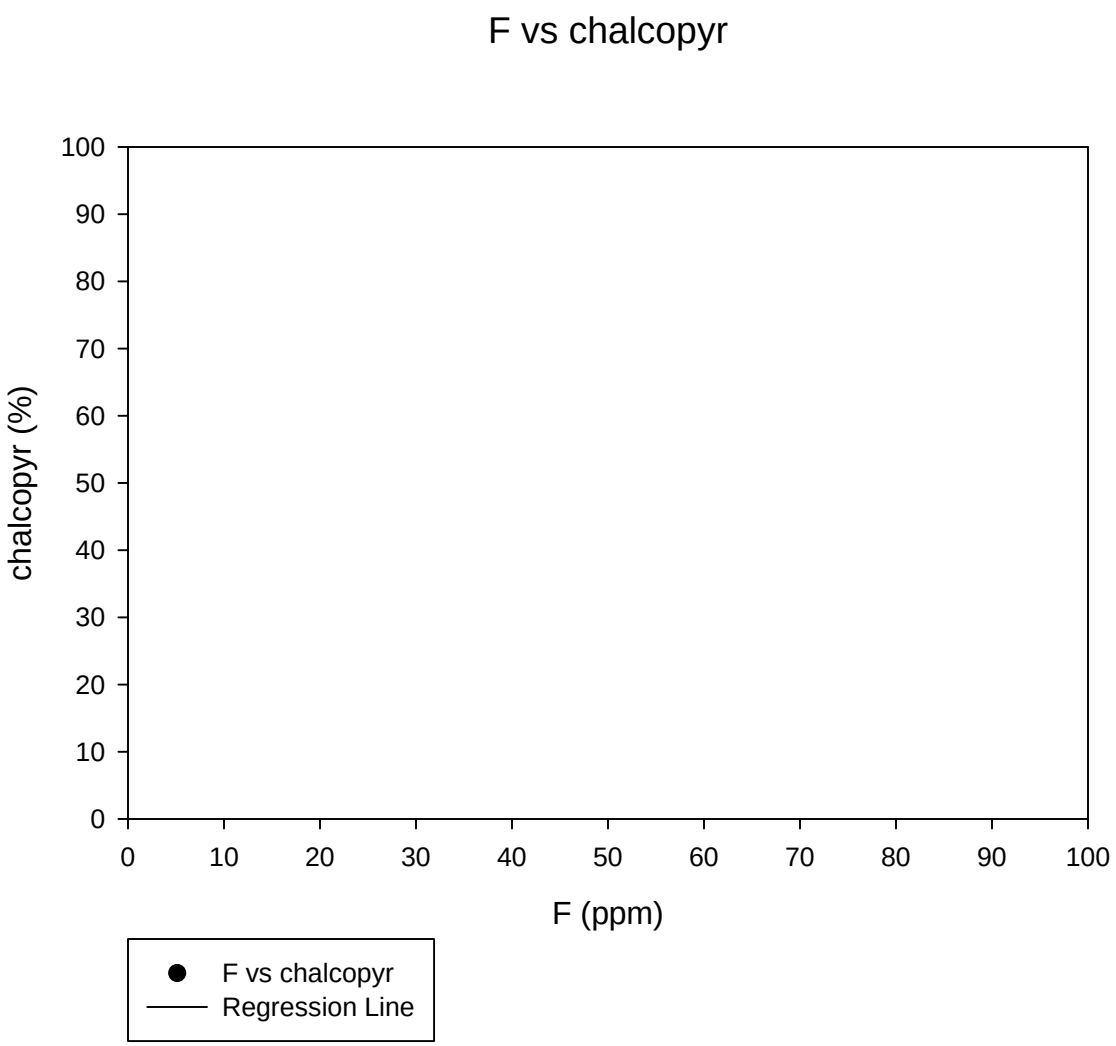
F vs chalcopyr
chalcopyr (%)
100
90
80
70
60
50
40
30
20
10
0
0
10
20
30
40
50
60
70
80
90
100
F (ppm)
F vs chalcopyr
Regression Line

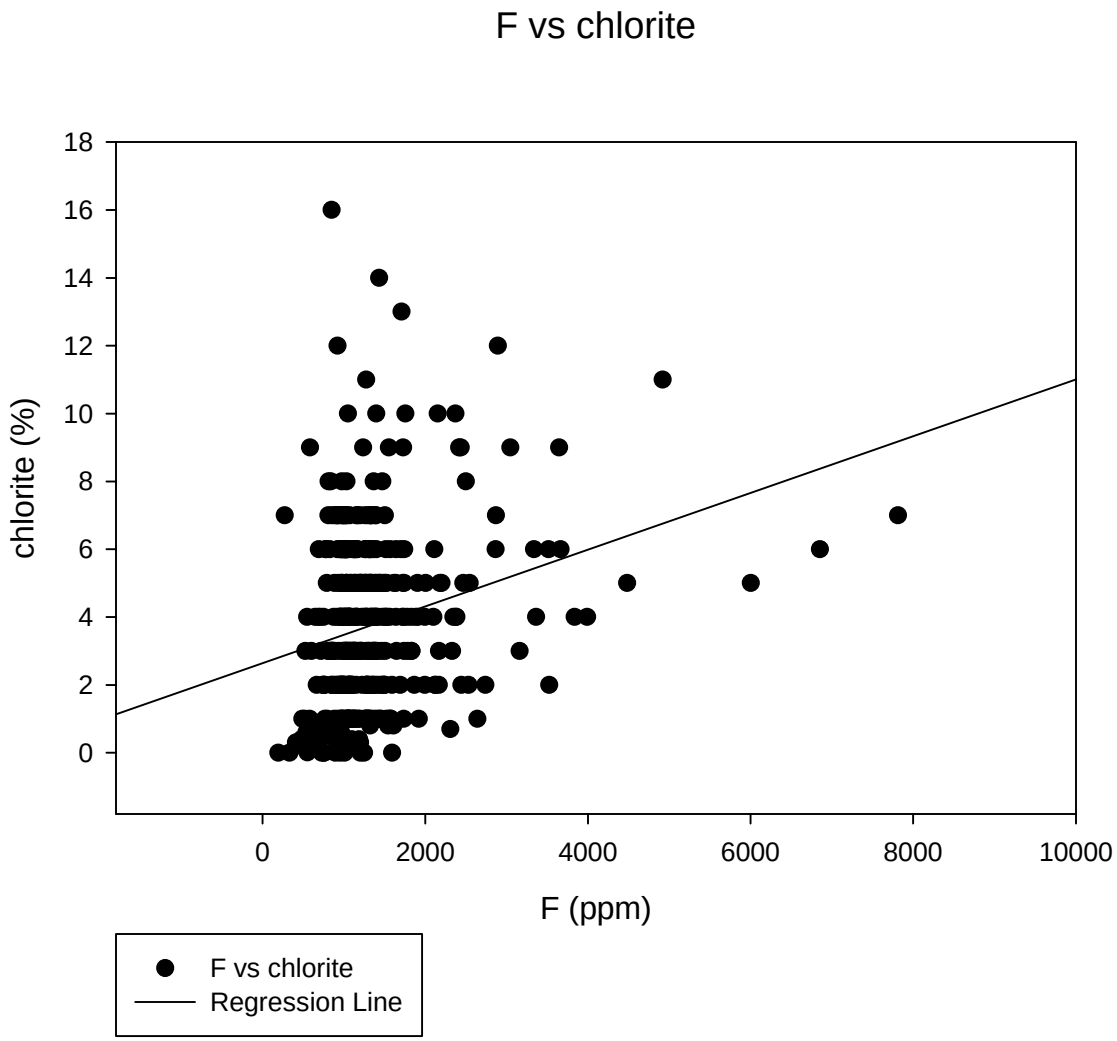
F vs chlorite
chlorite (%)
18
16
14
12
10
8
6
4
2
0
0
2000
4000
6000
8000
10000
F (ppm)
F vs chlorite
Regression Line

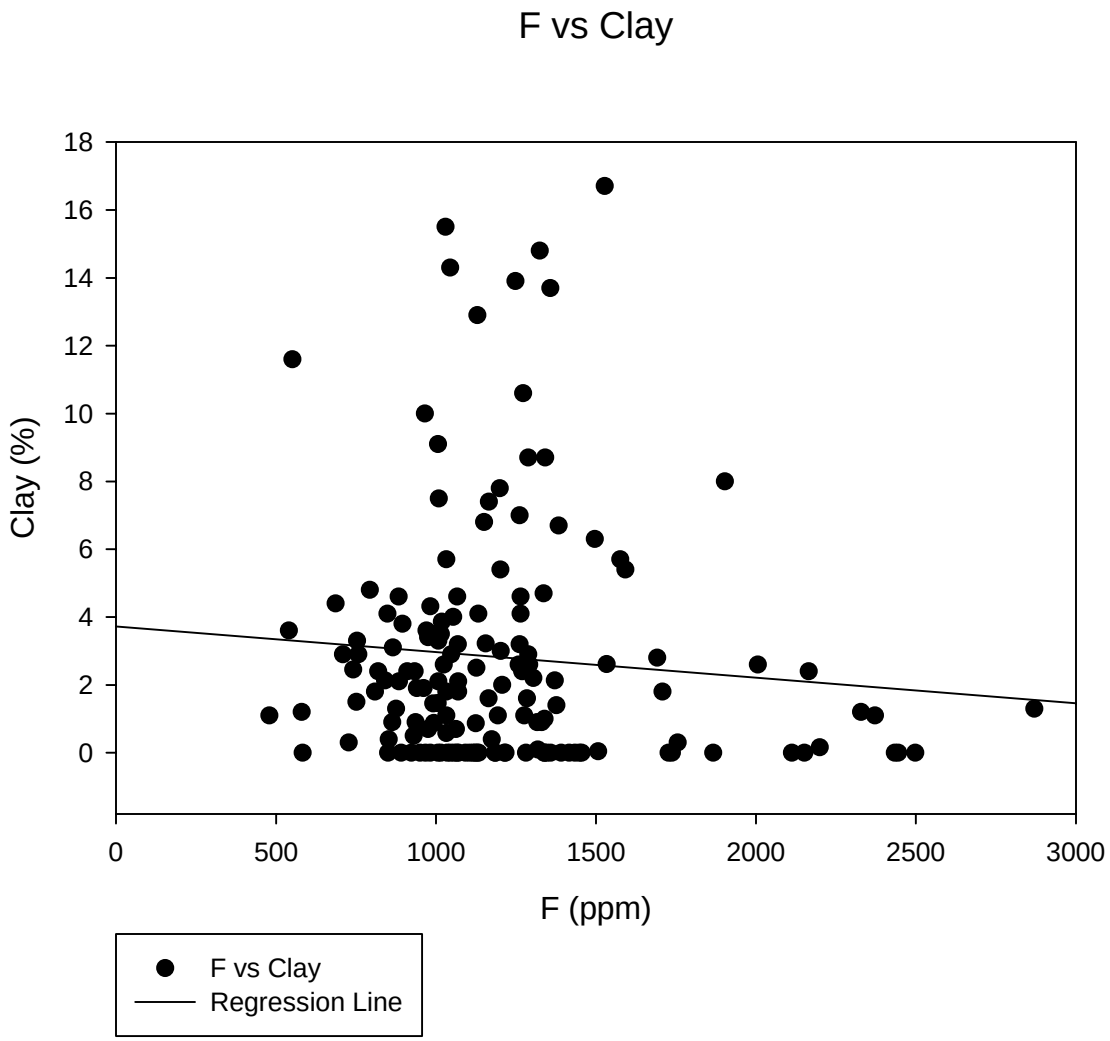
F vs Clay
Clay (%)
18
16
14
12
10
8
6
4
2
0
0
500
1000
1500
2000
2500
3000
F (ppm)
F vs Clay
Regression Line

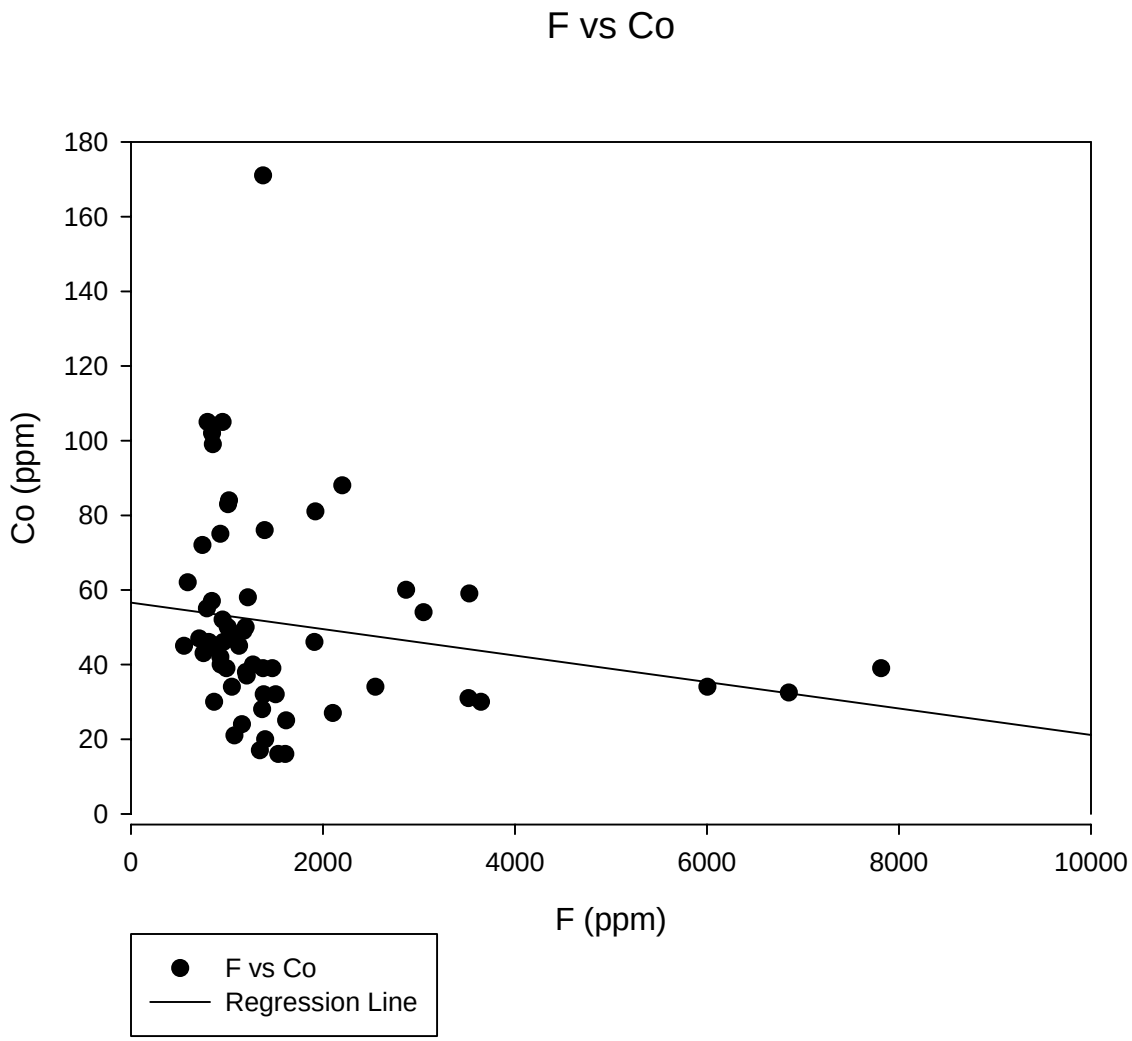
F vs Co
Co (ppm)
F (ppm)
0
20
40
60
80
100
120
140
160
180
0
2000
4000
6000
8000
10000
F vs Co
Regression Line

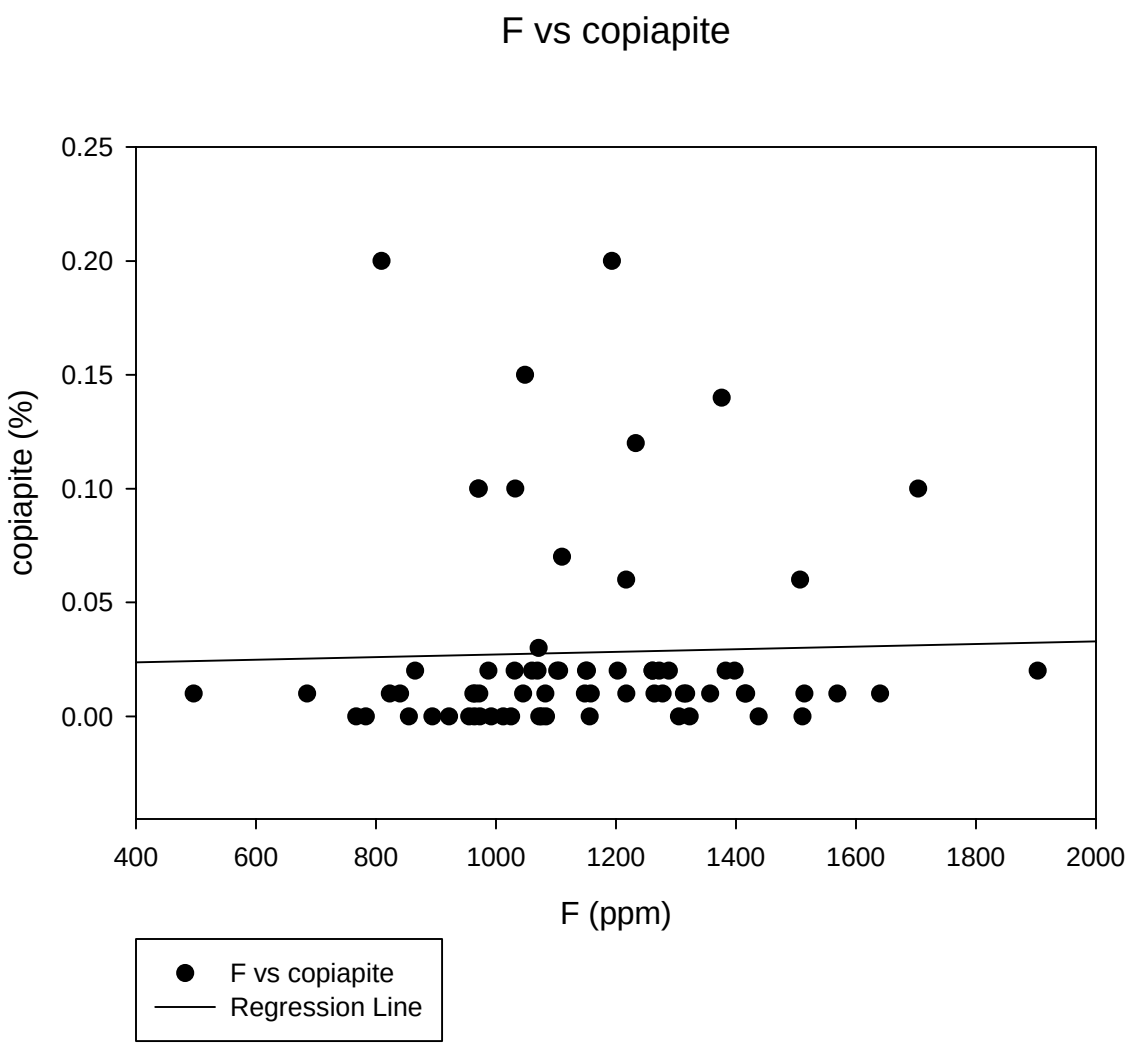
F vs copiapite
copiapite (%)
0.25
0.20
0.15
0.10
0.05
0.00
400
600
800
1000
1200
1400
1600
1800
2000
F (ppm)
F vs copiapite
Regression Line

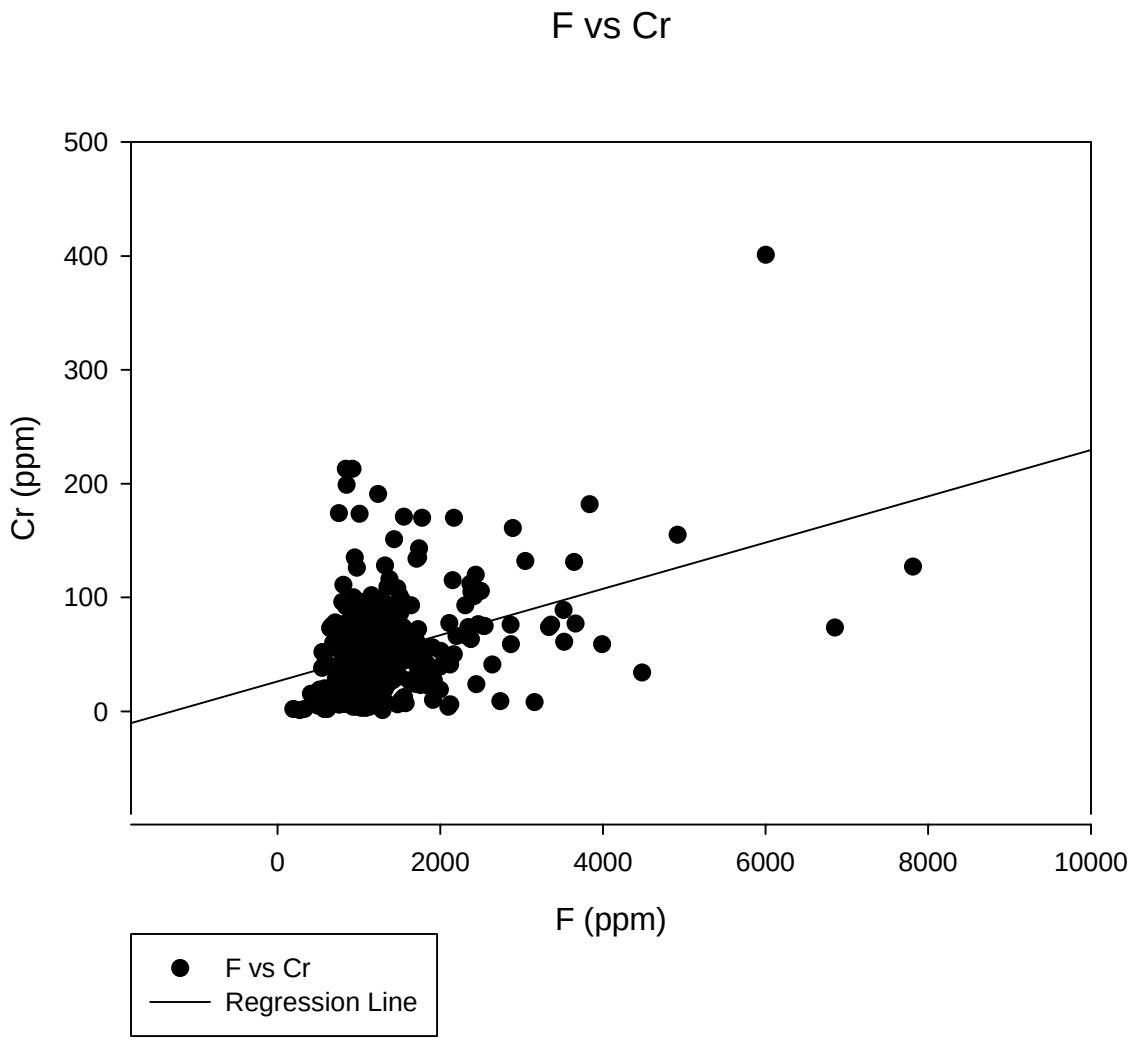
F vs Cr
500
400
300
200
100
0
Cr (ppm)
0
2000
4000
6000
8000
10000
F (ppm)
F vs Cr
Regression Line

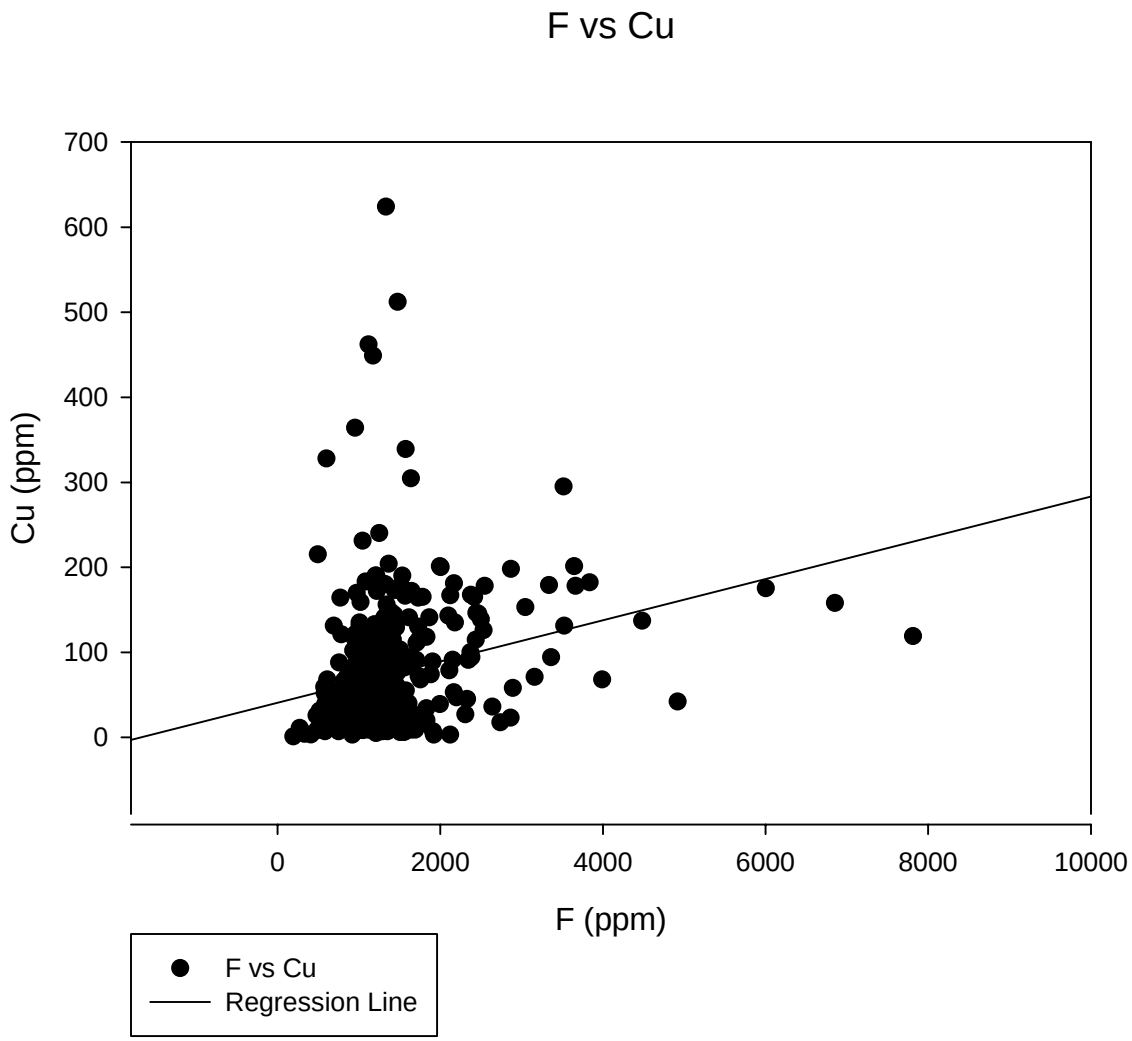
F vs Cu
700
600
500
400
300
200
100
0
Cu (ppm)
0
2000
4000
6000
8000
10000
F (ppm)
F vs Cu
Regression Line

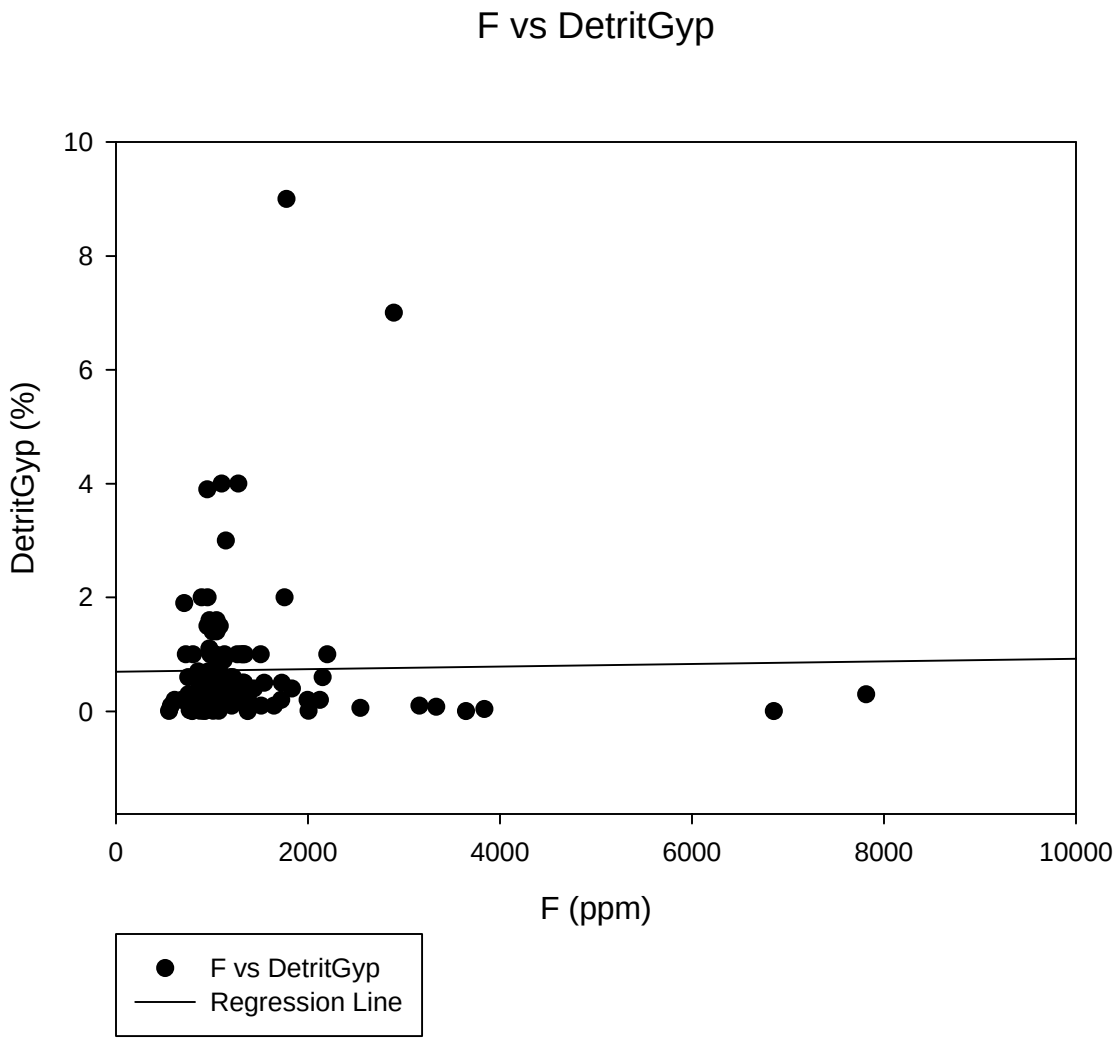
F vs DetritGyp
DetritGyp (%)
10
8
6
4
2
0
0
2000
4000
6000
8000
10000
F (ppm)
F vs DetritGyp
Regression Line

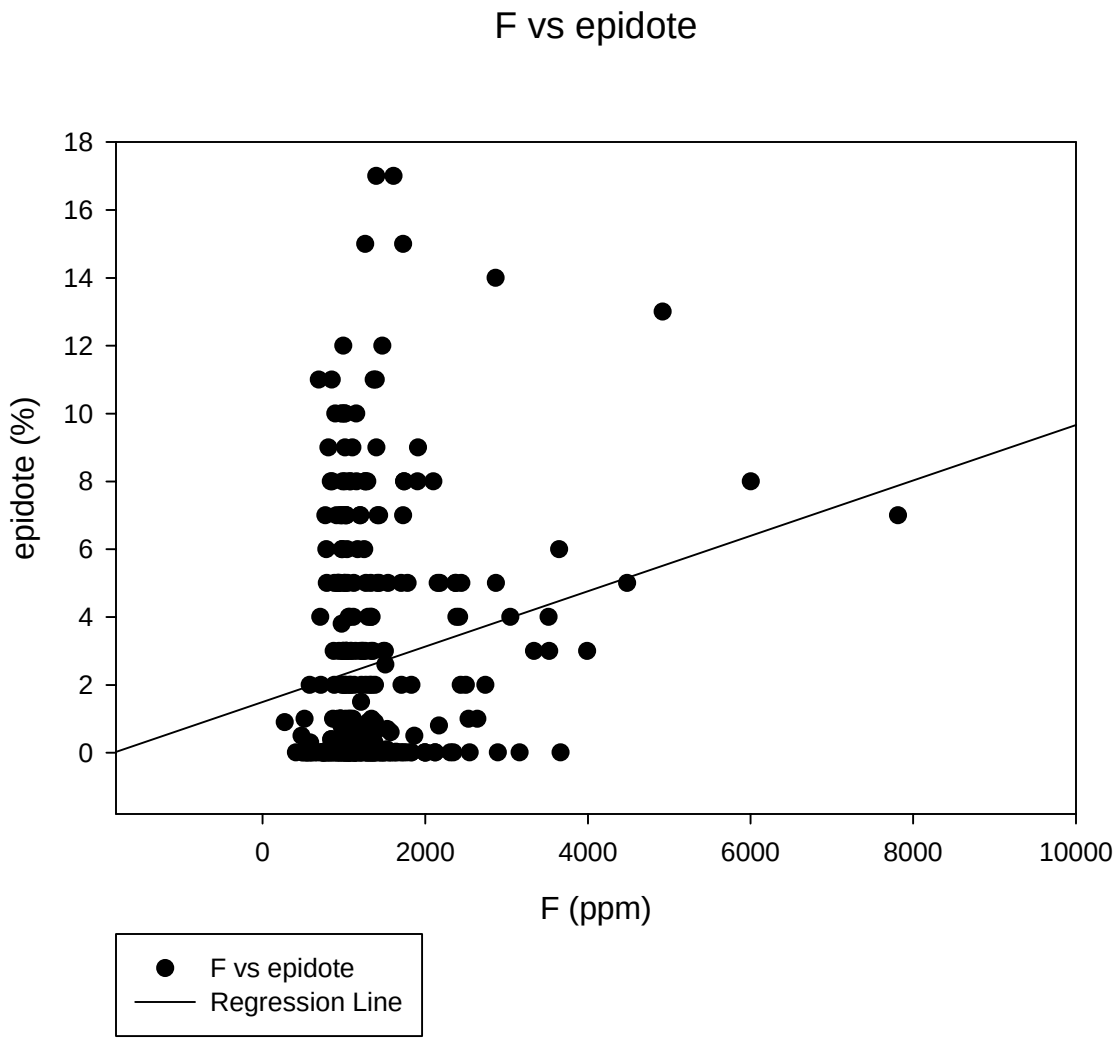
F vs epidote
epidote (%)
18
16
14
12
10
8
6
4
2
0
0
2000
4000
6000
8000
10000
F (ppm)
F vs epidote
Regression Line

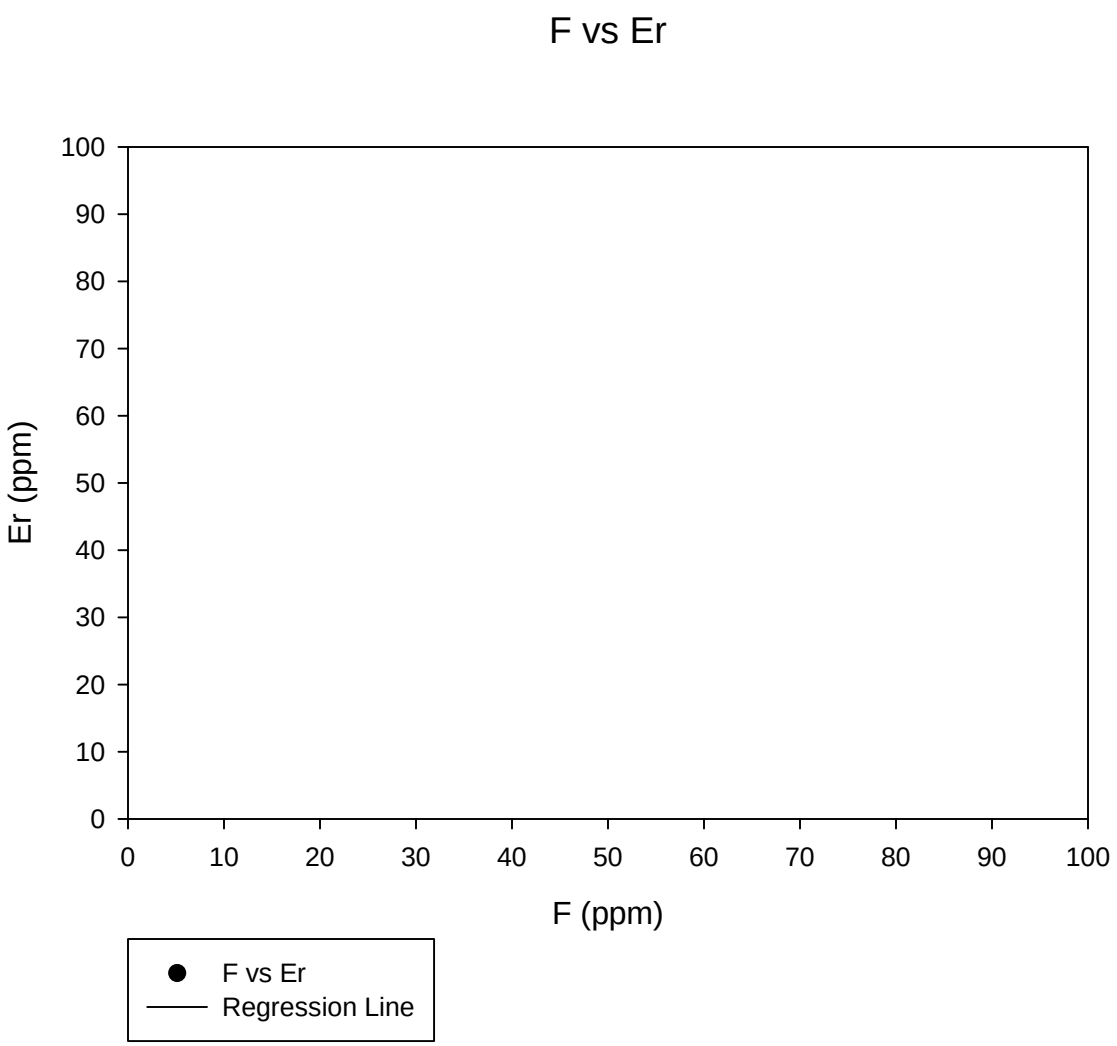
F vs Er
100
90
80
70
60
50
40
30
20
10
0
Er (ppm)
0
10
20
30
40
50
60
70
80
90
100
F (ppm)
F vs Er
Regression Line

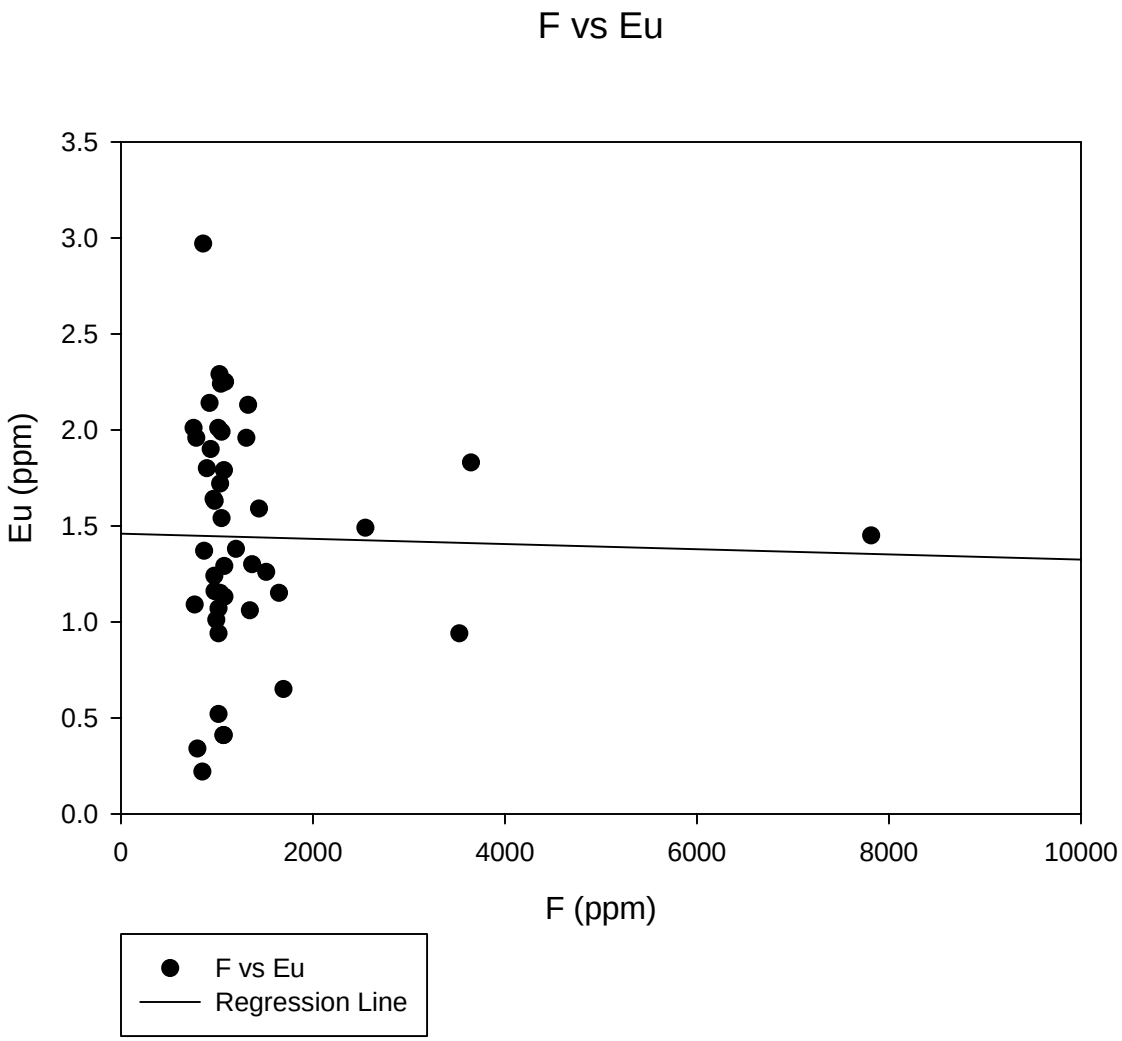
F vs Eu
3.5
3.0
2.5
2.0
1.5
1.0
0.5
0.0
Eu (ppm)
0
2000
4000
6000
8000
10000
F (ppm)
F vs Eu
Regression Line

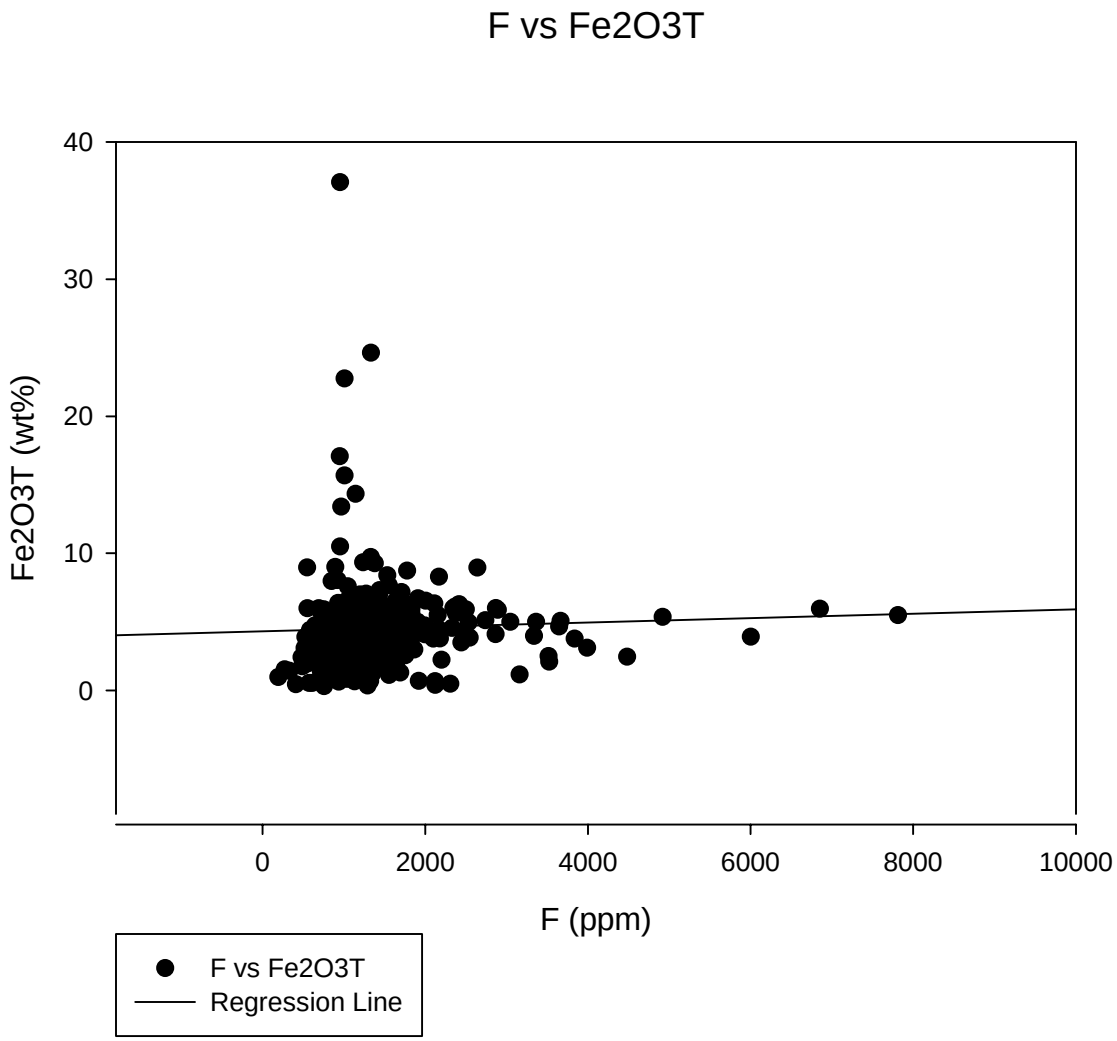
F vs Fe2O3T
40
30
20
10
0
Fe2O3T (wt%)
0
2000
4000
6000
8000
10000
F (ppm)
F vs Fe2O3T
Regression Line

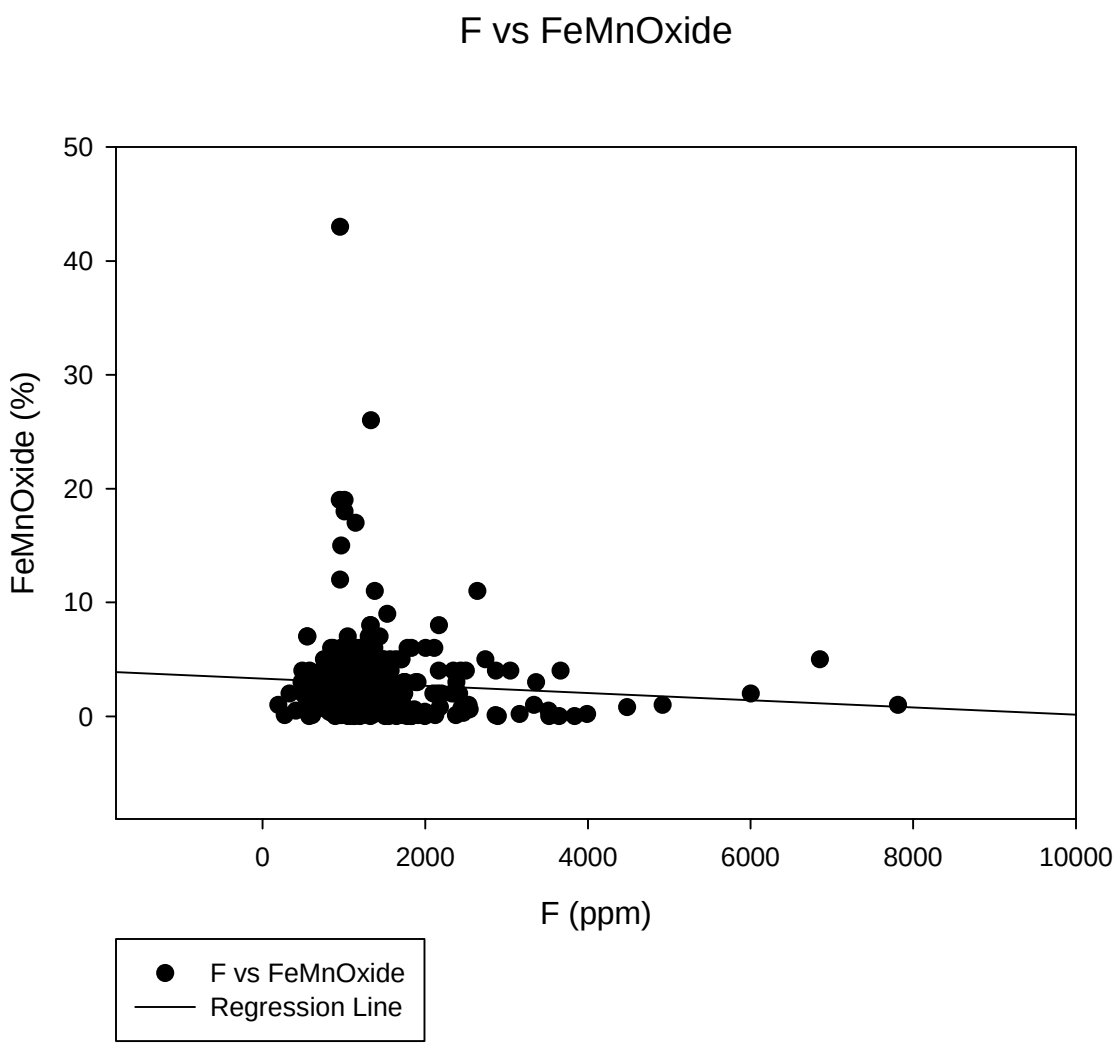
F vs FeMnOxide
50
40
30
20
10
0
FeMnOxide (%)
0
2000
4000
6000
8000
10000
F (ppm)
F vs FeMnOxide
Regression Line

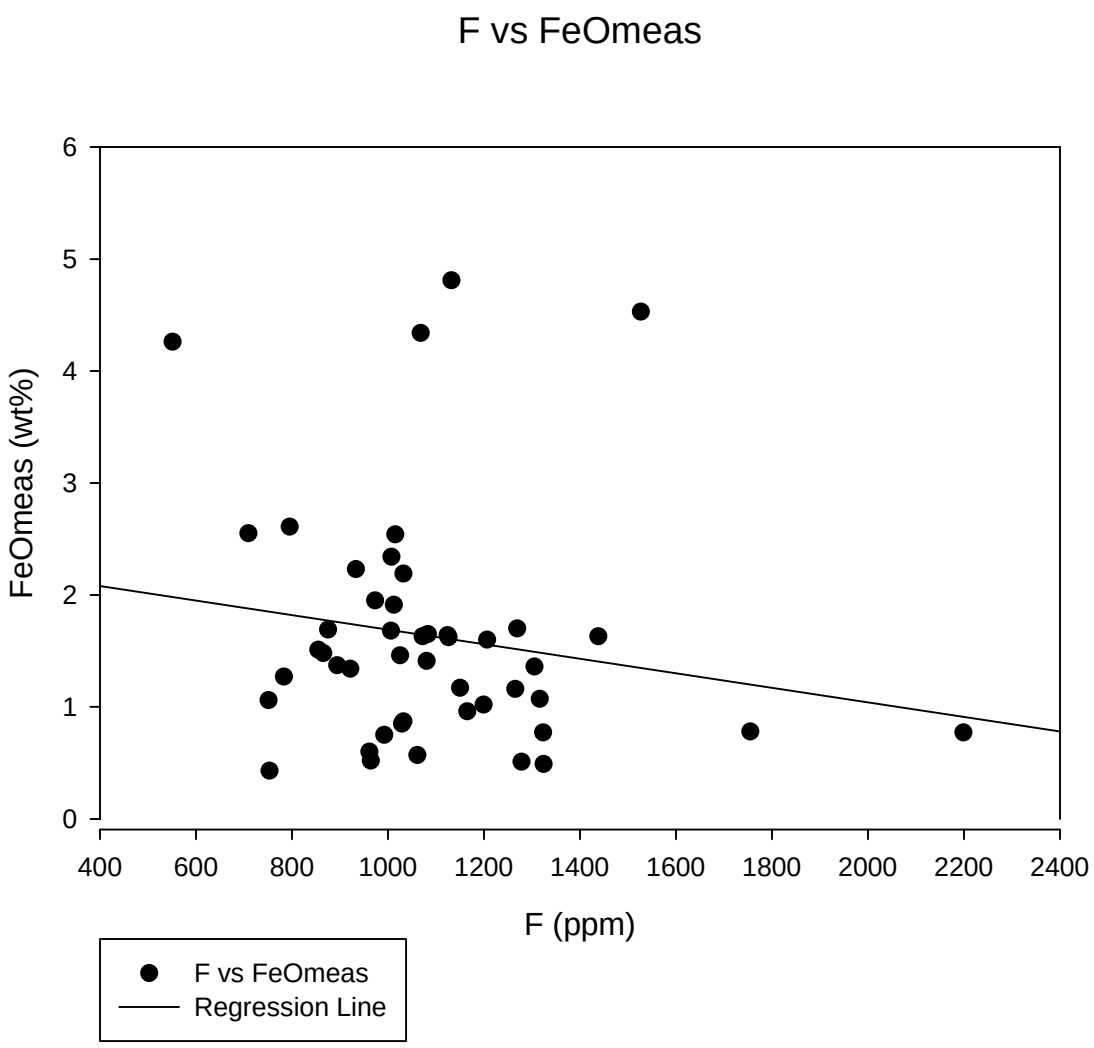
F vs FeOmeas
FeOmeas (wt%)
F (ppm)
0
1
2
3
4
5
6
400
600
800
1000
1200
1400
1600
1800
2000
2200
2400
F vs FeOmeas
Regression Line

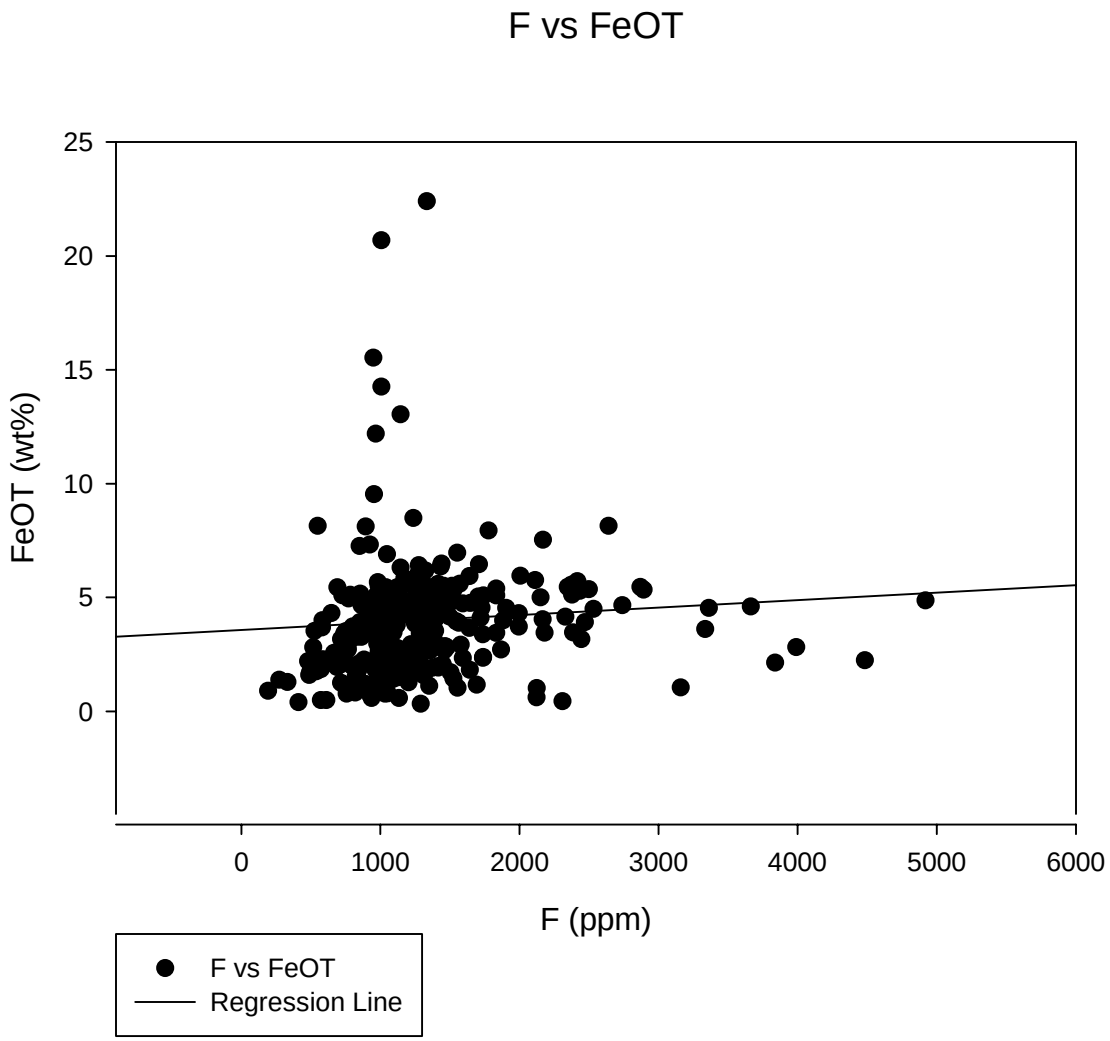
F vs FeOT
25
20
15
10
5
0
FeOT (wt%)
0
1000
2000
3000
4000
5000
6000
F (ppm)
F vs FeOT
Regression Line

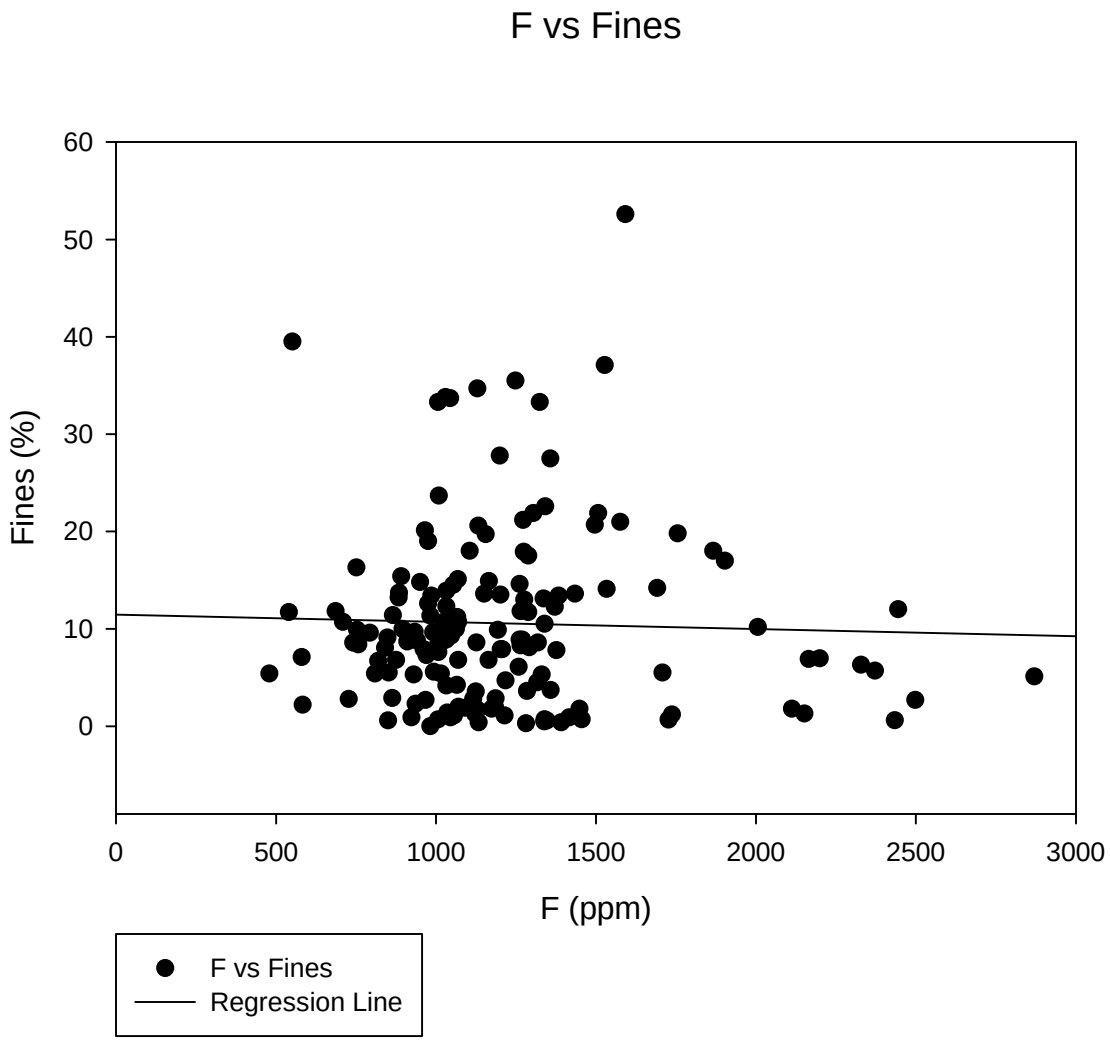
F vs Fines
60
50
40
30
20
10
0
Fines (%)
0
500
1000
1500
2000
2500
3000
F (ppm)
F vs Fines
Regression Line

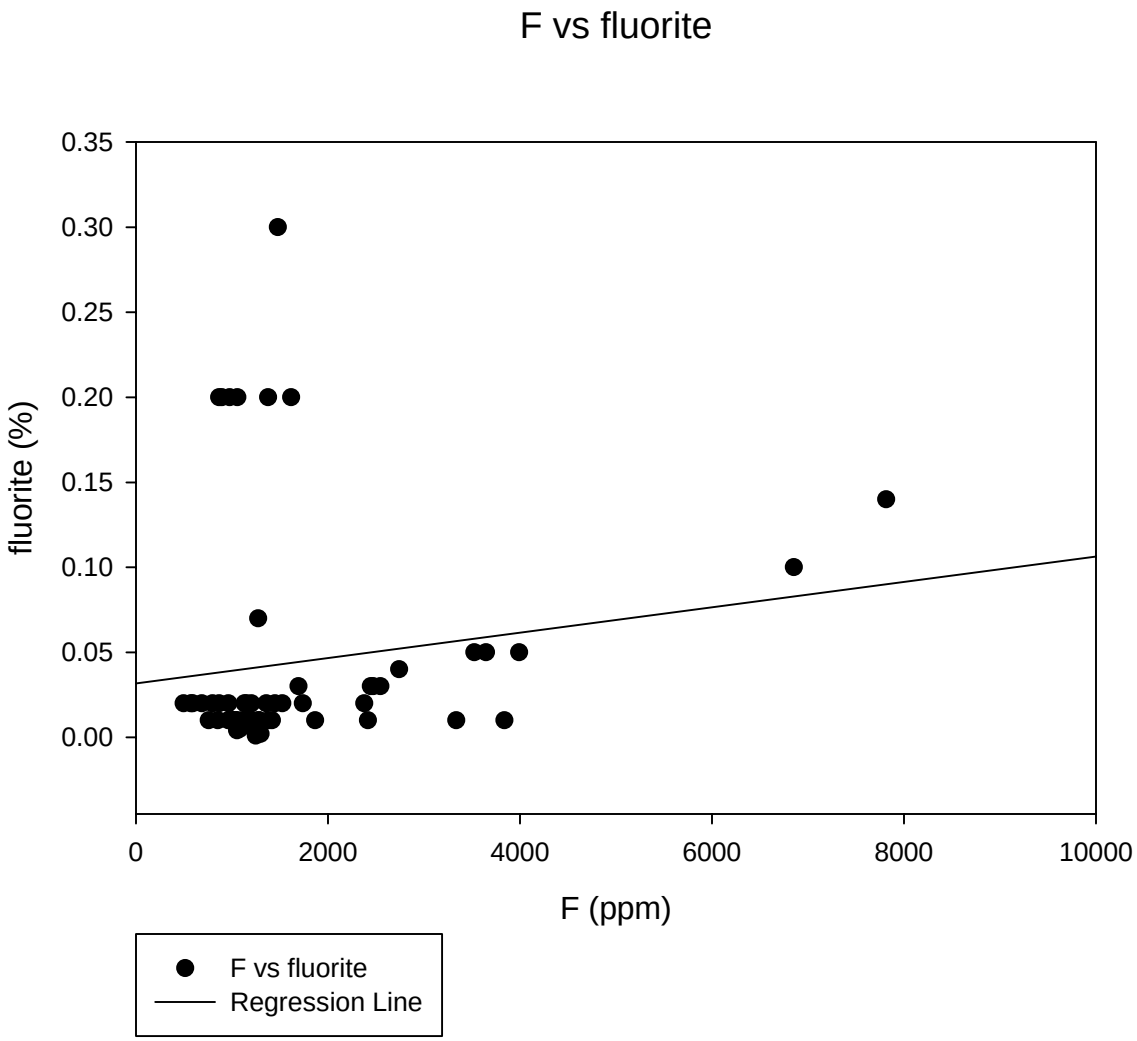
F vs fluorite
0.35
0.30
0.25
0.20
0.15
0.10
0.05
0.00
fluorite (%)
0
2000
4000
6000
8000
10000
F (ppm)
F vs fluorite
Regression Line

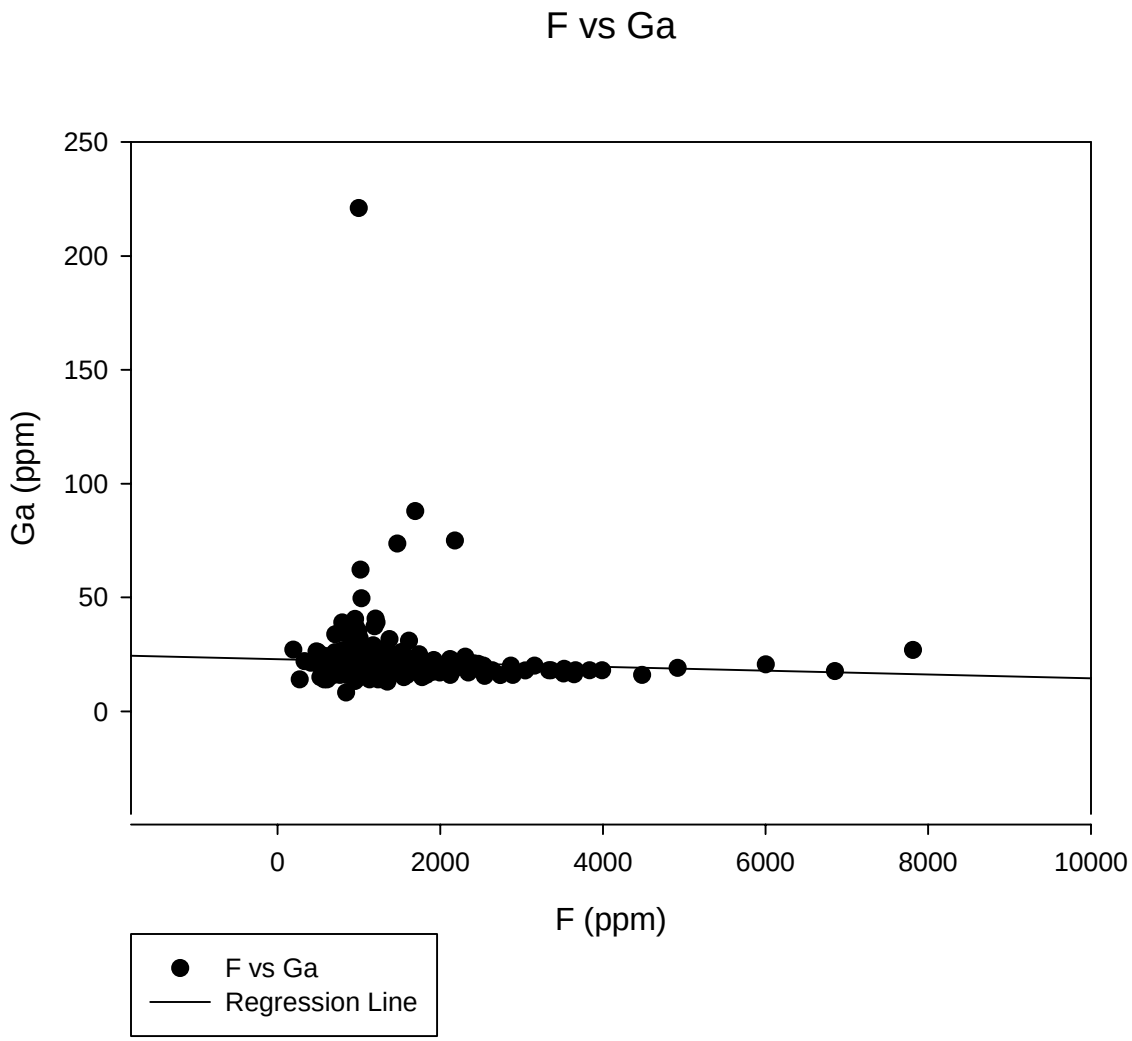
F vs Ga
250
200
150
100
50
0
Ga (ppm)
0
2000
4000
6000
8000
10000
F (ppm)
F vs Ga
Regression Line

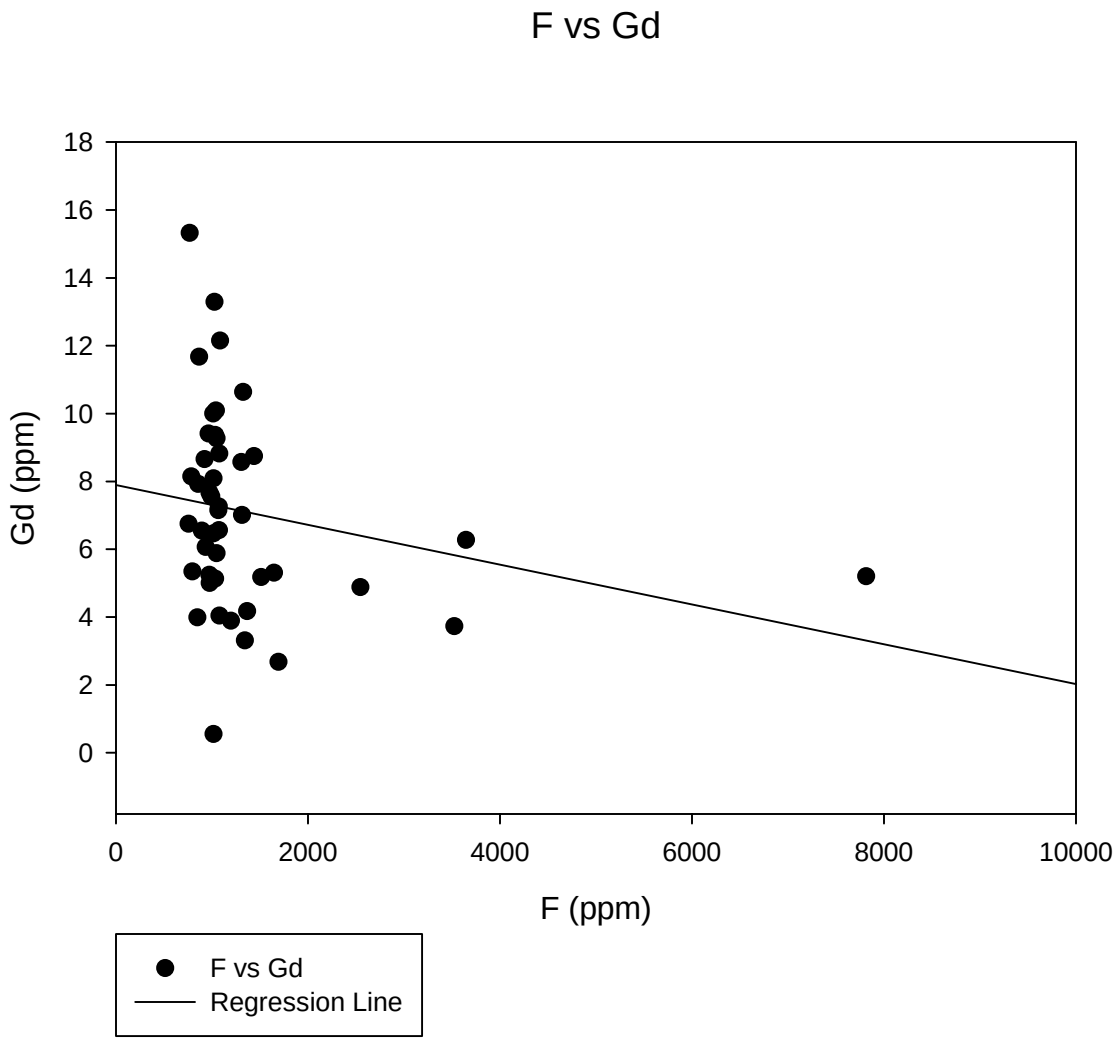
F vs Gd
Gd (ppm)
18
16
14
12
10
8
6
4
2
0
0
2000
4000
6000
8000
10000
F (ppm)
F vs Gd
Regression Line

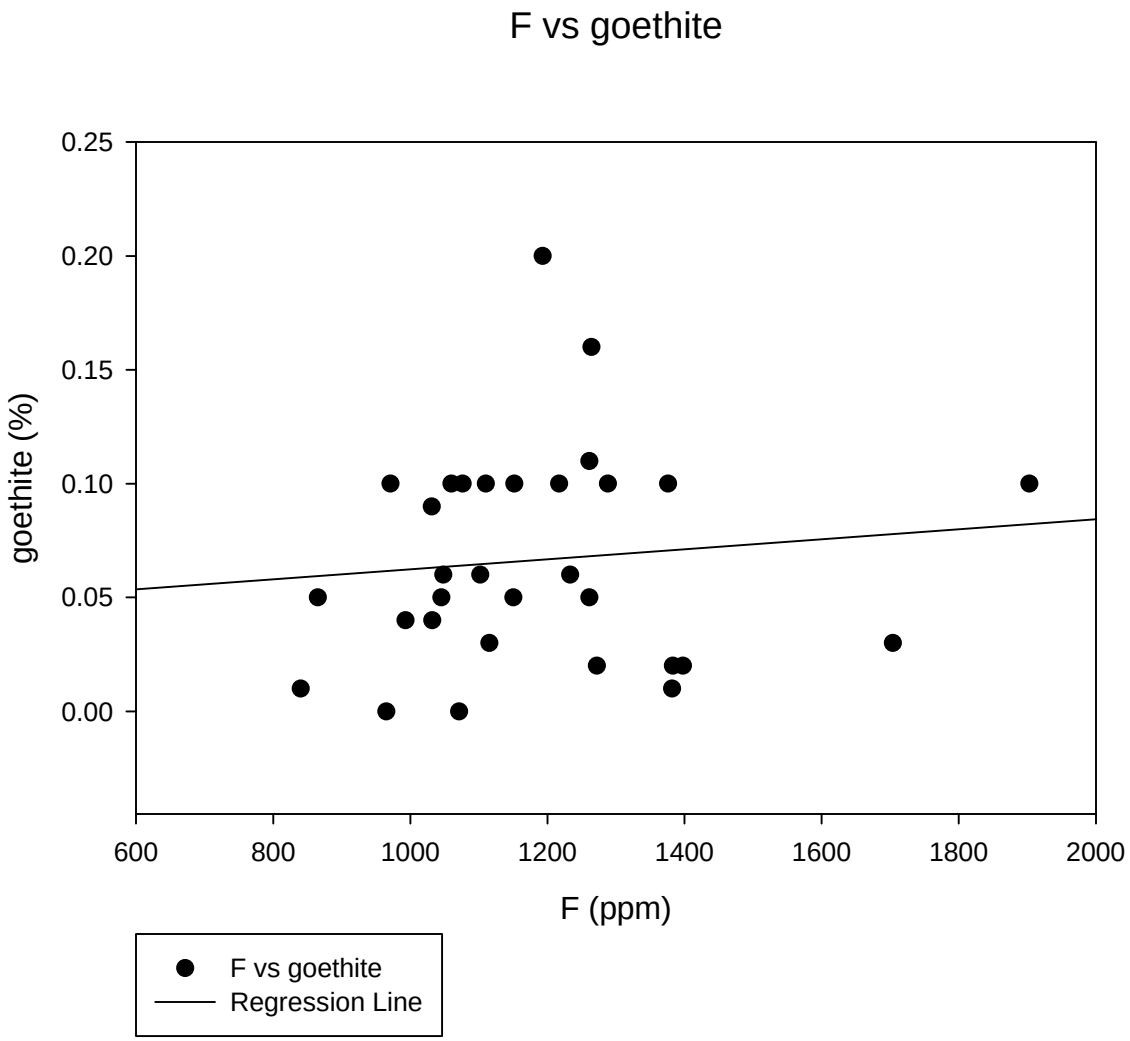
F vs goethite
0.25
0.20
0.15
0.10
0.05
0.00
goethite (%)
600
800
1000
1200
1400
1600
1800
2000
F (ppm)
F vs goethite
Regression Line

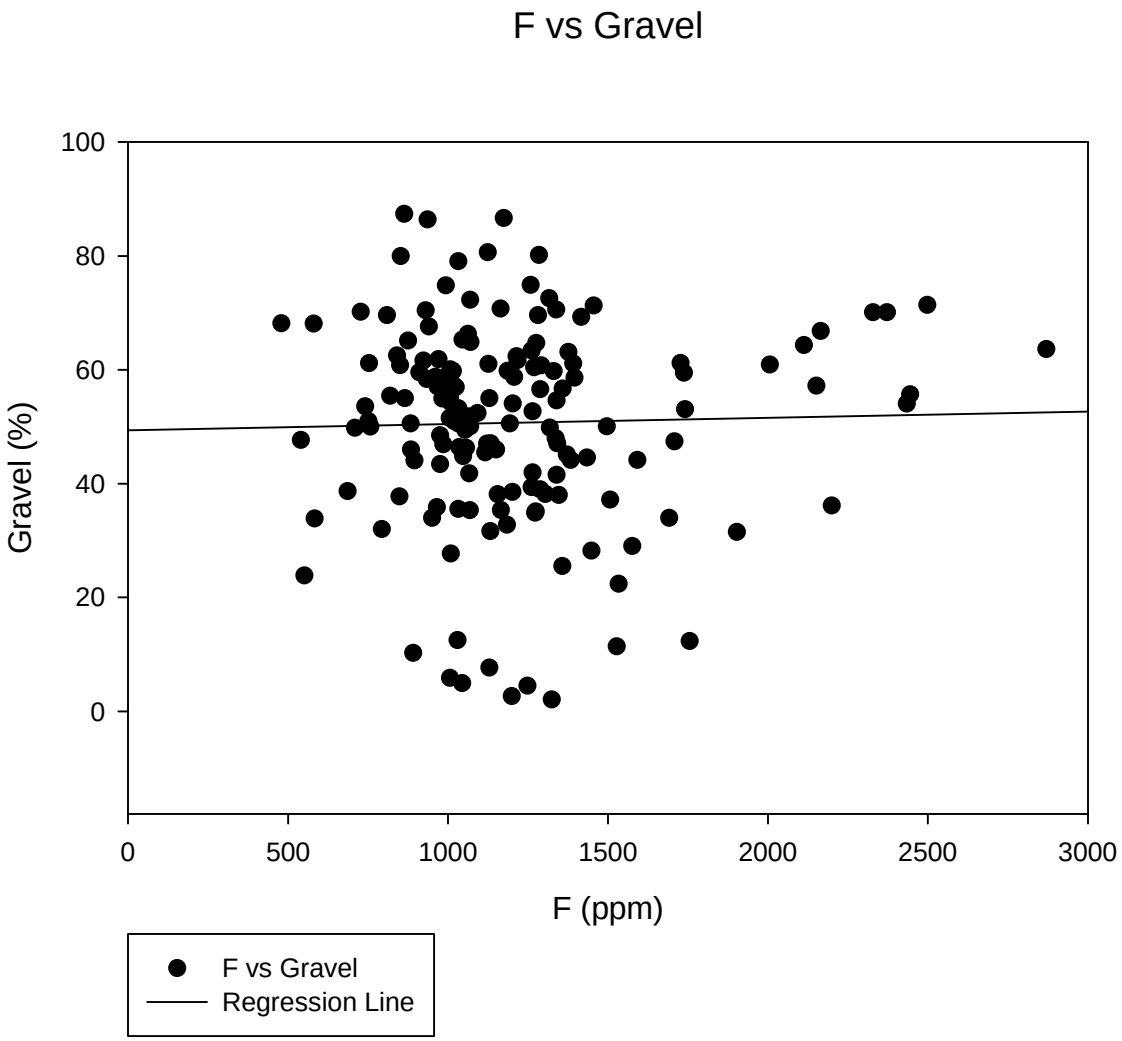
F vs Gravel
Gravel (%)
100
80
60
40
20
0
0
500
1000
1500
2000
2500
3000
F (ppm)
F vs Gravel
Regression Line

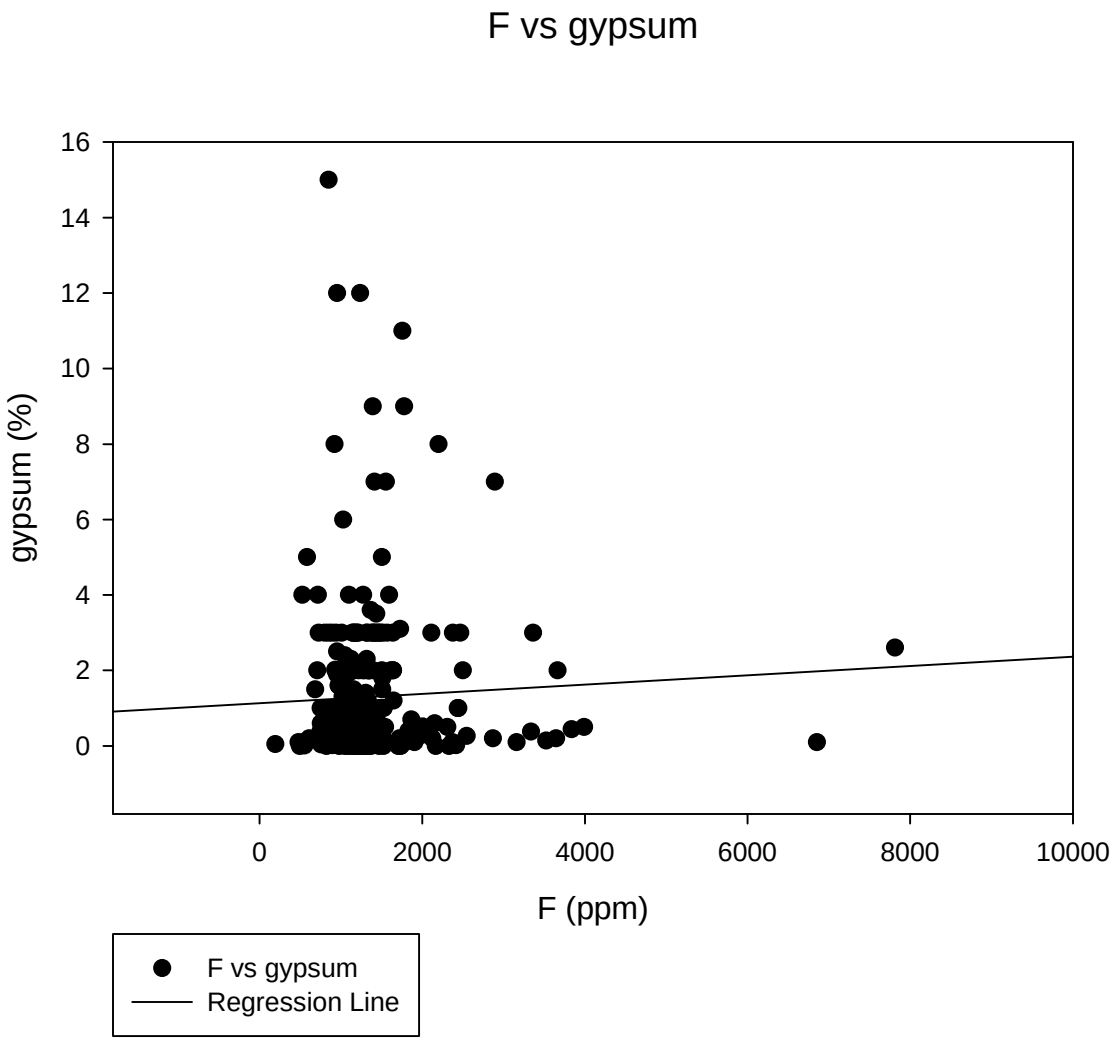
F vs gypsum
gypsum (%)
16
14
12
10
8
6
4
2
0
0
2000
4000
6000
8000
10000
F (ppm)
F vs gypsum
Regression Line

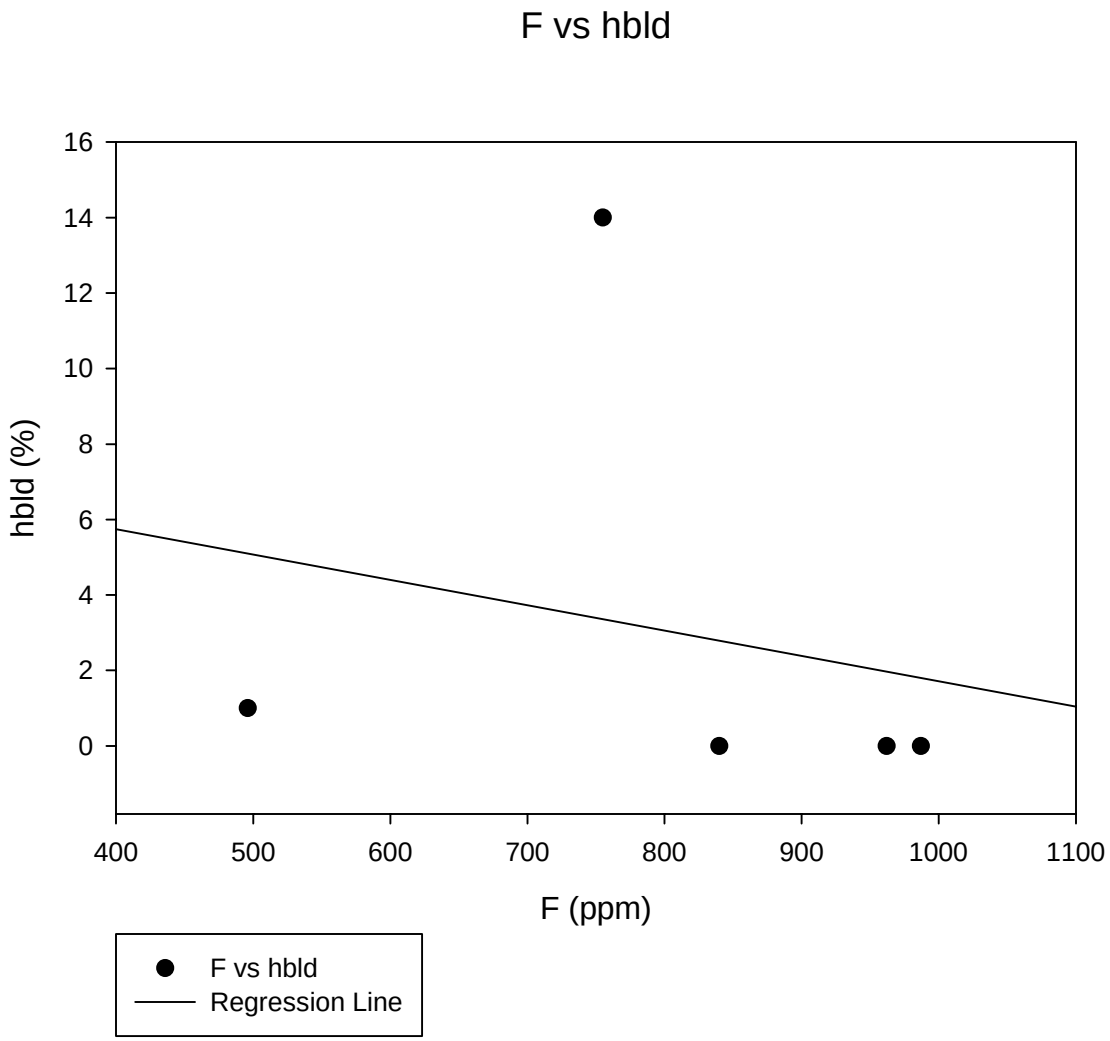
F vs hbld
16
14
12
10
8
6
4
2
0
hbld (%)
400
500
600
700
800
900
1000
1100
F (ppm)
F vs hbld
Regression Line

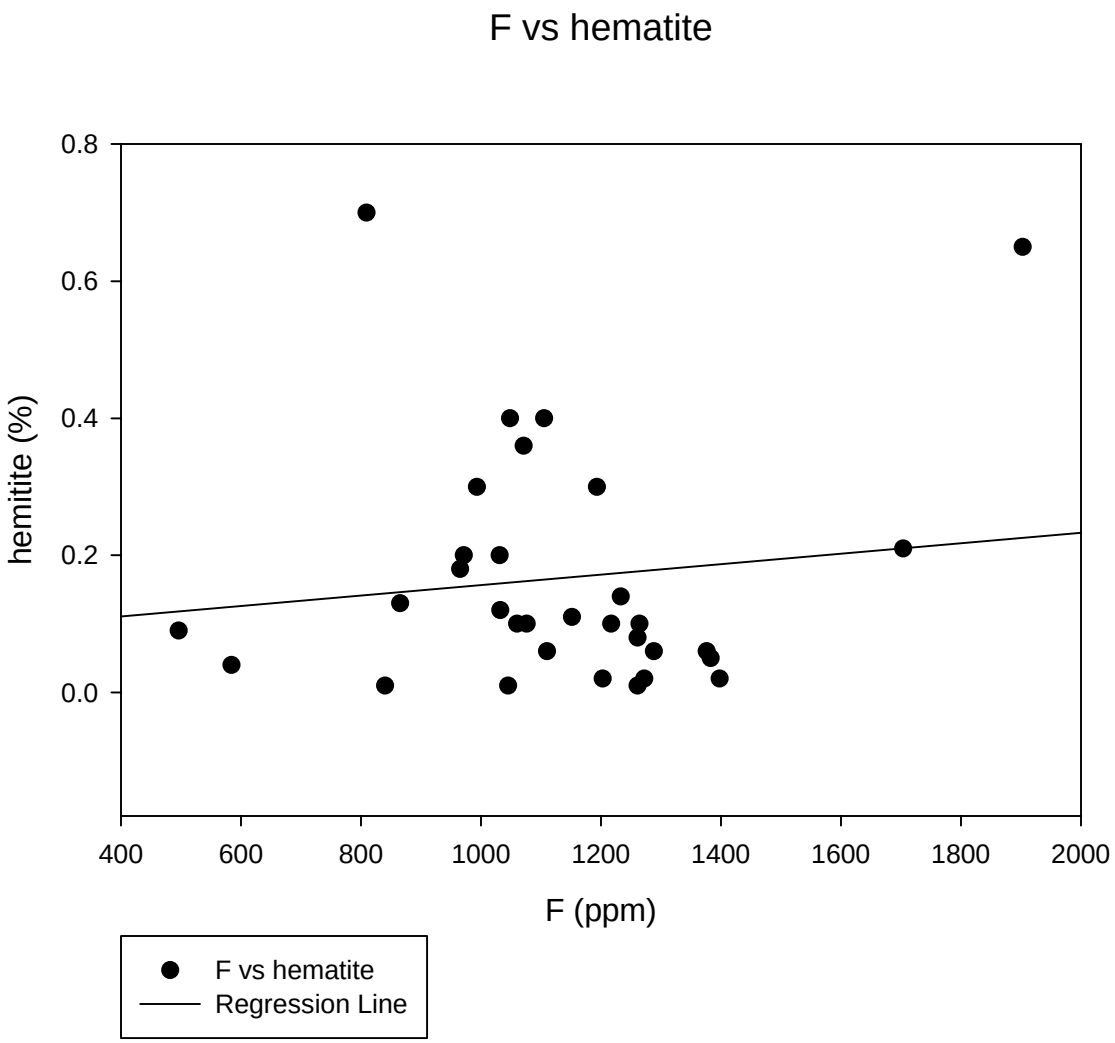
F vs hematite
0.8
0.6
0.4
0.2
0.0
hemitite (%)
400
600
800
1000
1200
1400
1600
1800
2000
F (ppm)
F vs hematite
Regression Line

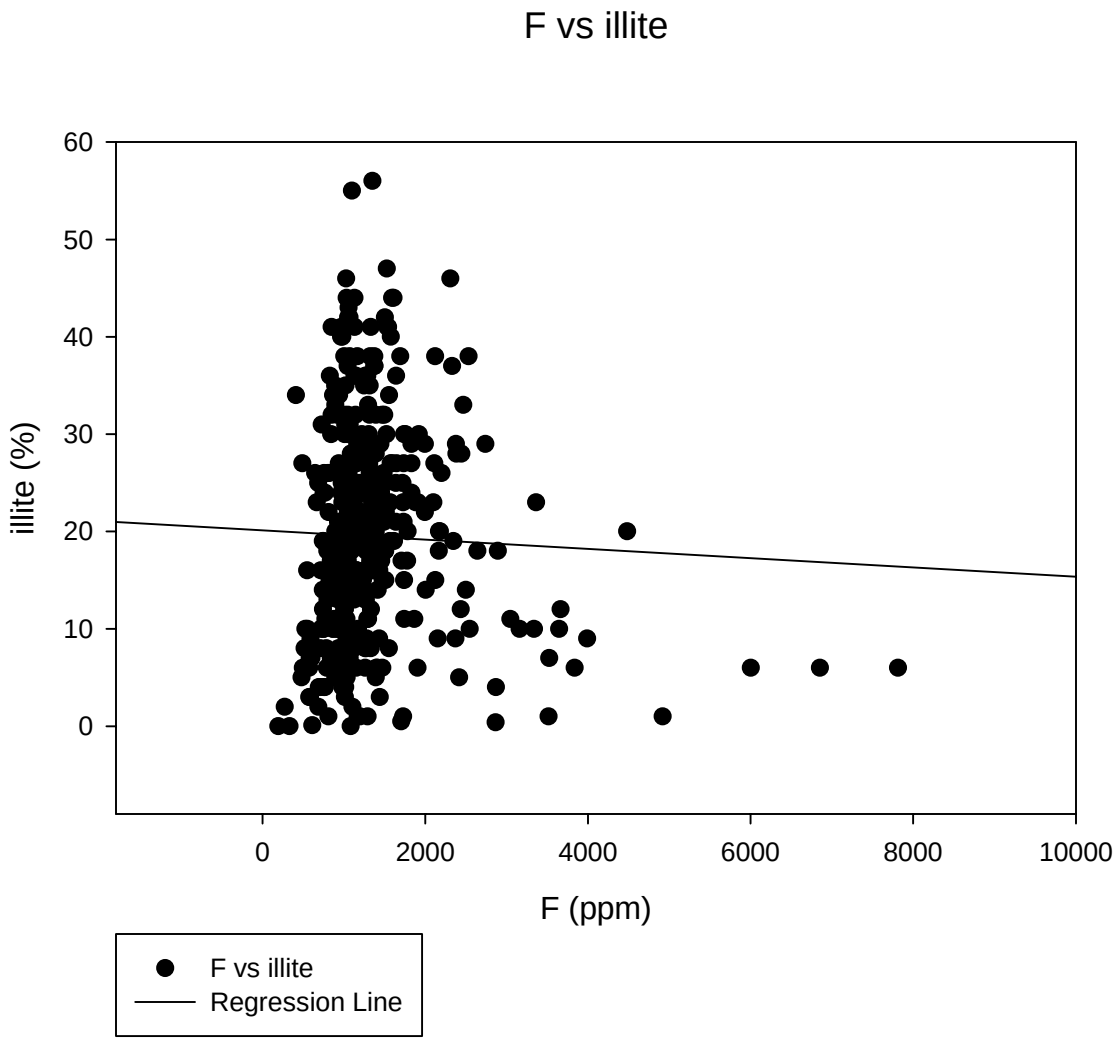
F vs illite
60
50
40
30
20
10
0
illite (%)
0
2000
4000
6000
8000
10000
F (ppm)
F vs illite
Regression Line

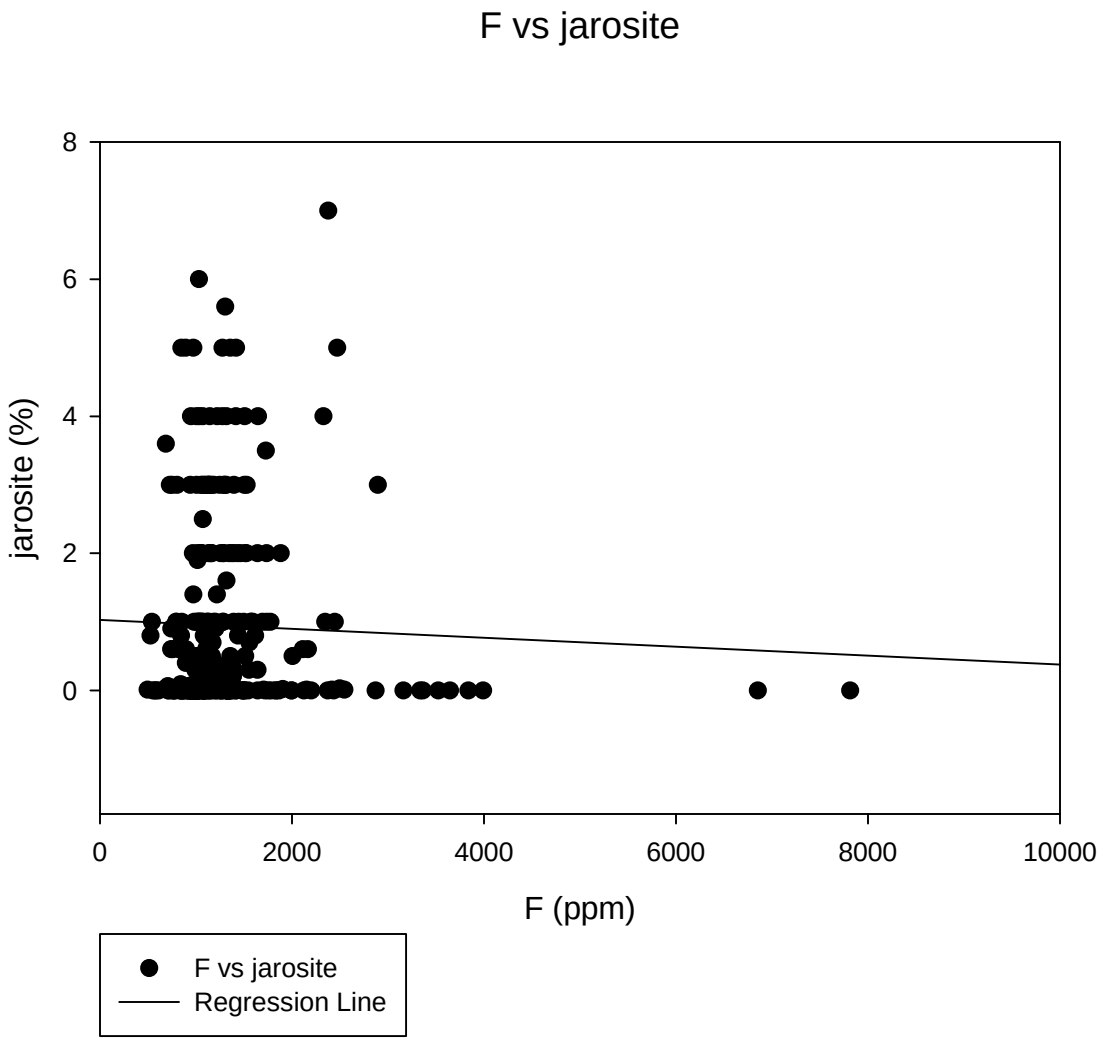
F vs jarosite
jarosite (%)
8
6
4
2
0
0
2000
4000
6000
8000
10000
F (ppm)
F vs jarosite
Regression Line

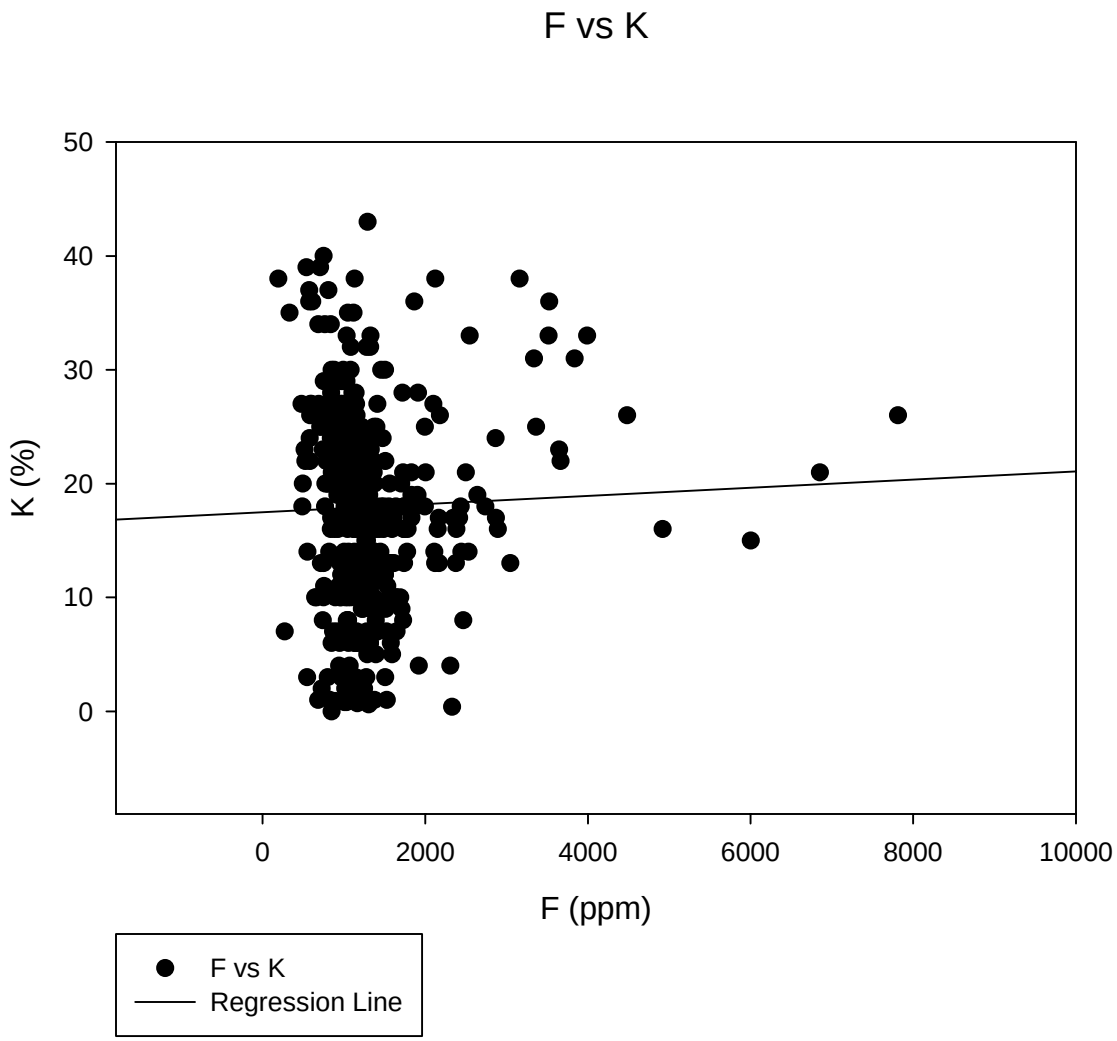
F vs K
50
40
30
20
10
0
K (%)
0
2000
4000
6000
8000
10000
F (ppm)
F vs K
Regression Line

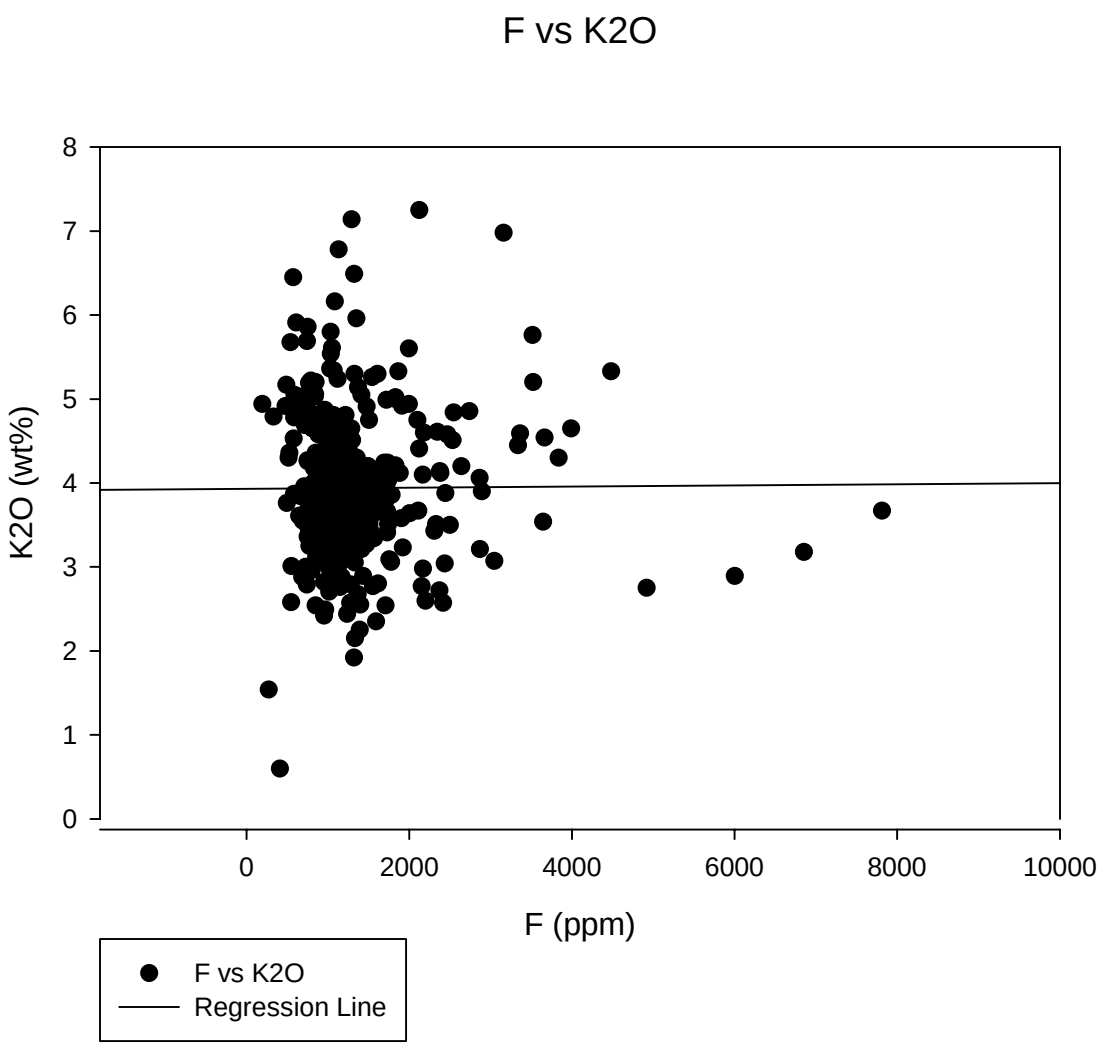
F vs K2O
K2O (wt%)
0
1
2
3
4
5
6
7
8
0
2000
4000
6000
8000
10000
F (ppm)
F vs K2O
Regression Line

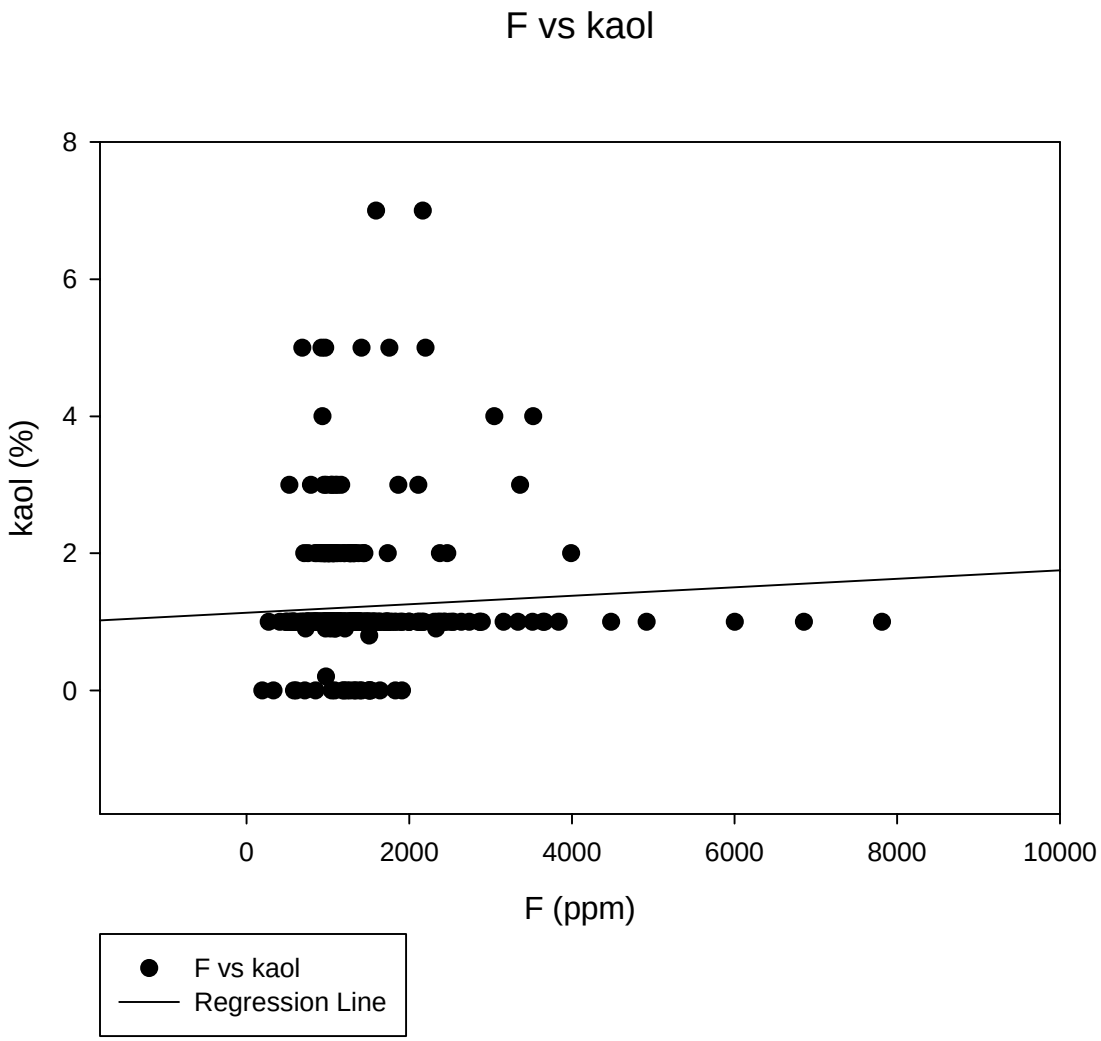
F vs kaol
kaol (%)
8
6
4
2
0
0
2000
4000
6000
8000
10000
F (ppm)
F vs kaol
Regression Line

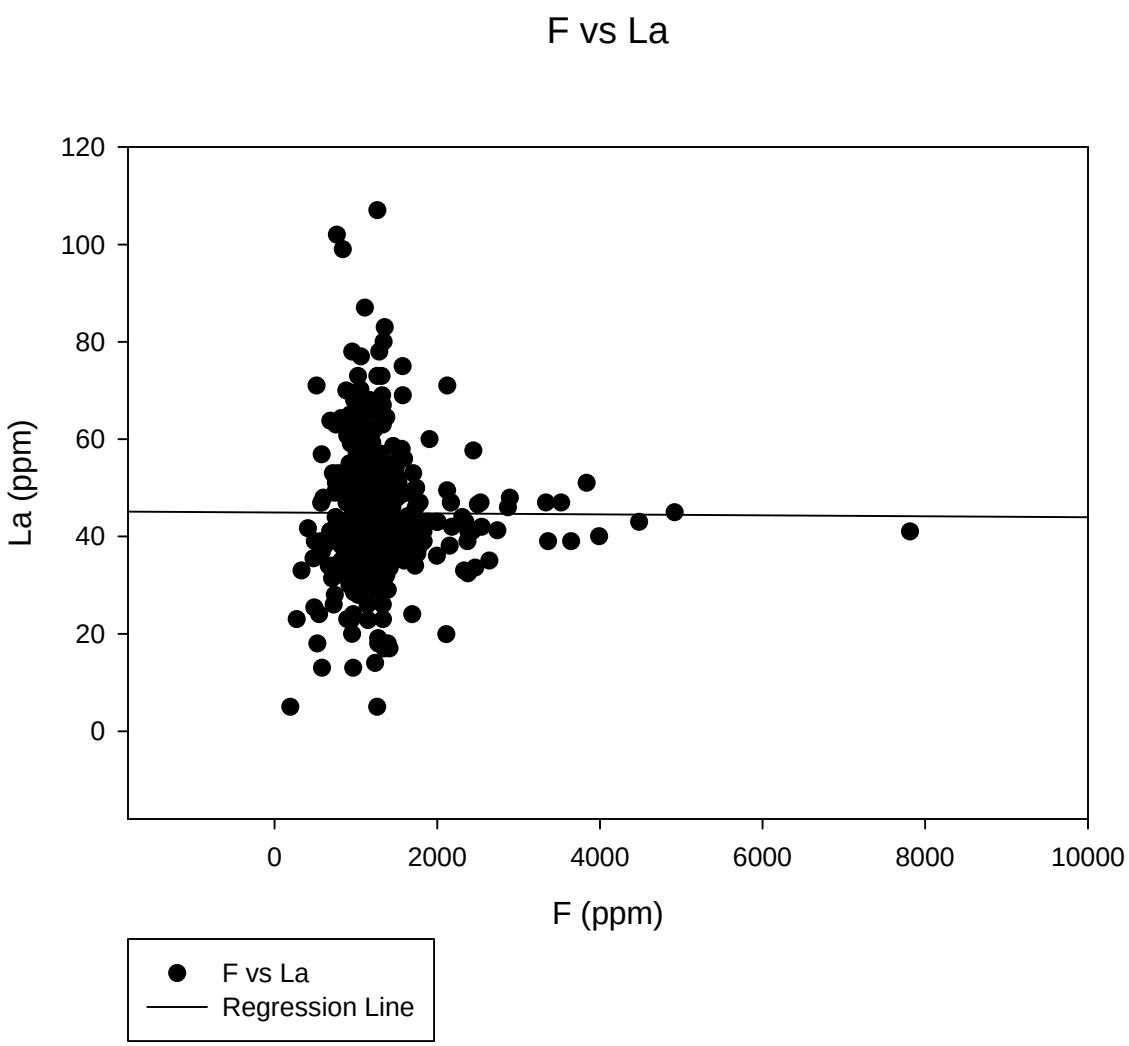
F vs La
120
100
80
60
40
20
0
La (ppm)
0
2000
4000
6000
8000
10000
F (ppm)
F vs La
Regression Line

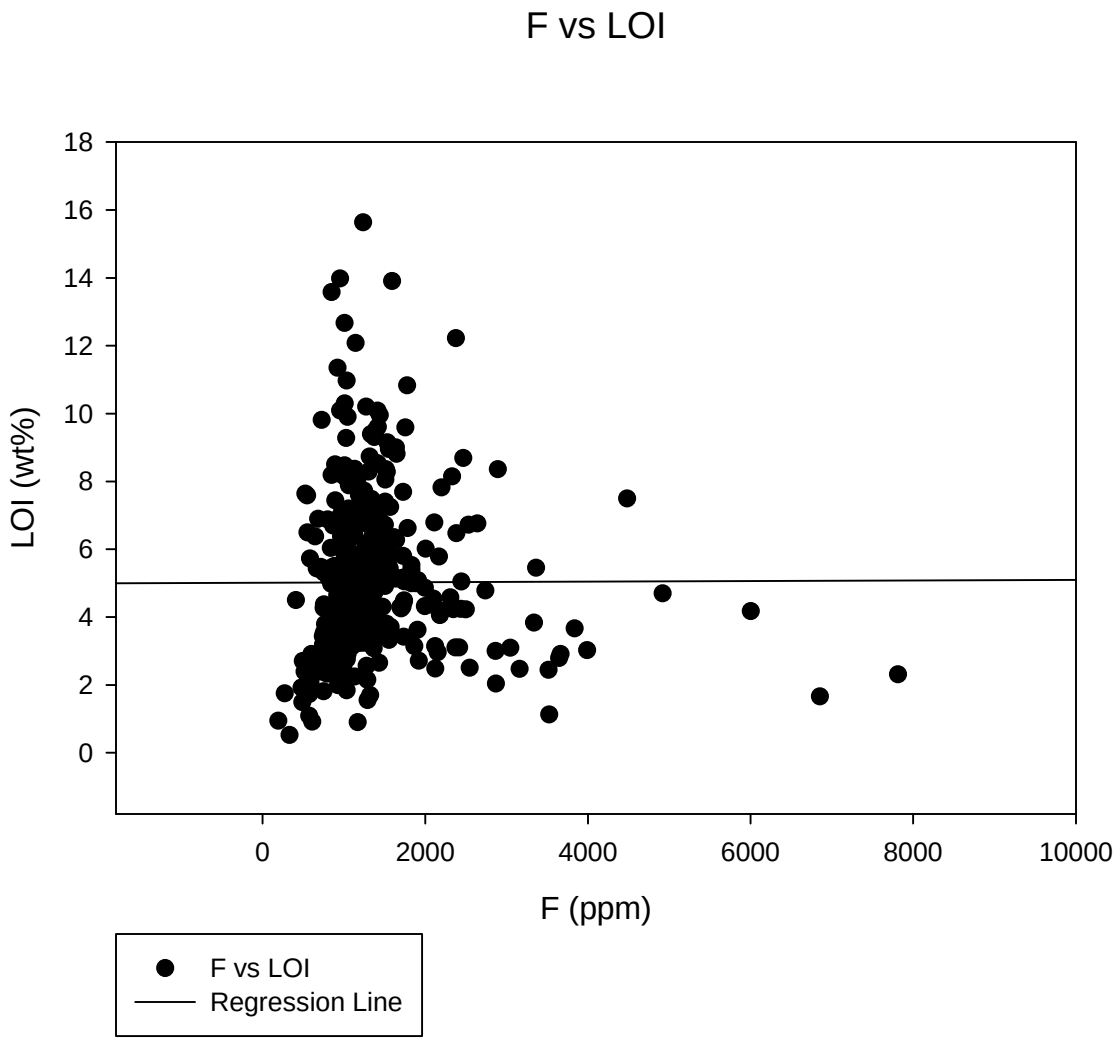
F vs LOI
LOI (wt%)
18
16
14
12
10
8
6
4
2
0
0
2000
4000
6000
8000
10000
F (ppm)
F vs LOI
Regression Line

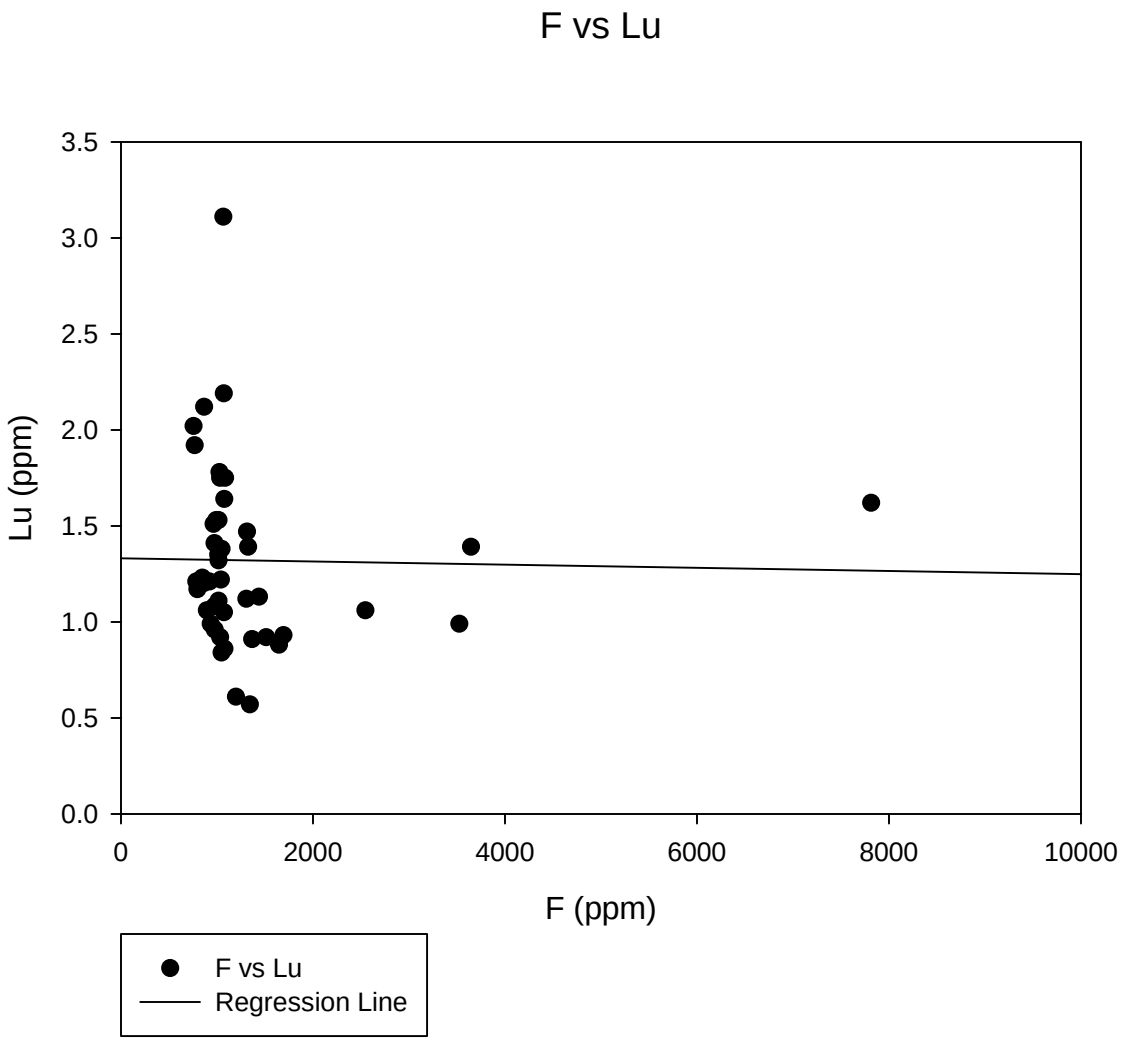
F vs Lu
3.5
3.0
2.5
2.0
1.5
1.0
0.5
0.0
Lu (ppm)
0
2000
4000
6000
8000
10000
F (ppm)
F vs Lu
Regression Line

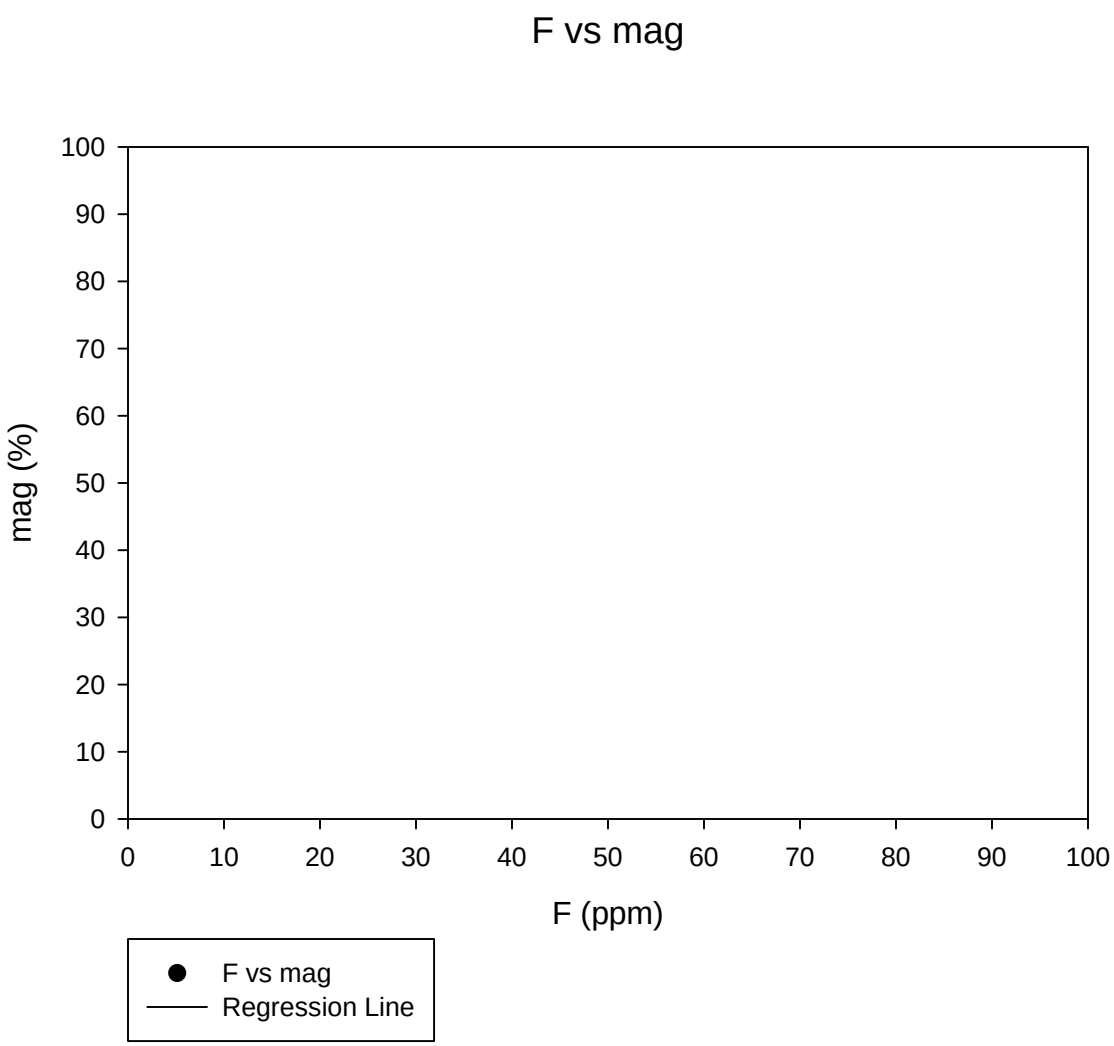
F vs mag
100
90
80
70
60
50
40
30
20
10
0
mag (%)
0
10
20
30
40
50
60
70
80
90
100
F (ppm)
F vs mag
Regression Line

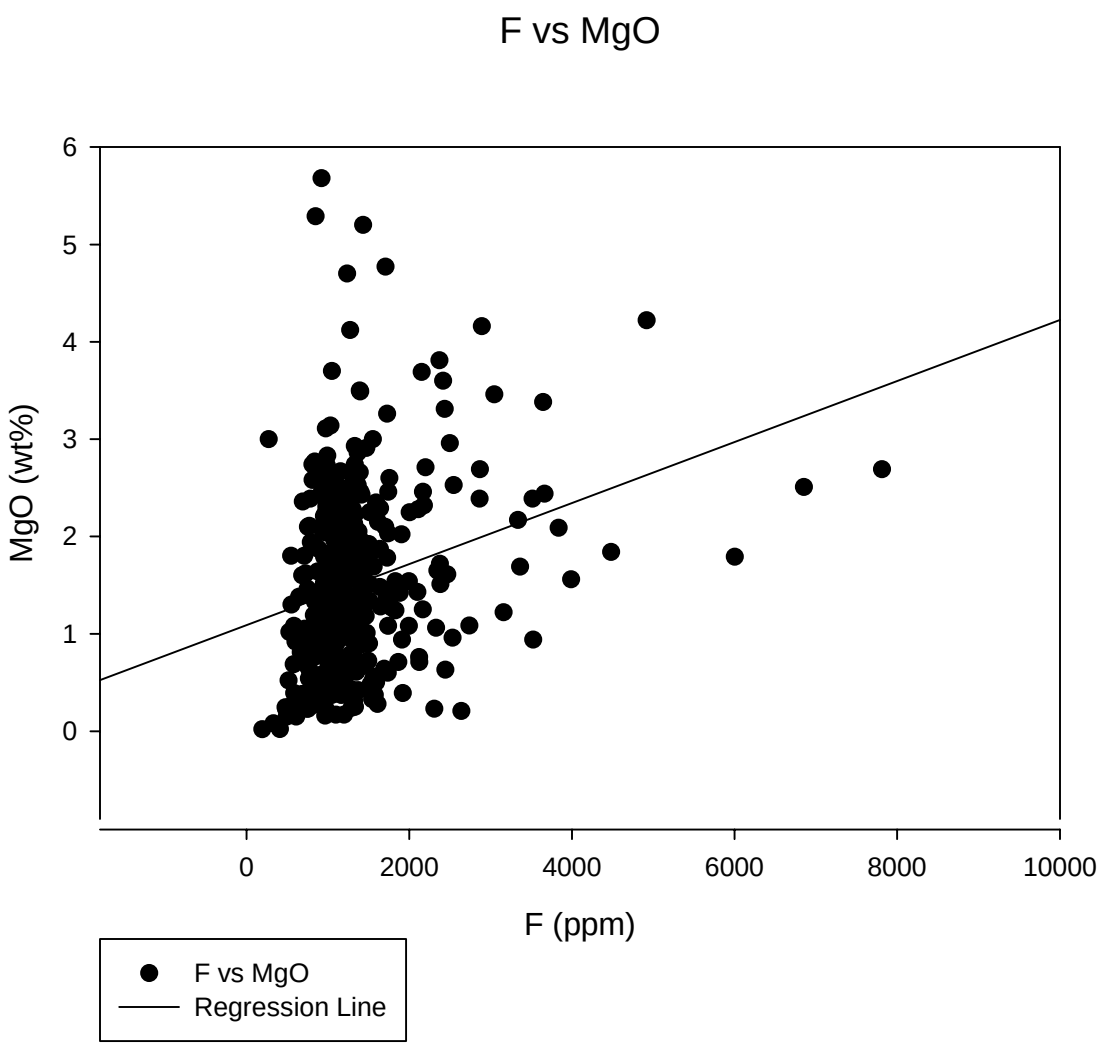
F vs MgO
MgO (wt%)
6
5
4
3
2
1
0
0
2000
4000
6000
8000
10000
F (ppm)
F vs MgO
Regression Line

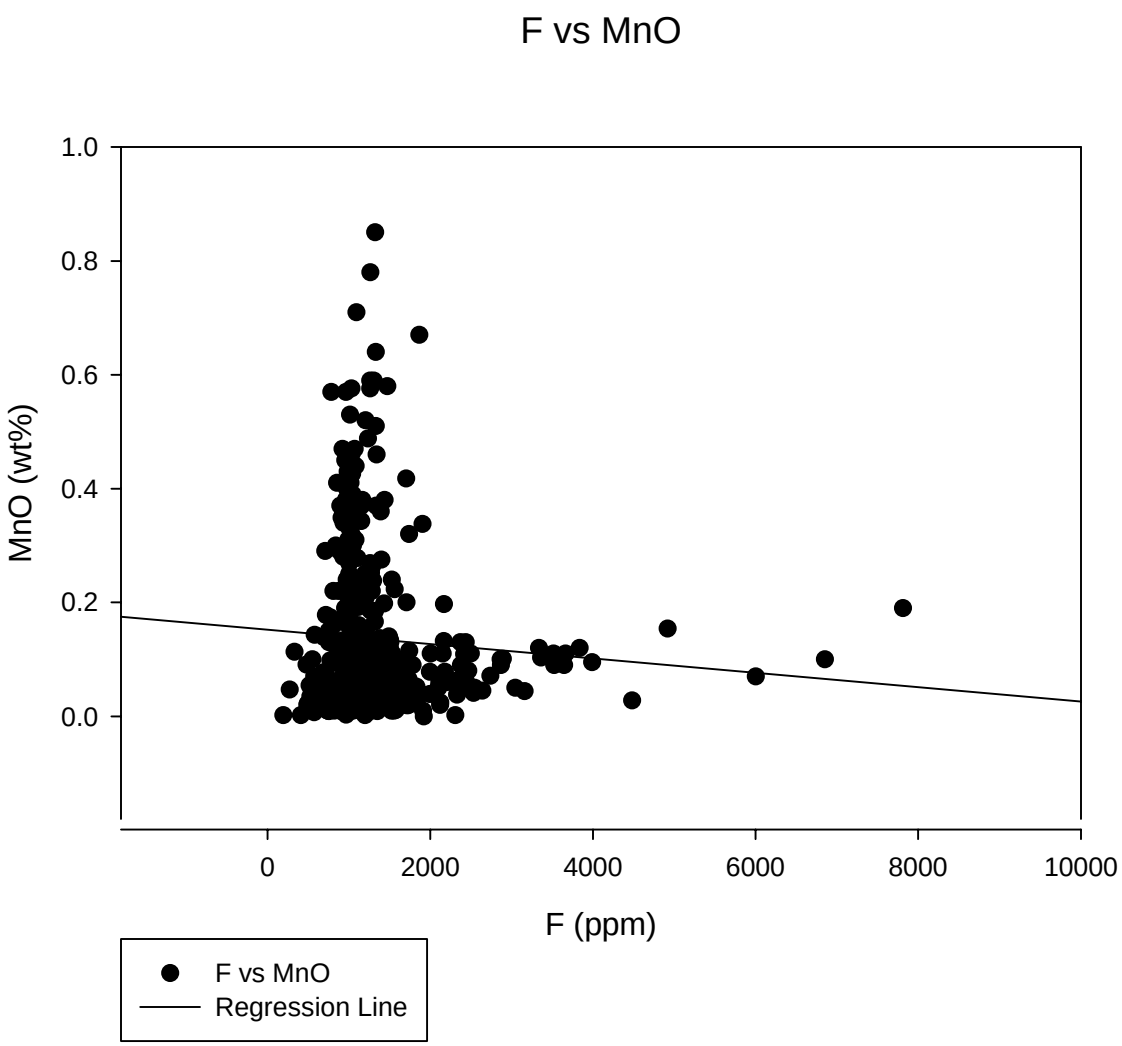
F vs MnO
1.0
0.8
0.6
0.4
0.2
0.0
MnO (wt%)
0
2000
4000
6000
8000
10000
F (ppm)
F vs MnO
Regression Line

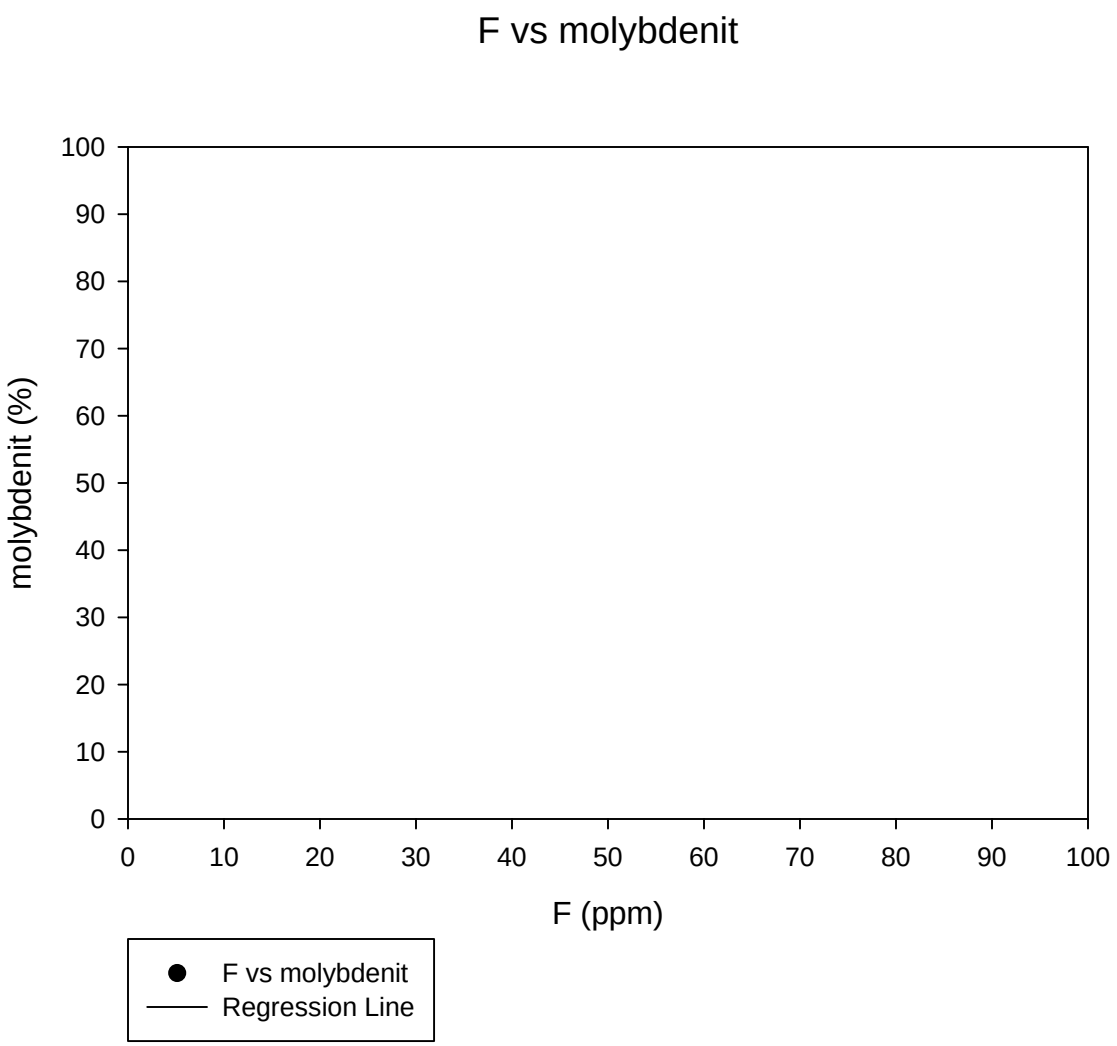
F vs molybdenit
molybdenit (%)
100
90
80
70
60
50
40
30
20
10
0
0
10
20
30
40
50
60
70
80
90
100
F (ppm)
F vs molybdenit
Regression Line

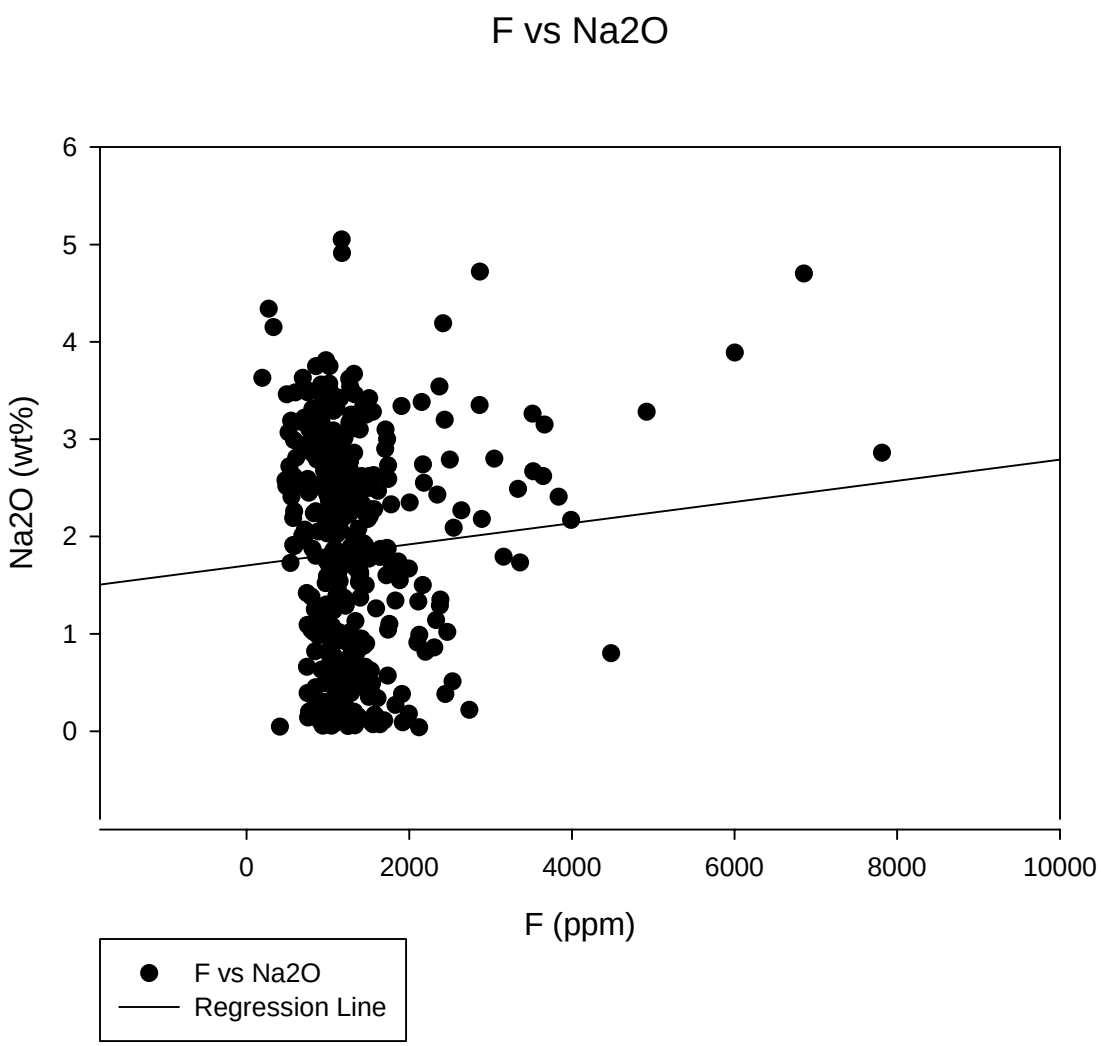
F vs Na2O
Na2O (wt%)
6
5
4
3
2
1
0
0
2000
4000
6000
8000
10000
F (ppm)
F vs Na2O
Regression Line

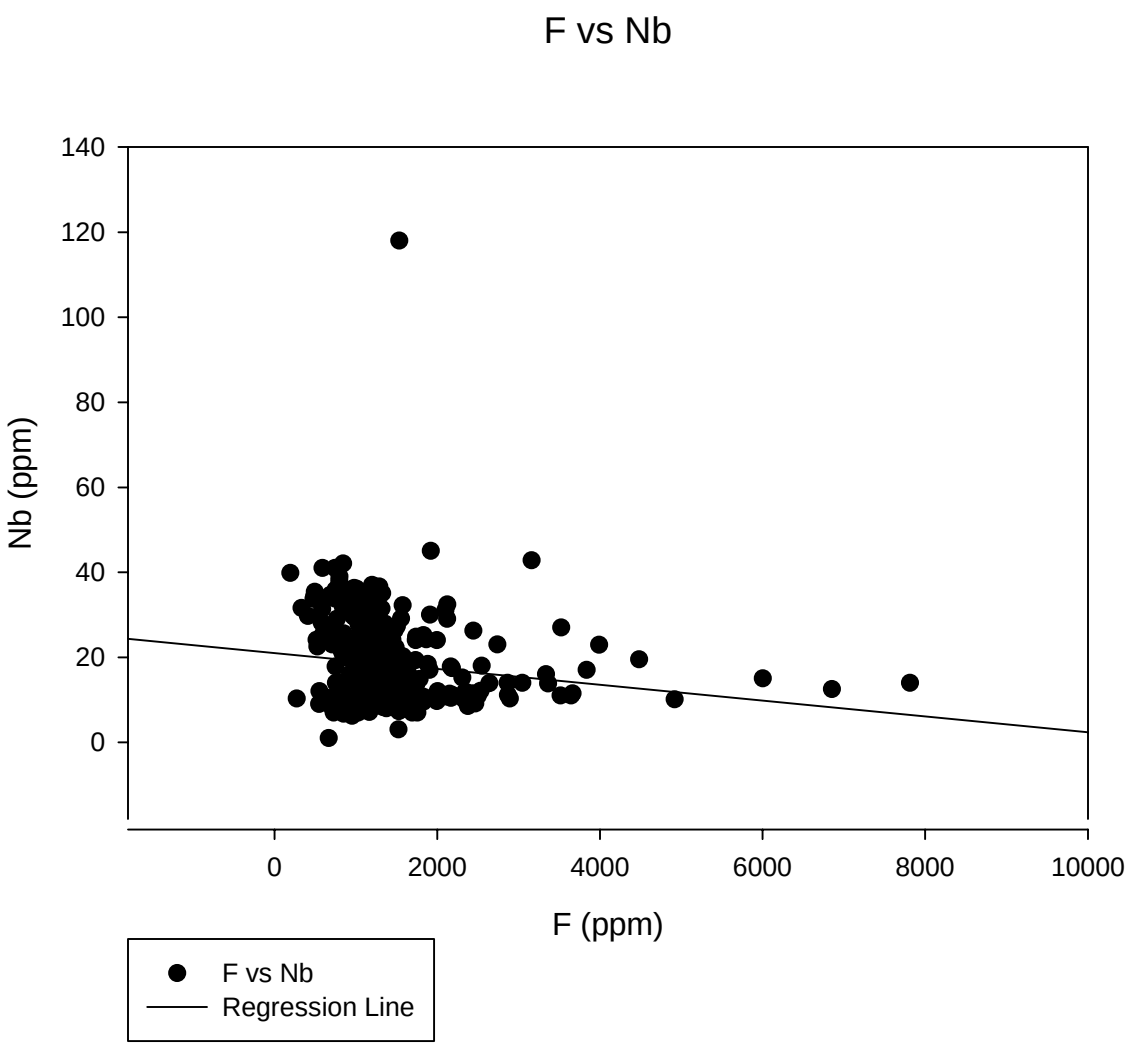
F vs Nb
140
120
100
80
60
40
20
0
Nb (ppm)
0
2000
4000
6000
8000
10000
F (ppm)
F vs Nb
Regression Line

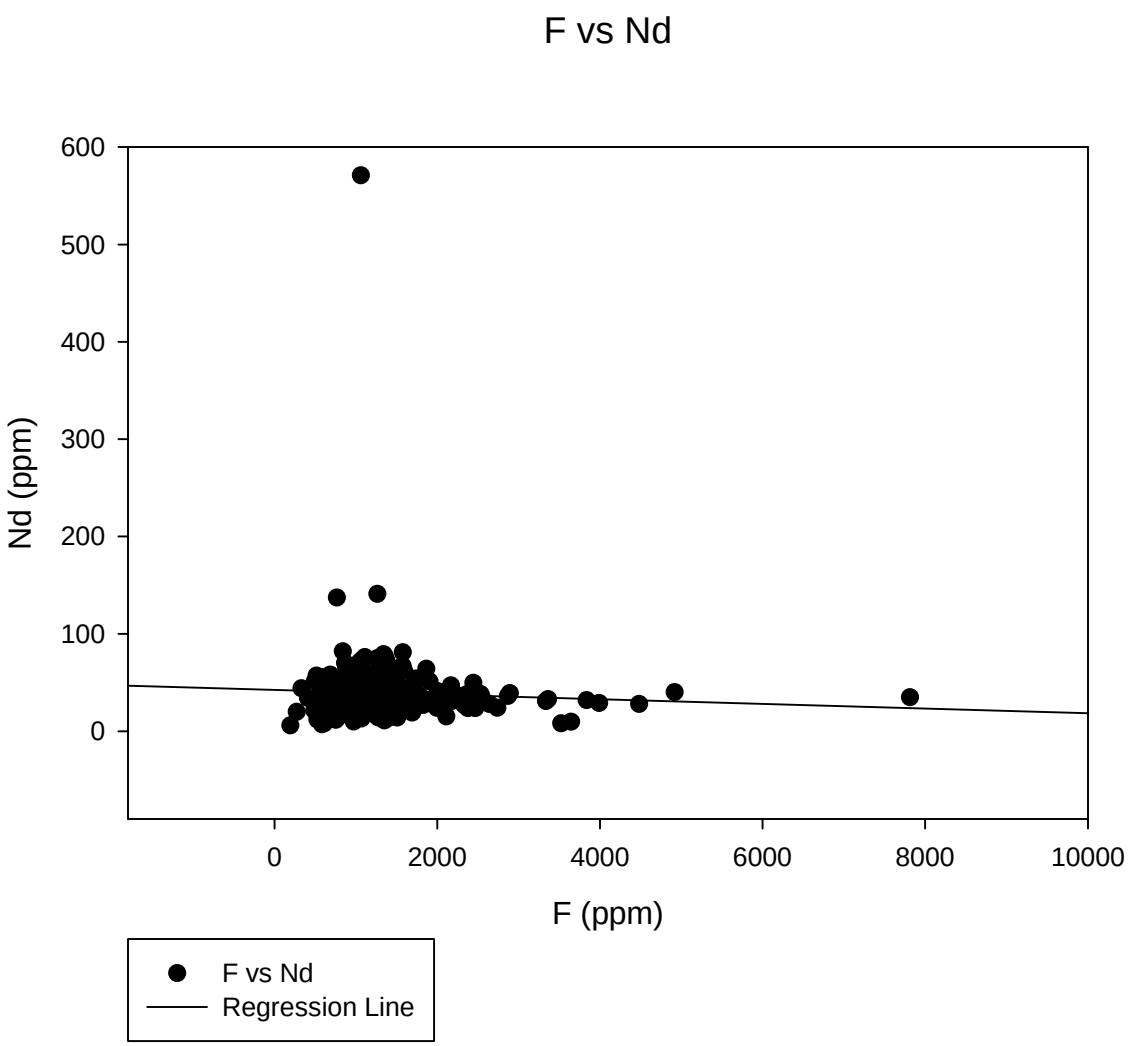
F vs Nd
600
500
400
300
200
100
0
Nd (ppm)
0
2000
4000
6000
8000
10000
F (ppm)
F vs Nd
Regression Line

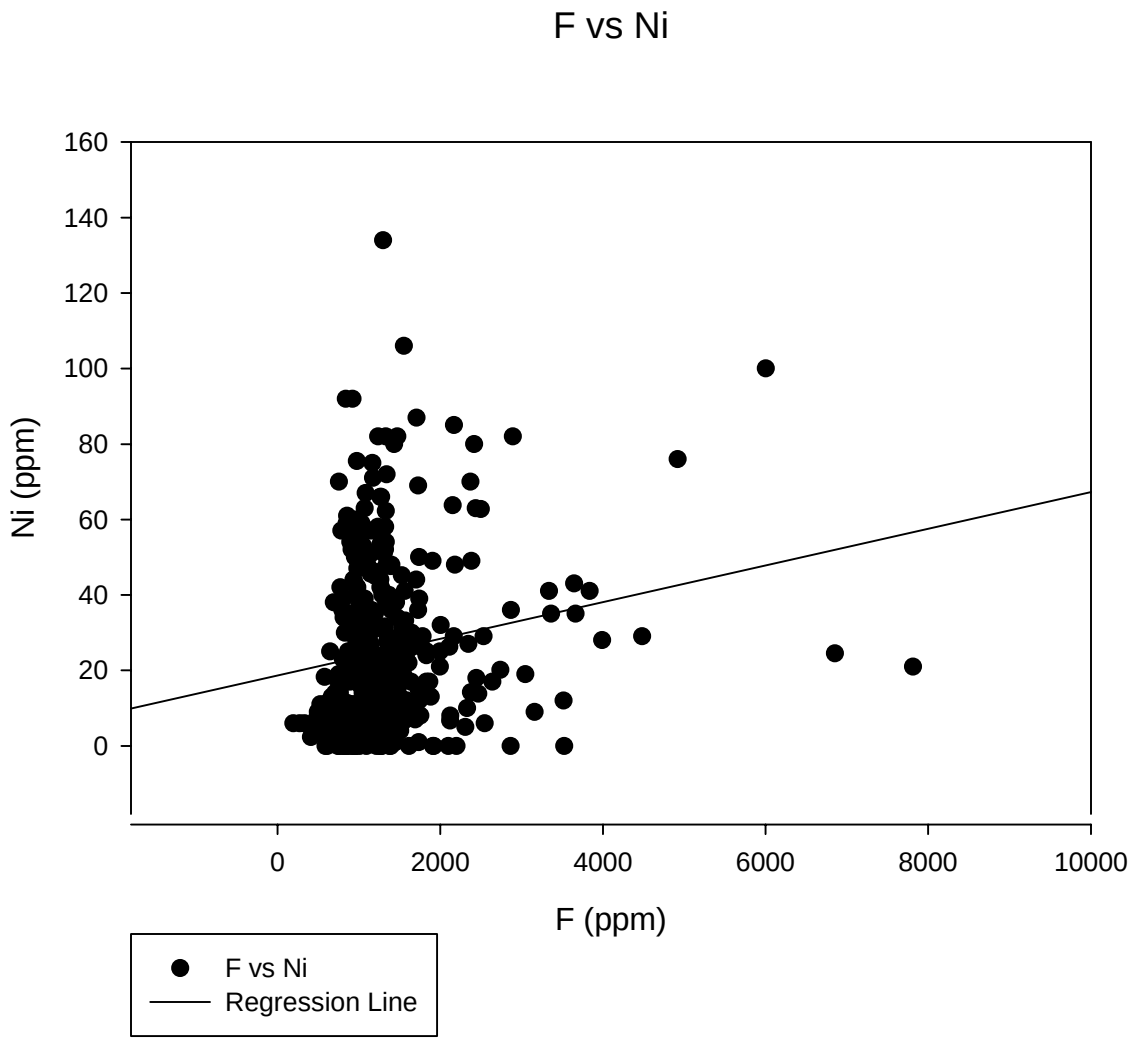
F vs Ni
160
140
120
100
80
60
40
20
0
Ni (ppm)
0
2000
4000
6000
8000
10000
F (ppm)
F vs Ni
Regression Line

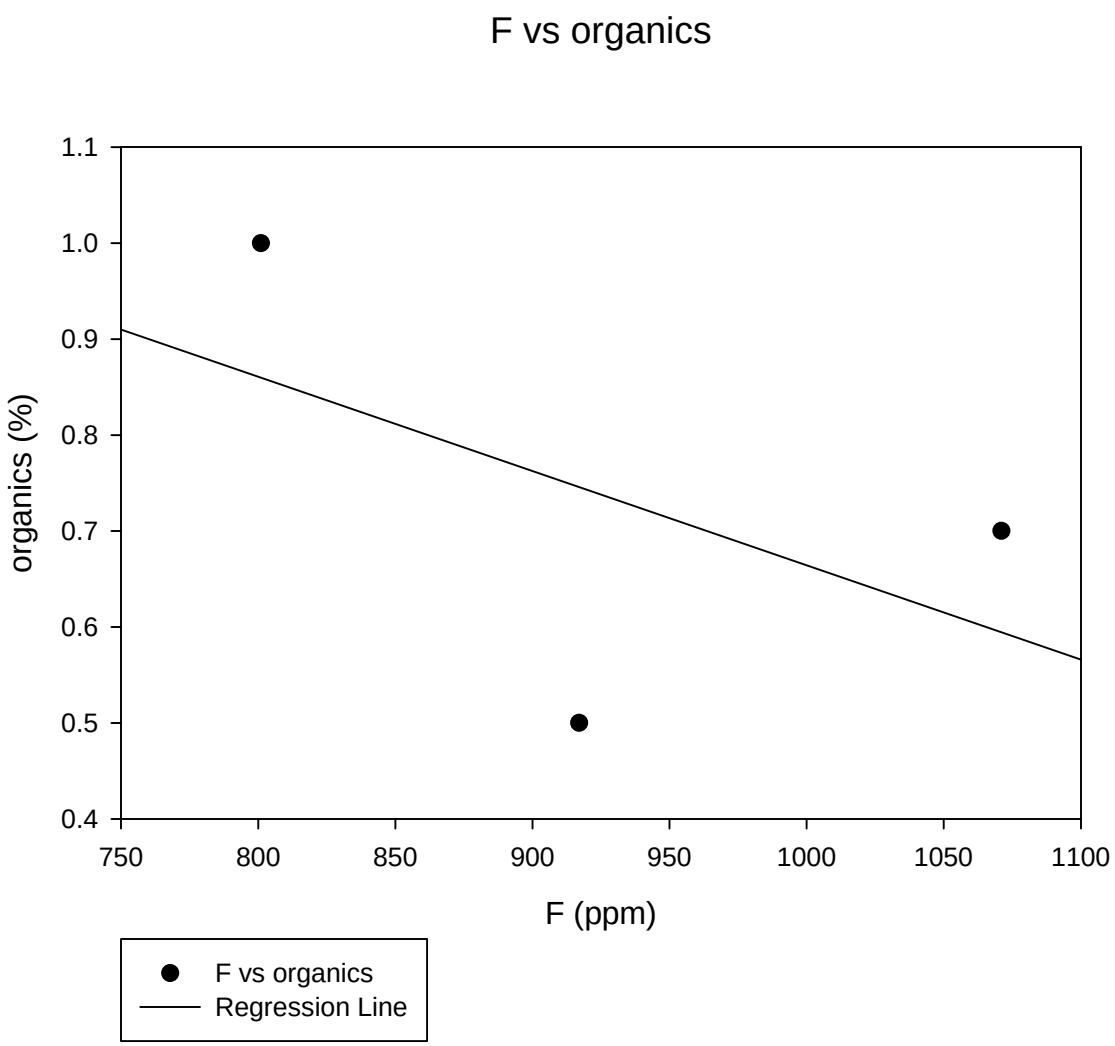
F vs organics
1.1
1.0
0.9
0.8
0.7
0.6
0.5
0.4
organics (%)
750
800
850
900
950
1000
1050
1100
F (ppm)
F vs organics
Regression Line

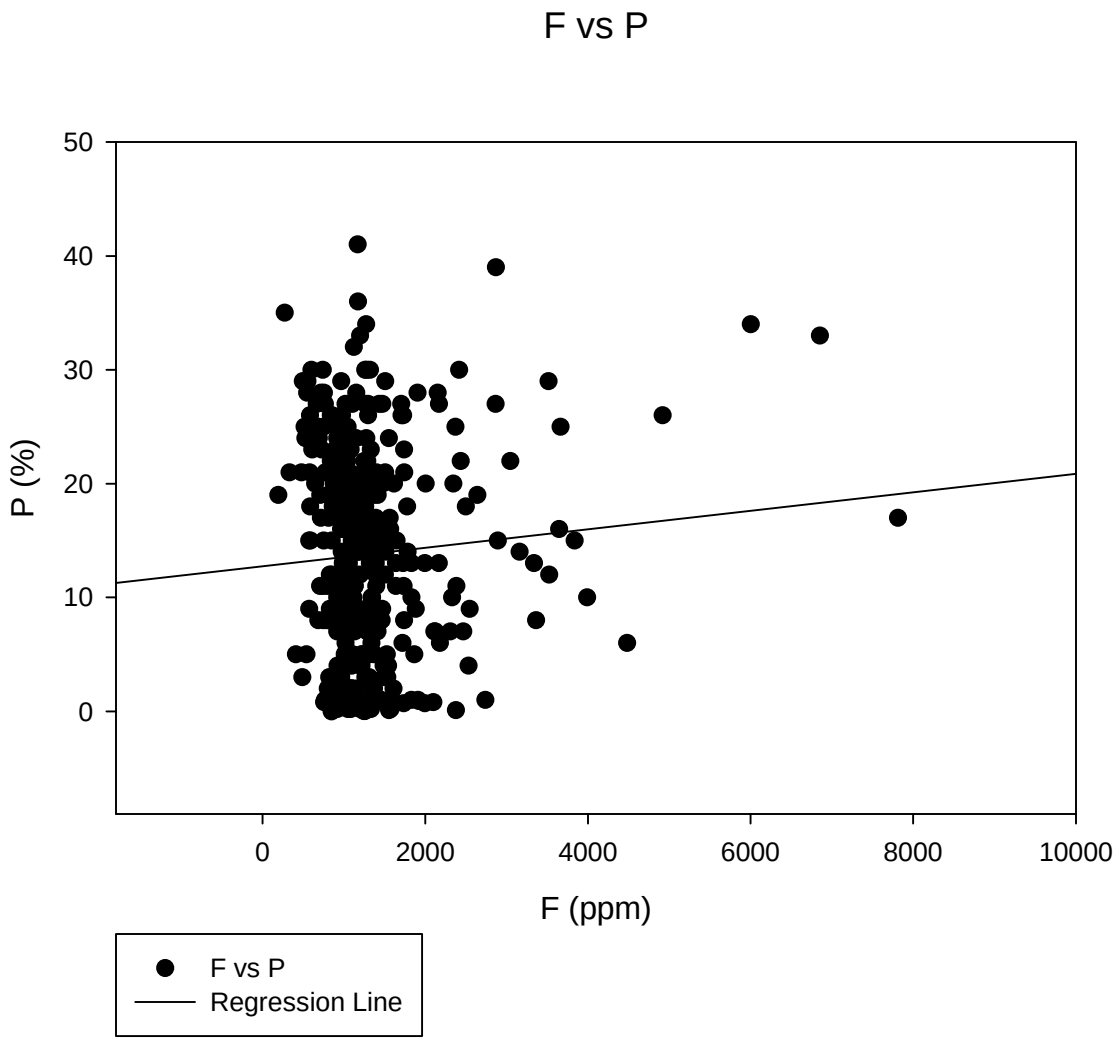
F vs P
50
40
30
20
10
0
P (%)
0
2000
4000
6000
8000
10000
F (ppm)
F vs P
Regression Line

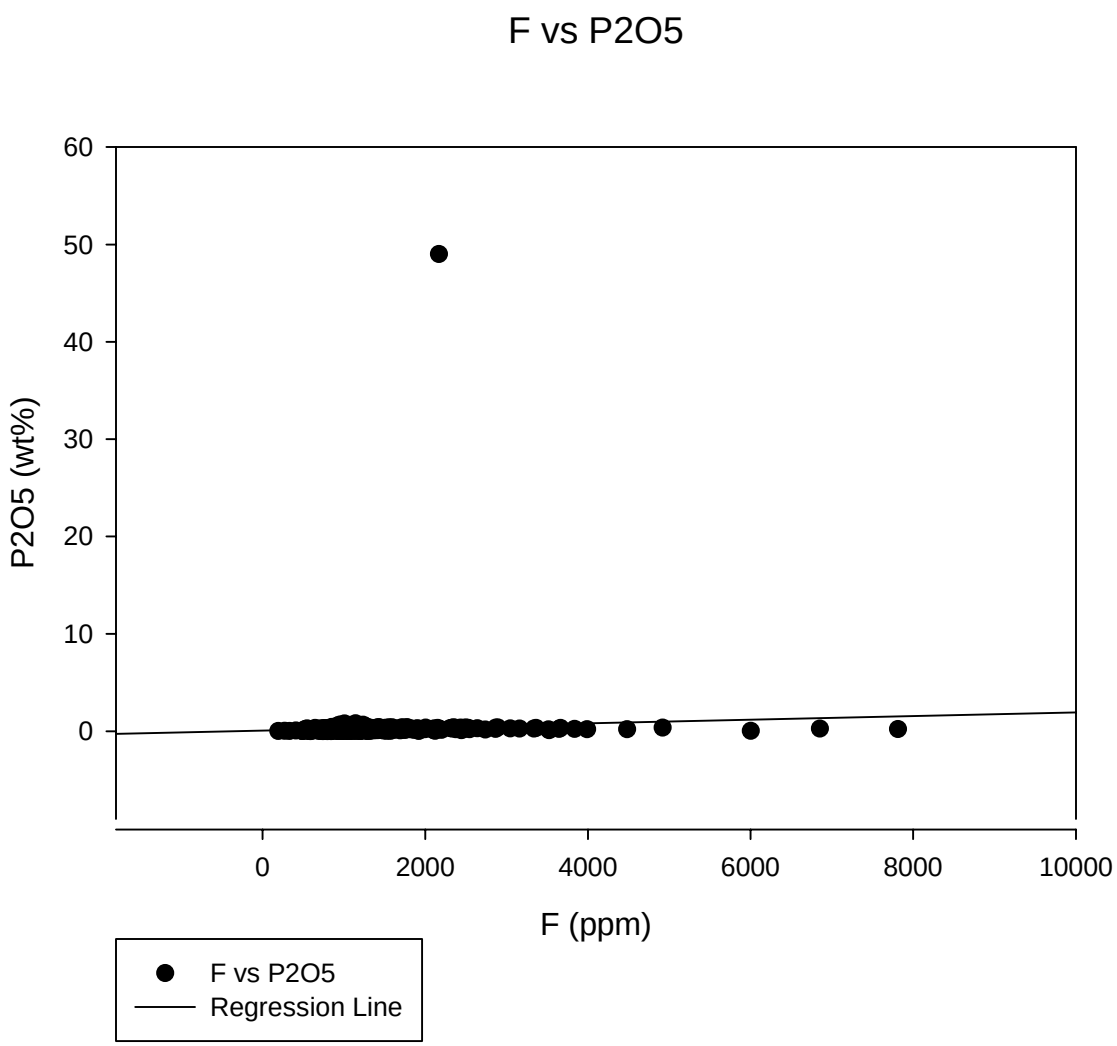
F vs P2O5
60
50
40
30
20
10
0
P2O5 (wt%)
0
2000
4000
6000
8000
10000
F (ppm)
F vs P2O5
Regression Line

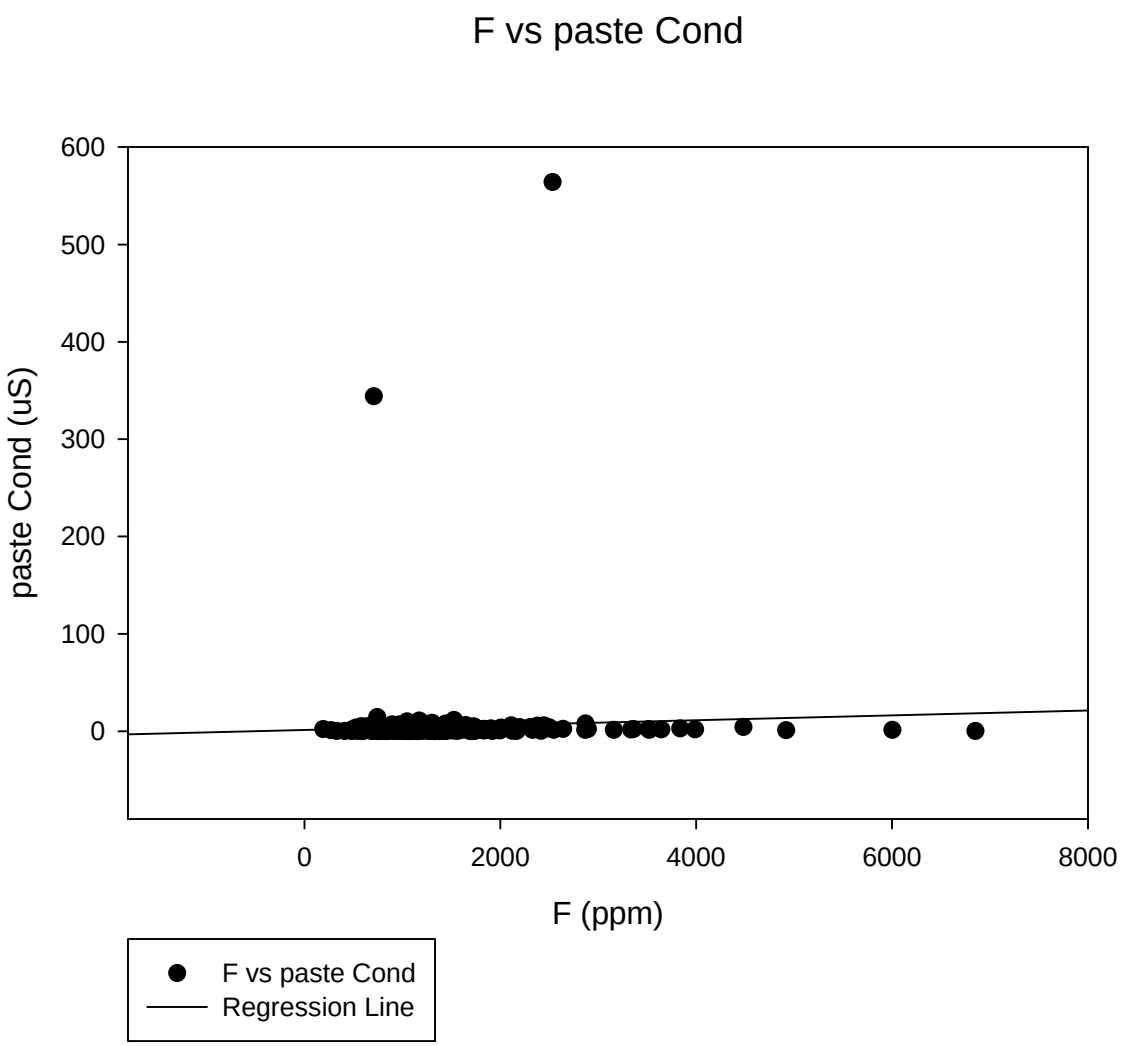
F vs paste Cond
600
500
400
300
200
100
0
paste Cond (uS)
0
2000
4000
6000
8000
F (ppm)
F vs paste Cond
Regression Line

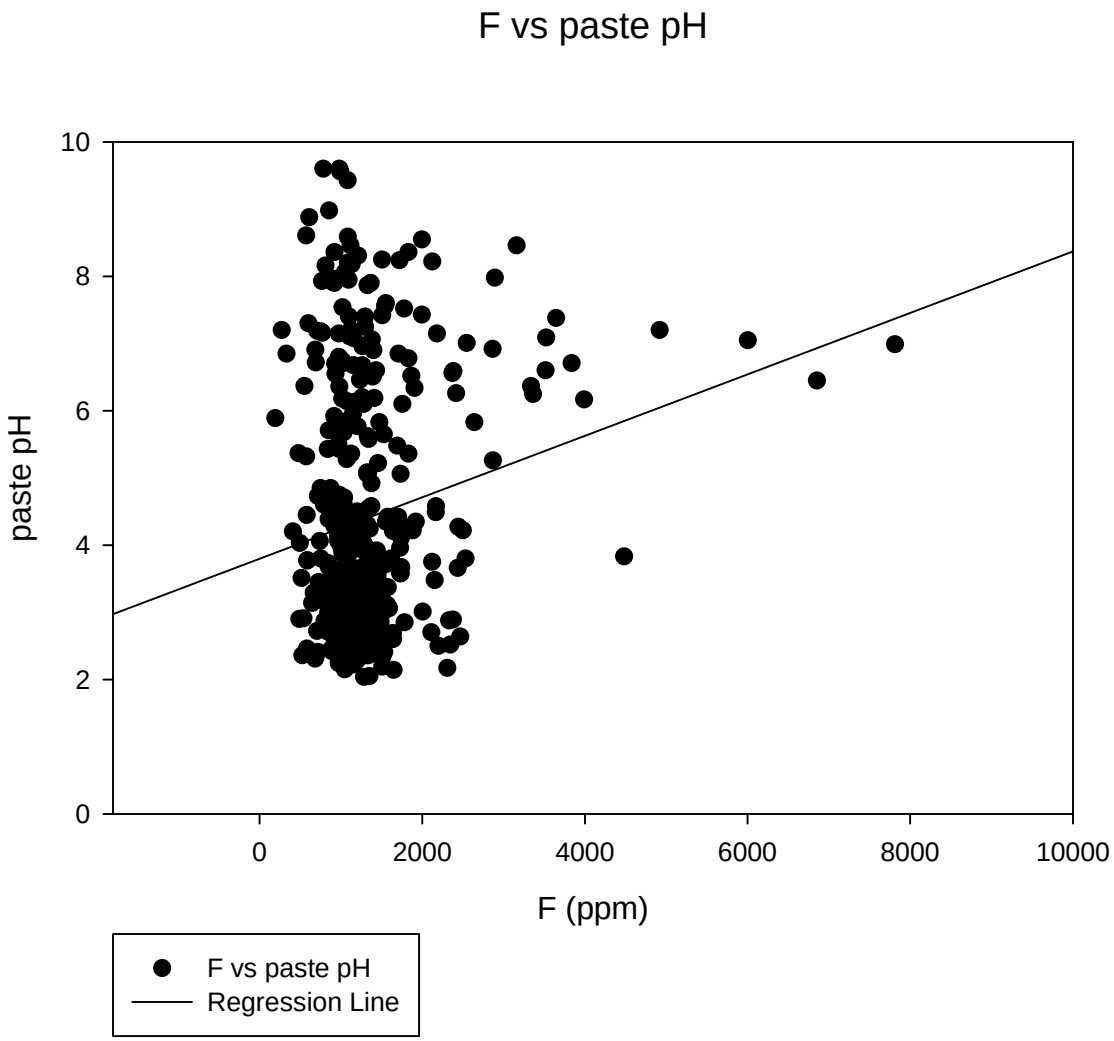
F vs paste pH
paste pH
10
8
6
4
2
0
0
2000
4000
6000
8000
10000
F (ppm)
F vs paste pH
Regression Line

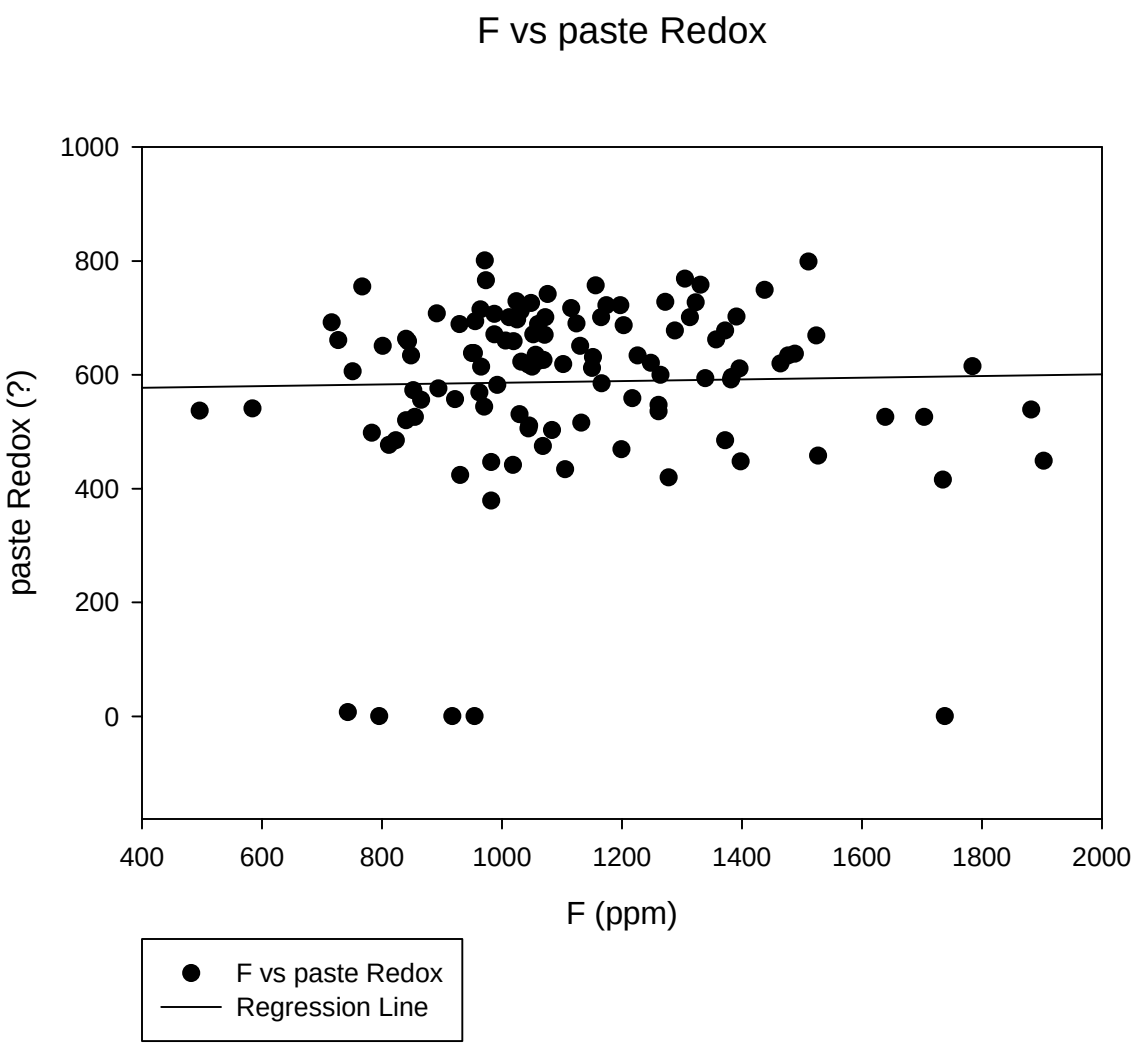
F vs paste Redox
paste Redox (?)
1000
800
600
400
200
0
400
600
800
1000
1200
1400
1600
1800
2000
F (ppm)
F vs paste Redox
Regression Line

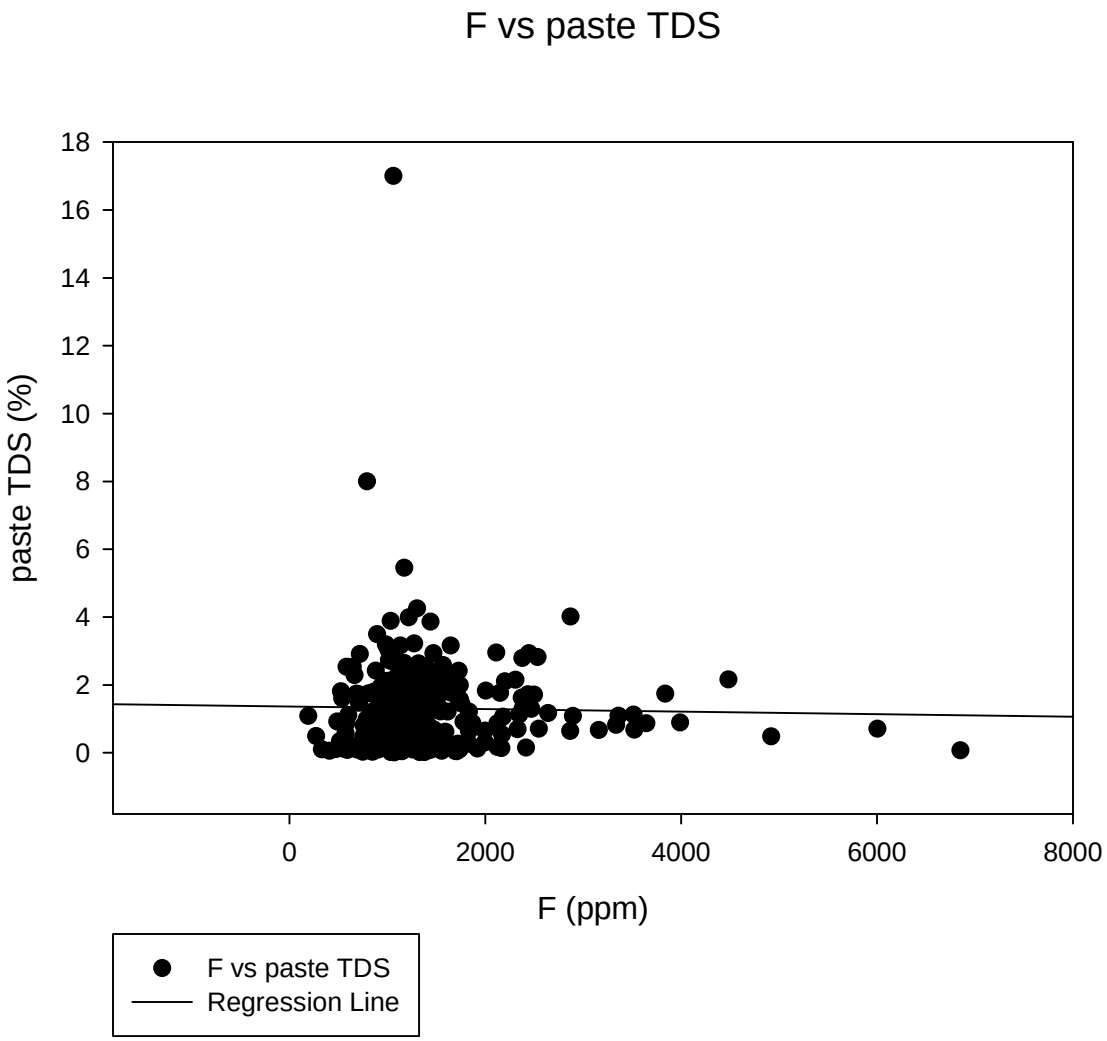
F vs paste TDS
paste TDS (%)
18
16
14
12
10
8
6
4
2
0
0
2000
4000
6000
8000
F (ppm)
F vs paste TDS
Regression Line

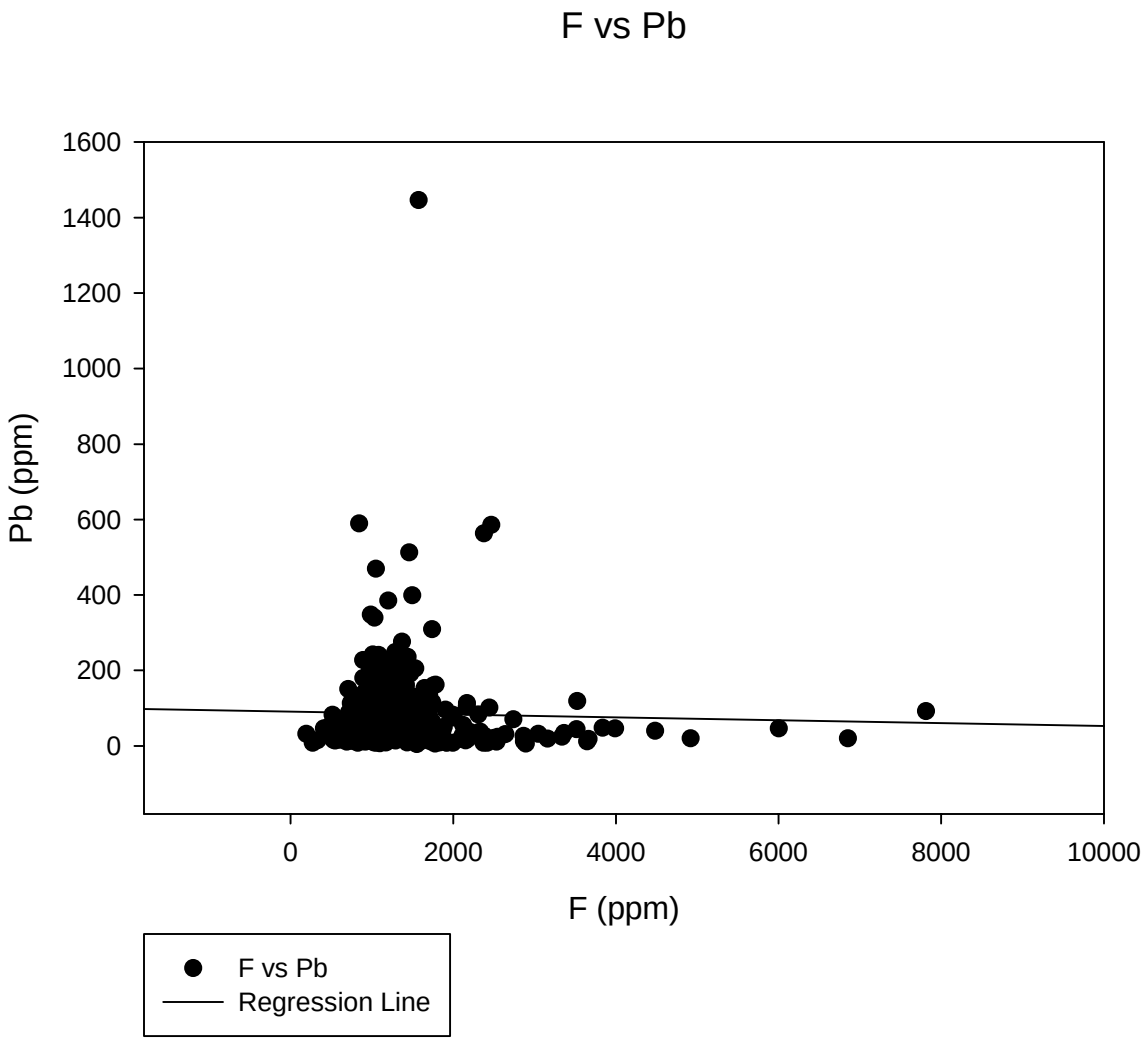
F vs Pb
1600
1400
1200
1000
800
600
400
200
0
Pb (ppm)
0
2000
4000
6000
8000
10000
F (ppm)
F vs Pb
Regression Line

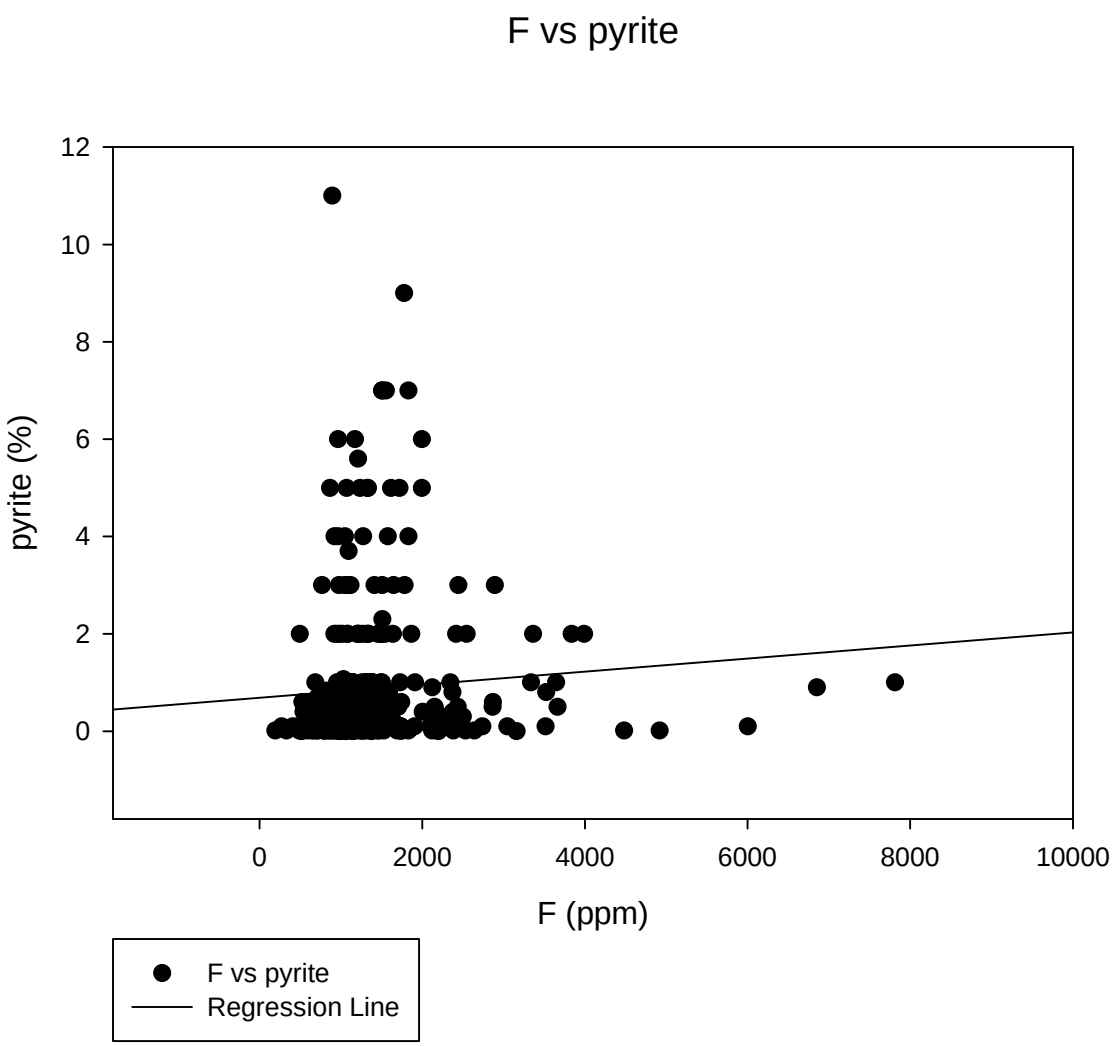
F vs pyrite
12
10
8
6
4
2
0
pyrite (%)
0
2000
4000
6000
8000
10000
F (ppm)
F vs pyrite
Regression Line

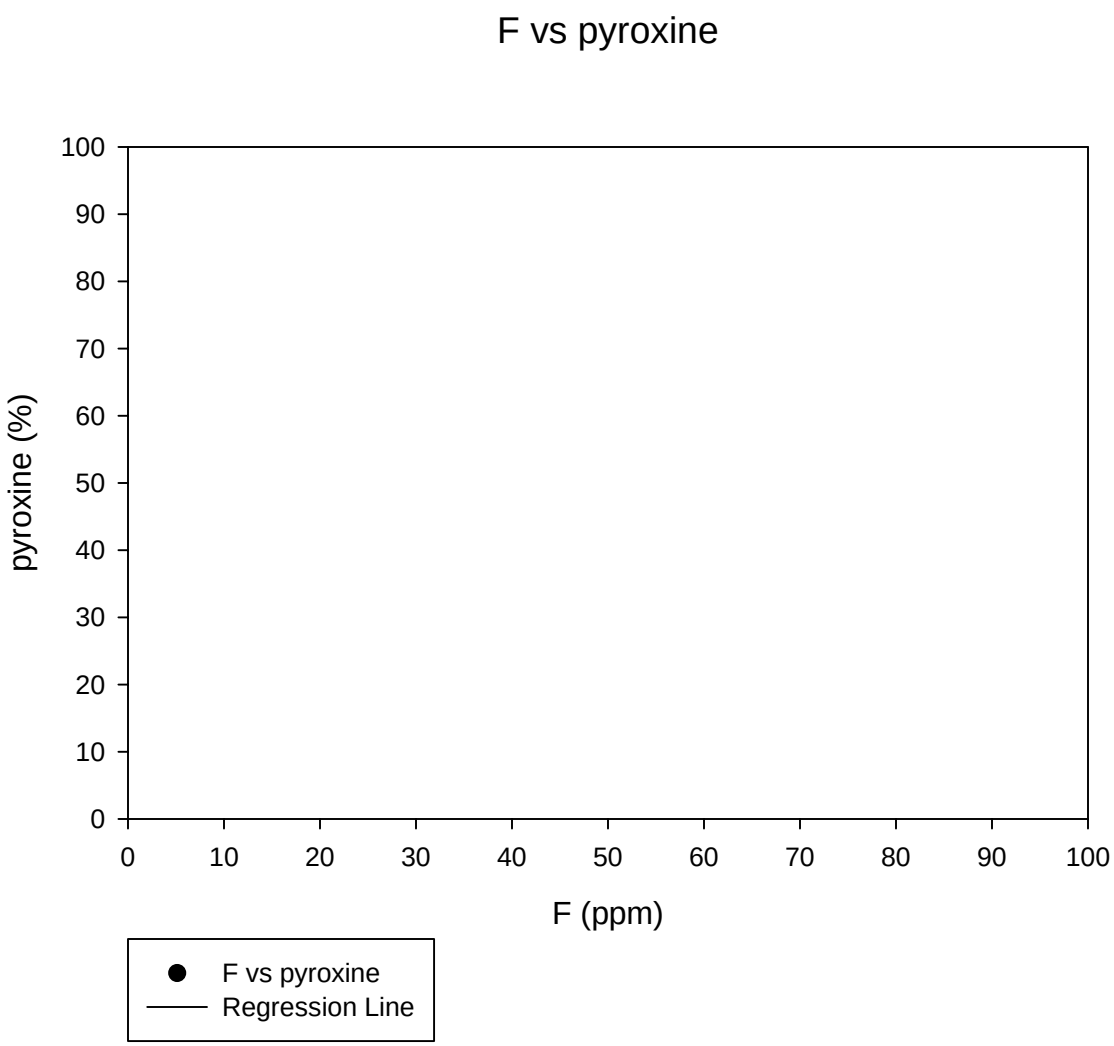
F vs pyroxine
pyroxine (%)
100
90
80
70
60
50
40
30
20
10
0
0
10
20
30
40
50
60
70
80
90
100
F (ppm)
F vs pyroxine
Regression Line

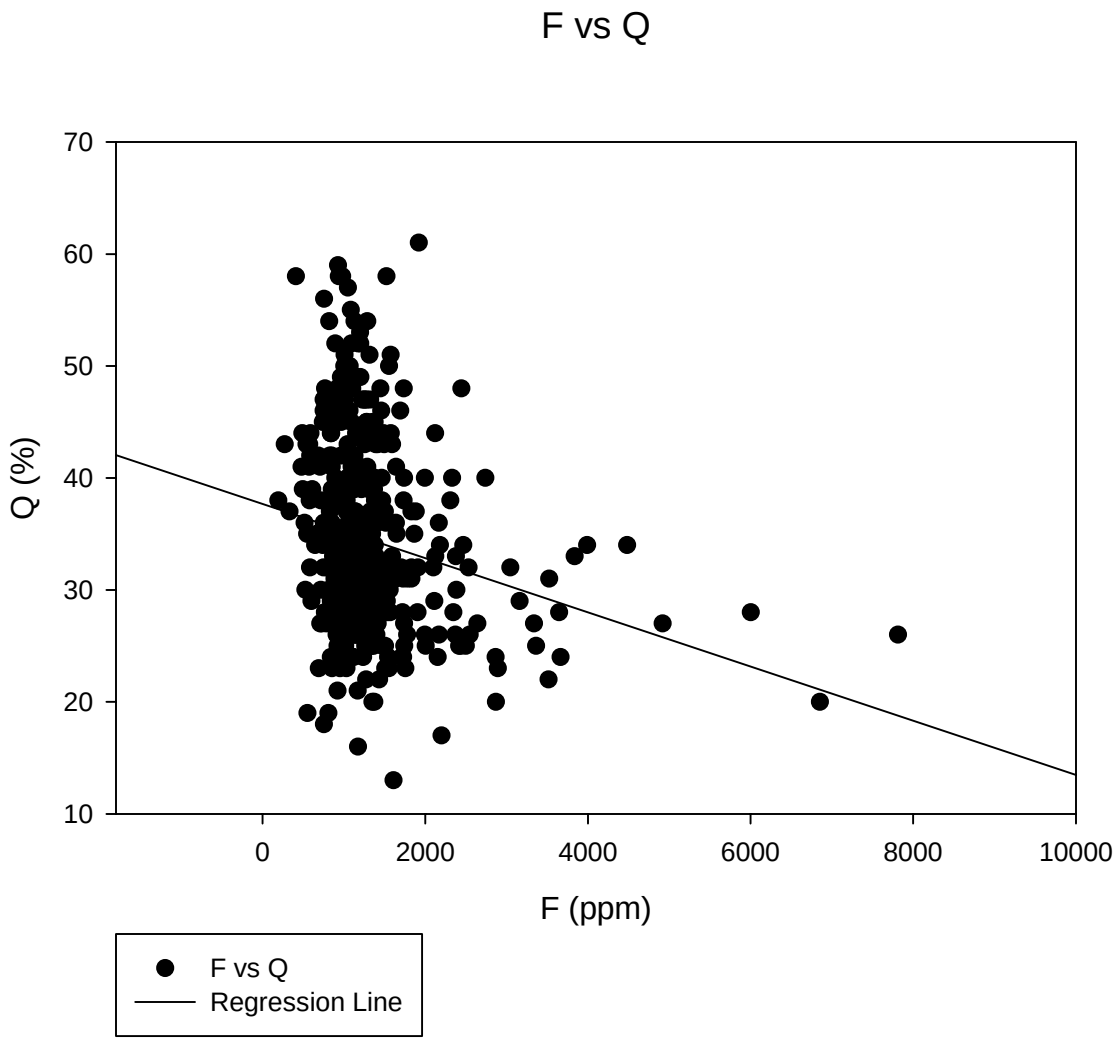
F vs Q
70
60
50
40
30
20
10
Q (%)
0
2000
4000
6000
8000
10000
F (ppm)
F vs Q
Regression Line

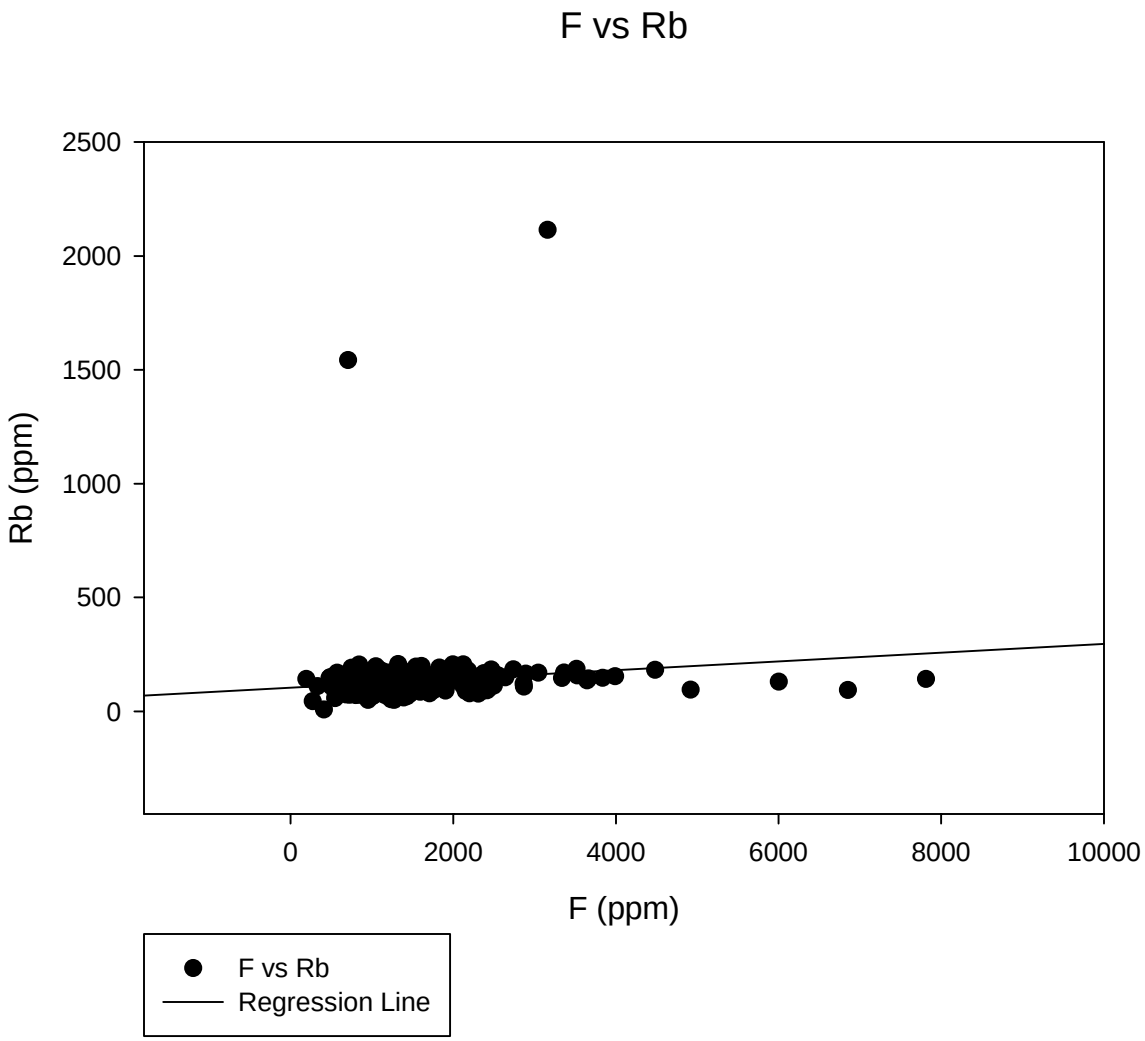
F vs Rb
2500
2000
1500
1000
500
0
Rb (ppm)
0
2000
4000
6000
8000
10000
F (ppm)
F vs Rb
Regression Line

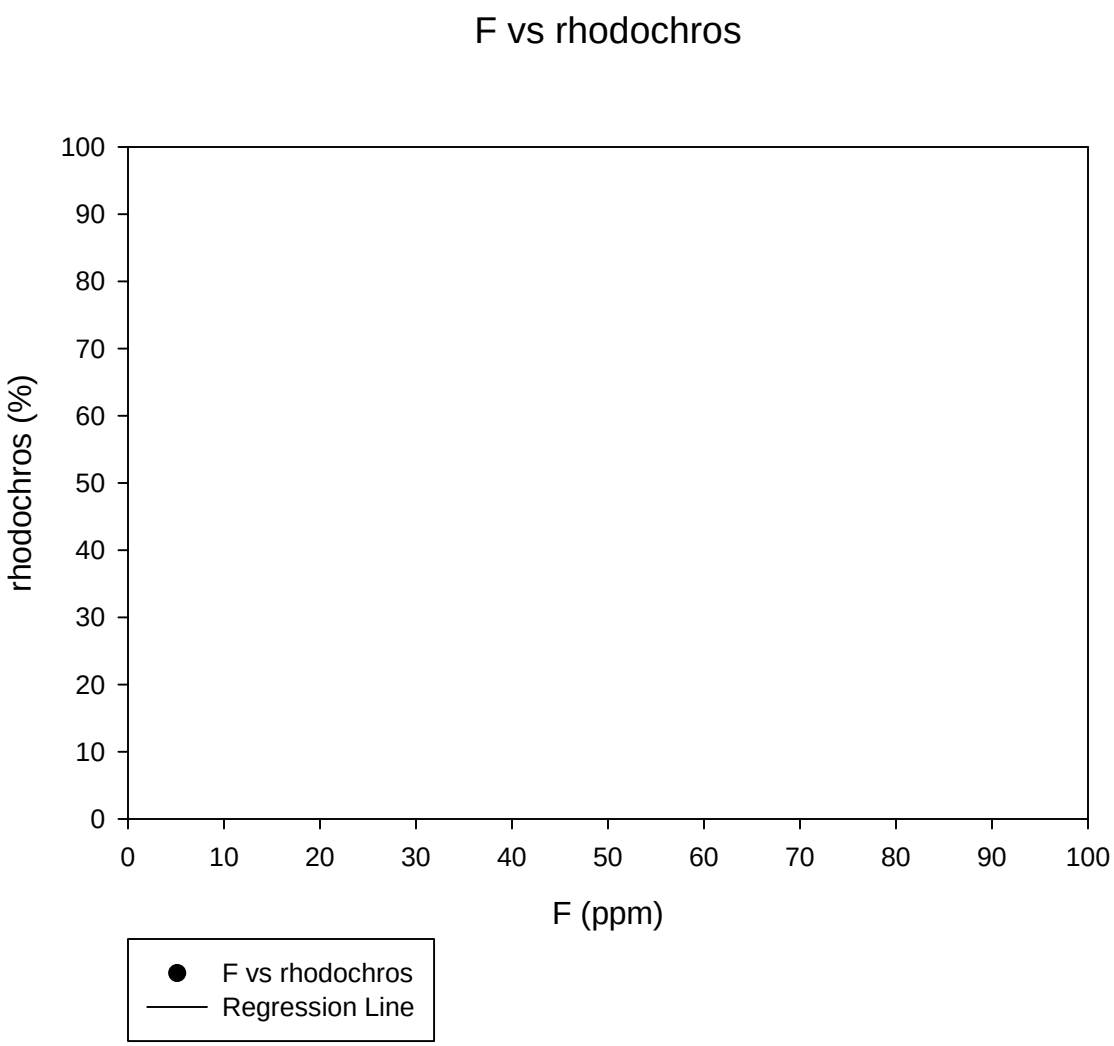
F vs rhodochros
rhodochros (%)
100
90
80
70
60
50
40
30
20
10
0
0
10
20
30
40
50
60
70
80
90
100
F (ppm)
F vs rhodochros
Regression Line

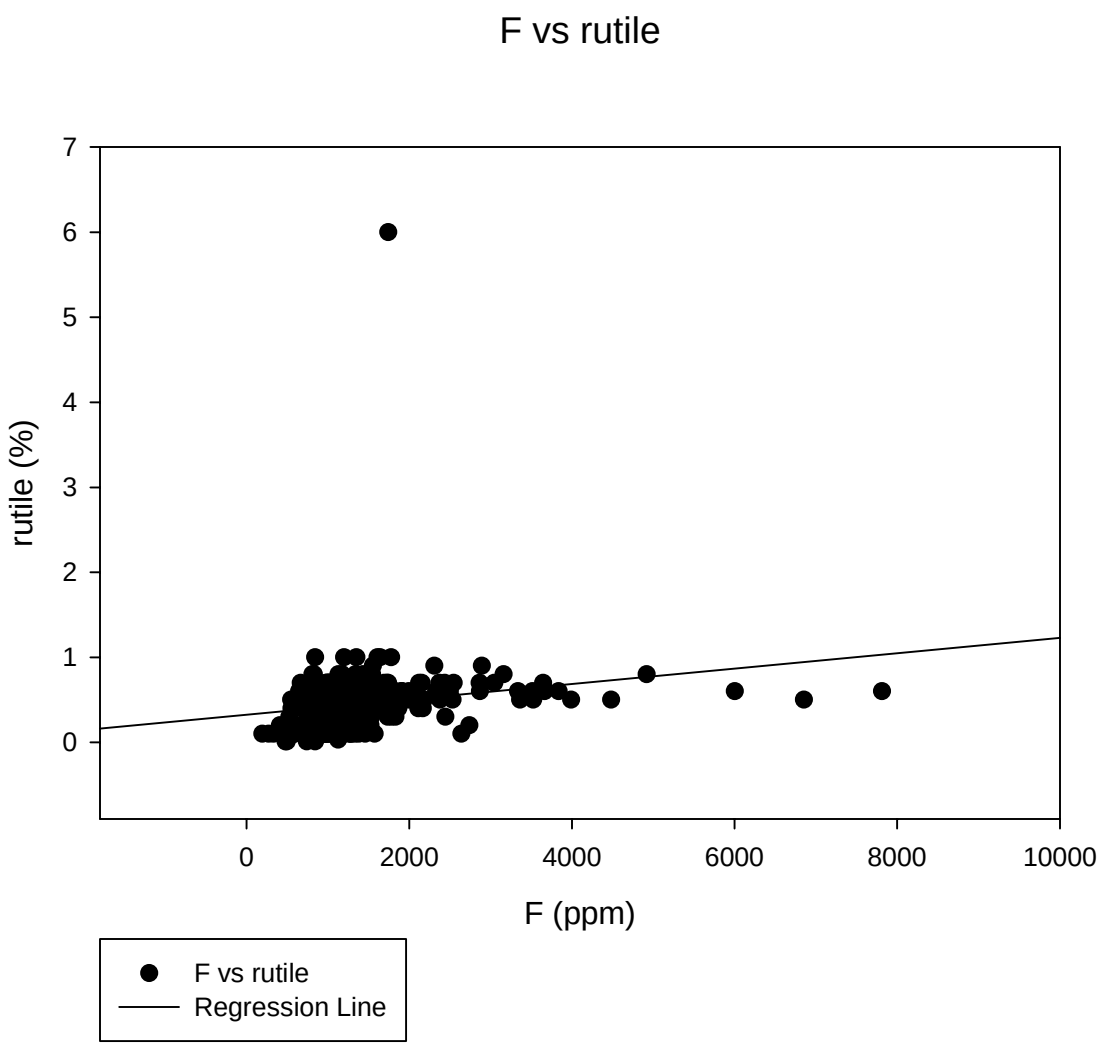
F vs rutile
rutile (%)
7
6
5
4
3
2
1
0
0
2000
4000
6000
8000
10000
F (ppm)
F vs rutile
Regression Line

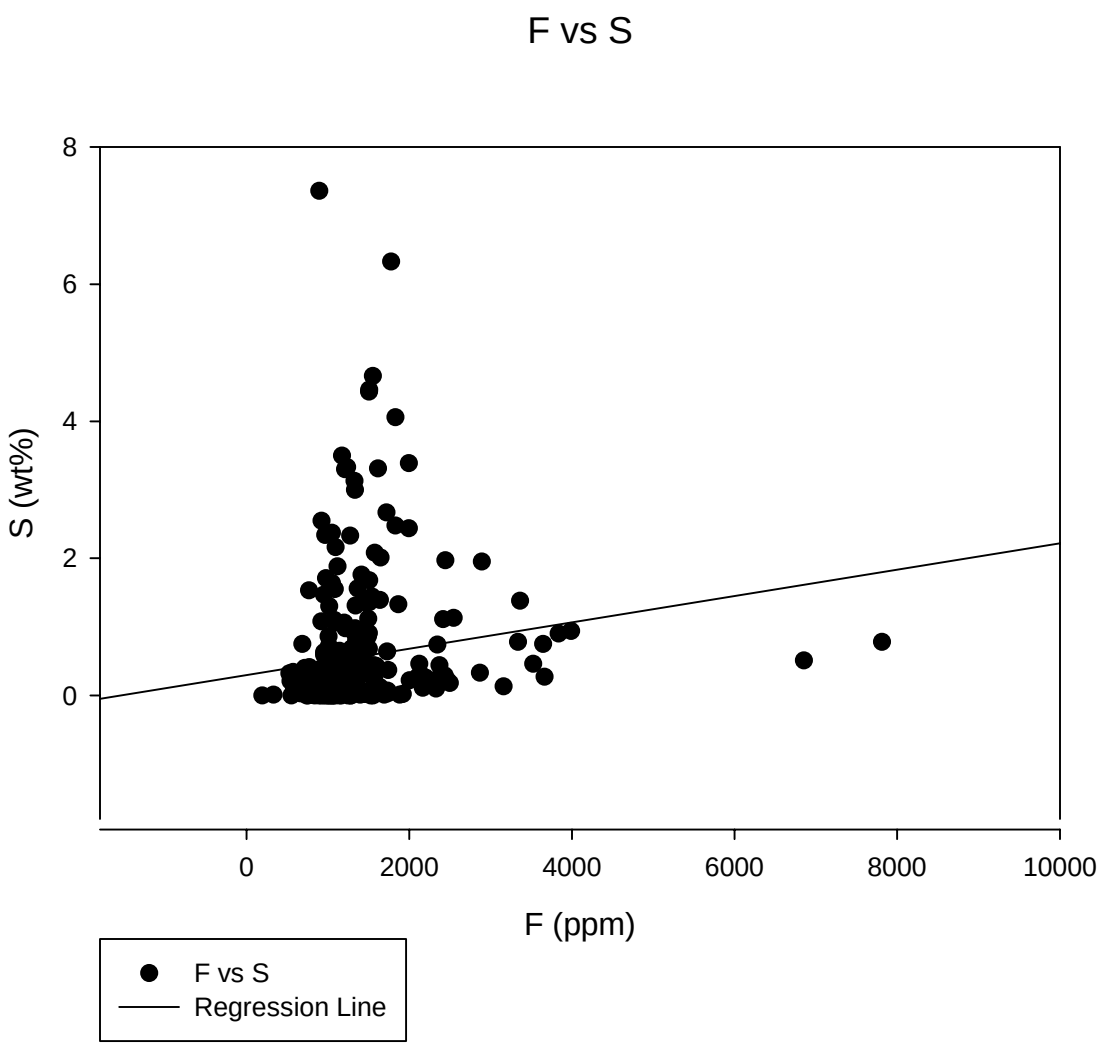
F vs S
8
6
4
2
0
S (wt%)
0
2000
4000
6000
8000
10000
F (ppm)
F vs S
Regression Line

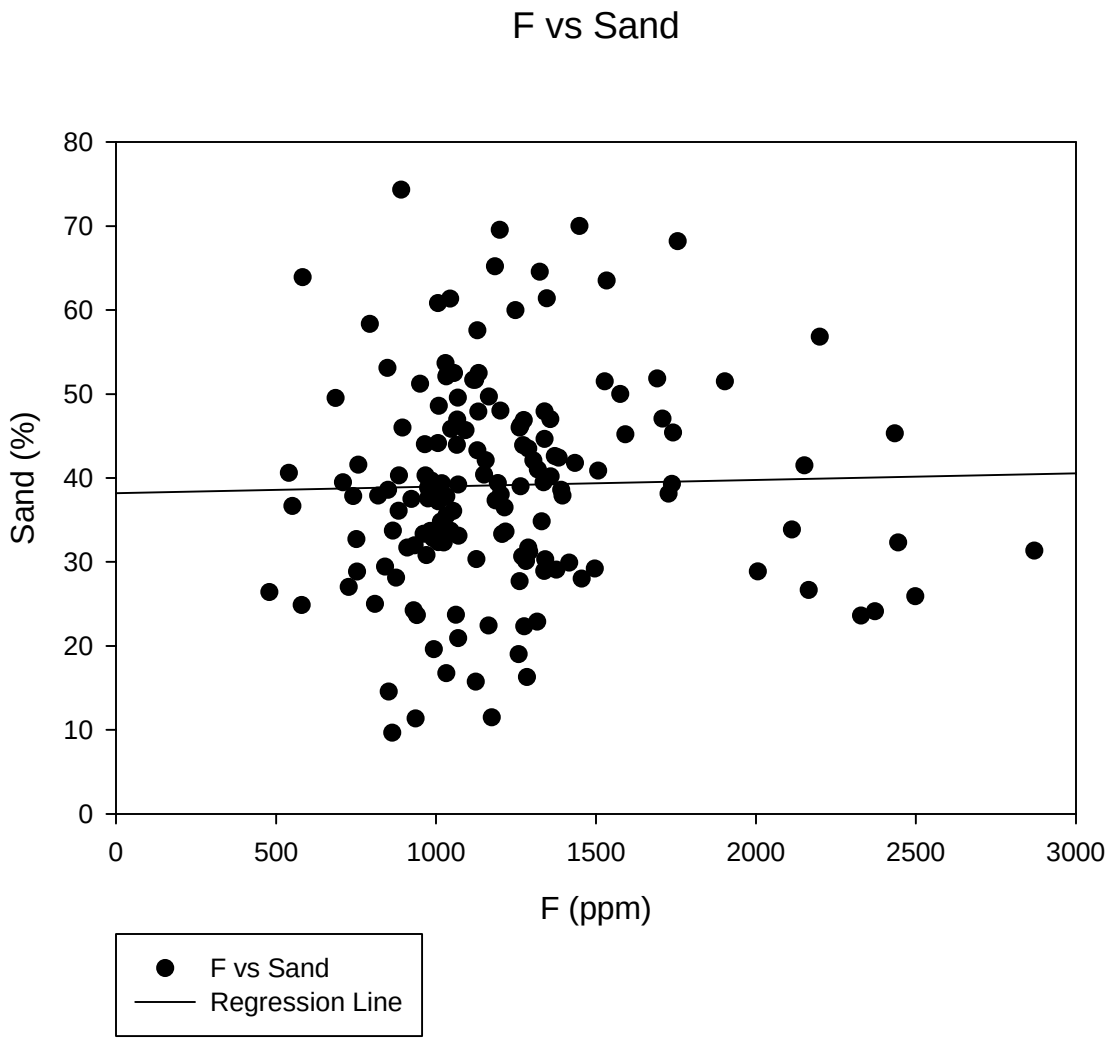
F vs Sand
Sand (%)
80
70
60
50
40
30
20
10
0
0
500
1000
1500
2000
2500
3000
F (ppm)
F vs Sand
Regression Line

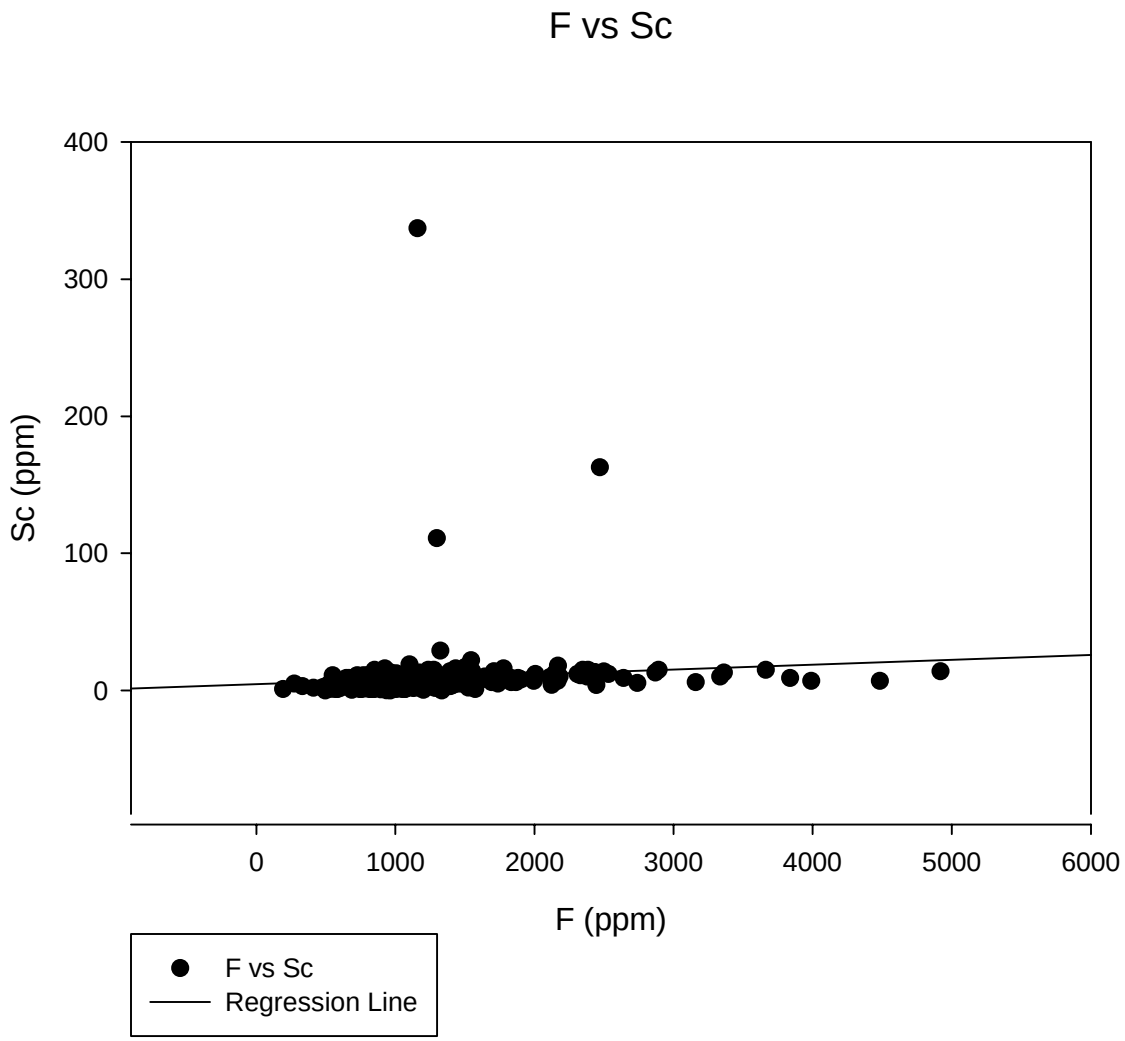
F vs Sc
400
300
200
100
0
Sc (ppm)
0
1000
2000
3000
4000
5000
6000
F (ppm)
F vs Sc
Regression Line

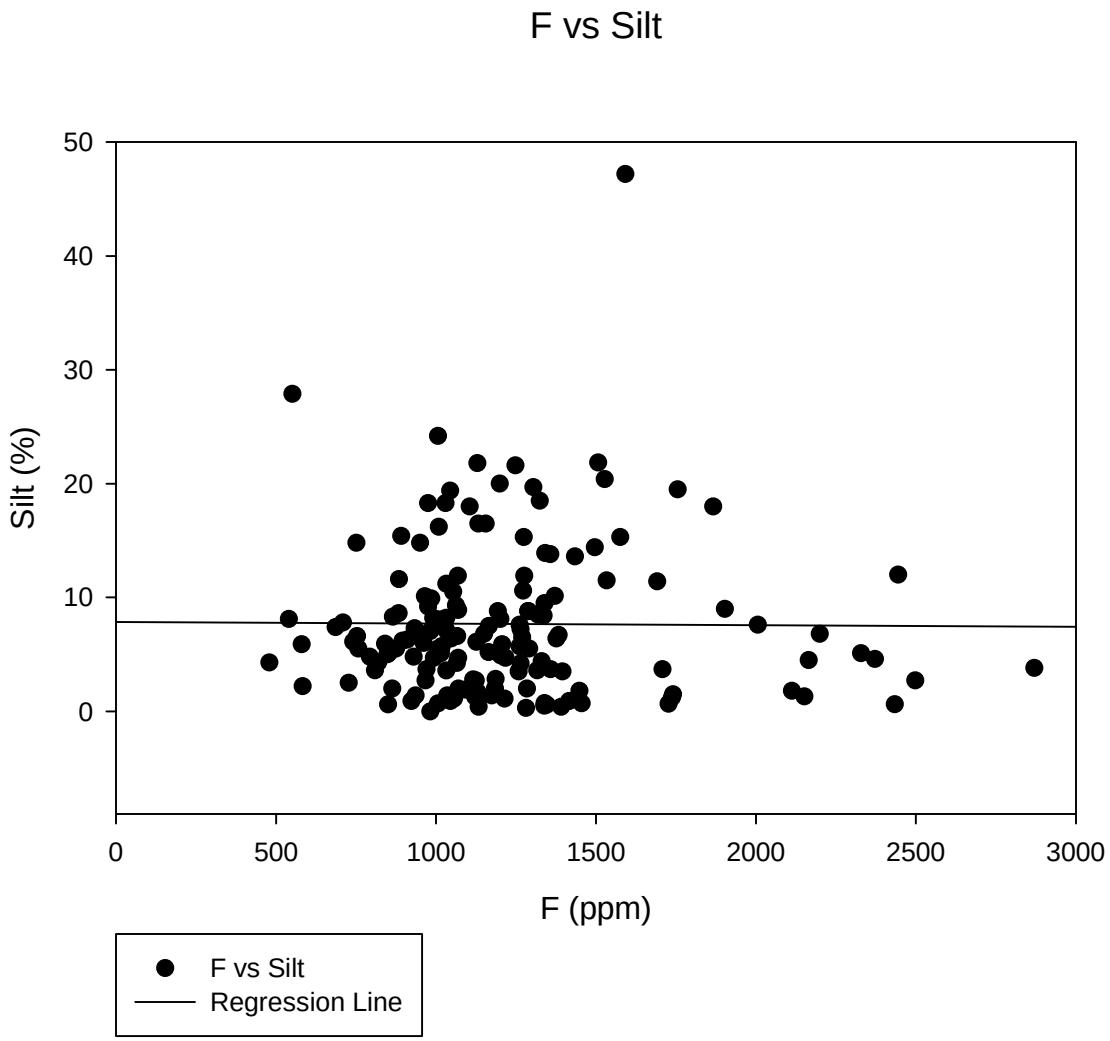
F vs Silt
50
40
30
20
10
0
Silt (%)
0
500
1000
1500
2000
2500
3000
F (ppm)
F vs Silt
Regression Line

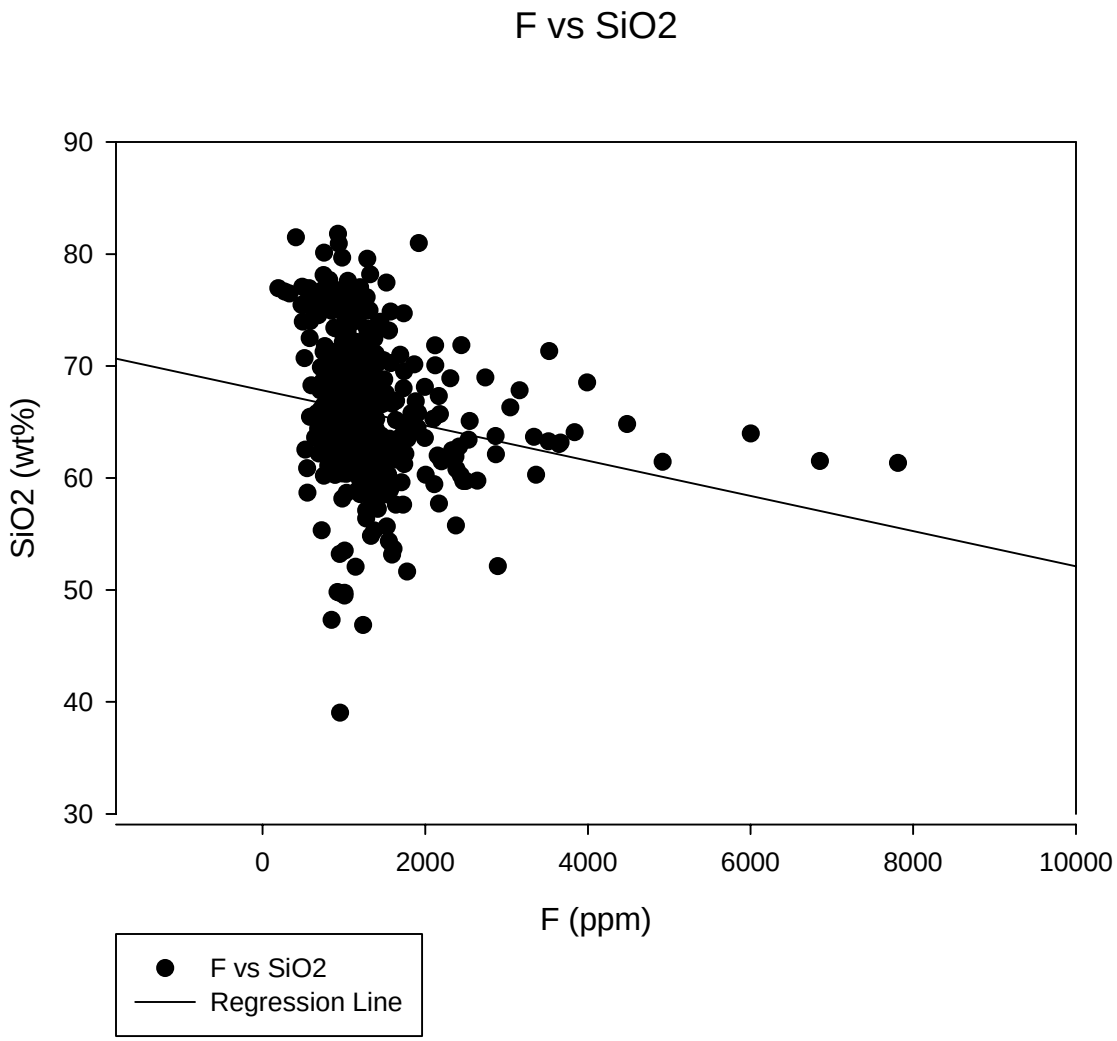
F vs SiO2
90
80
70
60
50
40
30
SiO2 (wt%)
0
2000
4000
6000
8000
10000
F (ppm)
F vs SiO2
Regression Line

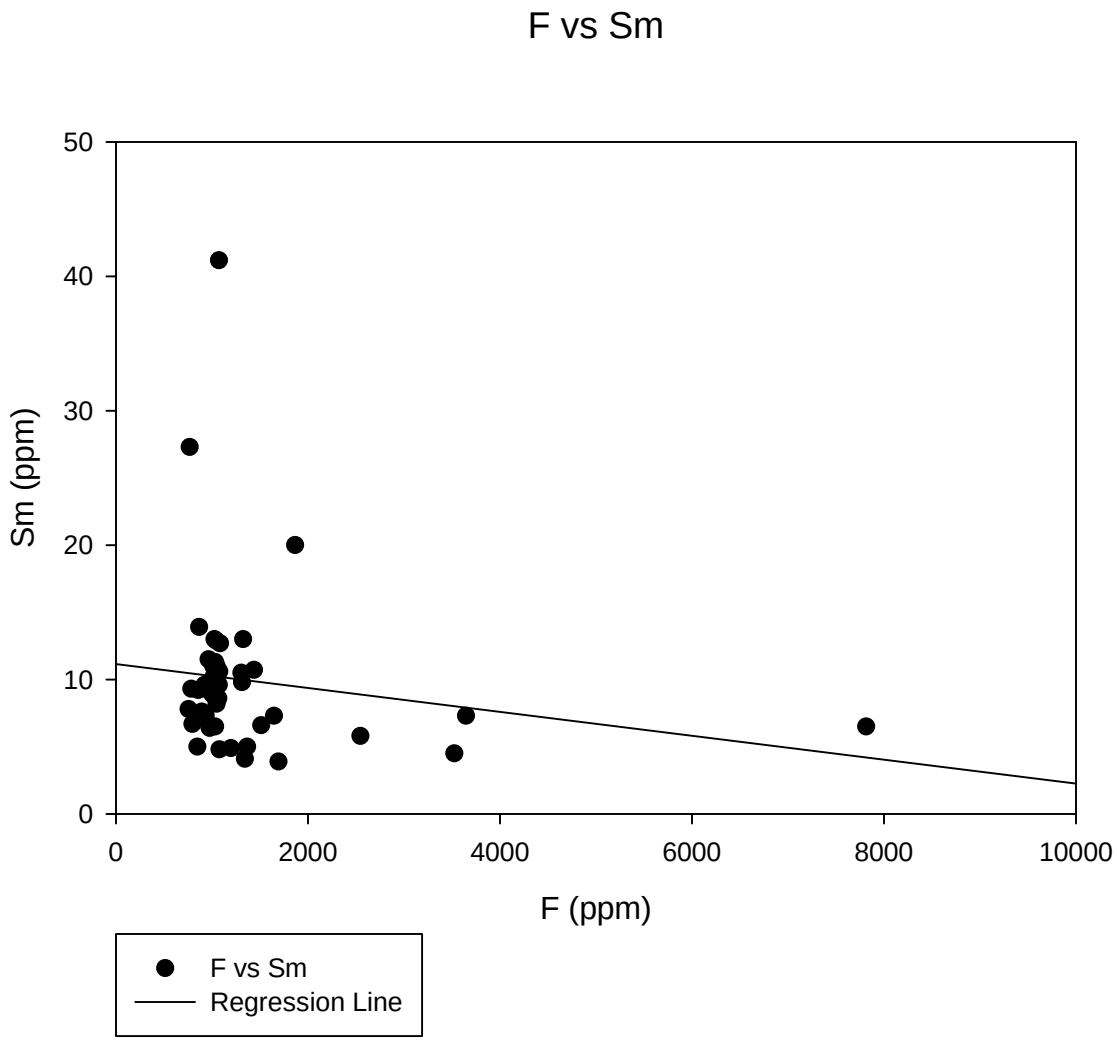
F vs Sm
50
40
30
20
10
0
Sm (ppm)
0
2000
4000
6000
8000
10000
F (ppm)
F vs Sm
Regression Line

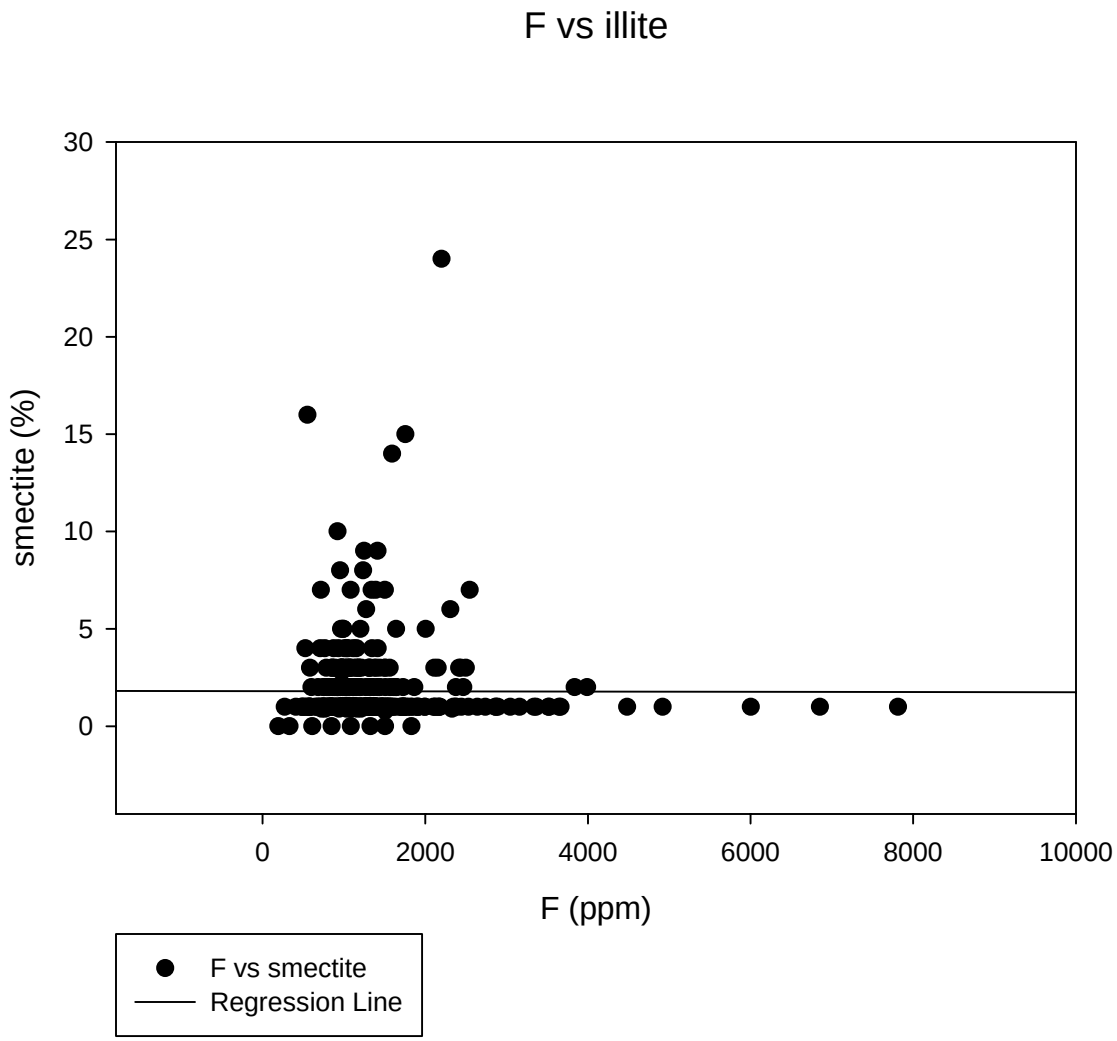
F vs illite
30
25
20
15
10
5
0
smectite (%)
0
2000
4000
6000
8000
10000
F (ppm)
F vs smectite
Regression Line

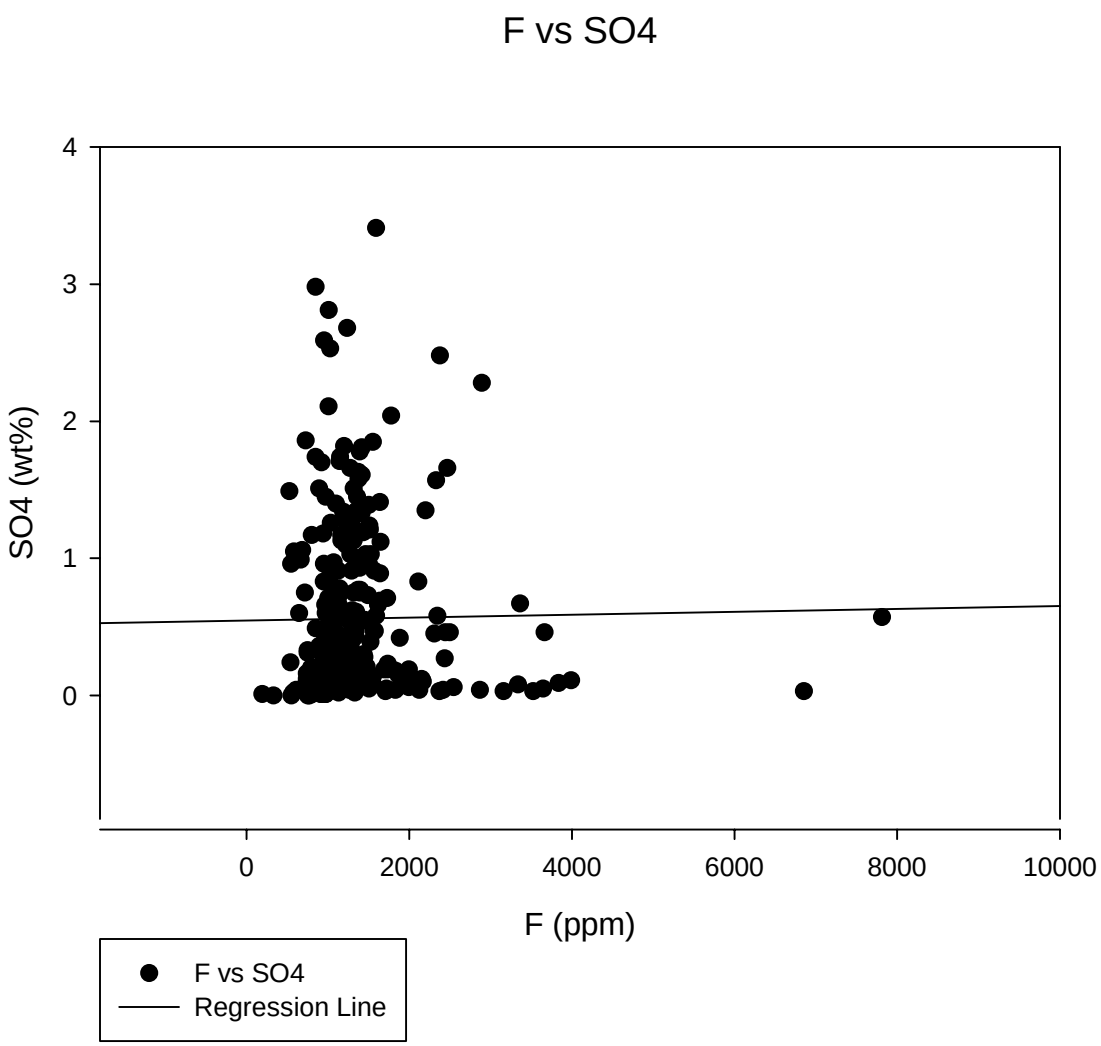
F vs SO4
SO4 (wt%)
4
3
2
1
0
0
2000
4000
6000
8000
10000
F (ppm)
F vs SO4
Regression Line

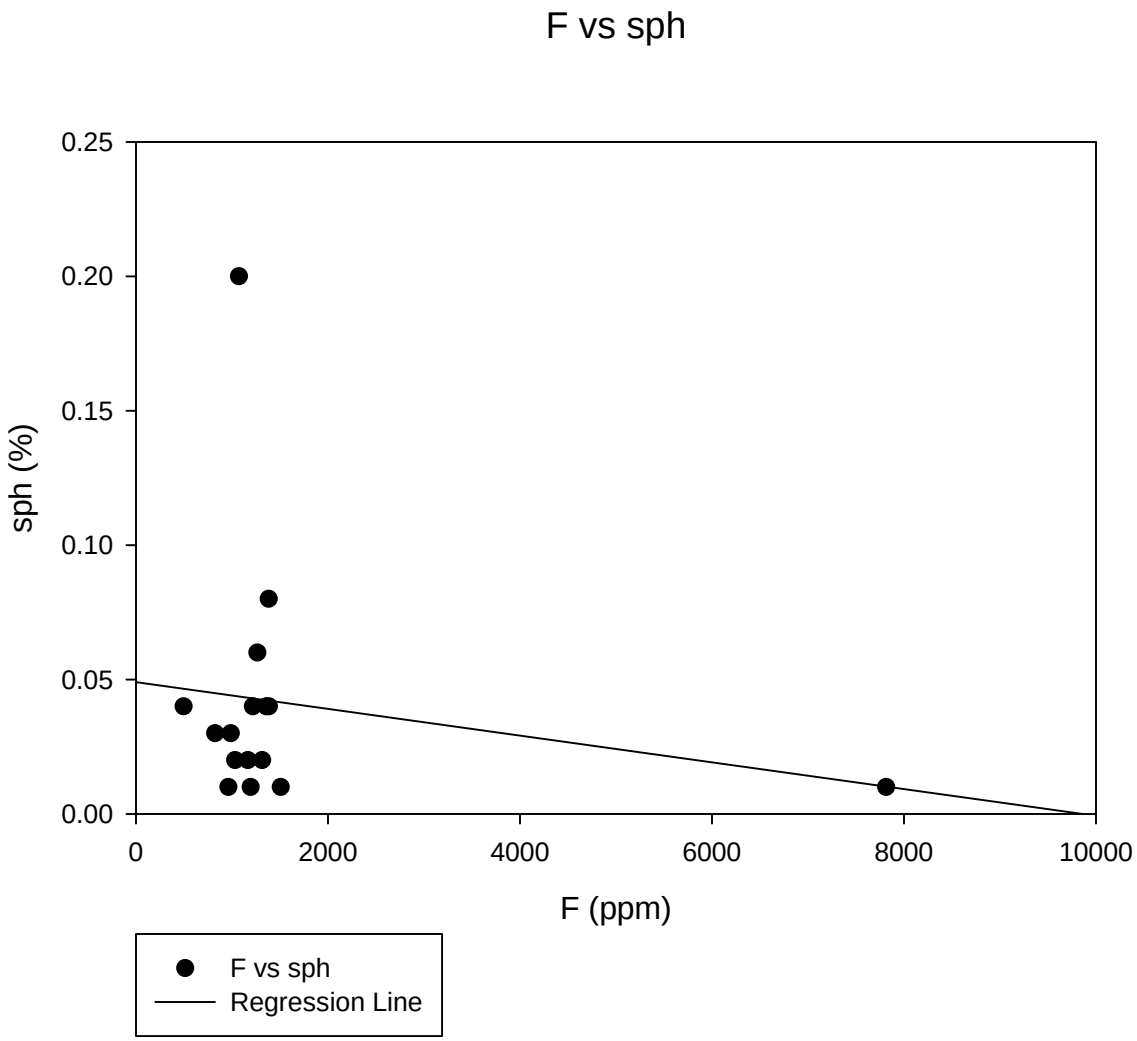
F vs sph
0.25
0.20
0.15
0.10
0.05
0.00
sph (%)
0
2000
4000
6000
8000
10000
F (ppm)
F vs sph
Regression Line

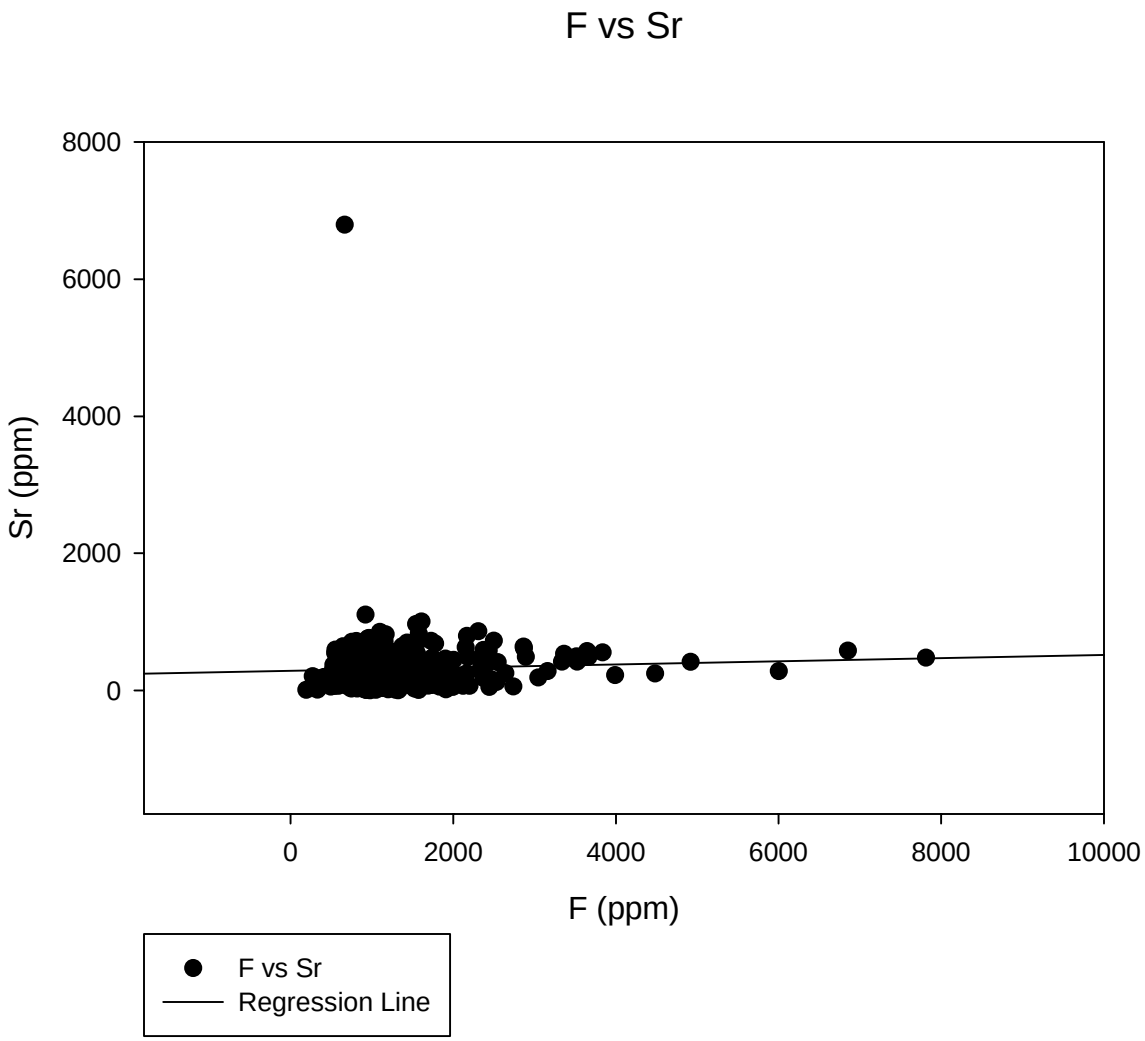
F vs Sr
8000
6000
4000
2000
0
Sr (ppm)
0
2000
4000
6000
8000
10000
F (ppm)
F vs Sr
Regression Line

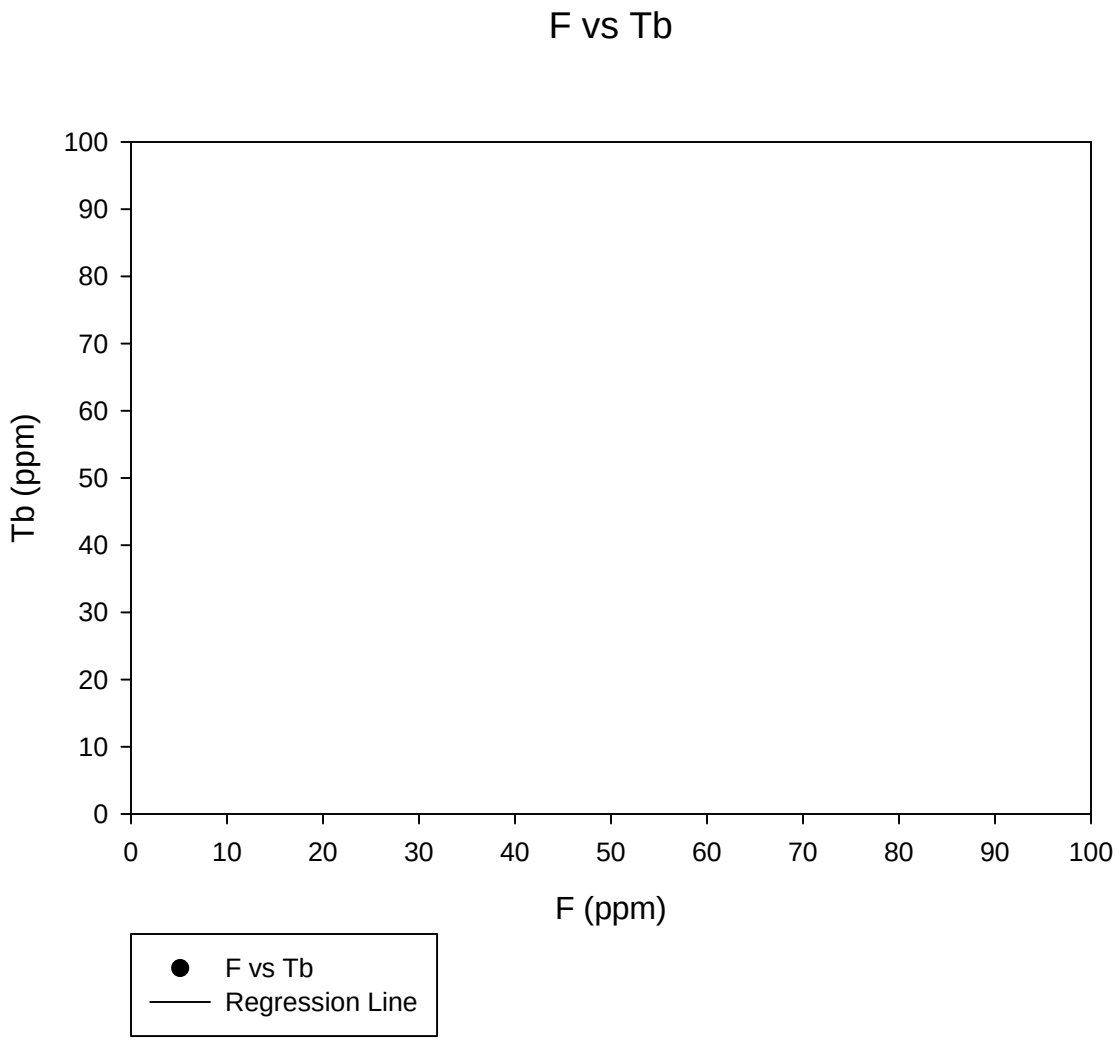
F vs Tb
Tb (ppm)
100
90
80
70
60
50
40
30
20
10
0
0
10
20
30
40
50
60
70
80
90
100
F (ppm)
F vs Tb
Regression Line

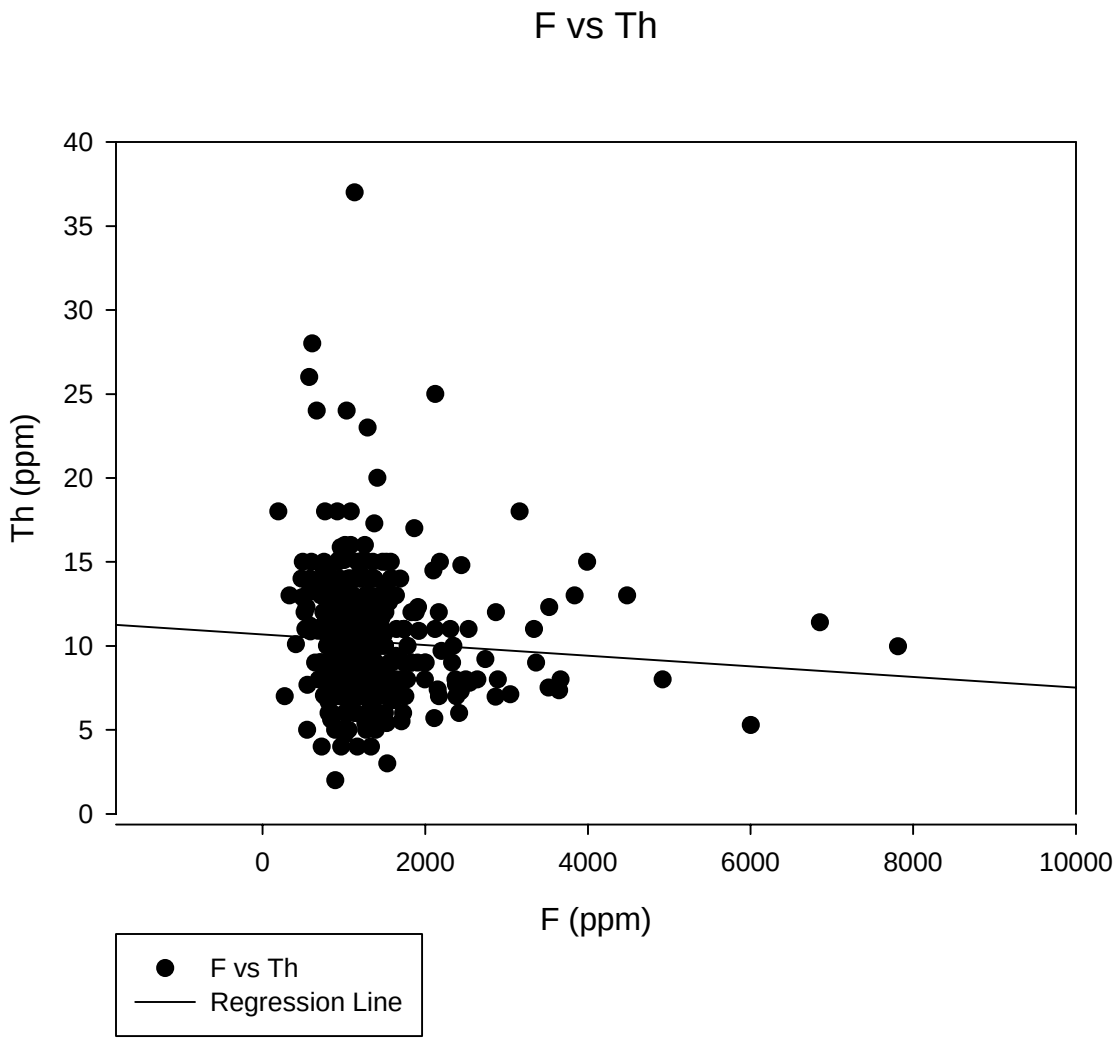
F vs Th
Th (ppm)
40
35
30
25
20
15
10
5
0
0
2000
4000
6000
8000
10000
F (ppm)
F vs Th
Regression Line

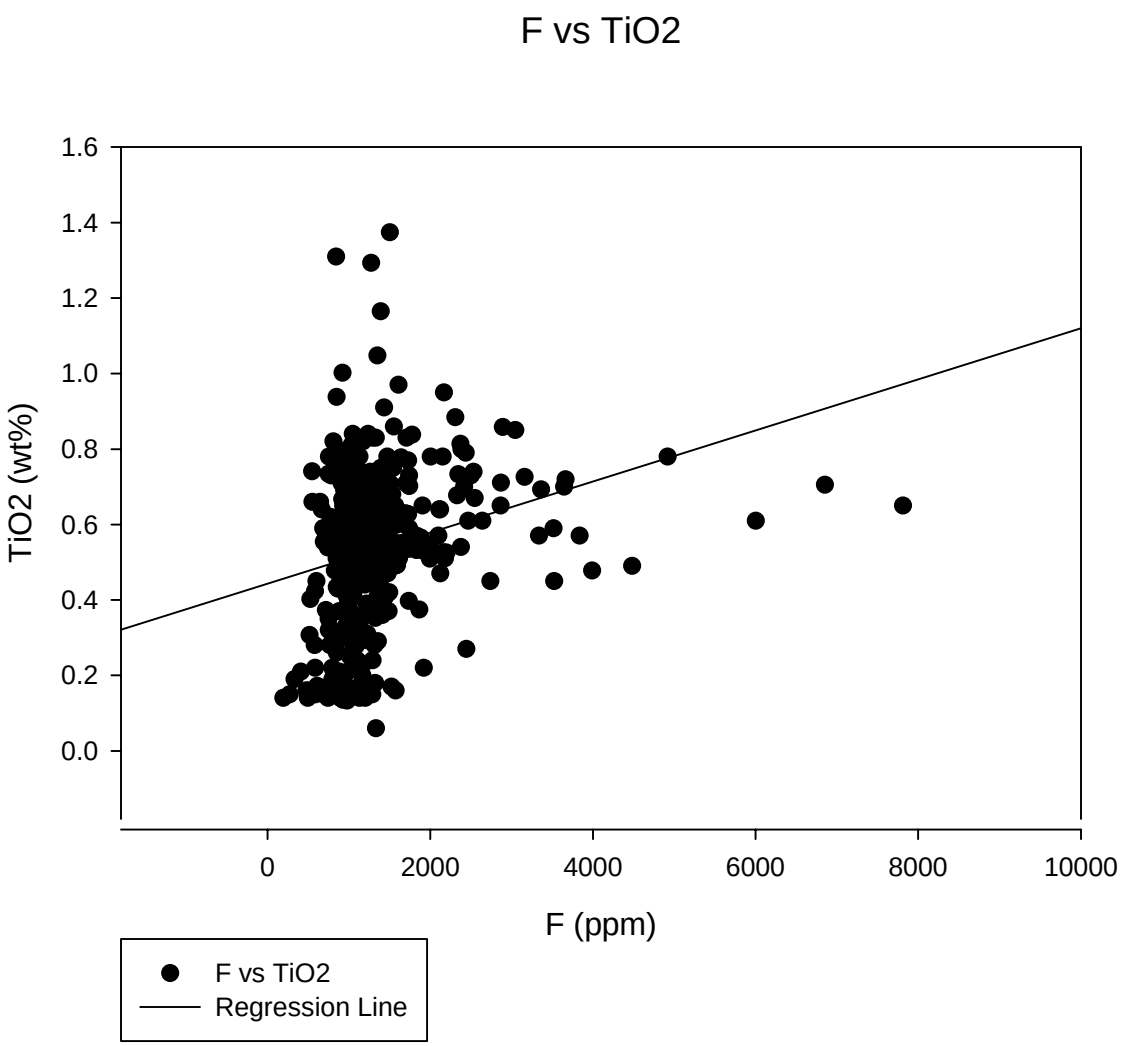
F vs TiO2
1.6
1.4
1.2
1.0
0.8
0.6
0.4
0.2
0.0
TiO2 (wt%)
0
2000
4000
6000
8000
10000
F (ppm)
F vs TiO2
Regression Line

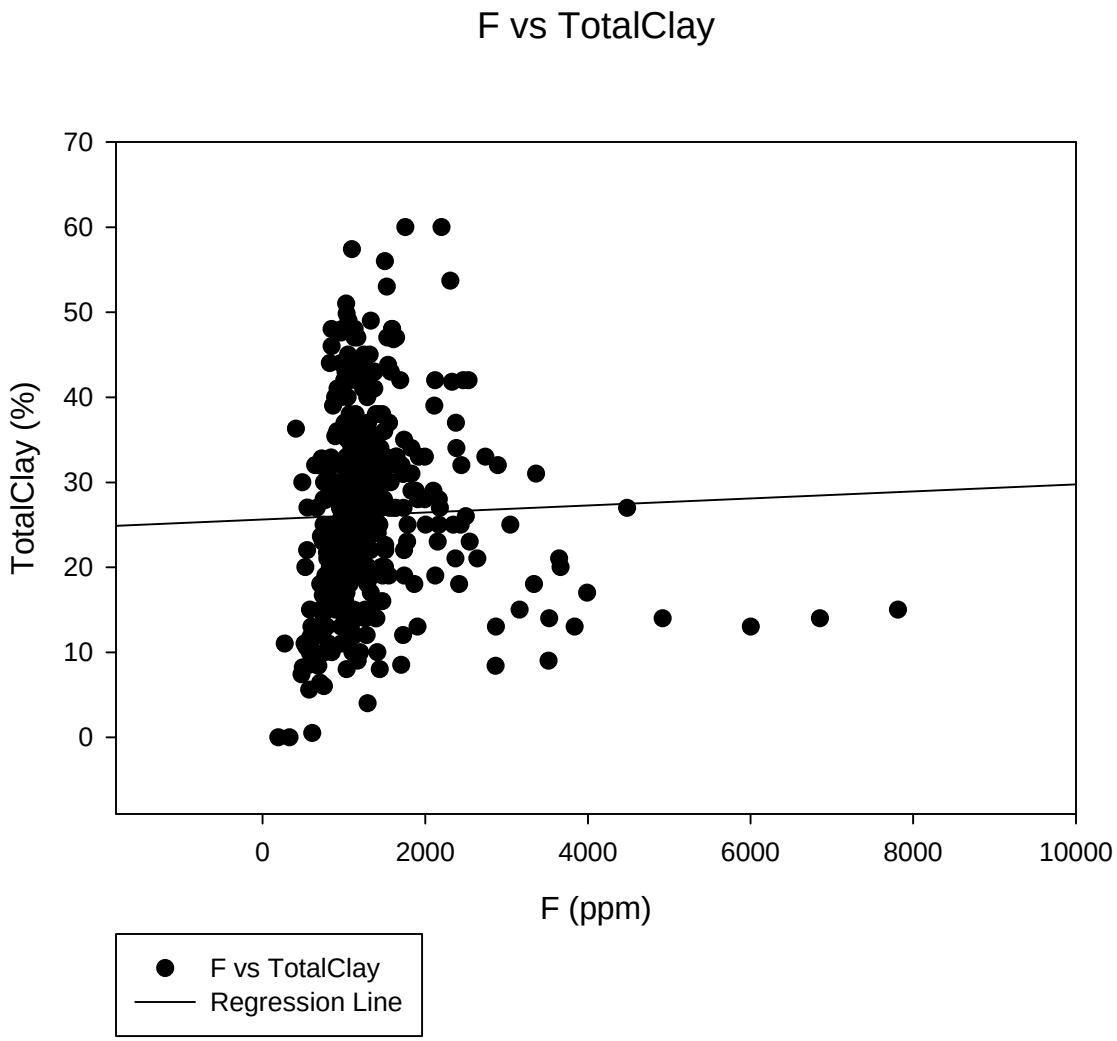
F vs TotalClay
70
60
50
40
30
20
10
0
TotalClay (%)
0
2000
4000
6000
8000
10000
F (ppm)
F vs TotalClay
Regression Line

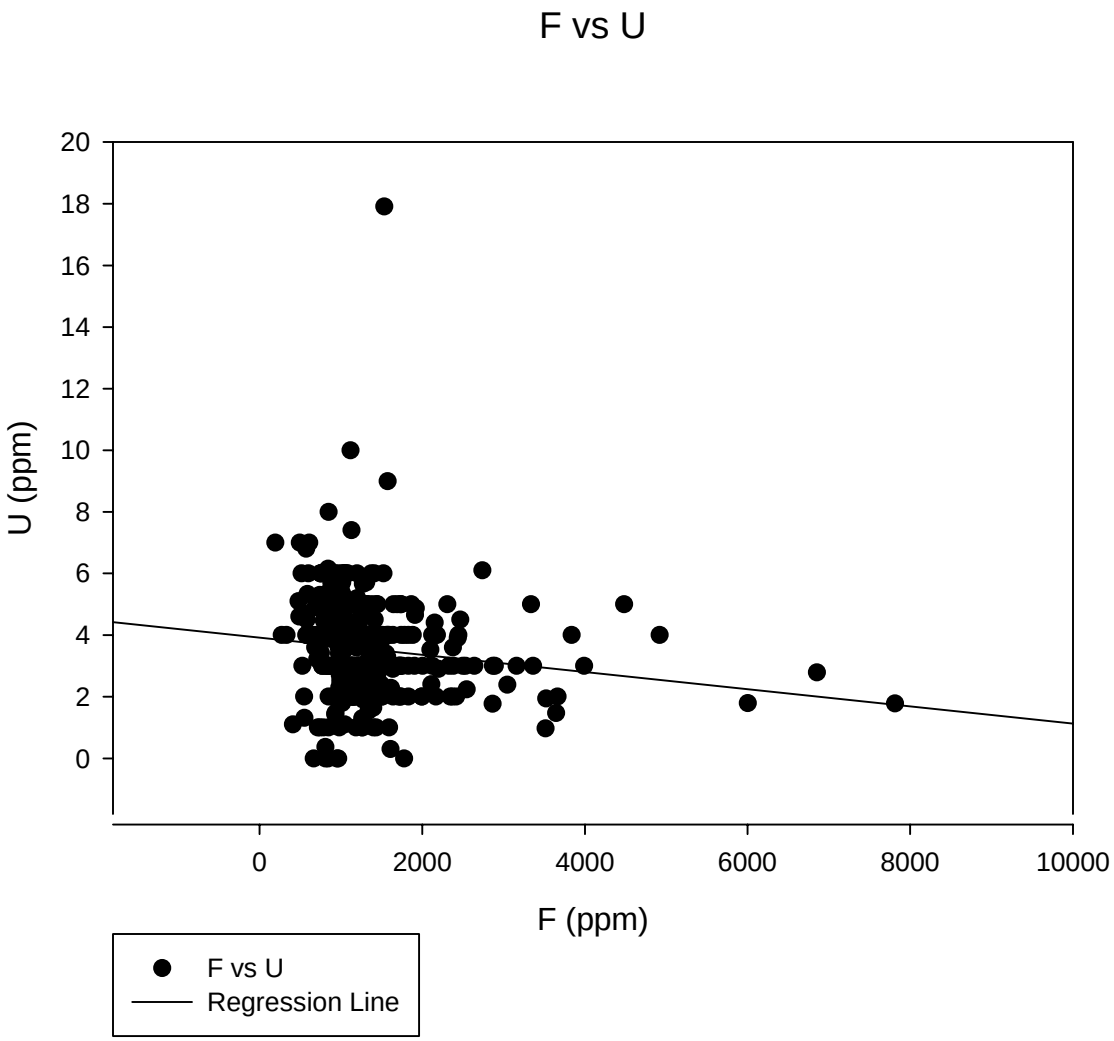
F vs U
20
18
16
14
12
10
8
6
4
2
0
U (ppm)
0
2000
4000
6000
8000
10000
F (ppm)
F vs U
Regression Line

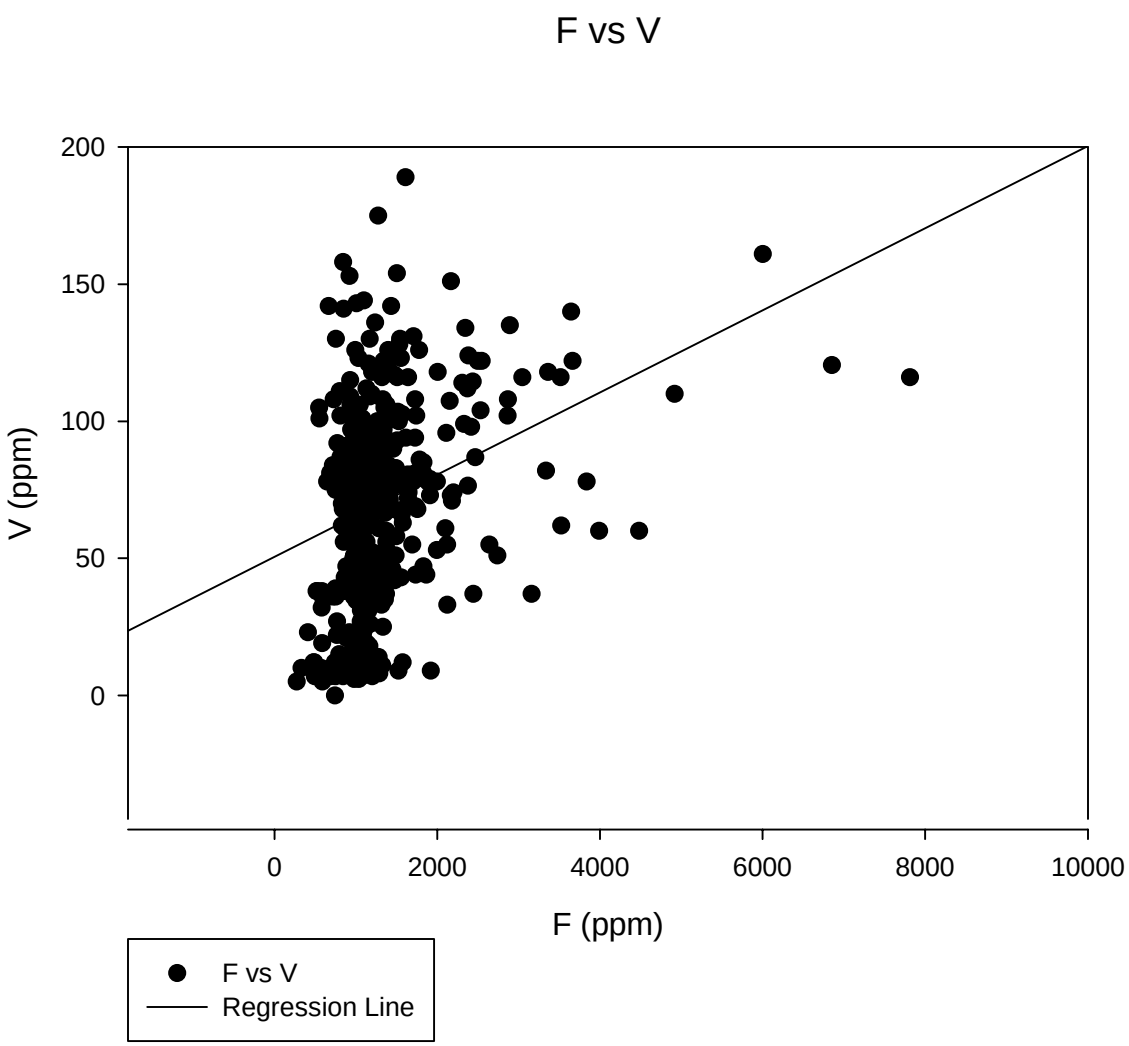
F vs V
200
150
100
50
0
V (ppm)
0
2000
4000
6000
8000
10000
F (ppm)
F vs V
Regression Line

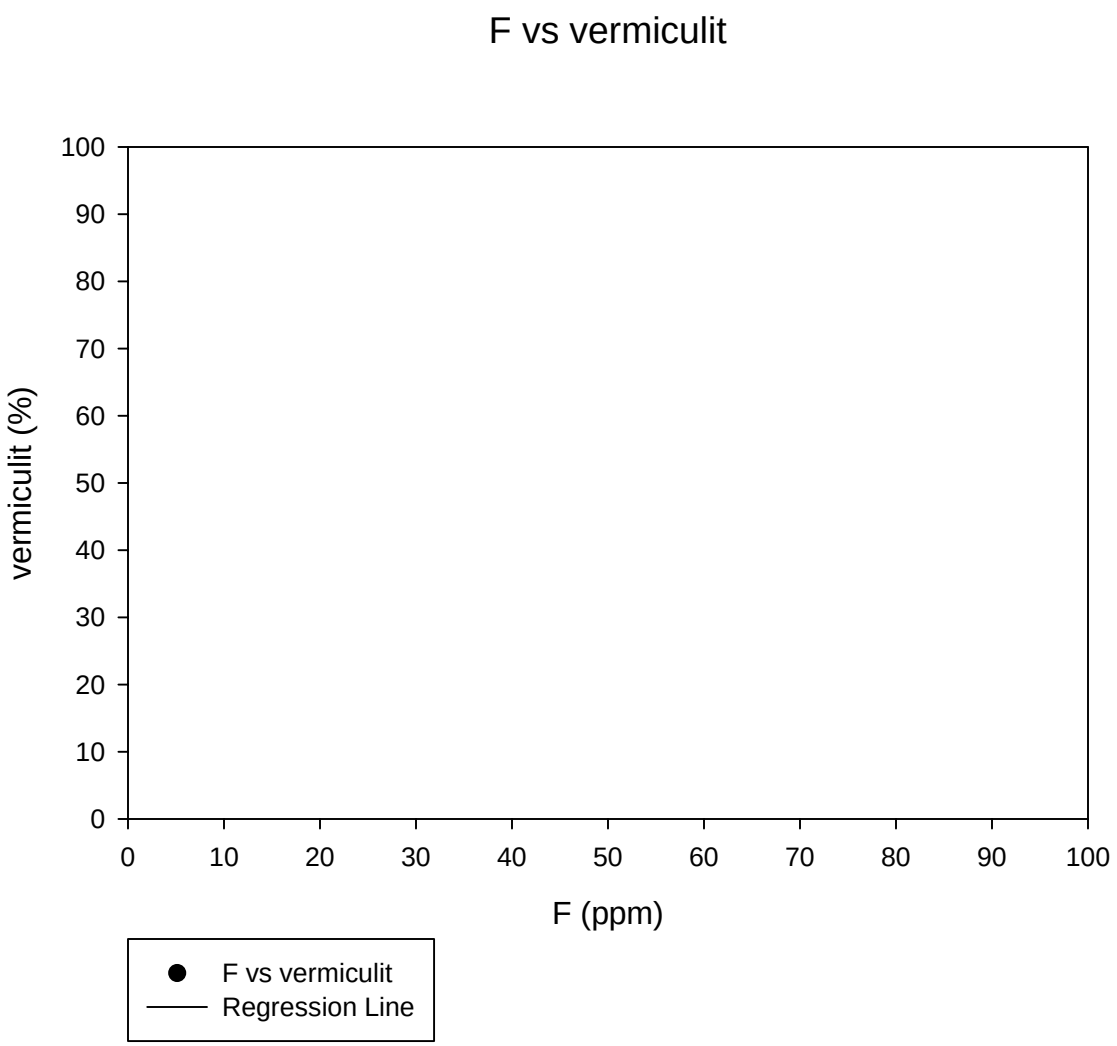
F vs vermiculit
vermiculit (%)
100
90
80
70
60
50
40
30
20
10
0
0
10
20
30
40
50
60
70
80
90
100
F (ppm)
F vs vermiculit
Regression Line

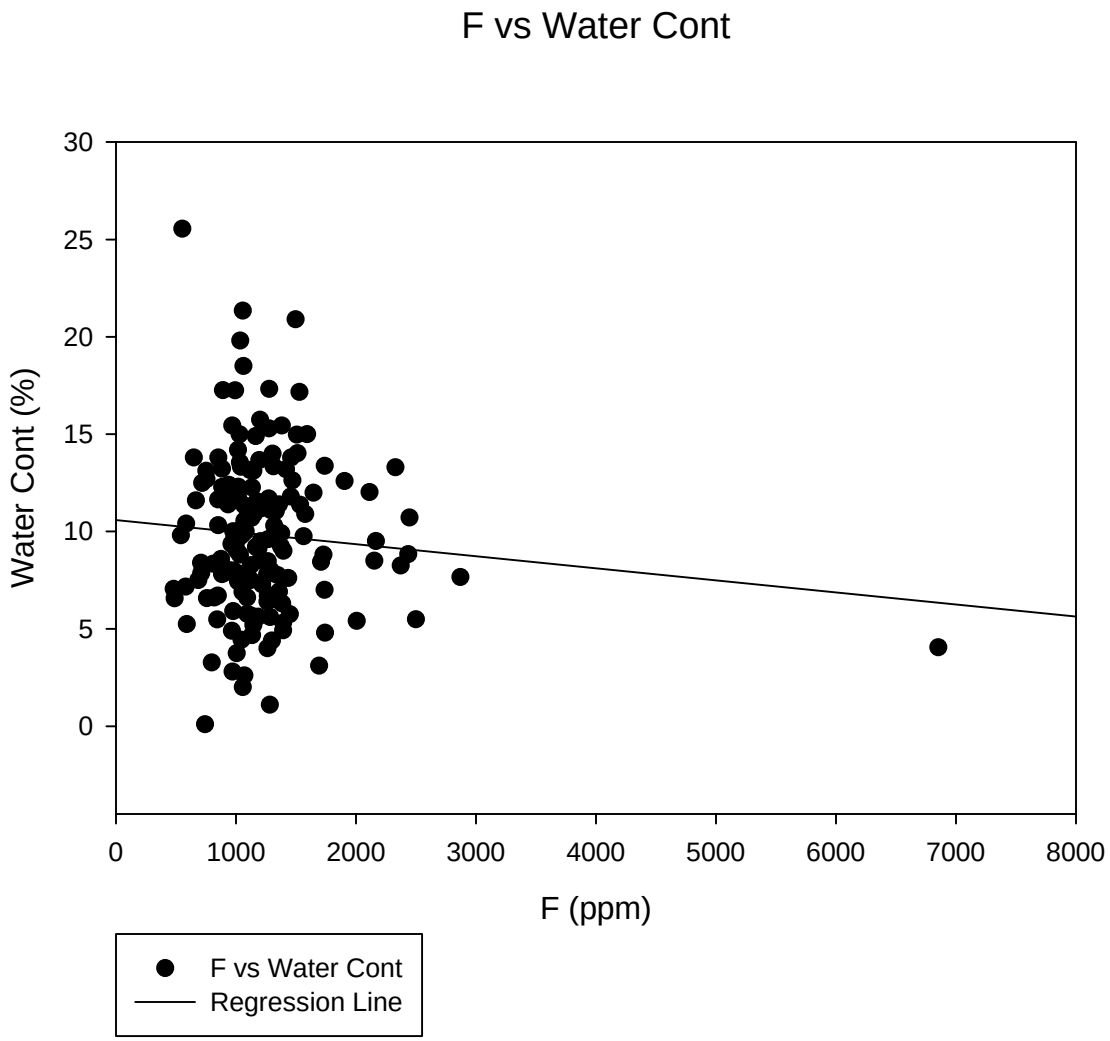
F vs Water Cont
Water Cont (%)
30
25
20
15
10
5
0
0
1000
2000
3000
4000
5000
6000
7000
8000
F (ppm)
F vs Water Cont
Regression Line

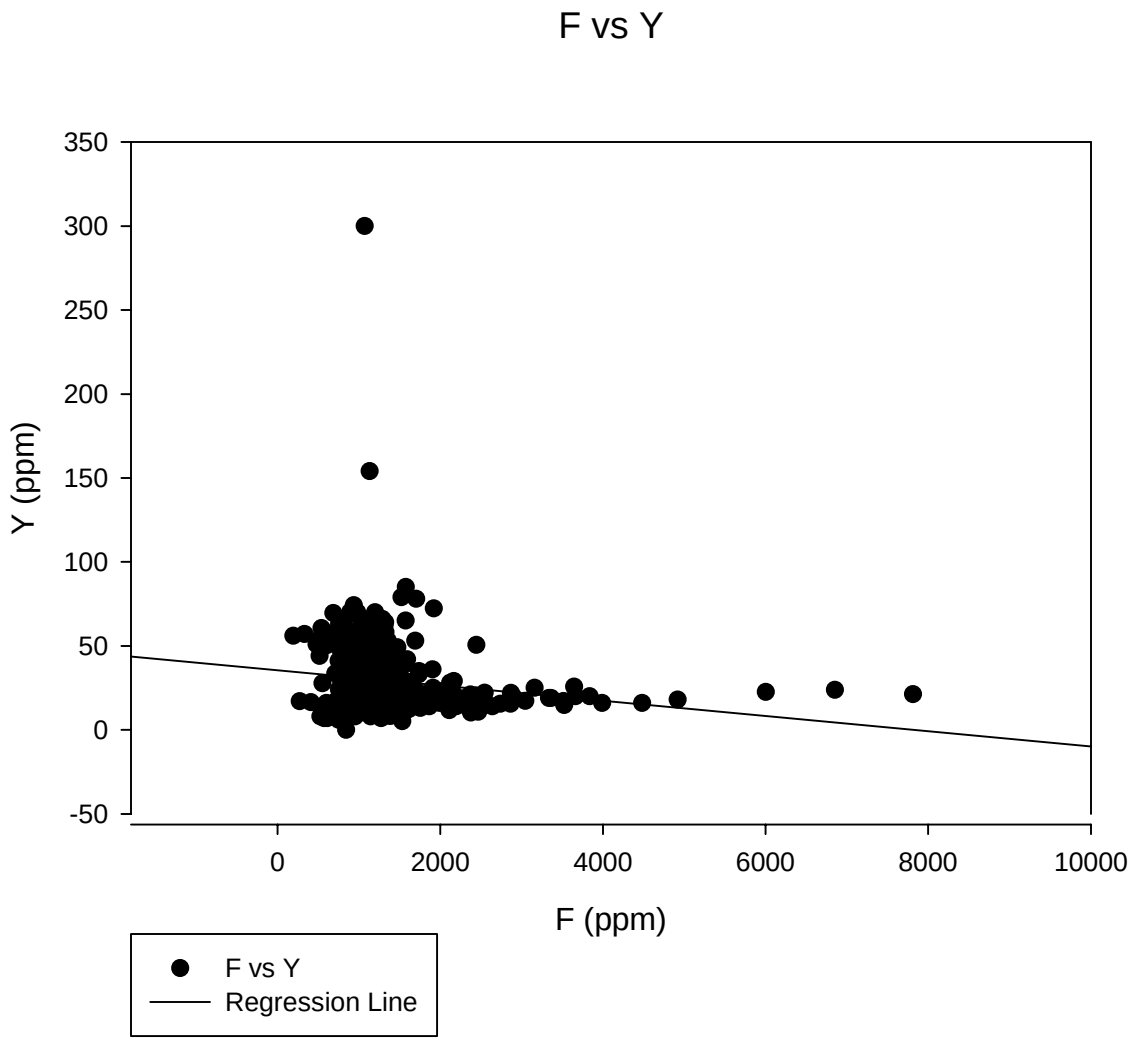
F vs Y
350
300
250
200
150
100
50
0
-50
Y (ppm)
0
2000
4000
6000
8000
10000
F (ppm)
F vs Y
Regression Line

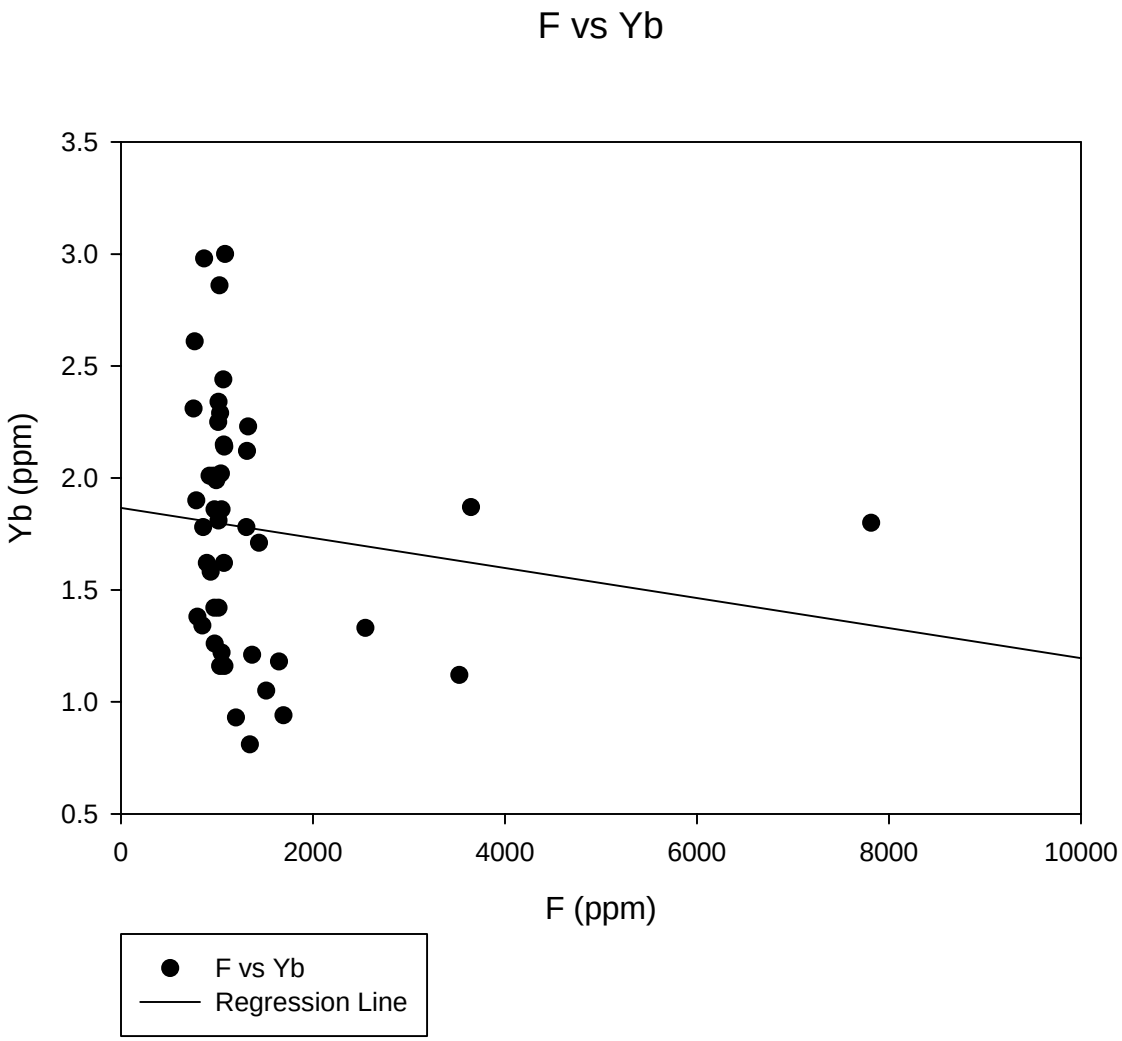
F vs Yb
3.5
3.0
2.5
2.0
1.5
1.0
0.5
Yb (ppm)
0
2000
4000
6000
8000
10000
F (ppm)
F vs Yb
Regression Line

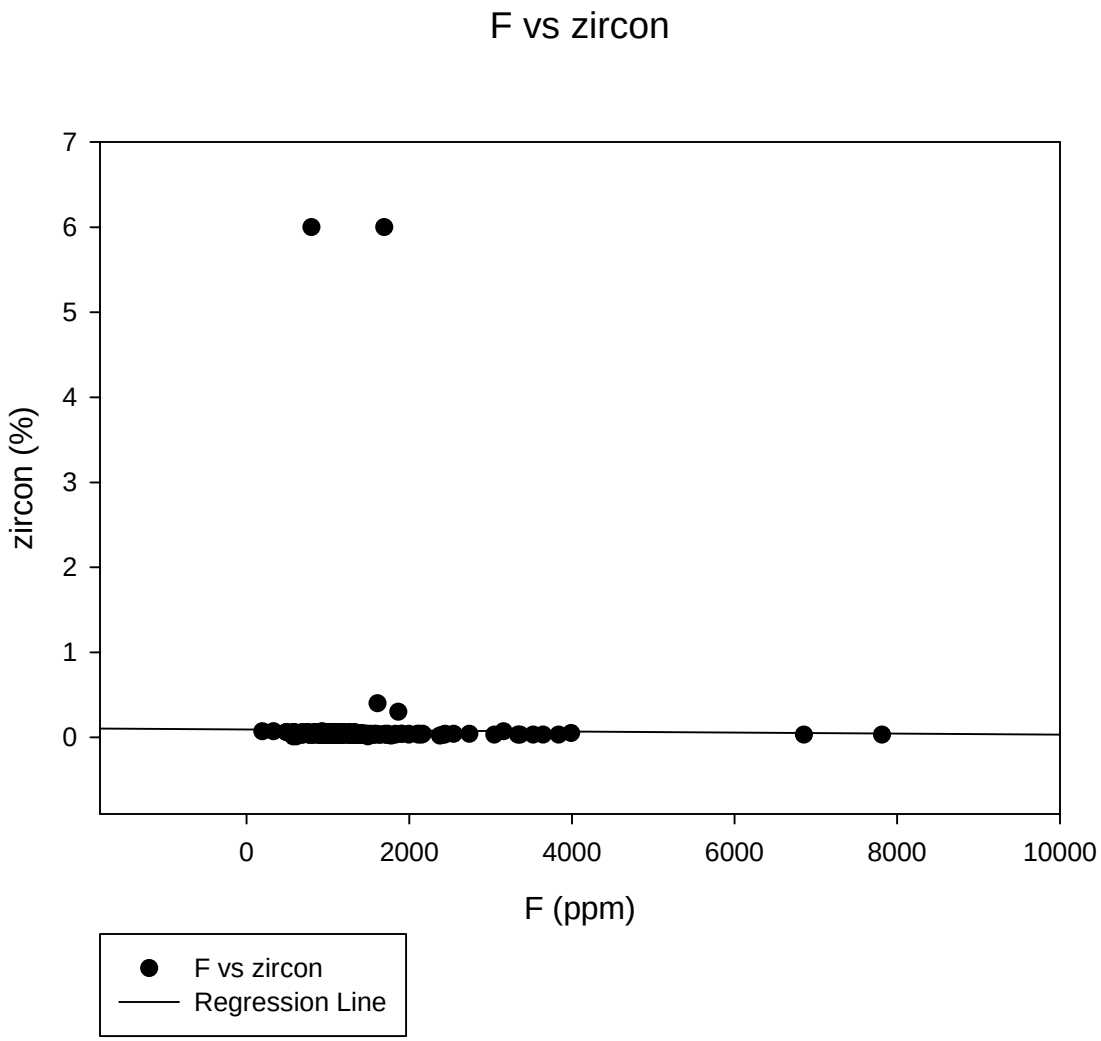
F vs zircon
zircon (%)
7
6
5
4
3
2
1
0
0
2000
4000
6000
8000
10000
F (ppm)
F vs zircon
Regression Line

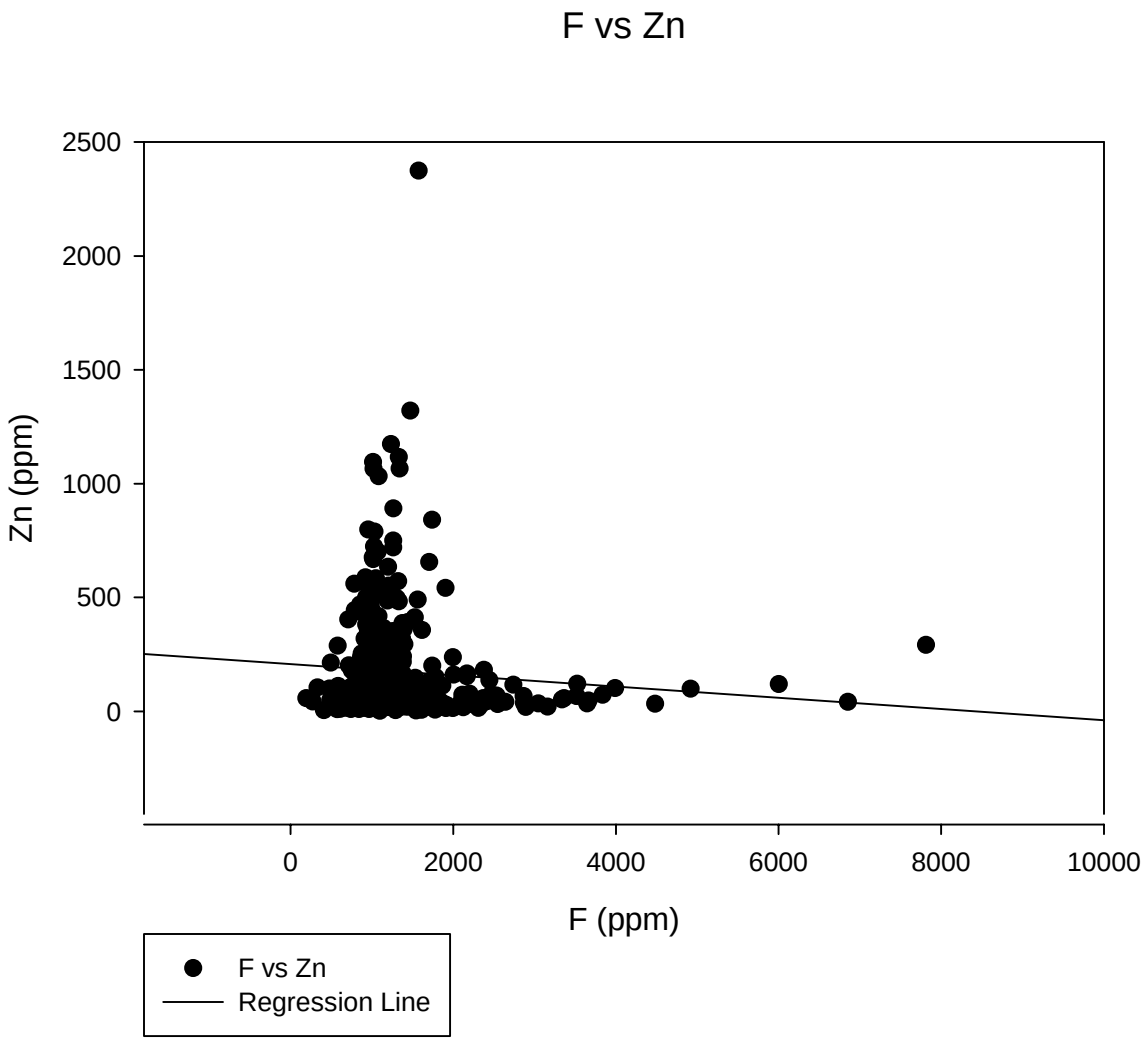
F vs Zn
2500
2000
1500
1000
500
0
Zn (ppm)
0
2000
4000
6000
8000
10000
F (ppm)
F vs Zn
Regression Line

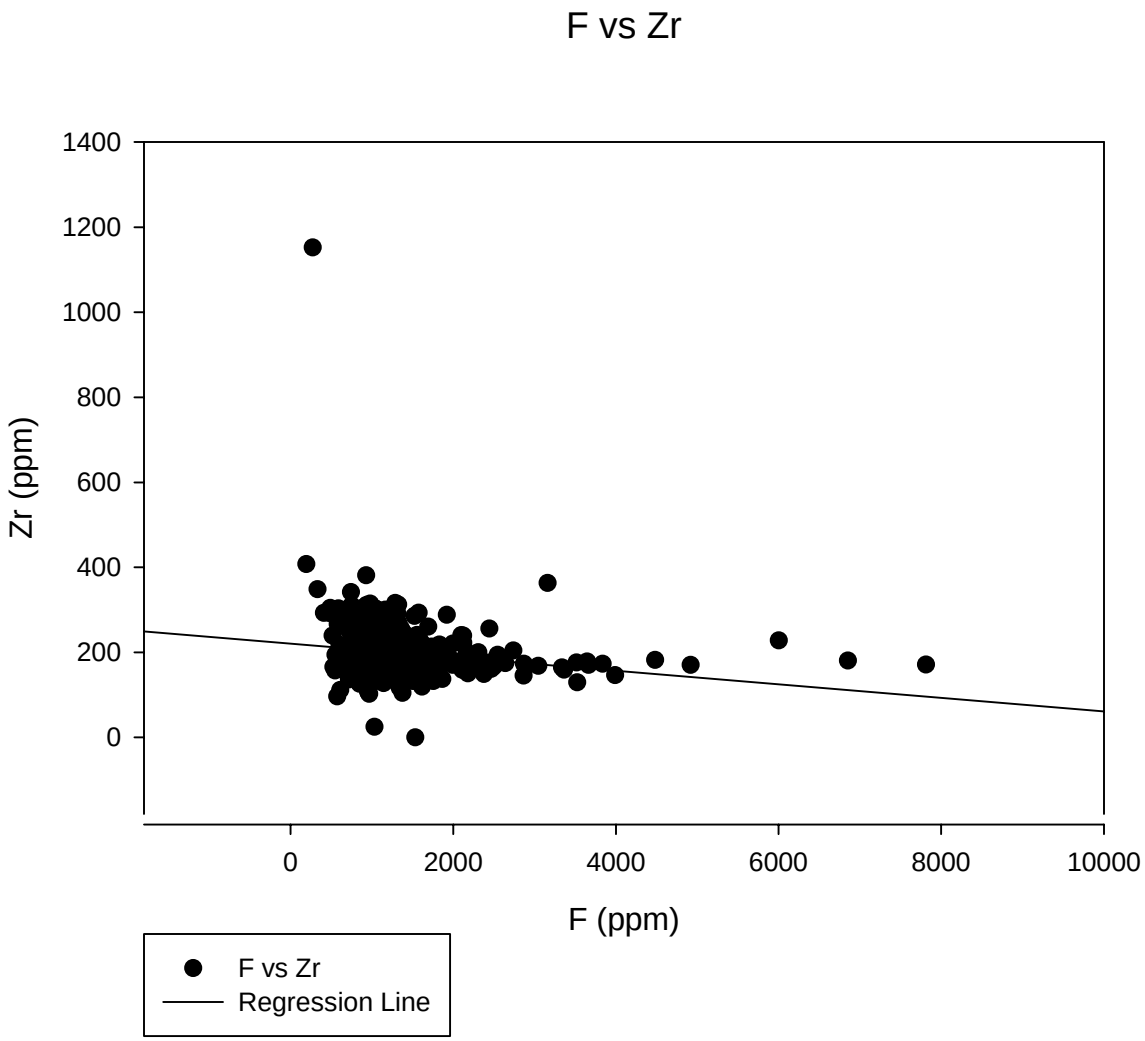
F vs Zr
1400
1200
1000
800
600
400
200
0
Zr (ppm)
0
2000
4000
6000
8000
10000
F (ppm)
F vs Zr
Regression Line

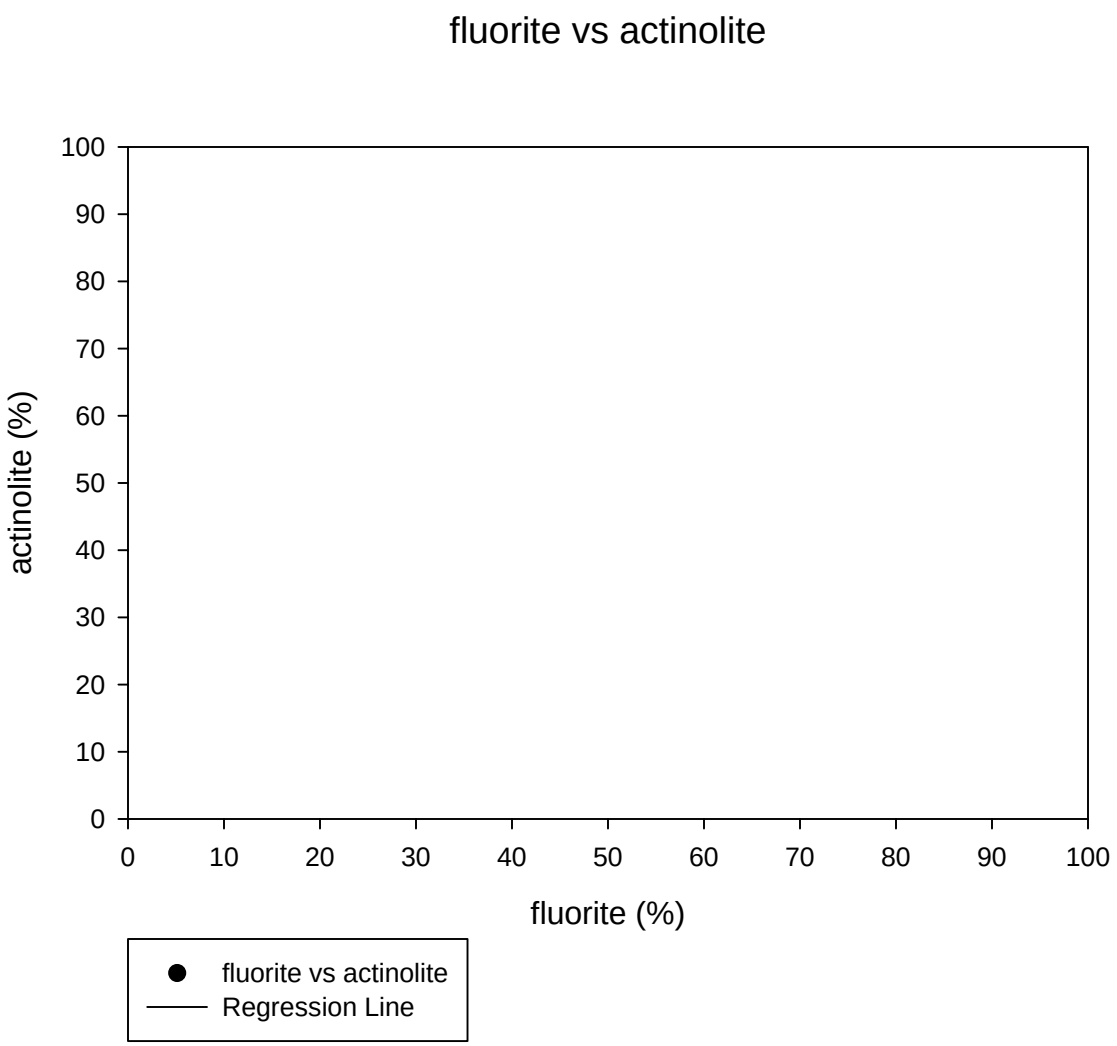
fluorite vs actinolite
actinolite (%)
100
90
80
70
60
50
40
30
20
10
0
0
10
20
30
40
50
60
70
80
90
100
fluorite (%)
fluorite vs actinolite
Regression Line

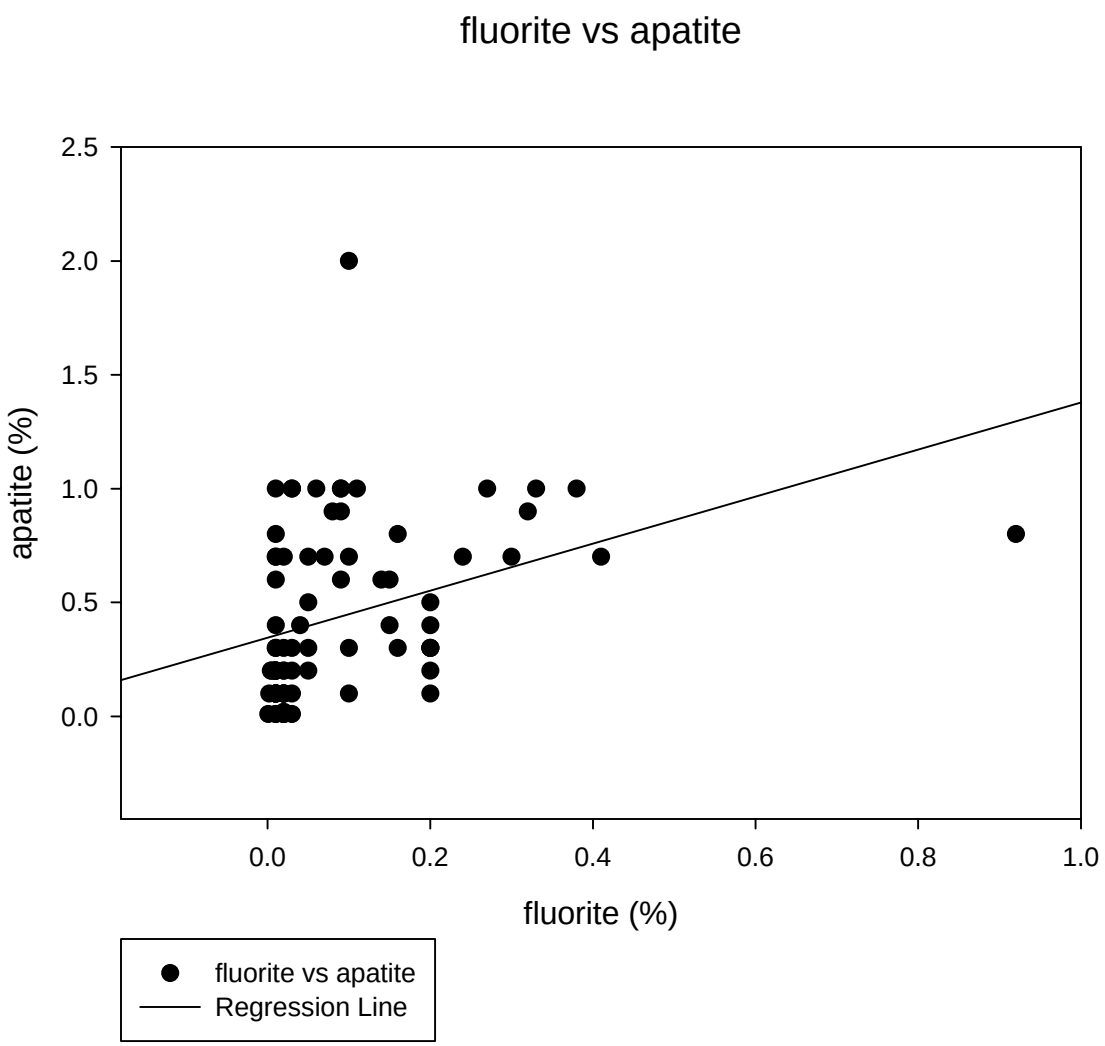
fluorite vs apatite
2.5
2.0
1.5
1.0
0.5
0.0
apatite (%)
0.0
0.2
0.4
0.6
0.8
1.0
fluorite (%)
fluorite vs apatite
Regression Line

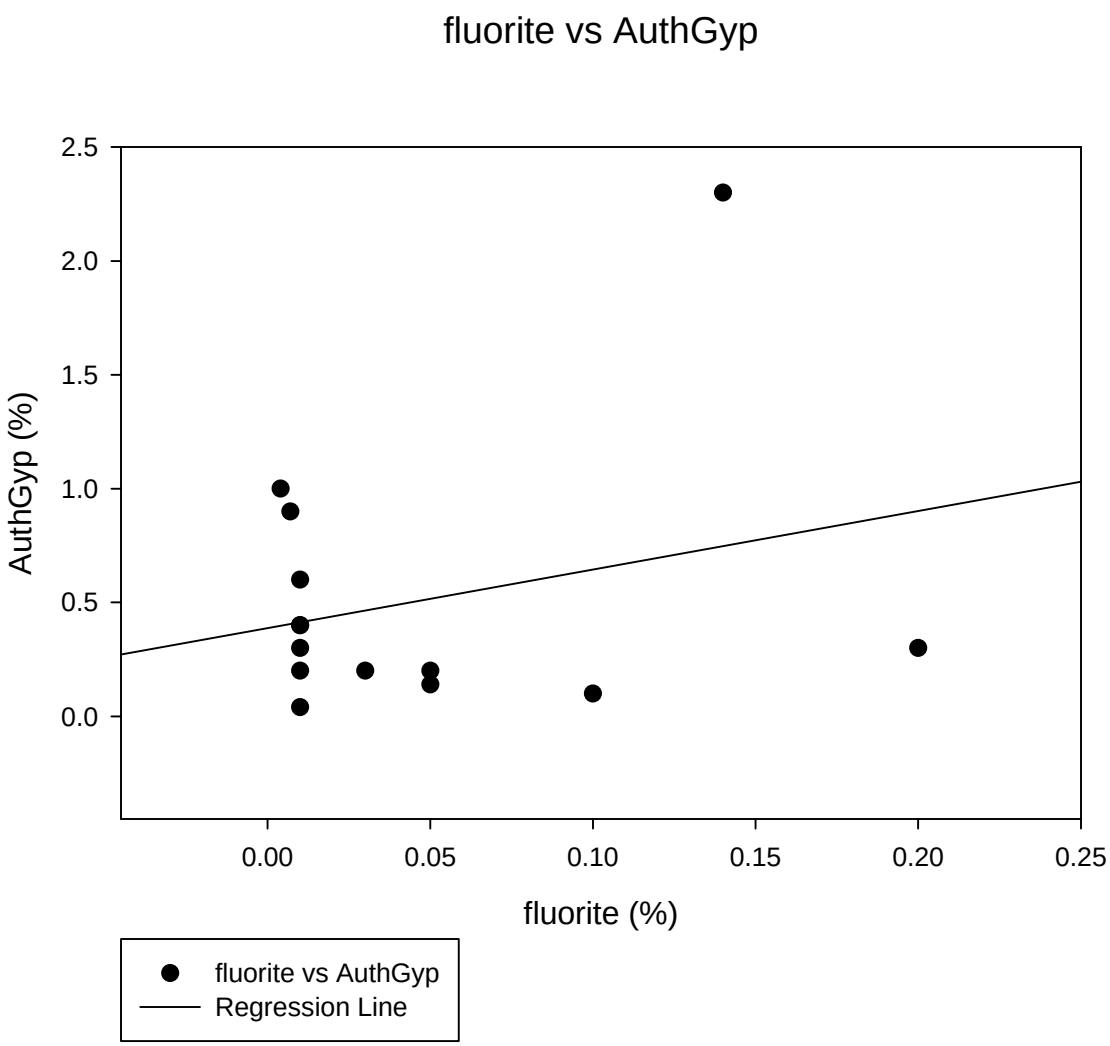
fluorite vs AuthGyp
2.5
2.0
1.5
1.0
0.5
0.0
AuthGyp (%)
0.00
0.05
0.10
0.15
0.20
0.25
fluorite (%)
fluorite vs AuthGyp
Regression Line

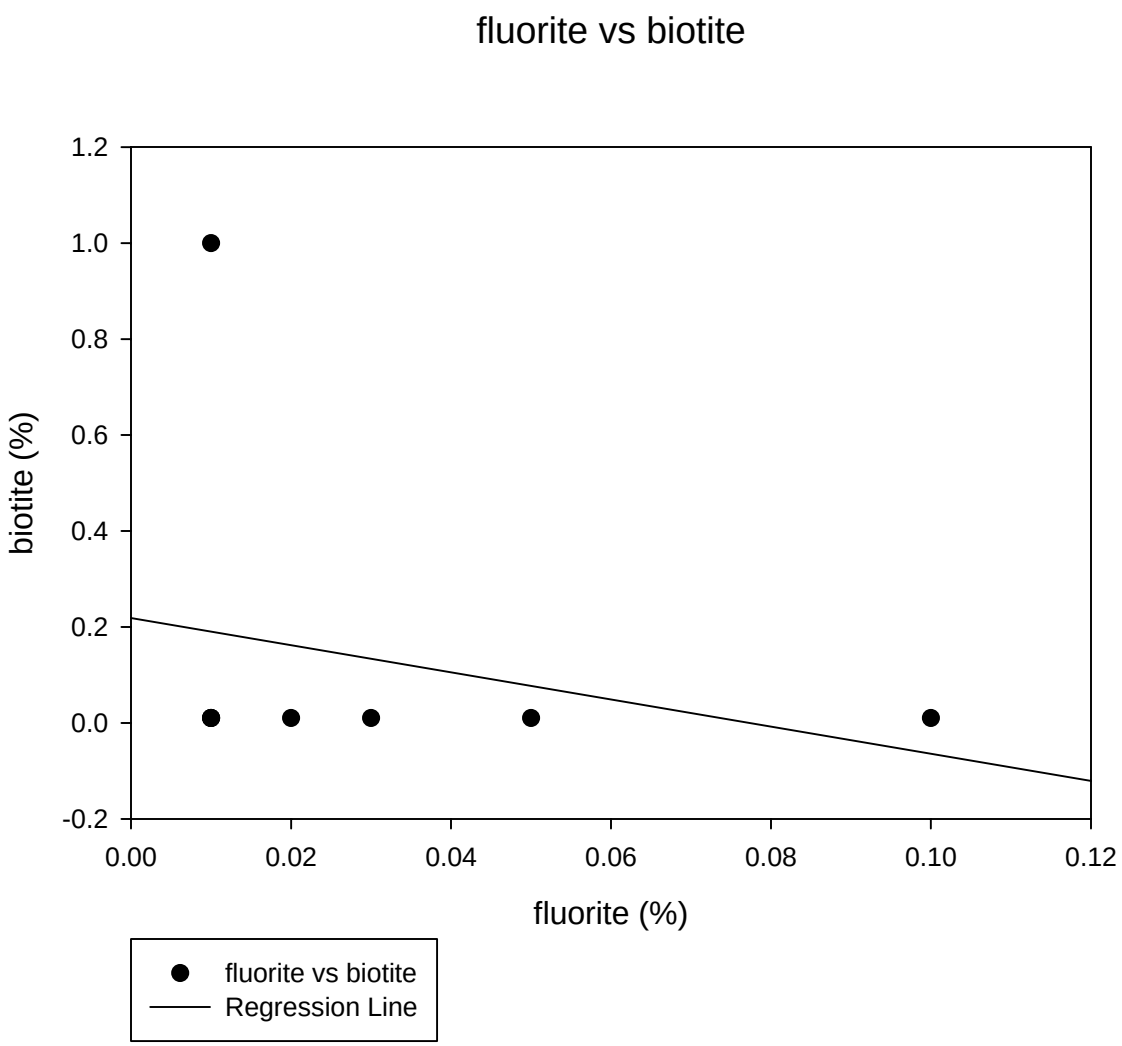
fluorite vs biotite
1.2
1.0
0.8
0.6
0.4
0.2
0.0
-0.2
biotite (%)
0.00
0.02
0.04
0.06
0.08
0.10
0.12
fluorite (%)
fluorite vs biotite
Regression Line

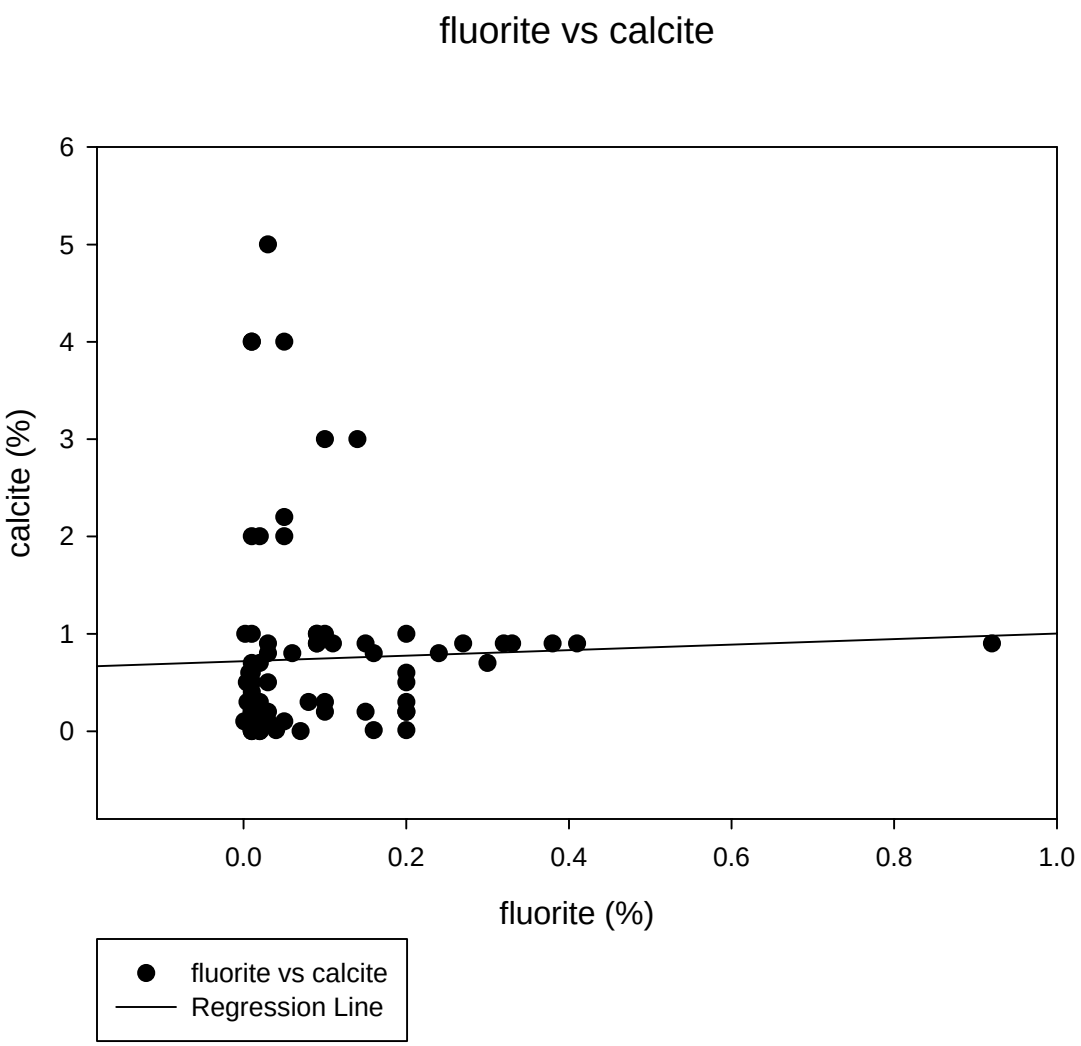
fluorite vs calcite
6
5
4
3
2
1
0
calcite (%)
0.0
0.2
0.4
0.6
0.8
1.0
fluorite (%)
fluorite vs calcite
Regression Line

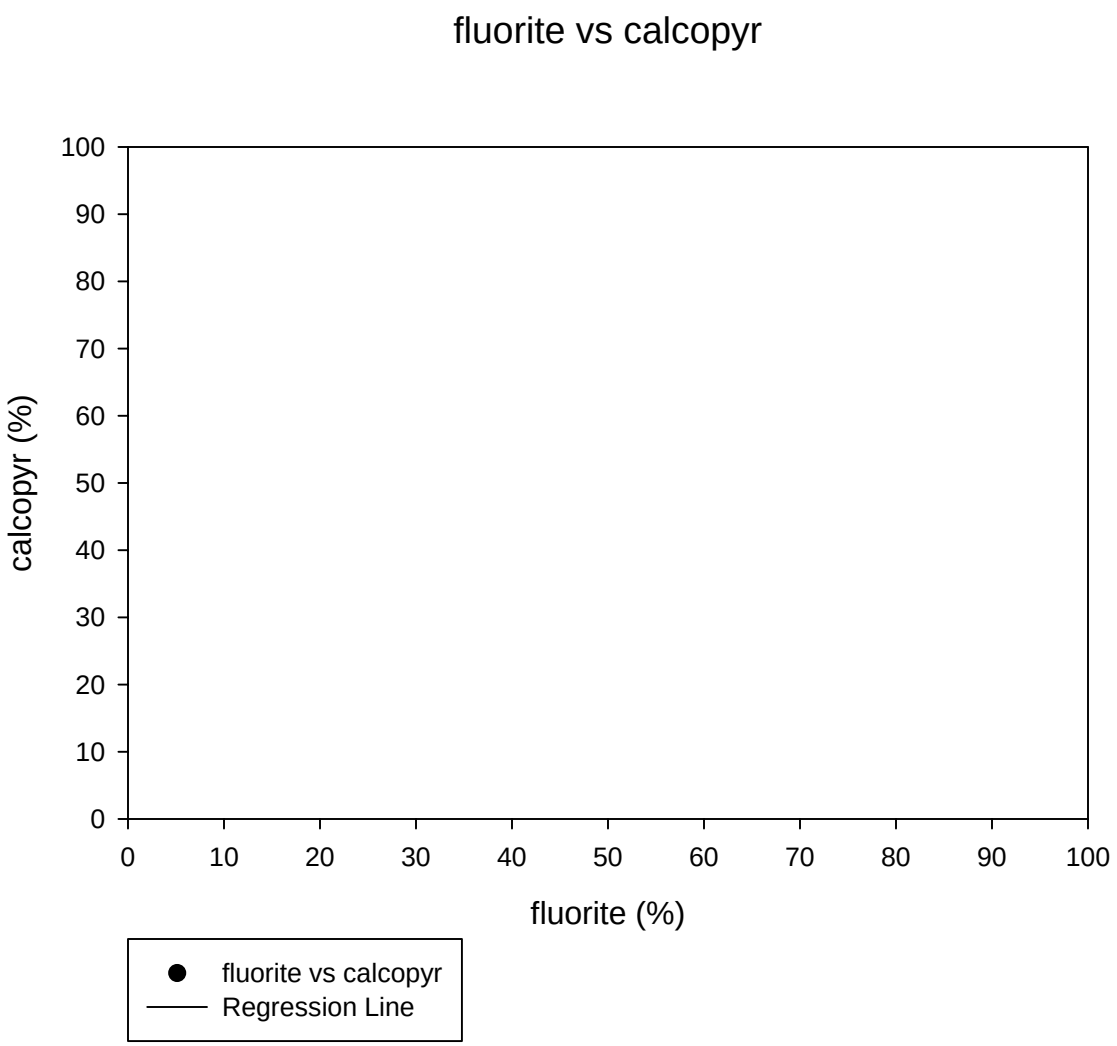
fluorite vs calcopyr
calcopyr (%)
100
90
80
70
60
50
40
30
20
10
0
0
10
20
30
40
50
60
70
80
90
100
fluorite (%)
fluorite vs calcopyr
Regression Line

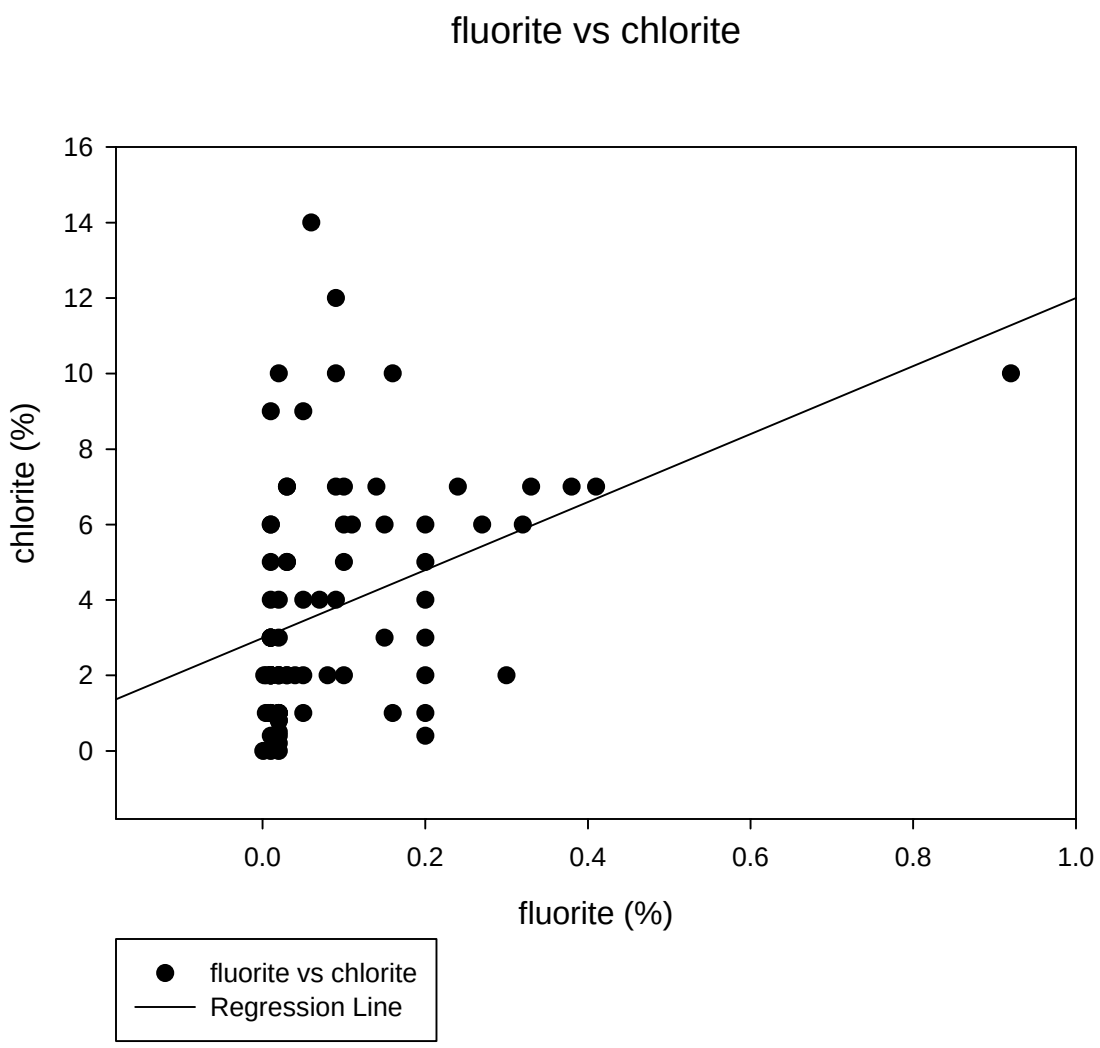
fluorite vs chlorite
chlorite (%)
16
14
12
10
8
6
4
2
0
0.0
0.2
0.4
0.6
0.8
1.0
fluorite (%)
fluorite vs chlorite
Regression Line

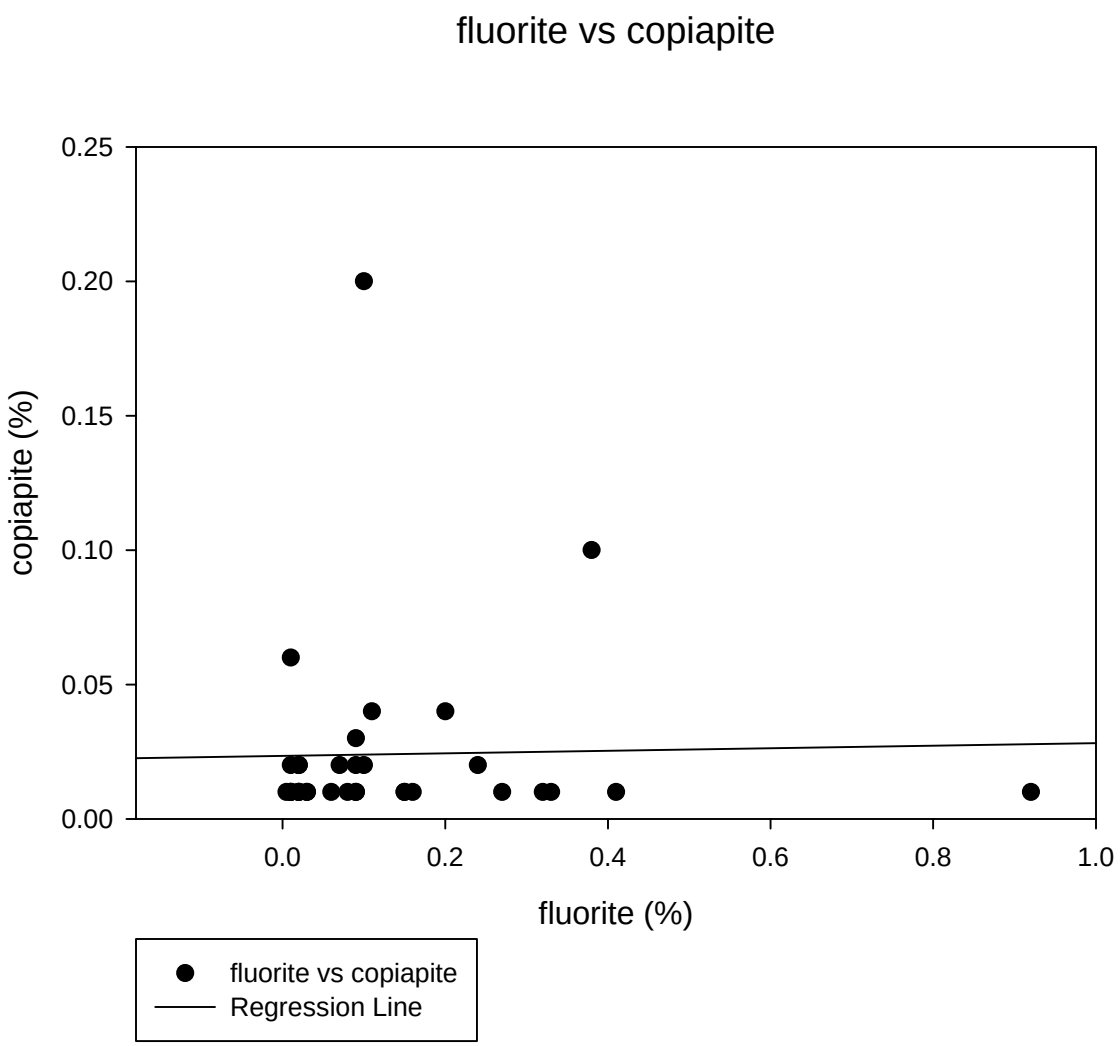
fluorite vs copiapite
0.25
0.20
0.15
0.10
0.05
0.00
copiapite (%)
0.0
0.2
0.4
0.6
0.8
1.0
fluorite (%)
fluorite vs copiapite
Regression Line

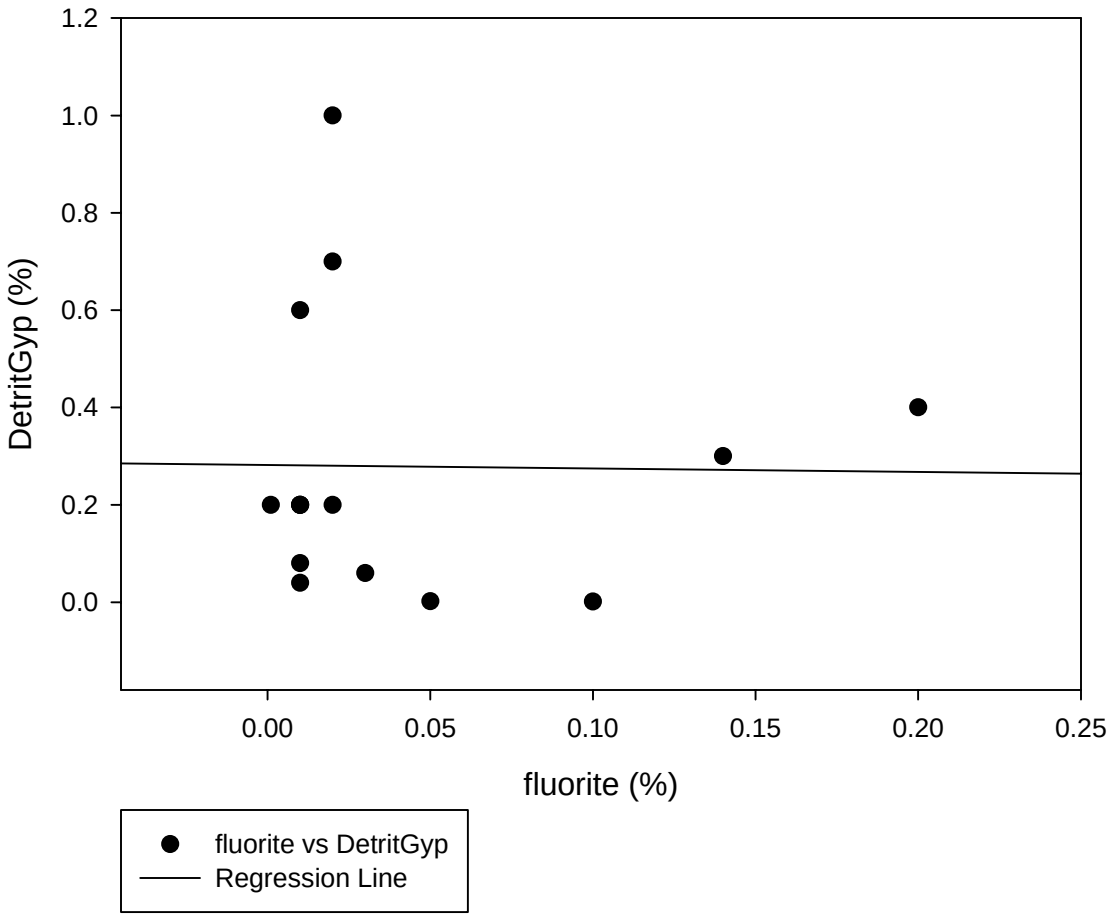
fluorite vs DetritGyp
1.2
1.0
0.8
0.6
0.4
0.2
0.0
DetritGyp (%)
0.00
0.05
0.10
0.15
0.20
0.25
fluorite (%)
fluorite vs DetritGyp
Regression Line

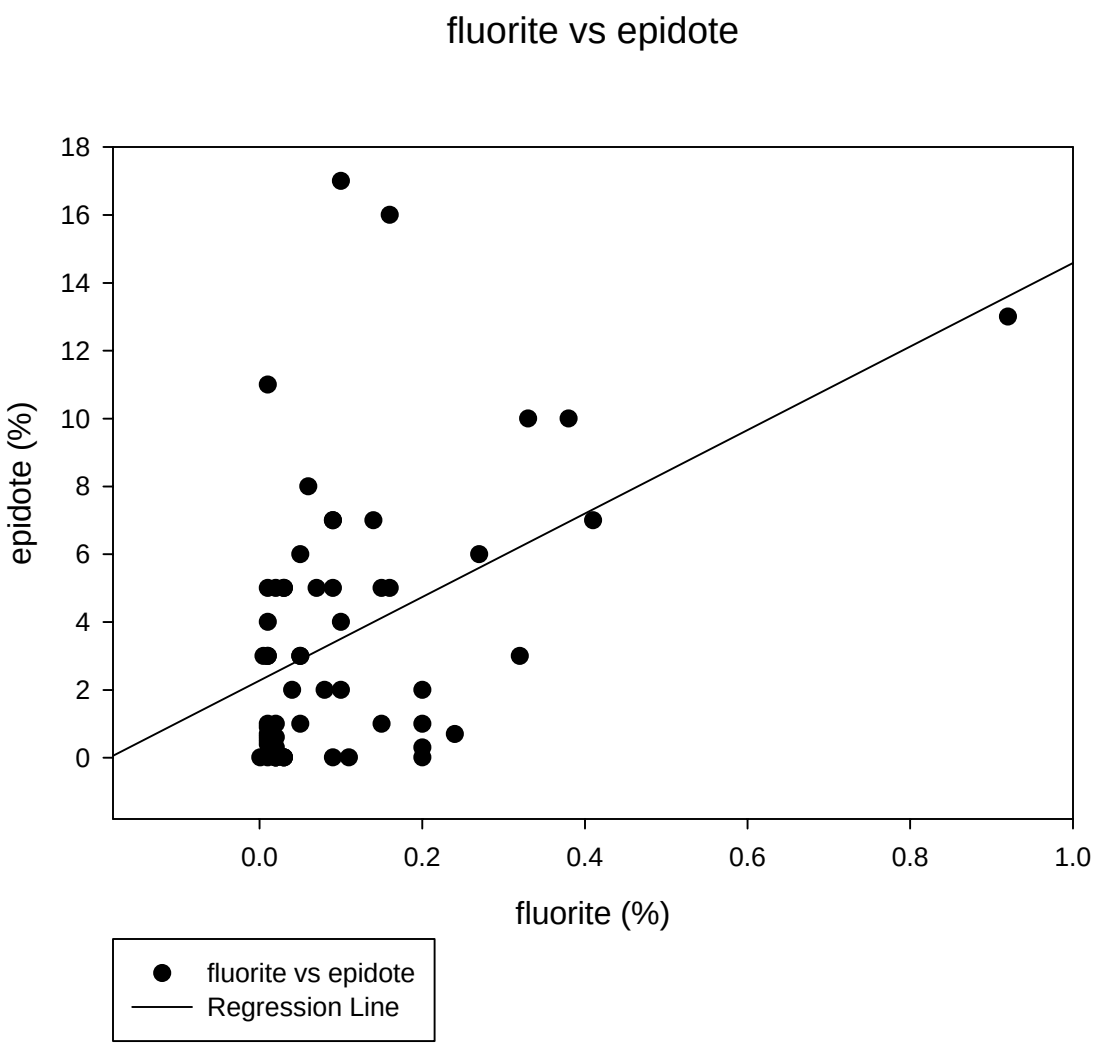
fluorite vs epidote
epidote (%)
fluorite (%)
0
2
4
6
8
10
12
14
16
18
0.0
0.2
0.4
0.6
0.8
1.0
fluorite vs epidote
Regression Line

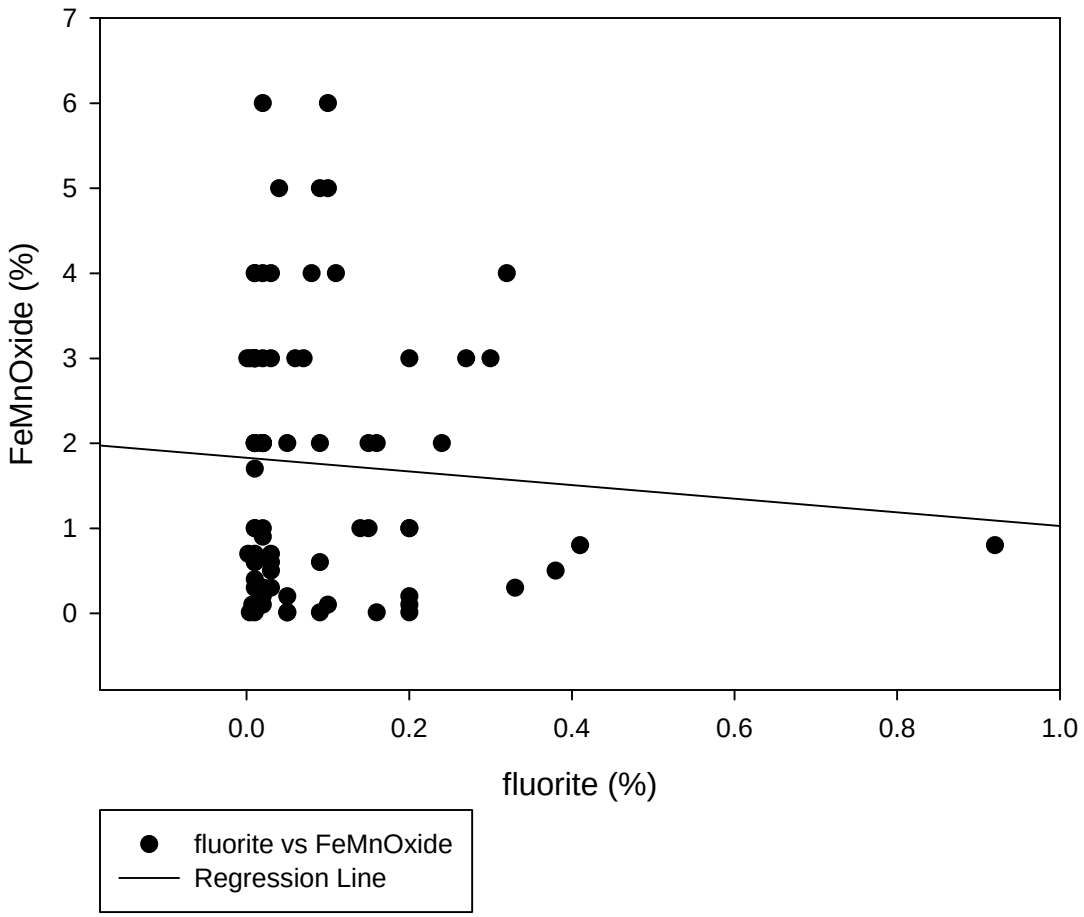
fluorite vs FeMnOxide
FeMnOxide (%)
7
6
5
4
3
2
1
0
0.0
0.2
0.4
0.6
0.8
1.0
fluorite (%)
fluorite vs FeMnOxide
Regression Line

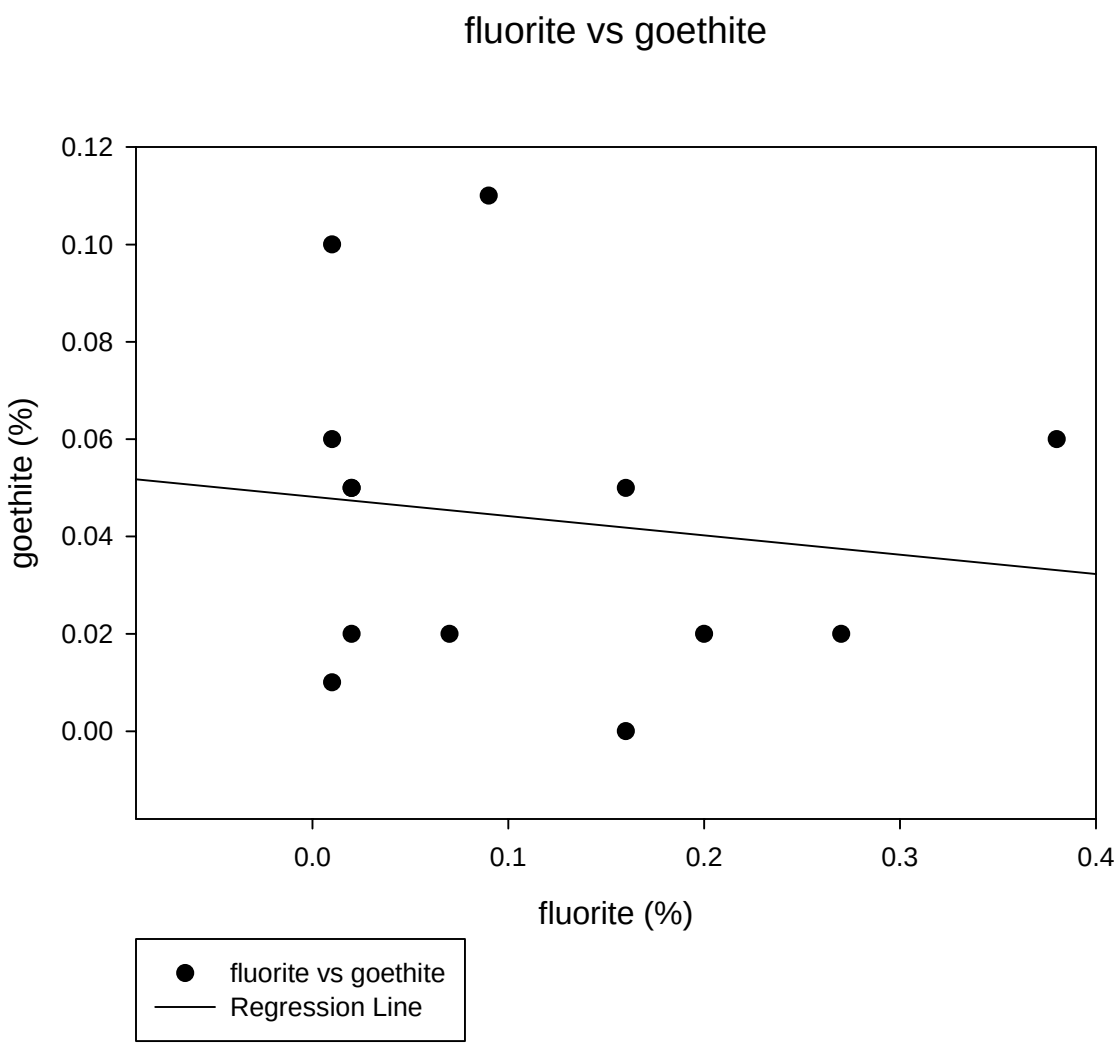
fluorite vs goethite
0.12
0.10
0.08
0.06
0.04
0.02
0.00
goethite (%)
0.0
0.1
0.2
0.3
0.4
fluorite (%)
fluorite vs goethite
Regression Line

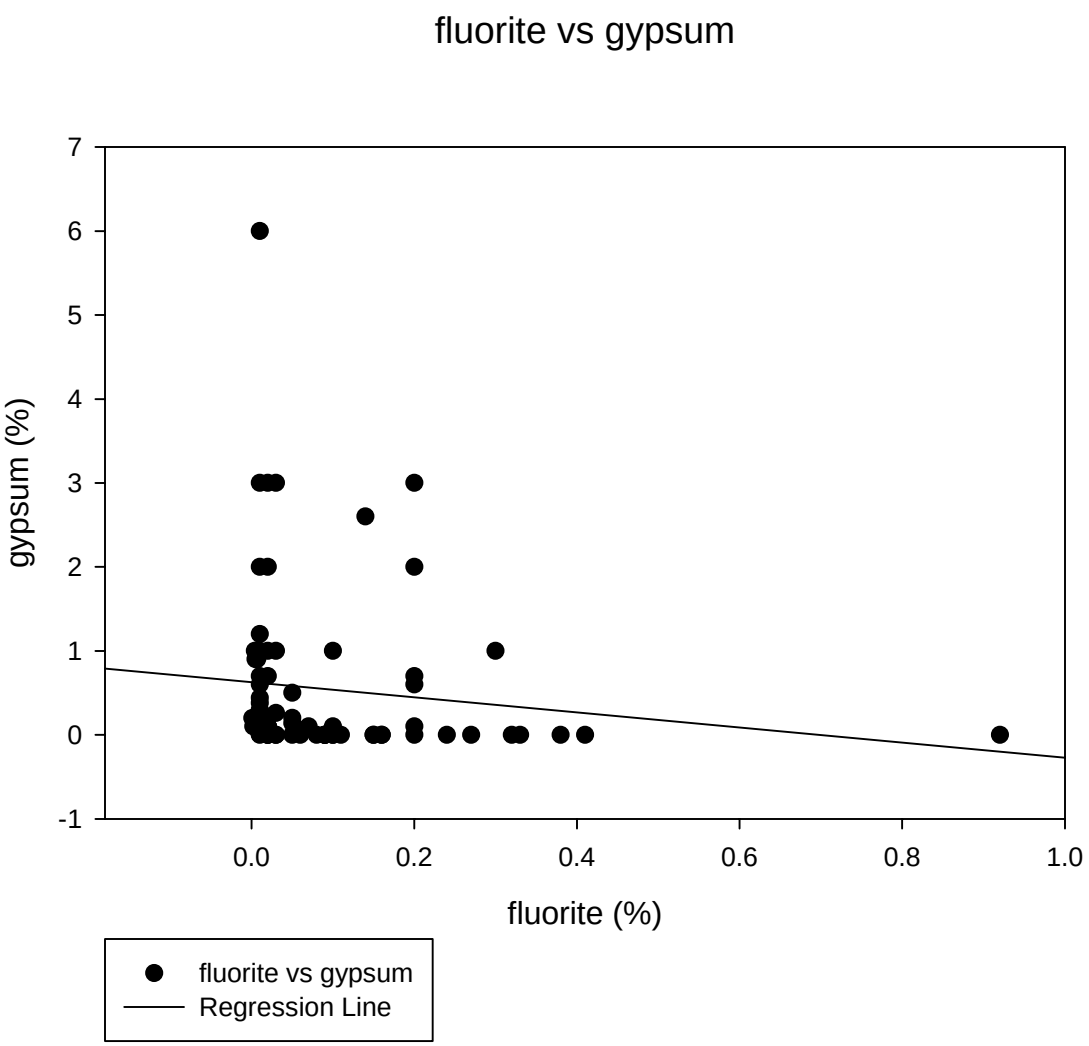
fluorite vs gypsum
gypsum (%)
7
6
5
4
3
2
1
0
-1
0.0
0.2
0.4
0.6
0.8
1.0
fluorite (%)
fluorite vs gypsum
Regression Line

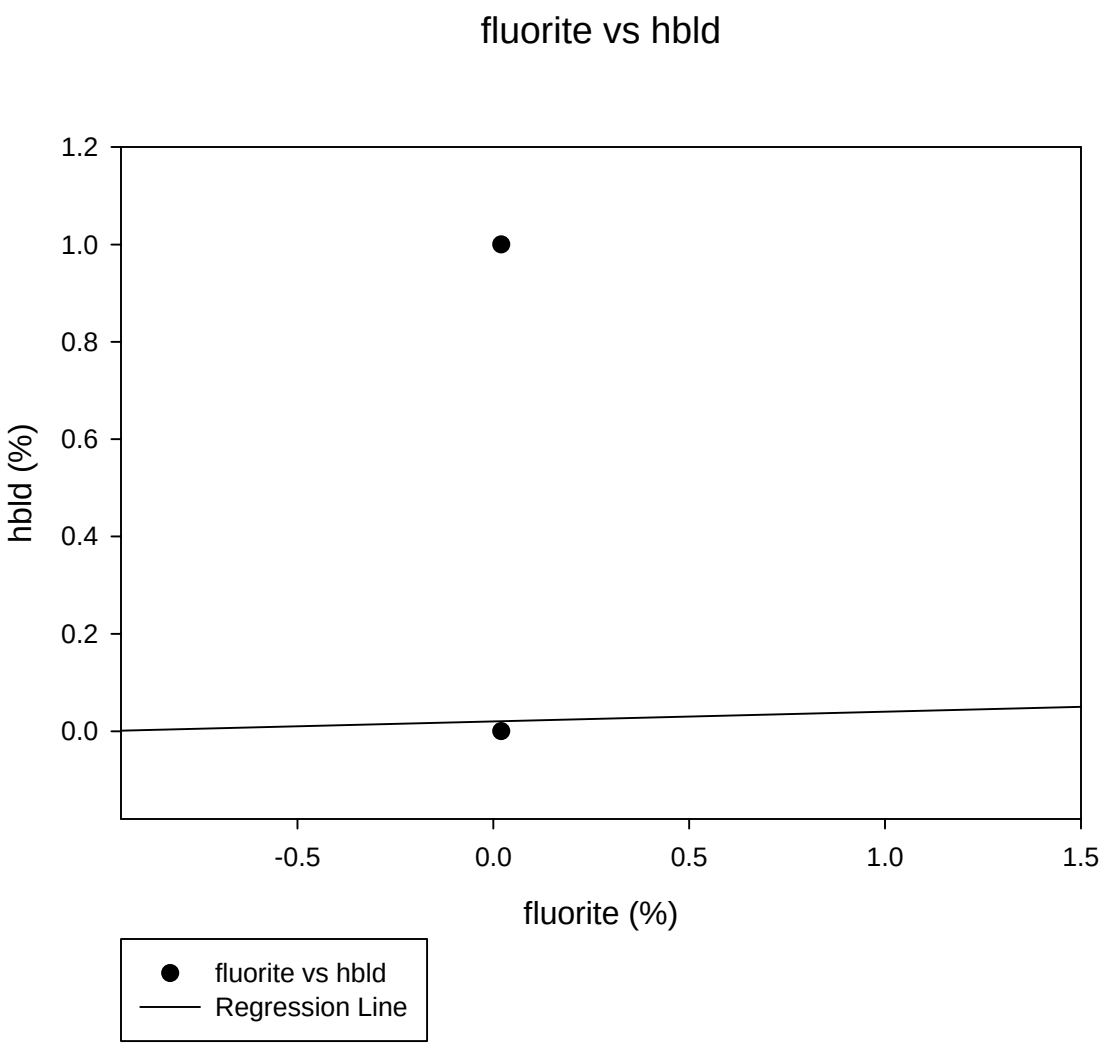
fluorite vs hbld
1.2
1.0
0.8
0.6
0.4
0.2
0.0
hbld (%)
-0.5
0.0
0.5
1.0
1.5
fluorite (%)
fluorite vs hbld
Regression Line

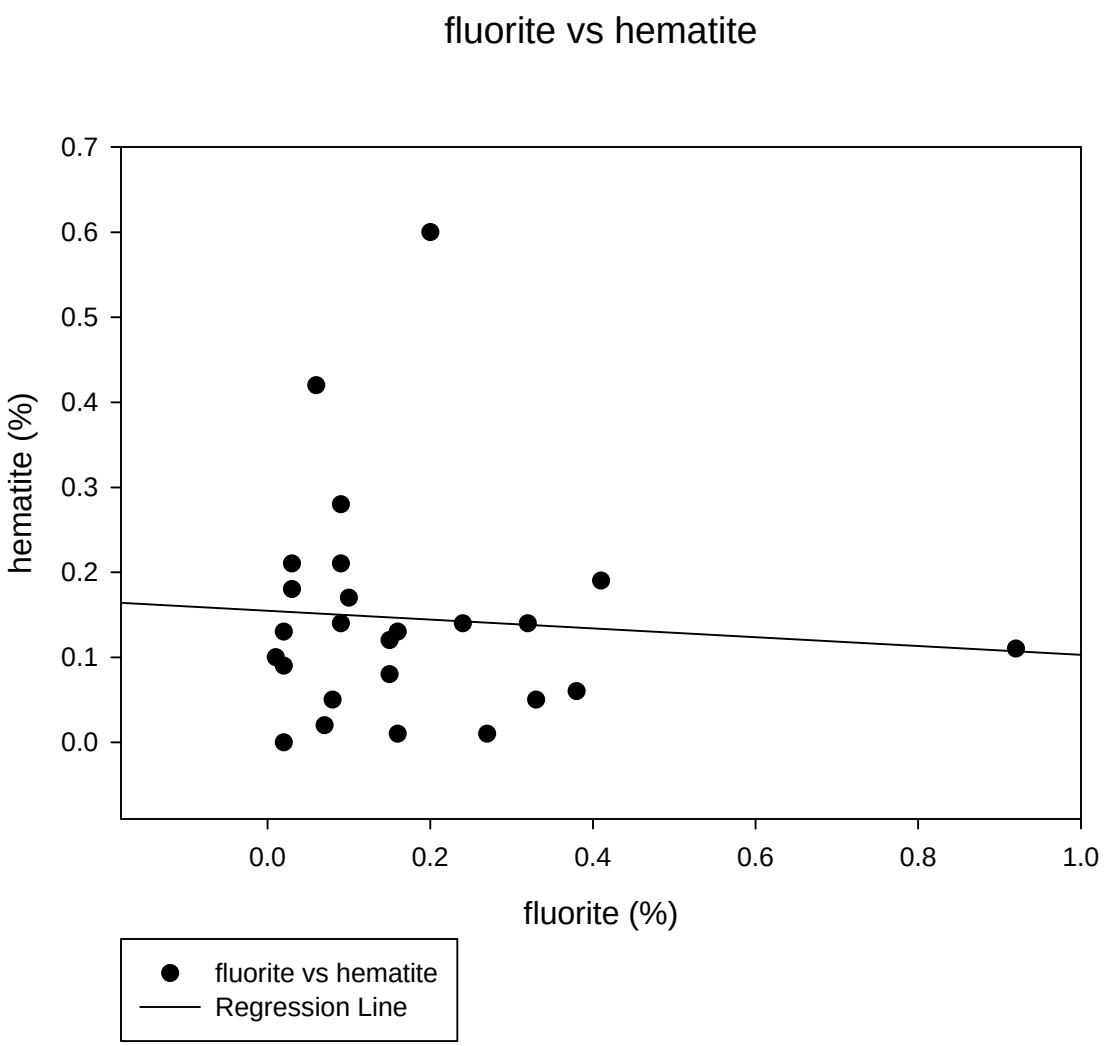
fluorite vs hematite
hematite (%)
0.7
0.6
0.5
0.4
0.3
0.2
0.1
0.0
0.0
0.2
0.4
0.6
0.8
1.0
fluorite (%)
fluorite vs hematite
Regression Line

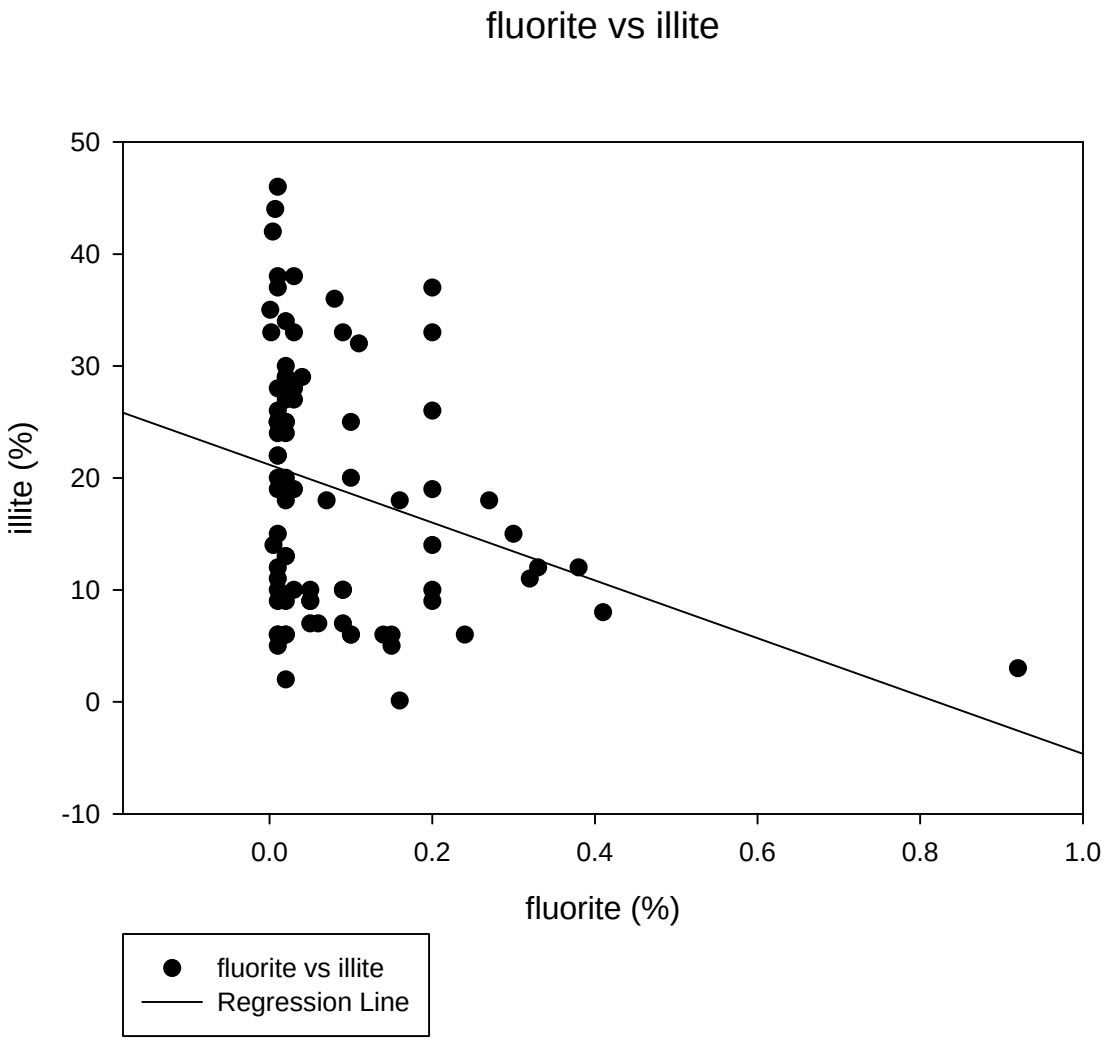
fluorite vs illite
illite (%)
50
40
30
20
10
0
-10
0.0
0.2
0.4
0.6
0.8
1.0
fluorite (%)
fluorite vs illite
Regression Line

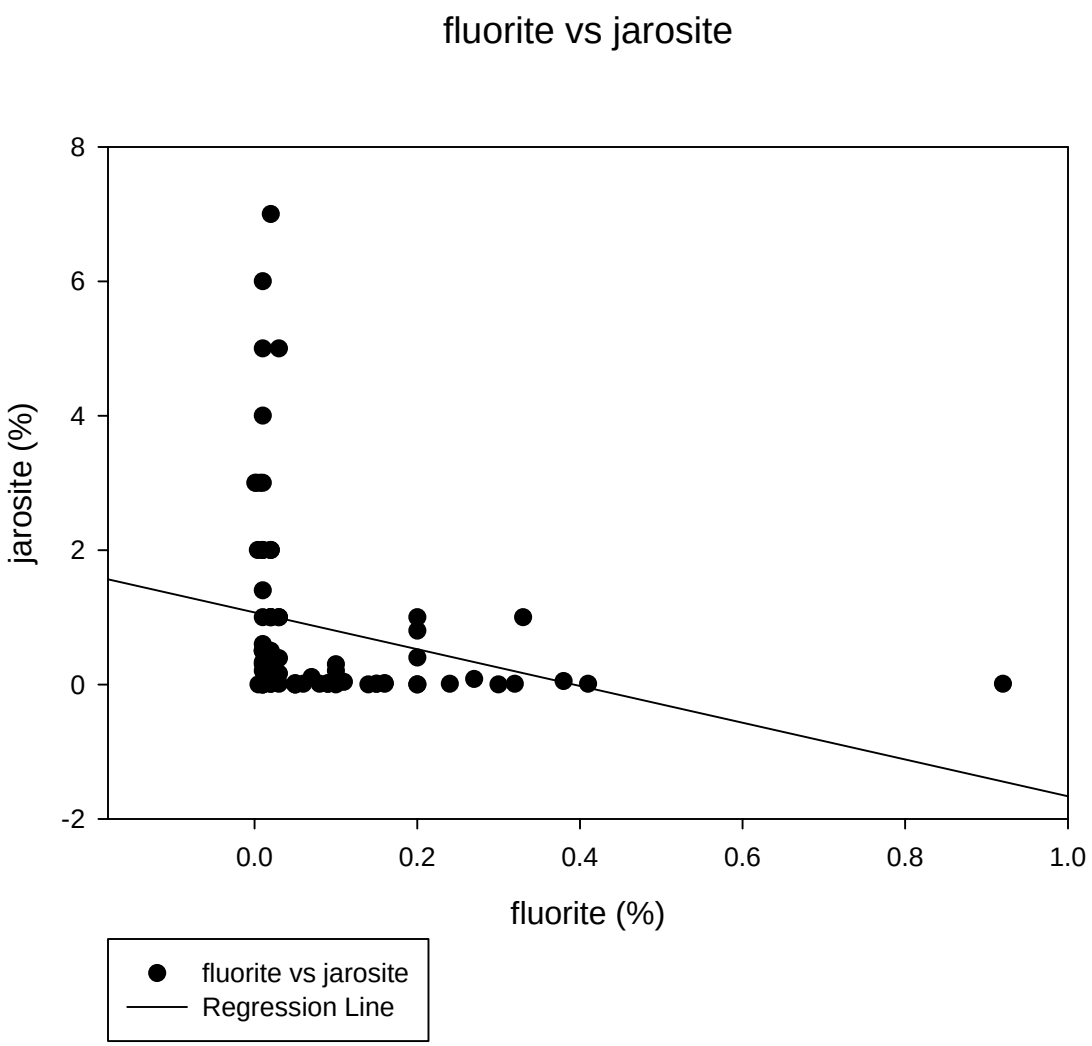
fluorite vs jarosite
jarosite (%)
8
6
4
2
0
-2
0.0
0.2
0.4
0.6
0.8
1.0
fluorite (%)
fluorite vs jarosite
Regression Line

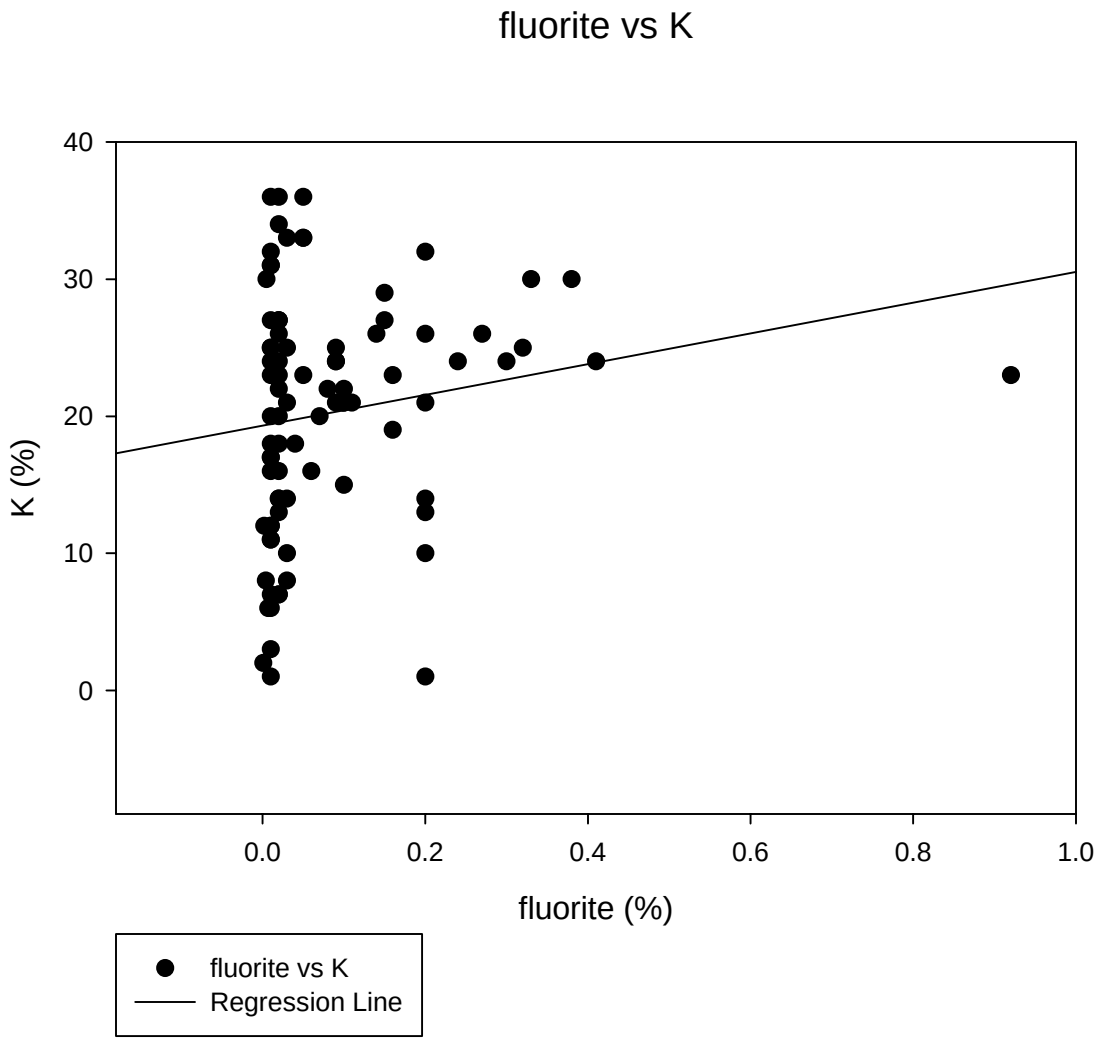
fluorite vs K
40
30
20
10
0
K (%)
0.0
0.2
0.4
0.6
0.8
1.0
fluorite (%)
fluorite vs K
Regression Line

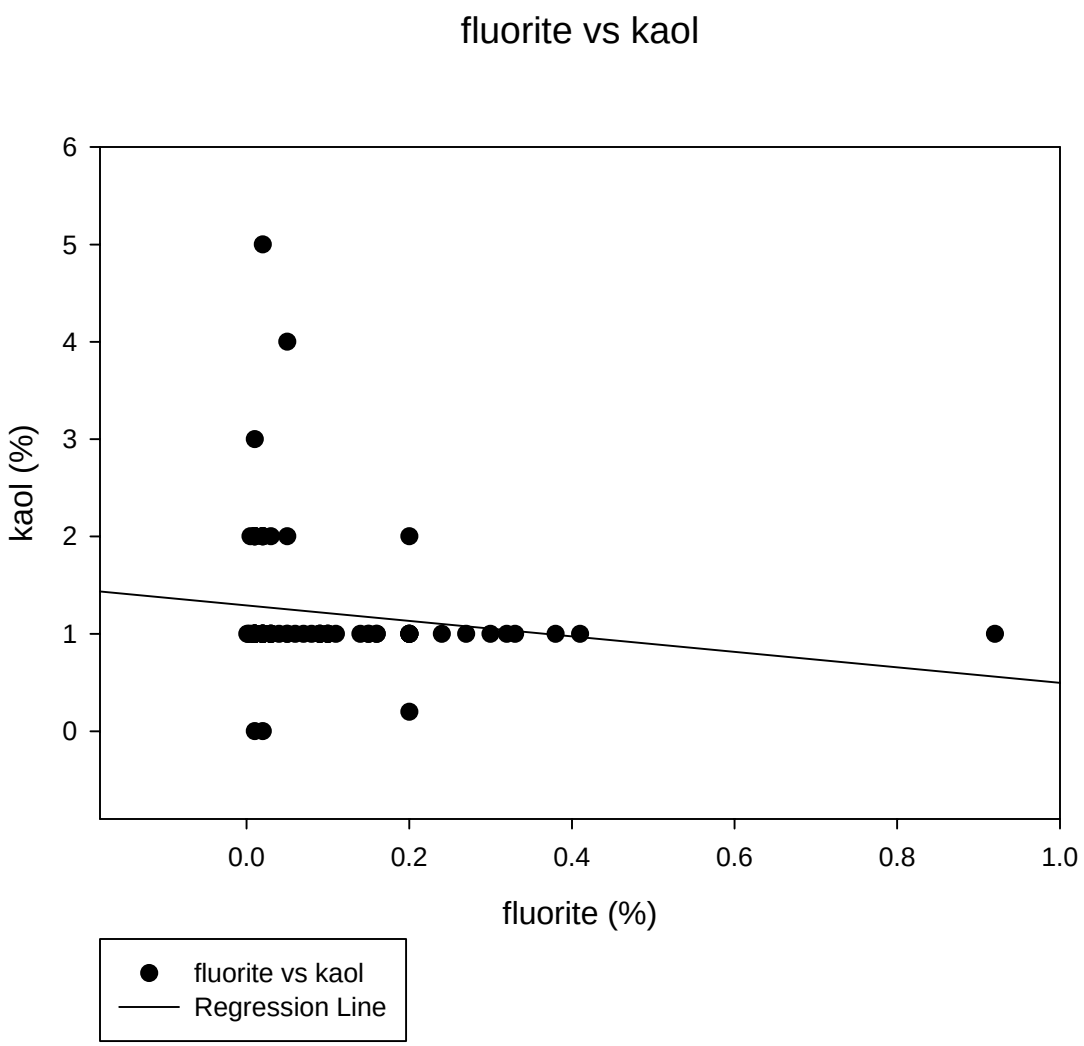
fluorite vs kaol
kaol (%)
6
5
4
3
2
1
0
0.0
0.2
0.4
0.6
0.8
1.0
fluorite (%)
fluorite vs kaol
Regression Line

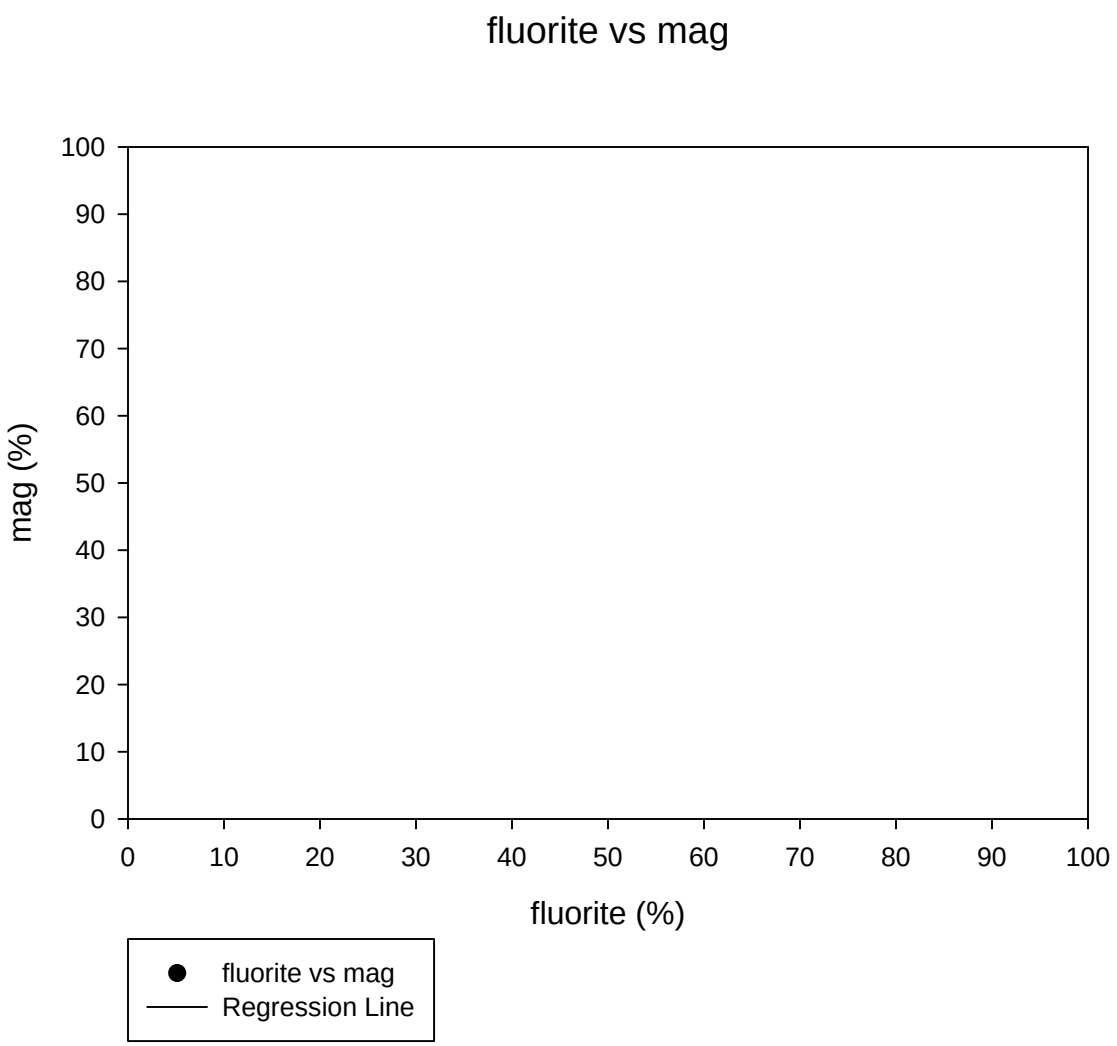
fluorite vs mag
100
90
80
70
60
50
40
30
20
10
0
mag (%)
0
10
20
30
40
50
60
70
80
90
100
fluorite (%)
fluorite vs mag
Regression Line

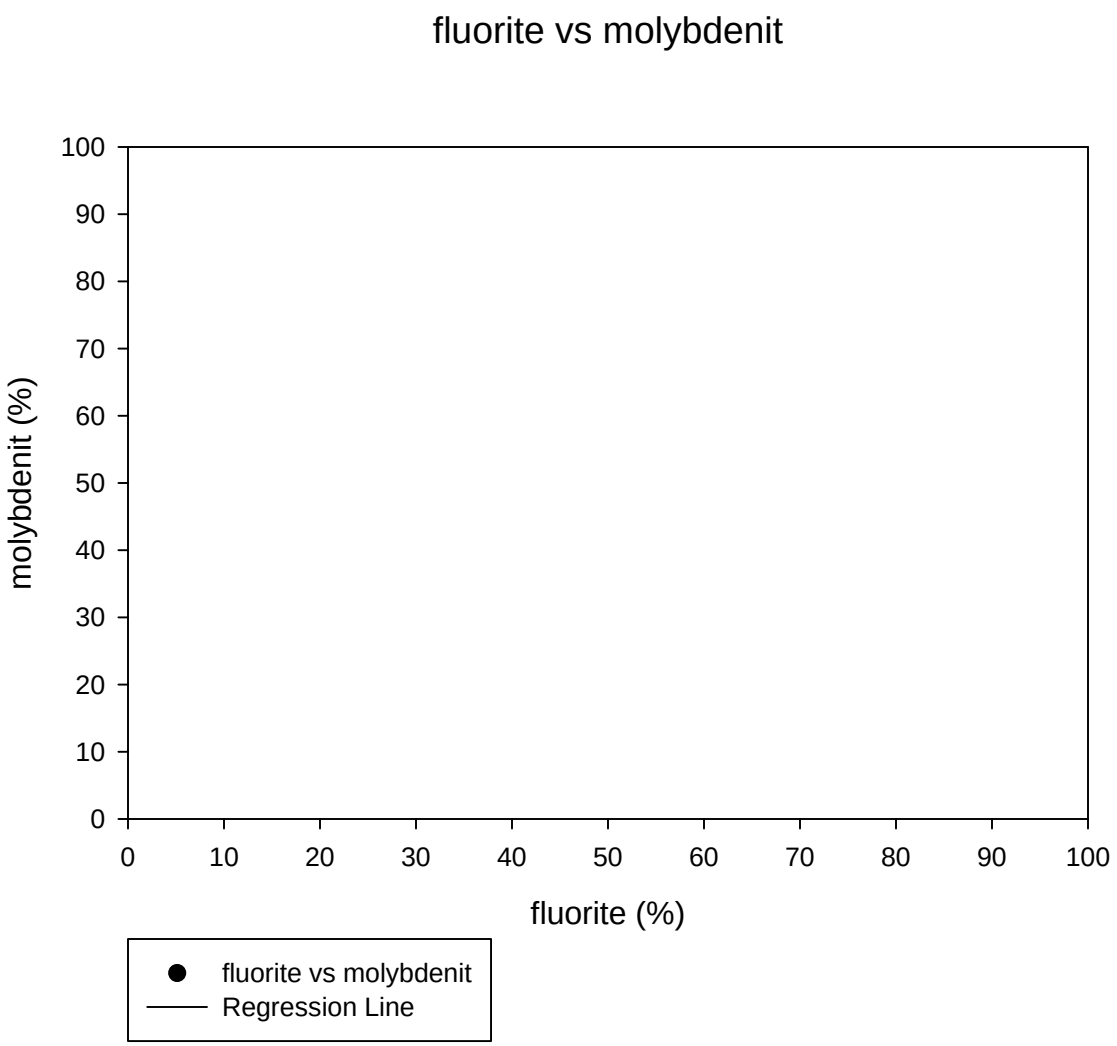
fluorite vs molybdenit
molybdenit (%)
100
90
80
70
60
50
40
30
20
10
0
0
10
20
30
40
50
60
70
80
90
100
fluorite (%)
fluorite vs molybdenit
Regression Line

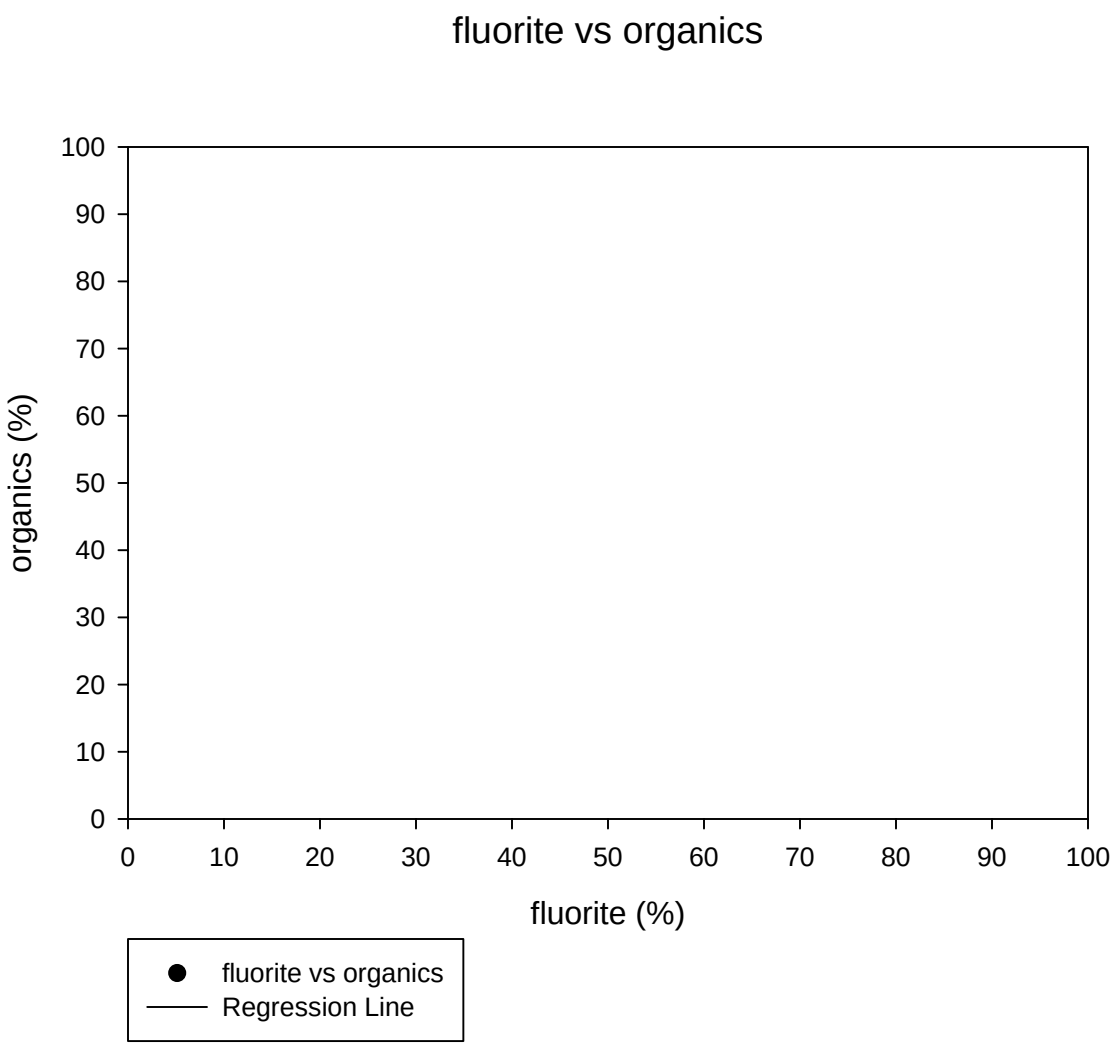
fluorite vs organics
organics (%)
100
90
80
70
60
50
40
30
20
10
0
0
10
20
30
40
50
60
70
80
90
100
fluorite (%)
fluorite vs organics
Regression Line

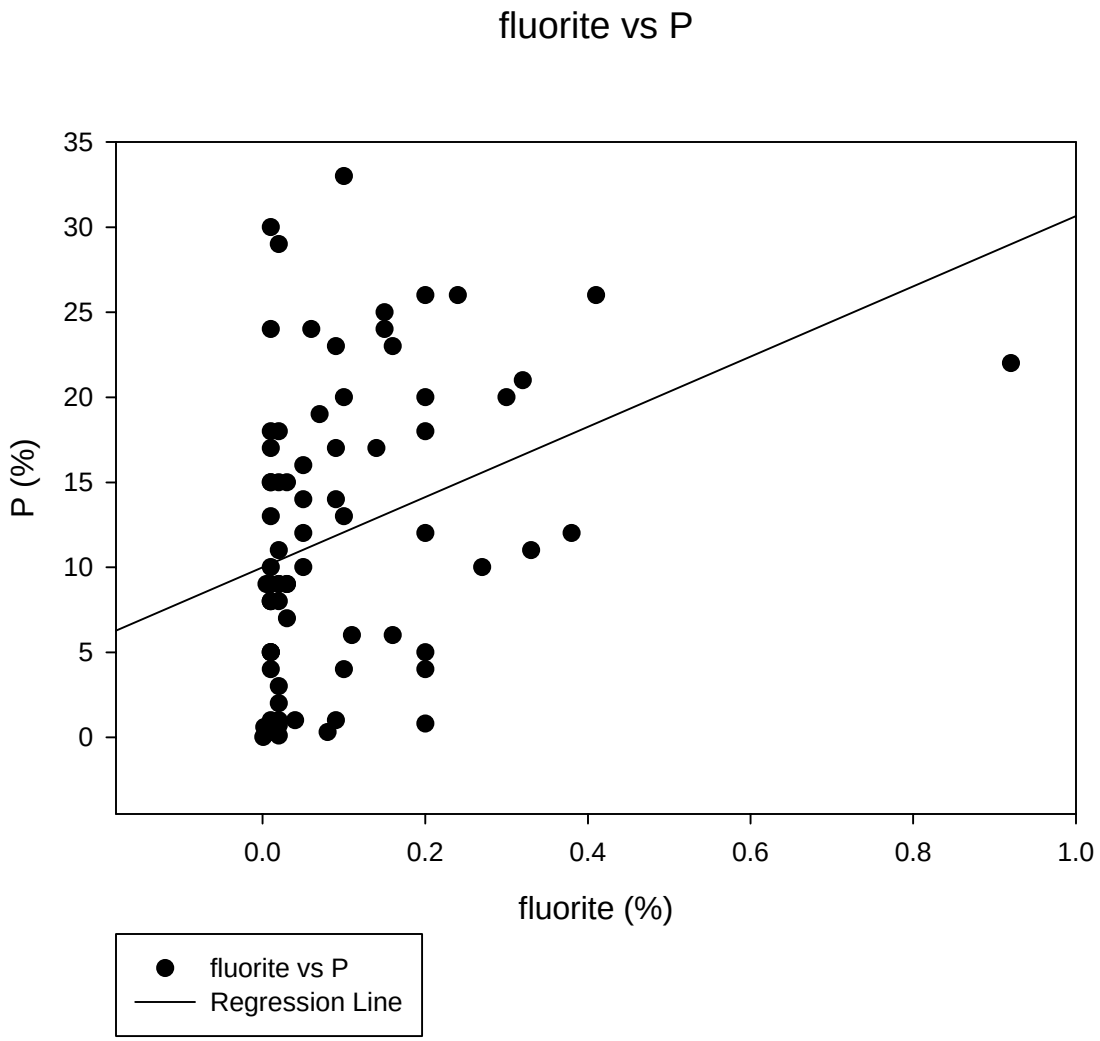
fluorite vs P
35
30
25
20
15
10
5
0
P (%)
0.0
0.2
0.4
0.6
0.8
1.0
fluorite (%)
fluorite vs P
Regression Line

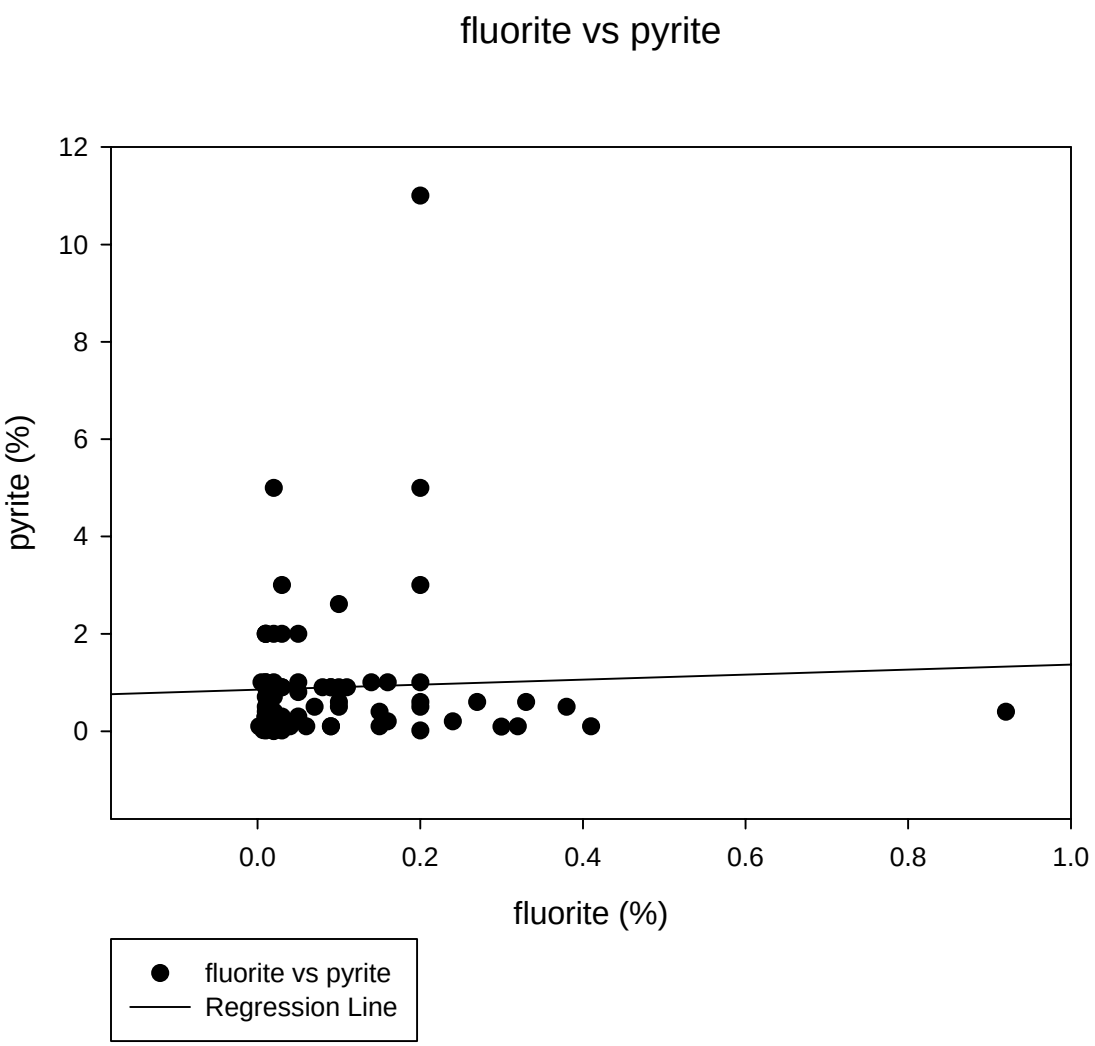
fluorite vs pyrite
12
10
8
6
4
2
0
pyrite (%)
0.0
0.2
0.4
0.6
0.8
1.0
fluorite (%)
fluorite vs pyrite
Regression Line

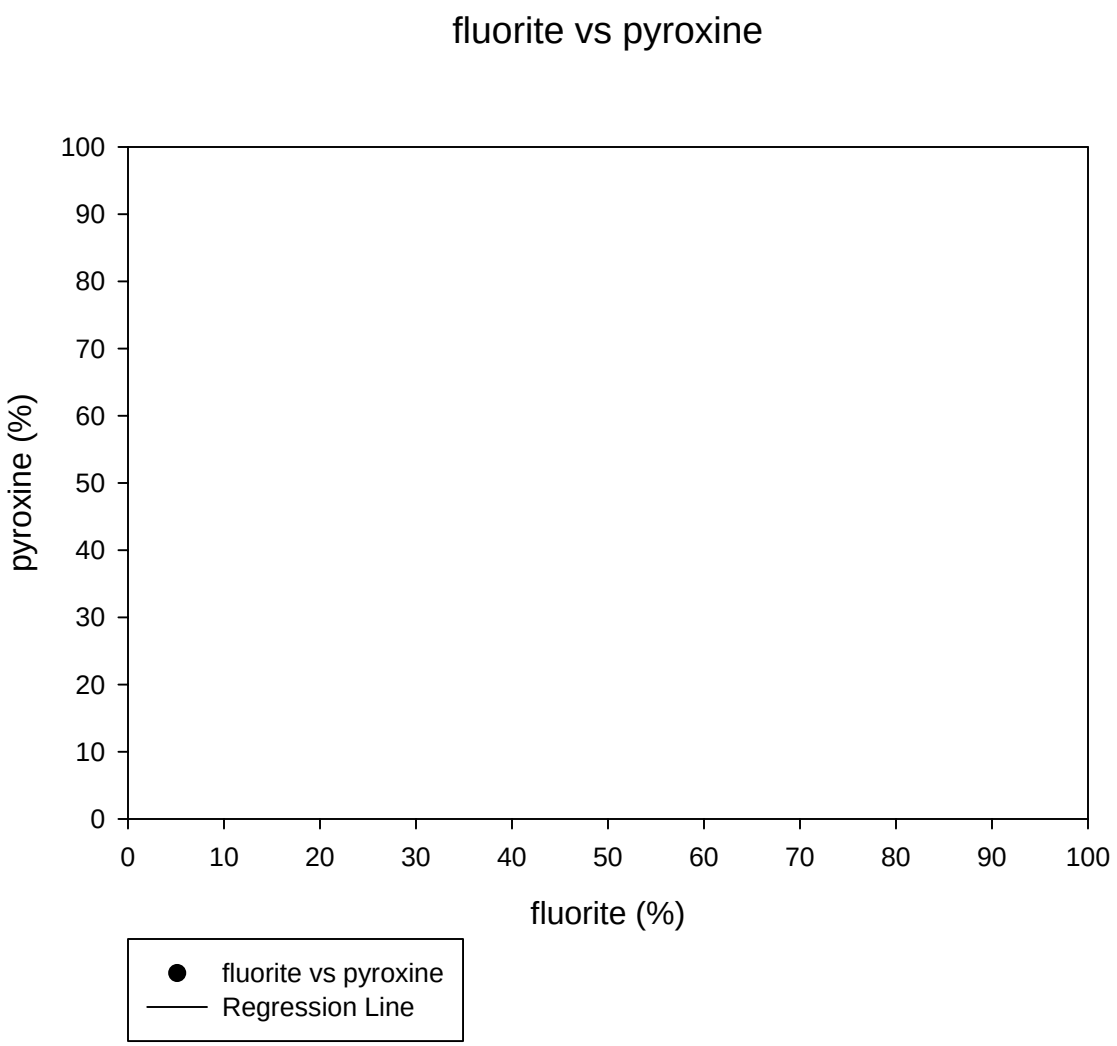
fluorite vs pyroxine
100
90
80
70
60
50
40
30
20
10
0
pyroxine (%)
0
10
20
30
40
50
60
70
80
90
100
fluorite (%)
fluorite vs pyroxine
Regression Line

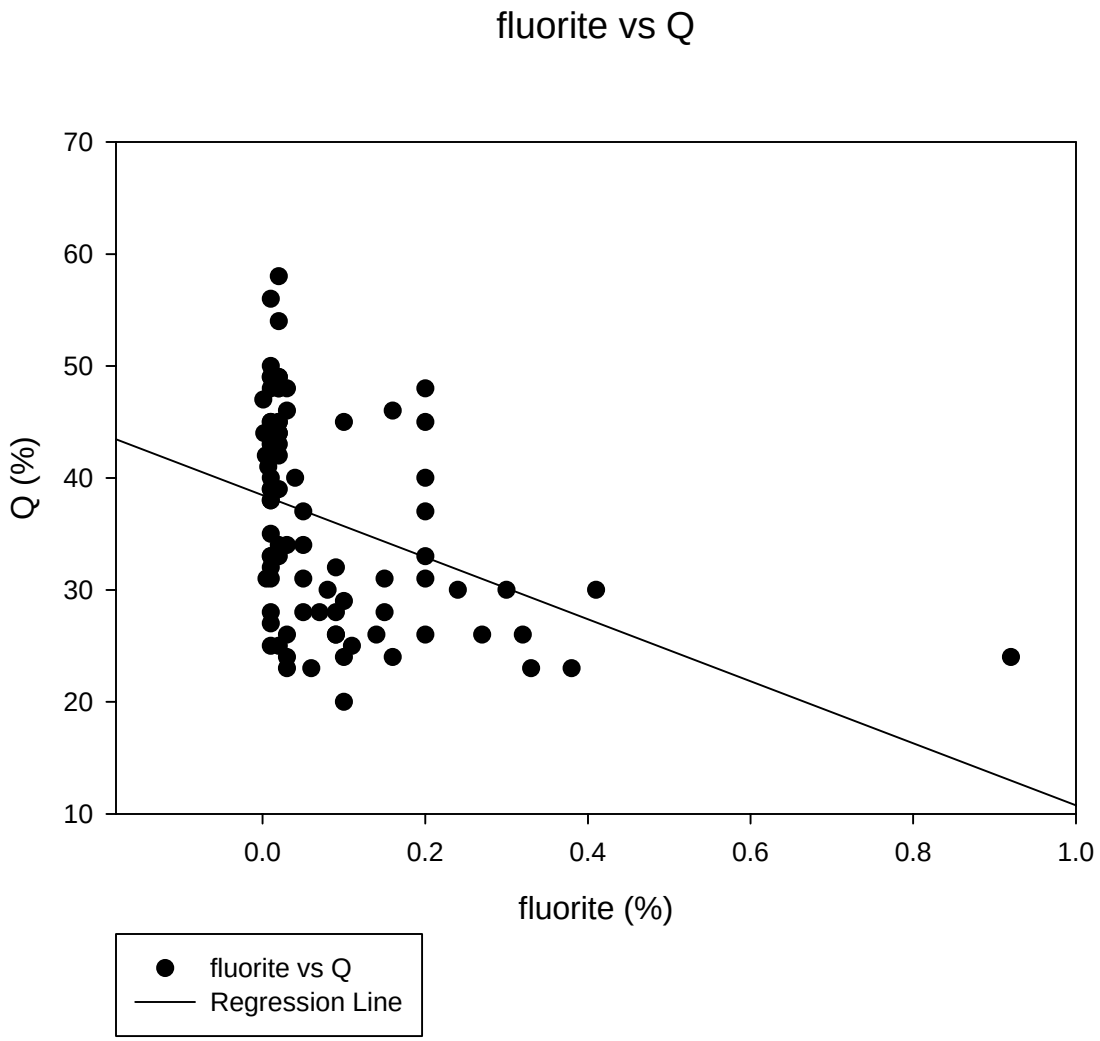
fluorite vs Q
70
60
50
40
30
20
10
Q (%)
0.0
0.2
0.4
0.6
0.8
1.0
fluorite (%)
fluorite vs Q
Regression Line

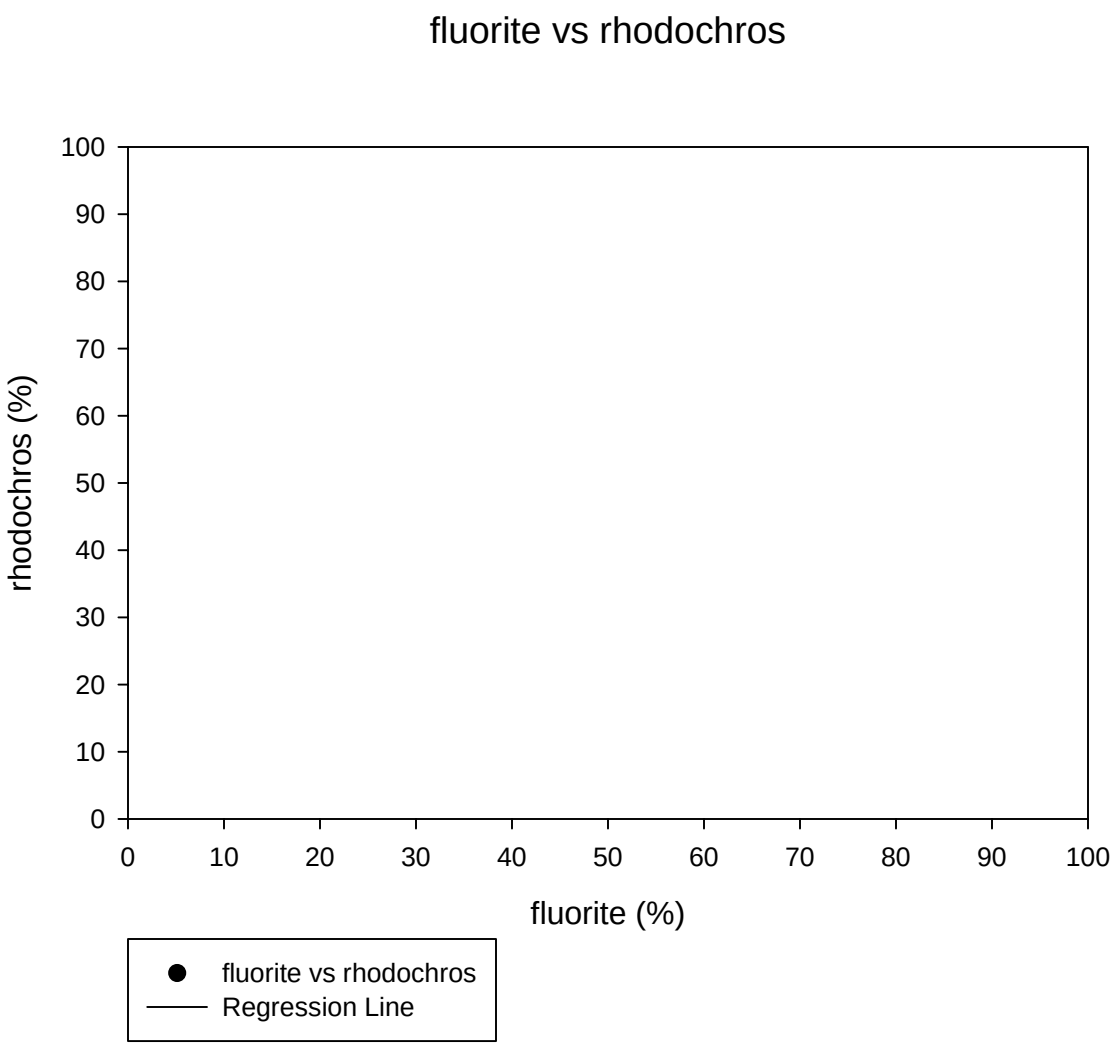
fluorite vs rhodochros
rhodochros (%)
100
90
80
70
60
50
40
30
20
10
0
0
10
20
30
40
50
60
70
80
90
100
fluorite (%)
fluorite vs rhodochros
Regression Line

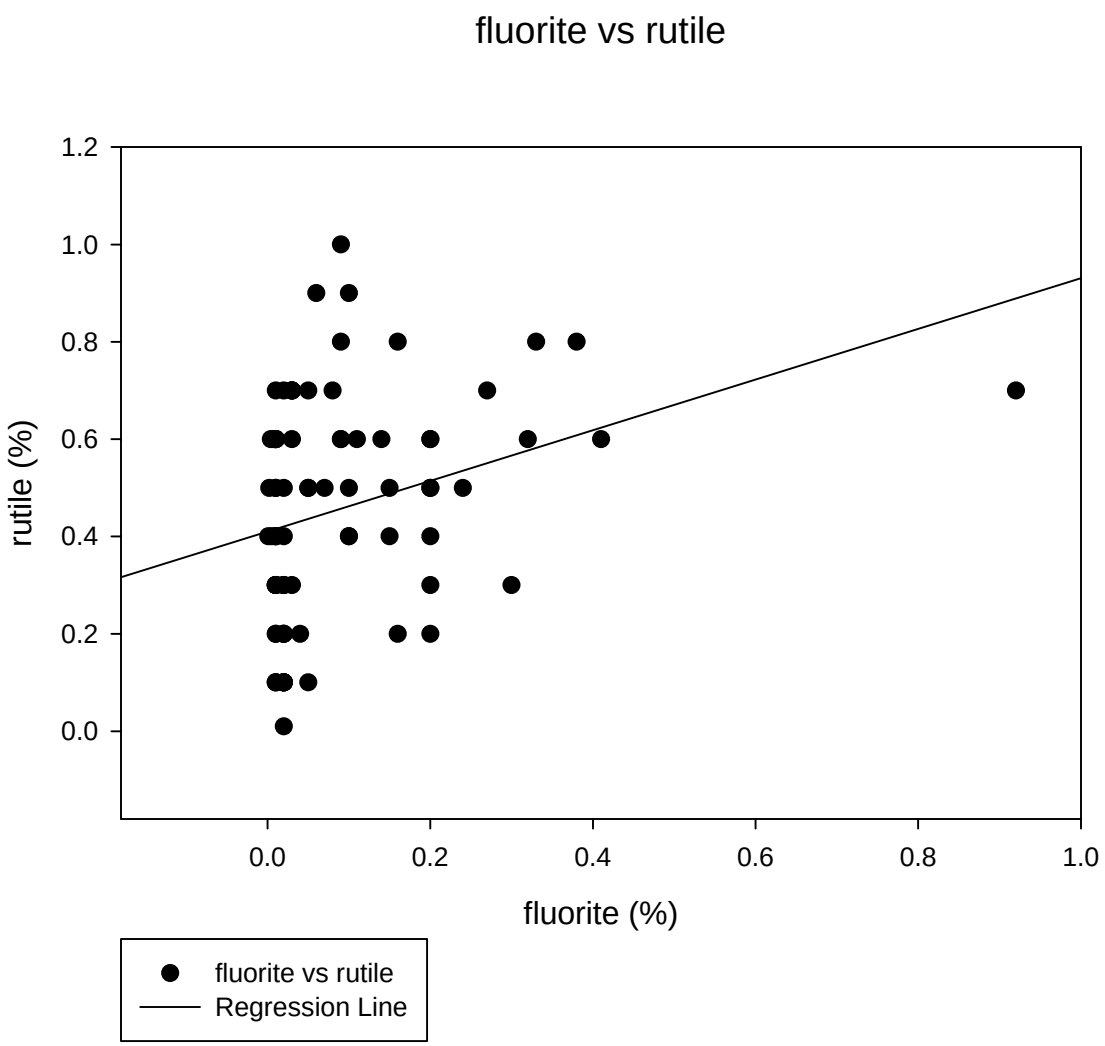
fluorite vs rutile
1.2
1.0
0.8
0.6
0.4
0.2
0.0
rutile (%)
0.0
0.2
0.4
0.6
0.8
1.0
fluorite (%)
fluorite vs rutile
Regression Line

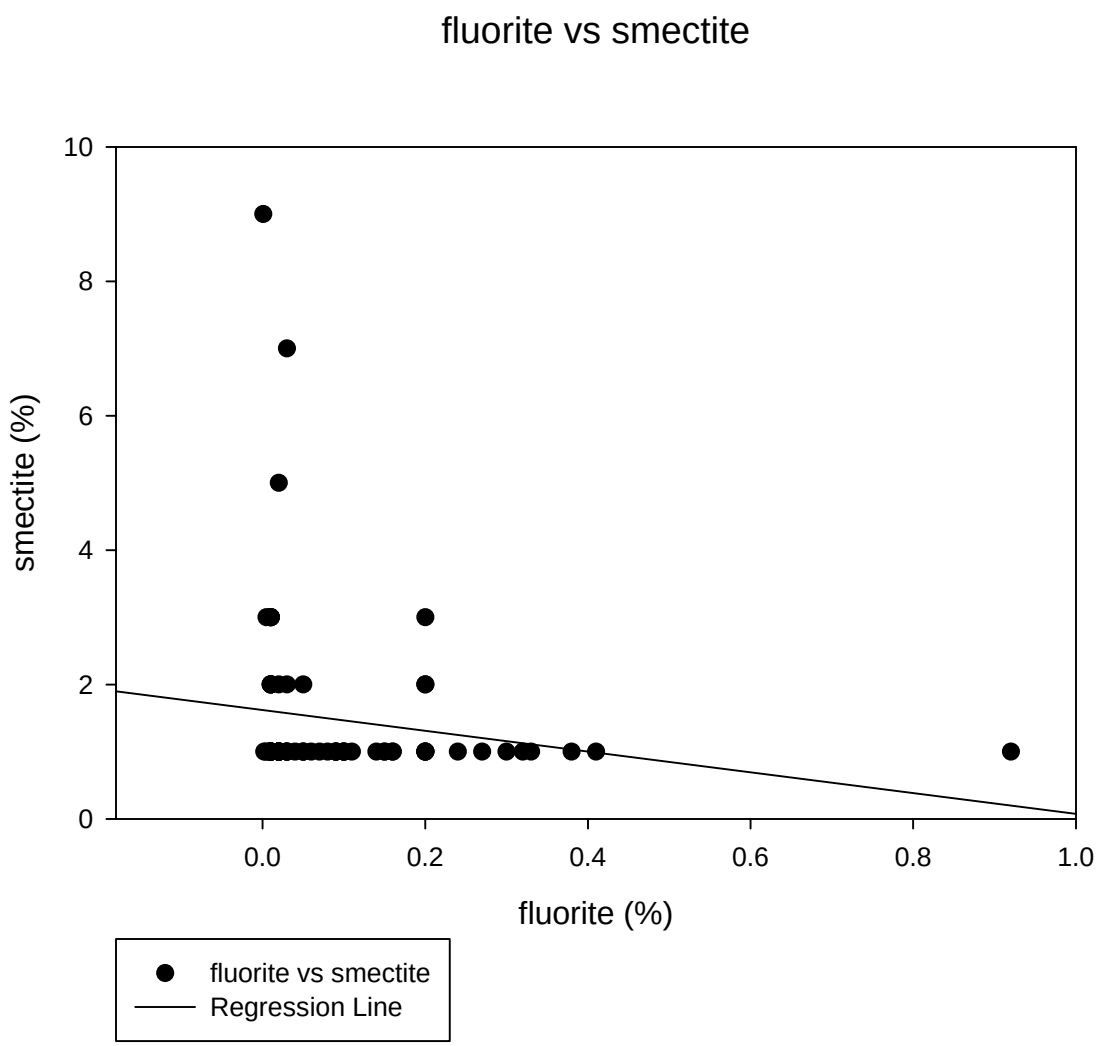
fluorite vs smectite
smectite (%)
10
8
6
4
2
0
0.0
0.2
0.4
0.6
0.8
1.0
fluorite (%)
fluorite vs smectite
Regression Line

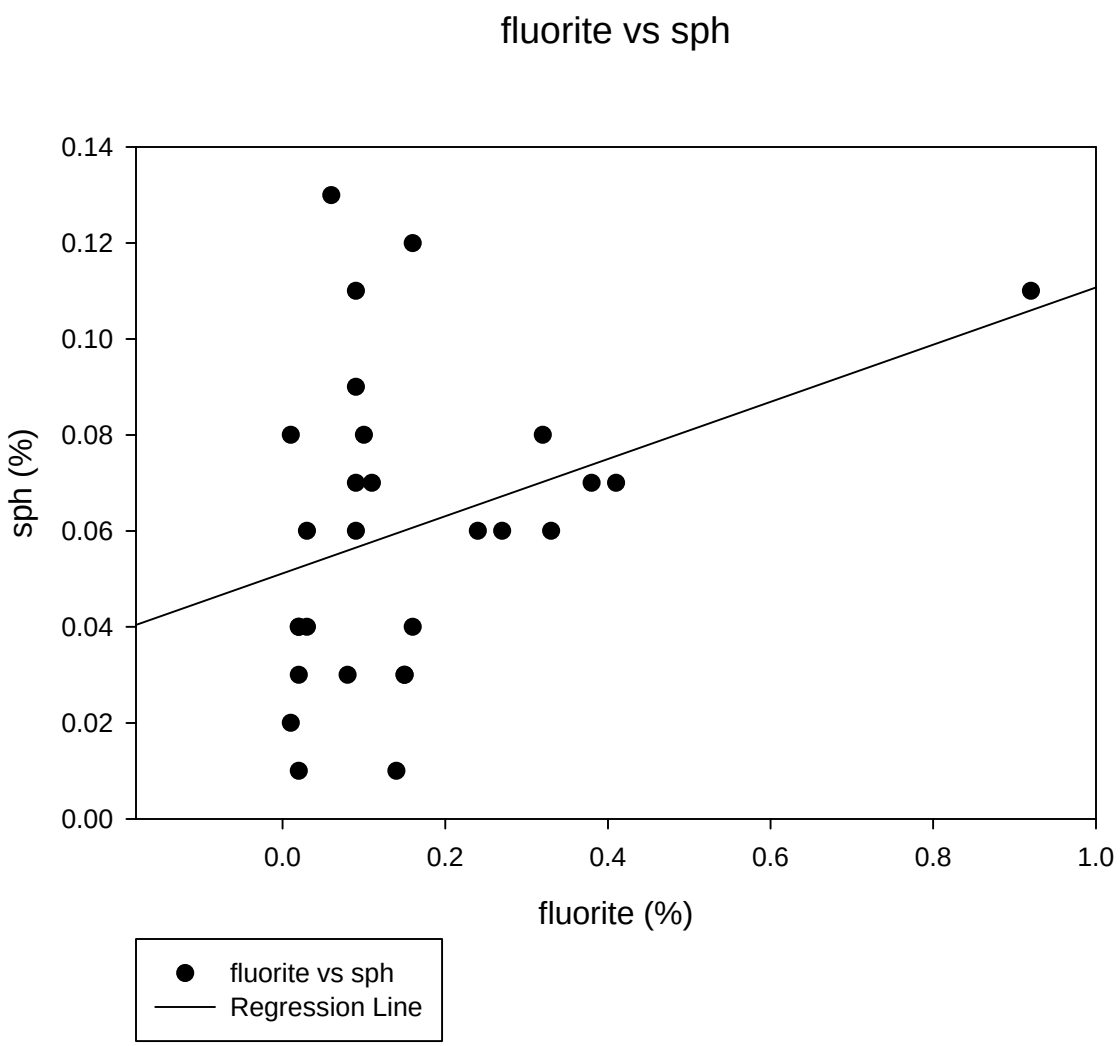
fluorite vs sph
0.14
0.12
0.10
0.08
0.06
0.04
0.02
0.00
sph (%)
0.0
0.2
0.4
0.6
0.8
1.0
fluorite (%)
fluorite vs sph
Regression Line

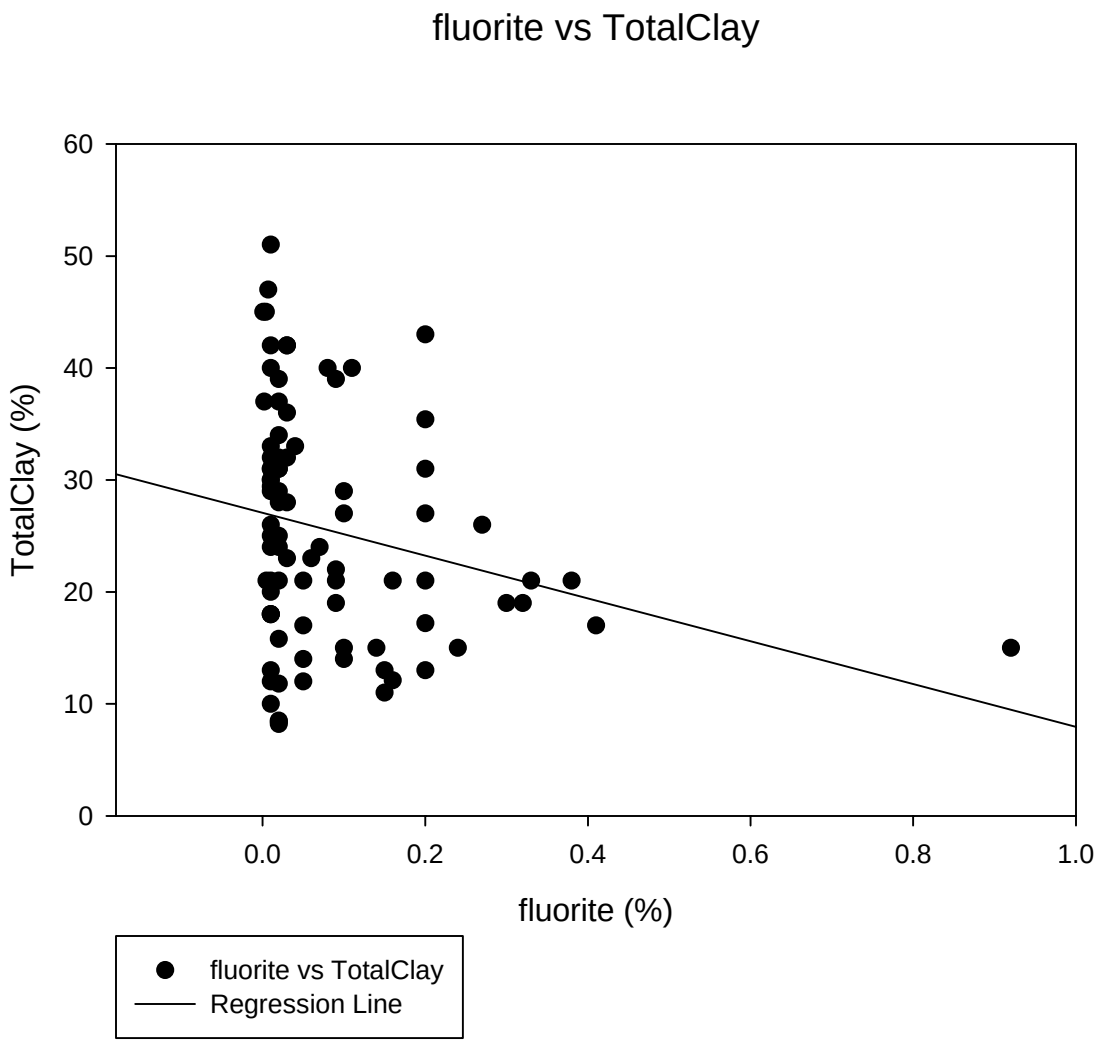
fluorite vs TotalClay
60
50
40
30
20
10
0
TotalClay (%)
0.0
0.2
0.4
0.6
0.8
1.0
fluorite (%)
fluorite vs TotalClay
Regression Line

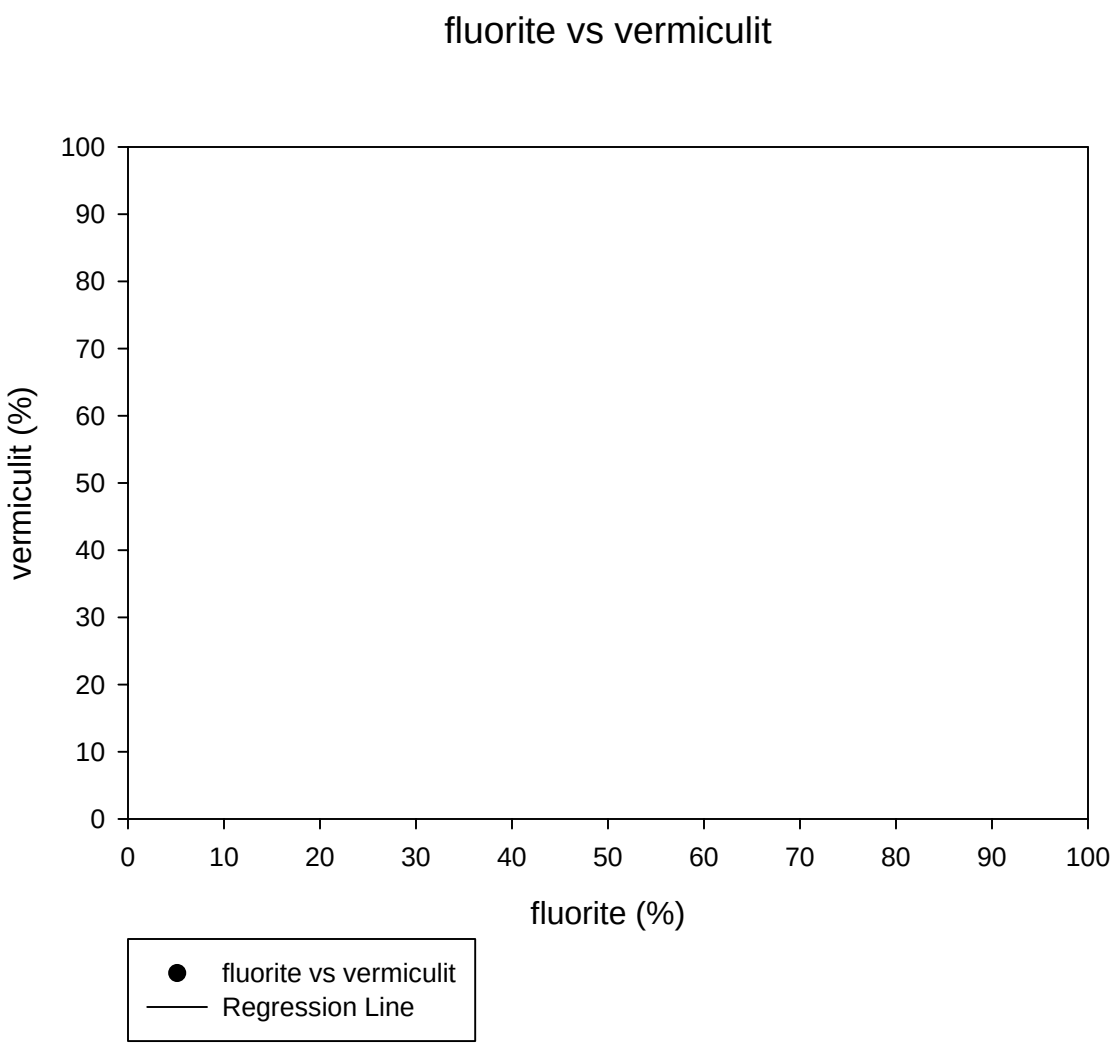
fluorite vs vermiculit
vermiculit (%)
100
90
80
70
60
50
40
30
20
10
0
0
10
20
30
40
50
60
70
80
90
100
fluorite (%)
fluorite vs vermiculit
Regression Line

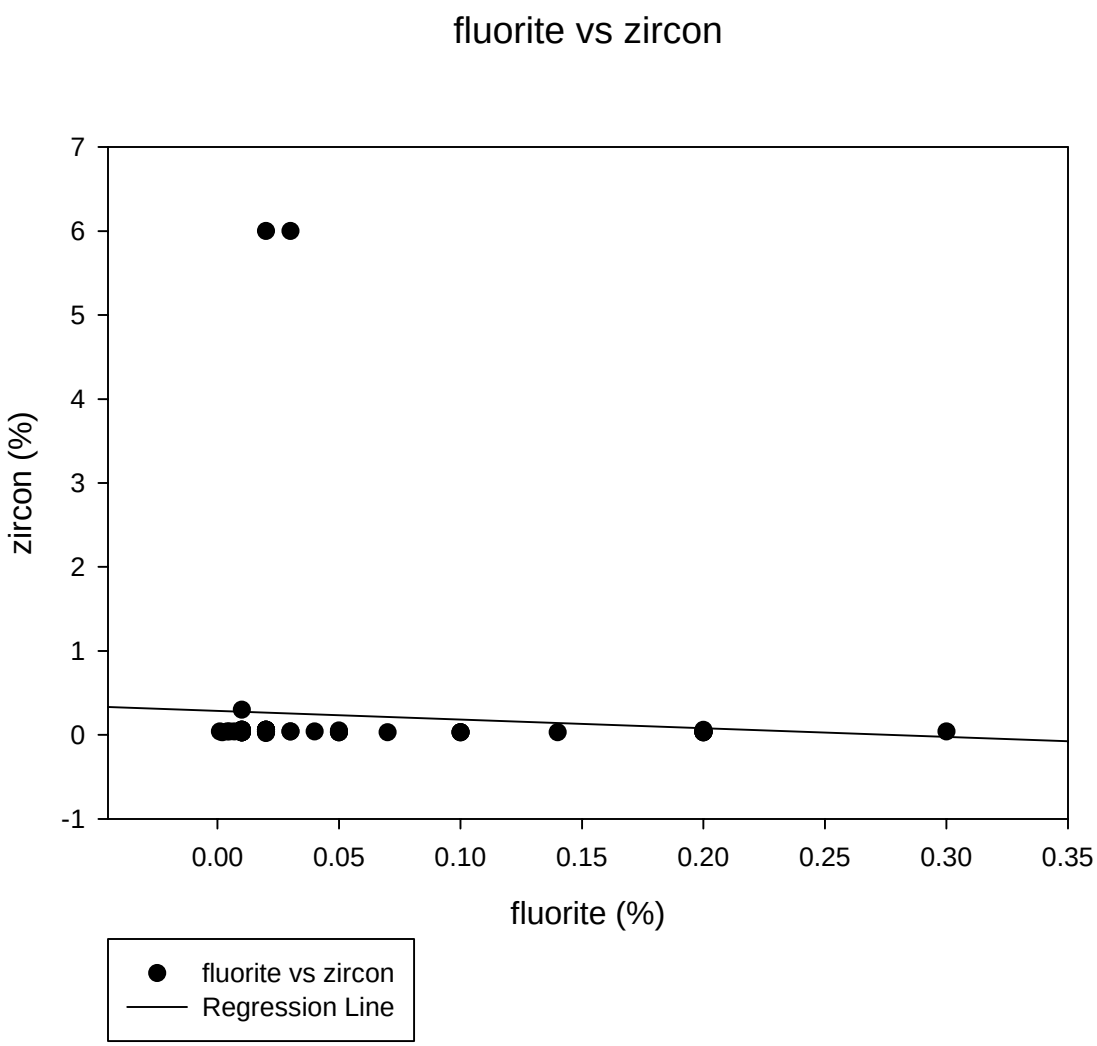
fluorite vs zircon
zircon (%)
7
6
5
4
3
2
1
0
-1
0.00
0.05
0.10
0.15
0.20
0.25
0.30
0.35
fluorite (%)
fluorite vs zircon
Regression Line

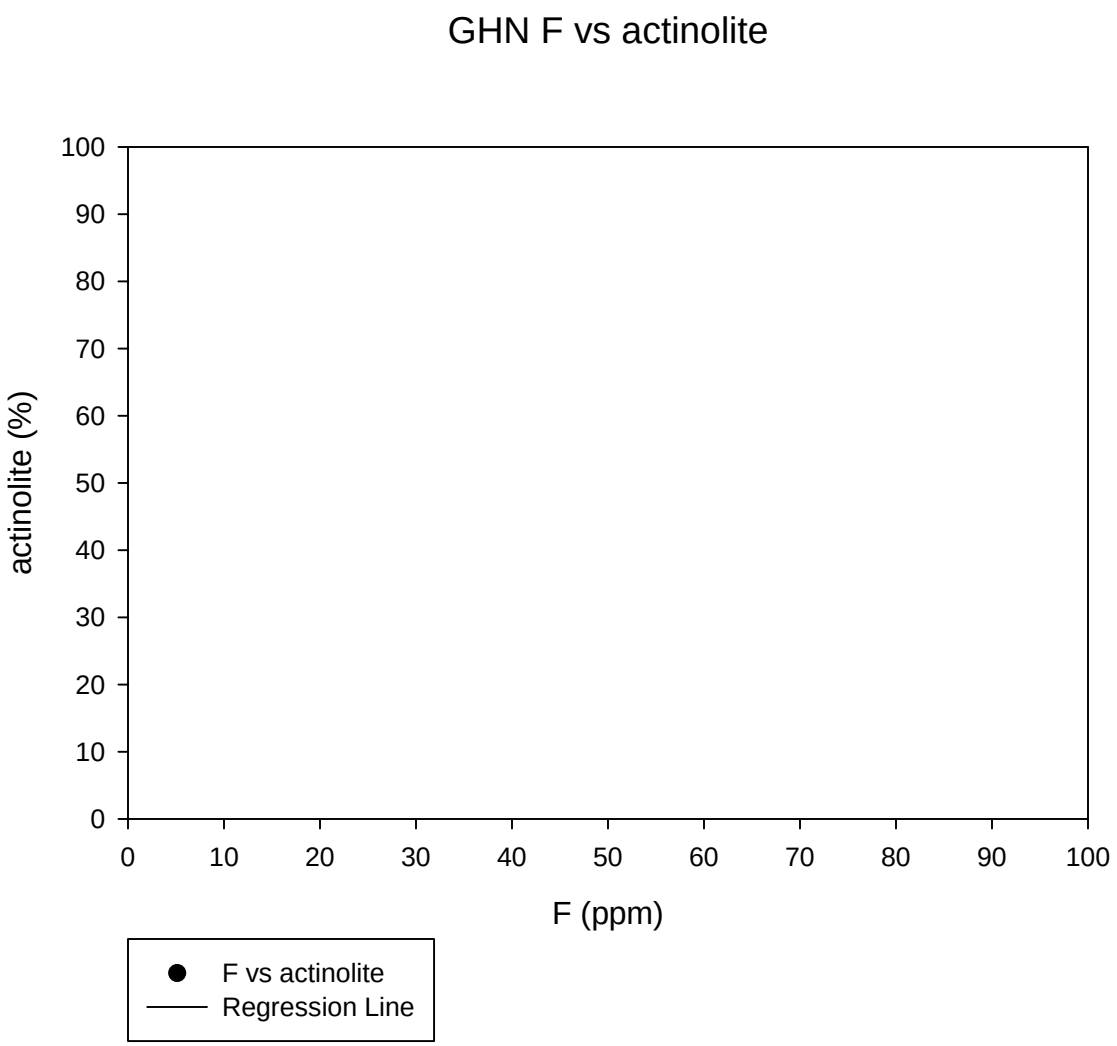
GHN F vs actinolite
actinolite (%)
100
90
80
70
60
50
40
30
20
10
0
0
10
20
30
40
50
60
70
80
90
100
F (ppm)
F vs actinolite
Regression Line

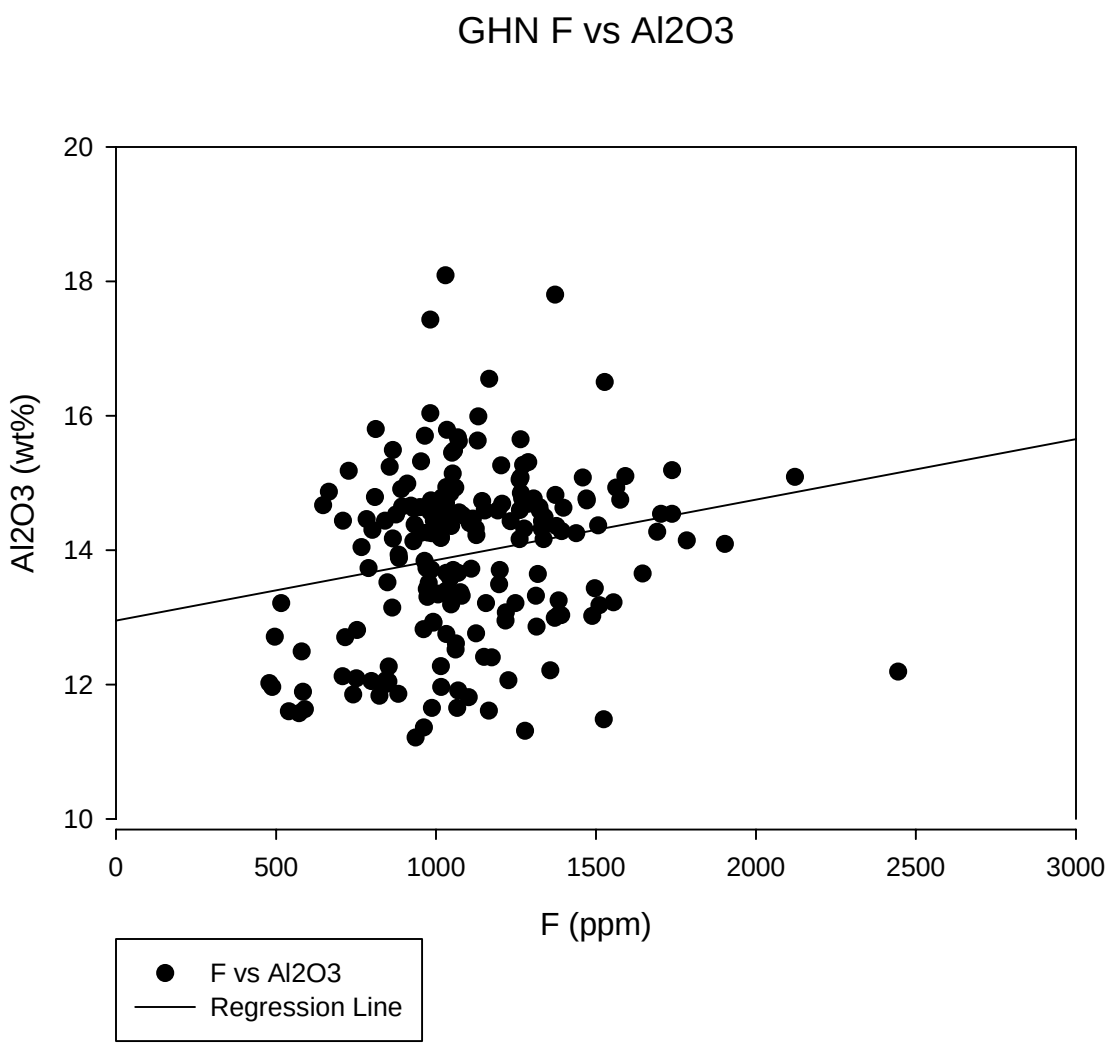
GHN F vs Al2O3
20
18
16
14
12
10
Al2O3 (wt%)
0
500
1000
1500
2000
2500
3000
F (ppm)
F vs Al2O3
Regression Line

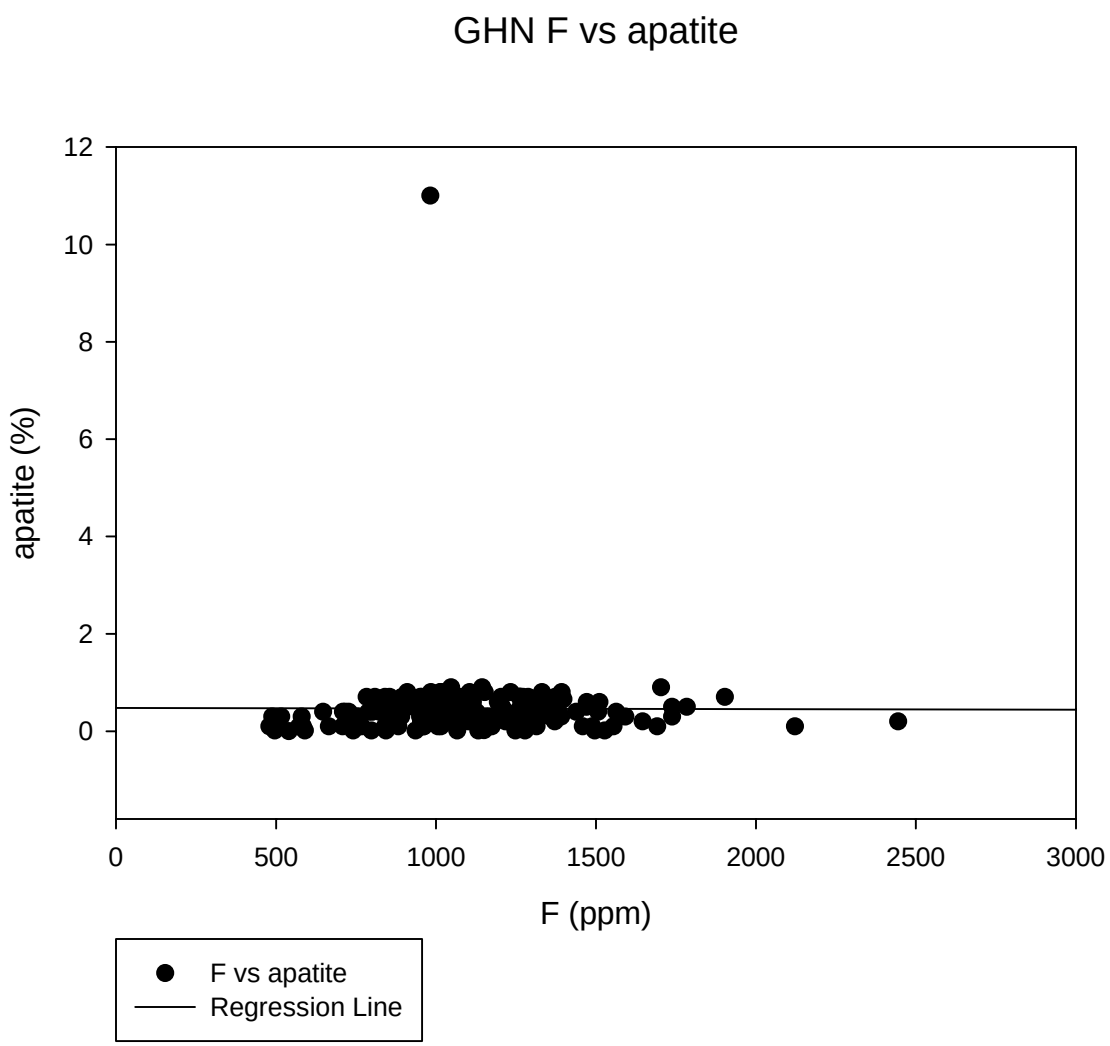
GHN F vs apatite
apatite (%)
12
10
8
6
4
2
0
0
500
1000
1500
2000
2500
3000
F (ppm)
F vs apatite
Regression Line

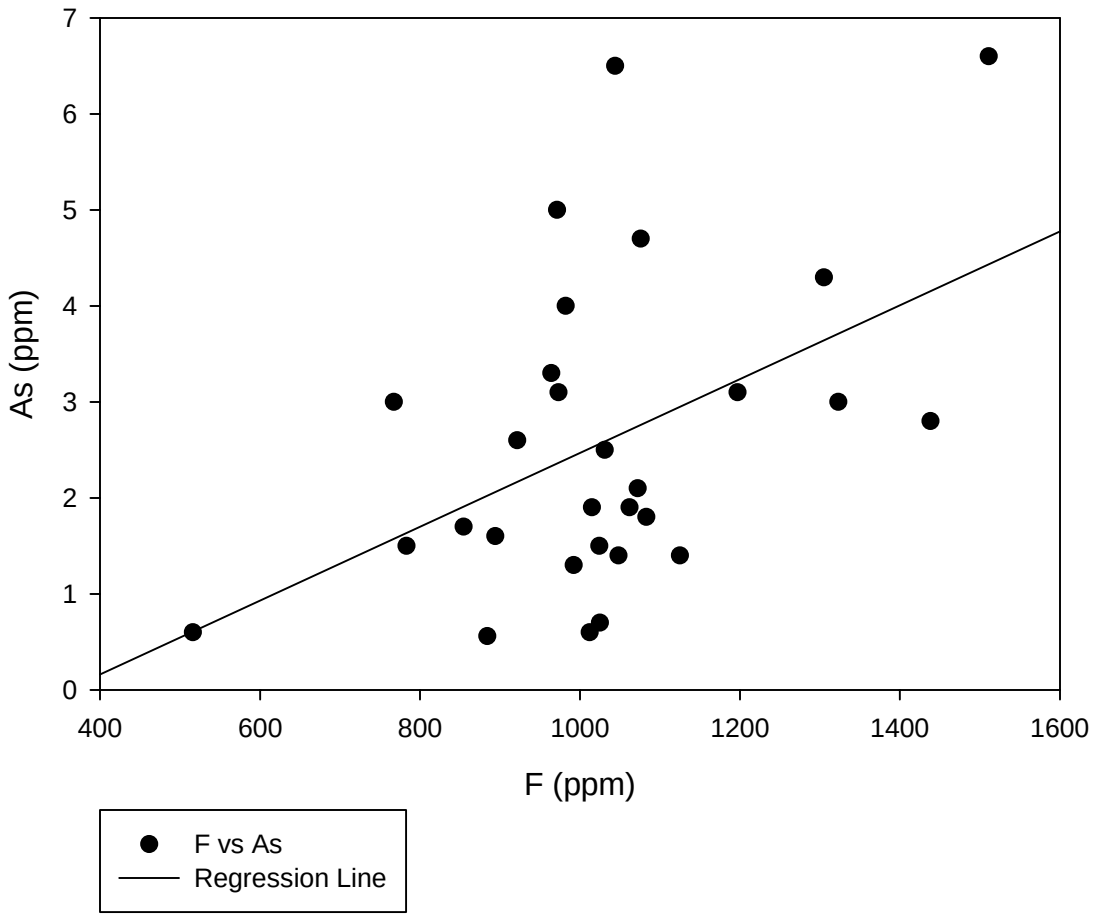
GHN F vs As
As (ppm)
F (ppm)
0
1
2
3
4
5
6
7
400
600
800
1000
1200
1400
1600
F vs As
Regression Line

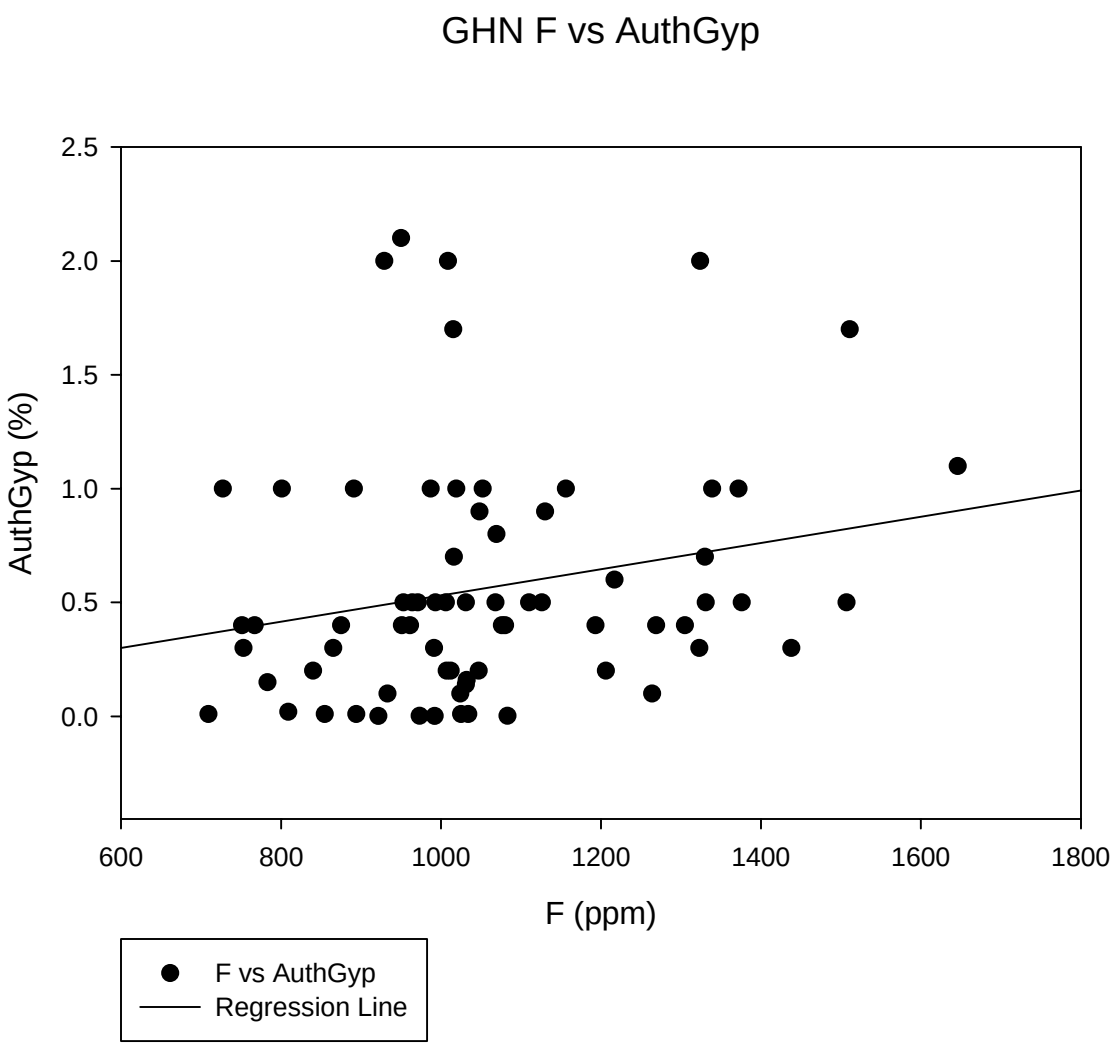
GHN F vs AuthGyp
AuthGyp (%)
2.5
2.0
1.5
1.0
0.5
0.0
600
800
1000
1200
1400
1600
1800
F (ppm)
F vs AuthGyp
Regression Line

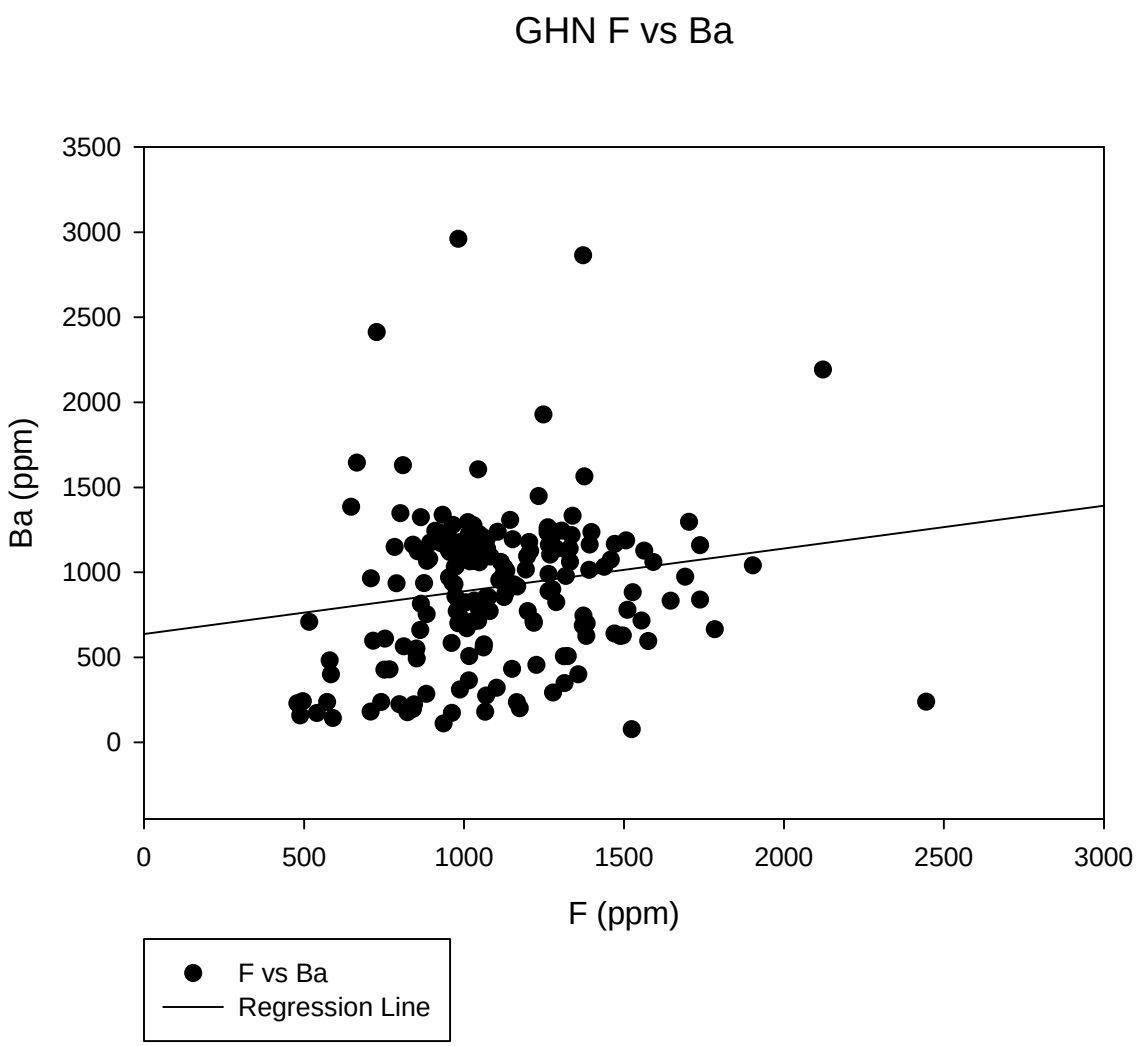
GHN F vs Ba
Ba (ppm)
3500
3000
2500
2000
1500
1000
500
0
0
500
1000
1500
2000
2500
3000
F (ppm)
F vs Ba
Regression Line

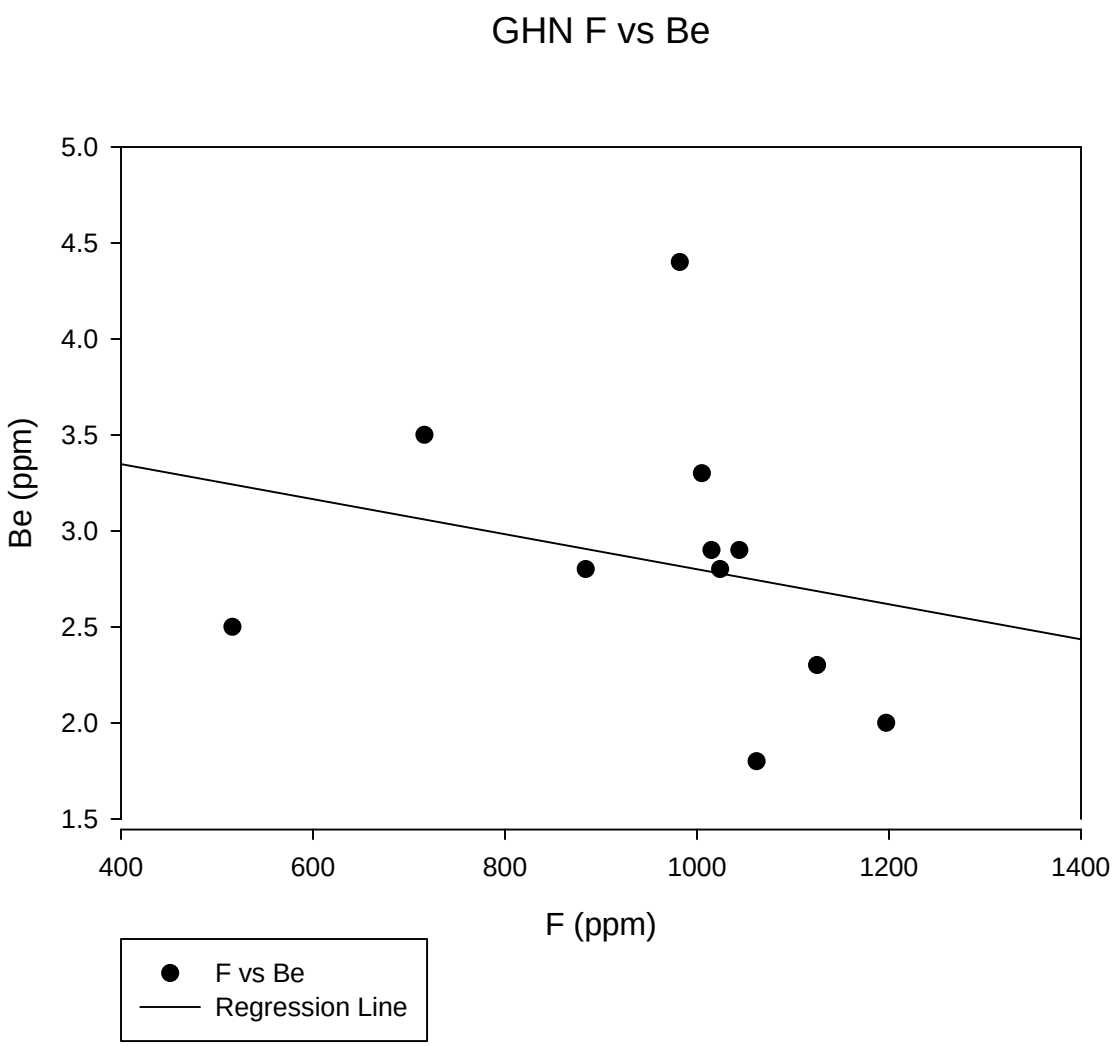
GHN F vs Be
5.0
4.5
4.0
3.5
3.0
2.5
2.0
1.5
Be (ppm)
400
600
800
1000
1200
1400
F (ppm)
F vs Be
Regression Line

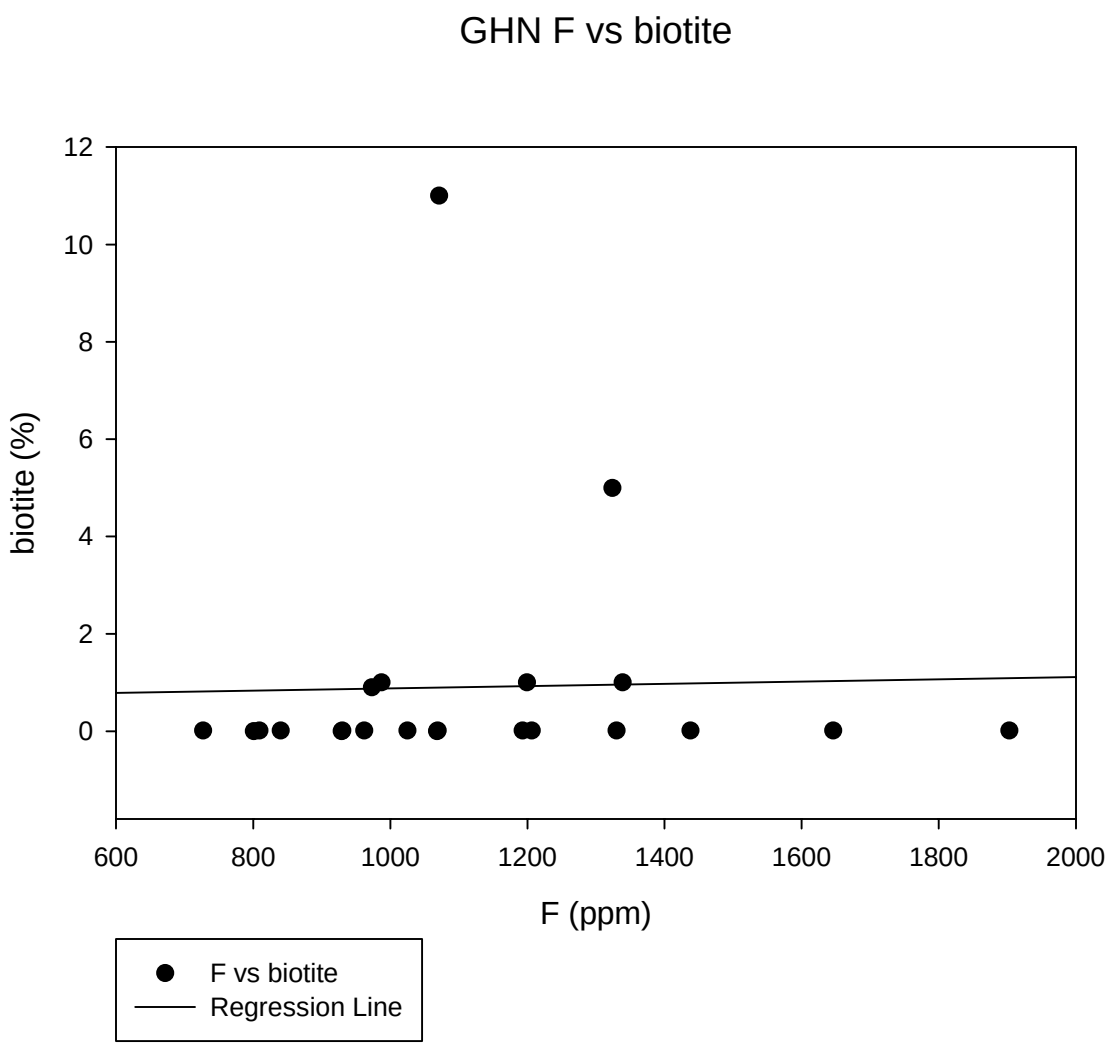
GHN F vs biotite
biotite (%)
12
10
8
6
4
2
0
600
800
1000
1200
1400
1600
1800
2000
F (ppm)
F vs biotite
Regression Line

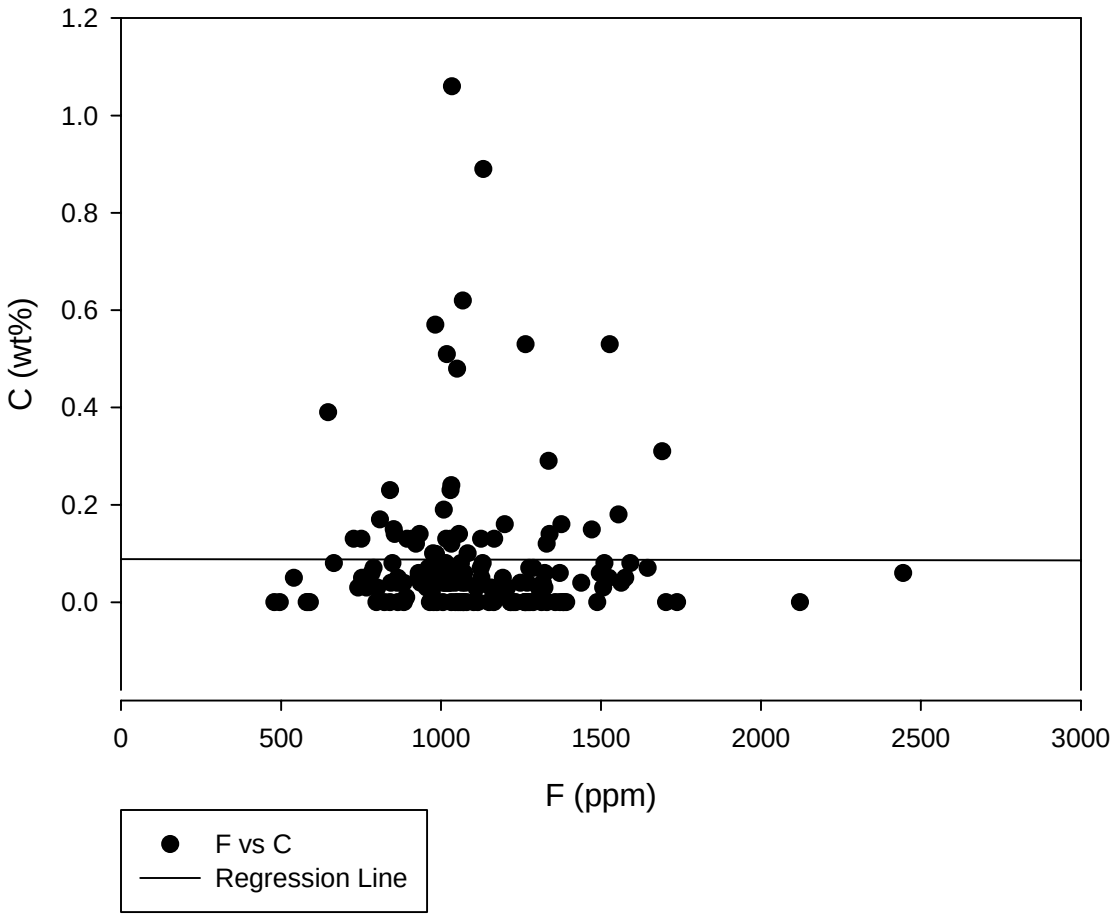
GHN F vs C
1.2
1.0
0.8
0.6
0.4
0.2
0.0
C (wt%)
0
500
1000
1500
2000
2500
3000
F (ppm)
F vs C
Regression Line

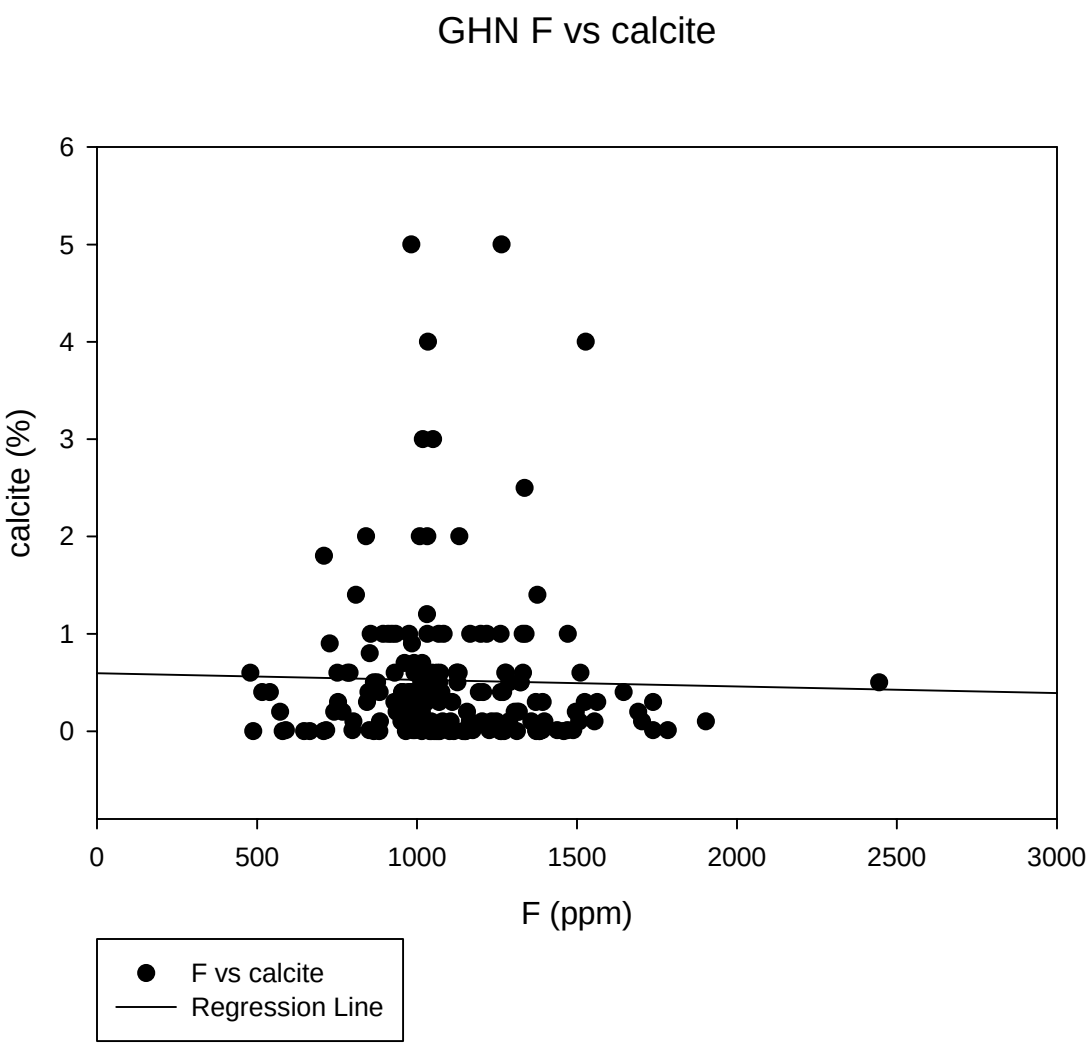
GHN F vs calcite
calcite (%)
6
5
4
3
2
1
0
0
500
1000
1500
2000
2500
3000
F (ppm)
F vs calcite
Regression Line

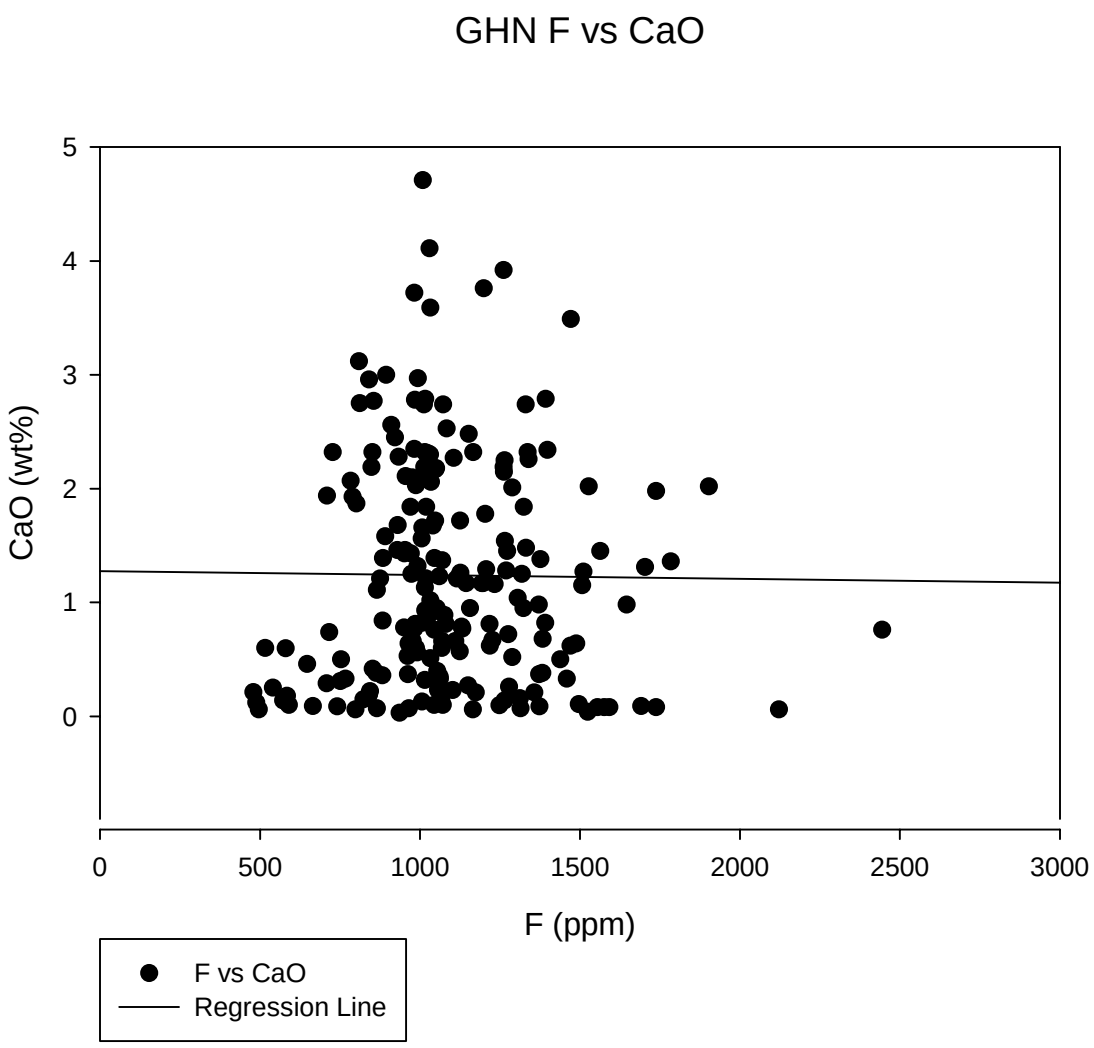
GHN F vs CaO
CaO (wt%)
5
4
3
2
1
0
0
500
1000
1500
2000
2500
3000
F (ppm)
F vs CaO
Regression Line

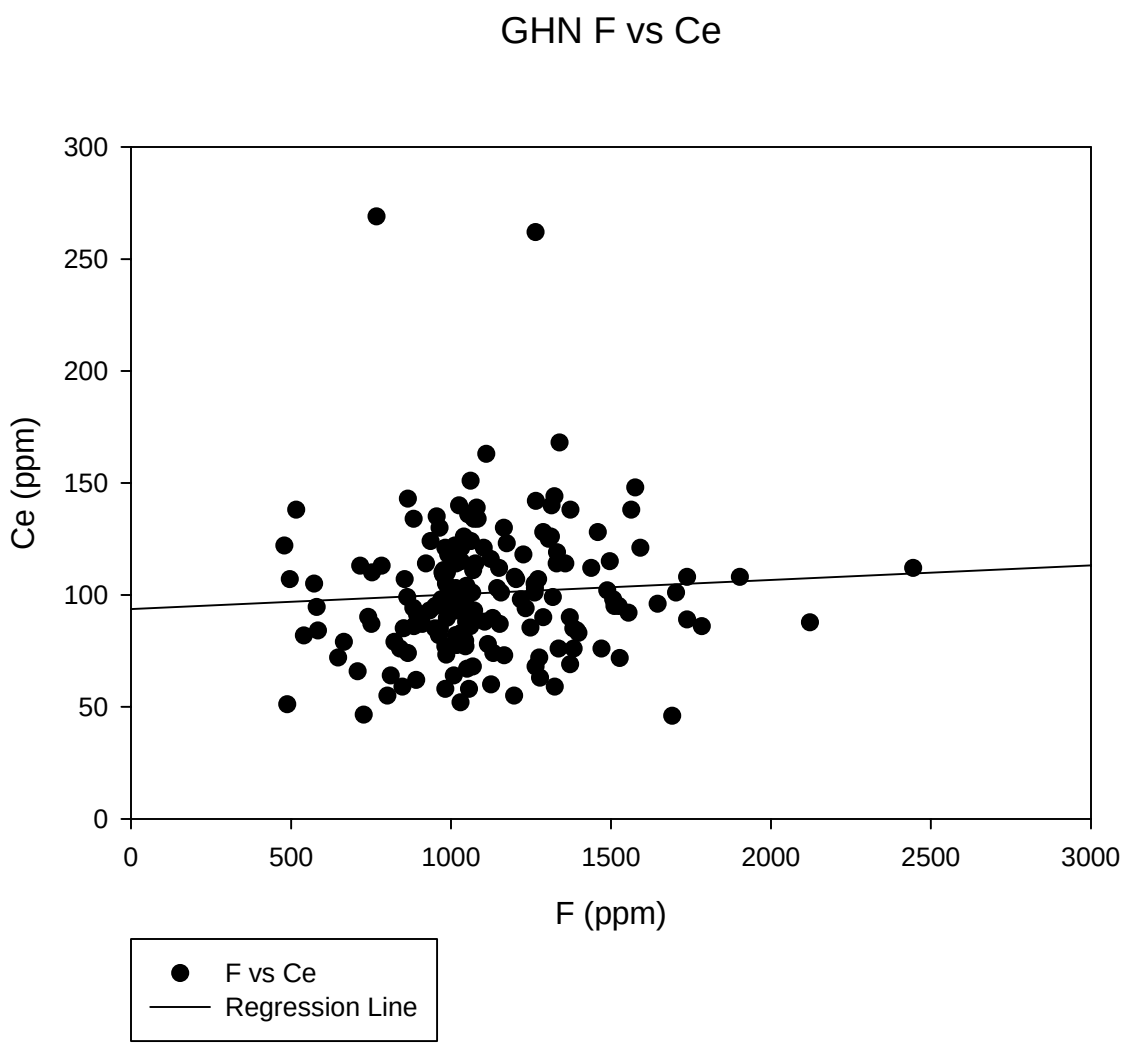
GHN F vs Ce
300
250
200
150
100
50
0
Ce (ppm)
0
500
1000
1500
2000
2500
3000
F (ppm)
F vs Ce
Regression Line

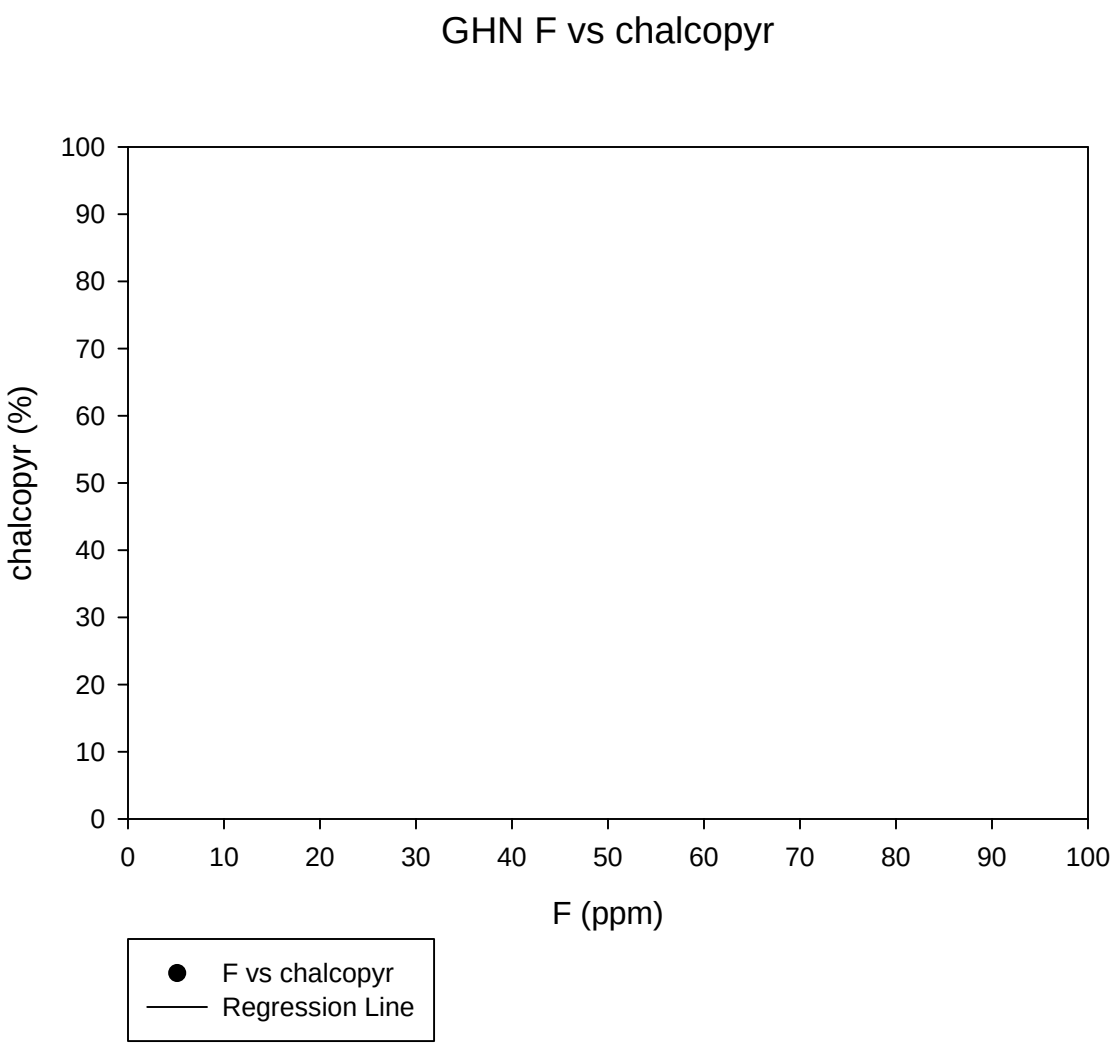
GHN F vs chalcopyr
chalcopyr (%)
100
90
80
70
60
50
40
30
20
10
0
0
10
20
30
40
50
60
70
80
90
100
F (ppm)
F vs chalcopyr
Regression Line

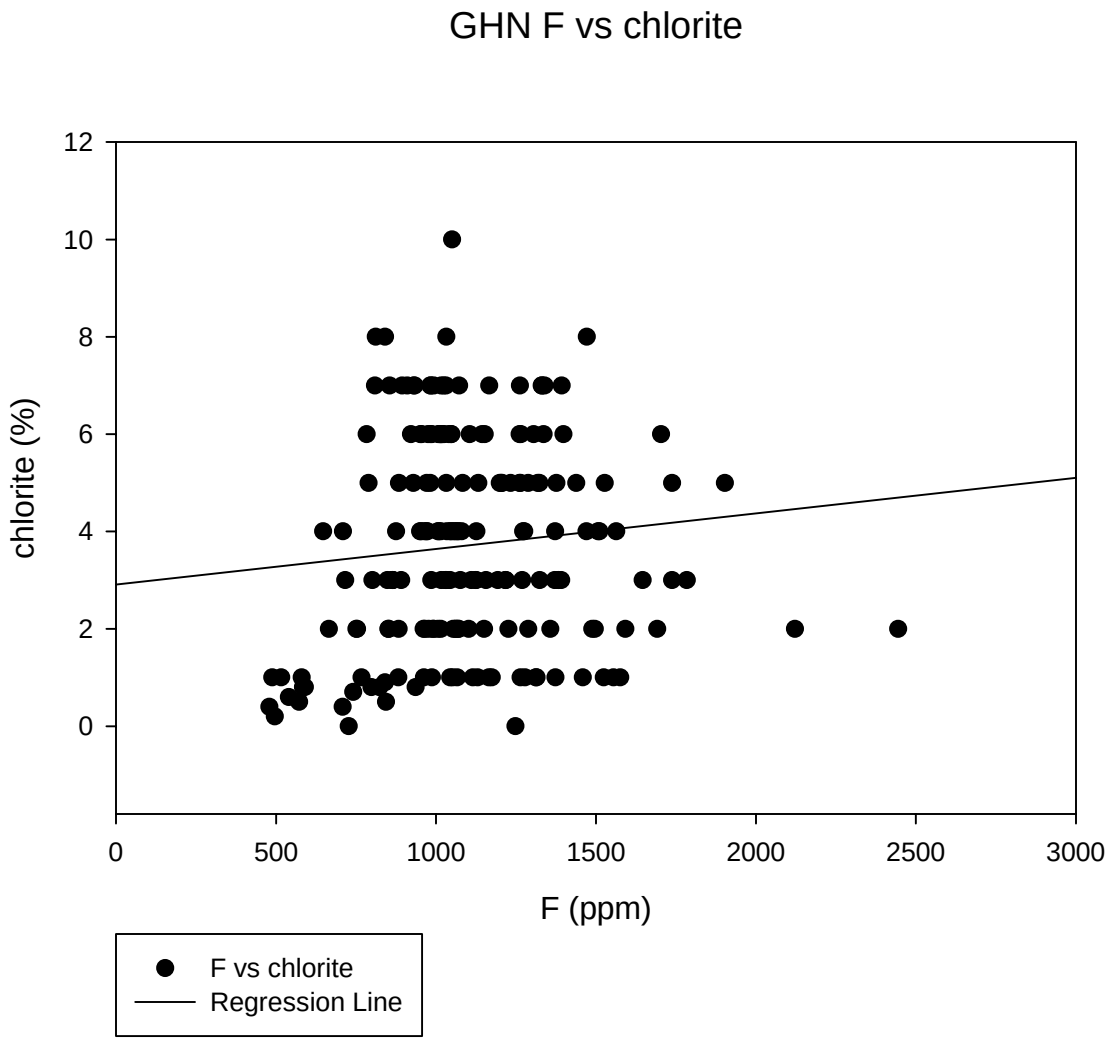
GHN F vs chlorite
chlorite (%)
12
10
8
6
4
2
0
0
500
1000
1500
2000
2500
3000
F (ppm)
F vs chlorite
Regression Line

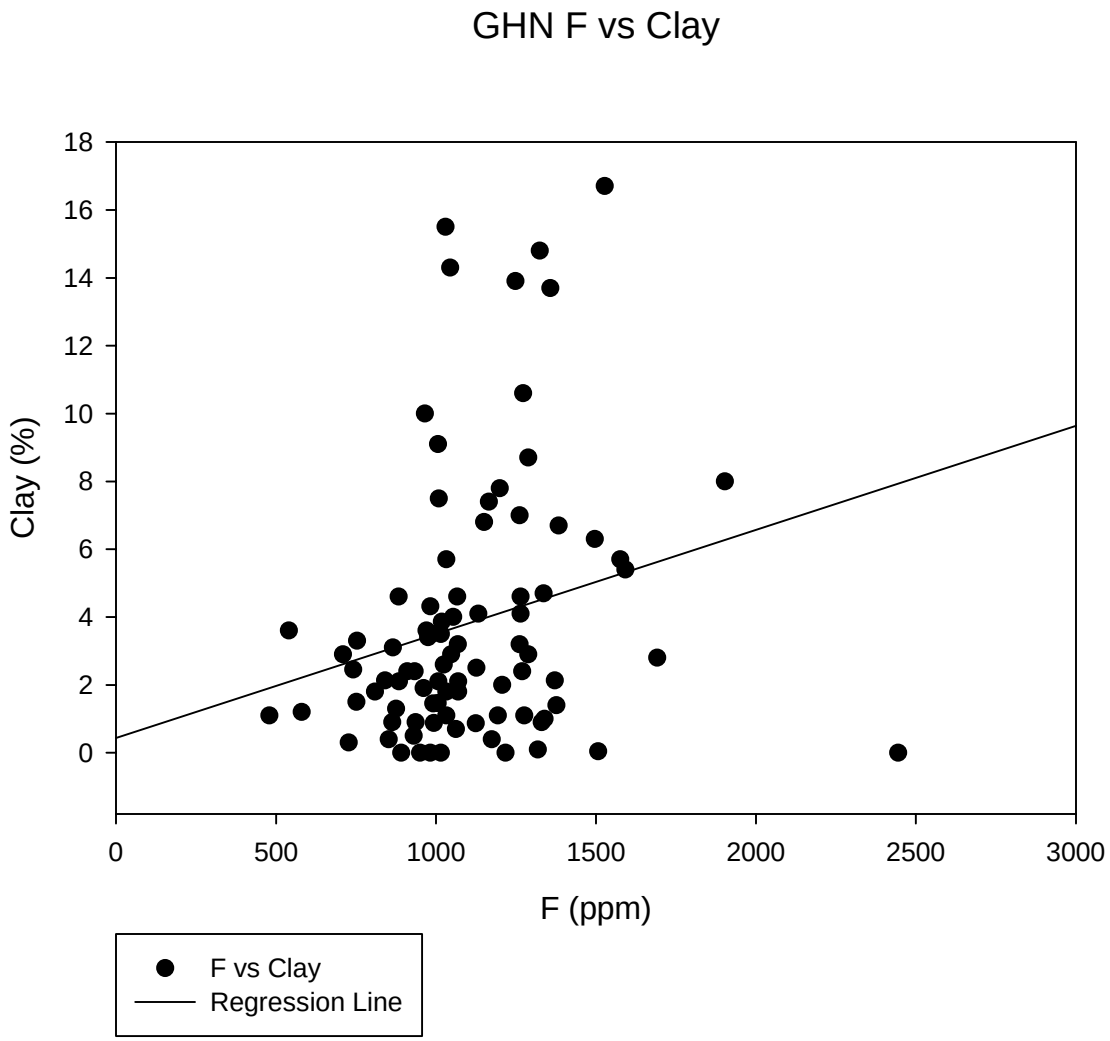
GHN F vs Clay
Clay (%)
18
16
14
12
10
8
6
4
2
0
0
500
1000
1500
2000
2500
3000
F (ppm)
F vs Clay
Regression Line

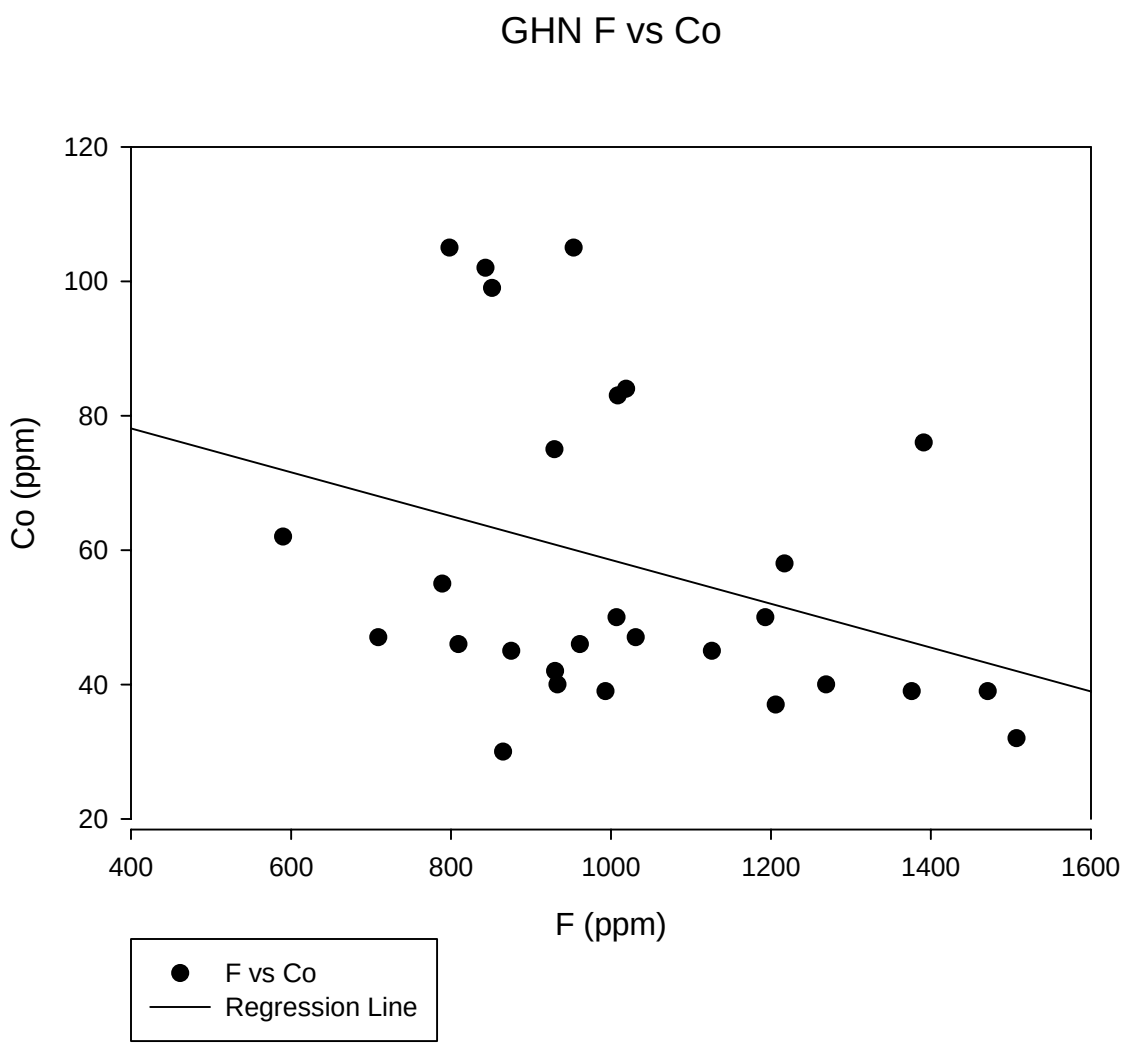
GHN F vs Co
120
100
80
60
40
20
Co (ppm)
400
600
800
1000
1200
1400
1600
F (ppm)
F vs Co
Regression Line

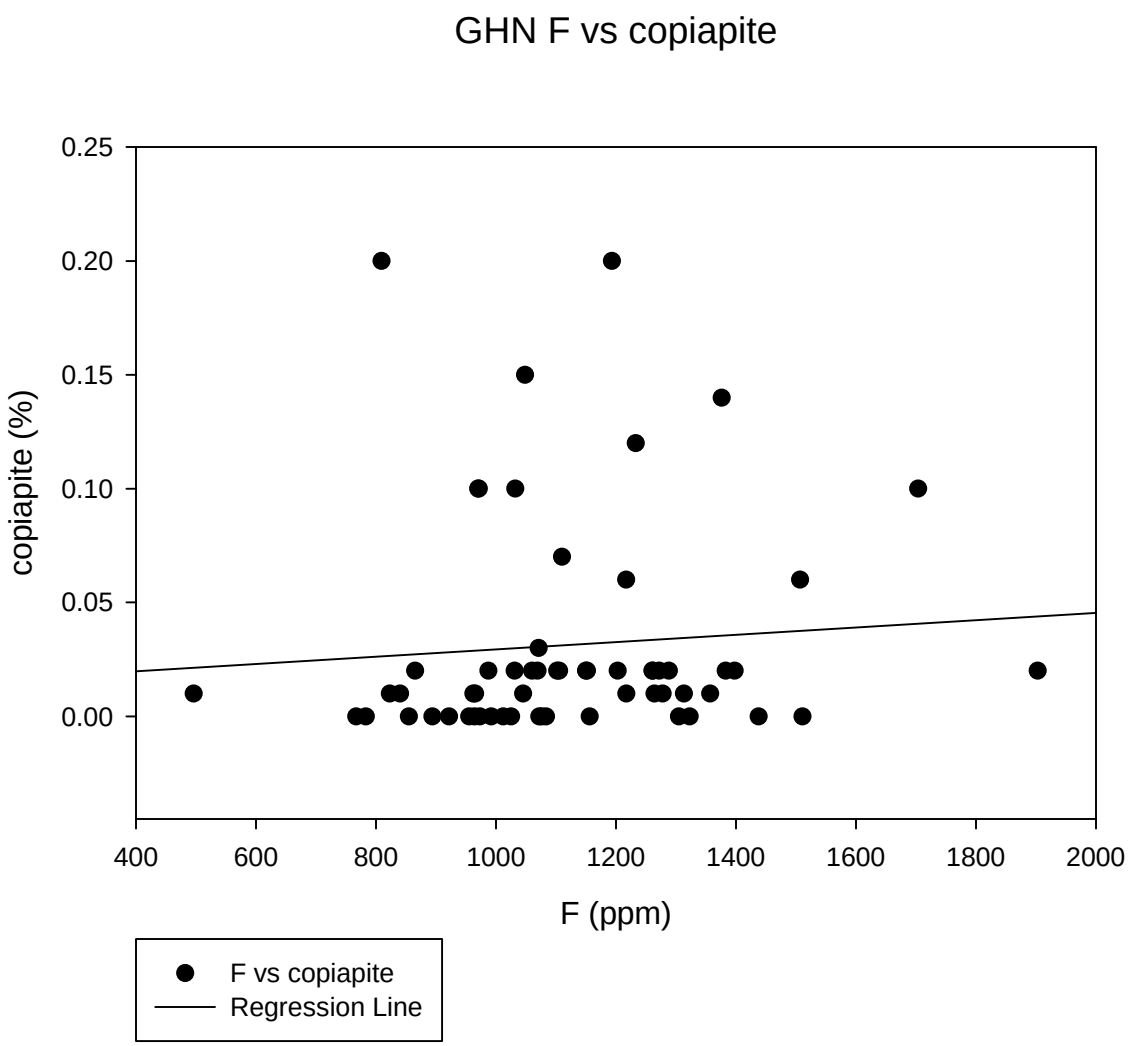
GHN F vs copiapite
0.25
0.20
0.15
0.10
0.05
0.00
copiapite (%)
400
600
800
1000
1200
1400
1600
1800
2000
F (ppm)
F vs copiapite
Regression Line

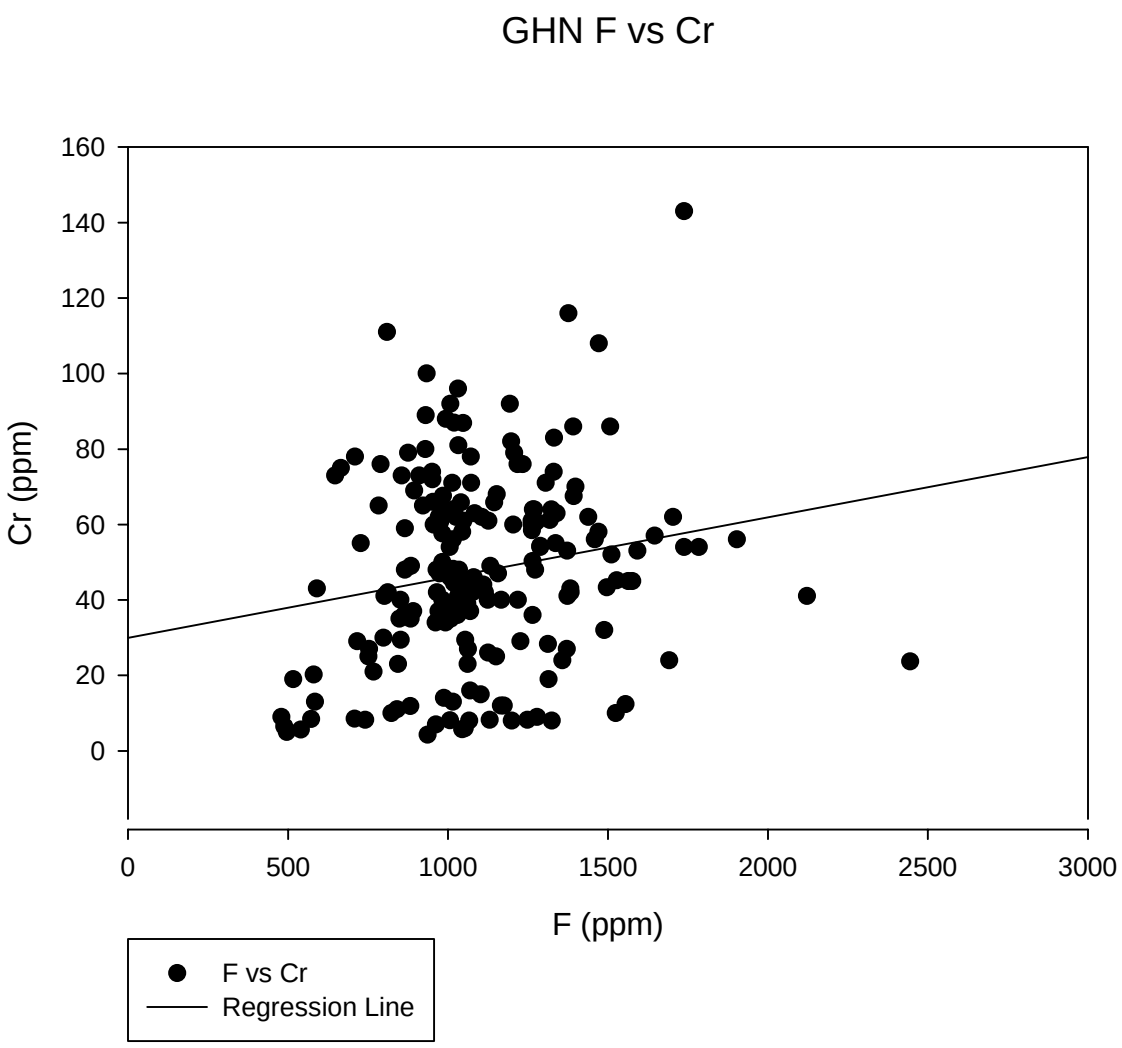
GHN F vs Cr
160
140
120
100
80
60
40
20
0
Cr (ppm)
0
500
1000
1500
2000
2500
3000
F (ppm)
F vs Cr
Regression Line

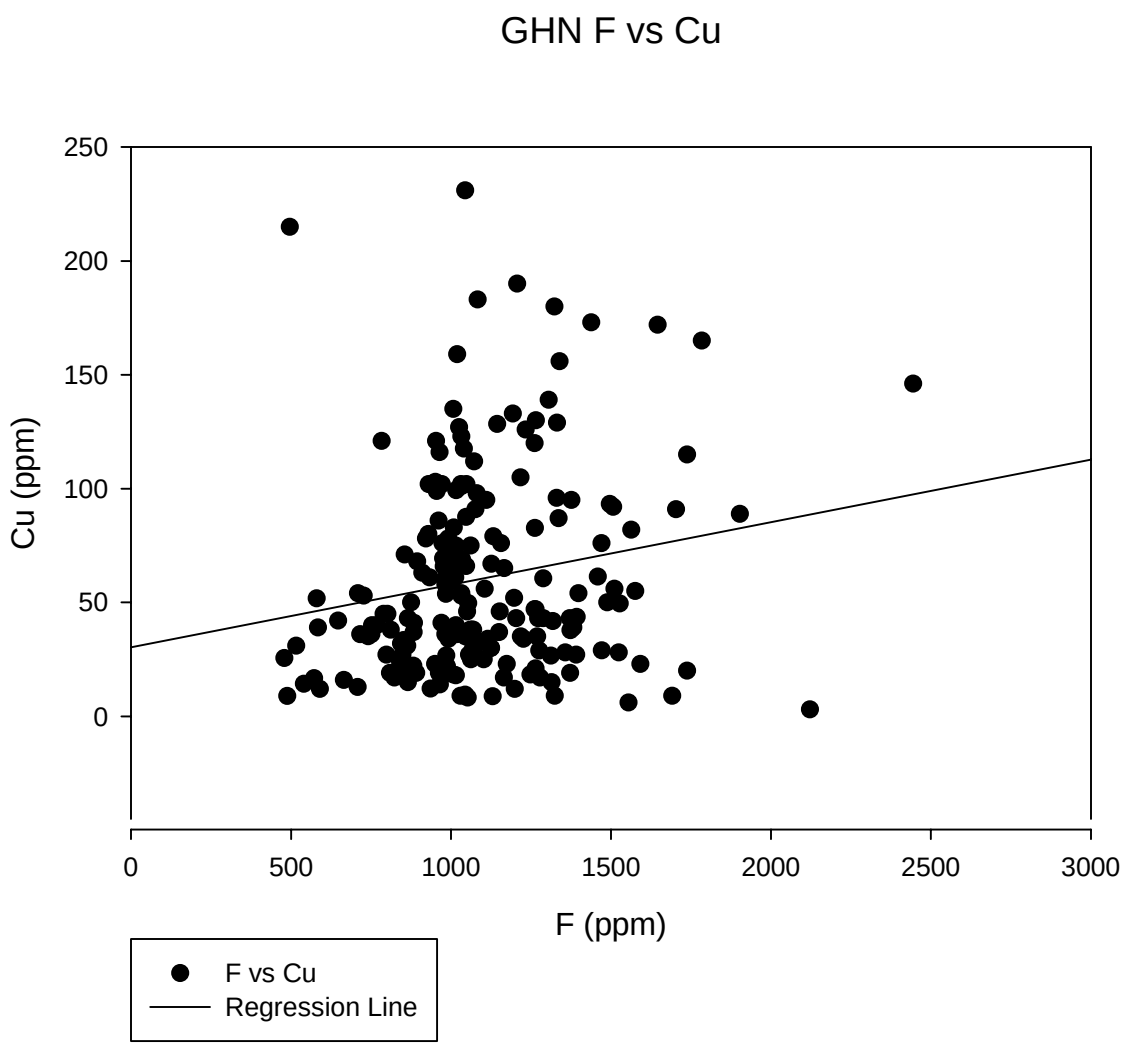
GHN F vs Cu
250
200
150
100
50
0
Cu (ppm)
0
500
1000
1500
2000
2500
3000
F (ppm)
F vs Cu
Regression Line

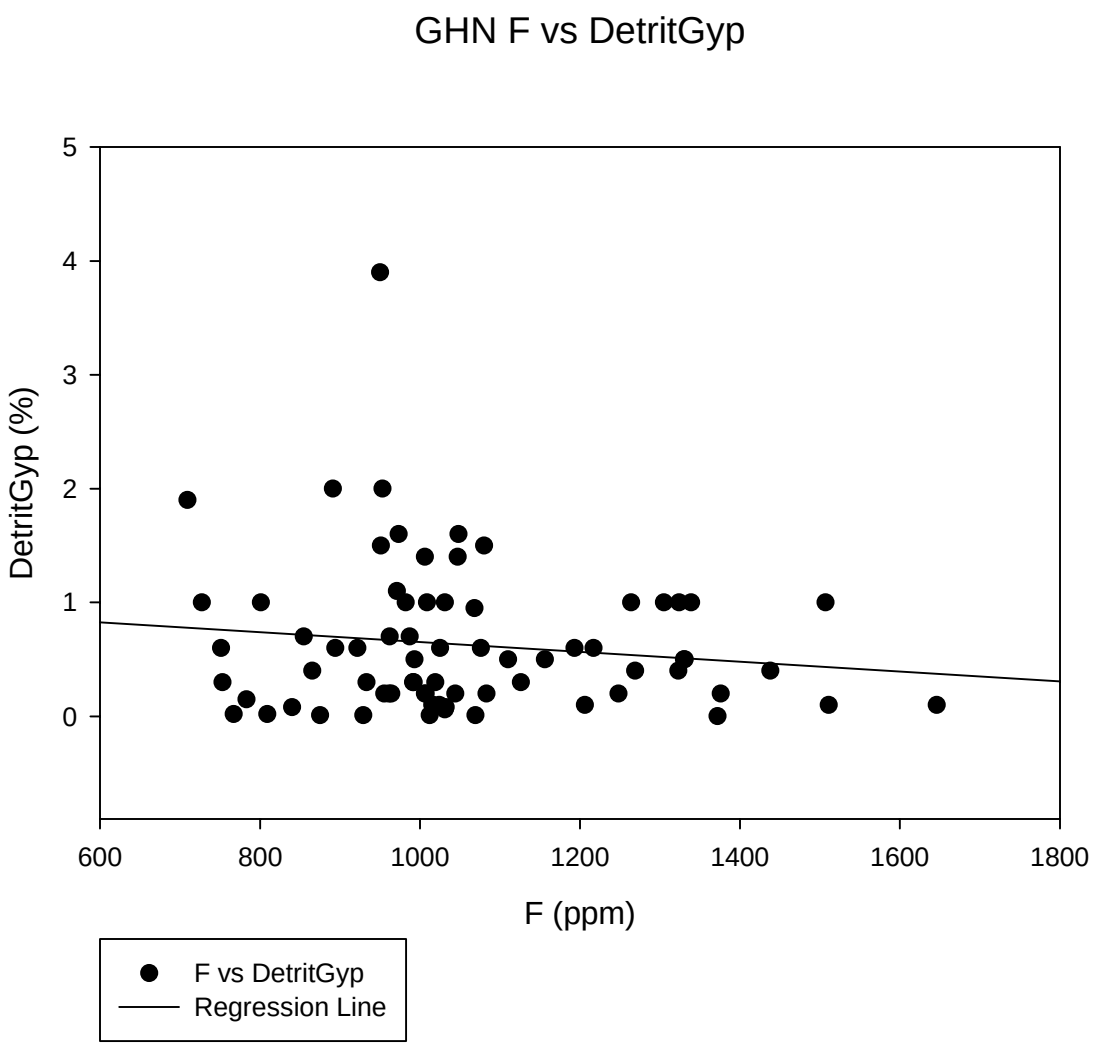
GHN F vs DetritGyp
DetritGyp (%)
5
4
3
2
1
0
600
800
1000
1200
1400
1600
1800
F (ppm)
F vs DetritGyp
Regression Line

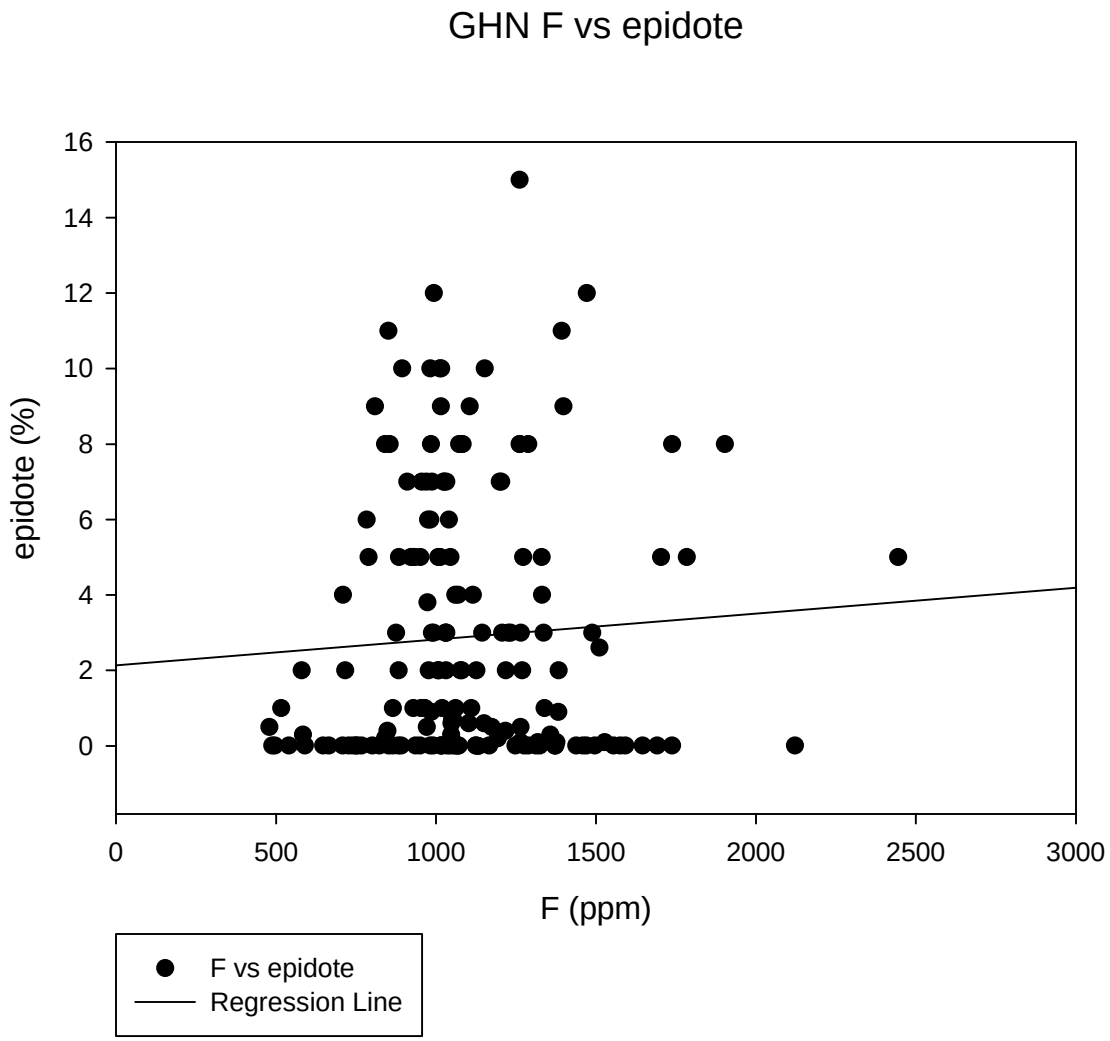
GHN F vs epidote
epidote (%)
16
14
12
10
8
6
4
2
0
0
500
1000
1500
2000
2500
3000
F (ppm)
F vs epidote
Regression Line

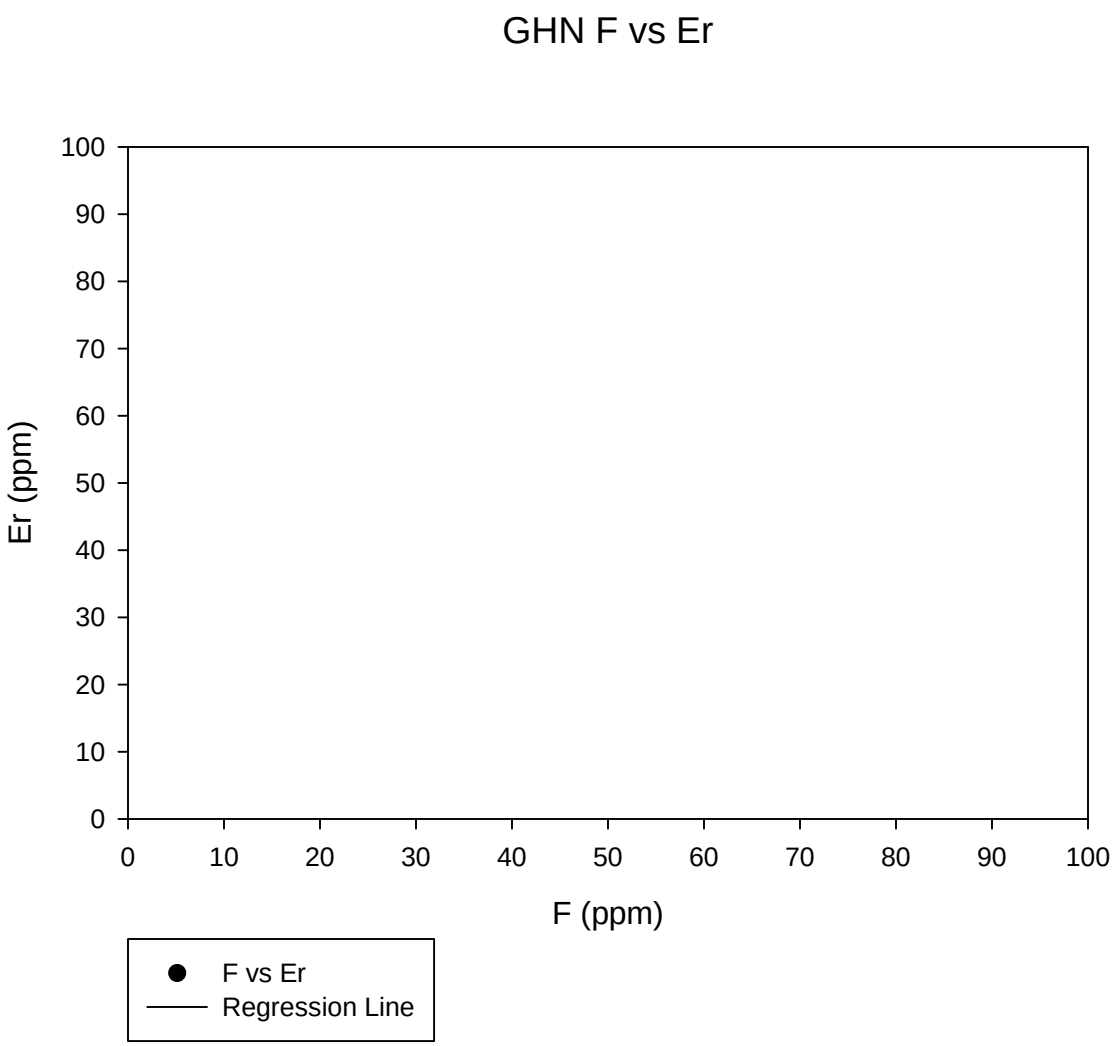
GHN F vs Er
Er (ppm)
F (ppm)
0
10
20
30
40
50
60
70
80
90
100
F vs Er
Regression Line

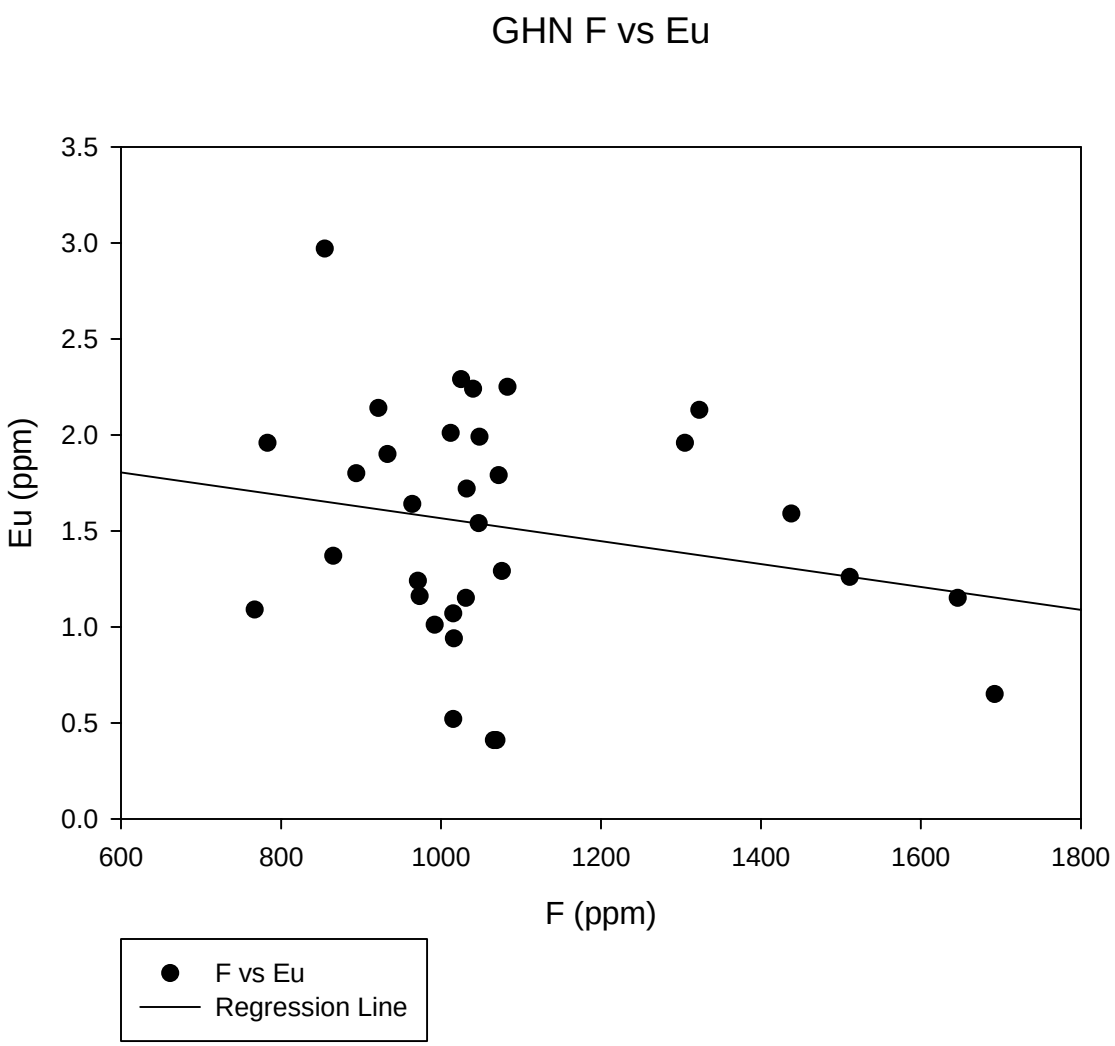
GHN F vs Eu
Eu (ppm)
F (ppm)
3.5
3.0
2.5
2.0
1.5
1.0
0.5
0.0
600
800
1000
1200
1400
1600
1800
F vs Eu
Regression Line

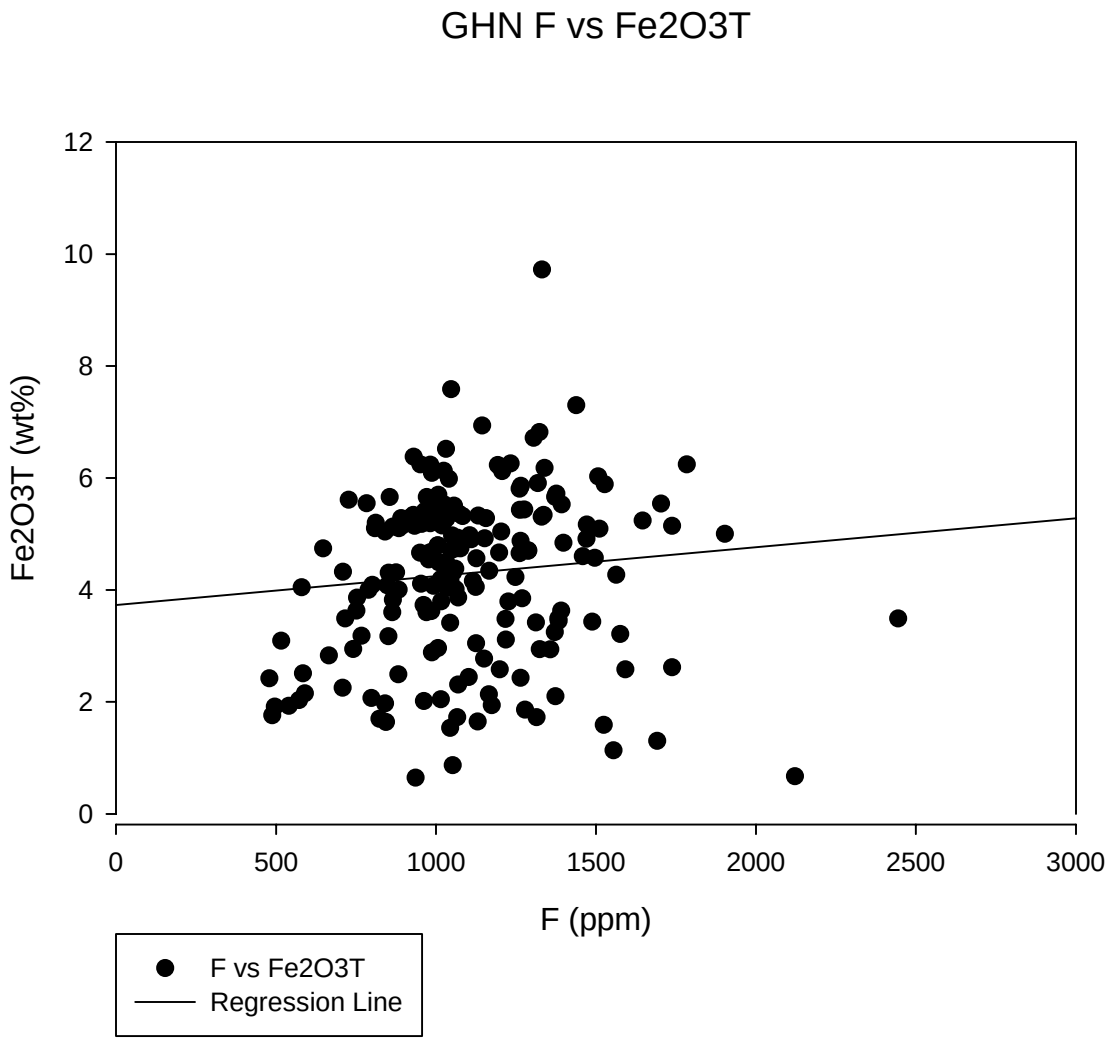
GHN F vs Fe2O3T
Fe2O3T (wt%)
F (ppm)
0
2
4
6
8
10
12
0
500
1000
1500
2000
2500
3000
F vs Fe2O3T
Regression Line

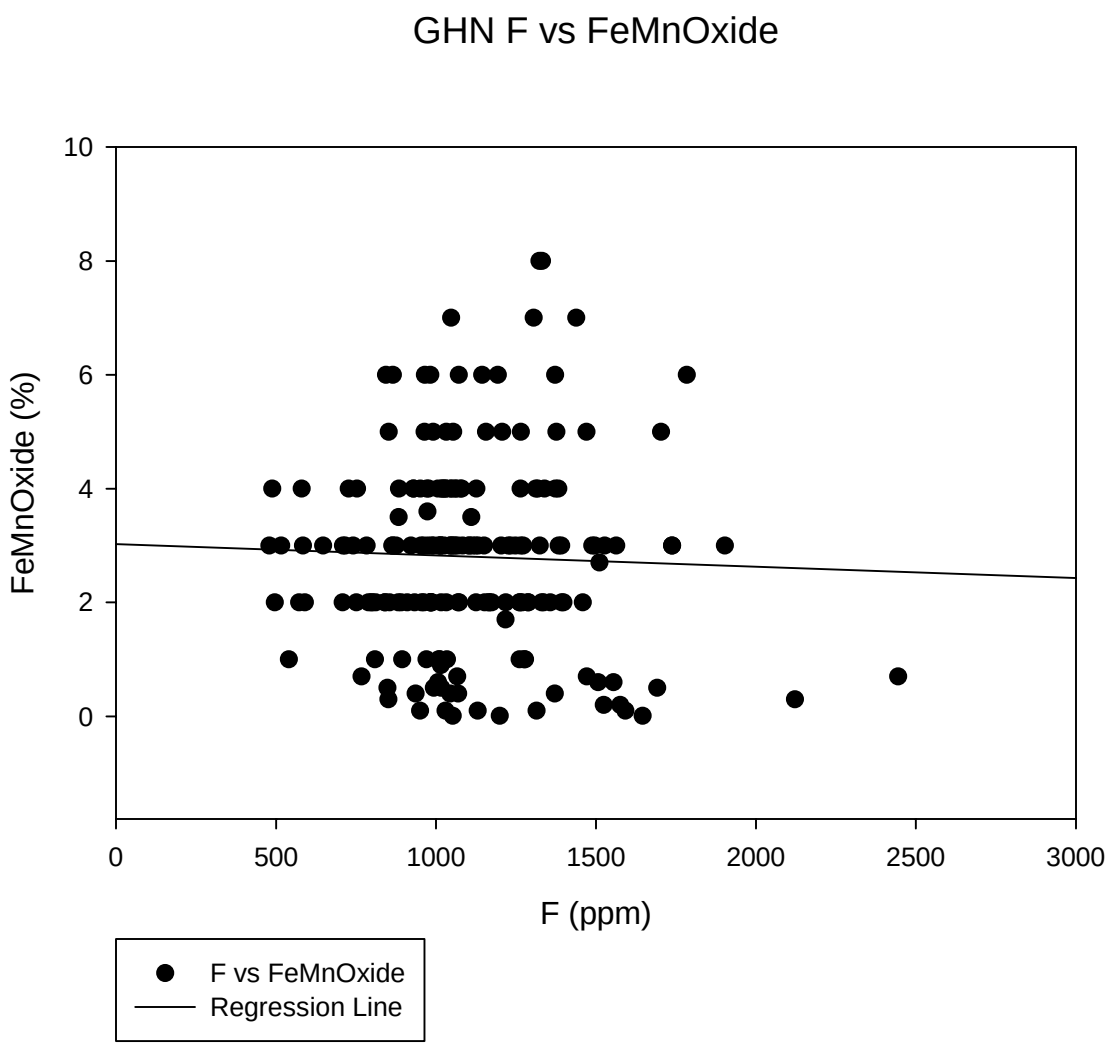
GHN F vs FeMnOxide
FeMnOxide (%)
10
8
6
4
2
0
0
500
1000
1500
2000
2500
3000
F (ppm)
F vs FeMnOxide
Regression Line

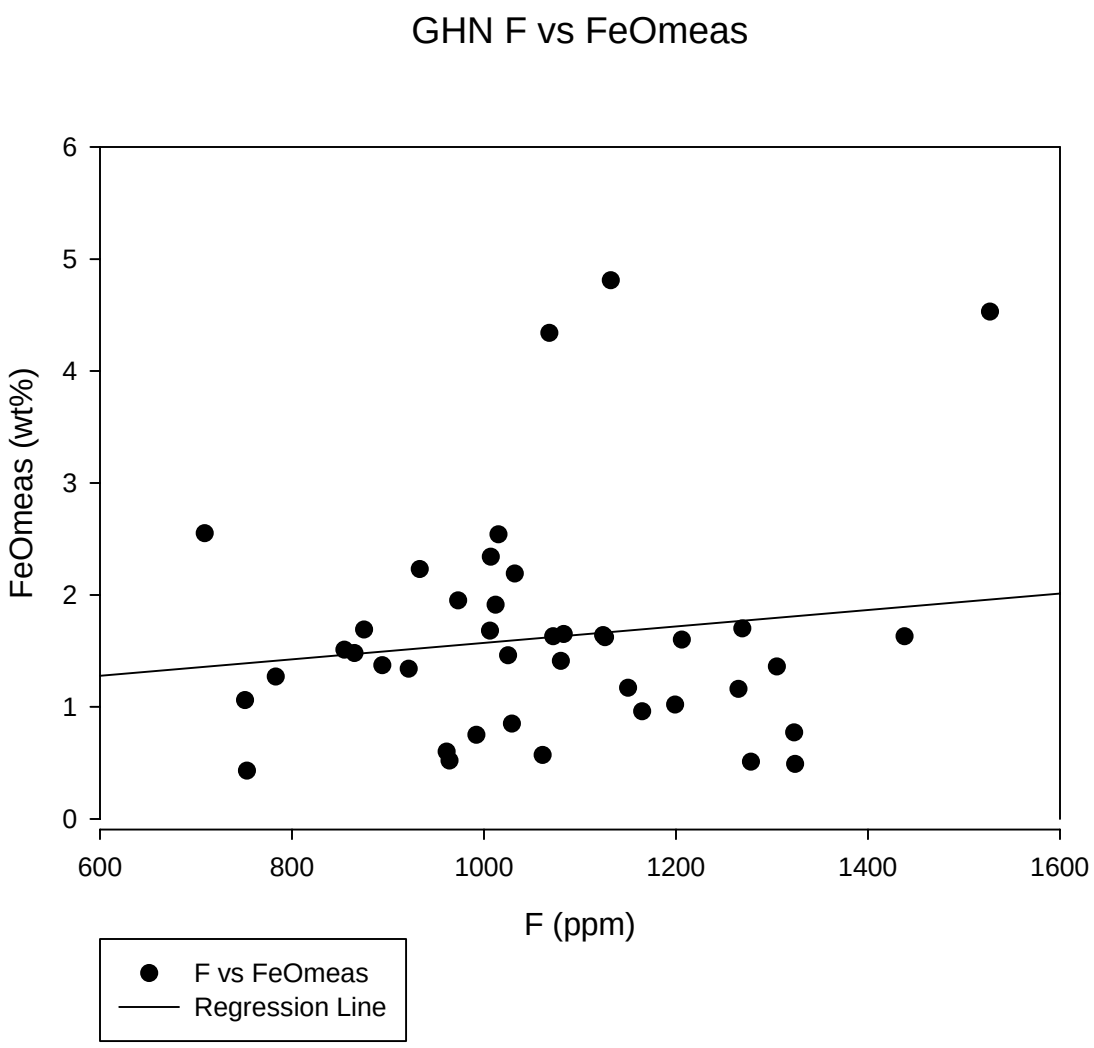
GHN F vs FeOmeas
FeOmeas (wt%)
F (ppm)
0
1
2
3
4
5
6
600
800
1000
1200
1400
1600
F vs FeOmeas
Regression Line

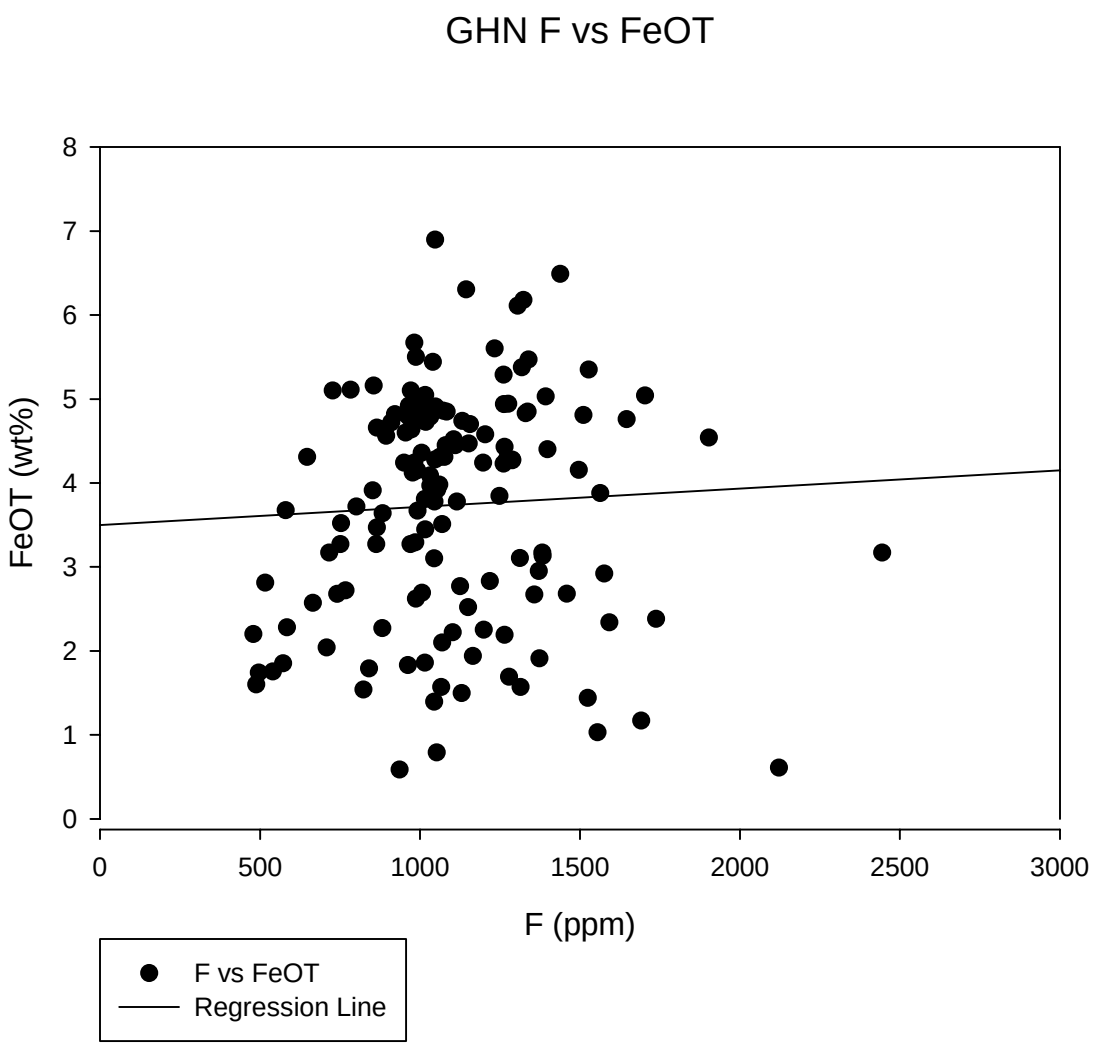
GHN F vs FeOT
FeOT (wt%)
F (ppm)
0
1
2
3
4
5
6
7
8
0
500
1000
1500
2000
2500
3000
F vs FeOT
Regression Line

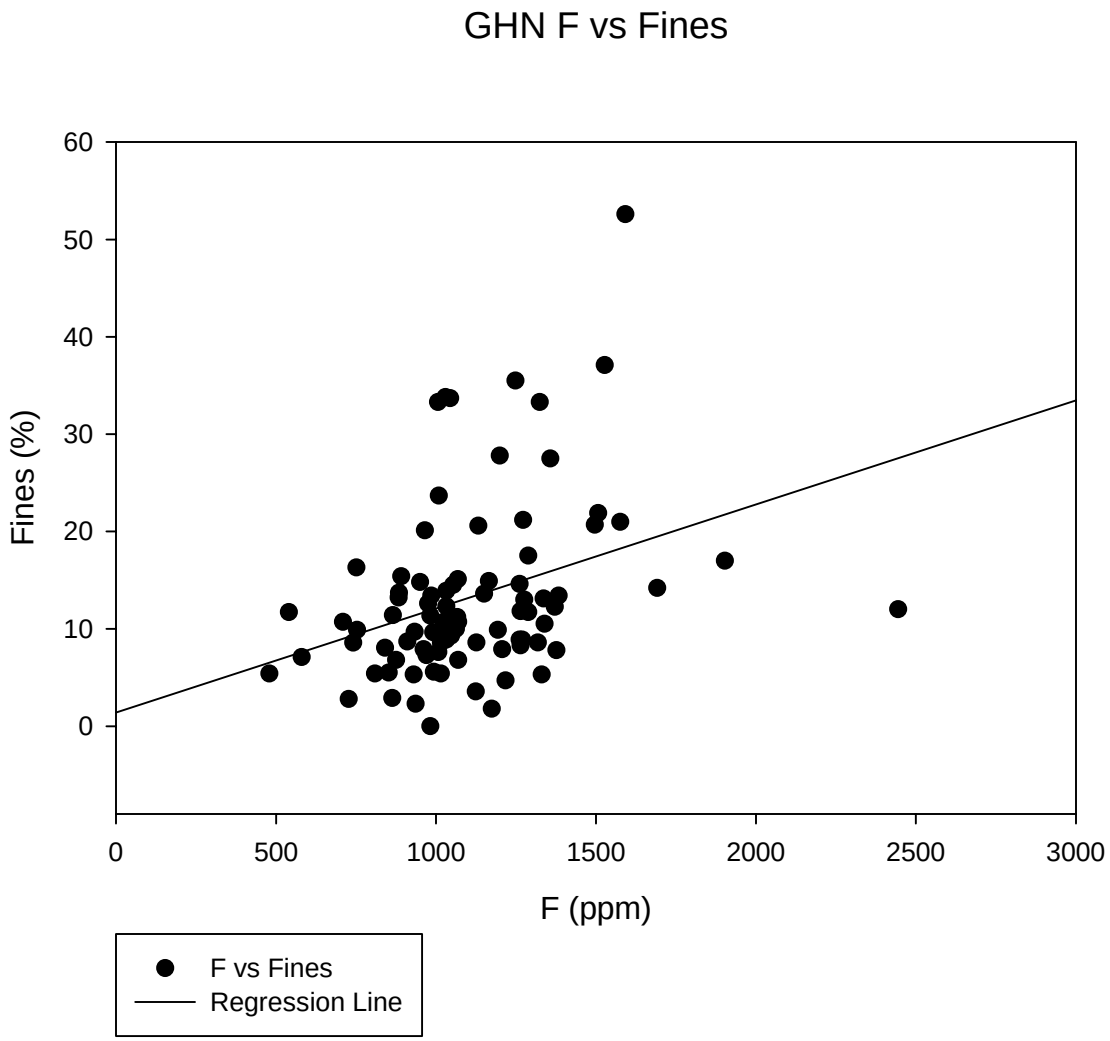
GHN F vs Fines
Fines (%)
60
50
40
30
20
10
0
0
500
1000
1500
2000
2500
3000
F (ppm)
F vs Fines
Regression Line

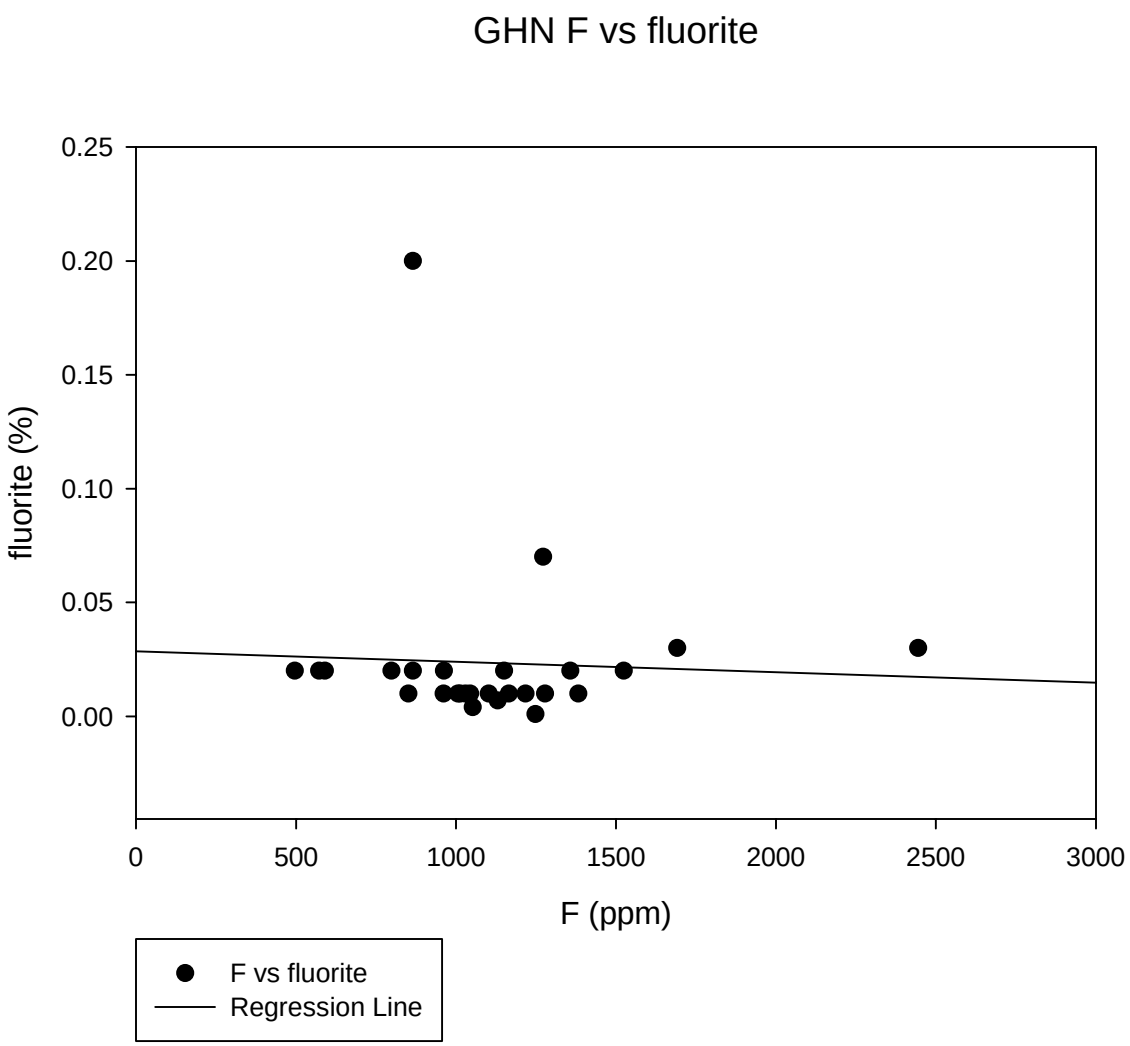
GHN F vs fluorite
0.25
0.20
0.15
0.10
0.05
0.00
fluorite (%)
0
500
1000
1500
2000
2500
3000
F (ppm)
F vs fluorite
Regression Line

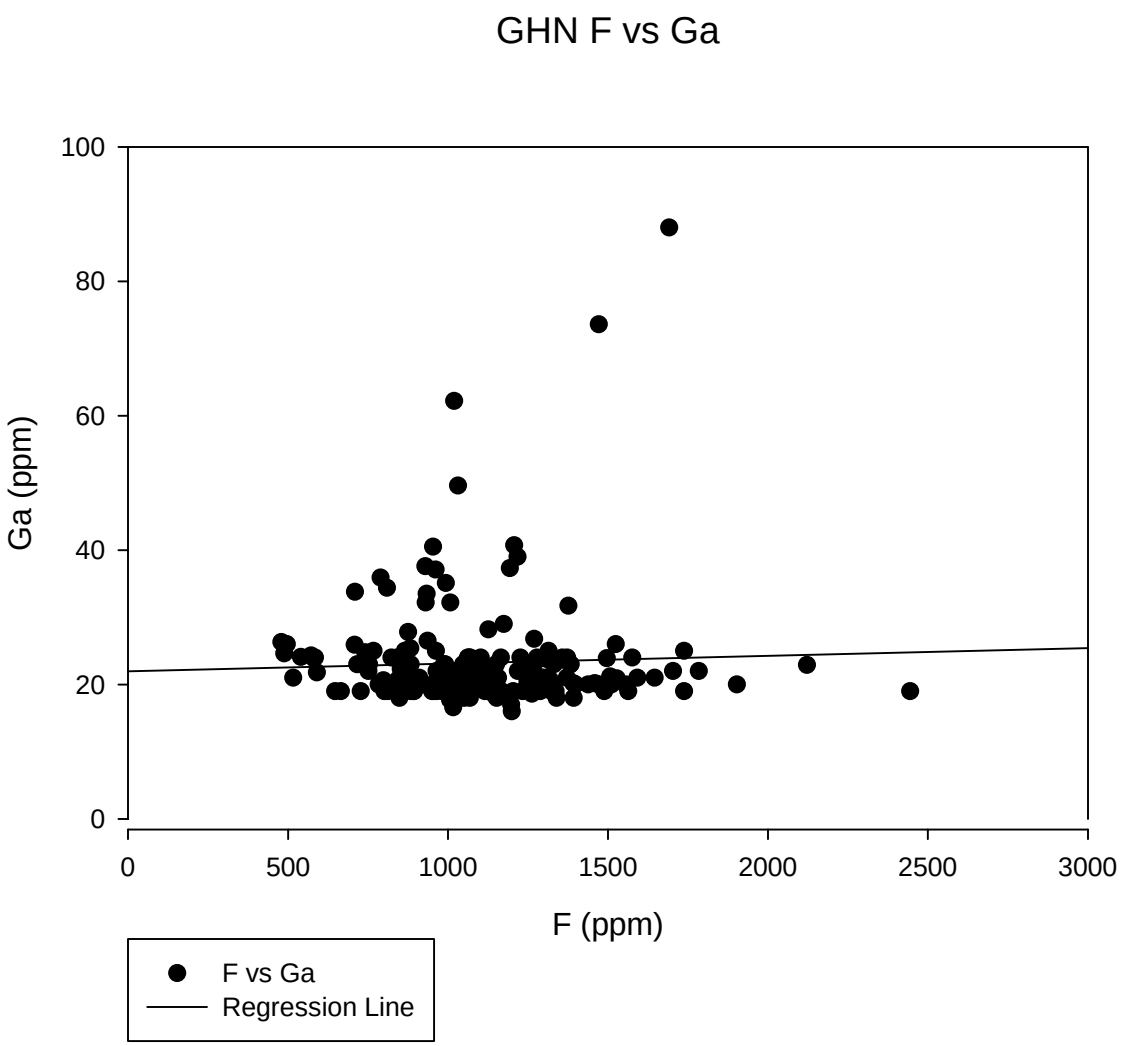
GHN F vs Ga
100
80
60
40
20
0
Ga (ppm)
0
500
1000
1500
2000
2500
3000
F (ppm)
F vs Ga
Regression Line

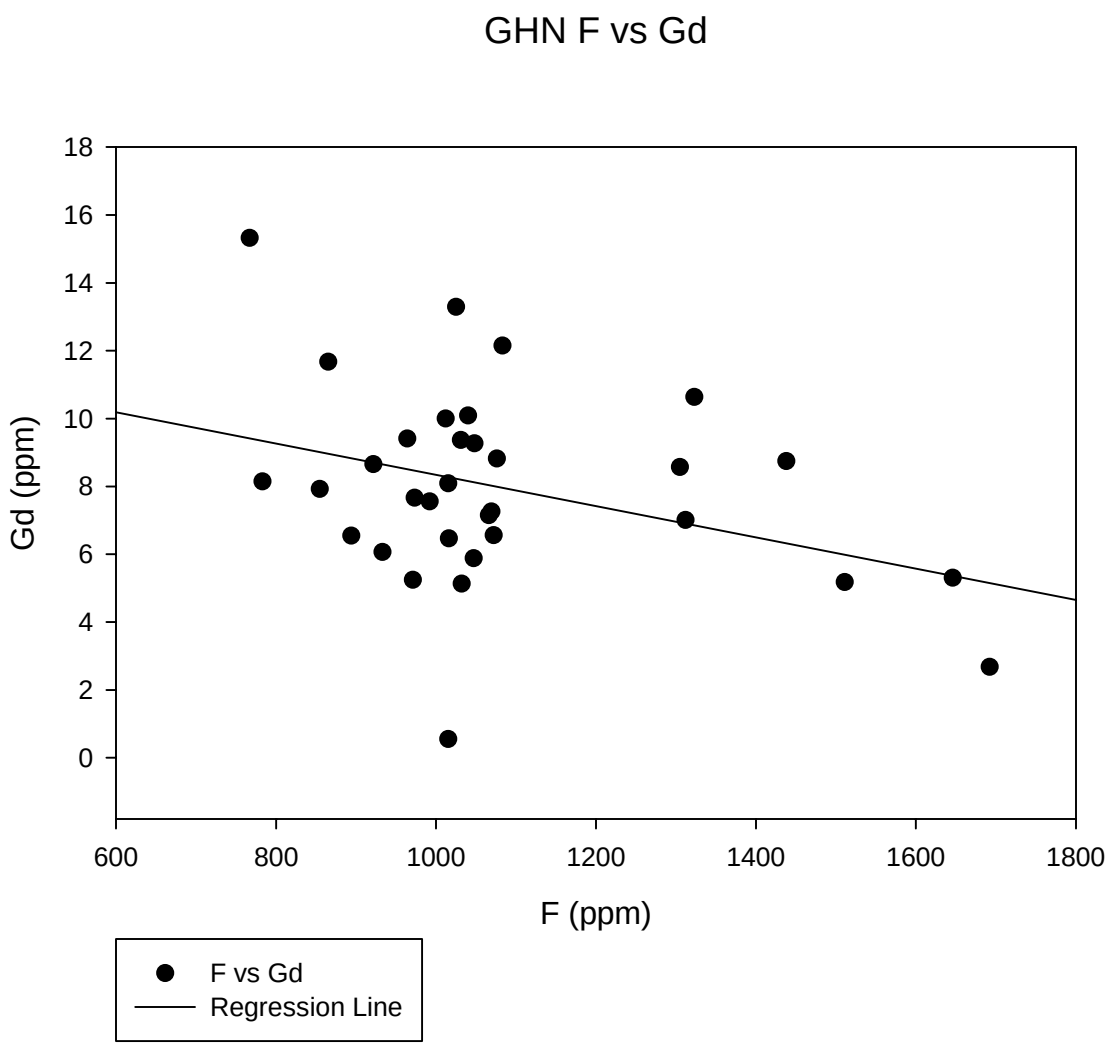
GHN F vs Gd
Gd (ppm)
F (ppm)
18
16
14
12
10
8
6
4
2
0
600
800
1000
1200
1400
1600
1800
F vs Gd
Regression Line

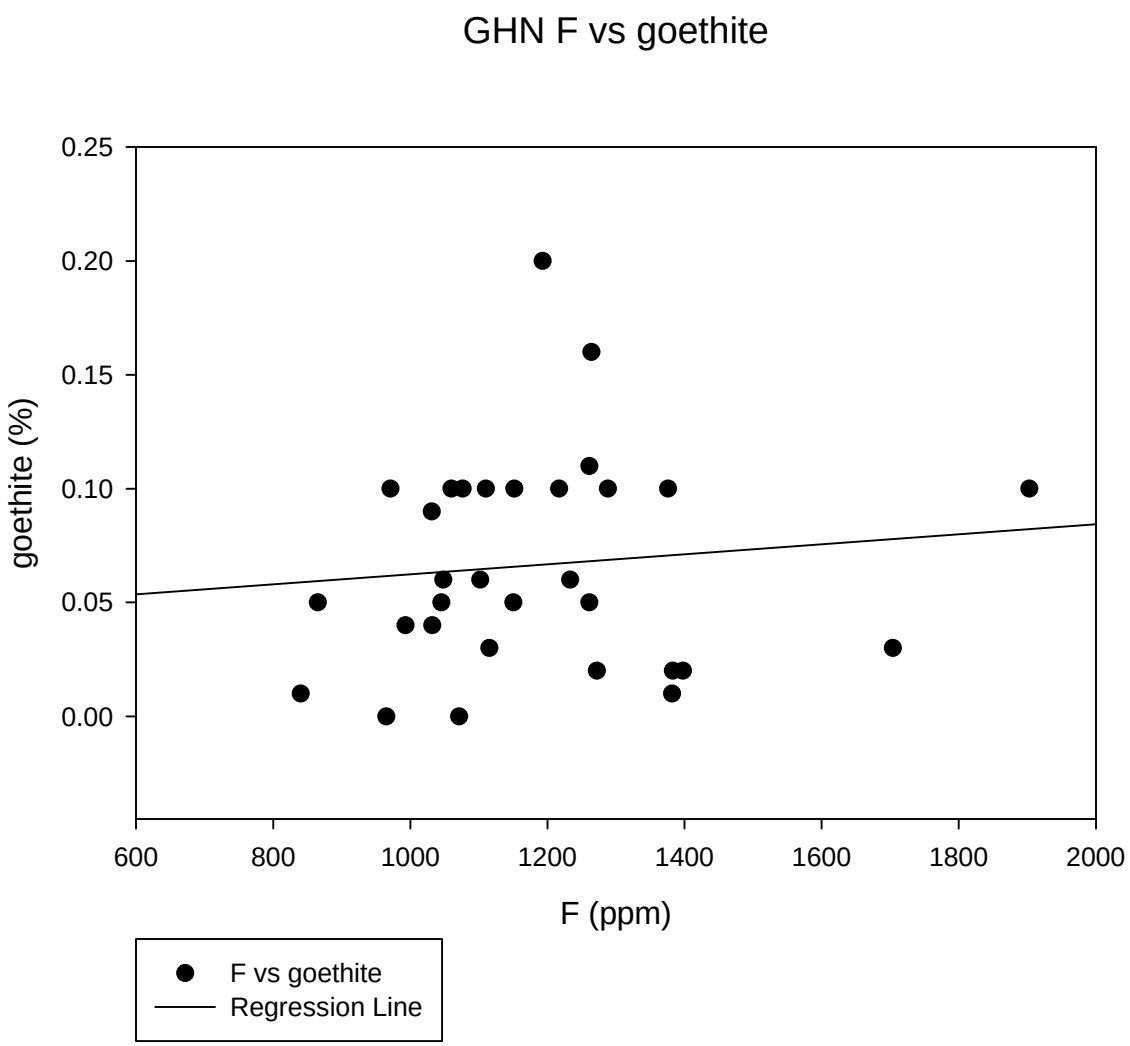
GHN F vs goethite
0.25
0.20
0.15
0.10
0.05
0.00
goethite (%)
600
800
1000
1200
1400
1600
1800
2000
F (ppm)
F vs goethite
Regression Line

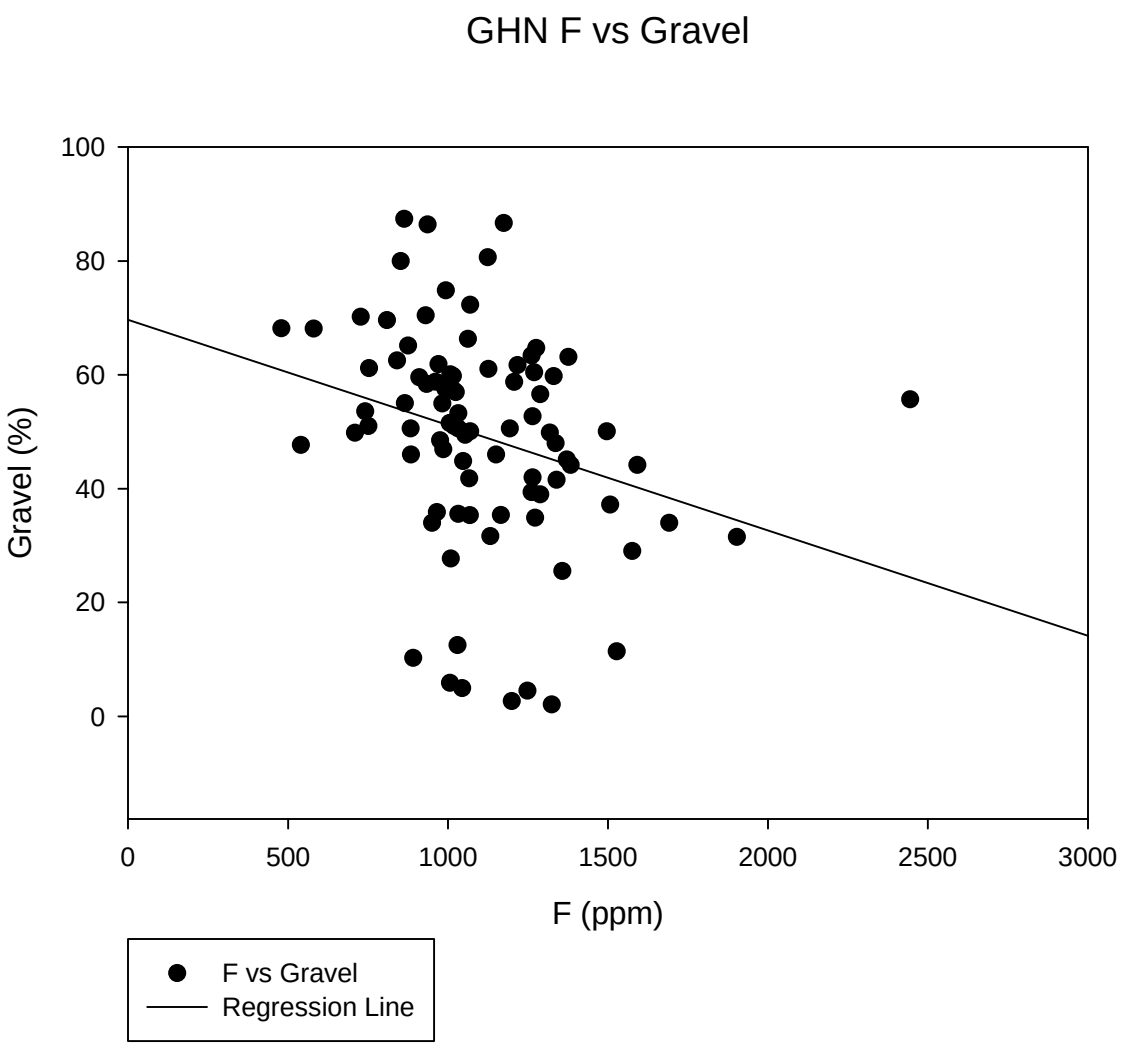
GHN F vs Gravel
Gravel (%)
100
80
60
40
20
0
0
500
1000
1500
2000
2500
3000
F (ppm)
F vs Gravel
Regression Line

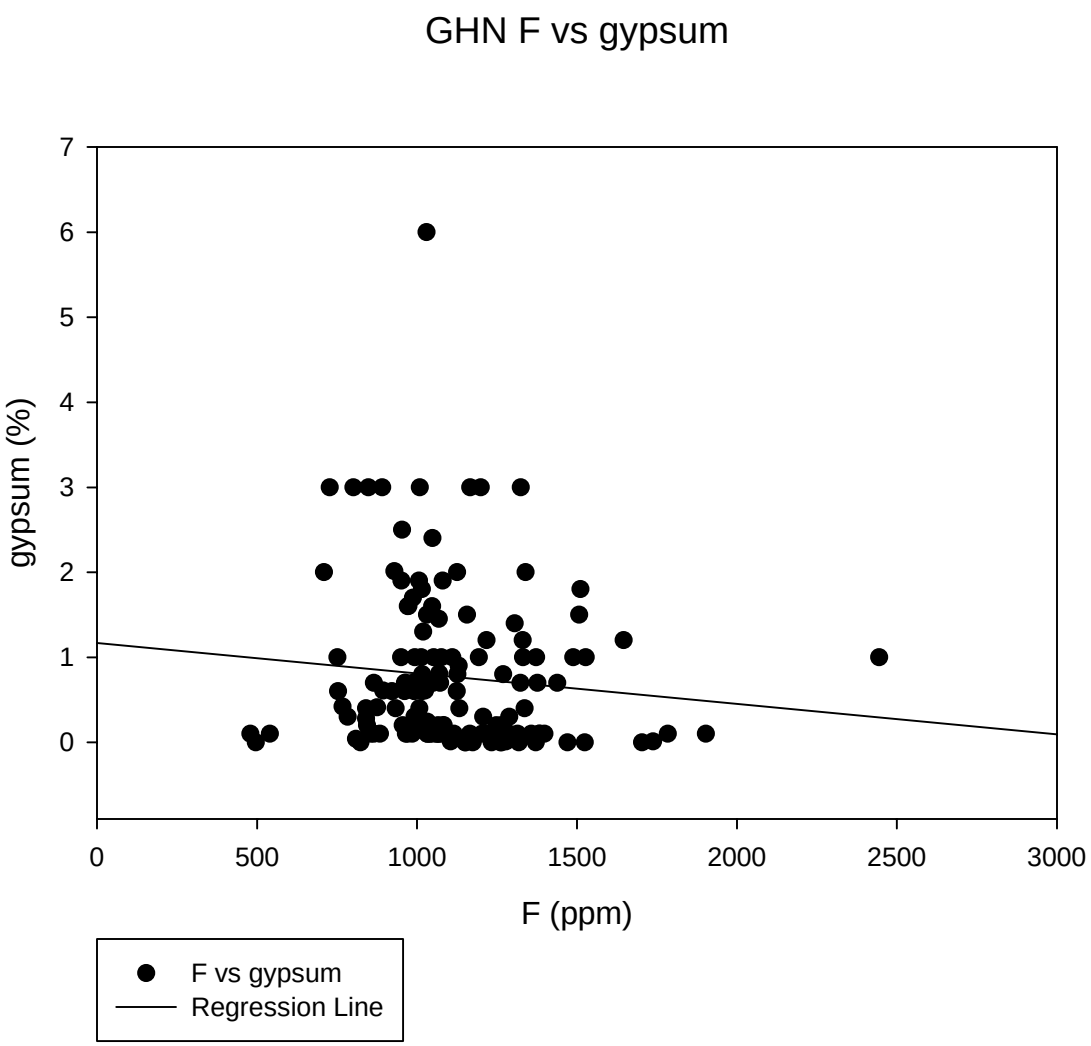
GHN F vs gypsum
gypsum (%)
7
6
5
4
3
2
1
0
0
500
1000
1500
2000
2500
3000
F (ppm)
F vs gypsum
Regression Line

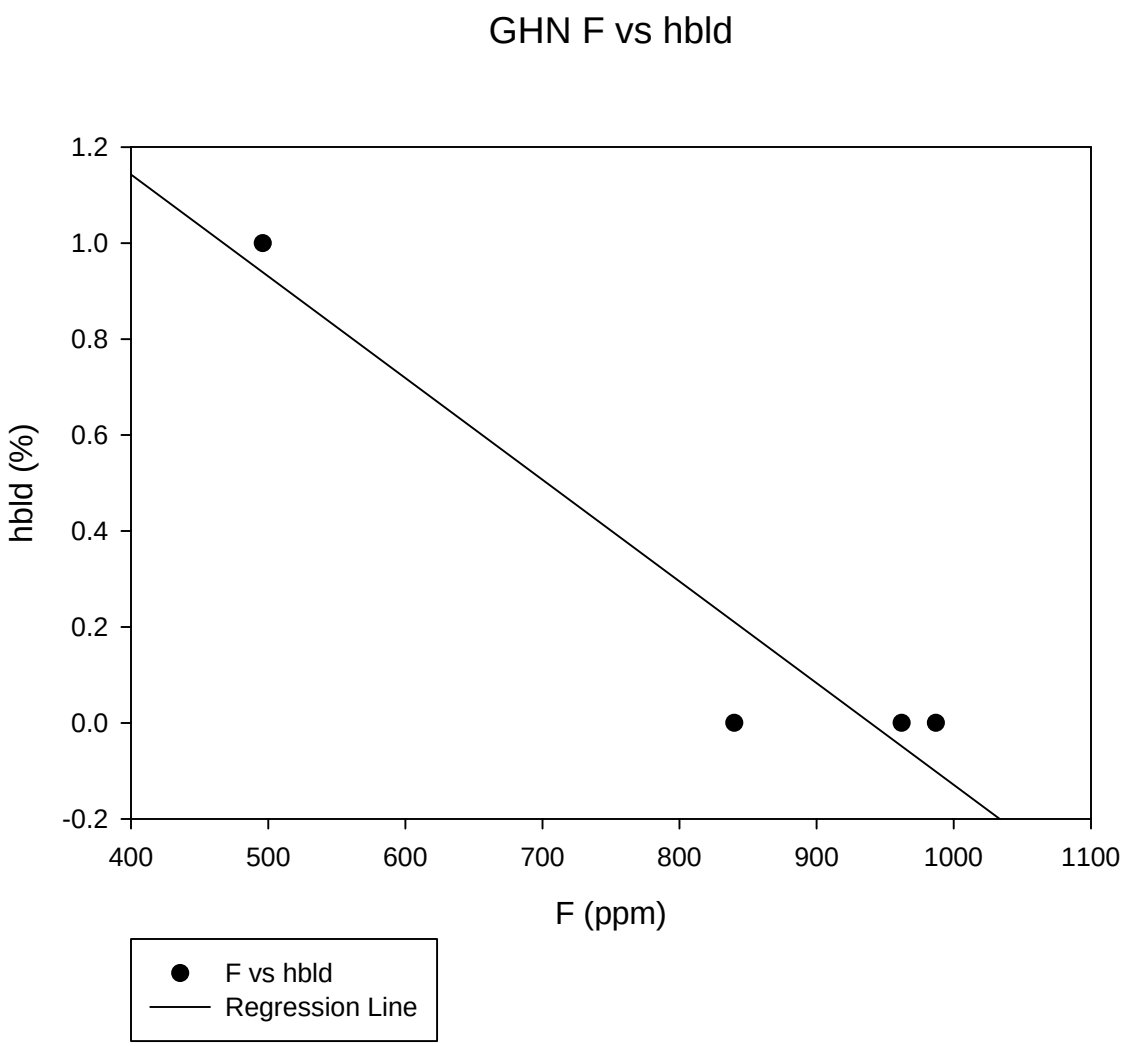
GHN F vs hbld
1.2
1.0
0.8
0.6
0.4
0.2
0.0
-0.2
hbld (%)
400
500
600
700
800
900
1000
1100
F (ppm)
F vs hbld
Regression Line

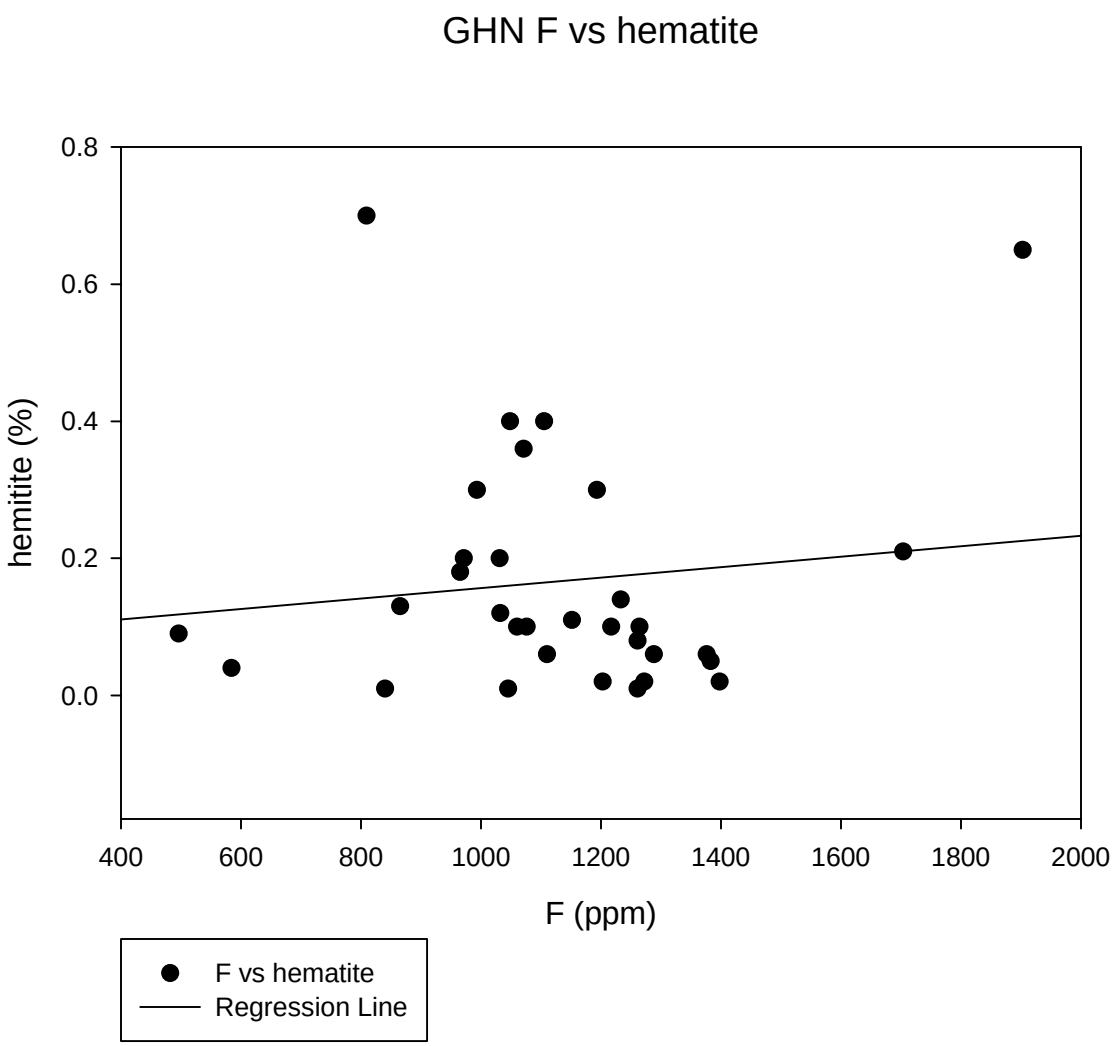
GHN F vs hematite
0.8
0.6
0.4
0.2
0.0
hemitite (%)
400
600
800
1000
1200
1400
1600
1800
2000
F (ppm)
F vs hematite
Regression Line

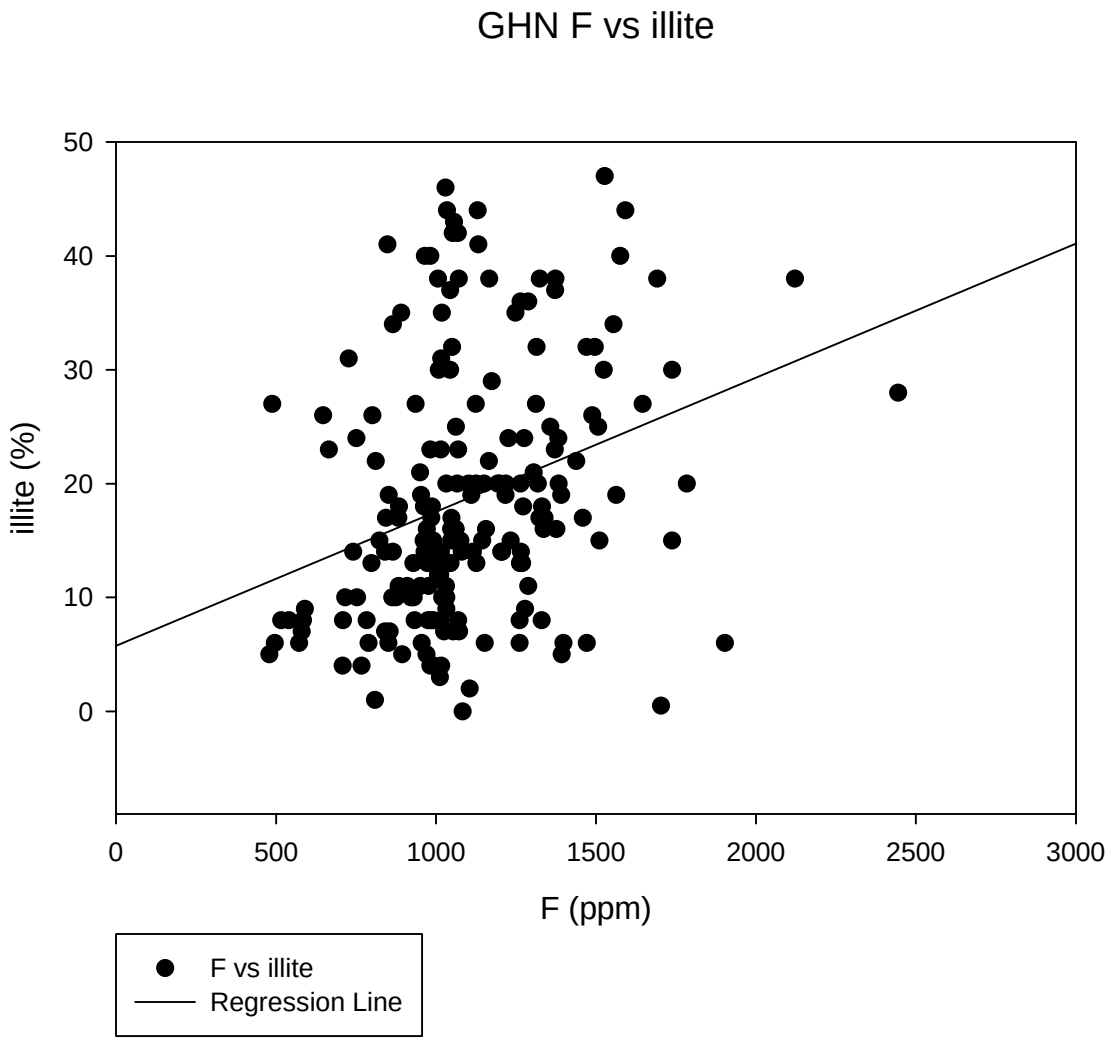
GHN F vs illite
illite (%)
50
40
30
20
10
0
0
500
1000
1500
2000
2500
3000
F (ppm)
F vs illite
Regression Line

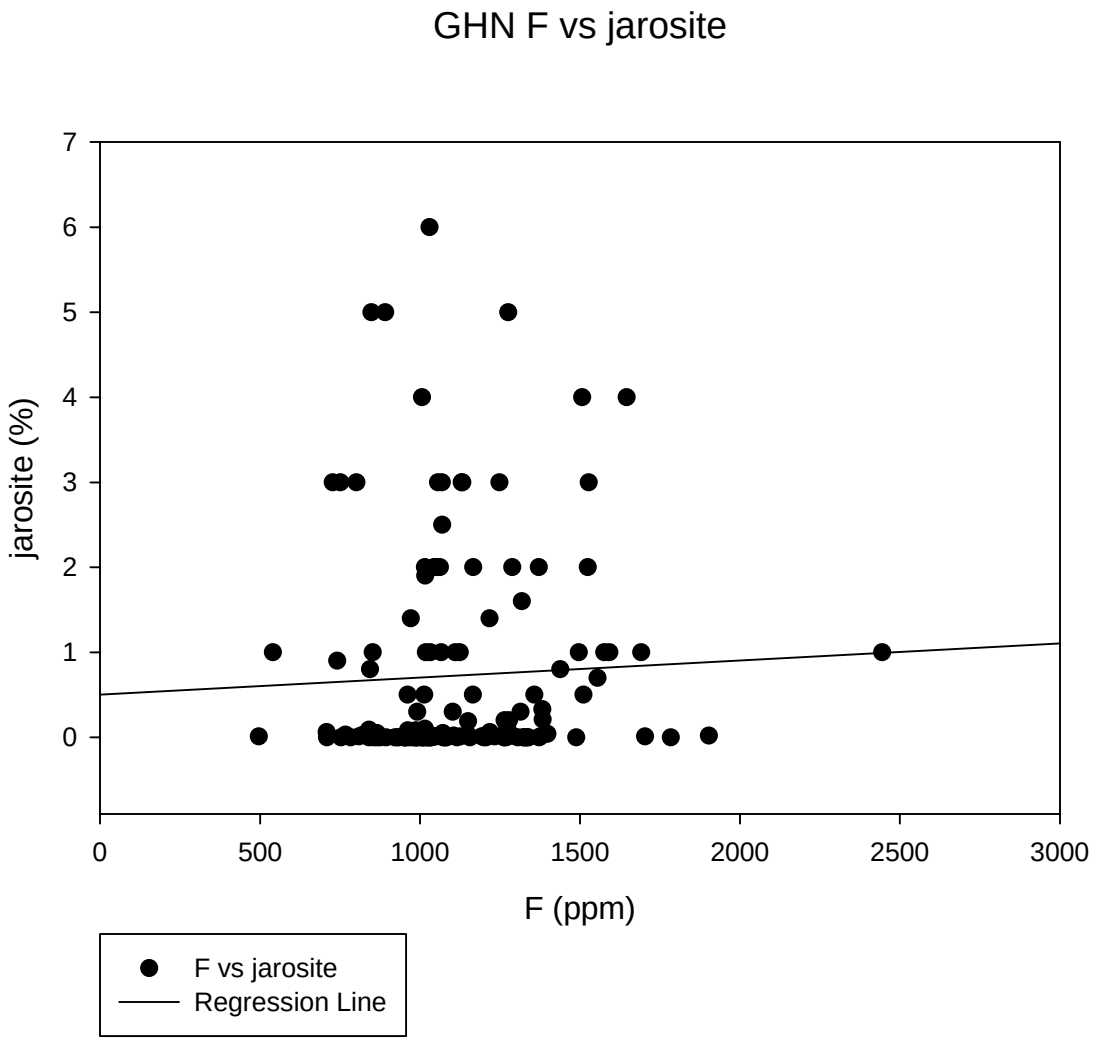
GHN F vs jarosite
jarosite (%)
F (ppm)
0
1
2
3
4
5
6
7
0
500
1000
1500
2000
2500
3000
F vs jarosite
Regression Line

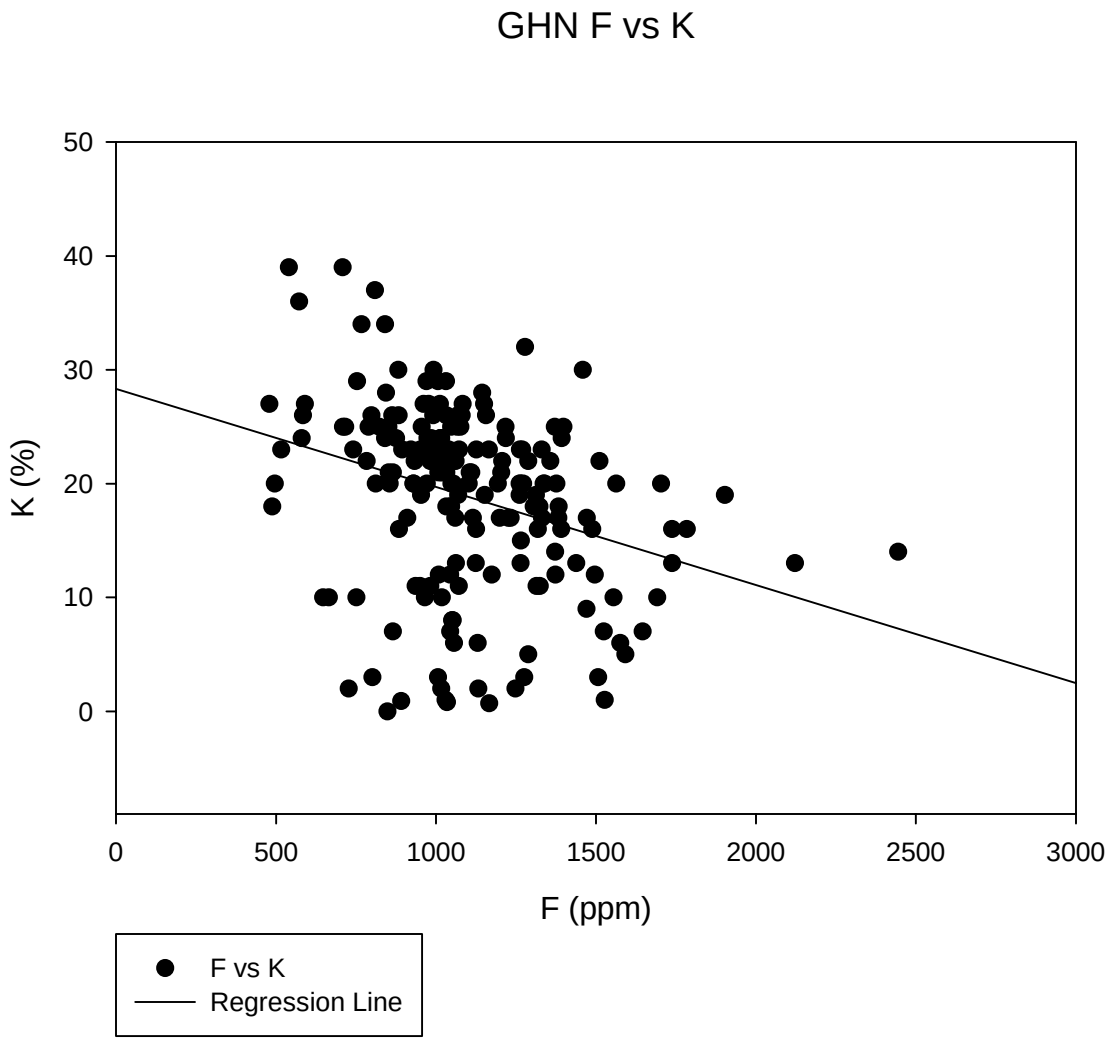
GHN F vs K
50
40
30
20
10
0
K (%)
0
500
1000
1500
2000
2500
3000
F (ppm)
F vs K
Regression Line

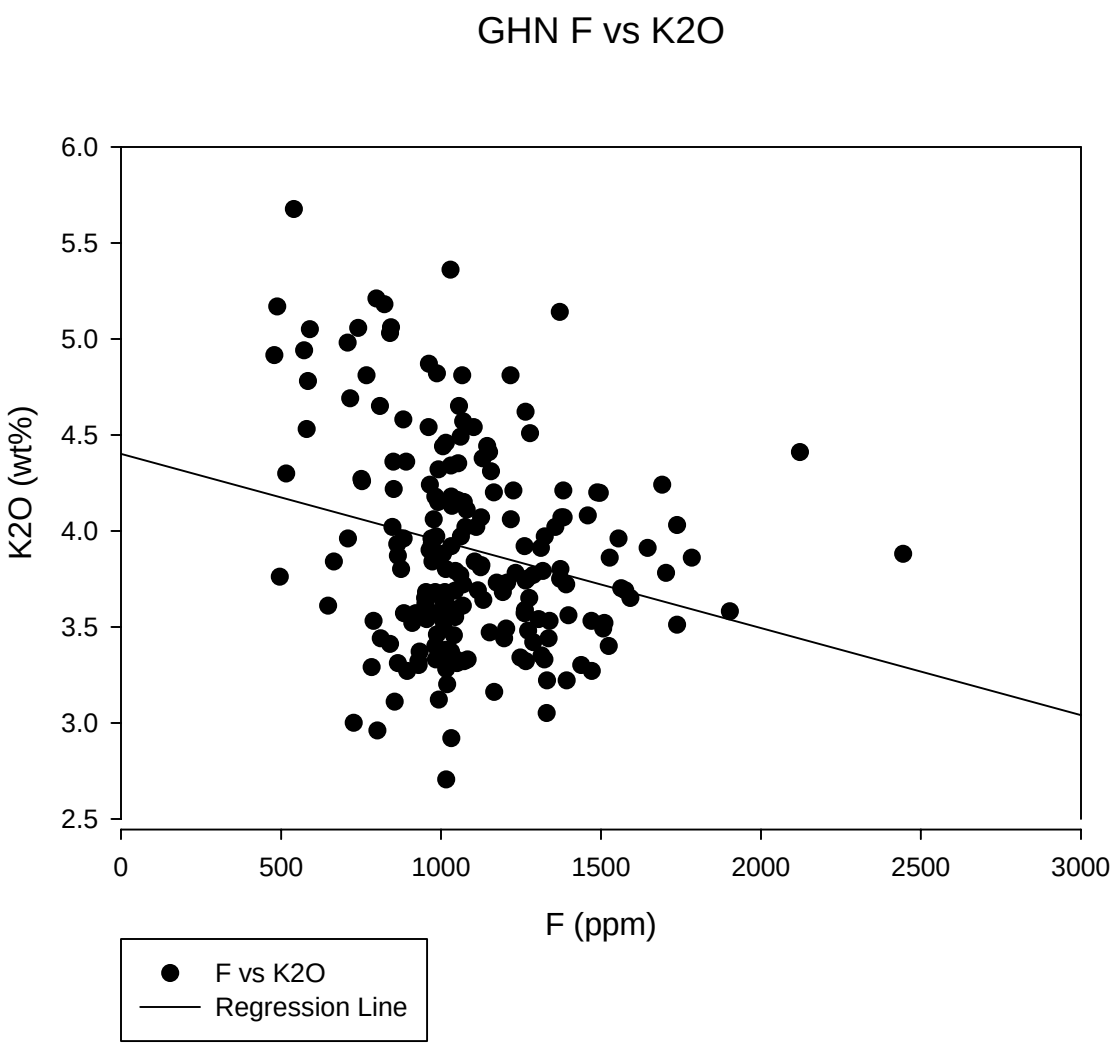
GHN F vs K2O
6.0
5.5
5.0
4.5
4.0
3.5
3.0
2.5
K2O (wt%)
0
500
1000
1500
2000
2500
3000
F (ppm)
F vs K2O
Regression Line

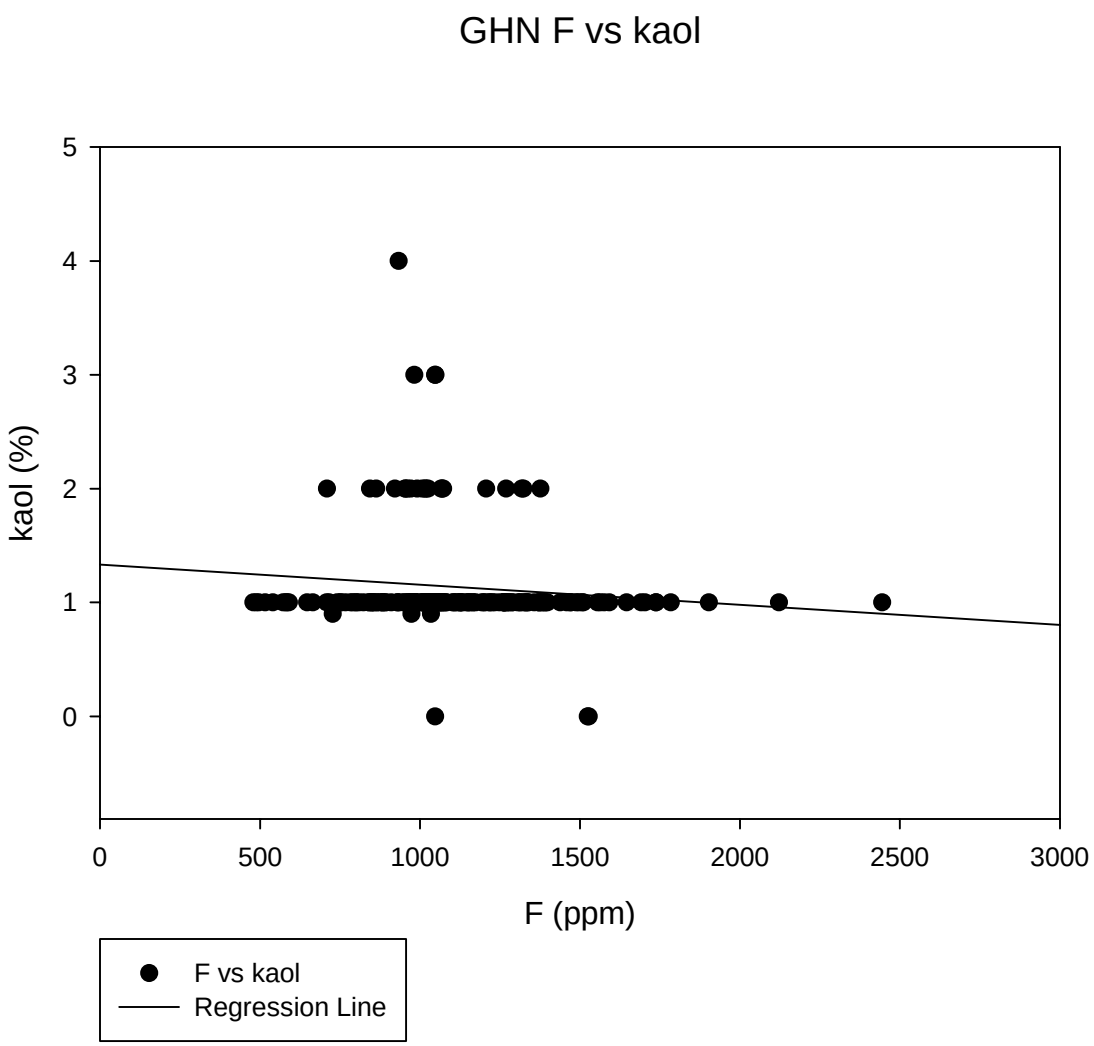
GHN F vs kaol
kaol (%)
5
4
3
2
1
0
0
500
1000
1500
2000
2500
3000
F (ppm)
F vs kaol
Regression Line

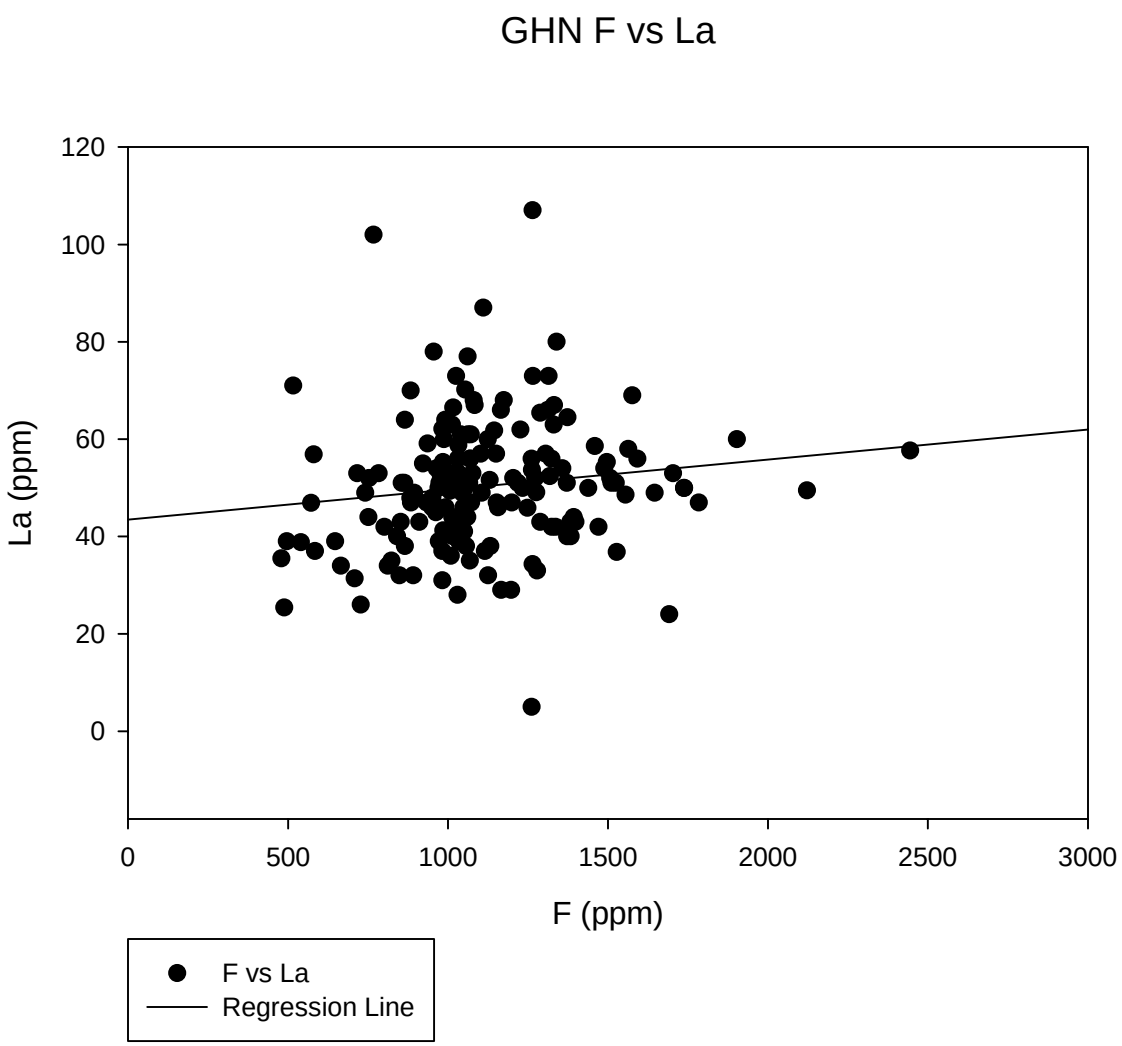
GHN F vs La
120
100
80
60
40
20
0
La (ppm)
0
500
1000
1500
2000
2500
3000
F (ppm)
F vs La
Regression Line

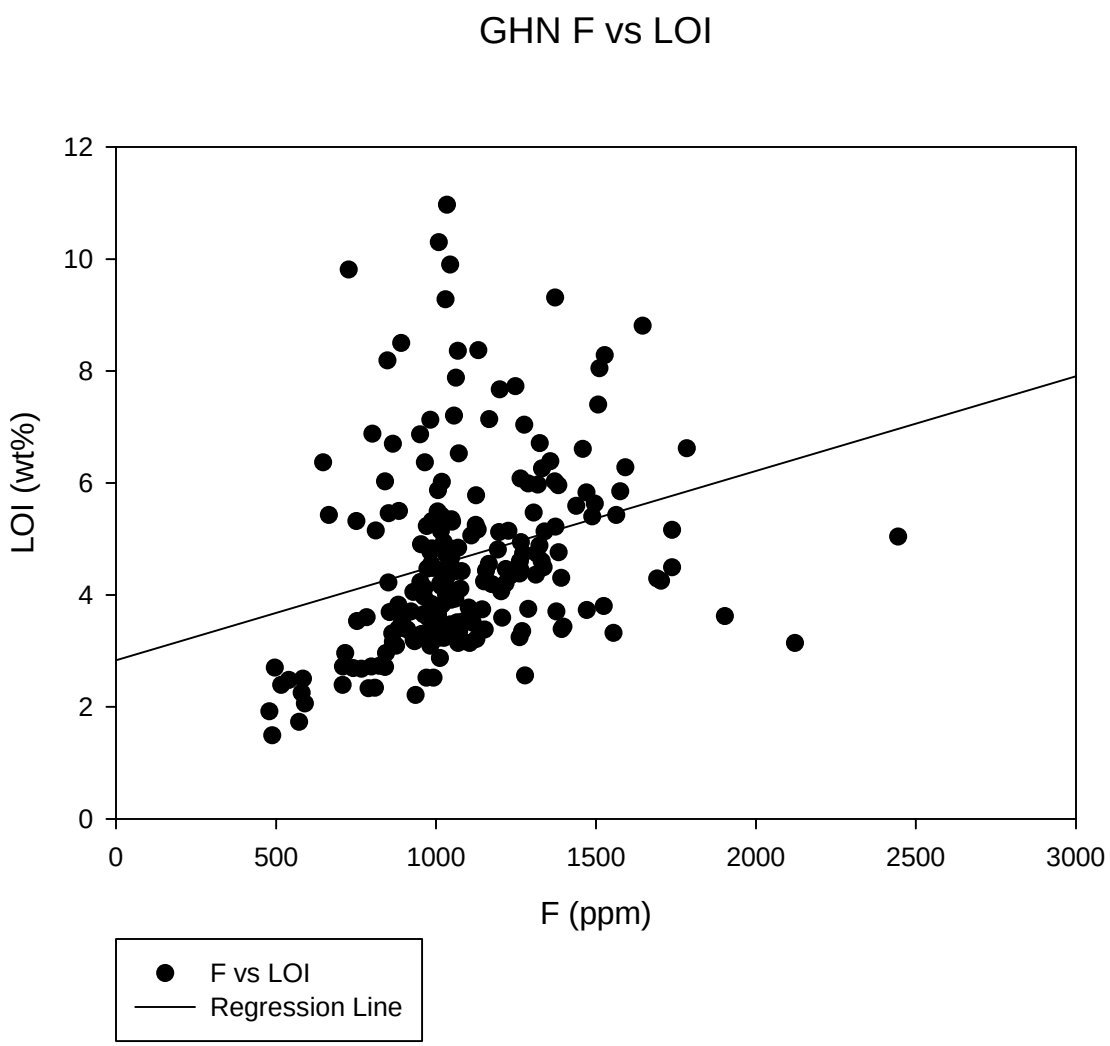
GHN F vs LOI
LOI (wt%)
F (ppm)
0
2
4
6
8
10
12
0
500
1000
1500
2000
2500
3000
F vs LOI
Regression Line

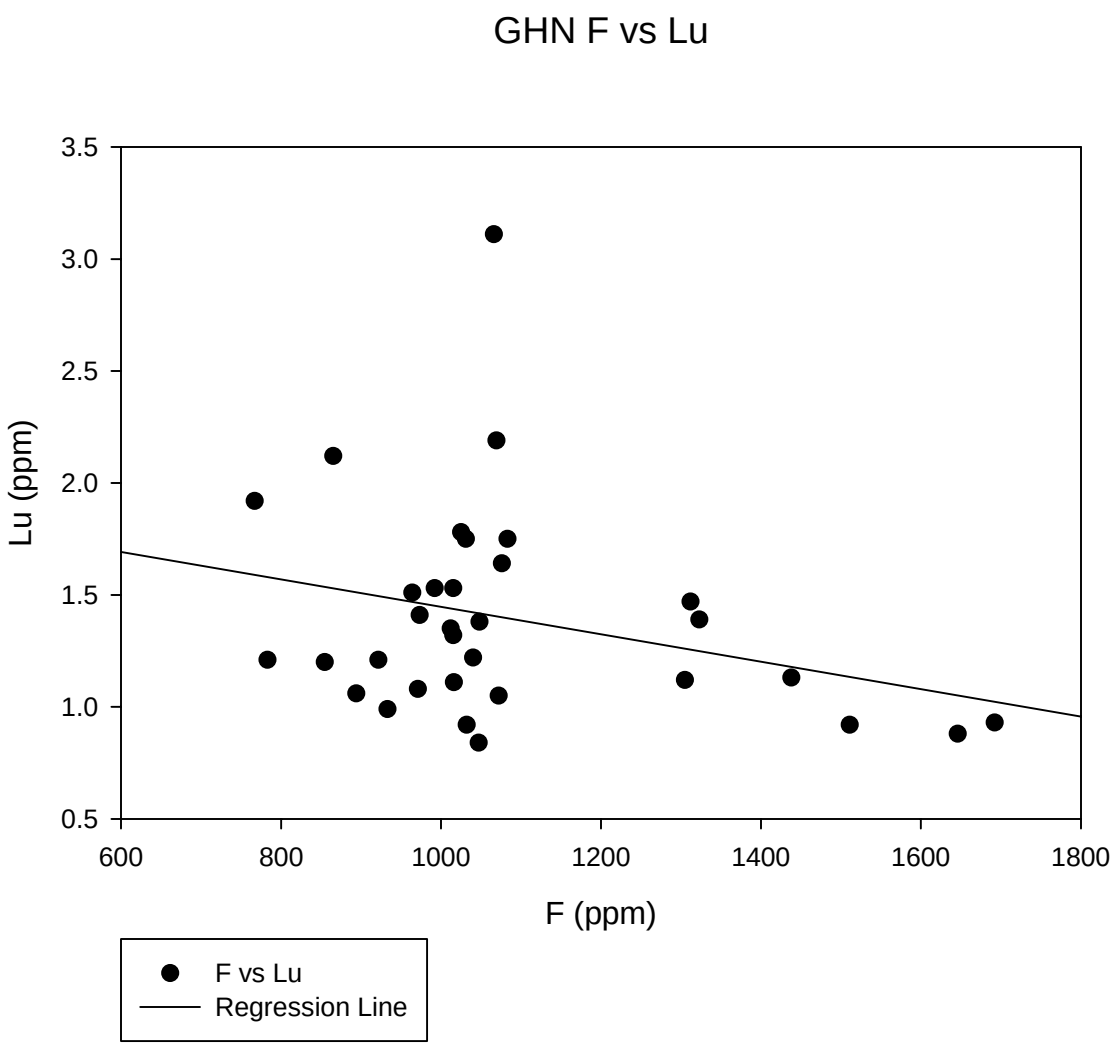
GHN F vs Lu
Lu (ppm)
3.5
3.0
2.5
2.0
1.5
1.0
0.5
600
800
1000
1200
1400
1600
1800
F (ppm)
F vs Lu
Regression Line

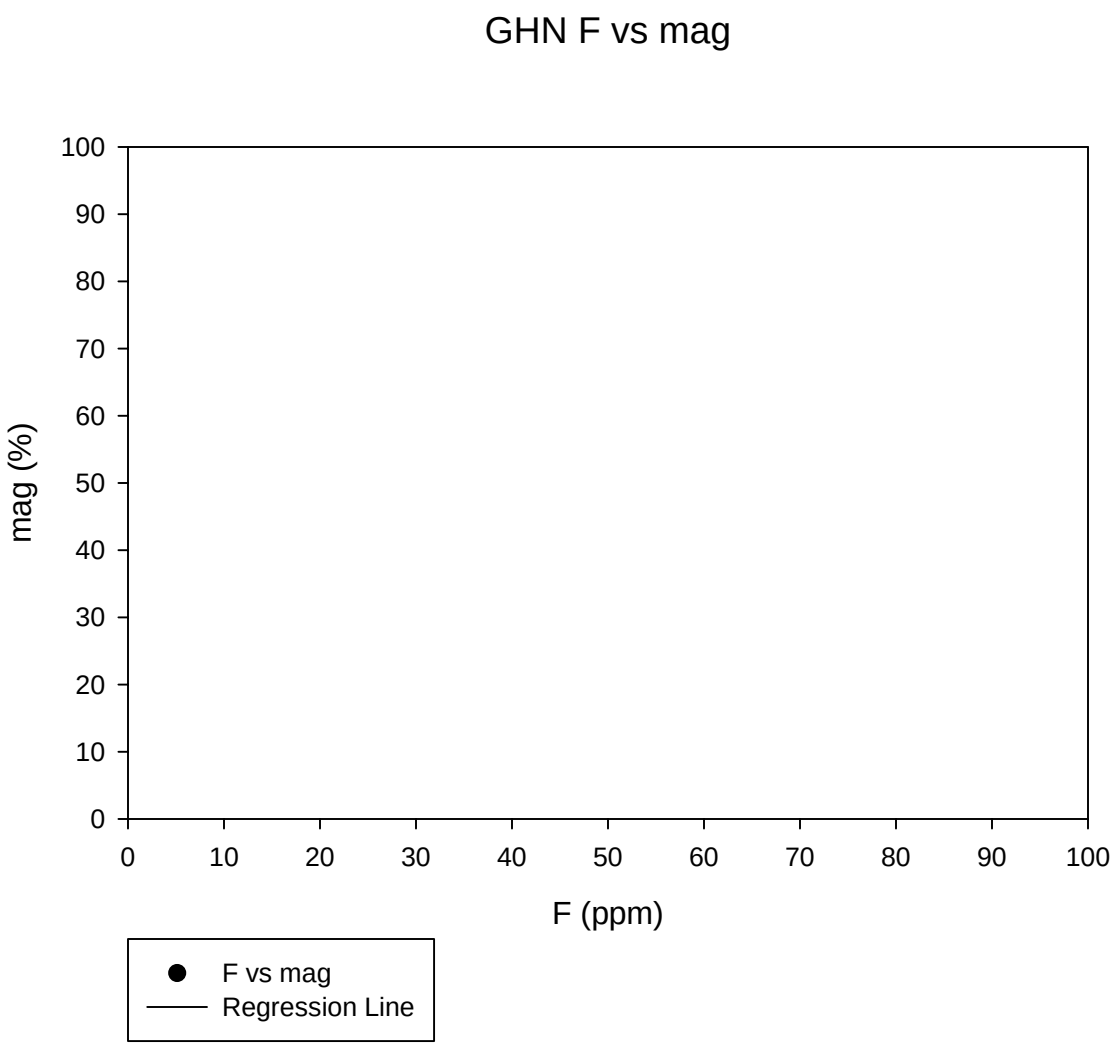
GHN F vs mag
mag (%)
100
90
80
70
60
50
40
30
20
10
0
0
10
20
30
40
50
60
70
80
90
100
F (ppm)
F vs mag
Regression Line

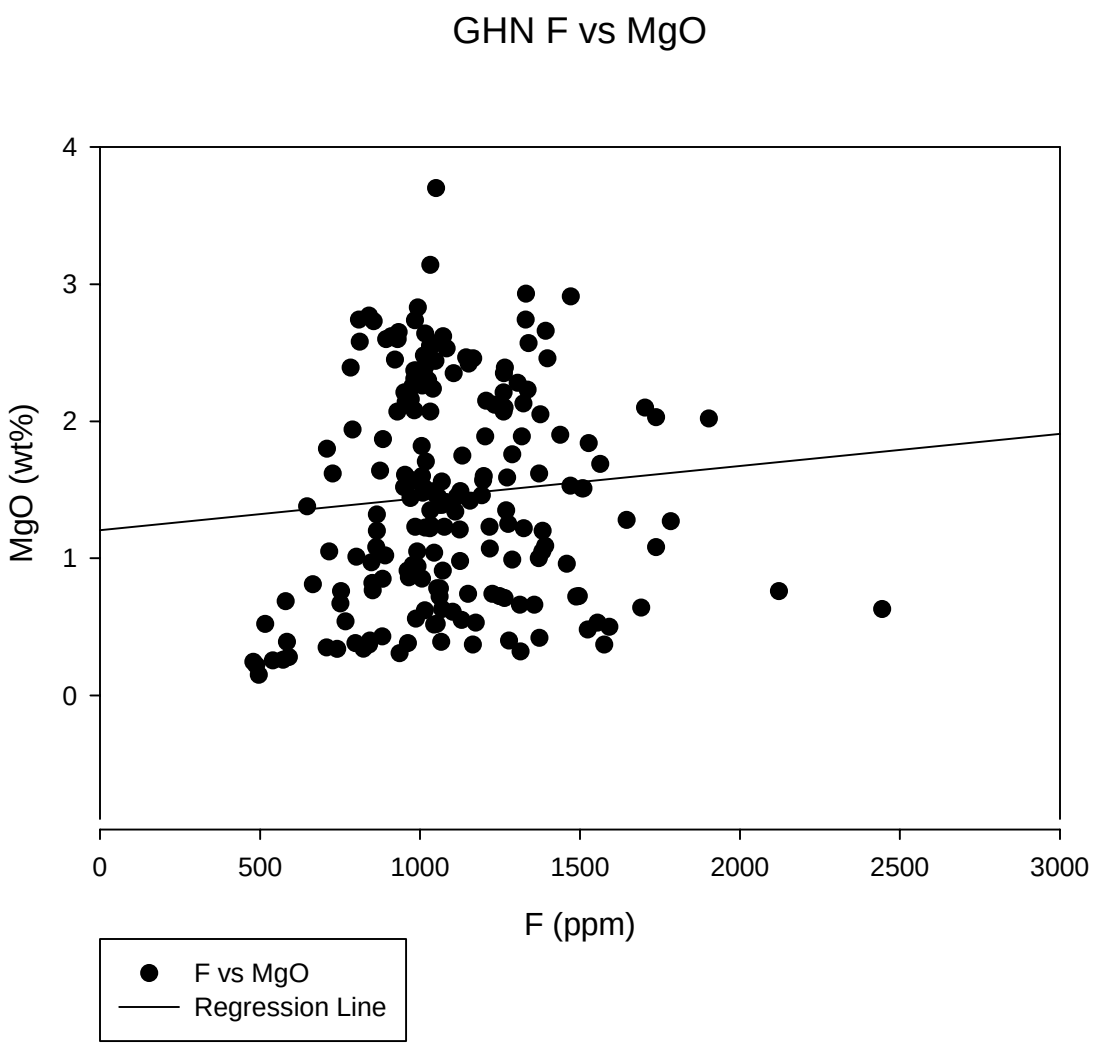
GHN F vs MgO
MgO (wt%)
4
3
2
1
0
0
500
1000
1500
2000
2500
3000
F (ppm)
F vs MgO
Regression Line

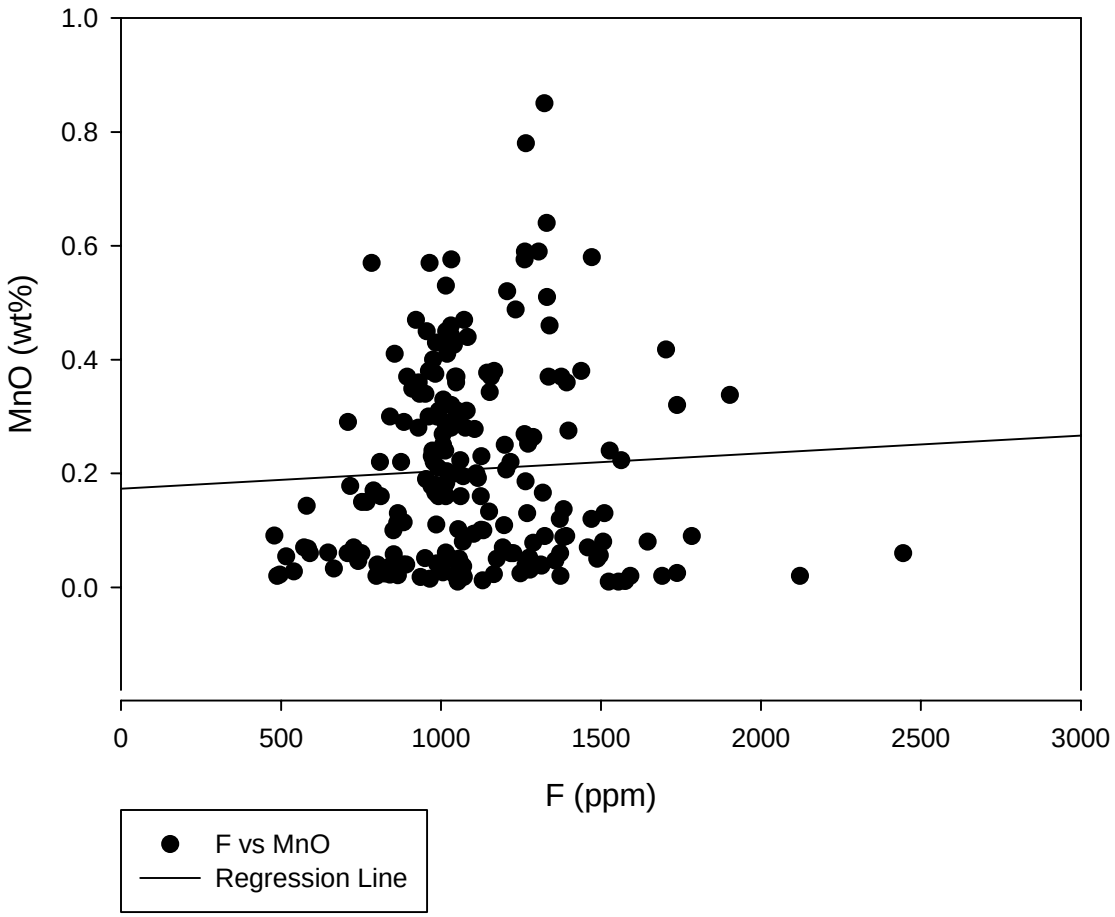
GHN F vs MnO
1.0
0.8
0.6
0.4
0.2
0.0
MnO (wt%)
0
500
1000
1500
2000
2500
3000
F (ppm)
F vs MnO
Regression Line

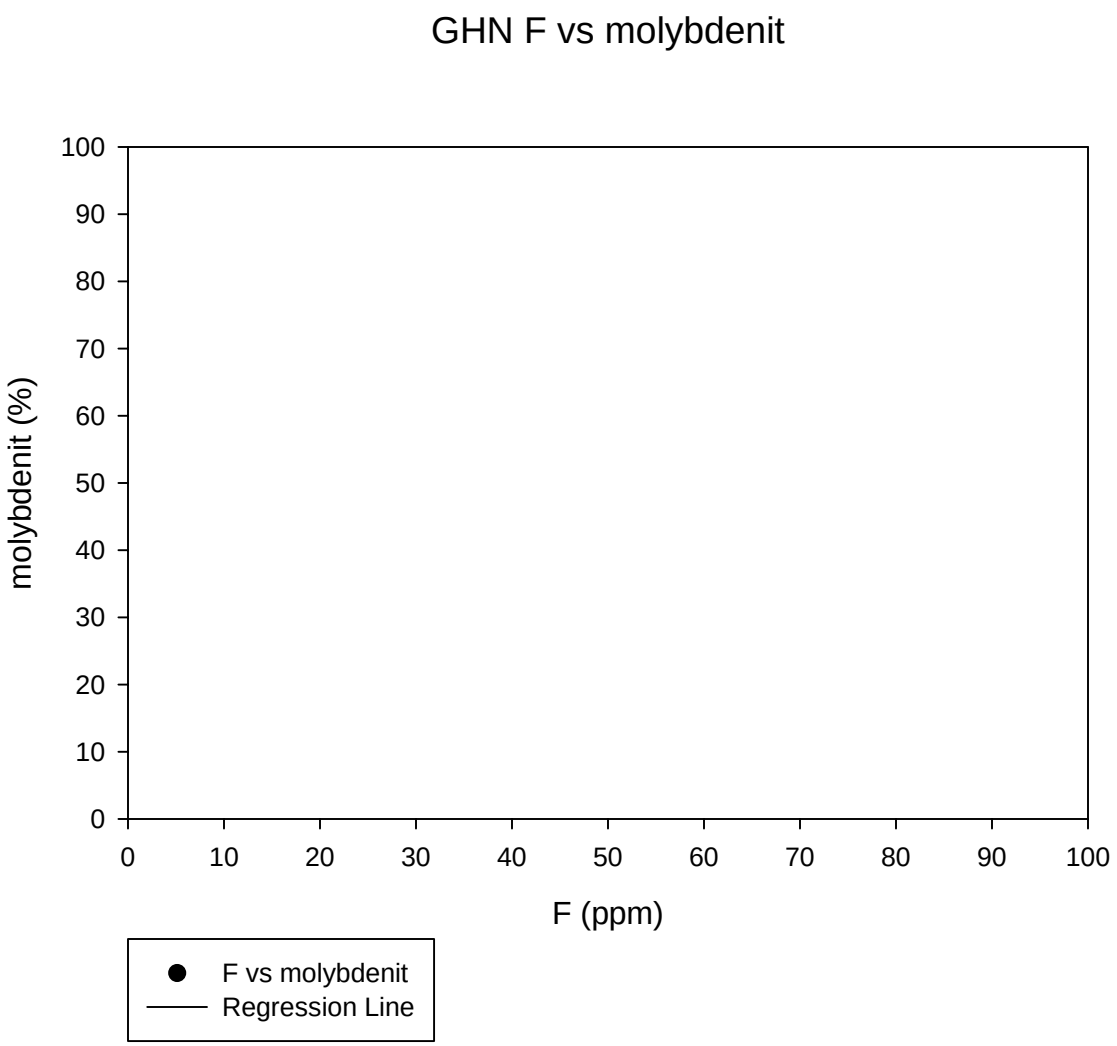
GHN F vs molybdenit
molybdenit (%)
100
90
80
70
60
50
40
30
20
10
0
0
10
20
30
40
50
60
70
80
90
100
F (ppm)
F vs molybdenit
Regression Line

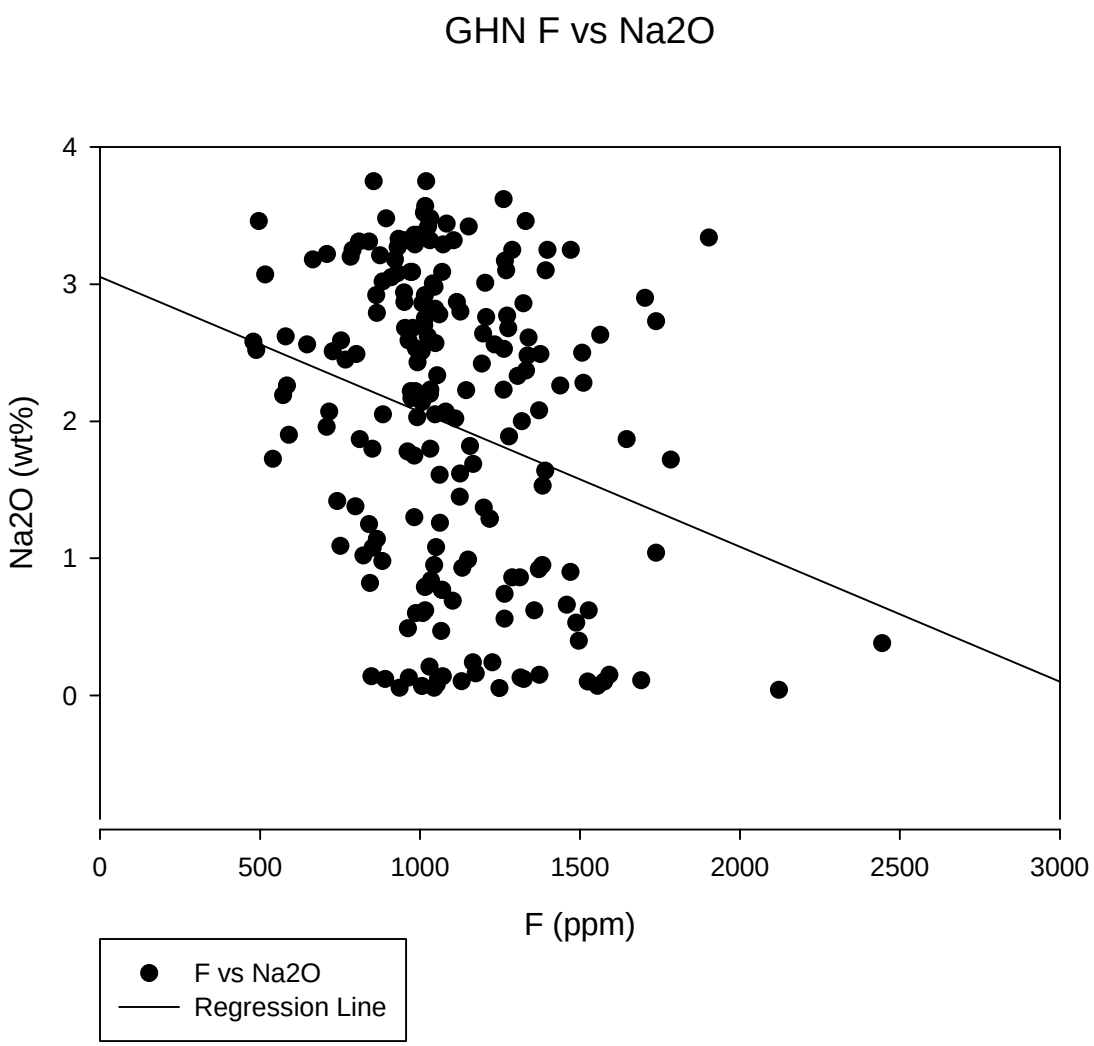
GHN F vs Na2O
Na2O (wt%)
4
3
2
1
0
0
500
1000
1500
2000
2500
3000
F (ppm)
F vs Na2O
Regression Line

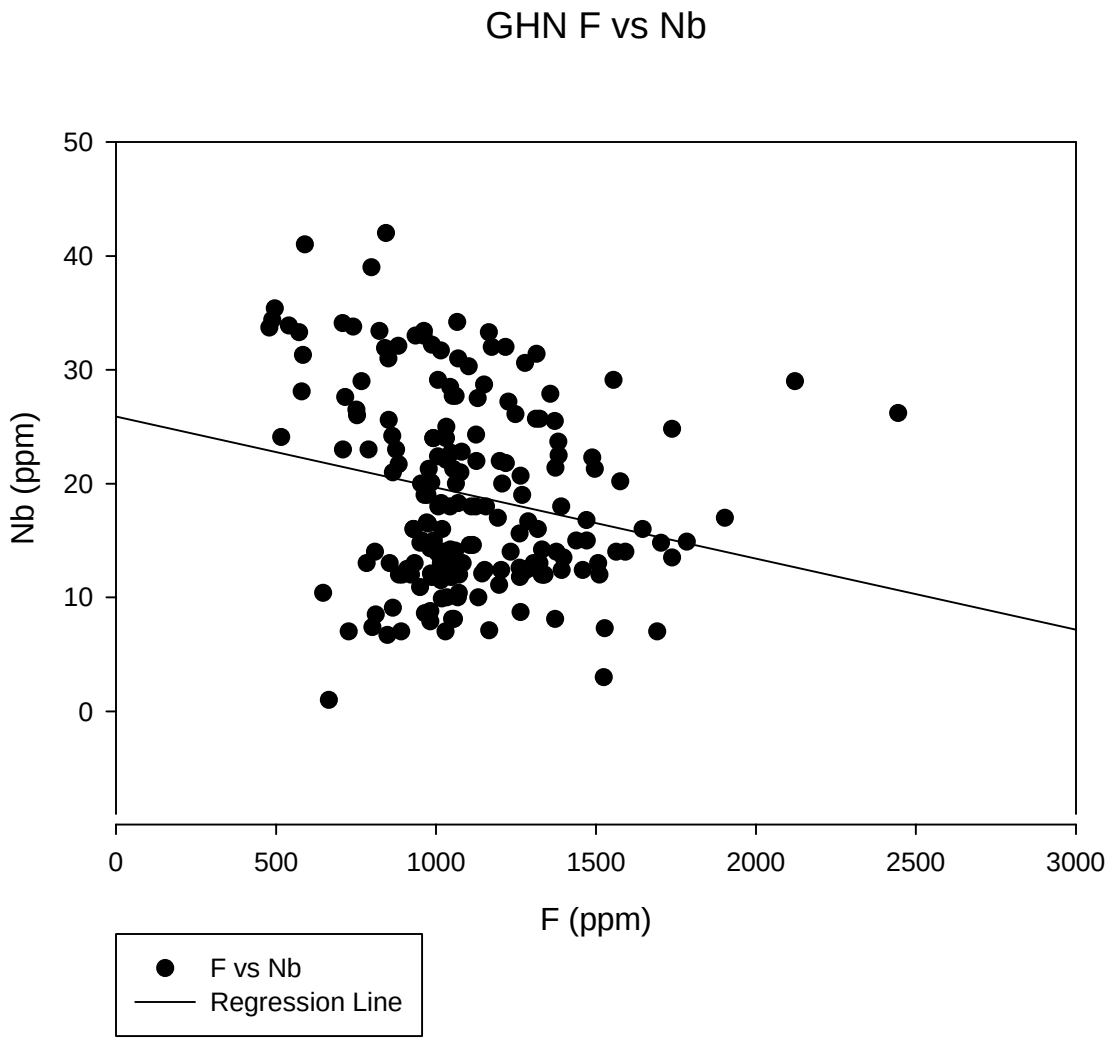
GHN F vs Nb
Nb (ppm)
50
40
30
20
10
0
0
500
1000
1500
2000
2500
3000
F (ppm)
F vs Nb
Regression Line

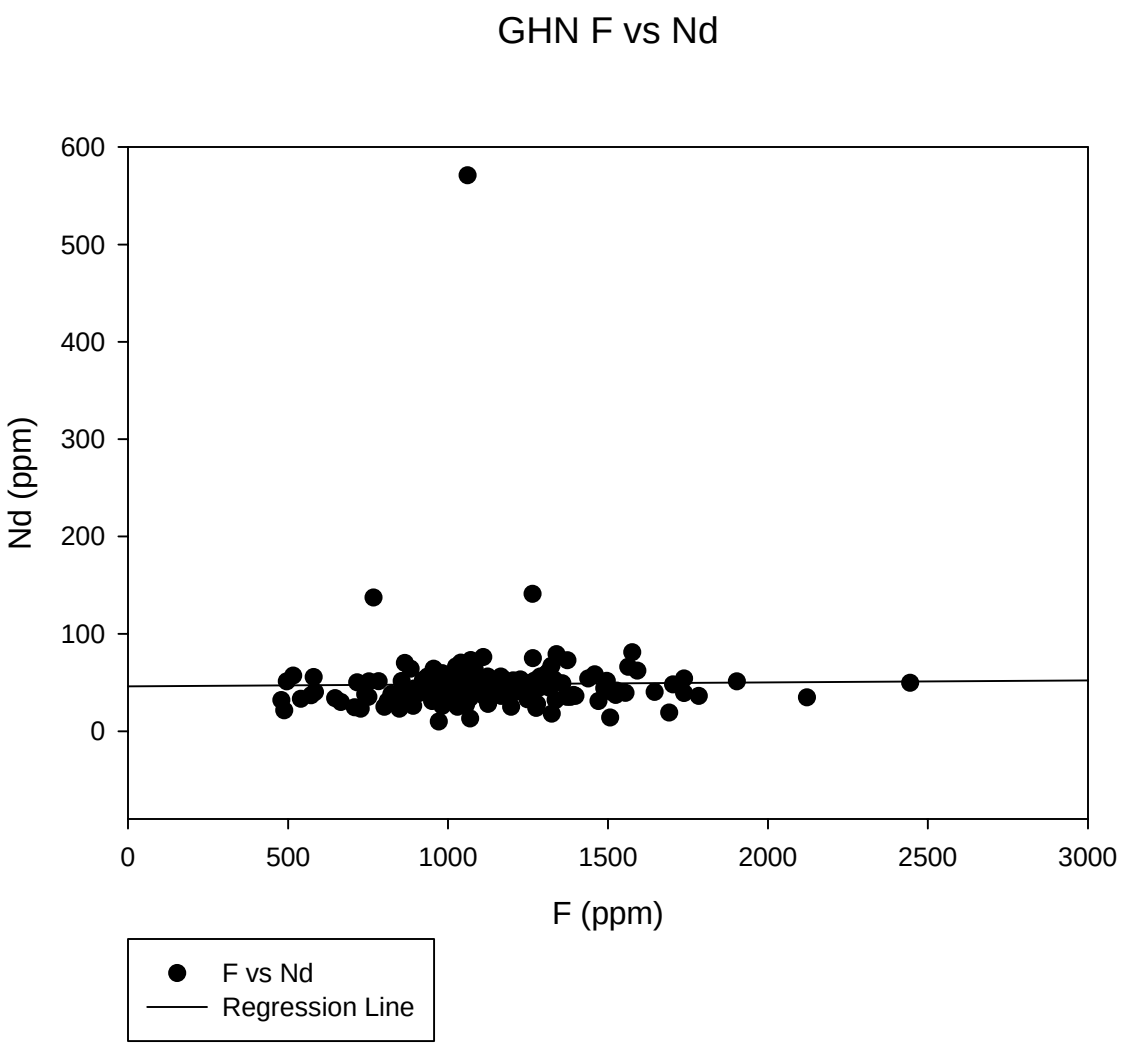
GHN F vs Nd
600
500
400
300
200
100
0
Nd (ppm)
0
500
1000
1500
2000
2500
3000
F (ppm)
F vs Nd
Regression Line

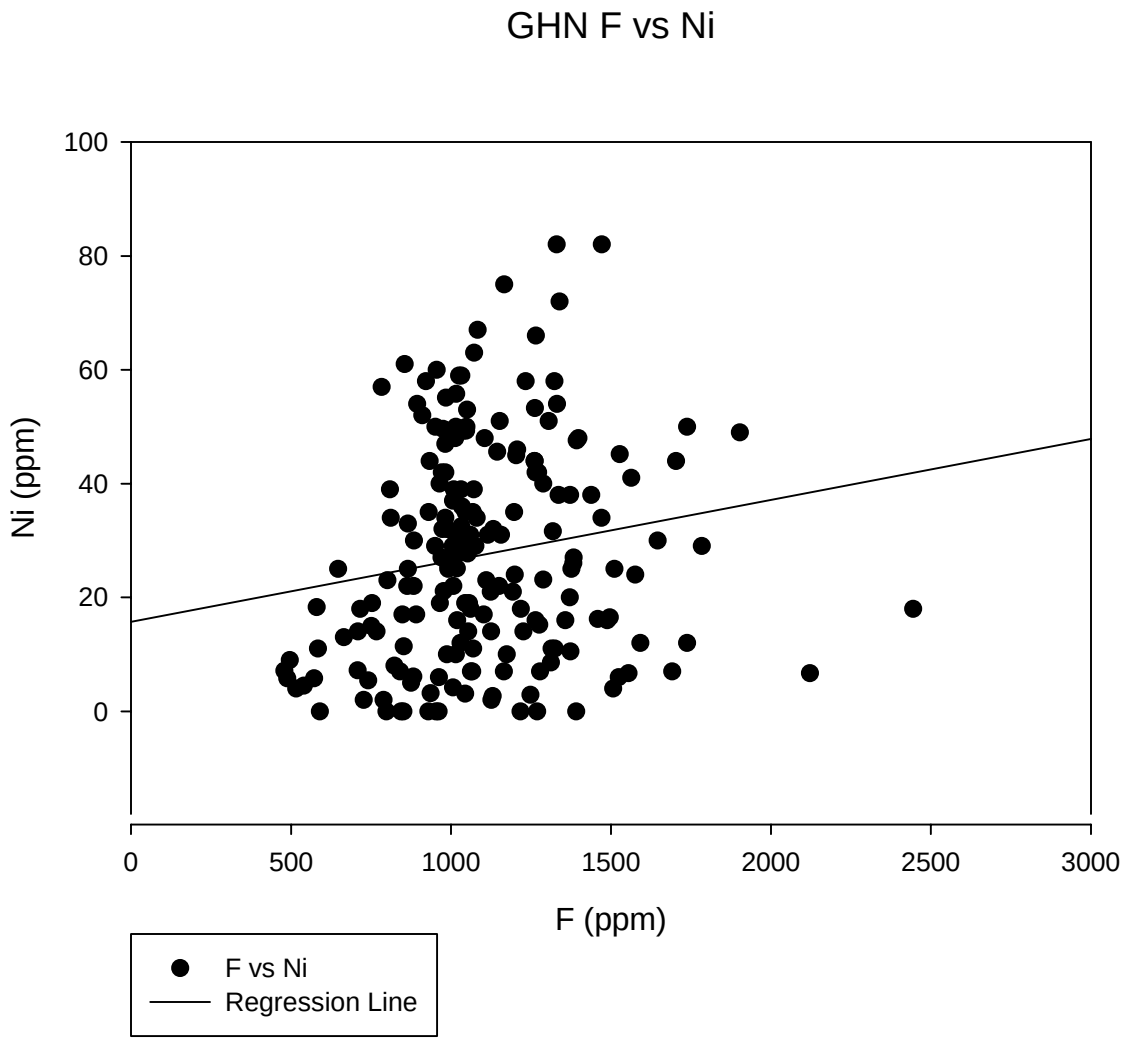
GHN F vs Ni
100
80
60
40
20
0
Ni (ppm)
0
500
1000
1500
2000
2500
3000
F (ppm)
F vs Ni
Regression Line

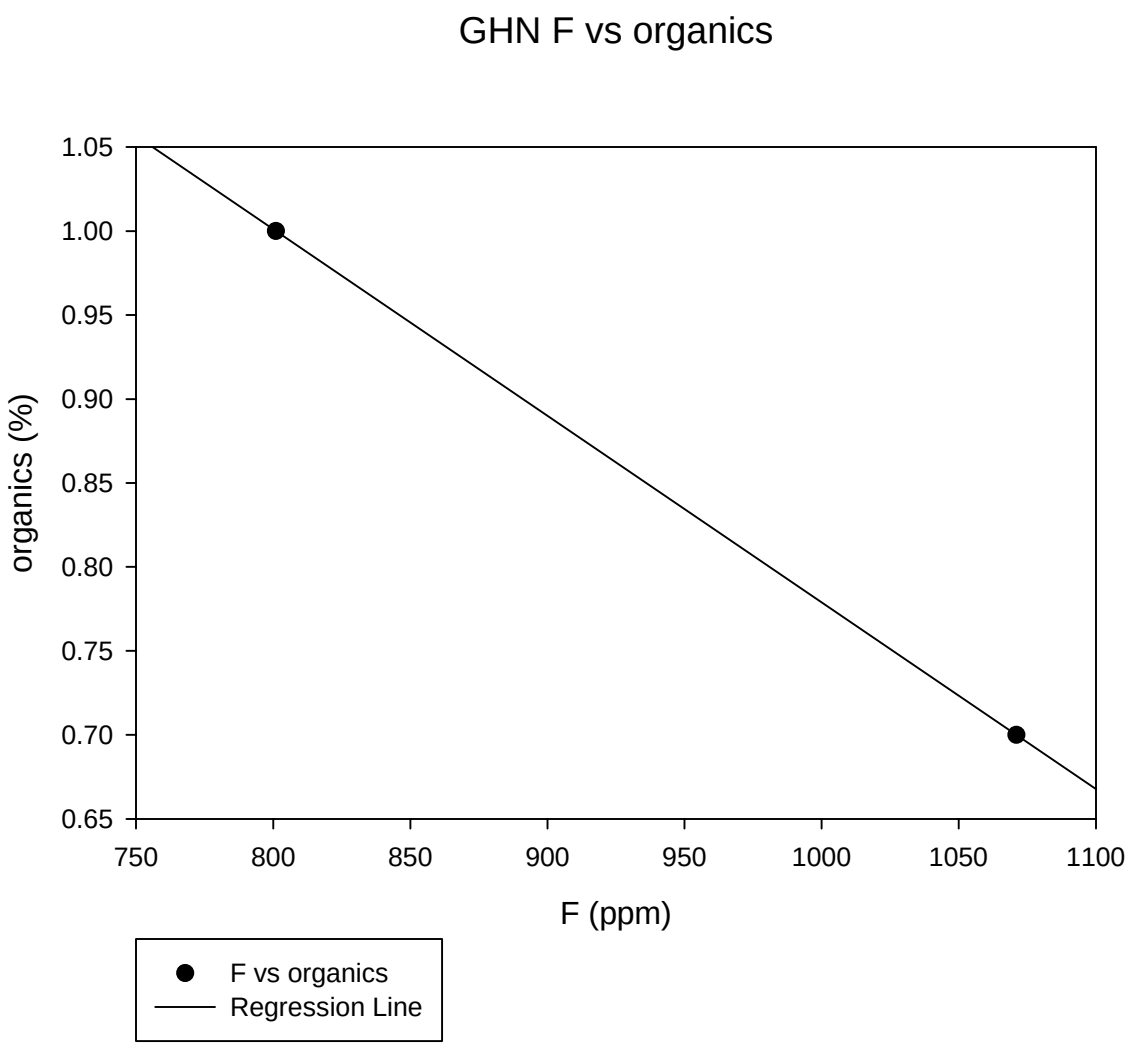
GHN F vs organics
1.05
1.00
0.95
0.90
0.85
0.80
0.75
0.70
0.65
organics (%)
750
800
850
900
950
1000
1050
1100
F (ppm)
F vs organics
Regression Line

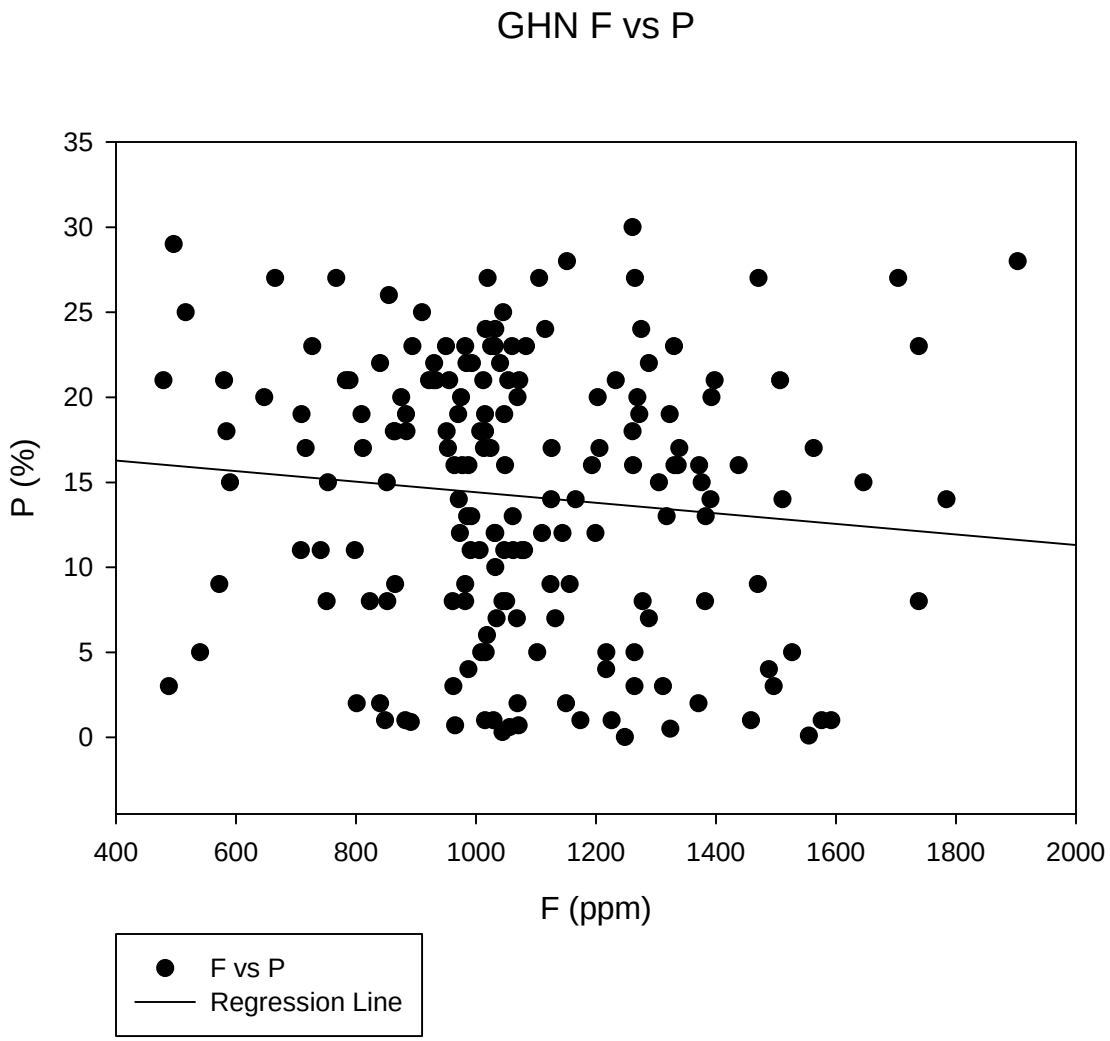
GHN F vs P
35
30
25
20
15
10
5
0
P (%)
400
600
800
1000
1200
1400
1600
1800
2000
F (ppm)
F vs P
Regression Line

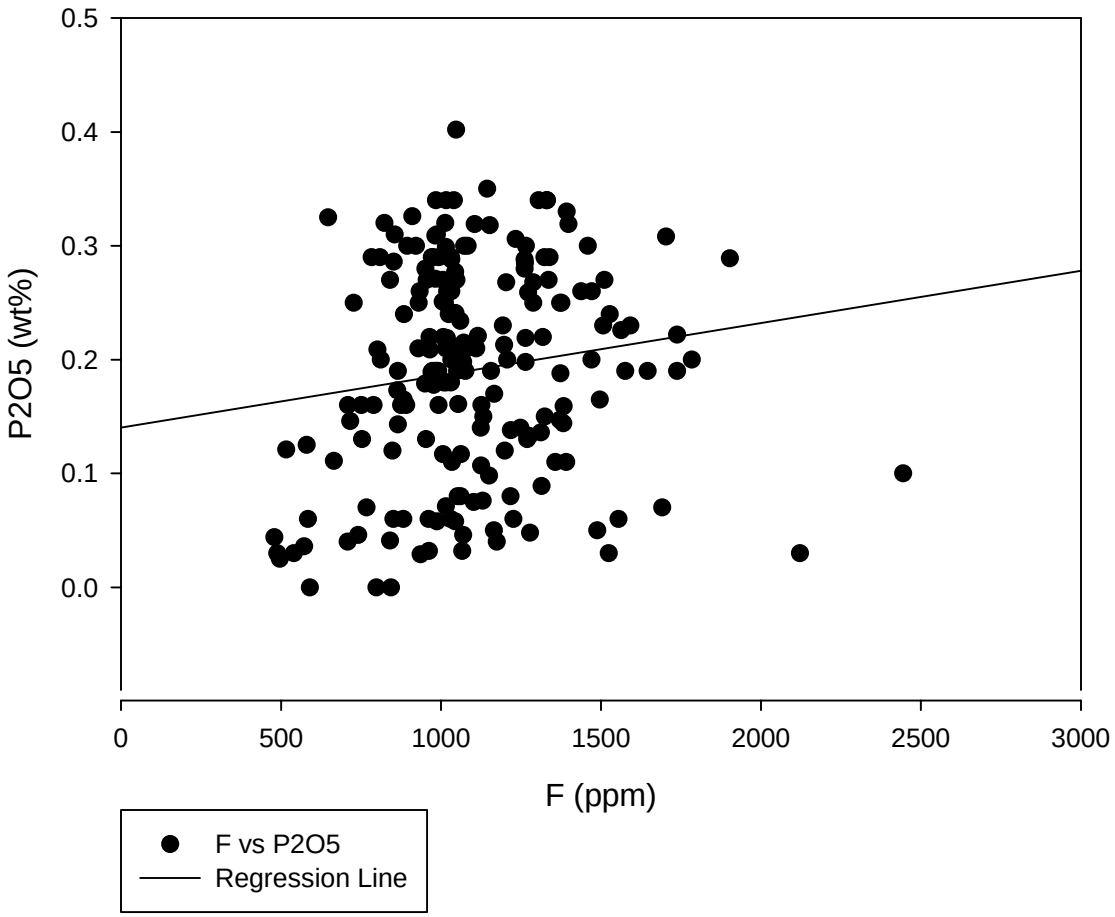
GHN F vs P2O5
0.5
0.4
0.3
0.2
0.1
0.0
P2O5 (wt%)
0
500
1000
1500
2000
2500
3000
F (ppm)
F vs P2O5
Regression Line

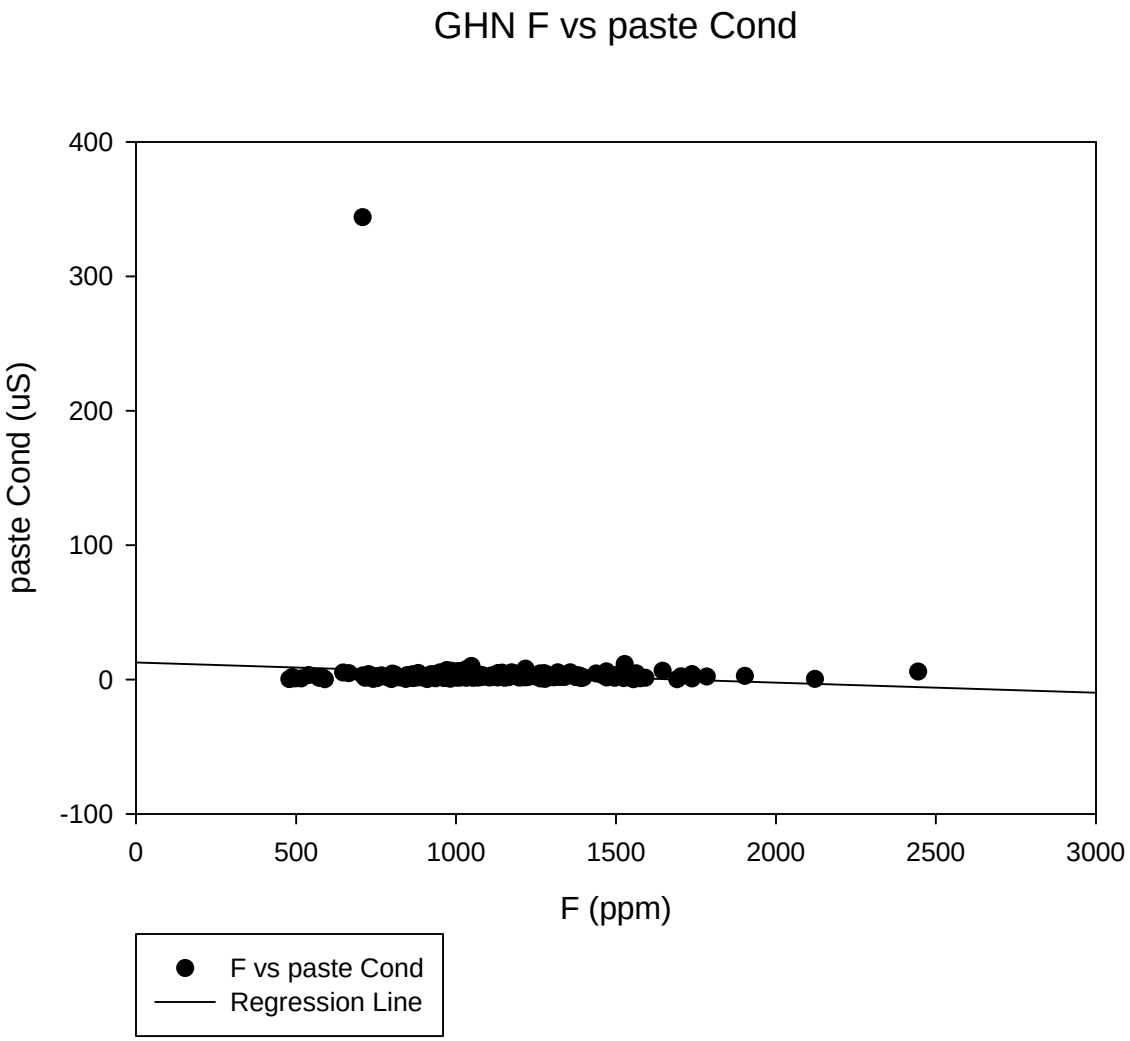
GHN F vs paste Cond
400
300
200
100
0
-100
paste Cond (uS)
0
500
1000
1500
2000
2500
3000
F (ppm)
F vs paste Cond
Regression Line

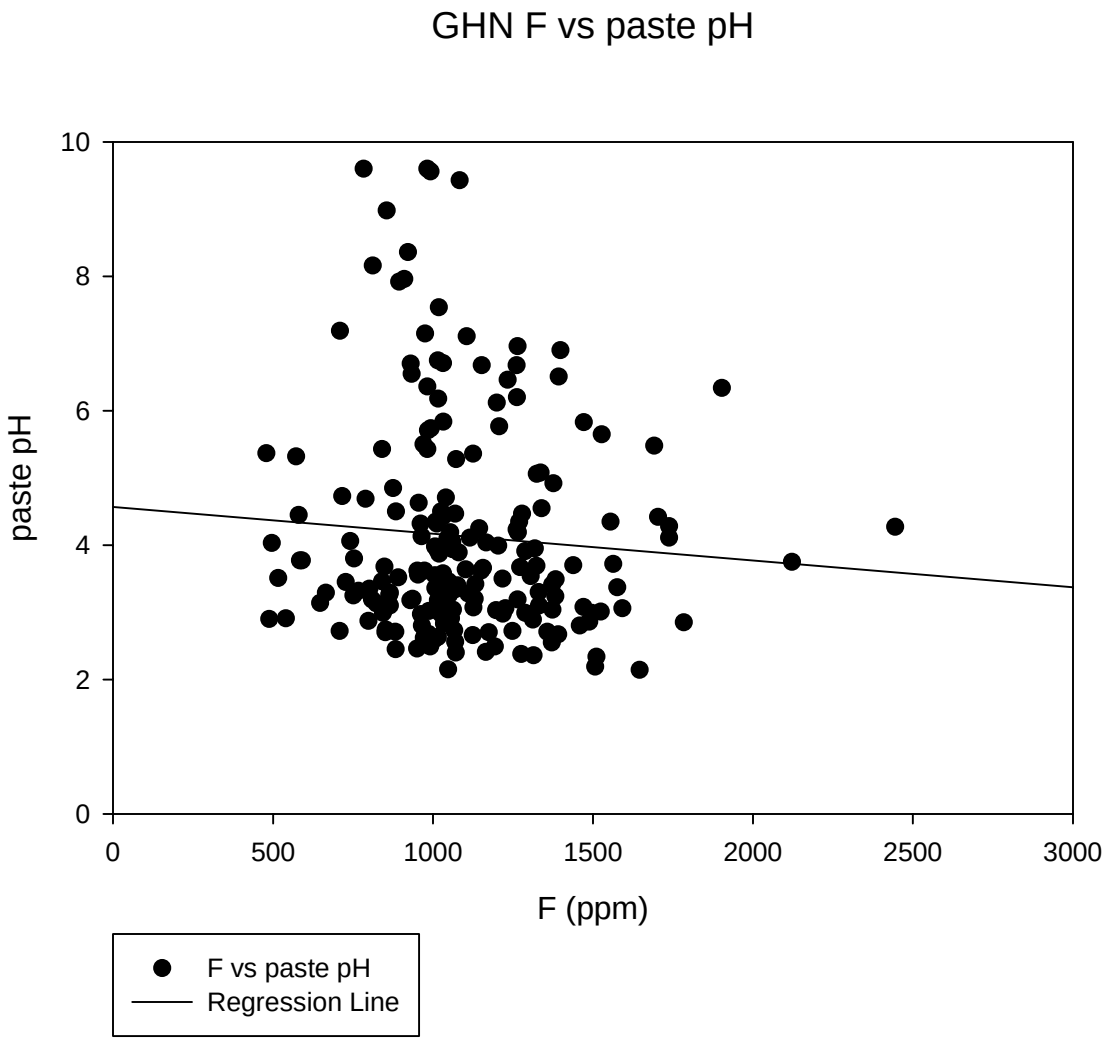
GHN F vs paste pH
paste pH
F (ppm)
0
2
4
6
8
10
0
500
1000
1500
2000
2500
3000
F vs paste pH
Regression Line

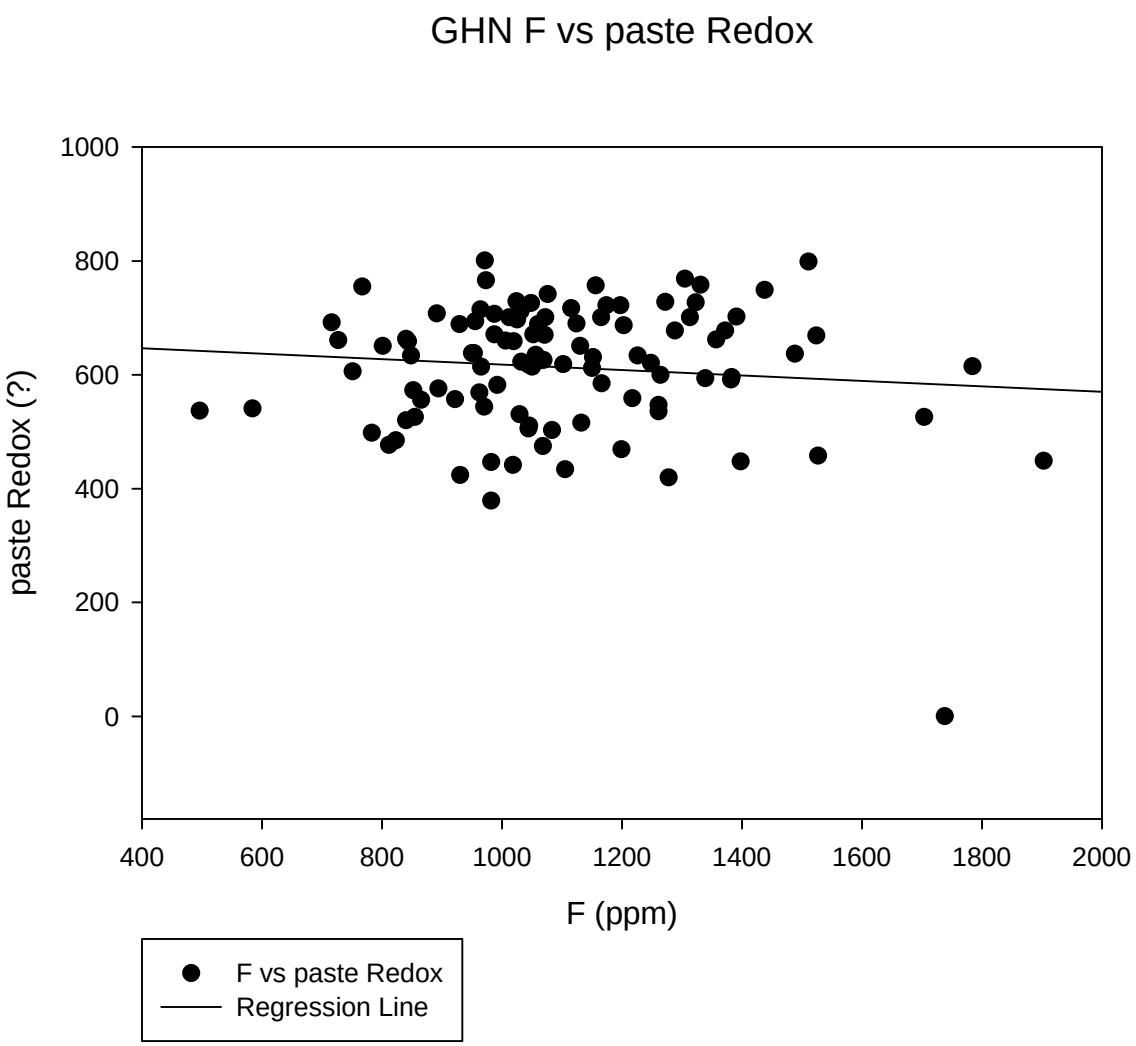
GHN F vs paste Redox
paste Redox (?)
1000
800
600
400
200
0
400
600
800
1000
1200
1400
1600
1800
2000
F (ppm)
F vs paste Redox
Regression Line

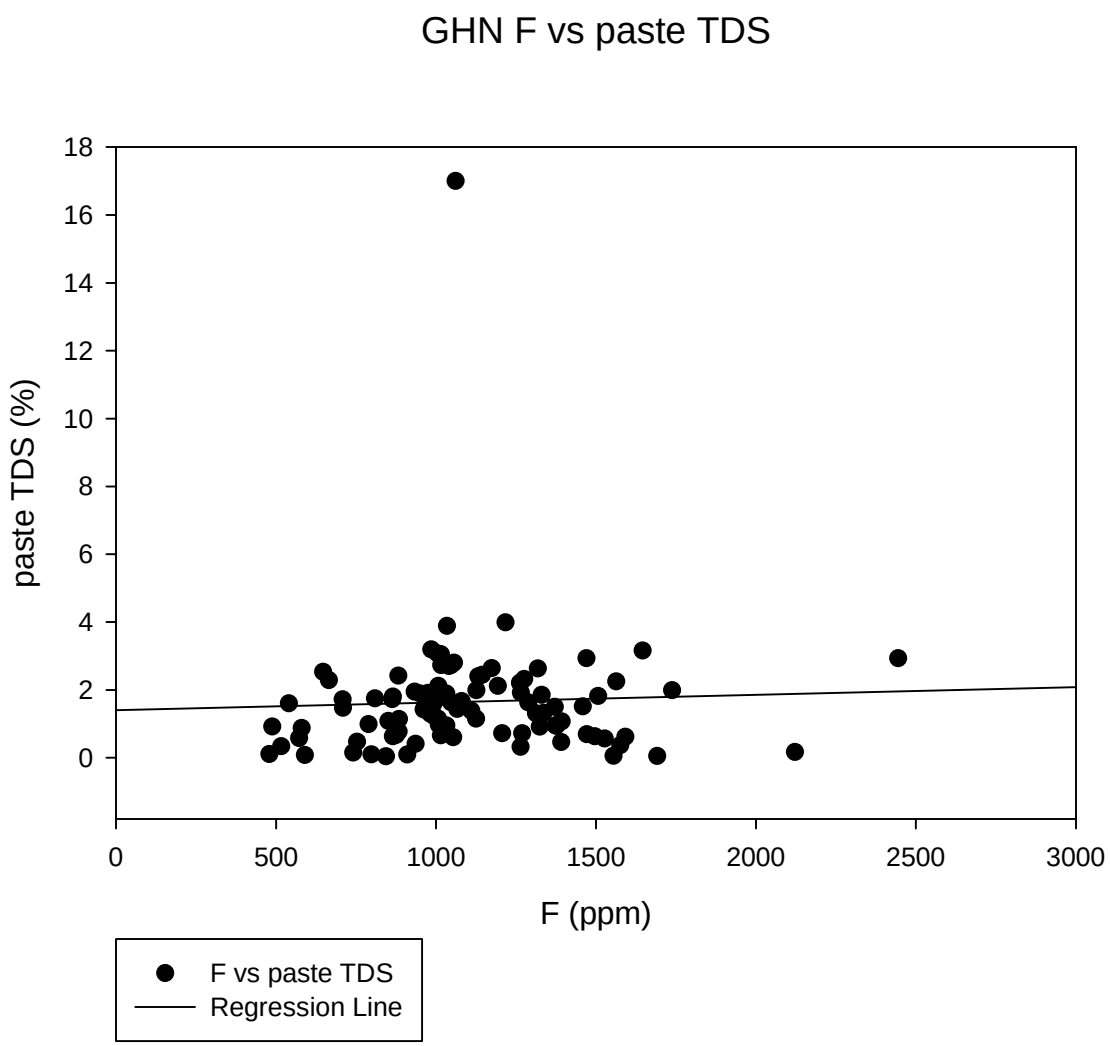
GHN F vs paste TDS
paste TDS (%)
18
16
14
12
10
8
6
4
2
0
0
500
1000
1500
2000
2500
3000
F (ppm)
F vs paste TDS
Regression Line

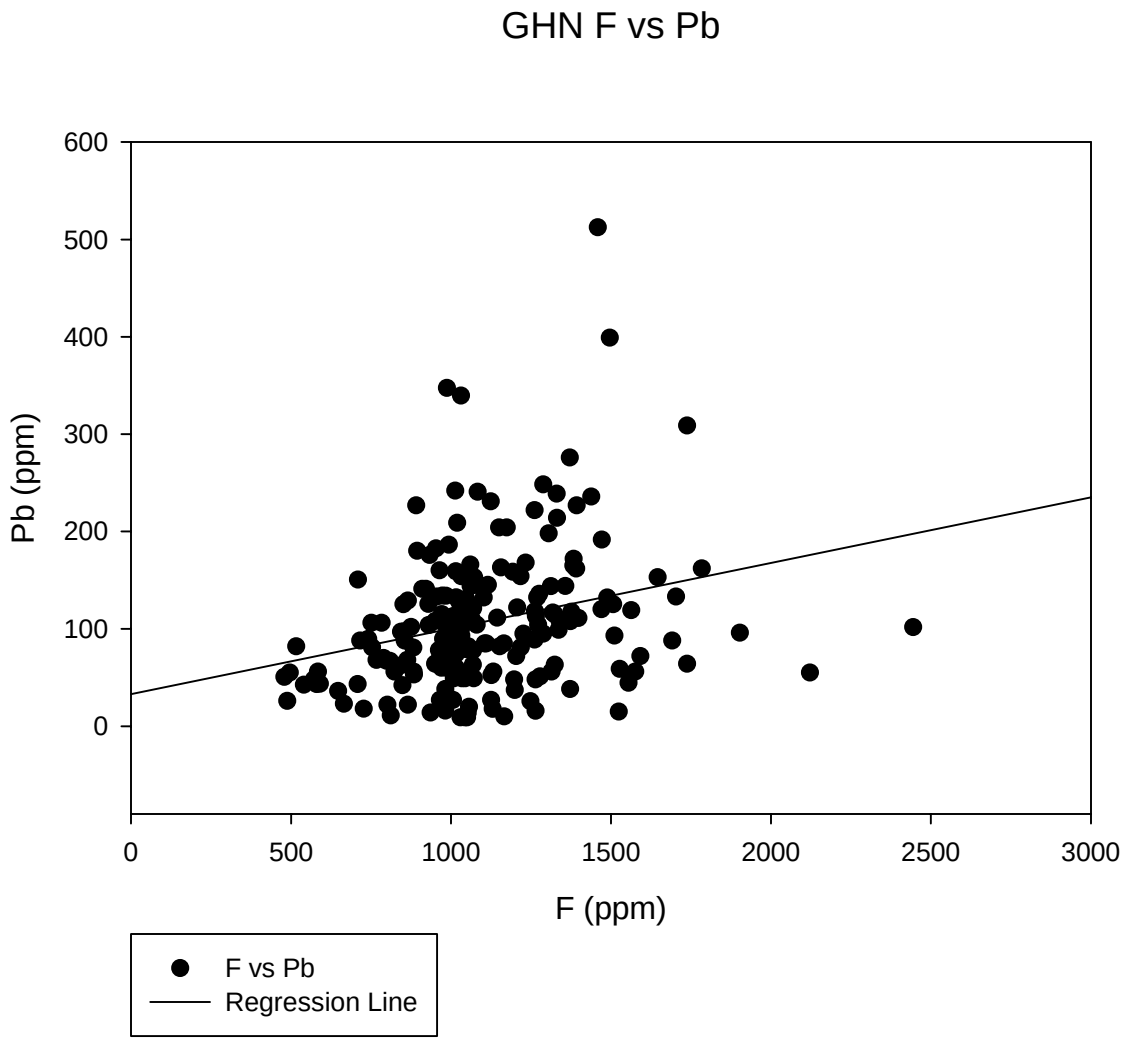
GHN F vs Pb
600
500
400
300
200
100
0
Pb (ppm)
0
500
1000
1500
2000
2500
3000
F (ppm)
F vs Pb
Regression Line

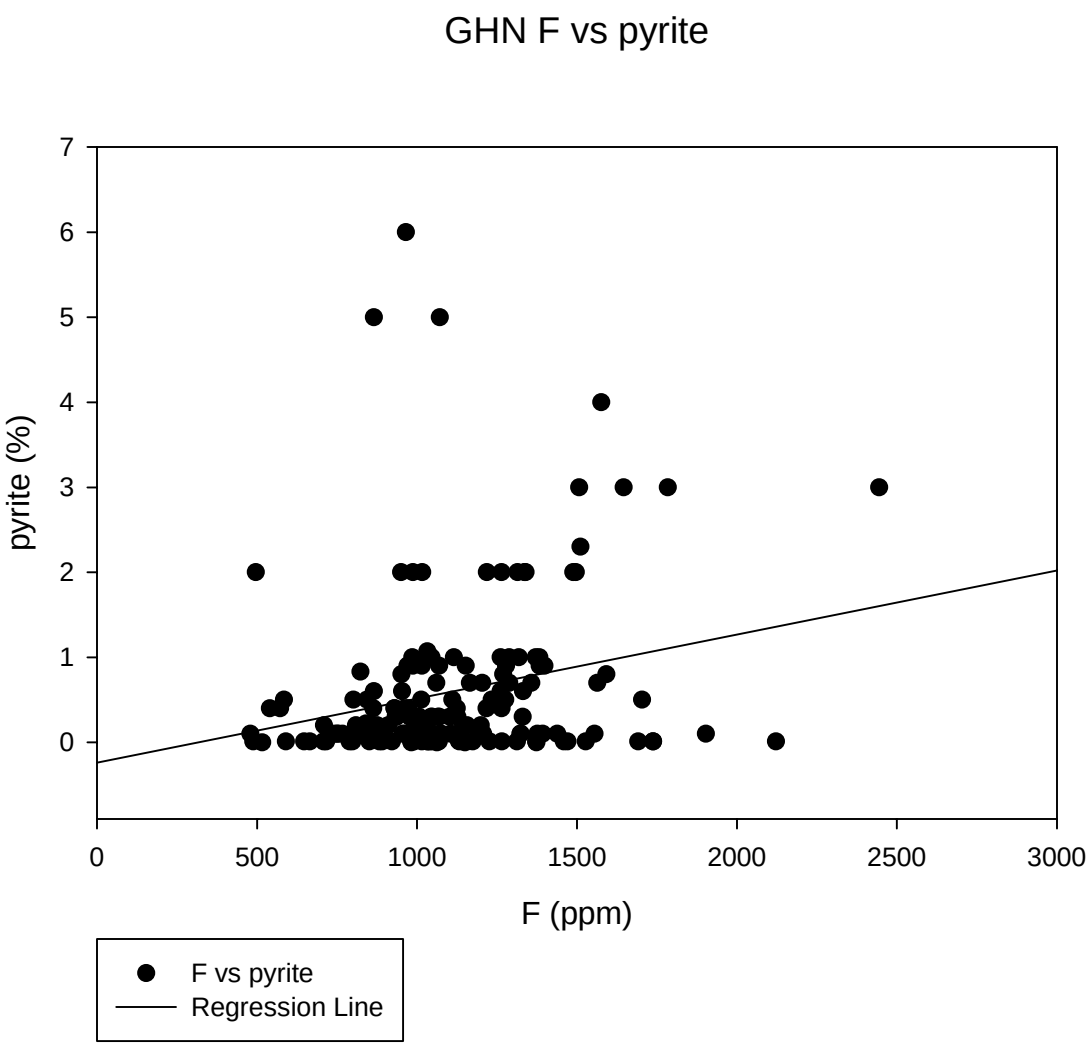
GHN F vs pyrite
pyrite (%)
7
6
5
4
3
2
1
0
0
500
1000
1500
2000
2500
3000
F (ppm)
F vs pyrite
Regression Line

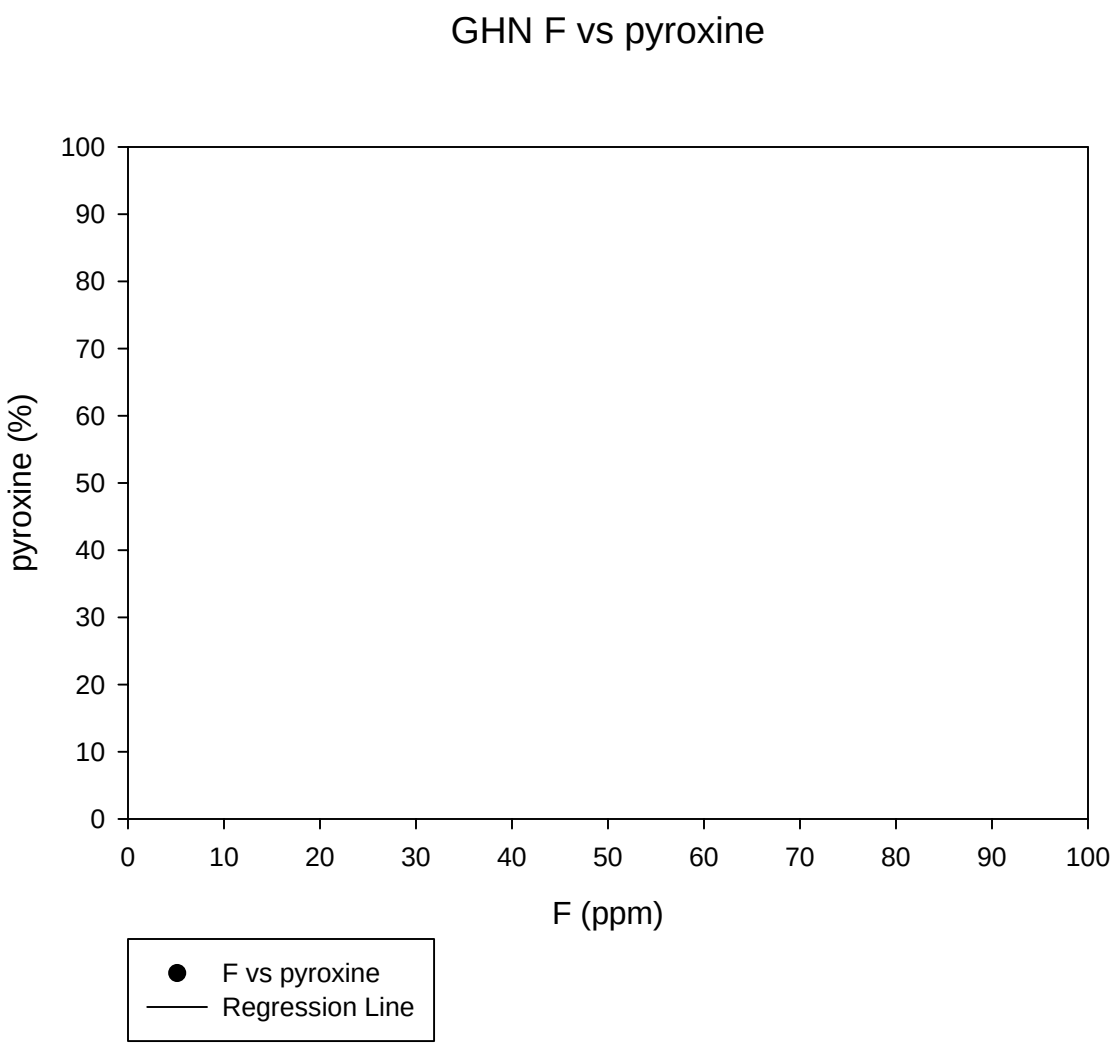
GHN F vs pyroxine
pyroxine (%)
100
90
80
70
60
50
40
30
20
10
0
0
10
20
30
40
50
60
70
80
90
100
F (ppm)
F vs pyroxine
Regression Line

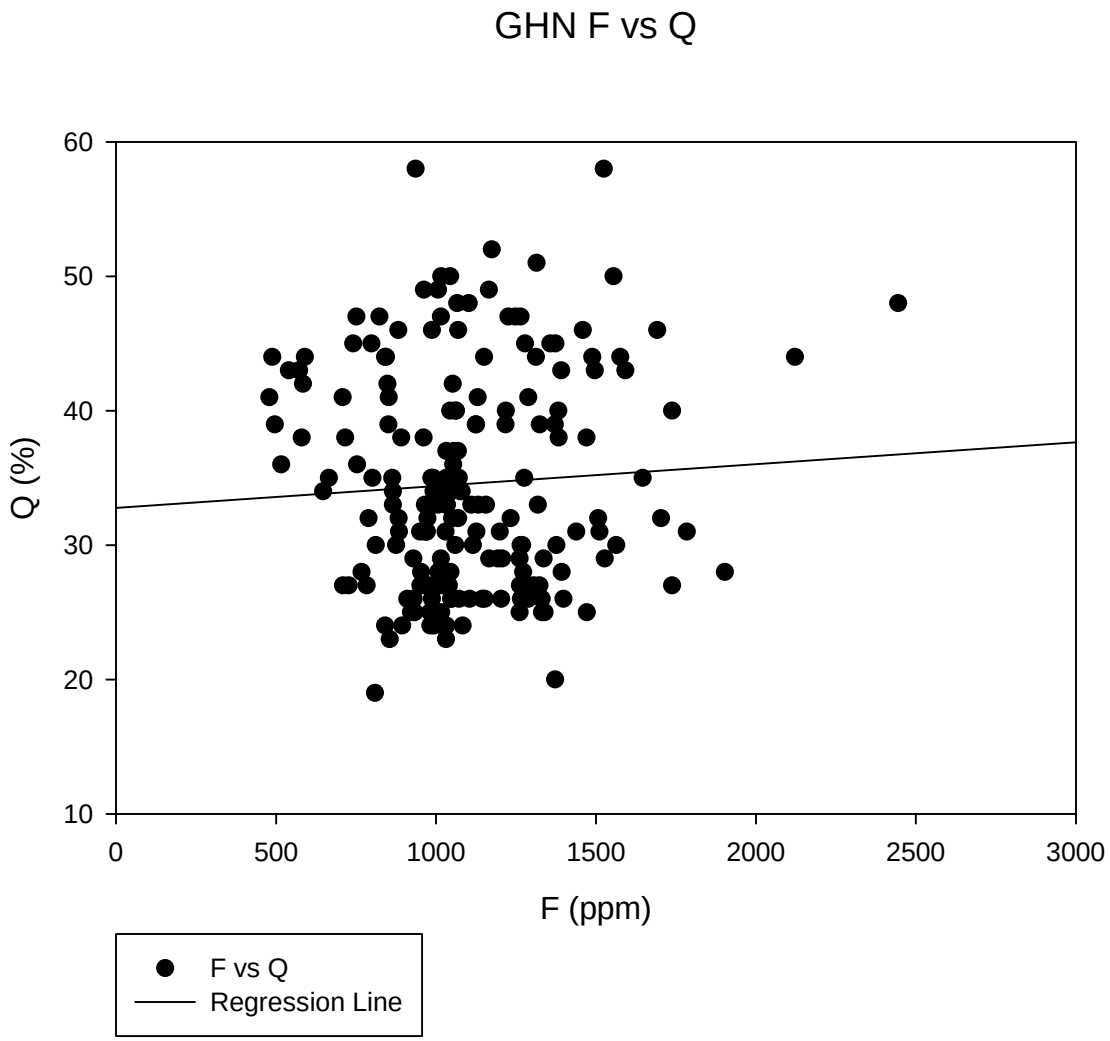
GHN F vs Q
60
50
40
30
20
10
Q (%)
0
500
1000
1500
2000
2500
3000
F (ppm)
F vs Q
Regression Line

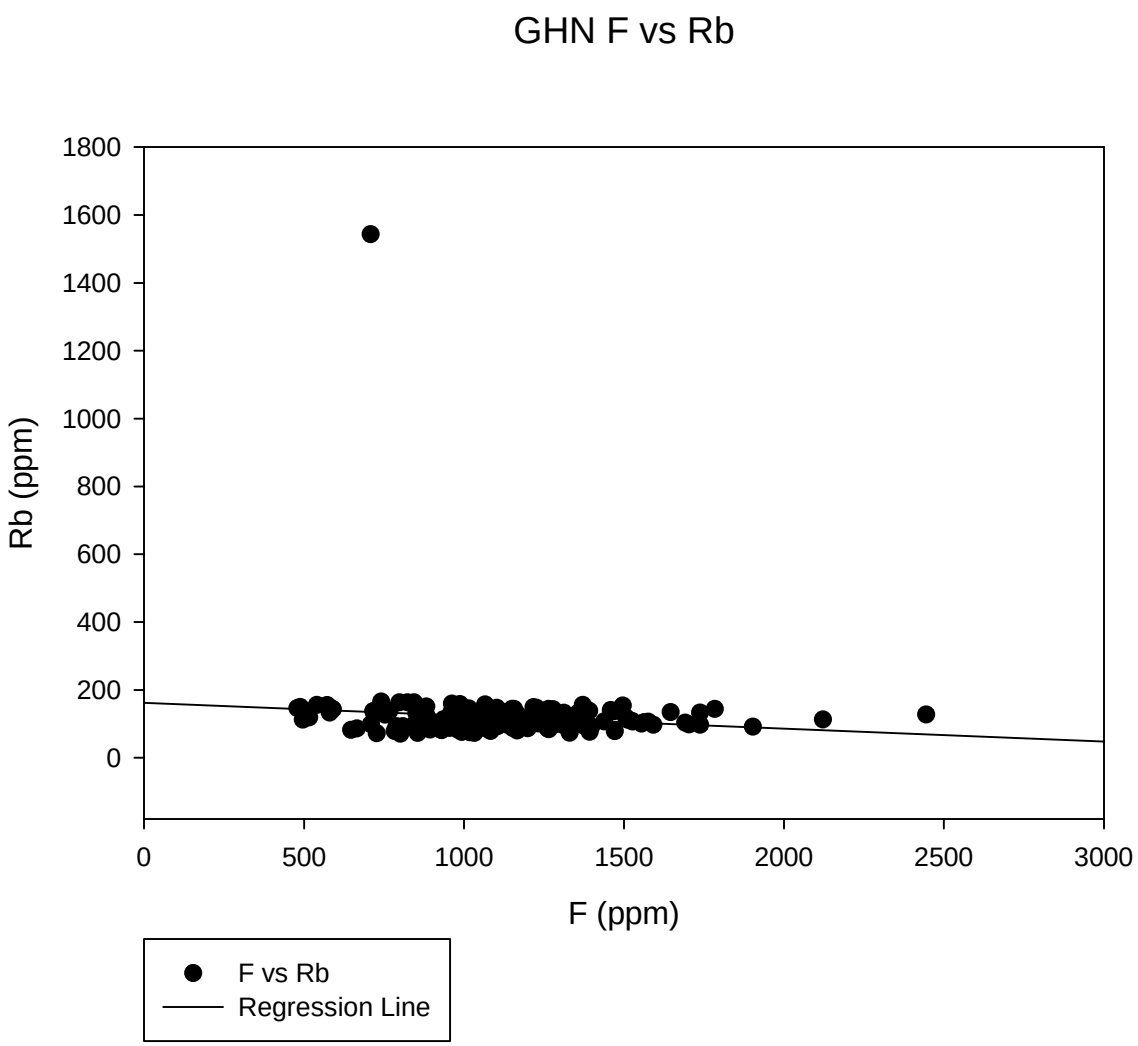
GHN F vs Rb
Rb (ppm)
1800
1600
1400
1200
1000
800
600
400
200
0
0
500
1000
1500
2000
2500
3000
F (ppm)
F vs Rb
Regression Line

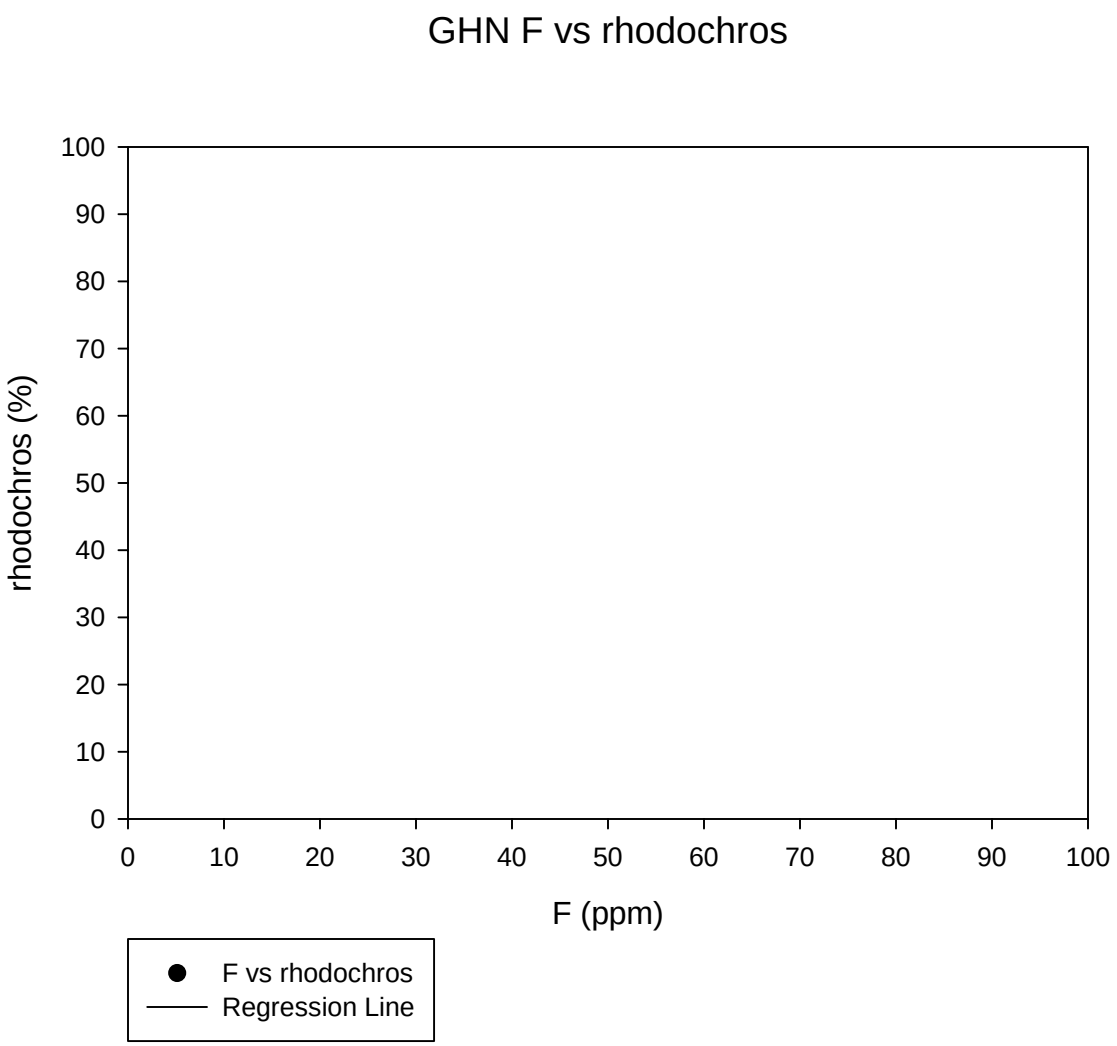
GHN F vs rhodochros
rhodochros (%)
100
90
80
70
60
50
40
30
20
10
0
0
10
20
30
40
50
60
70
80
90
100
F (ppm)
F vs rhodochros
Regression Line

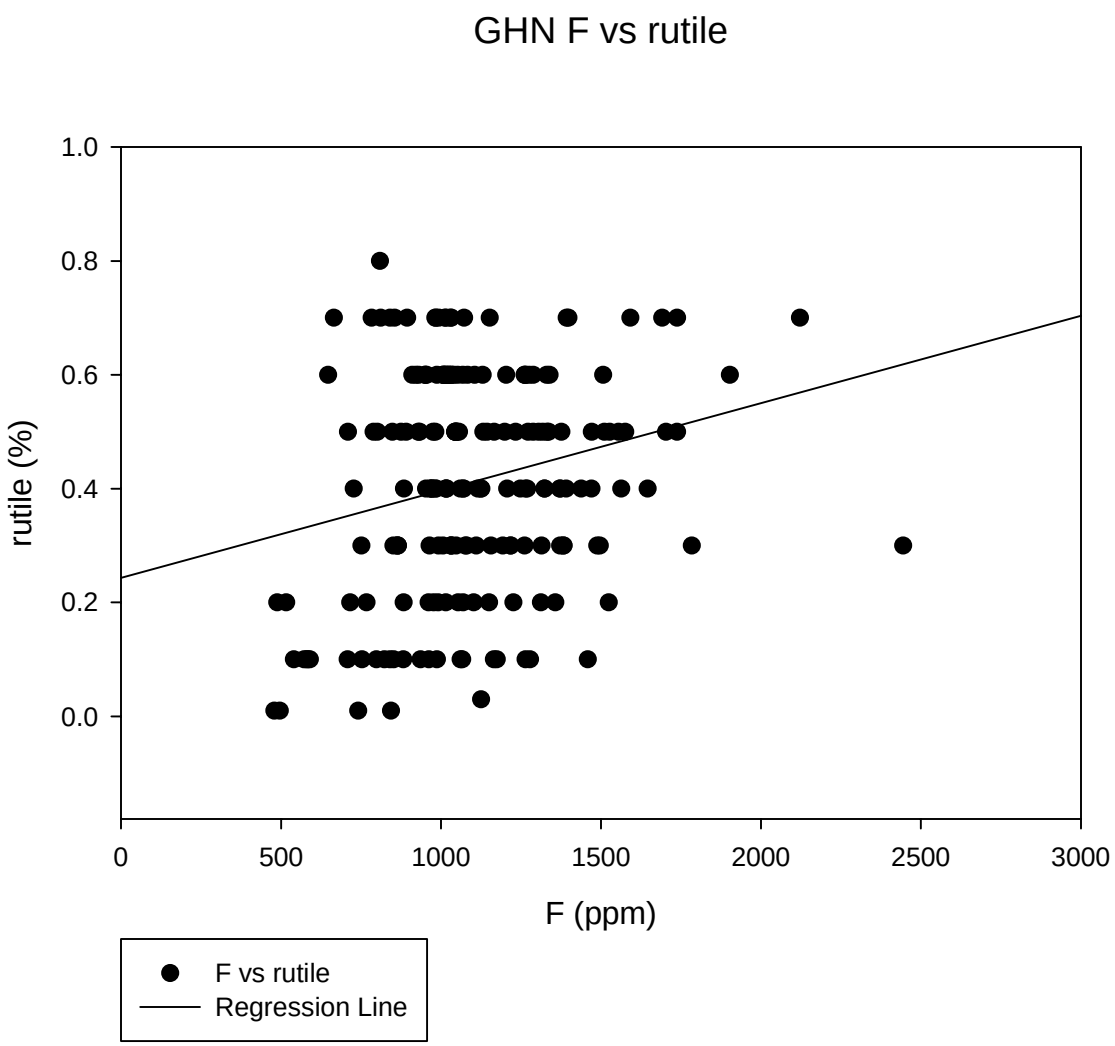
GHN F vs rutile
1.0
0.8
0.6
0.4
0.2
0.0
rutile (%)
0
500
1000
1500
2000
2500
3000
F (ppm)
F vs rutile
Regression Line

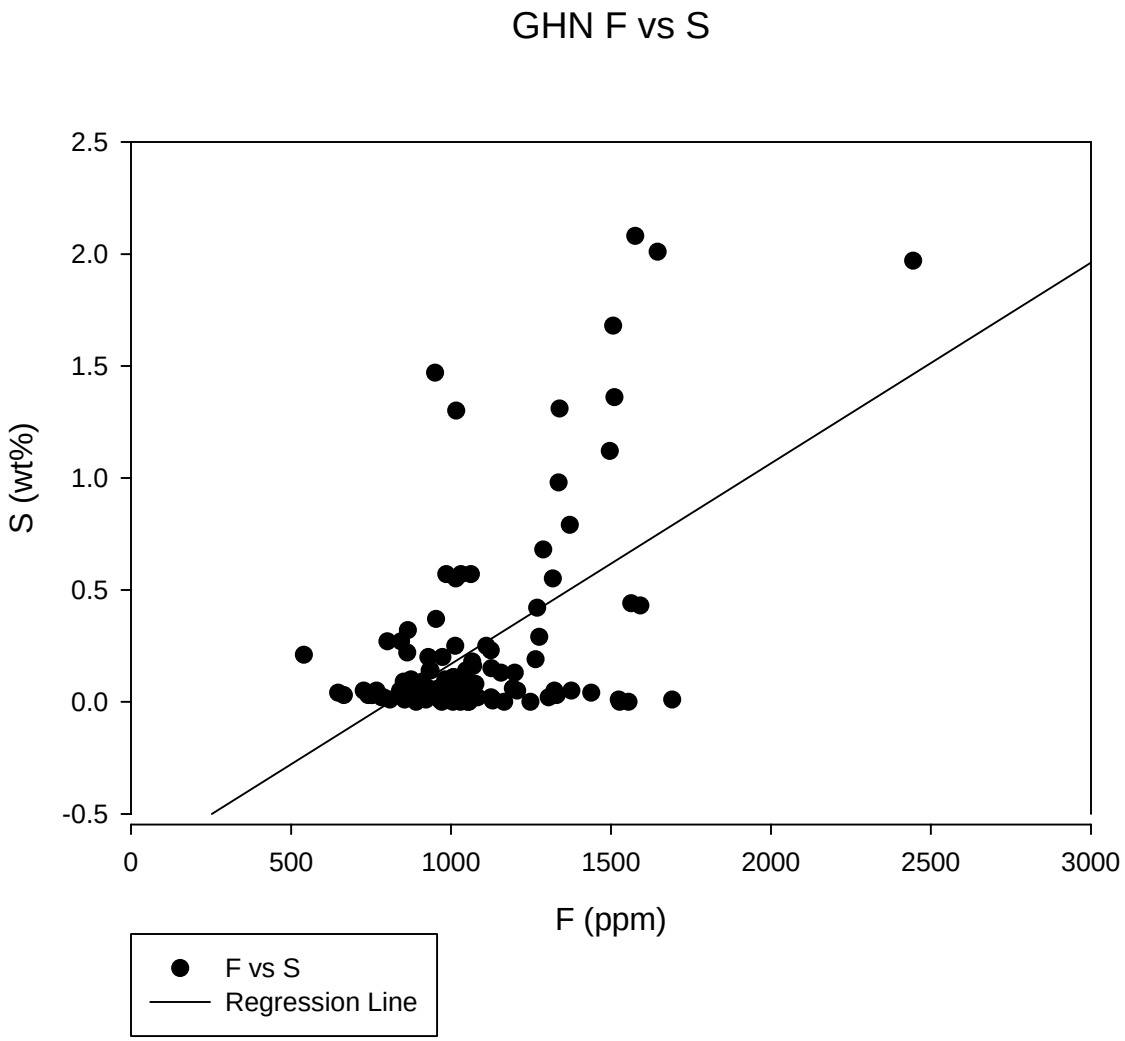
GHN F vs S
2.5
2.0
1.5
1.0
0.5
0.0
-0.5
S (wt%)
0
500
1000
1500
2000
2500
3000
F (ppm)
F vs S
Regression Line

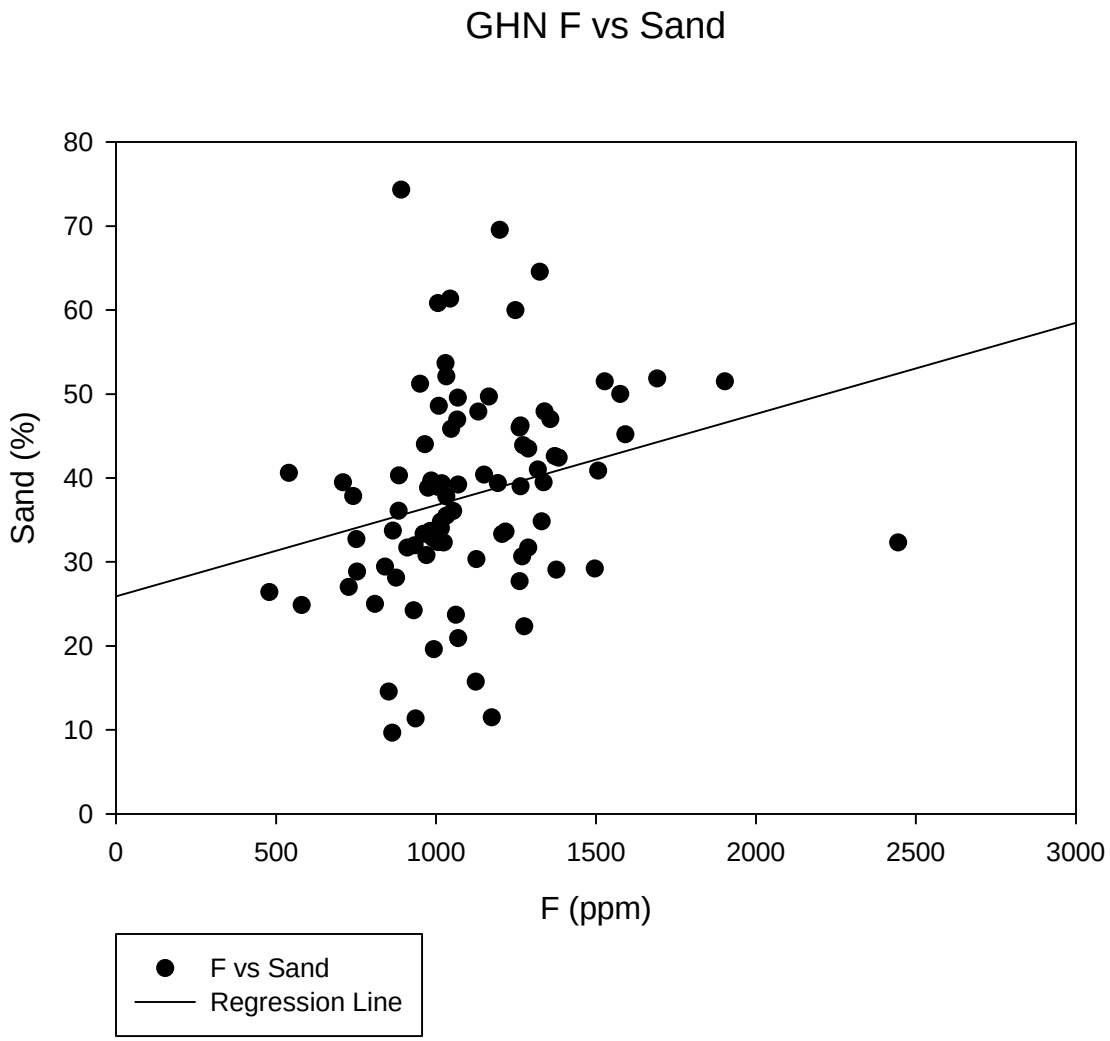
GHN F vs Sand
Sand (%)
F (ppm)
0
10
20
30
40
50
60
70
80
0
500
1000
1500
2000
2500
3000
F vs Sand
Regression Line

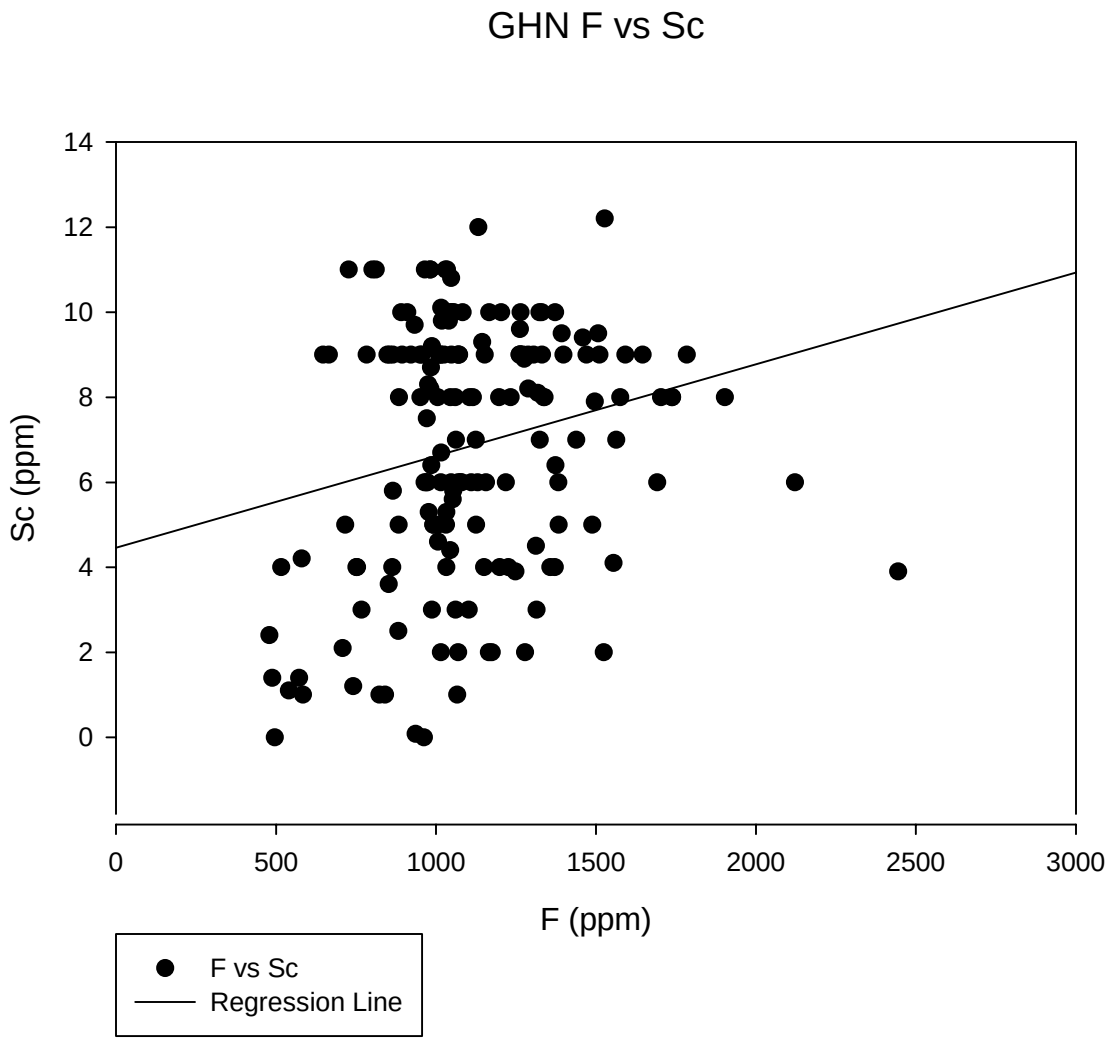
GHN F vs Sc
Sc (ppm)
14
12
10
8
6
4
2
0
0
500
1000
1500
2000
2500
3000
F (ppm)
F vs Sc
Regression Line

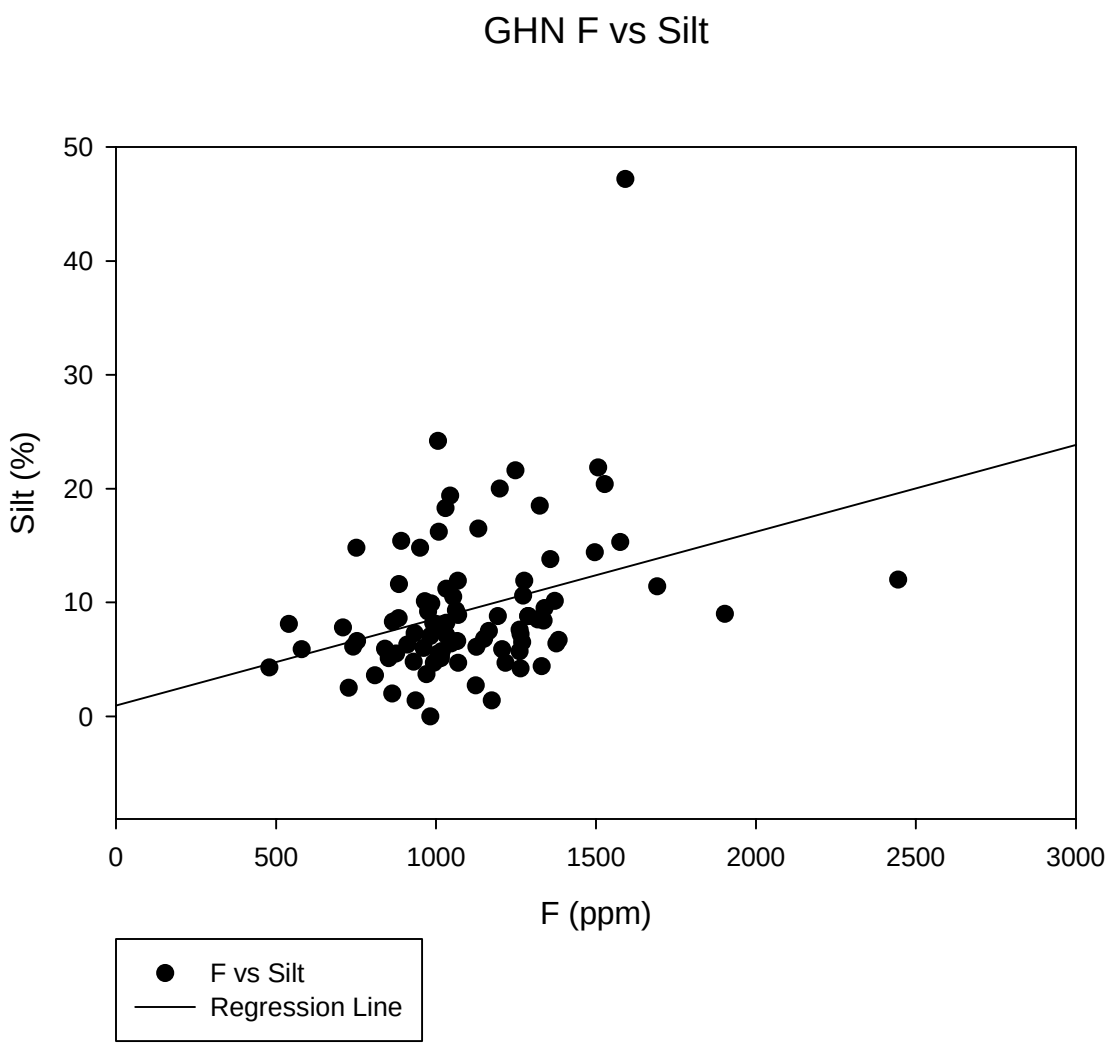
GHN F vs Silt
Silt (%)
50
40
30
20
10
0
0
500
1000
1500
2000
2500
3000
F (ppm)
F vs Silt
Regression Line

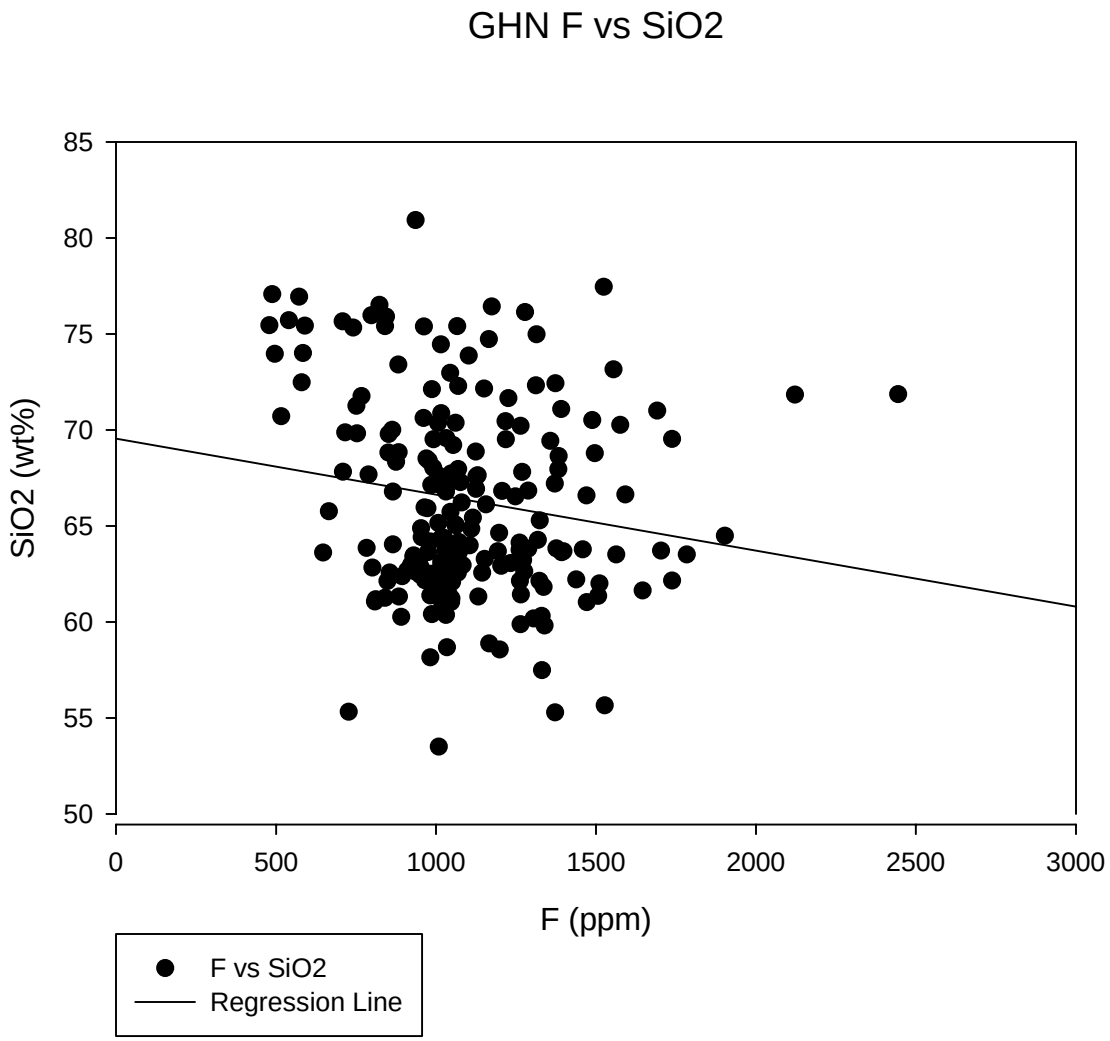
GHN F vs SiO2
85
80
75
70
65
60
55
50
SiO2 (wt%)
0
500
1000
1500
2000
2500
3000
F (ppm)
F vs SiO2
Regression Line

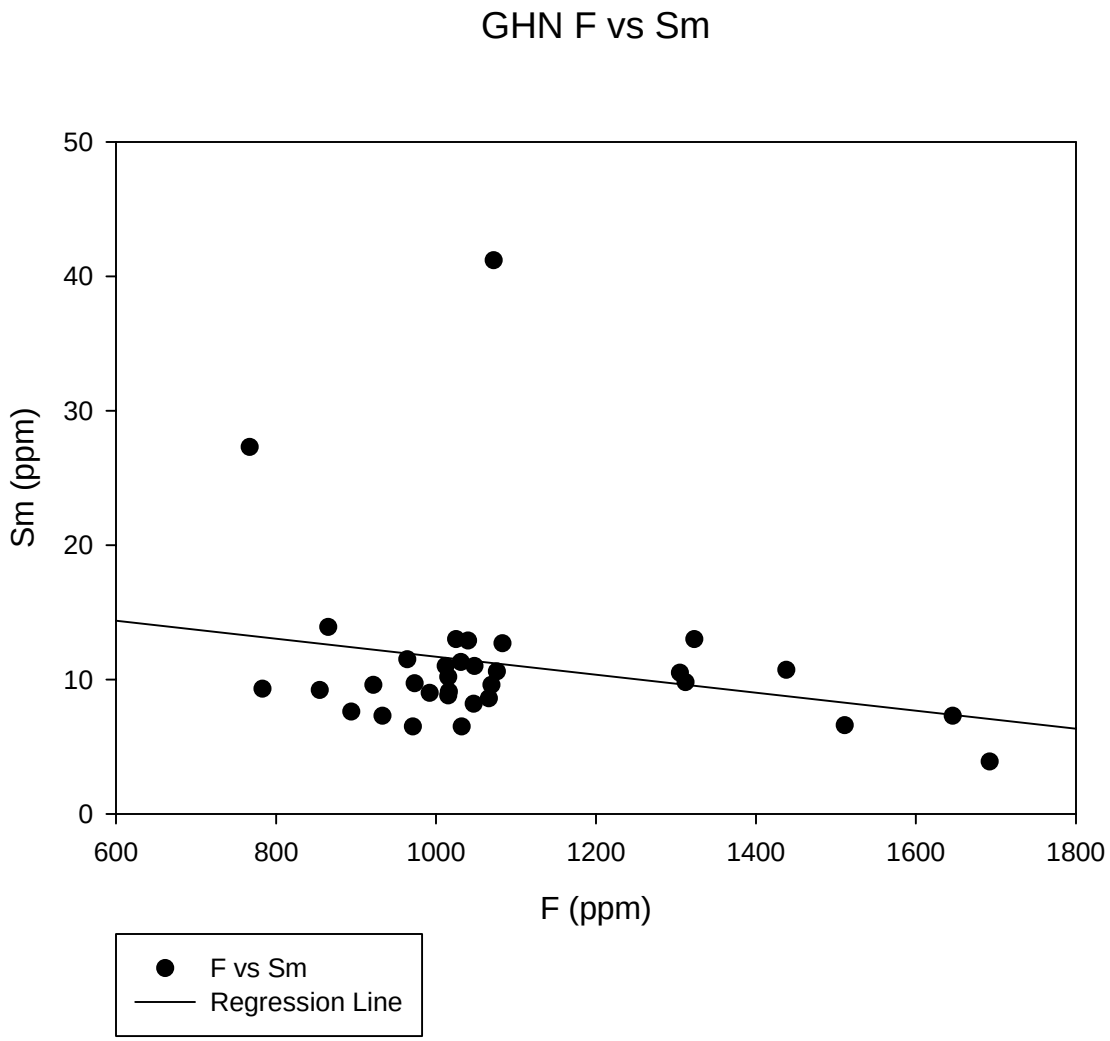
GHN F vs Sm
Sm (ppm)
F (ppm)
0
10
20
30
40
50
600
800
1000
1200
1400
1600
1800
F vs Sm
Regression Line

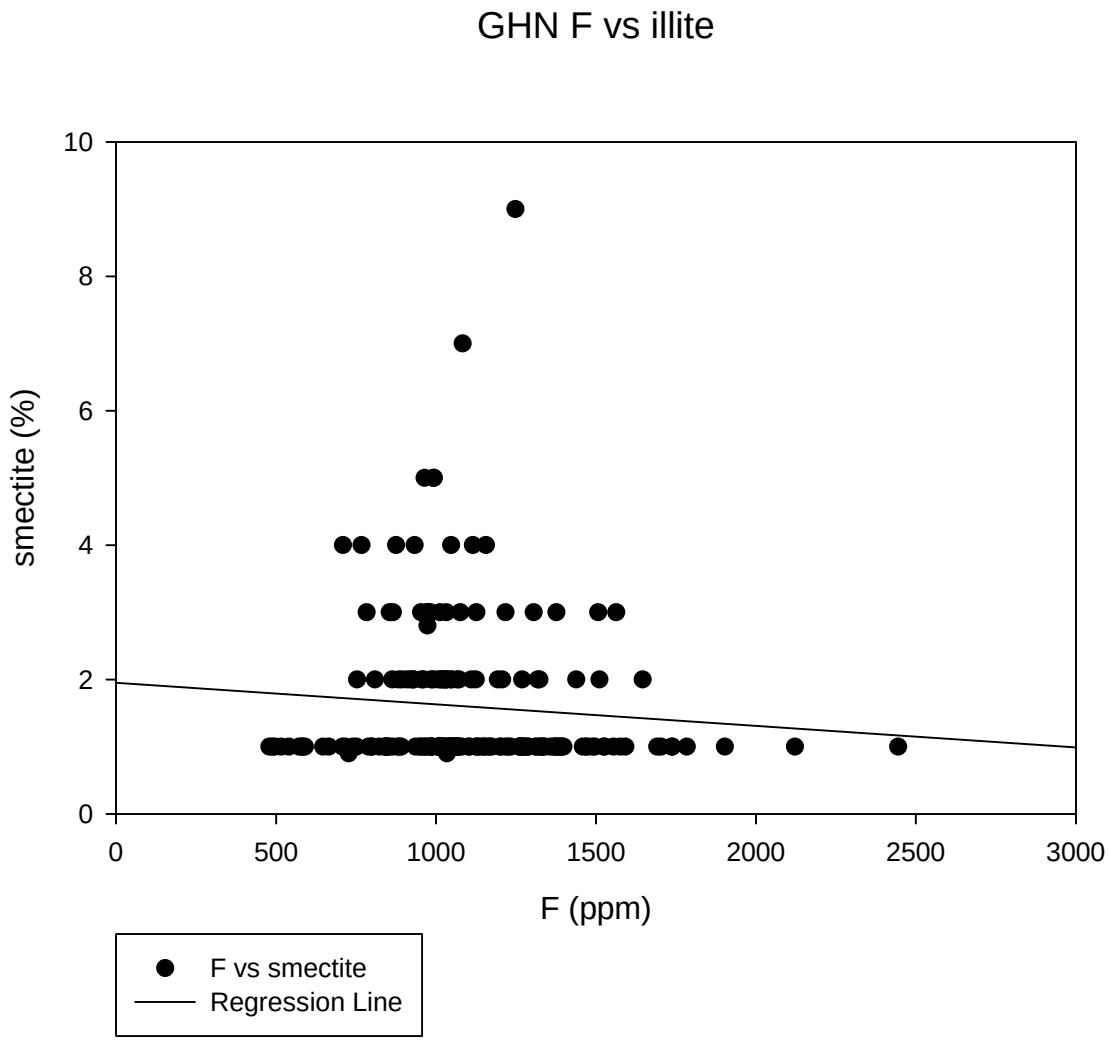
GHN F vs illite
smectite (%)
10
8
6
4
2
0
0
500
1000
1500
2000
2500
3000
F (ppm)
F vs smectite
Regression Line

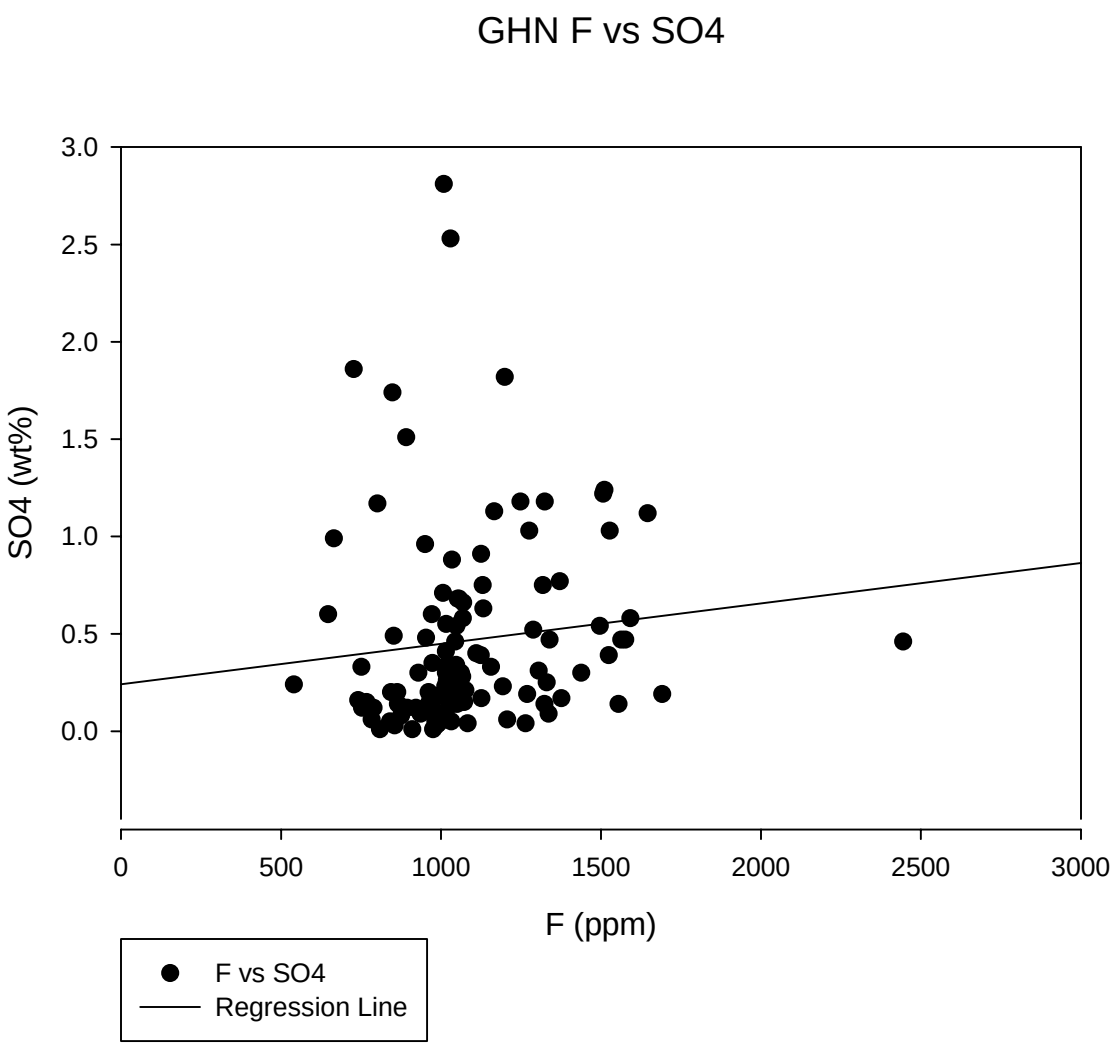
GHN F vs SO4
SO4 (wt%)
3.0
2.5
2.0
1.5
1.0
0.5
0.0
0
500
1000
1500
2000
2500
3000
F (ppm)
F vs SO4
Regression Line

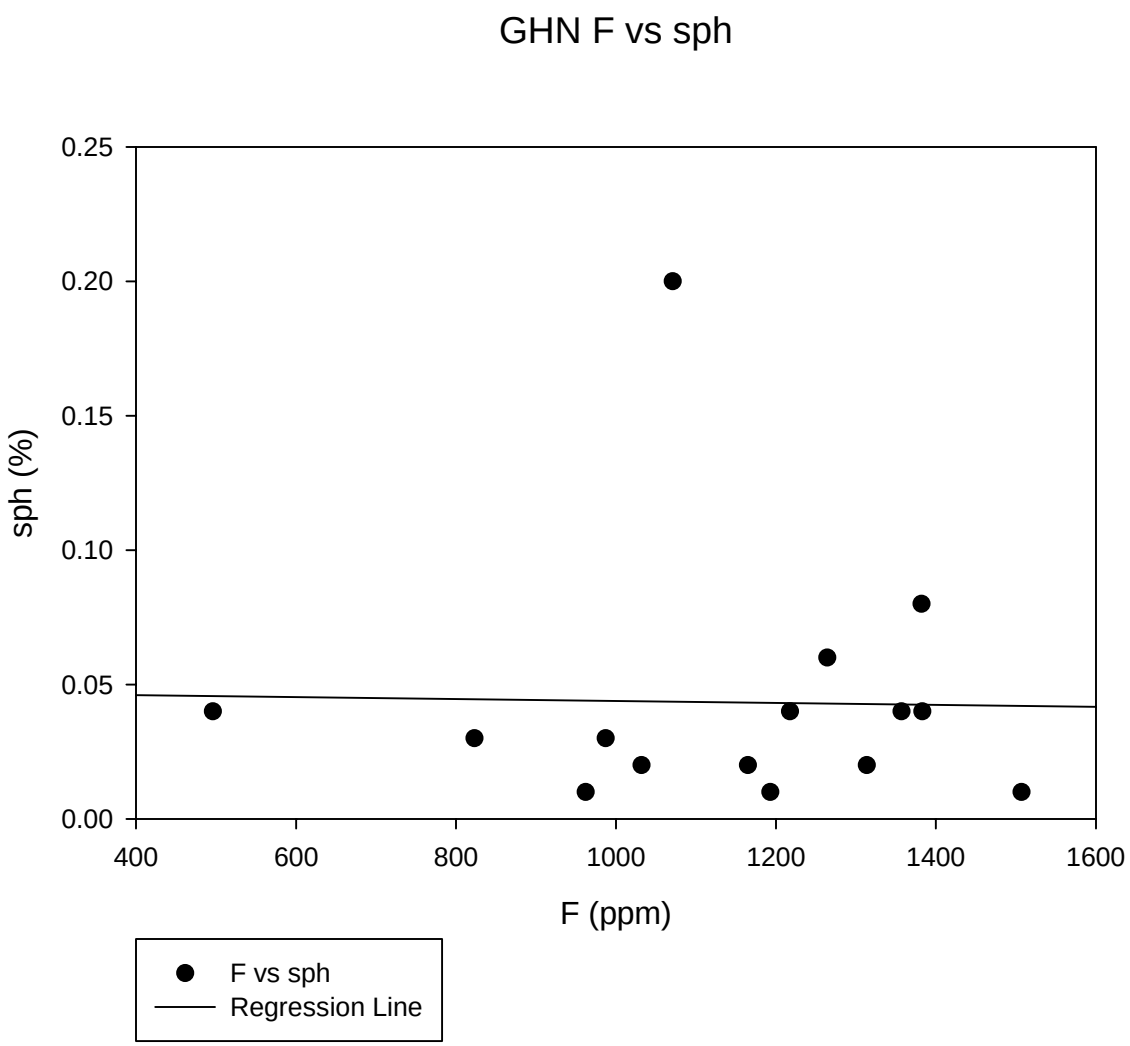
GHN F vs sph
0.25
0.20
0.15
0.10
0.05
0.00
sph (%)
400
600
800
1000
1200
1400
1600
F (ppm)
F vs sph
Regression Line

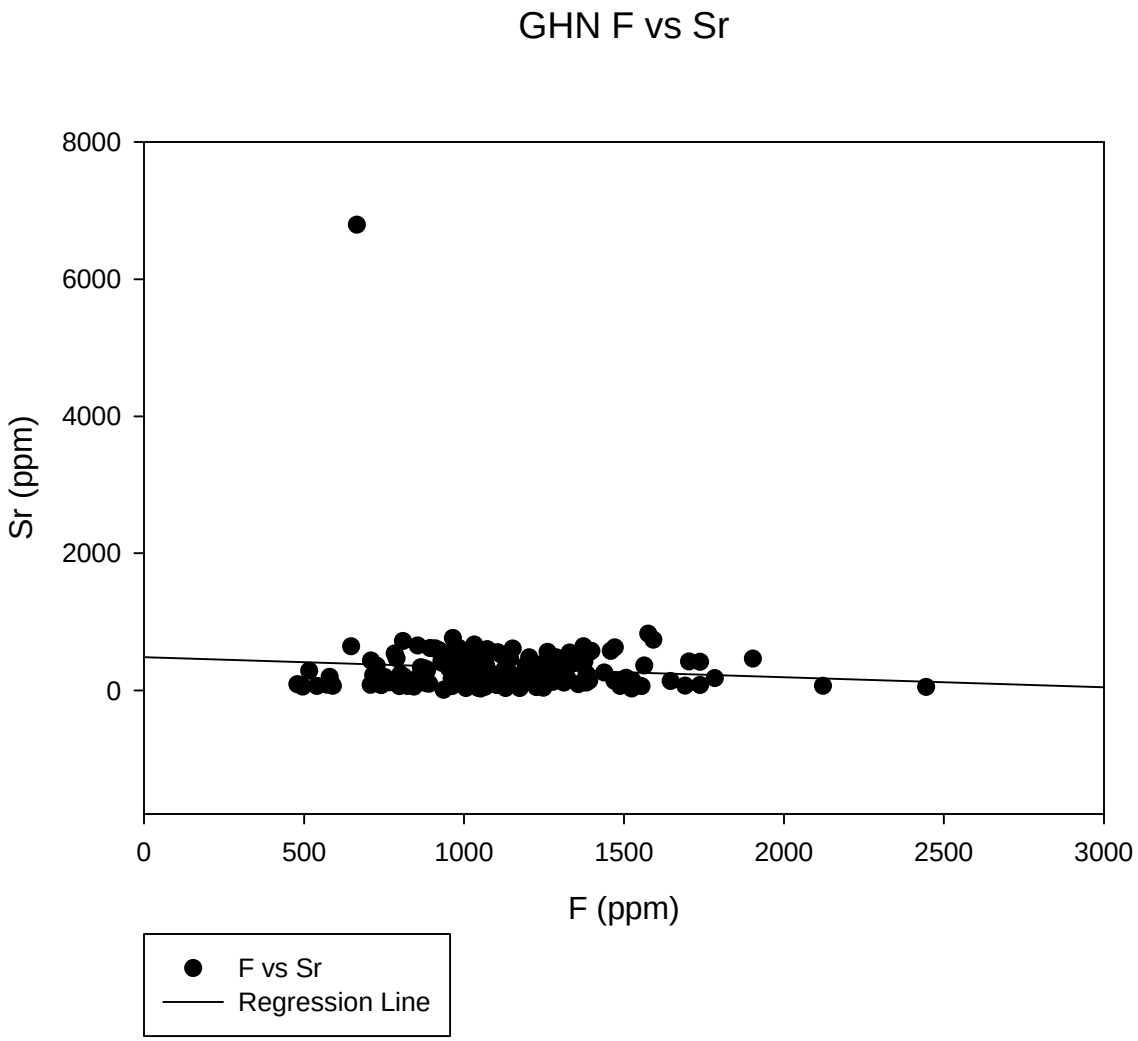
GHN F vs Sr
8000
6000
4000
2000
0
Sr (ppm)
0
500
1000
1500
2000
2500
3000
F (ppm)
F vs Sr
Regression Line

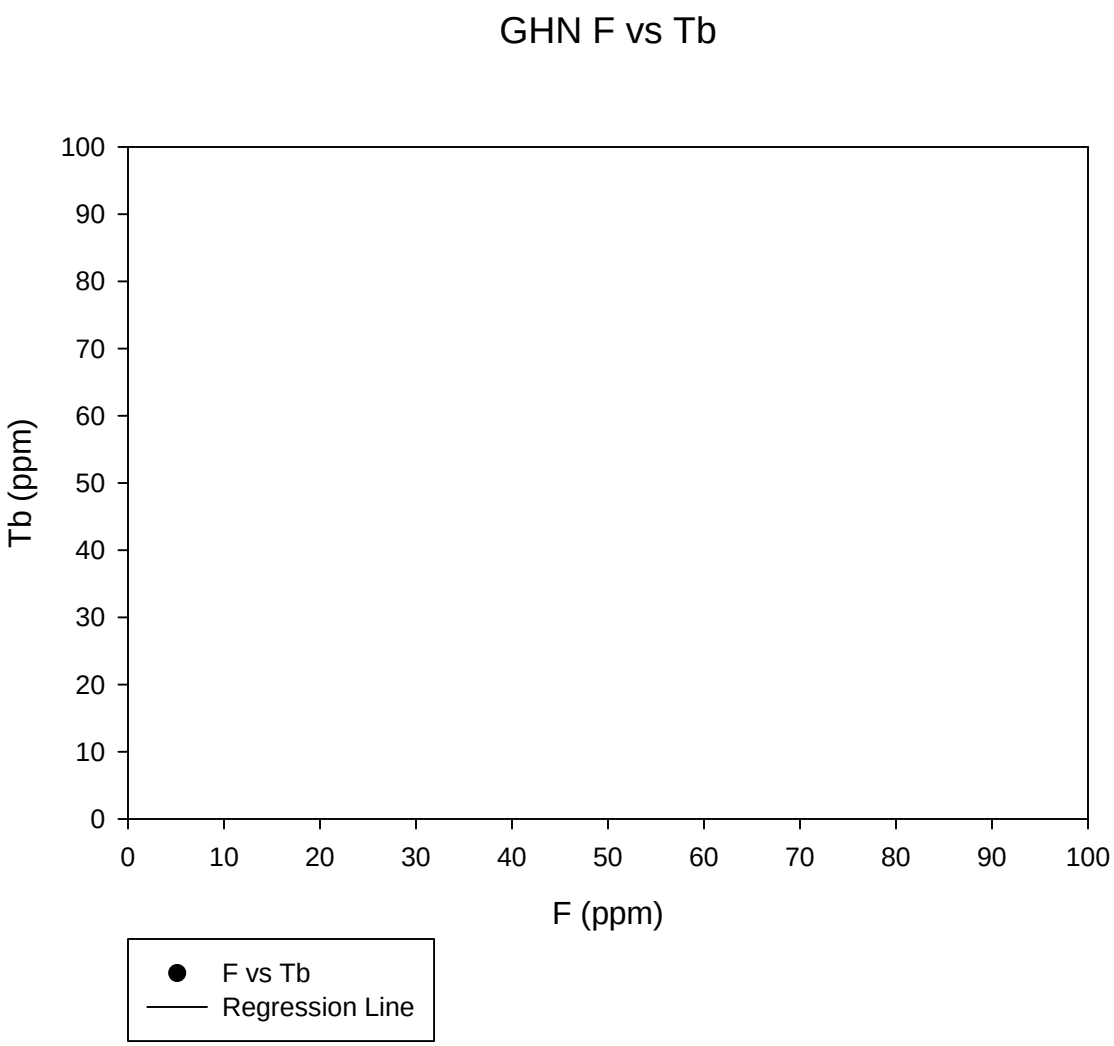
GHN F vs Tb
Tb (ppm)
F (ppm)
0
10
20
30
40
50
60
70
80
90
100
F vs Tb
Regression Line

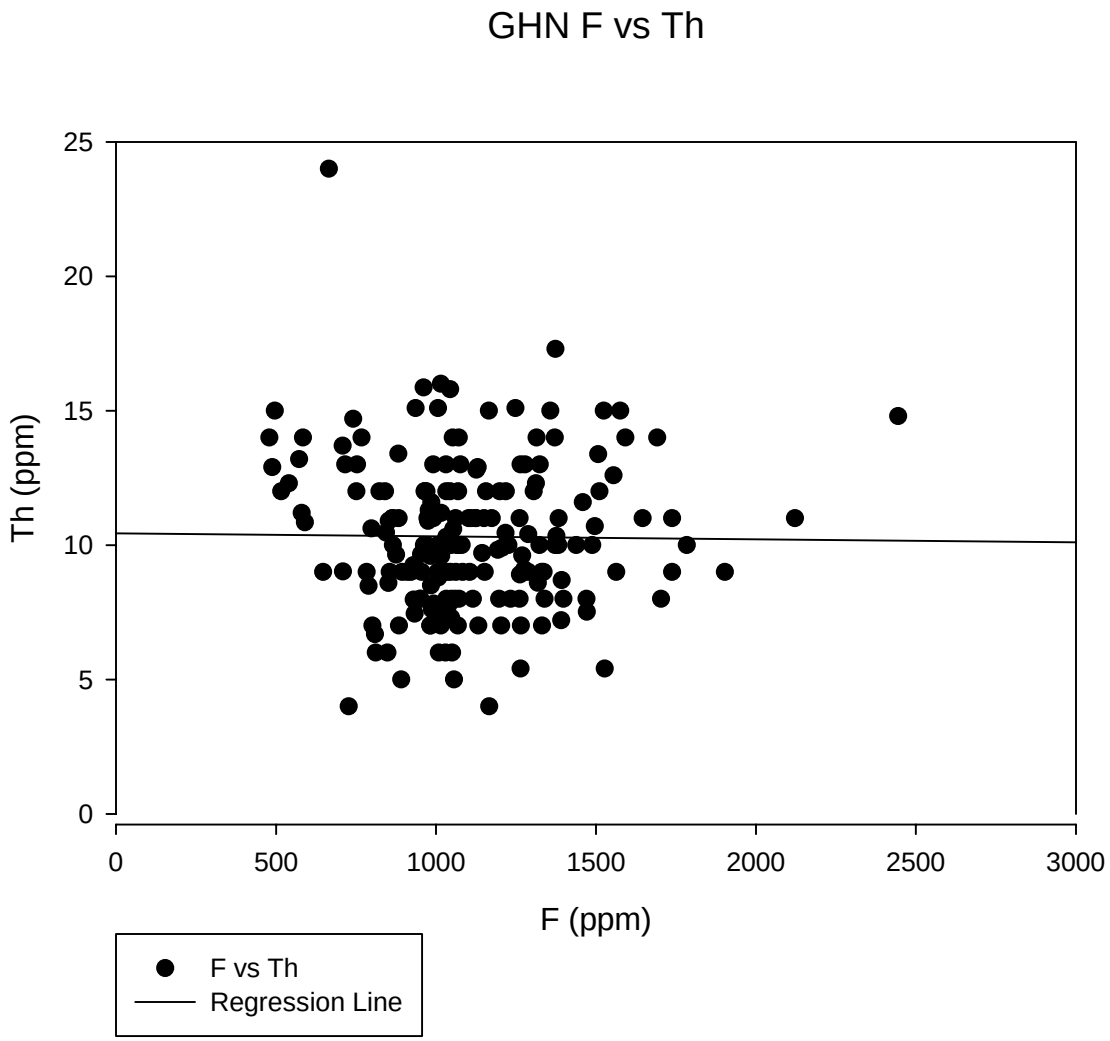
GHN F vs Th
Th (ppm)
25
20
15
10
5
0
0
500
1000
1500
2000
2500
3000
F (ppm)
F vs Th
Regression Line

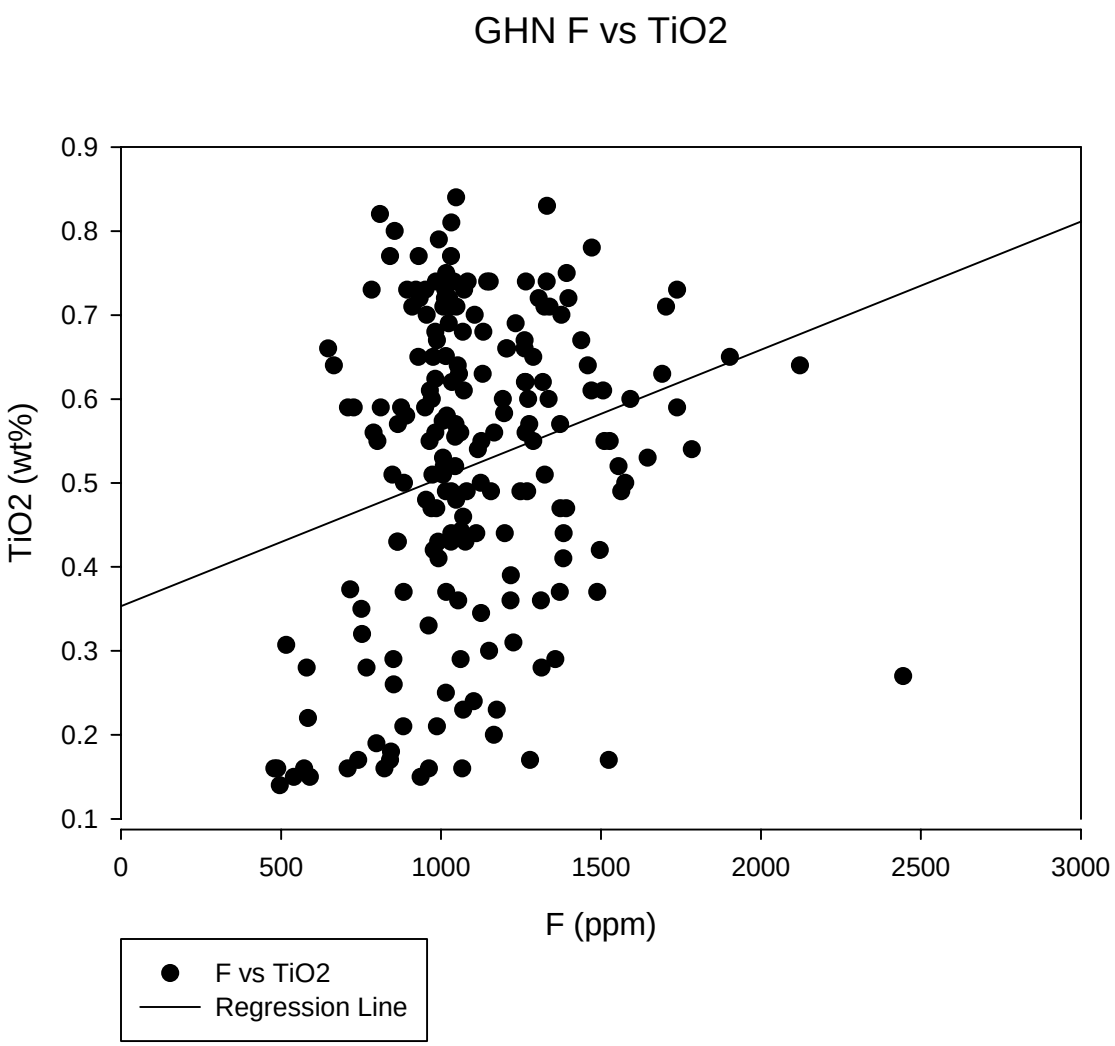
GHN F vs TiO2
TiO2 (wt%)
0.9
0.8
0.7
0.6
0.5
0.4
0.3
0.2
0.1
0
500
1000
1500
2000
2500
3000
F (ppm)
F vs TiO2
Regression Line

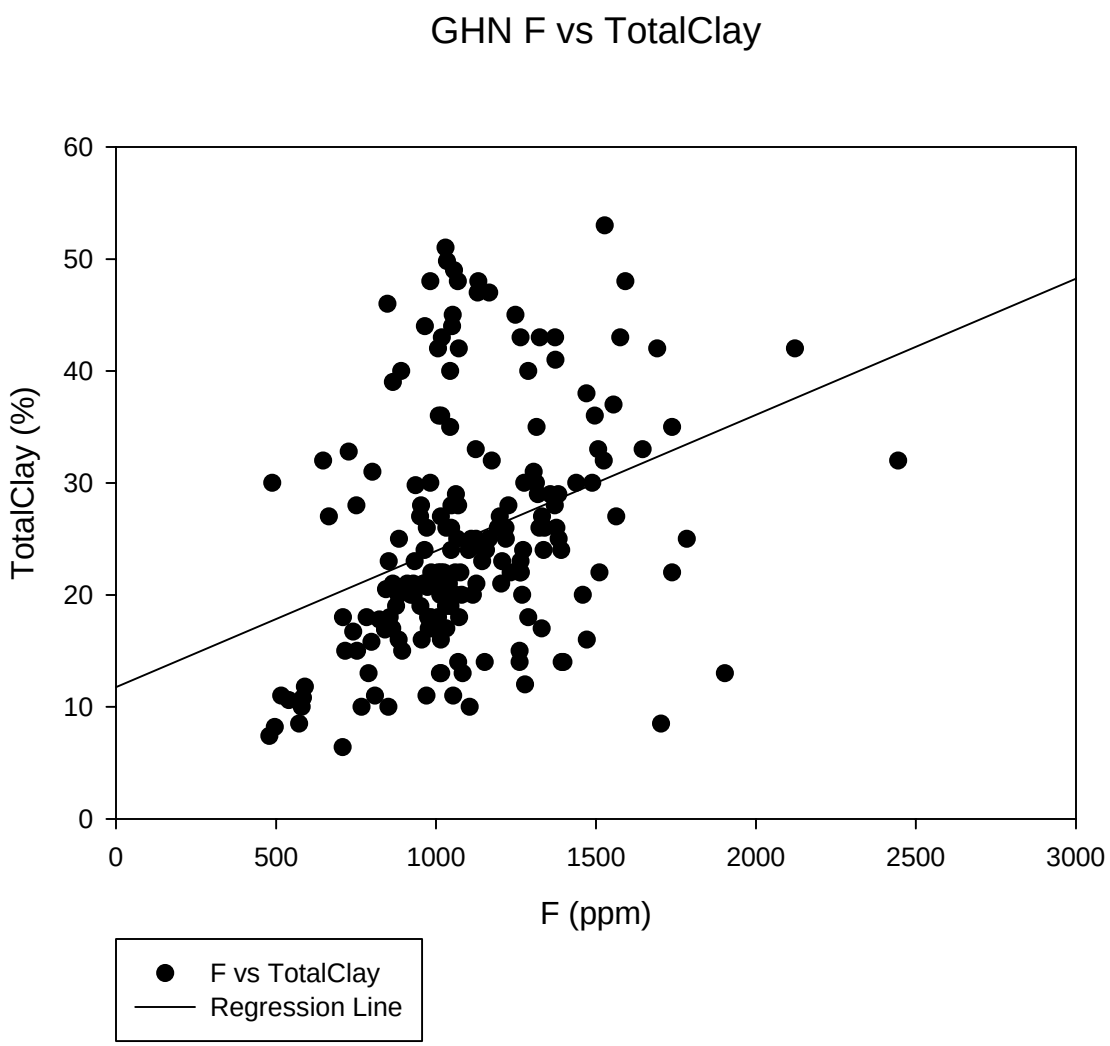
GHN F vs TotalClay
TotalClay (%)
F (ppm)
0
10
20
30
40
50
60
0
500
1000
1500
2000
2500
3000
F vs TotalClay
Regression Line

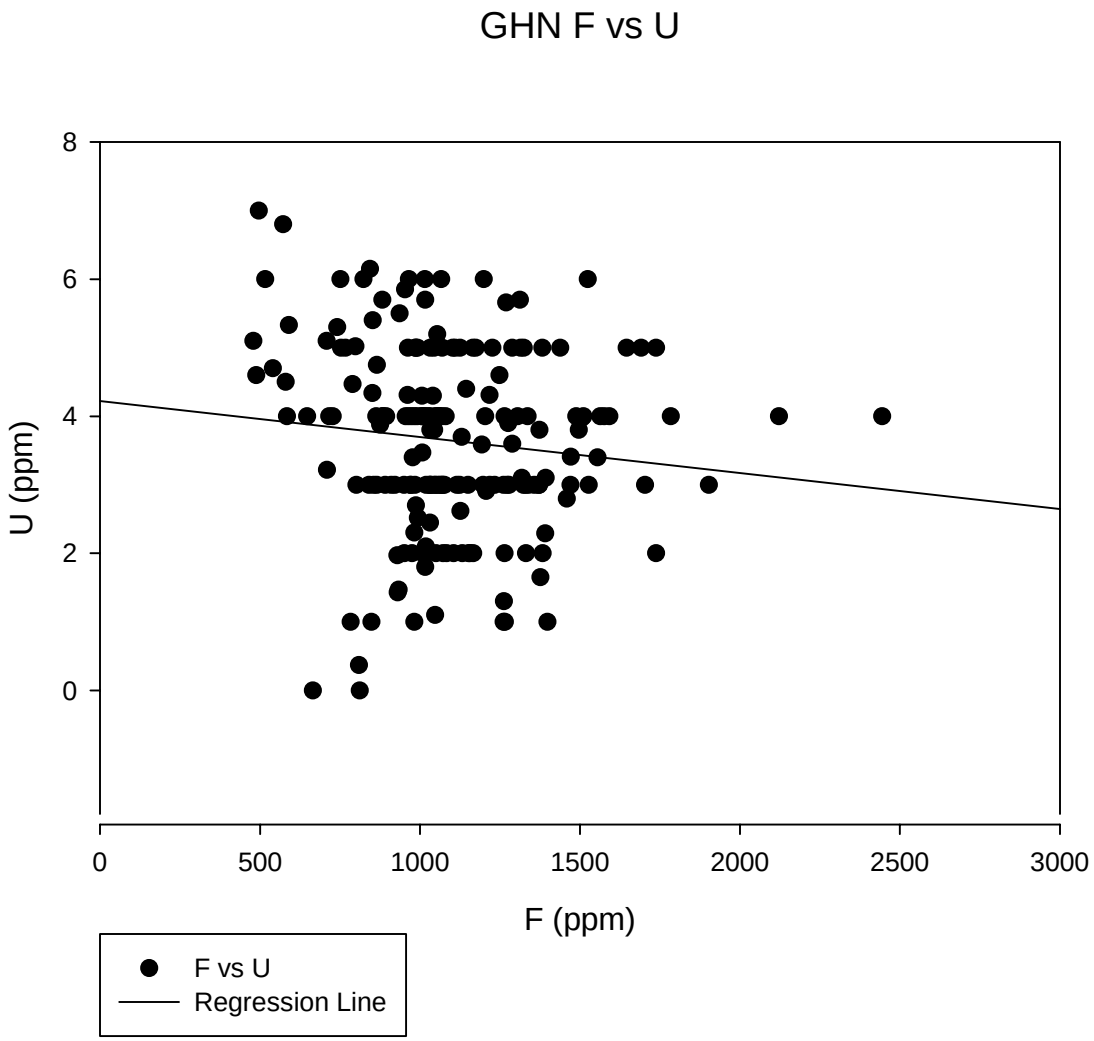
GHN F vs U
8
6
4
2
0
U (ppm)
0
500
1000
1500
2000
2500
3000
F (ppm)
F vs U
Regression Line

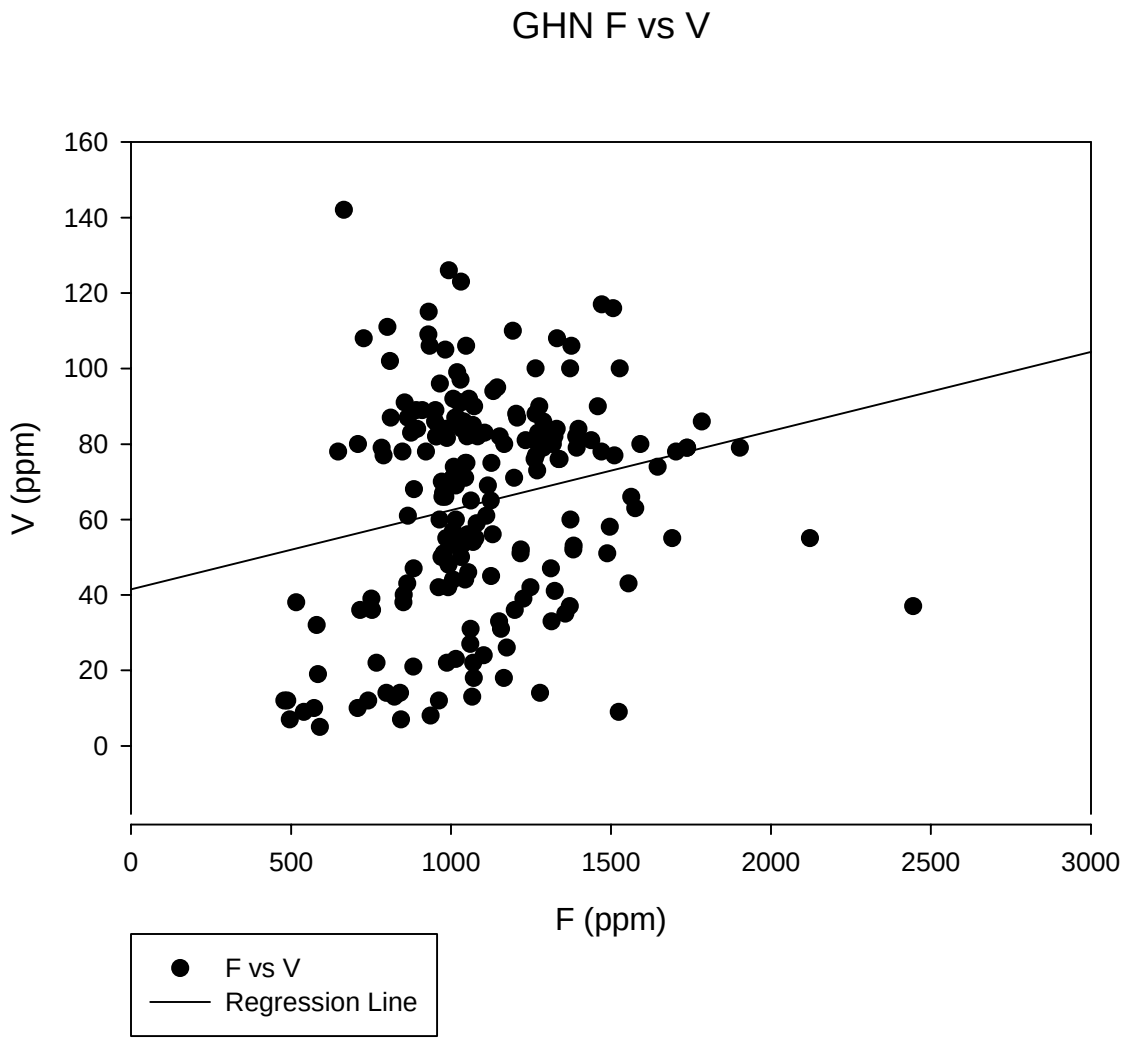
GHN F vs V
160
140
120
100
80
60
40
20
0
V (ppm)
0
500
1000
1500
2000
2500
3000
F (ppm)
F vs V
Regression Line

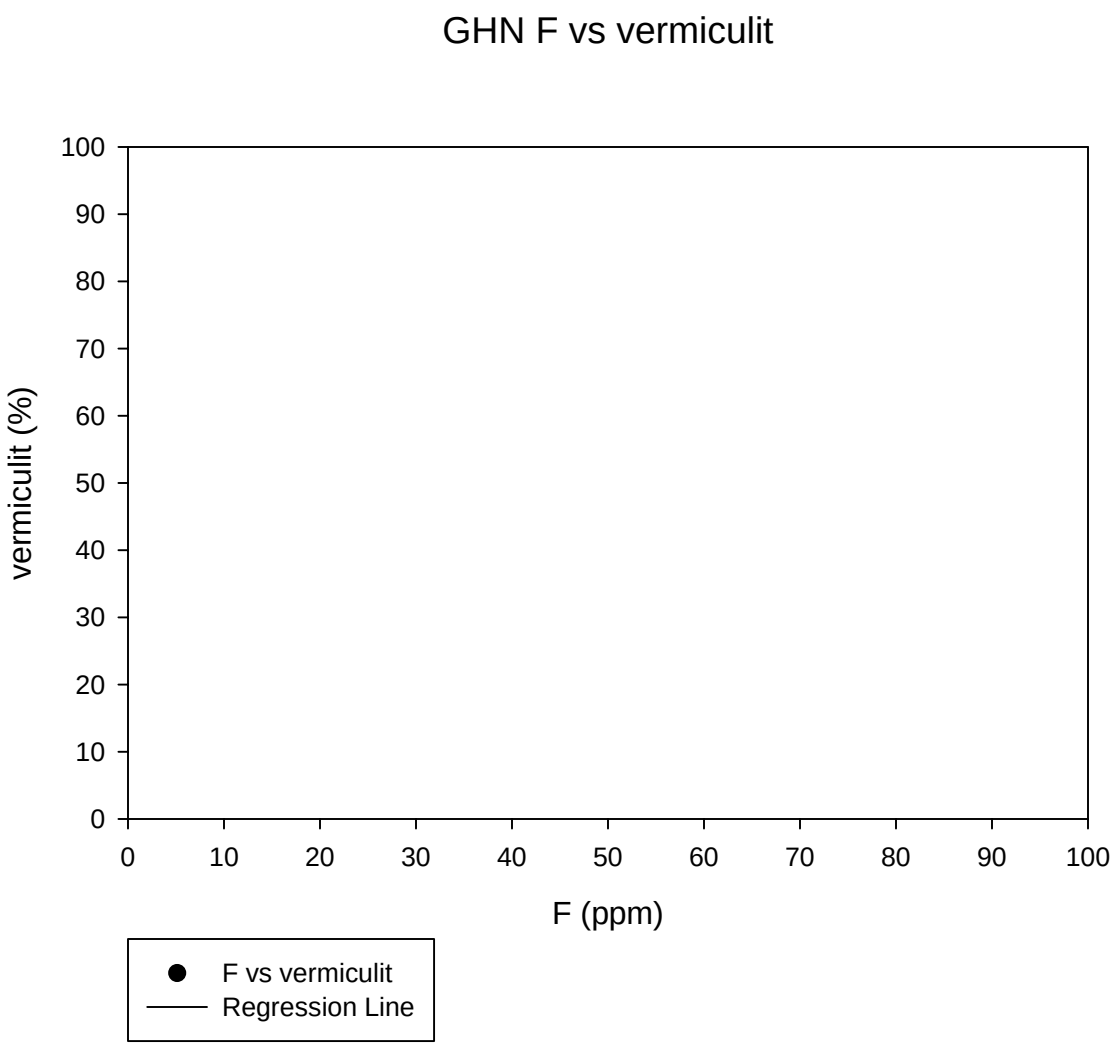
GHN F vs vermiculit
vermiculit (%)
100
90
80
70
60
50
40
30
20
10
0
0
10
20
30
40
50
60
70
80
90
100
F (ppm)
F vs vermiculit
Regression Line

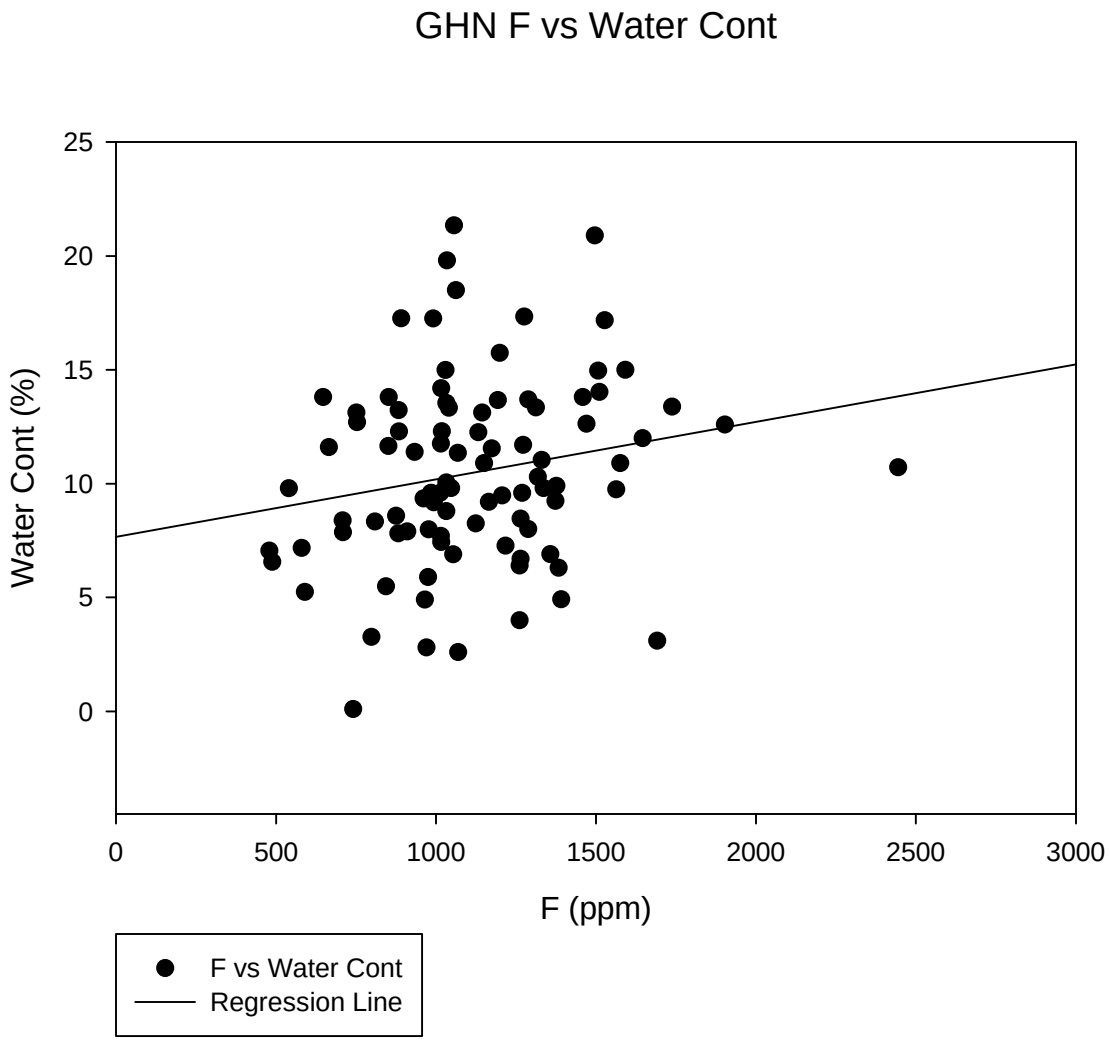
GHN F vs Water Cont
Water Cont (%)
25
20
15
10
5
0
0
500
1000
1500
2000
2500
3000
F (ppm)
F vs Water Cont
Regression Line

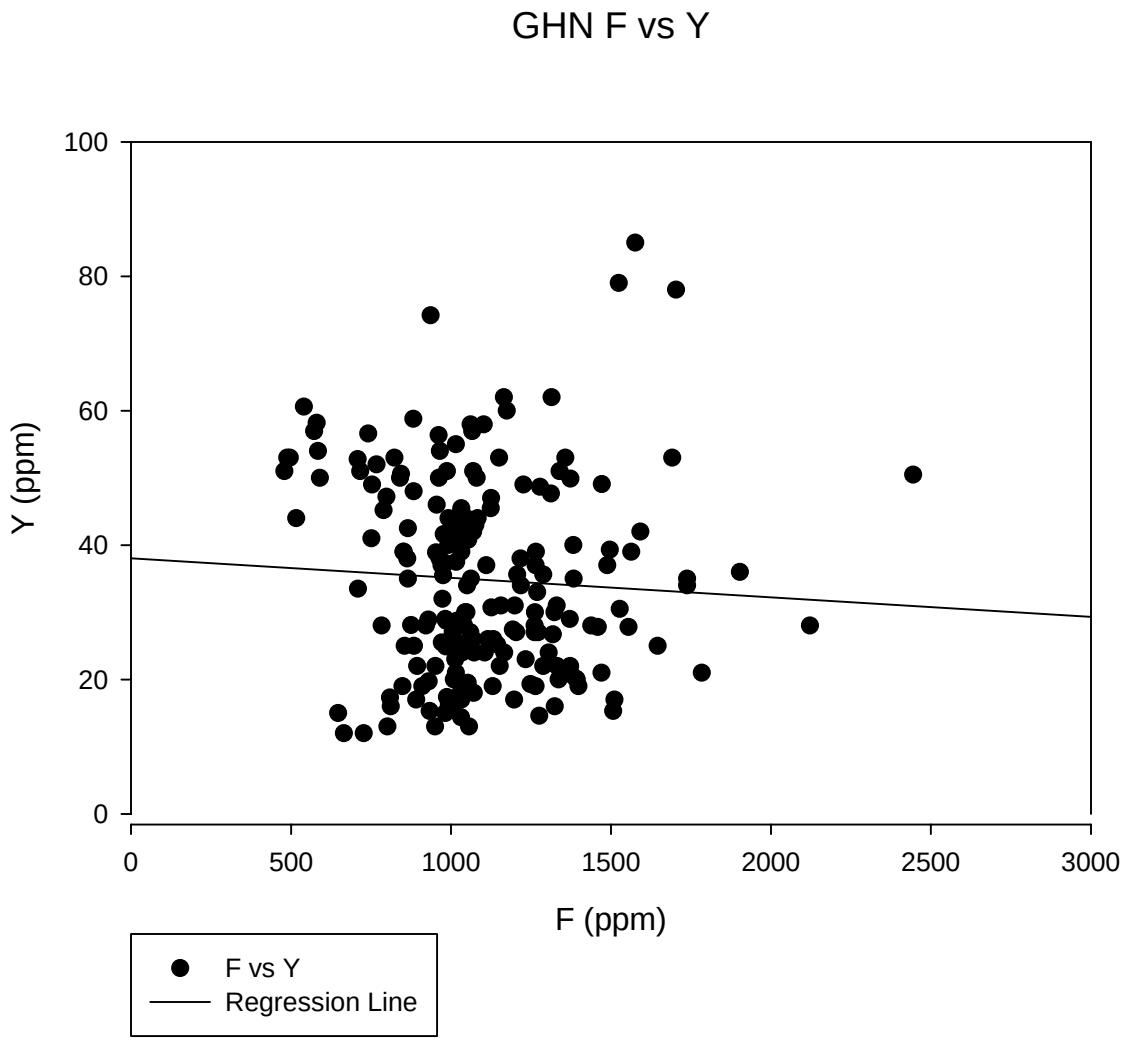
GHN F vs Y
100
80
60
40
20
0
Y (ppm)
0
500
1000
1500
2000
2500
3000
F (ppm)
F vs Y
Regression Line

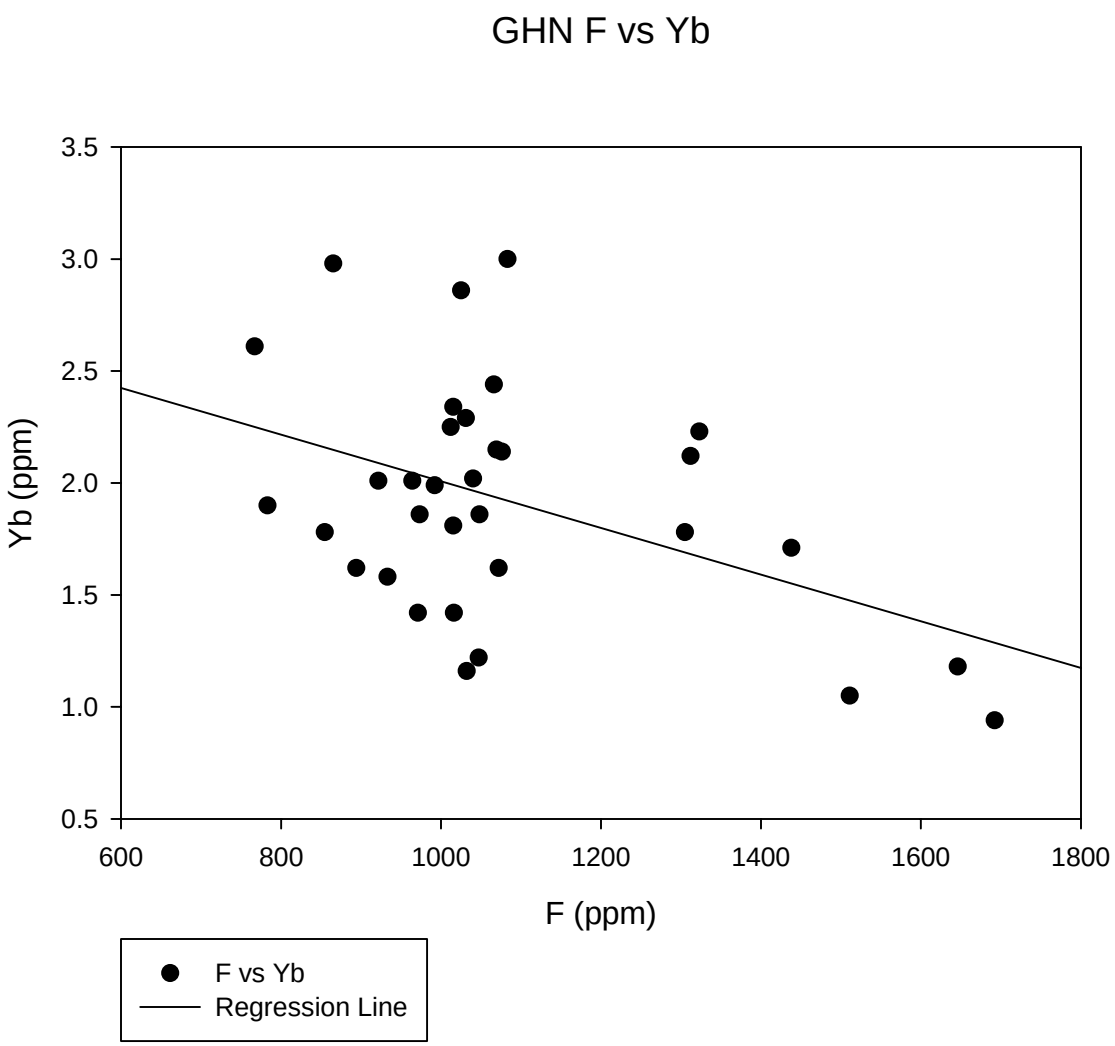
GHN F vs Yb
3.5
3.0
2.5
2.0
1.5
1.0
0.5
Yb (ppm)
600
800
1000
1200
1400
1600
1800
F (ppm)
F vs Yb
Regression Line

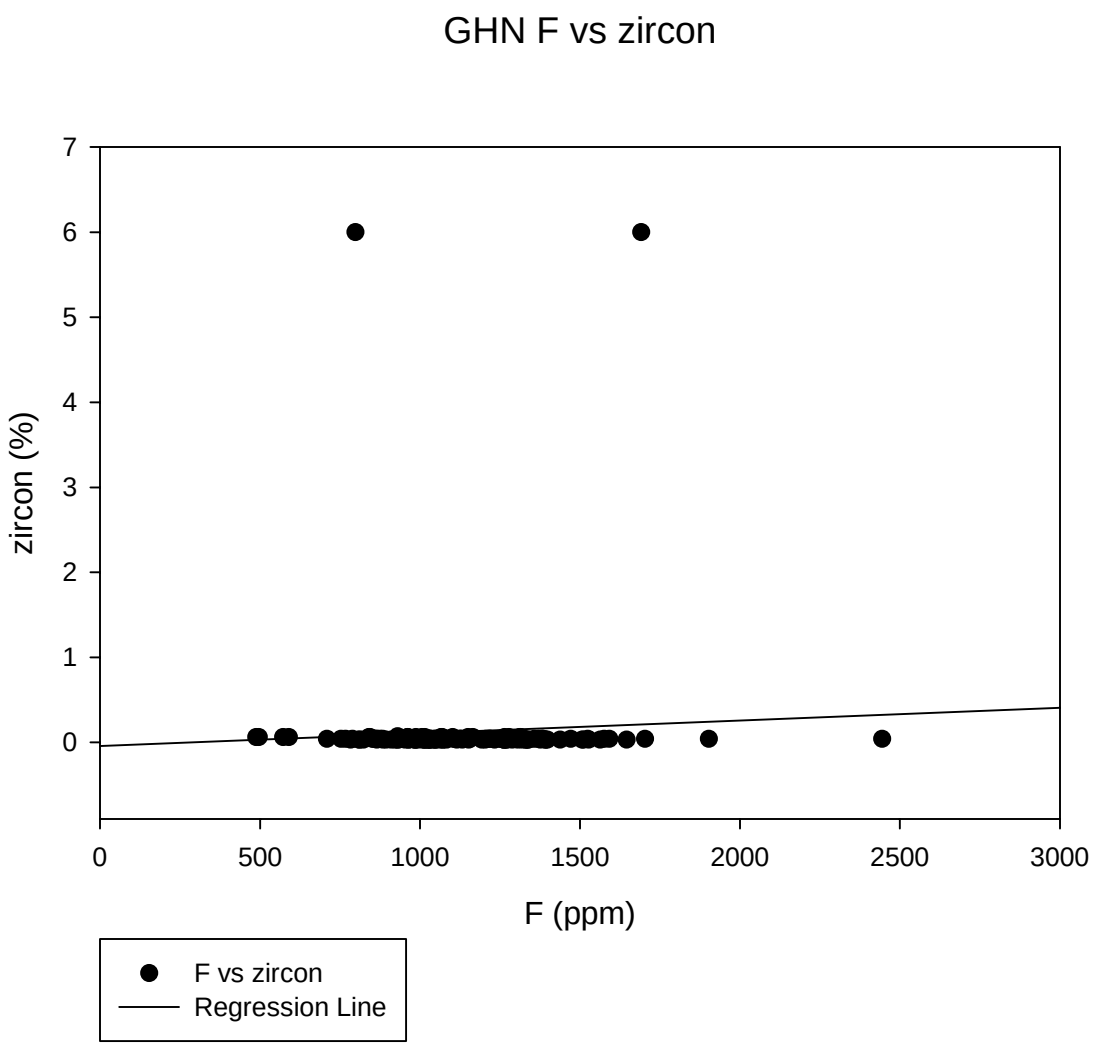
GHN F vs zircon
zircon (%)
7
6
5
4
3
2
1
0
0
500
1000
1500
2000
2500
3000
F (ppm)
F vs zircon
Regression Line

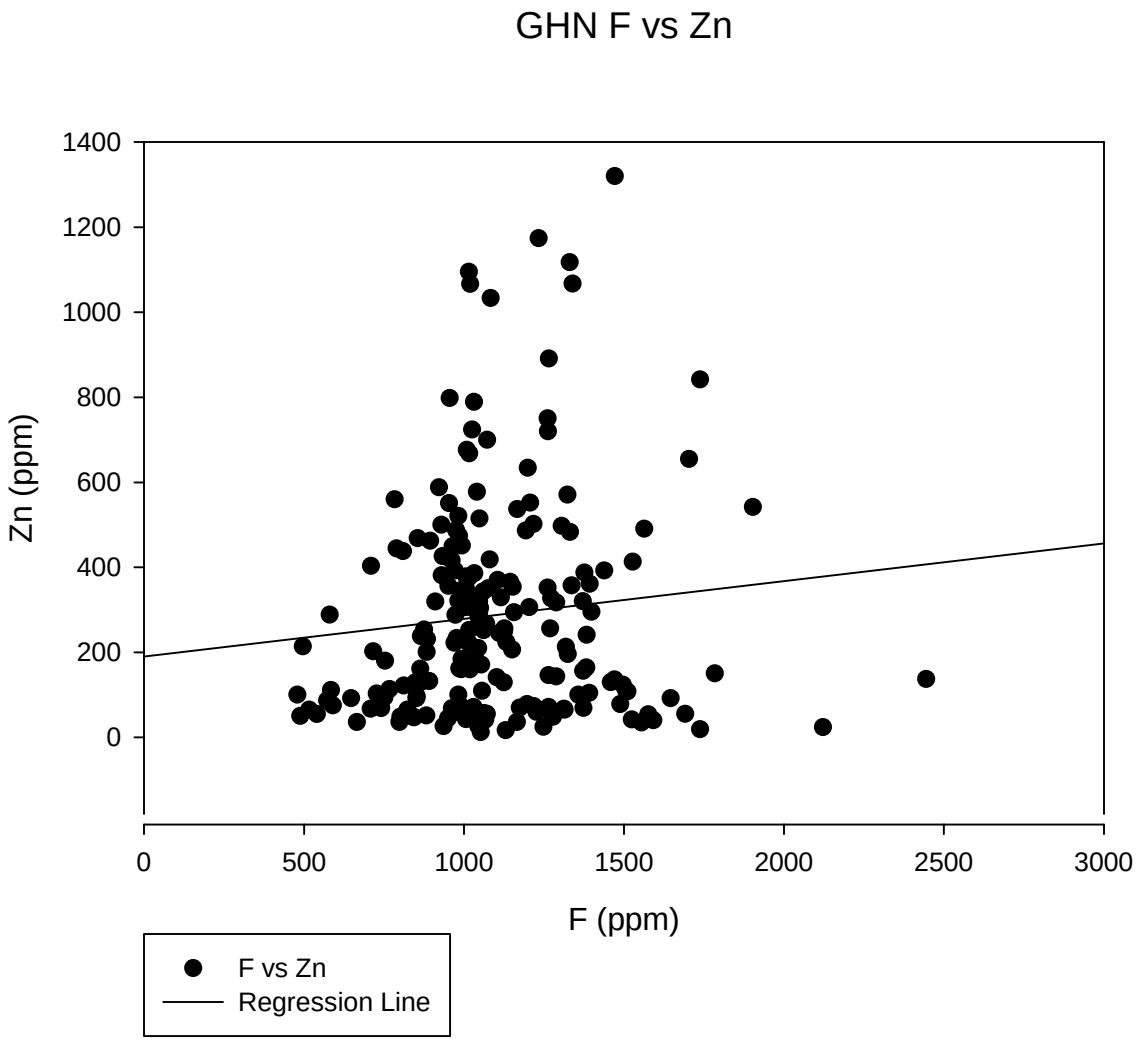
GHN F vs Zn
1400
1200
1000
800
600
400
200
0
Zn (ppm)
0
500
1000
1500
2000
2500
3000
F (ppm)
F vs Zn
Regression Line

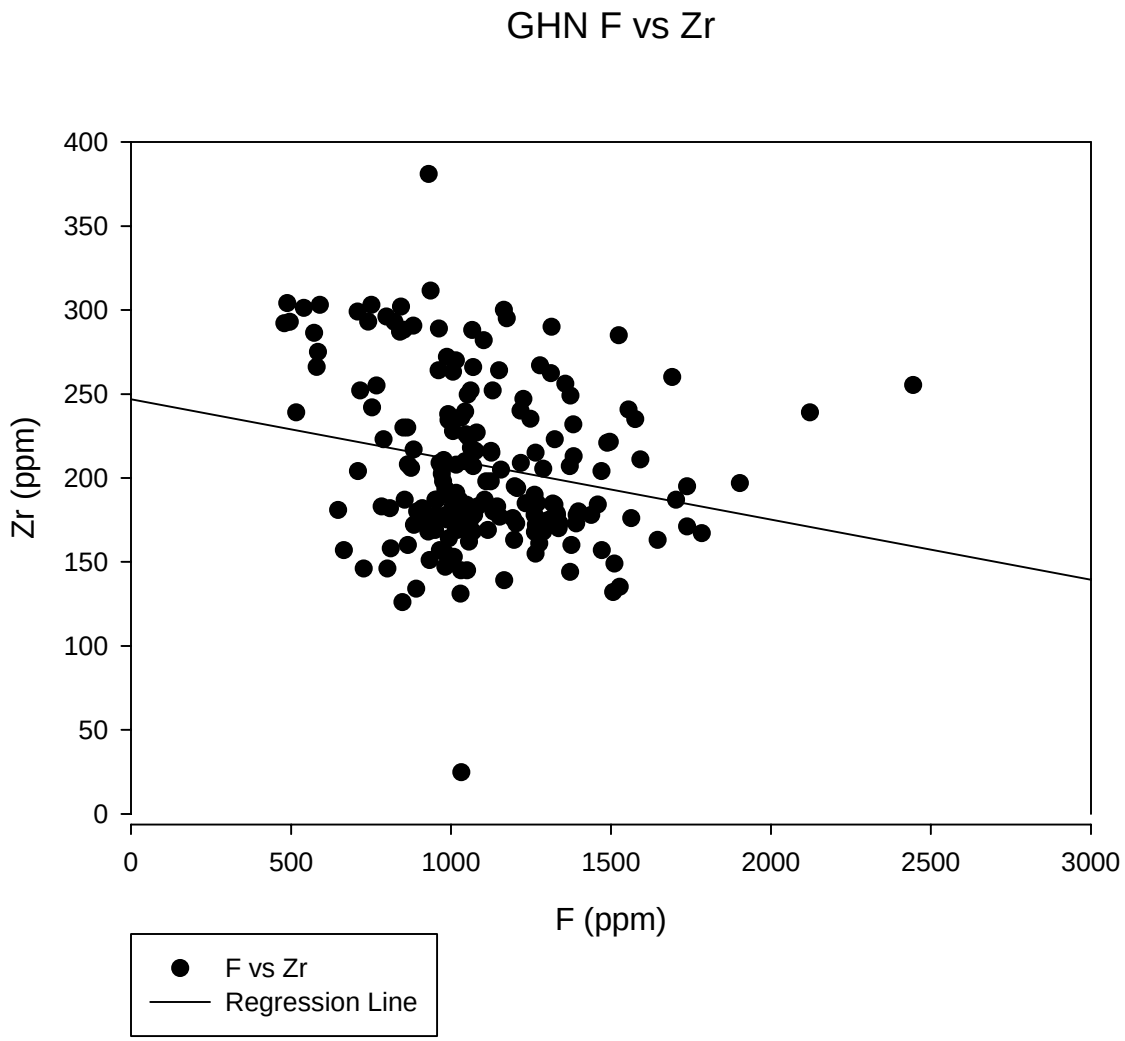
GHN F vs Zr
400
350
300
250
200
150
100
50
0
Zr (ppm)
0
500
1000
1500
2000
2500
3000
F (ppm)
F vs Zr
Regression Line

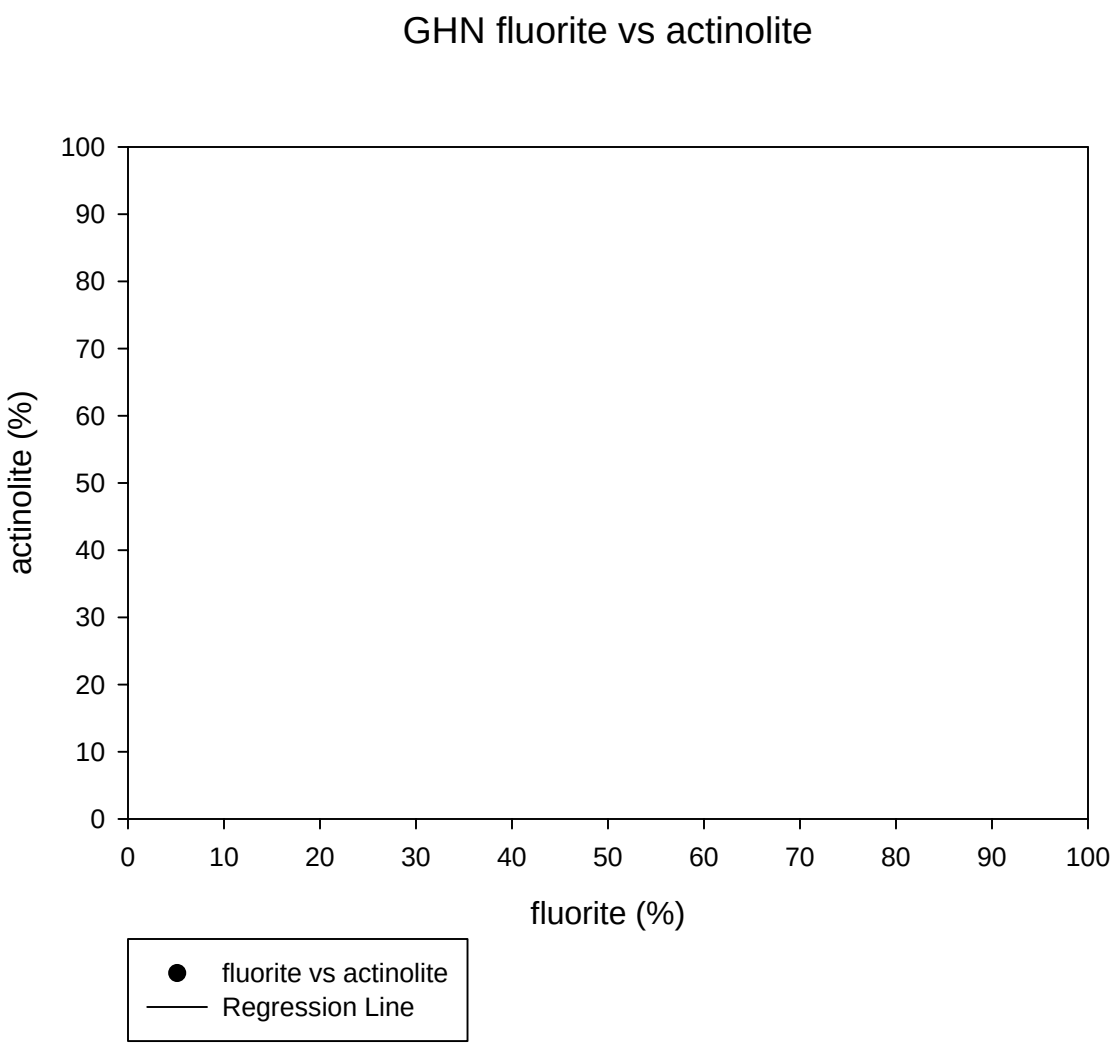
GHN fluorite vs actinolite
actinolite (%)
fluorite (%)
0
10
20
30
40
50
60
70
80
90
100
fluorite vs actinolite
Regression Line

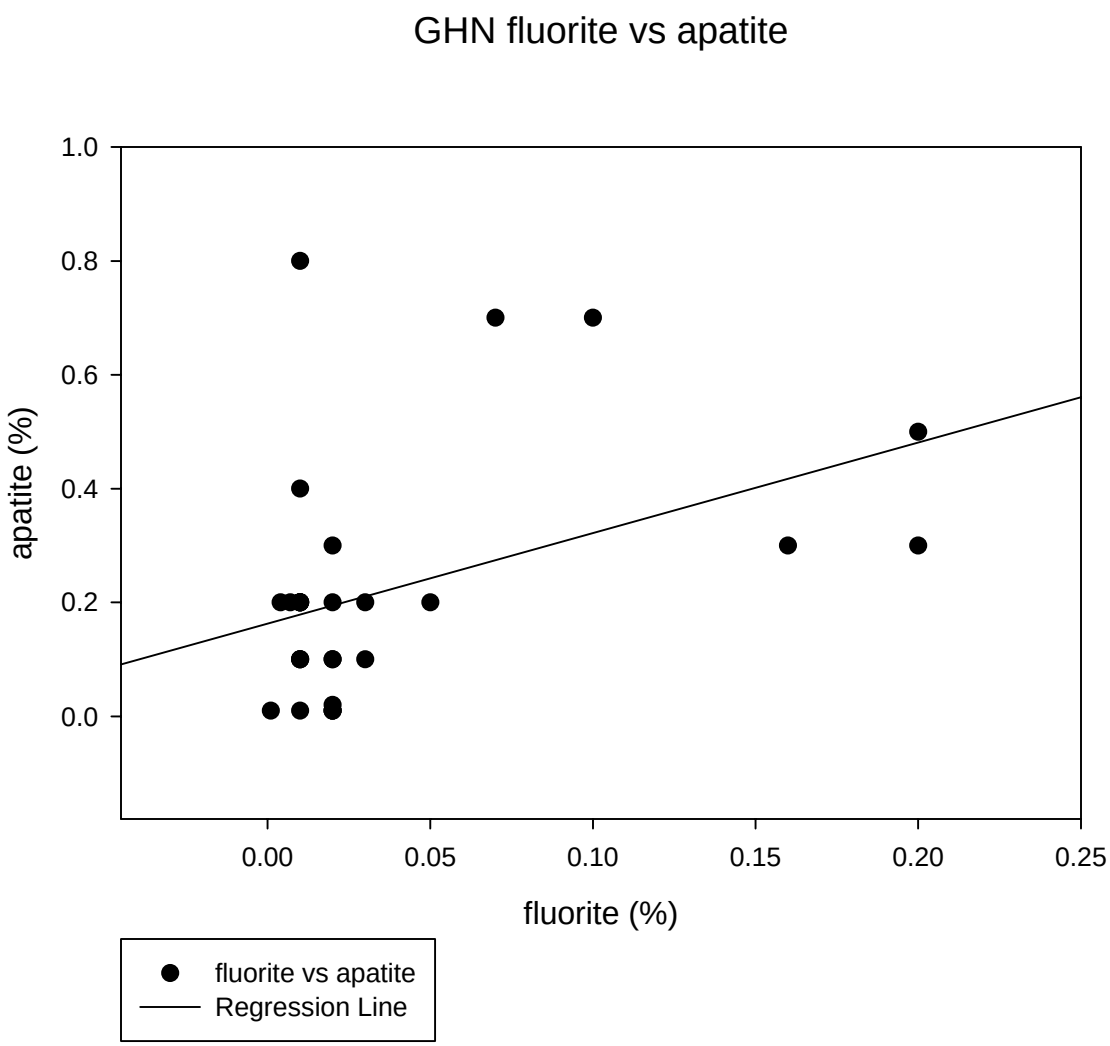
GHN fluorite vs apatite
1.0
0.8
0.6
0.4
0.2
0.0
apatite (%)
0.00
0.05
0.10
0.15
0.20
0.25
fluorite (%)
fluorite vs apatite
Regression Line

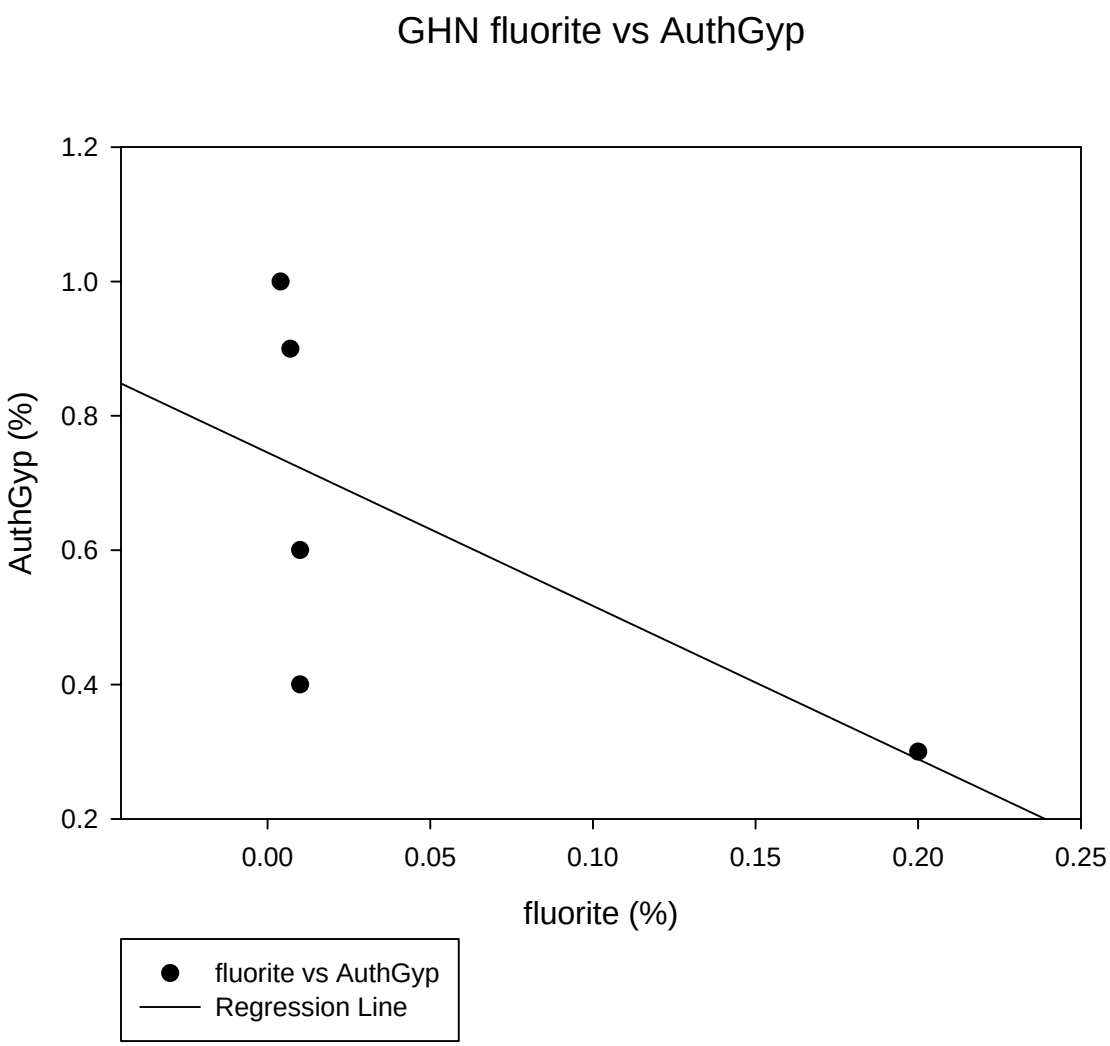
GHN fluorite vs AuthGyp
1.2
1.0
0.8
0.6
0.4
0.2
AuthGyp (%)
0.00
0.05
0.10
0.15
0.20
0.25
fluorite (%)
fluorite vs AuthGyp
Regression Line

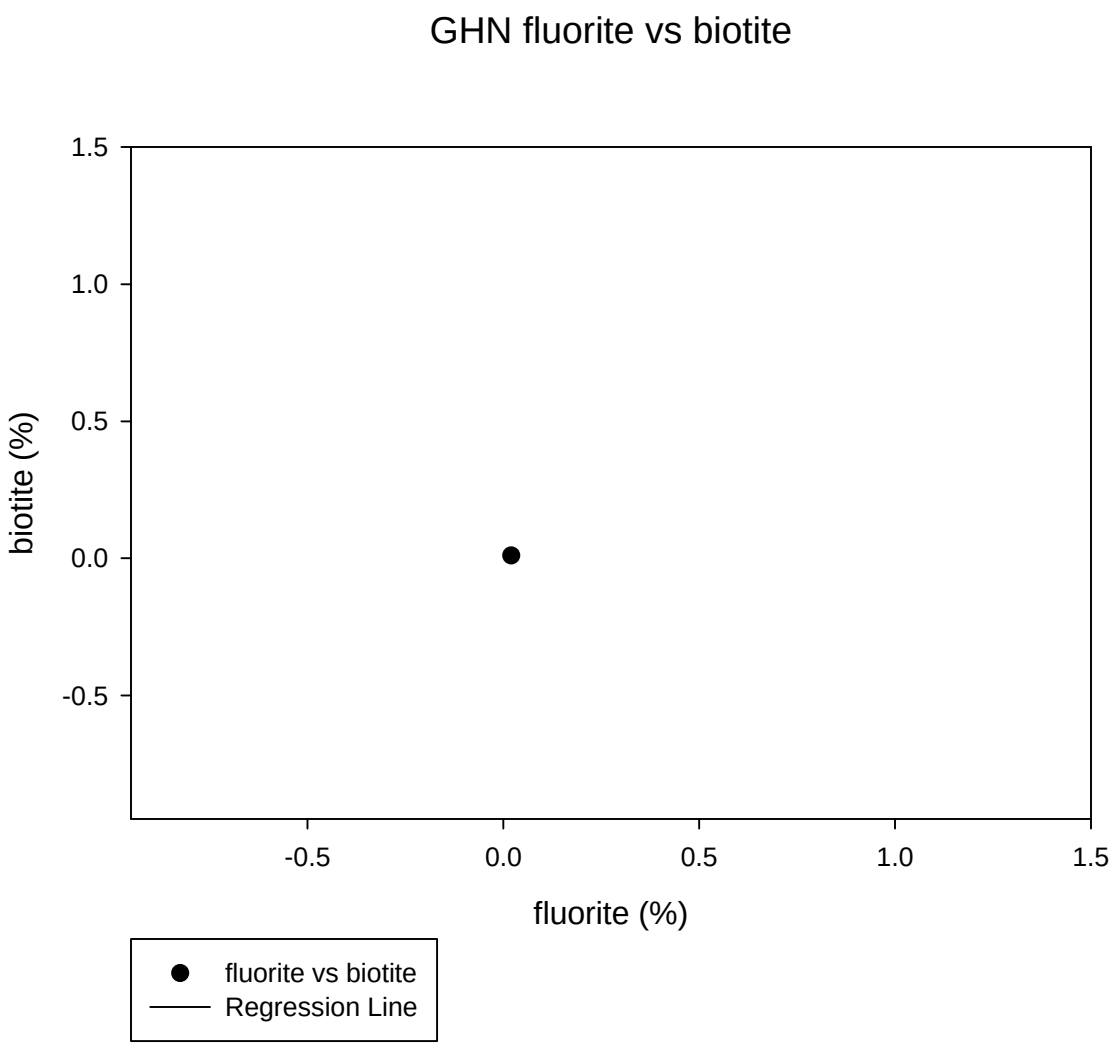
GHN fluorite vs biotite
1.5
1.0
0.5
0.0
-0.5
biotite (%)
-0.5
0.0
0.5
1.0
1.5
fluorite (%)
fluorite vs biotite
Regression Line

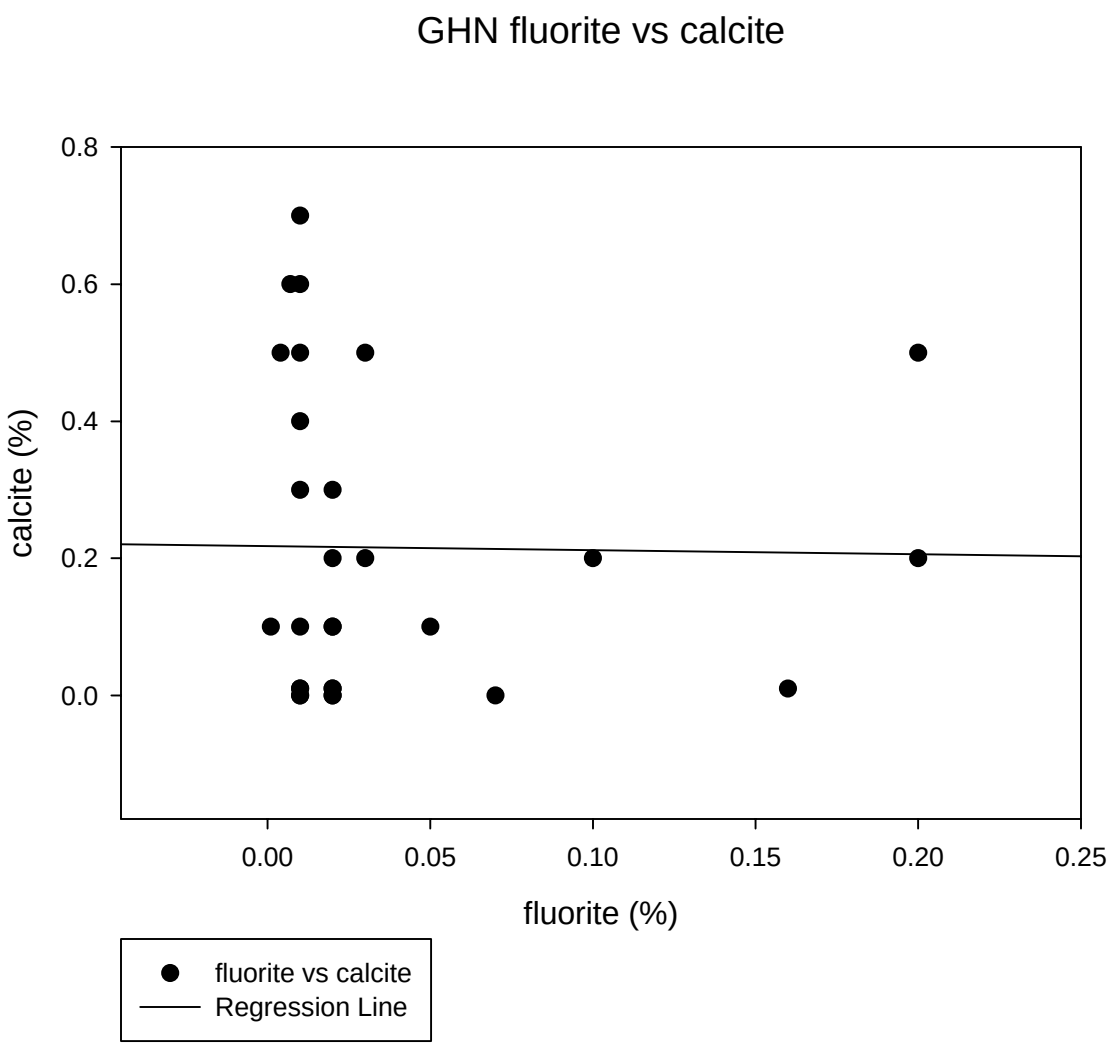
GHN fluorite vs calcite
0.8
0.6
0.4
0.2
0.0
calcite (%)
0.00
0.05
0.10
0.15
0.20
0.25
fluorite (%)
fluorite vs calcite
Regression Line

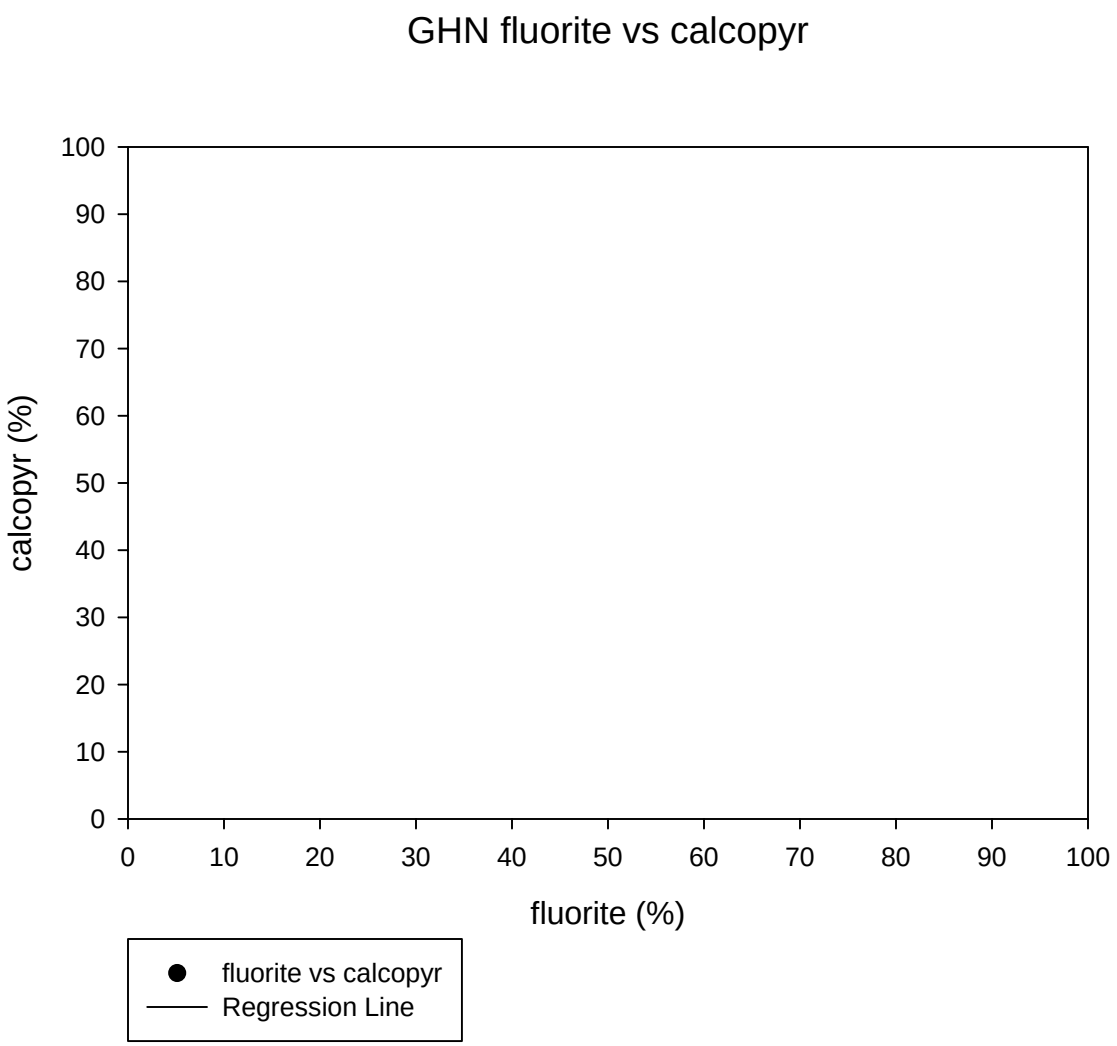
GHN fluorite vs calcopyr
calcopyr (%)
fluorite (%)
0
10
20
30
40
50
60
70
80
90
100
fluorite vs calcopyr
Regression Line

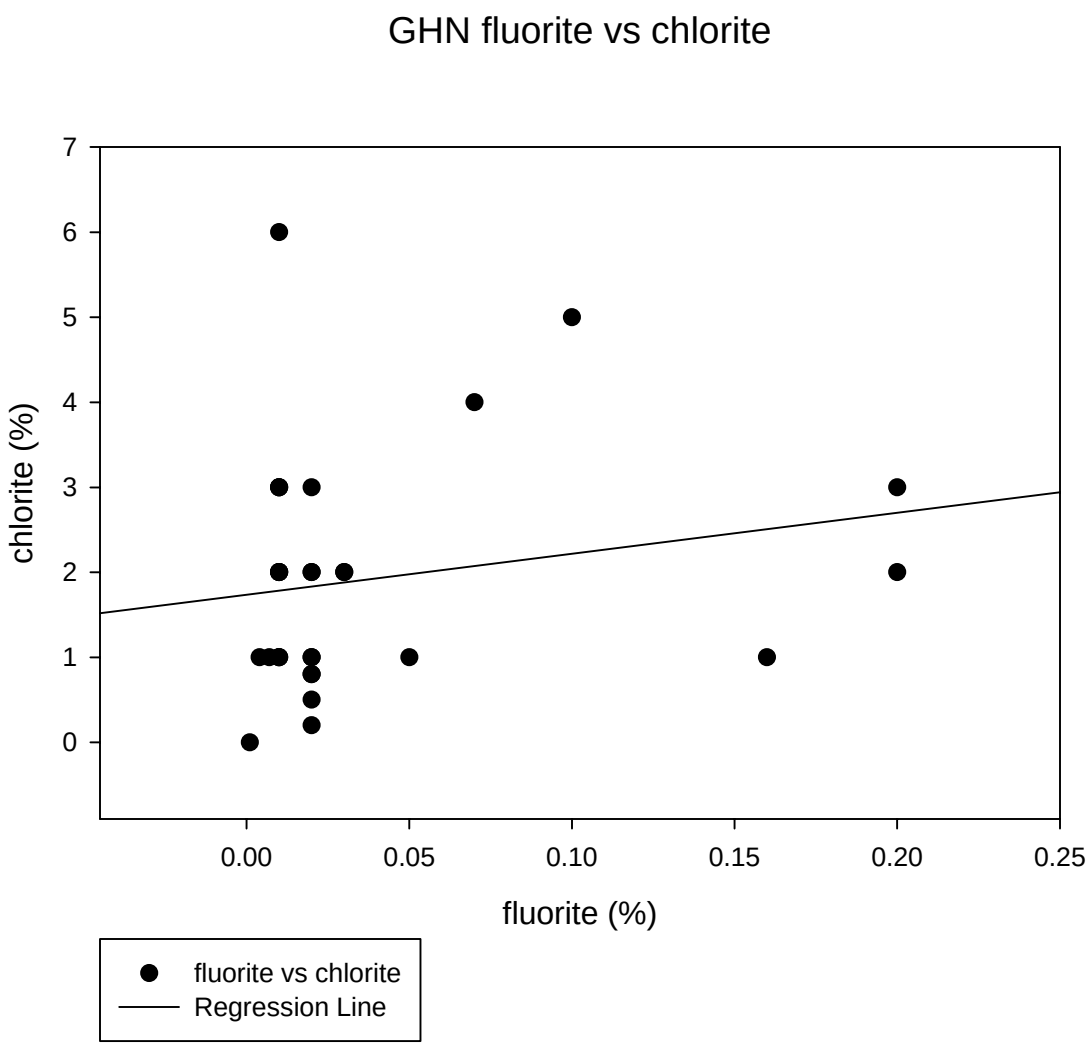
GHN fluorite vs chlorite
chlorite (%)
fluorite (%)
0
1
2
3
4
5
6
7
0.00
0.05
0.10
0.15
0.20
0.25
fluorite vs chlorite
Regression Line

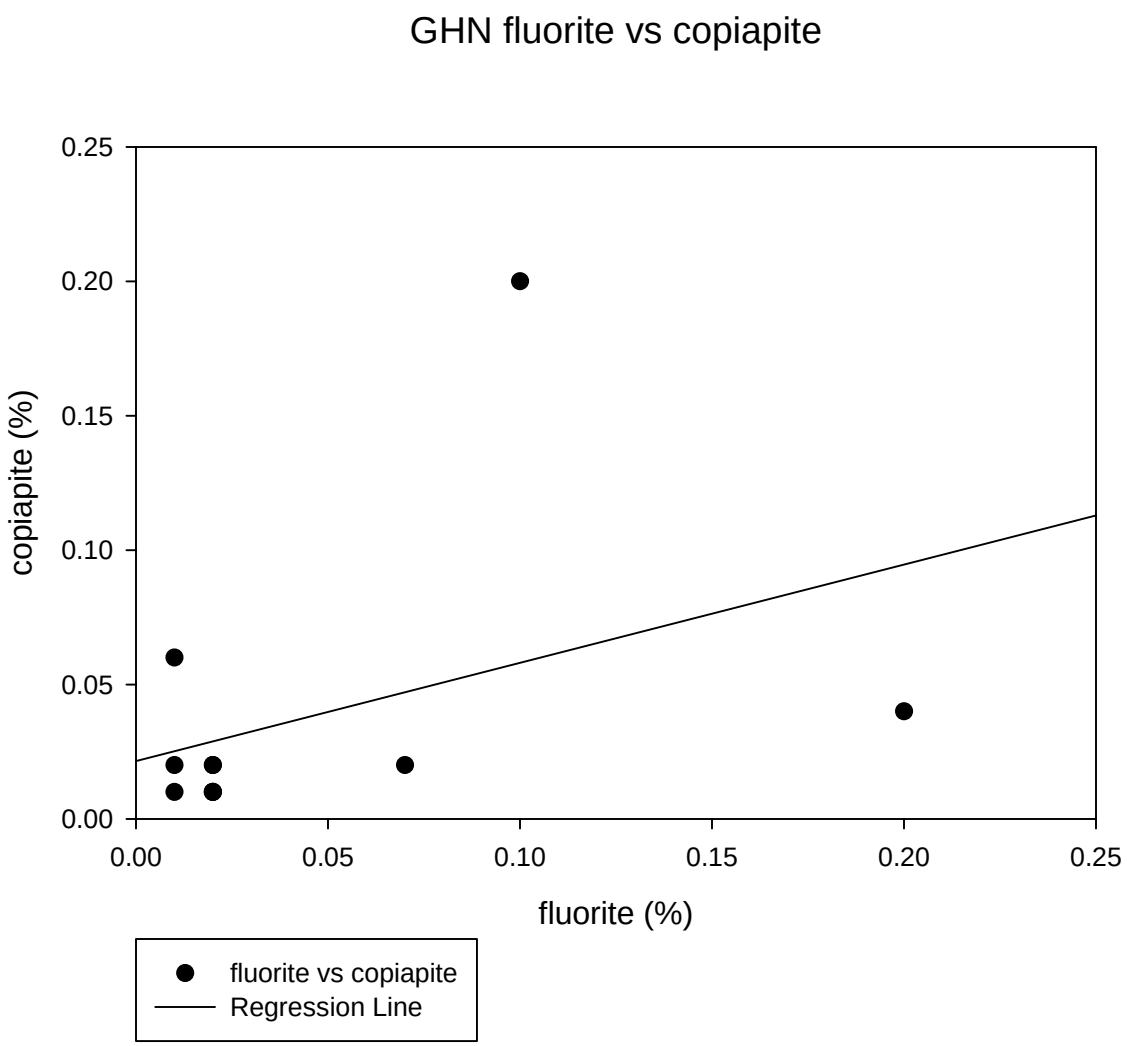
GHN fluorite vs copiapite
0.25
0.20
0.15
0.10
0.05
0.00
copiapite (%)
0.00
0.05
0.10
0.15
0.20
0.25
fluorite (%)
fluorite vs copiapite
Regression Line

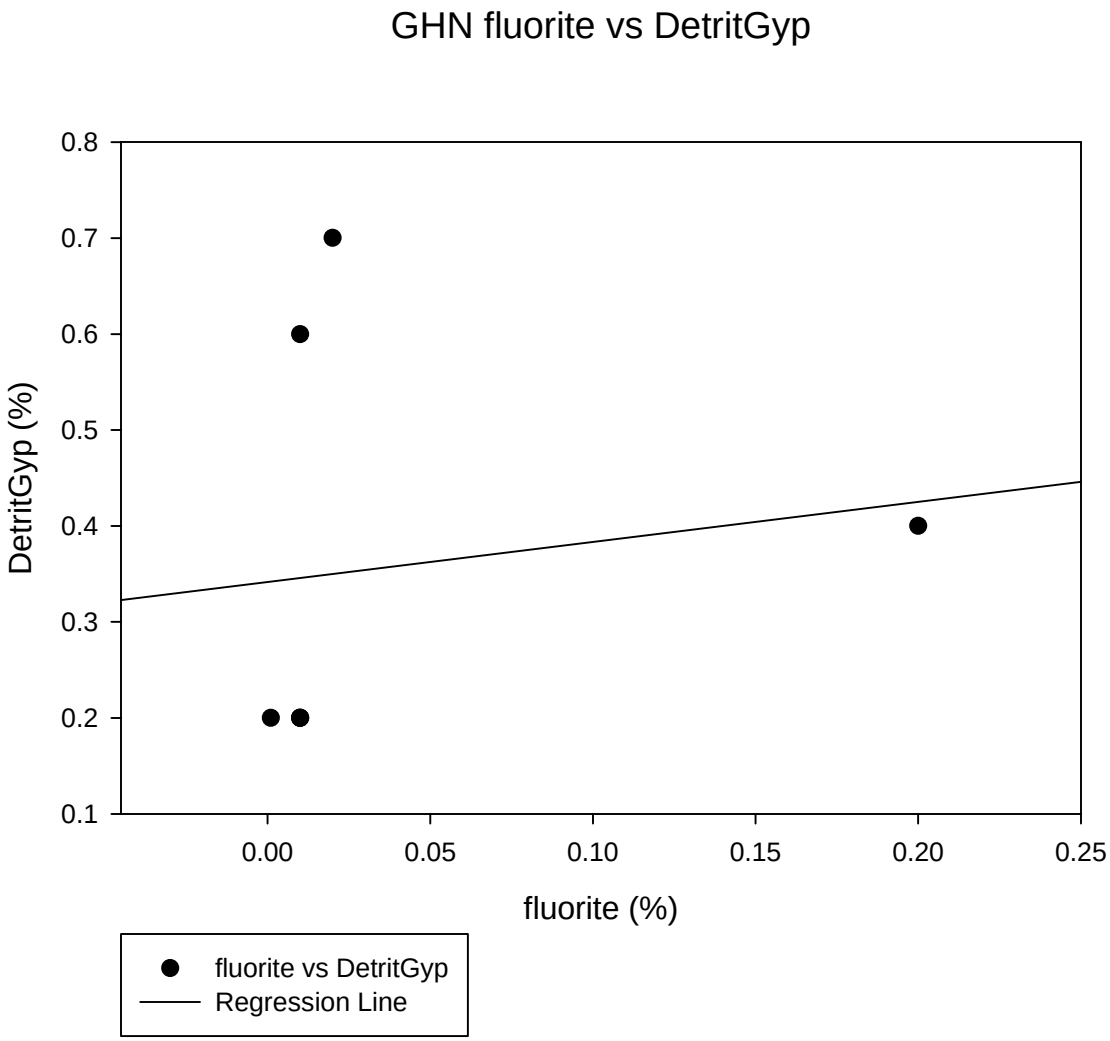
GHN fluorite vs DetritGyp
DetritGyp (%)
0.8
0.7
0.6
0.5
0.4
0.3
0.2
0.1
0.00
0.05
0.10
0.15
0.20
0.25
fluorite (%)
fluorite vs DetritGyp
Regression Line

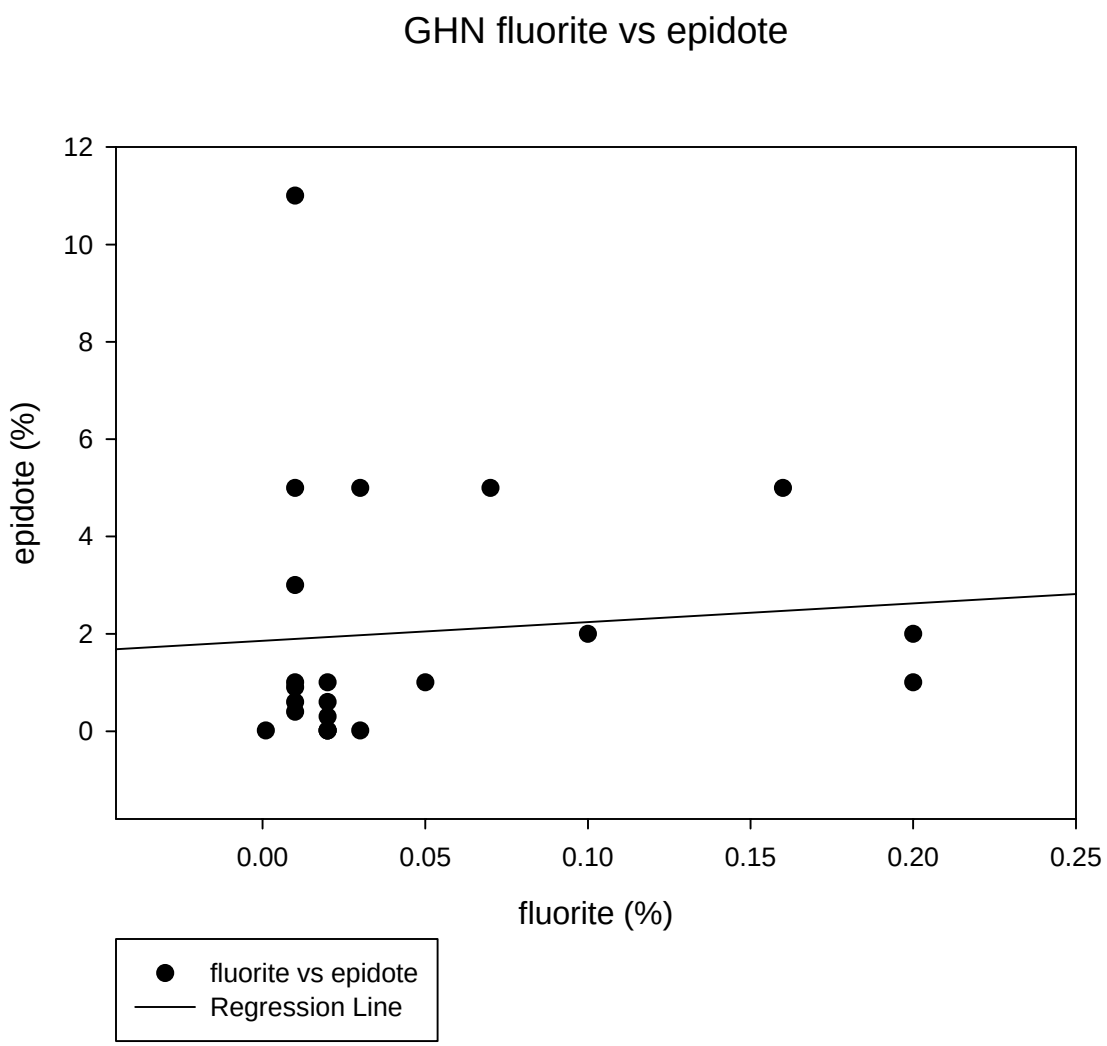
GHN fluorite vs epidote
epidote (%)
12
10
8
6
4
2
0
0.00
0.05
0.10
0.15
0.20
0.25
fluorite (%)
fluorite vs epidote
Regression Line

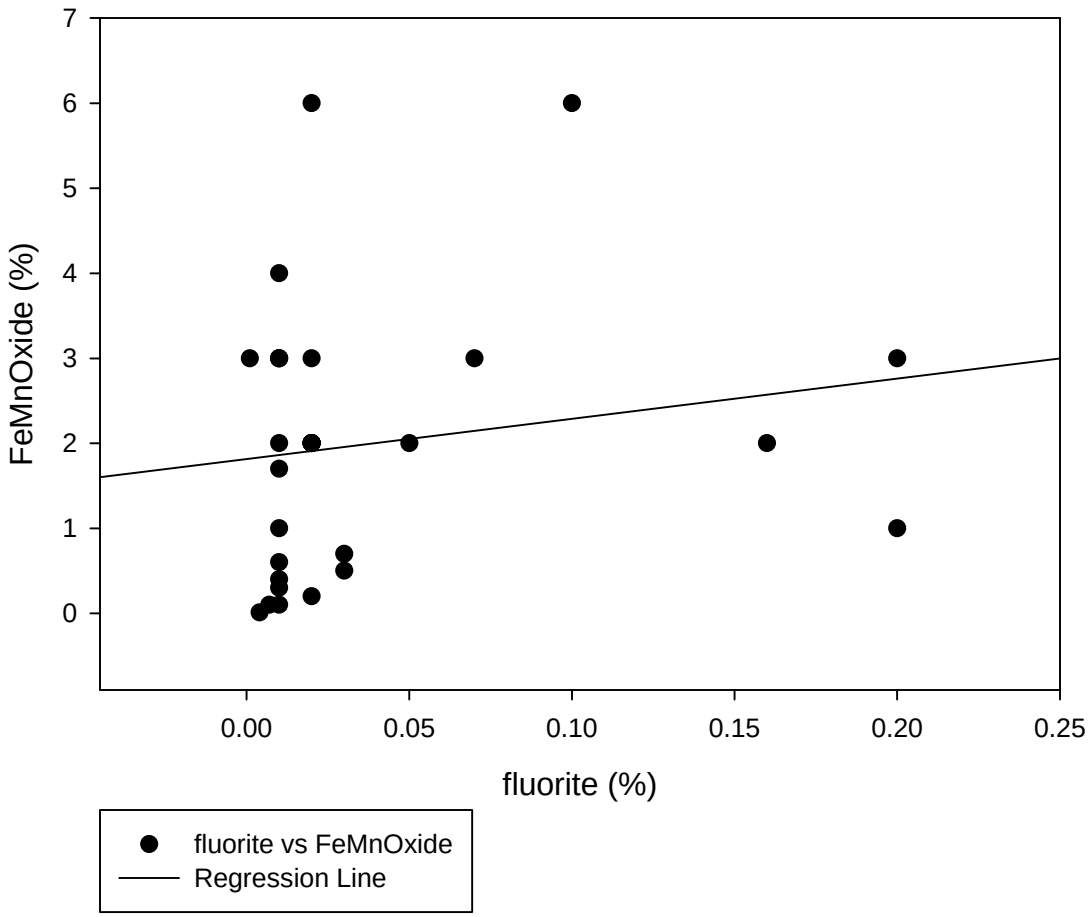
GHN fluorite vs FeMnOxide
FeMnOxide (%)
7
6
5
4
3
2
1
0
0.00
0.05
0.10
0.15
0.20
0.25
fluorite (%)
fluorite vs FeMnOxide
Regression Line

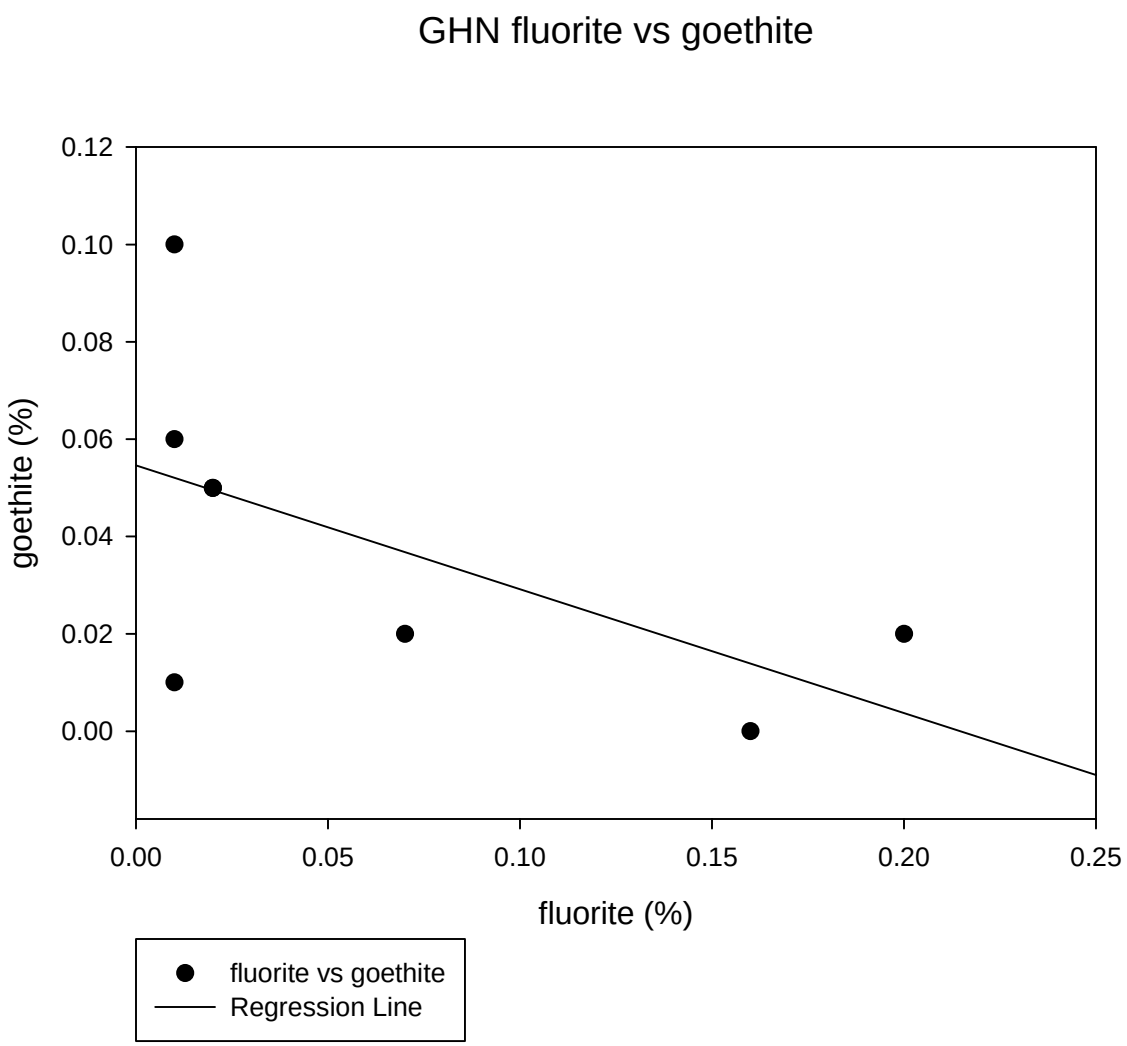
GHN fluorite vs goethite
0.12
0.10
0.08
0.06
0.04
0.02
0.00
goethite (%)
0.00
0.05
0.10
0.15
0.20
0.25
fluorite (%)
fluorite vs goethite
Regression Line

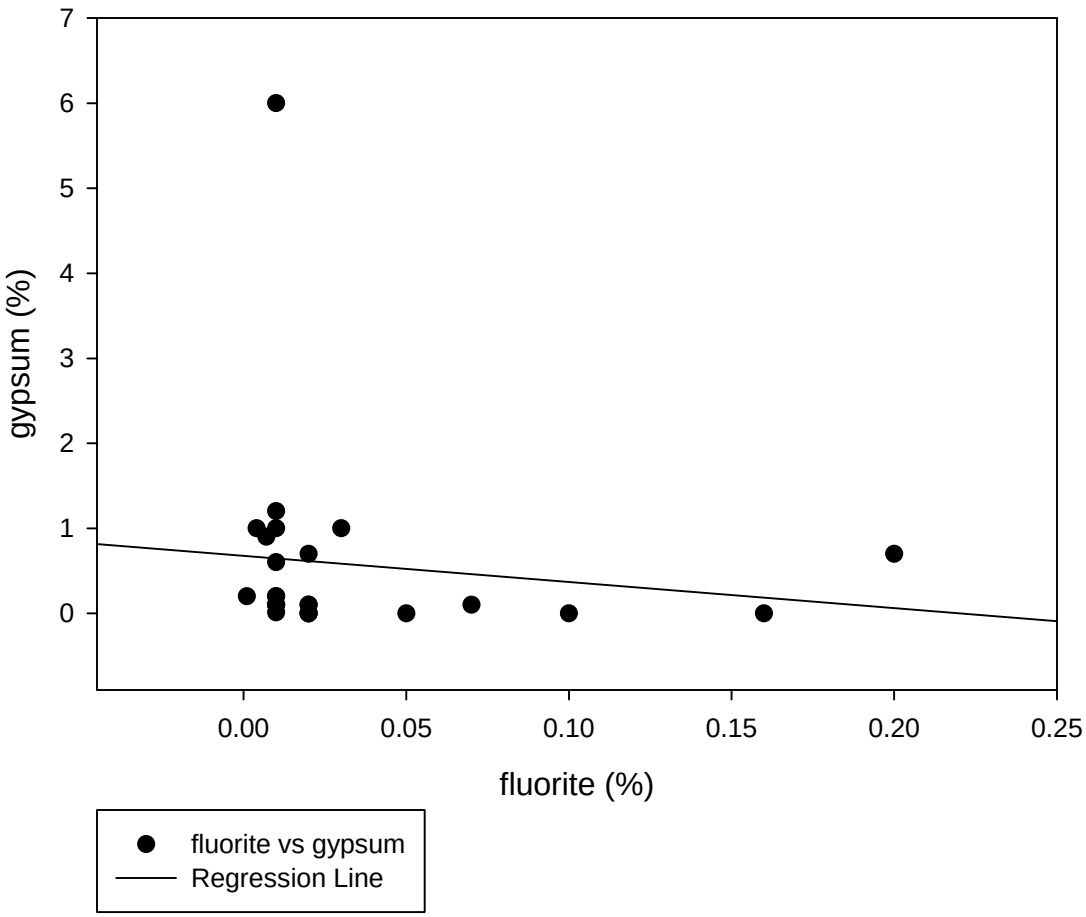
GHN fluorite vs gypsum
gypsum (%)
7
6
5
4
3
2
1
0
0.00
0.05
0.10
0.15
0.20
0.25
fluorite (%)
fluorite vs gypsum
Regression Line

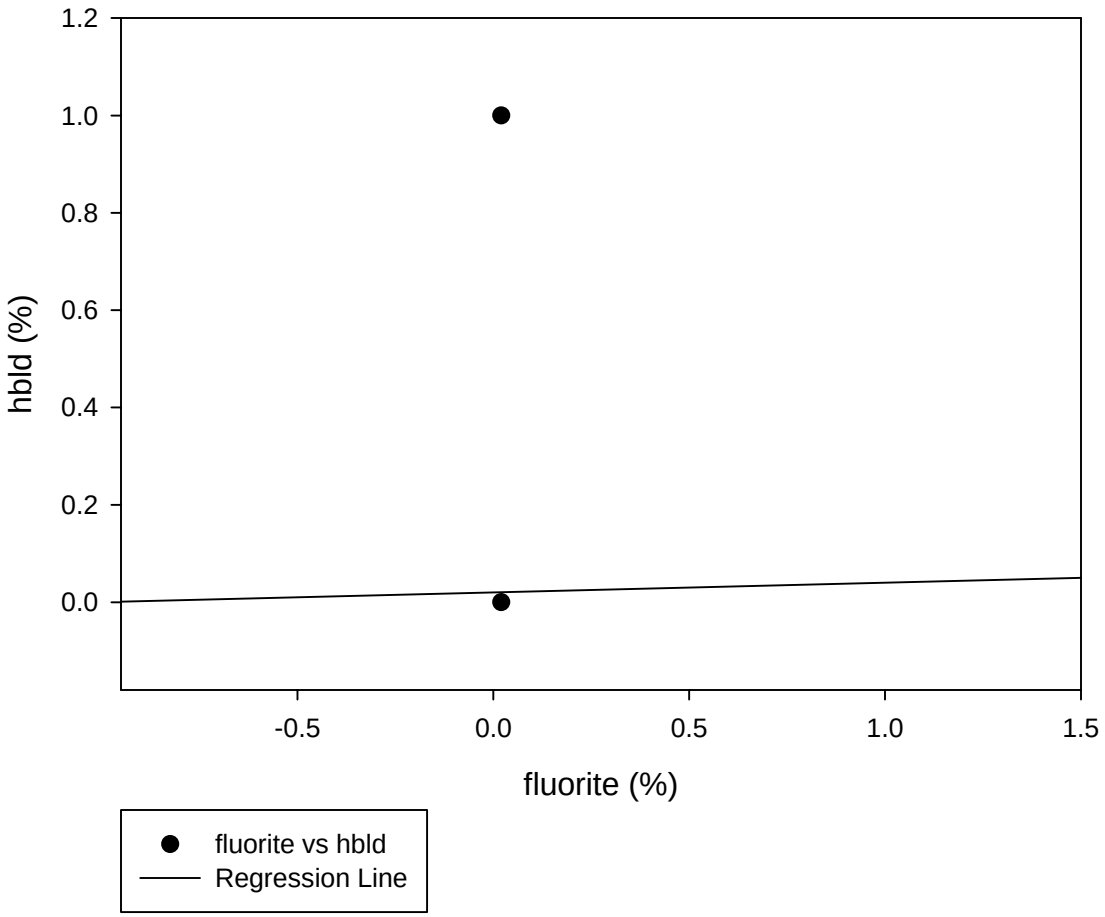
GHN fluorite vs hbld
1.2
1.0
0.8
0.6
0.4
0.2
0.0
hbld (%)
-0.5
0.0
0.5
1.0
1.5
fluorite (%)
fluorite vs hbld
Regression Line

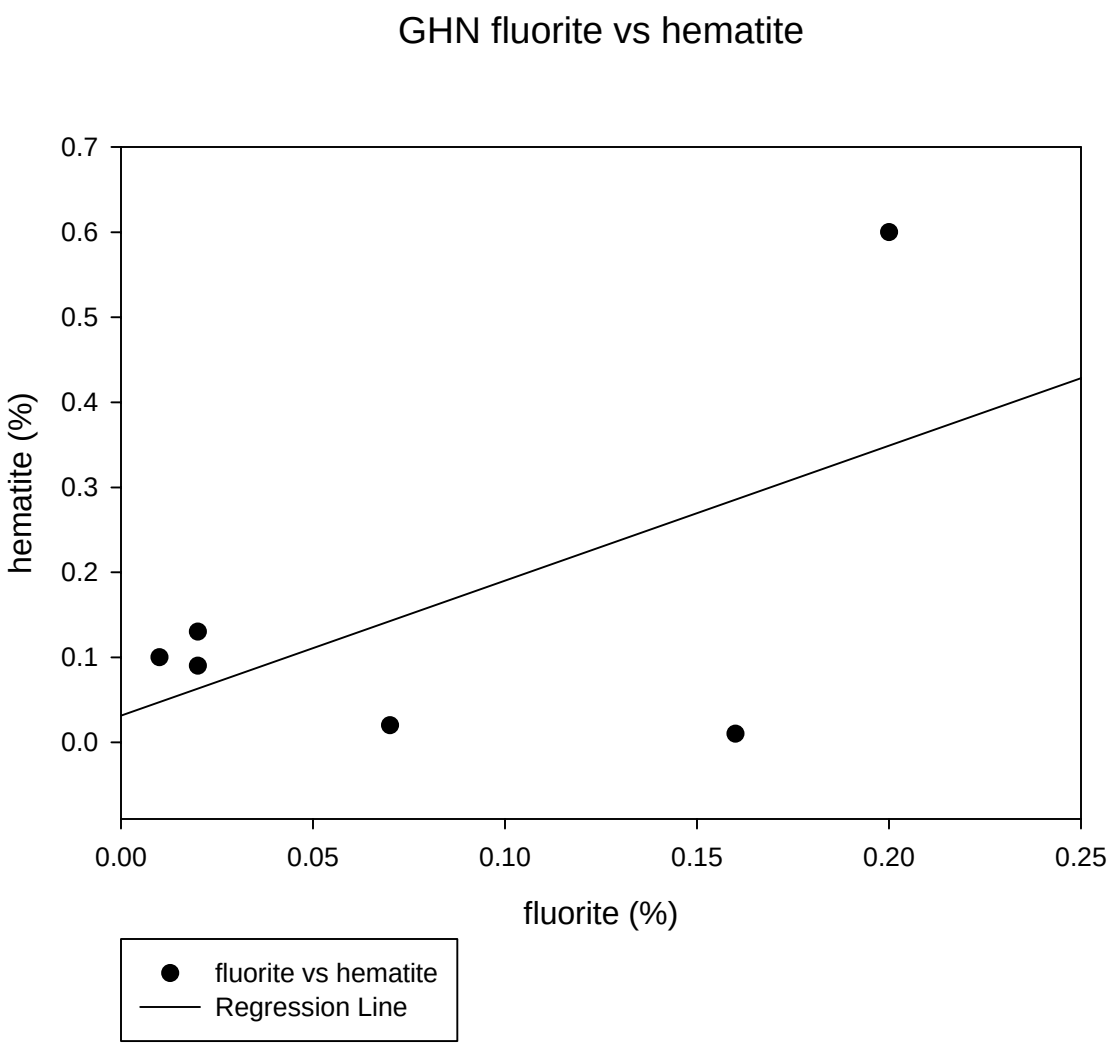
GHN fluorite vs hematite
0.7
0.6
0.5
0.4
0.3
0.2
0.1
0.0
hematite (%)
0.00
0.05
0.10
0.15
0.20
0.25
fluorite (%)
fluorite vs hematite
Regression Line

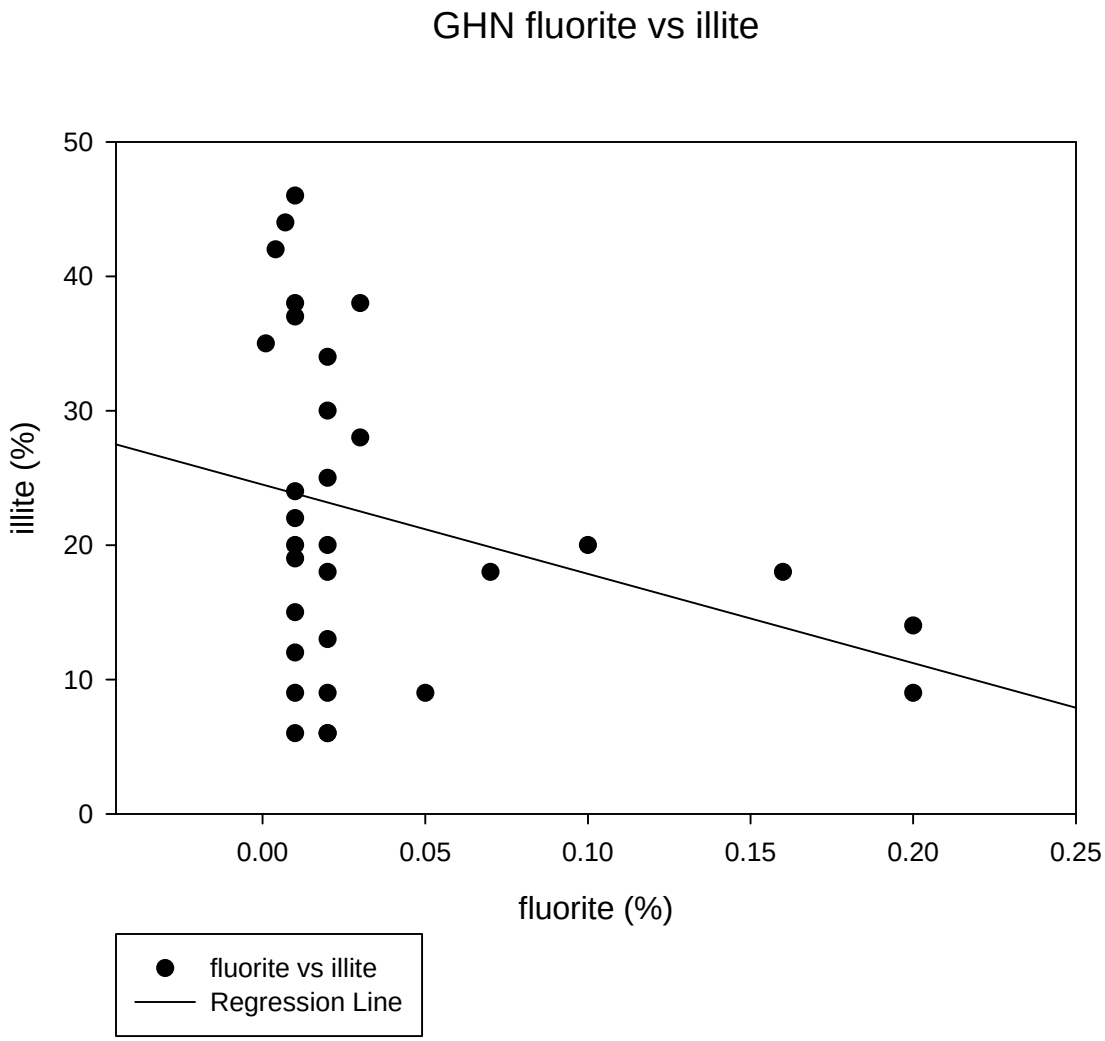
GHN fluorite vs illite
illite (%)
fluorite (%)
0
10
20
30
40
50
0.00
0.05
0.10
0.15
0.20
0.25
fluorite vs illite
Regression Line

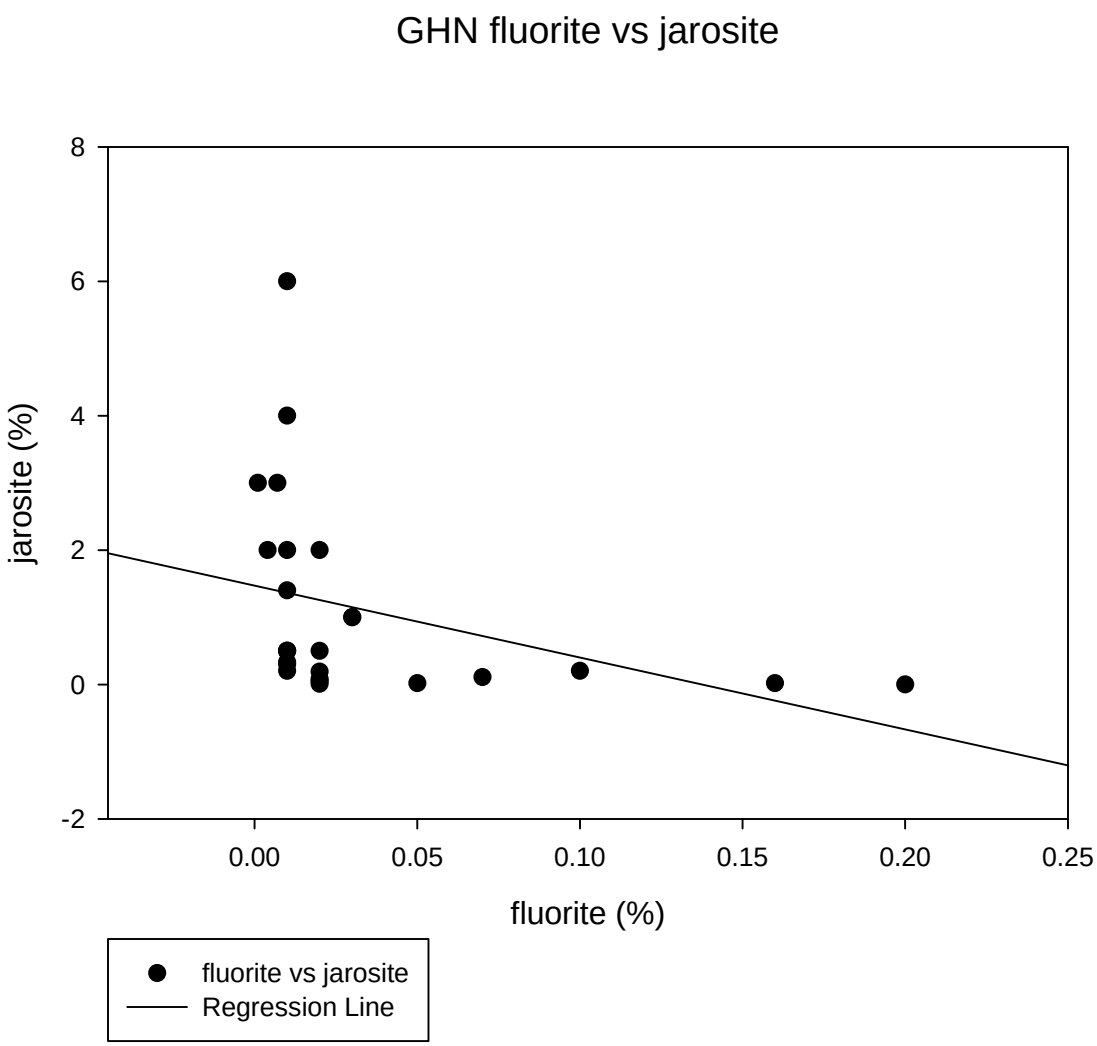
GHN fluorite vs jarosite
8
6
4
2
0
-2
jarosite (%)
0.00
0.05
0.10
0.15
0.20
0.25
fluorite (%)
fluorite vs jarosite
Regression Line

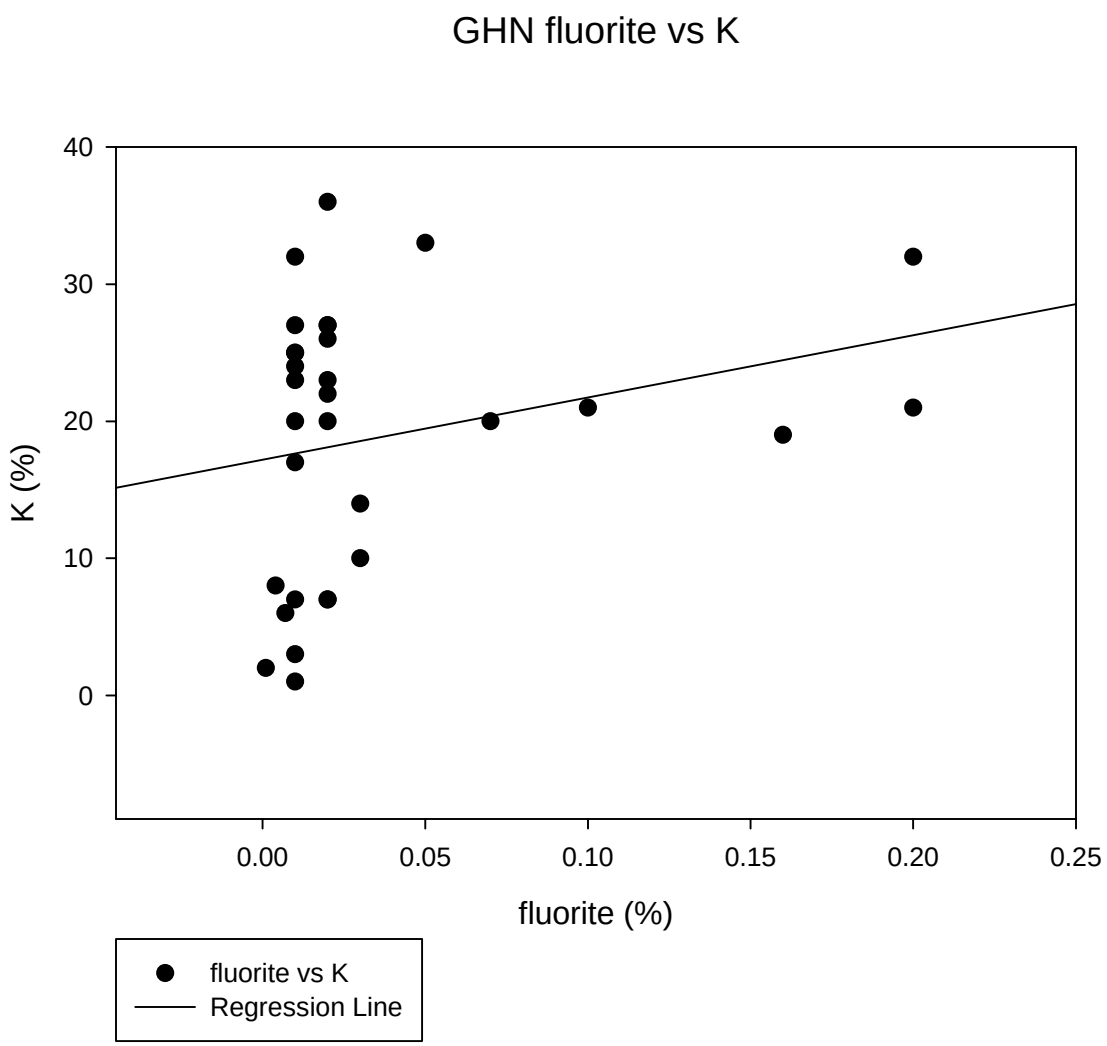
GHN fluorite vs K
40
30
20
10
0
K (%)
0.00
0.05
0.10
0.15
0.20
0.25
fluorite (%)
fluorite vs K
Regression Line

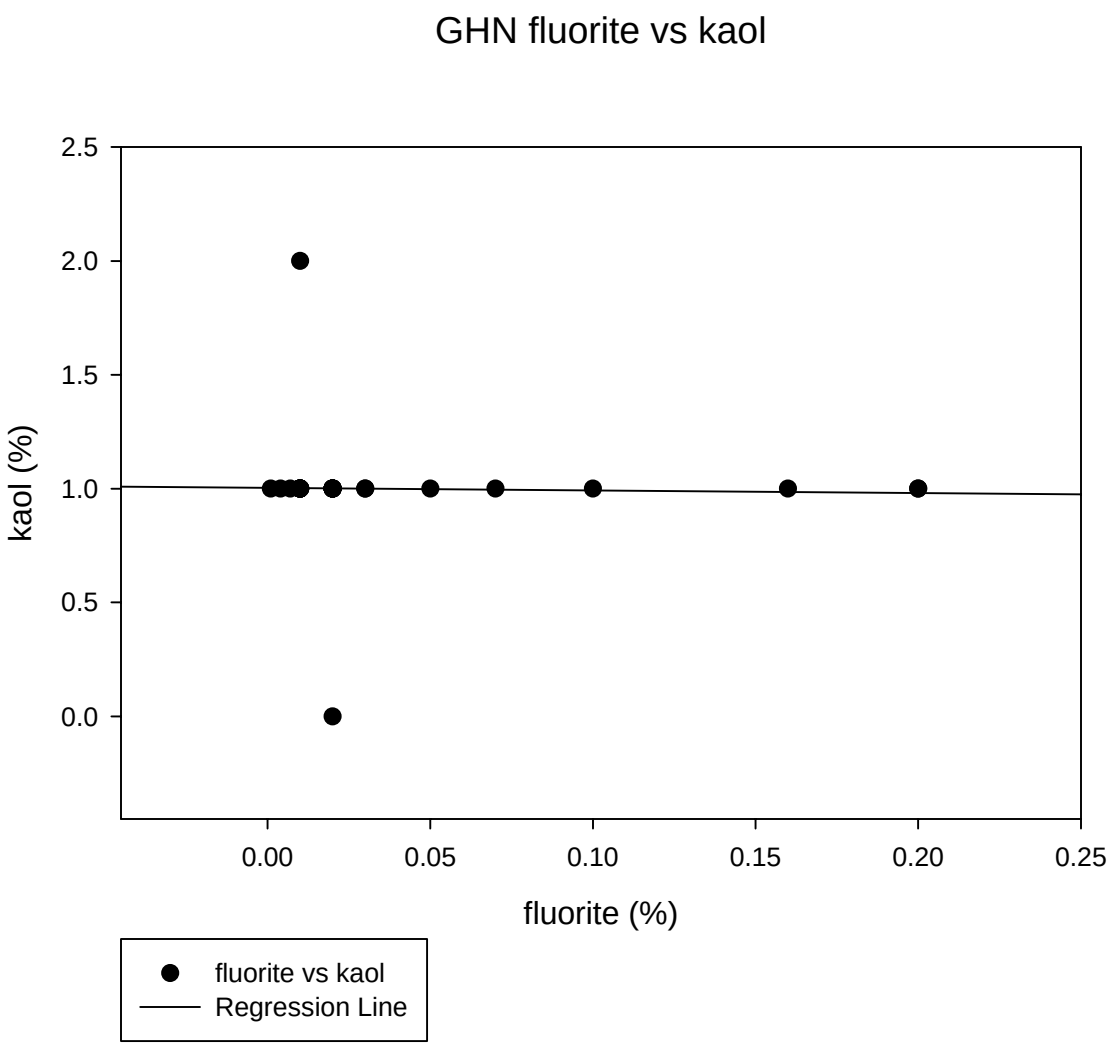
GHN fluorite vs kaol
2.5
2.0
1.5
1.0
0.5
0.0
kaol (%)
0.00
0.05
0.10
0.15
0.20
0.25
fluorite (%)
fluorite vs kaol
Regression Line

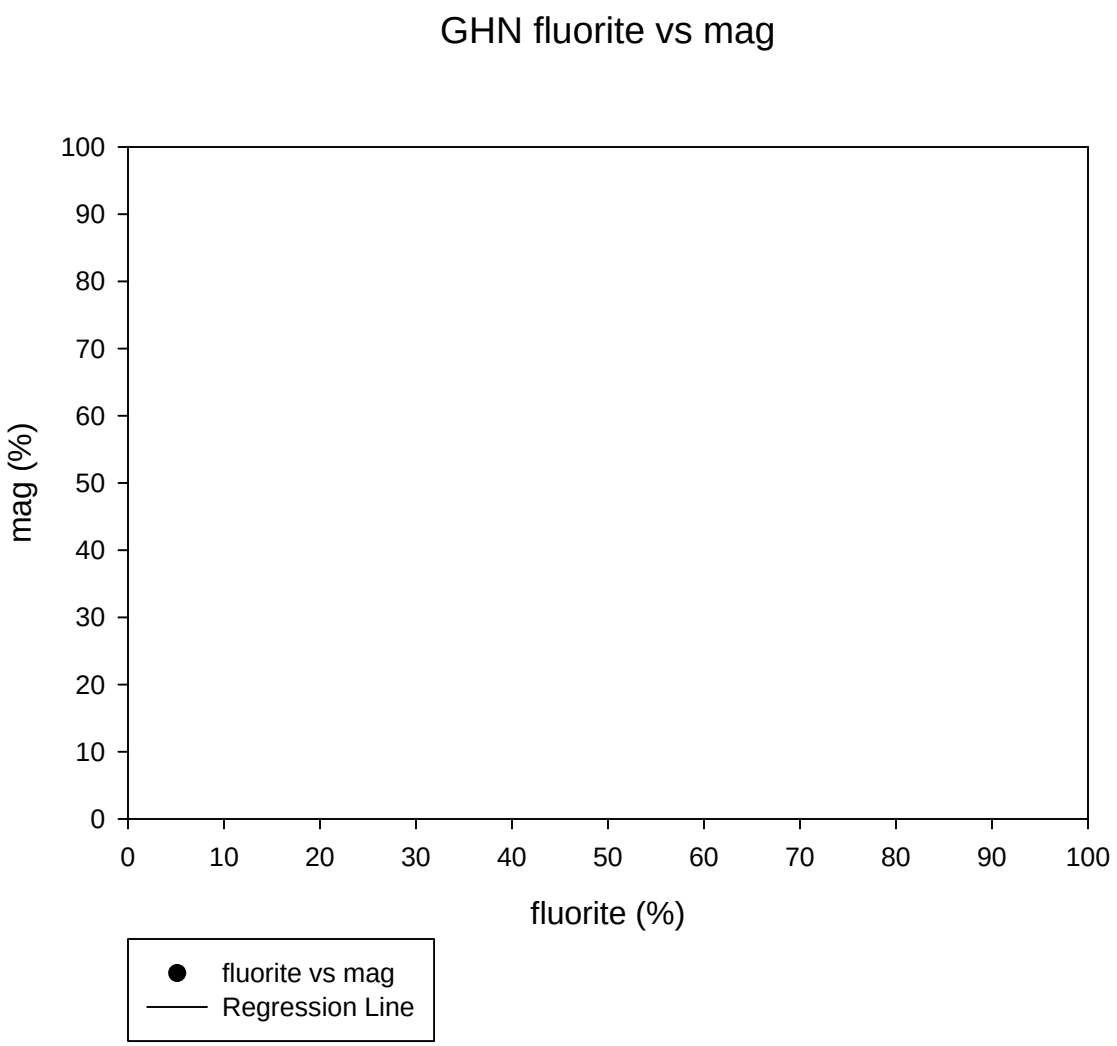
GHN fluorite vs mag
mag (%)
100
90
80
70
60
50
40
30
20
10
0
0
10
20
30
40
50
60
70
80
90
100
fluorite (%)
fluorite vs mag
Regression Line

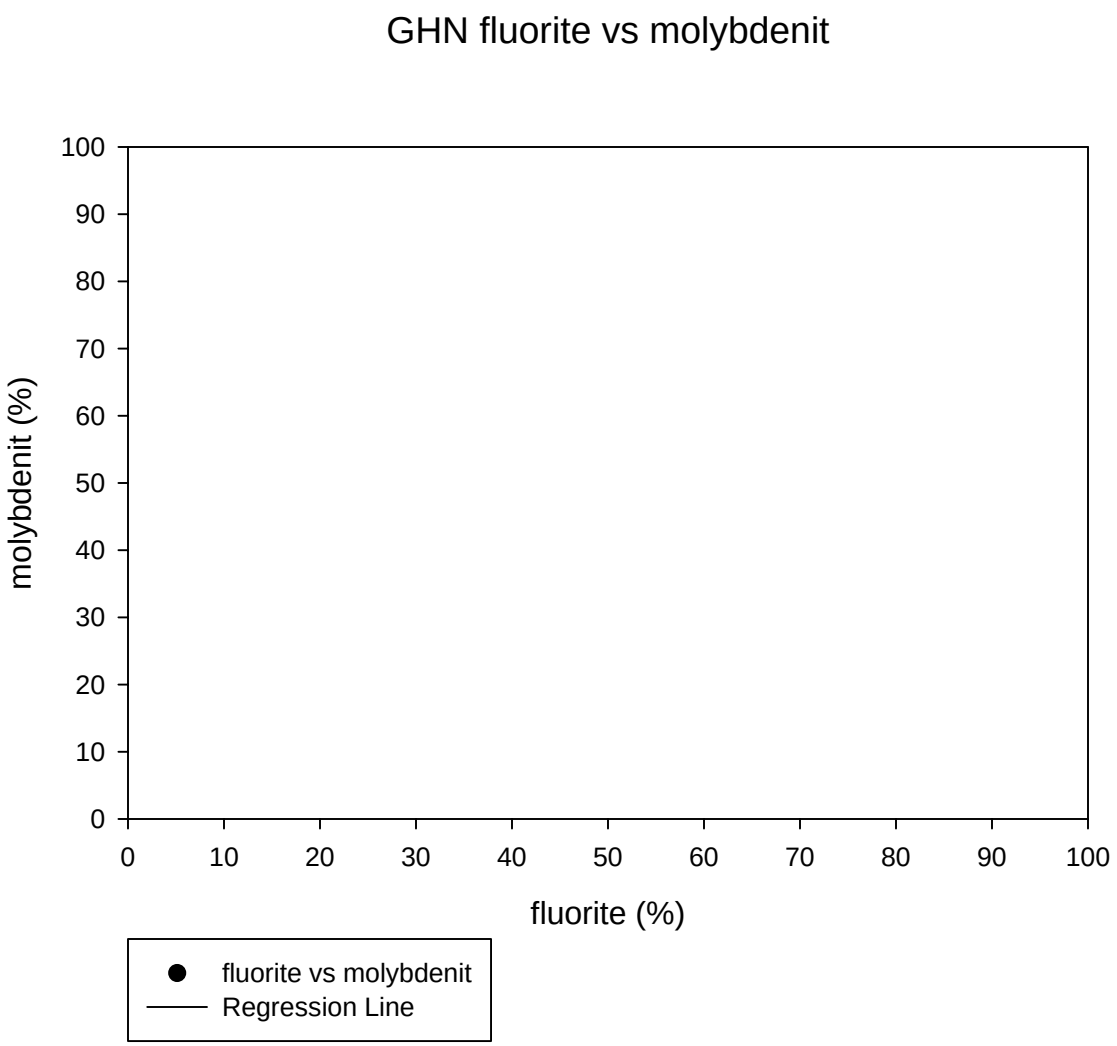
GHN fluorite vs molybdenit
molybdenit (%)
fluorite (%)
0
10
20
30
40
50
60
70
80
90
100
fluorite vs molybdenit
Regression Line

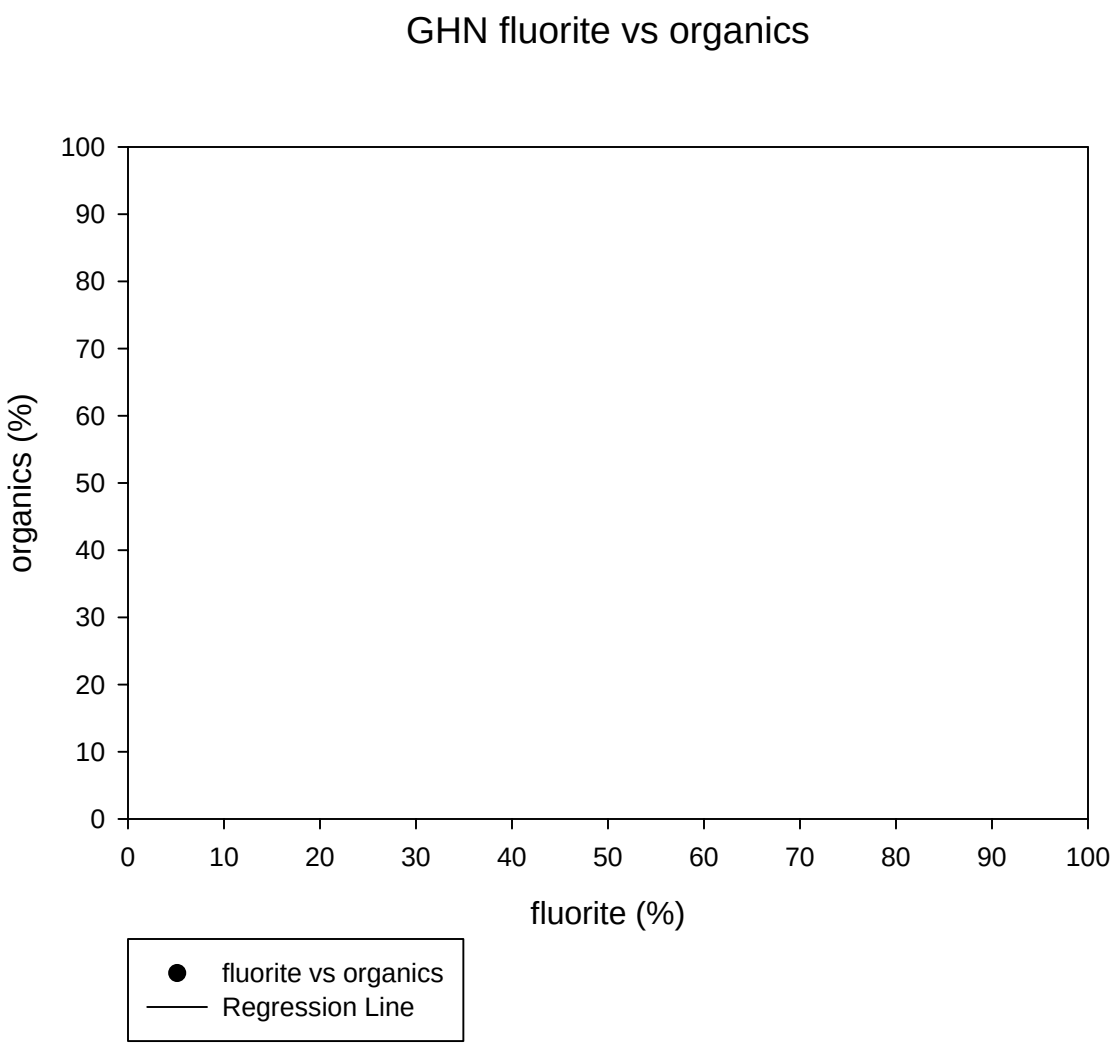
GHN fluorite vs organics
organics (%)
100
90
80
70
60
50
40
30
20
10
0
0
10
20
30
40
50
60
70
80
90
100
fluorite (%)
fluorite vs organics
Regression Line

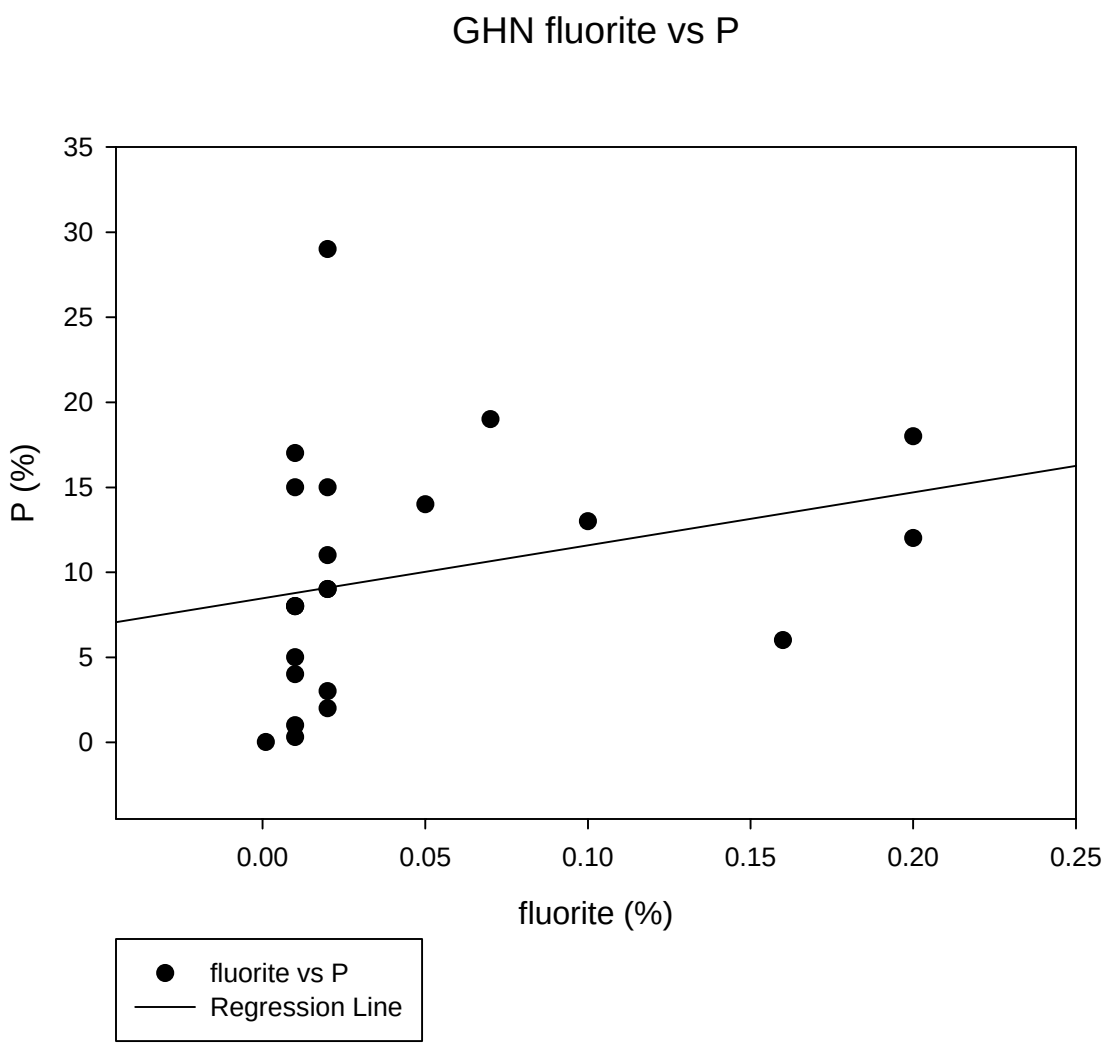
GHN fluorite vs P
35
30
25
20
15
10
5
0
P (%)
0.00
0.05
0.10
0.15
0.20
0.25
fluorite (%)
fluorite vs P
Regression Line

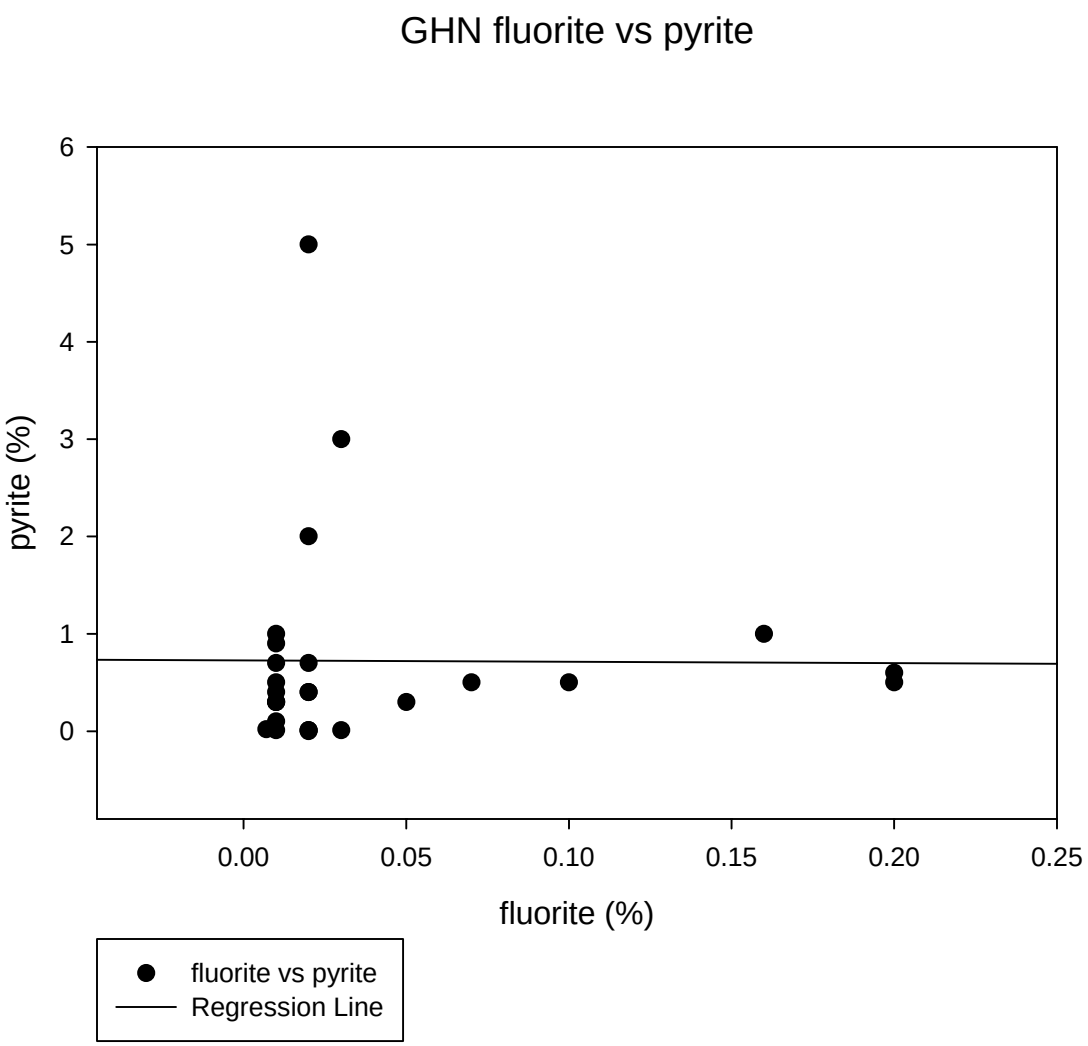
GHN fluorite vs pyrite
pyrite (%)
6
5
4
3
2
1
0
0.00
0.05
0.10
0.15
0.20
0.25
fluorite (%)
fluorite vs pyrite
Regression Line

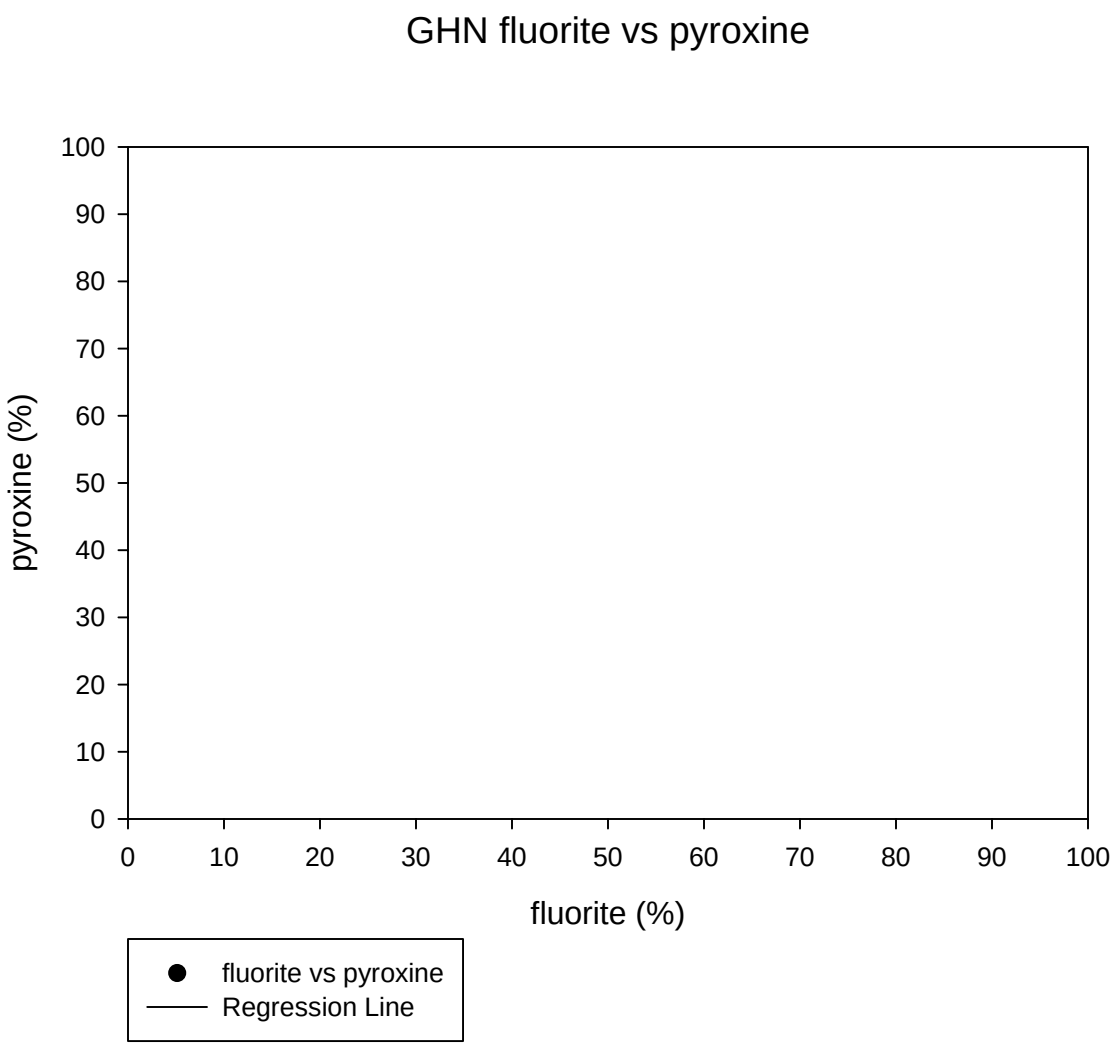
GHN fluorite vs pyroxine
pyroxine (%)
fluorite (%)
0
10
20
30
40
50
60
70
80
90
100
fluorite vs pyroxine
Regression Line

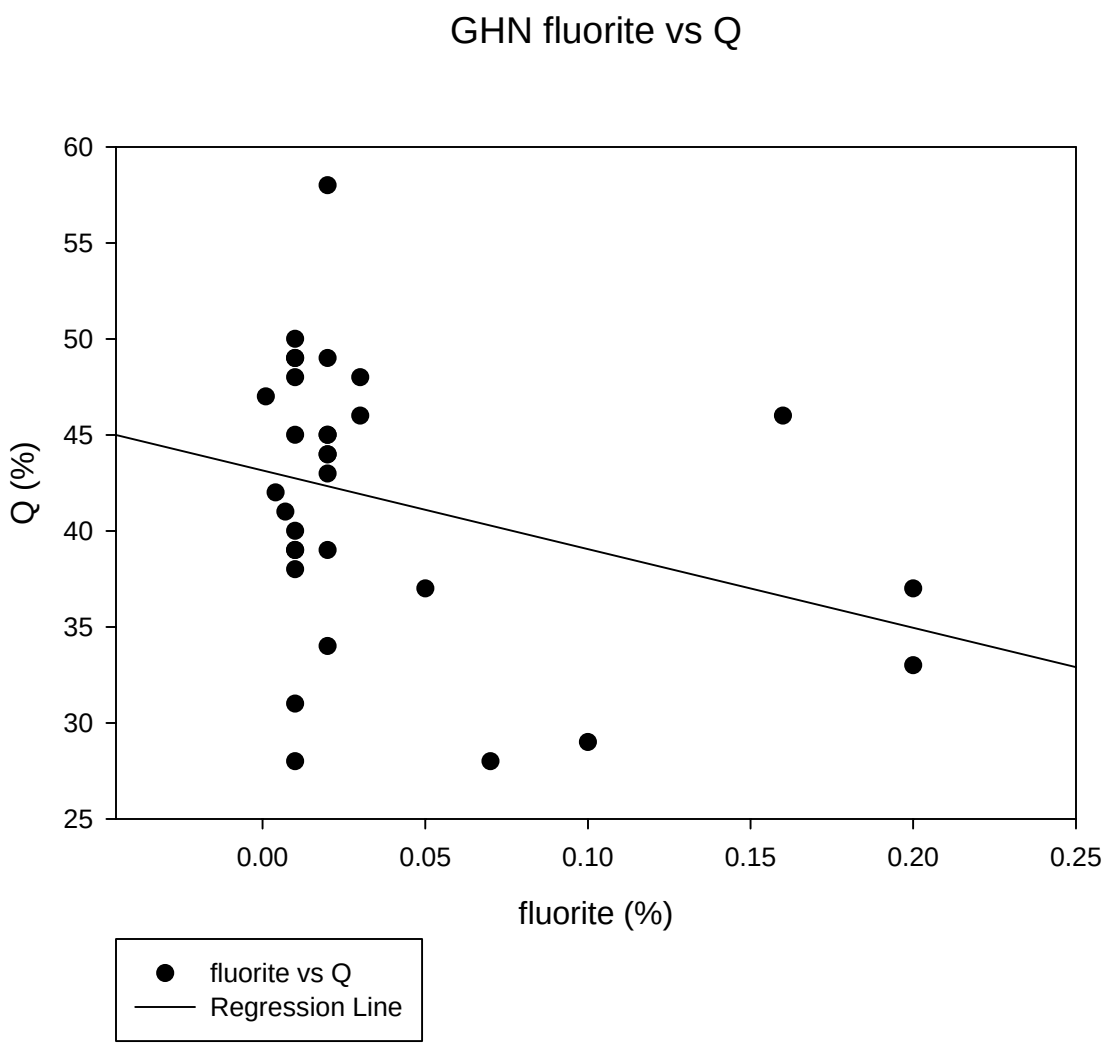
GHN fluorite vs Q
60
55
50
45
40
35
30
25
Q (%)
0.00
0.05
0.10
0.15
0.20
0.25
fluorite (%)
fluorite vs Q
Regression Line

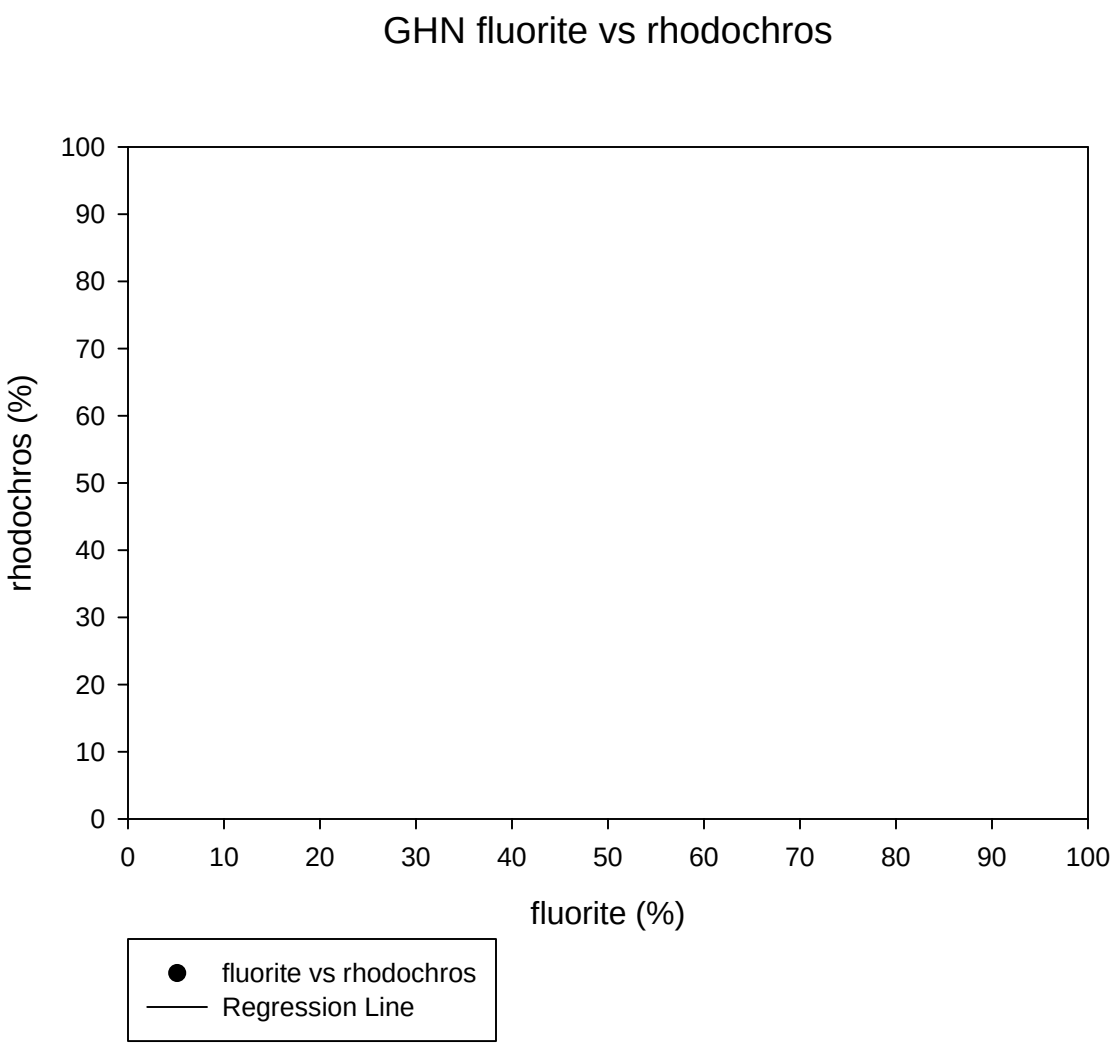
GHN fluorite vs rhodochros
rhodochros (%)
100
90
80
70
60
50
40
30
20
10
0
0
10
20
30
40
50
60
70
80
90
100
fluorite (%)
fluorite vs rhodochros
Regression Line

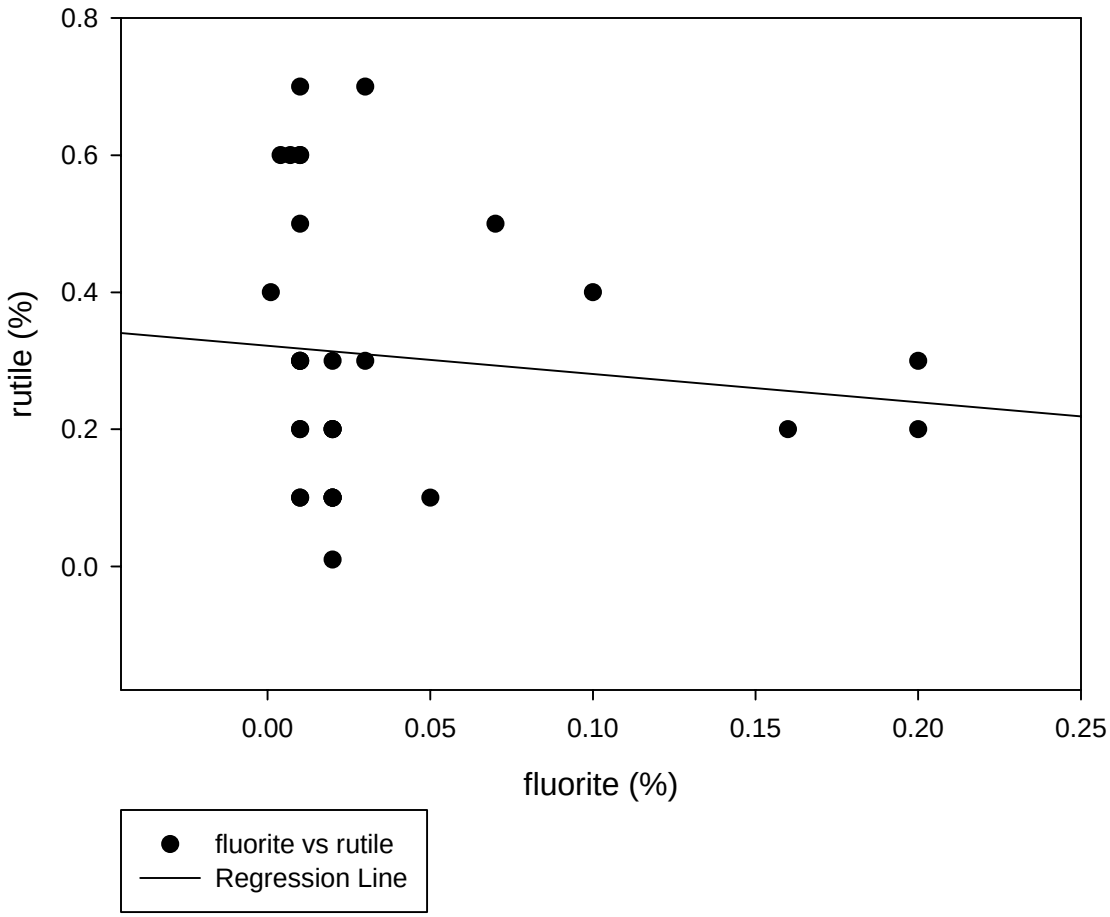
GHN fluorite vs rutile
0.8
0.6
0.4
0.2
0.0
rutile (%)
0.00
0.05
0.10
0.15
0.20
0.25
fluorite (%)
fluorite vs rutile
Regression Line

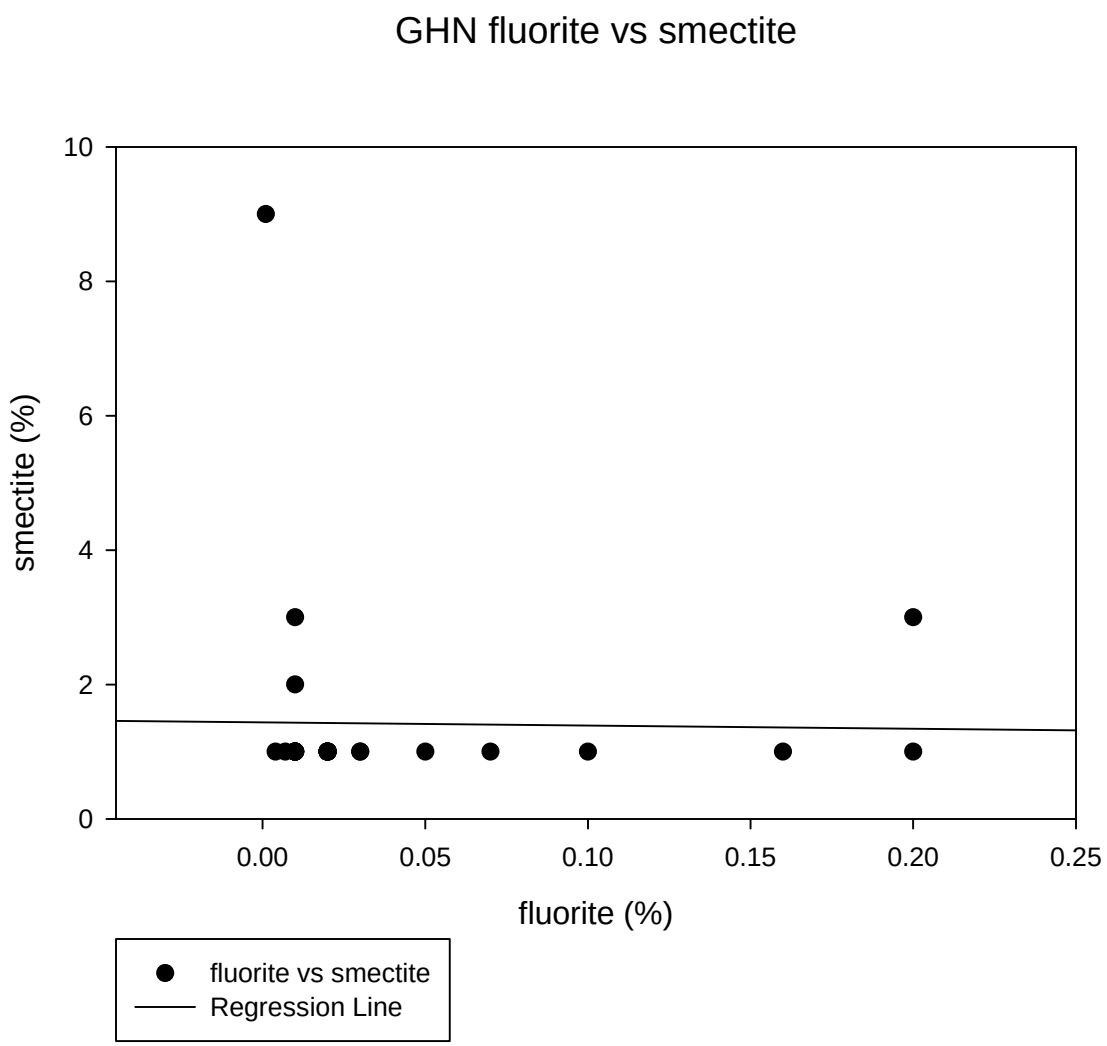
GHN fluorite vs smectite
smectite (%)
10
8
6
4
2
0
0.00
0.05
0.10
0.15
0.20
0.25
fluorite (%)
fluorite vs smectite
Regression Line

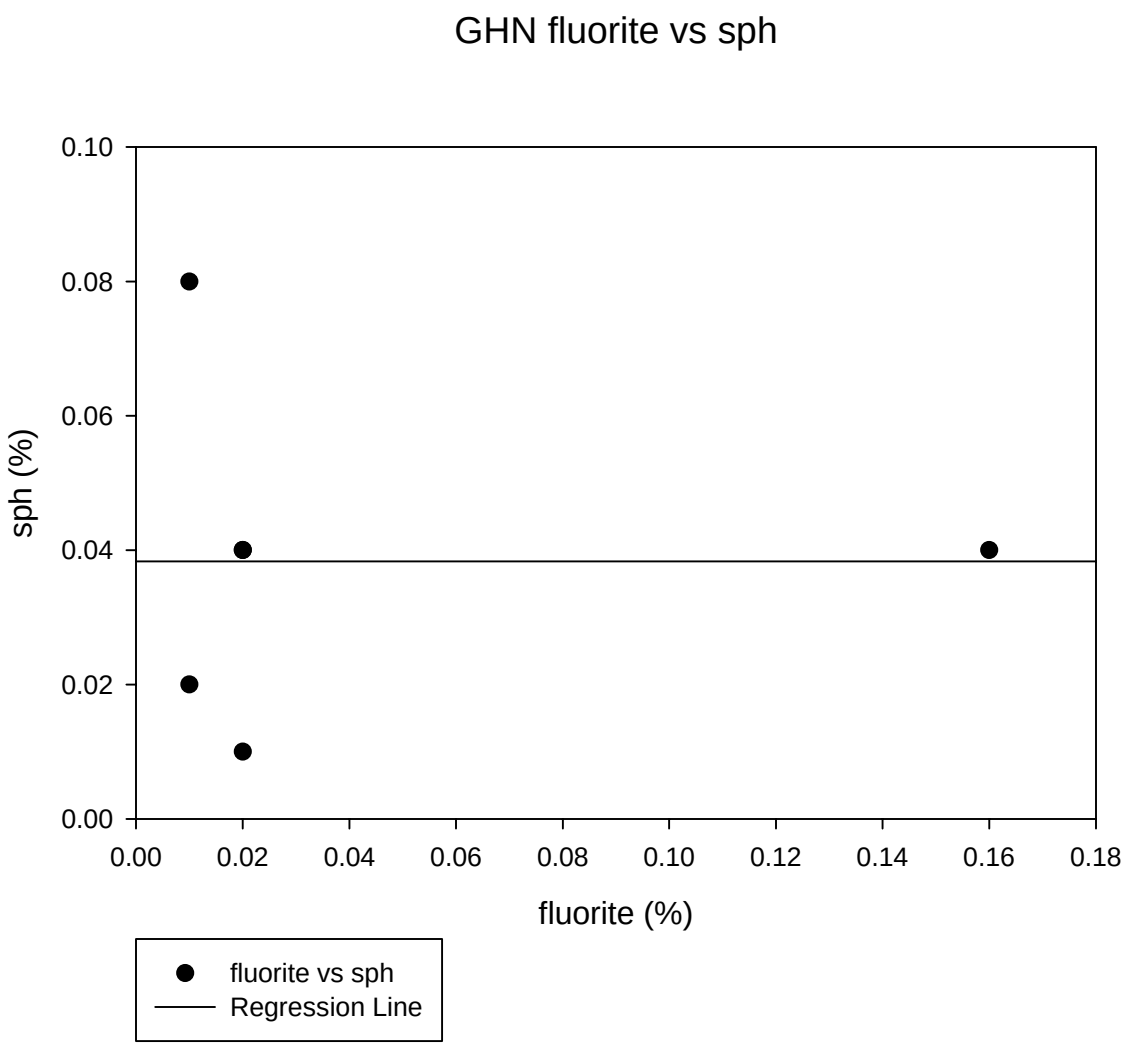
GHN fluorite vs sph
0.10
0.08
0.06
0.04
0.02
0.00
sph (%)
0.00
0.02
0.04
0.06
0.08
0.10
0.12
0.14
0.16
0.18
fluorite (%)
fluorite vs sph
Regression Line

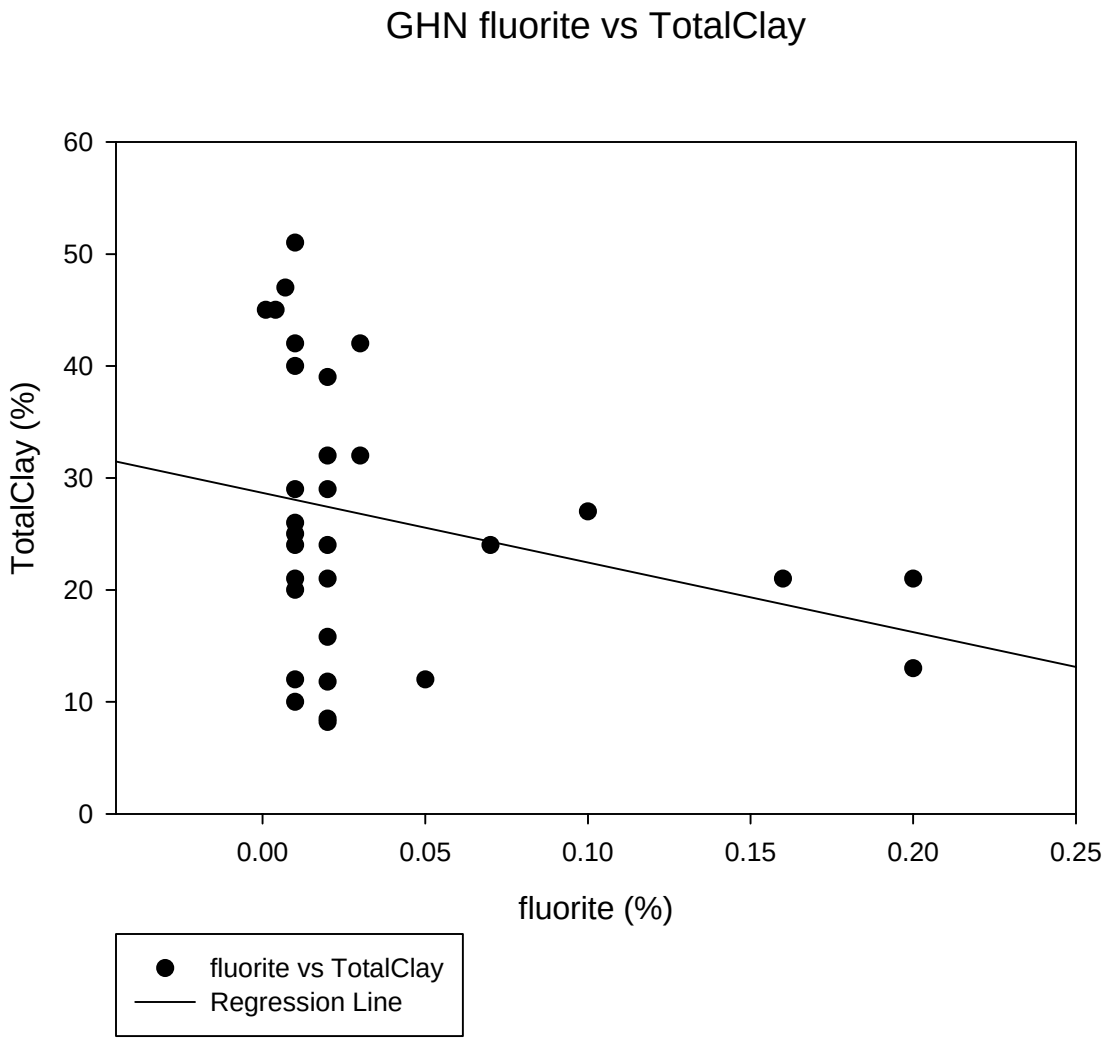
GHN fluorite vs TotalClay
TotalClay (%)
60
50
40
30
20
10
0
0.00
0.05
0.10
0.15
0.20
0.25
fluorite (%)
fluorite vs TotalClay
Regression Line

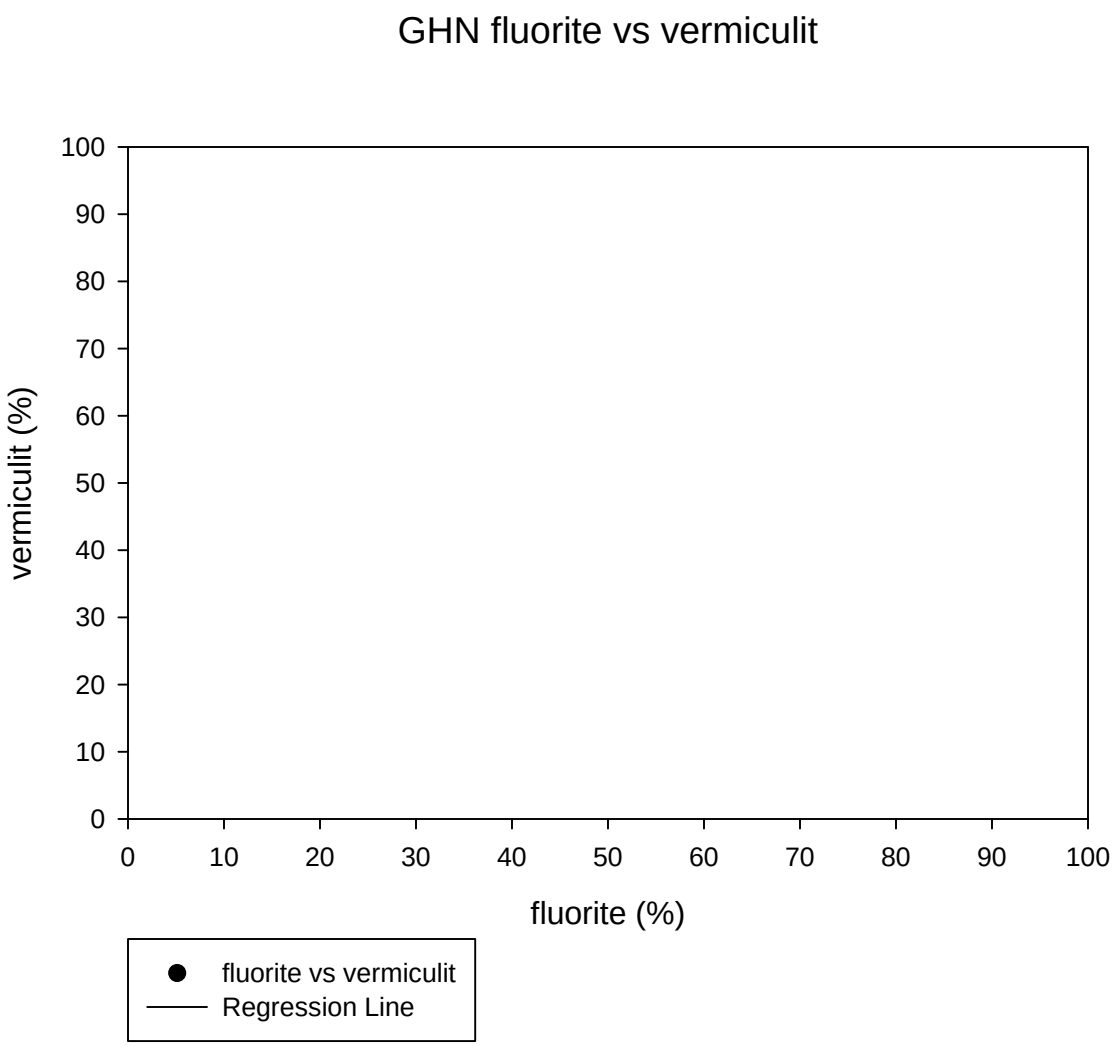
GHN fluorite vs vermiculit
vermiculit (%)
fluorite (%)
0
10
20
30
40
50
60
70
80
90
100
fluorite vs vermiculit
Regression Line

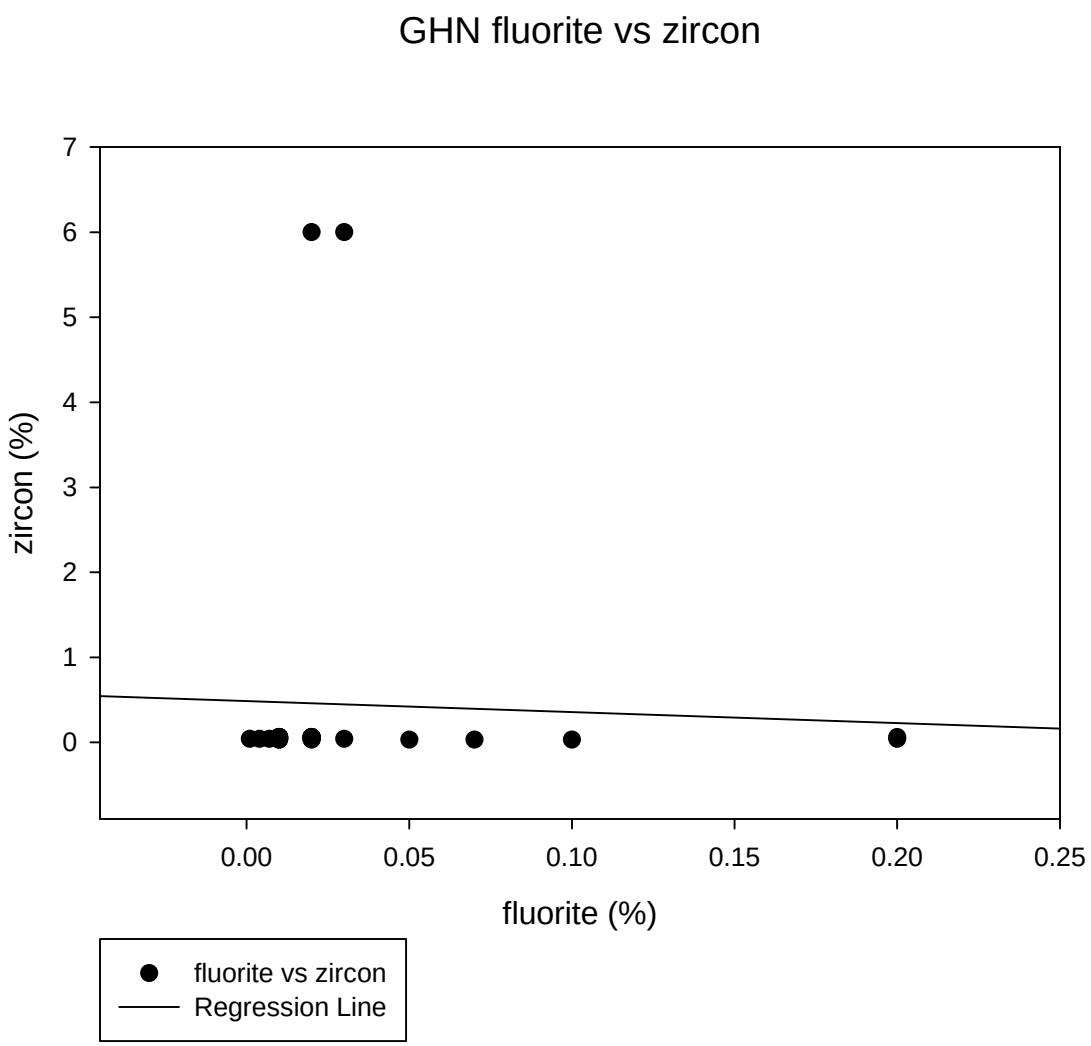
GHN fluorite vs zircon
zircon (%)
7
6
5
4
3
2
1
0
0.00
0.05
0.10
0.15
0.20
0.25
fluorite (%)
fluorite vs zircon
Regression Line

APPENDIX 4 – GIS MODEL ITERATIONS

Goathill North Rock Pile Modeling

Fluoride Concentration (ppm)

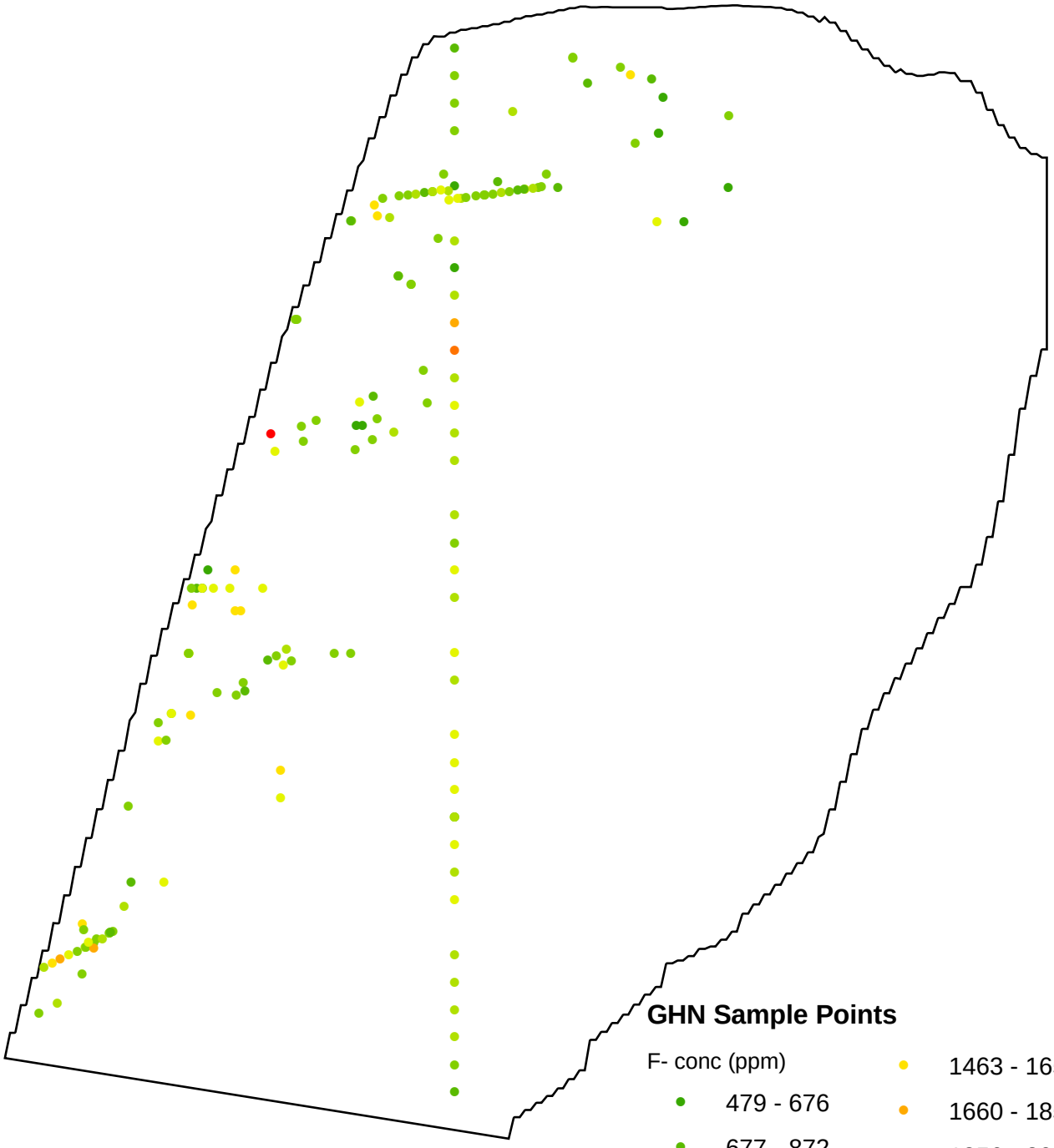

Goathill North Rock Pile Modeling

Inverse Distance Weighting #1

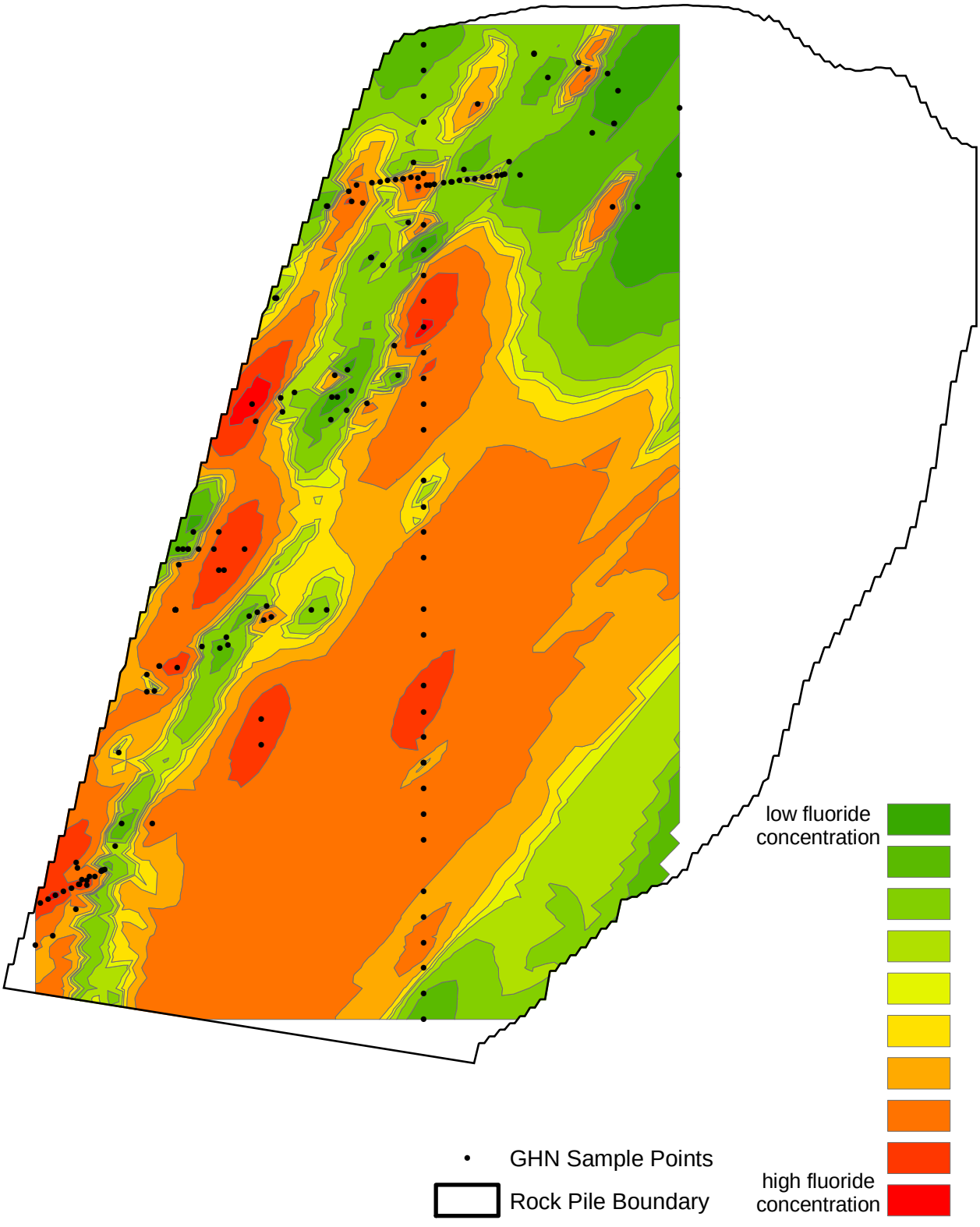

Goathill North Rock Pile Modeling

Inverse Distance Weighting #2

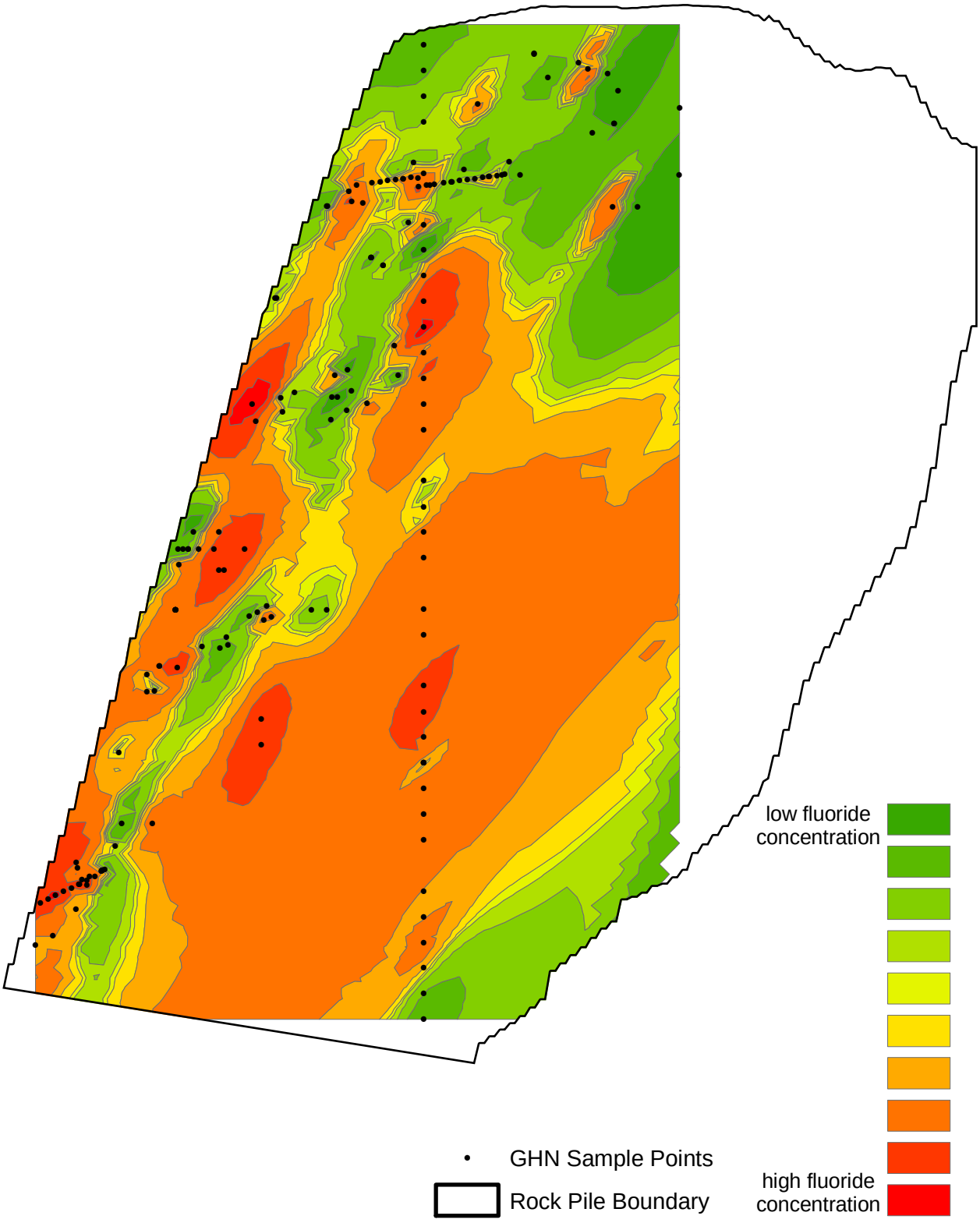

Goathill North Rock Pile Modeling

Inverse Distance Weighting #3

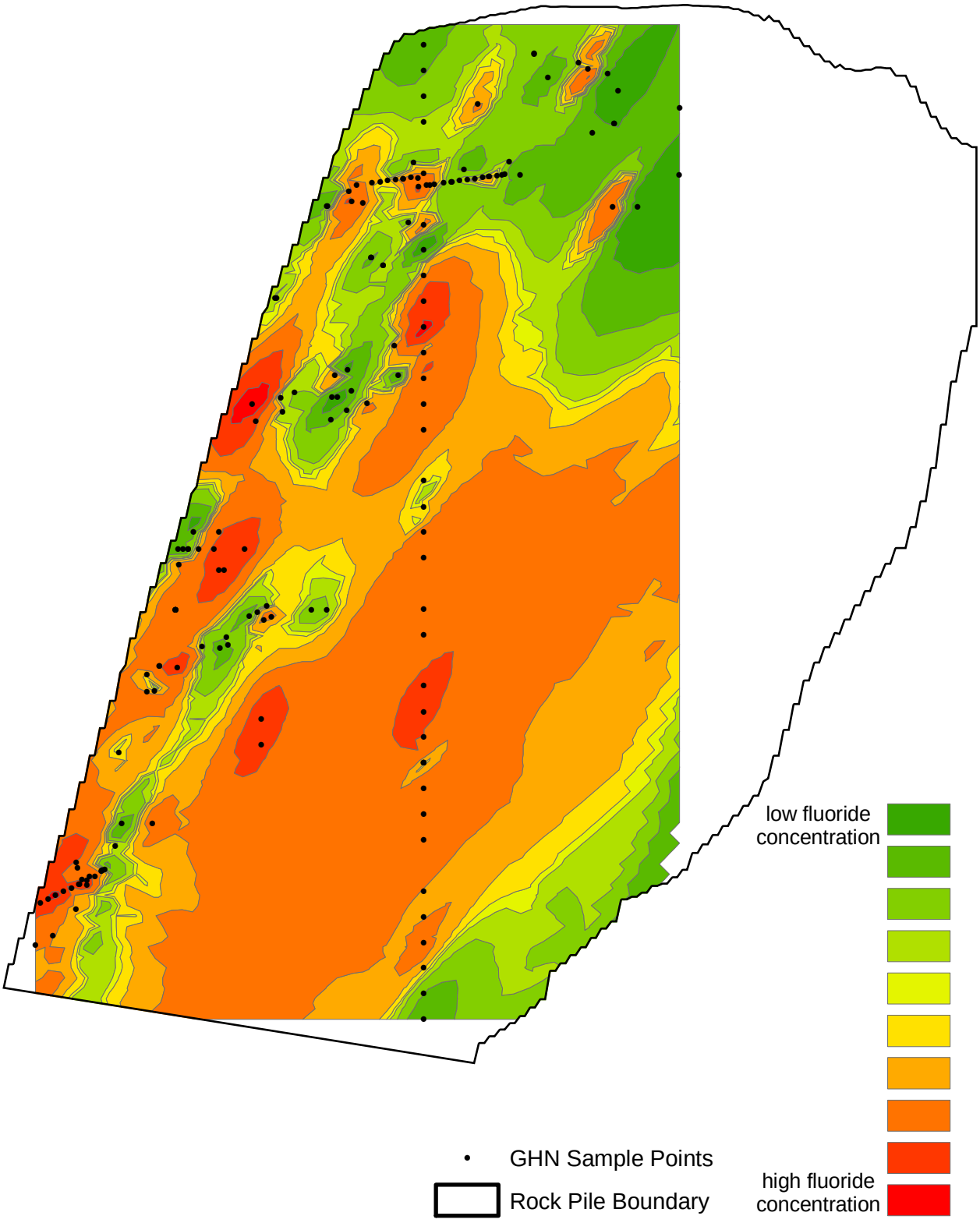

Goathill North Rock Pile Modeling

Inverse Distance Weighting #4

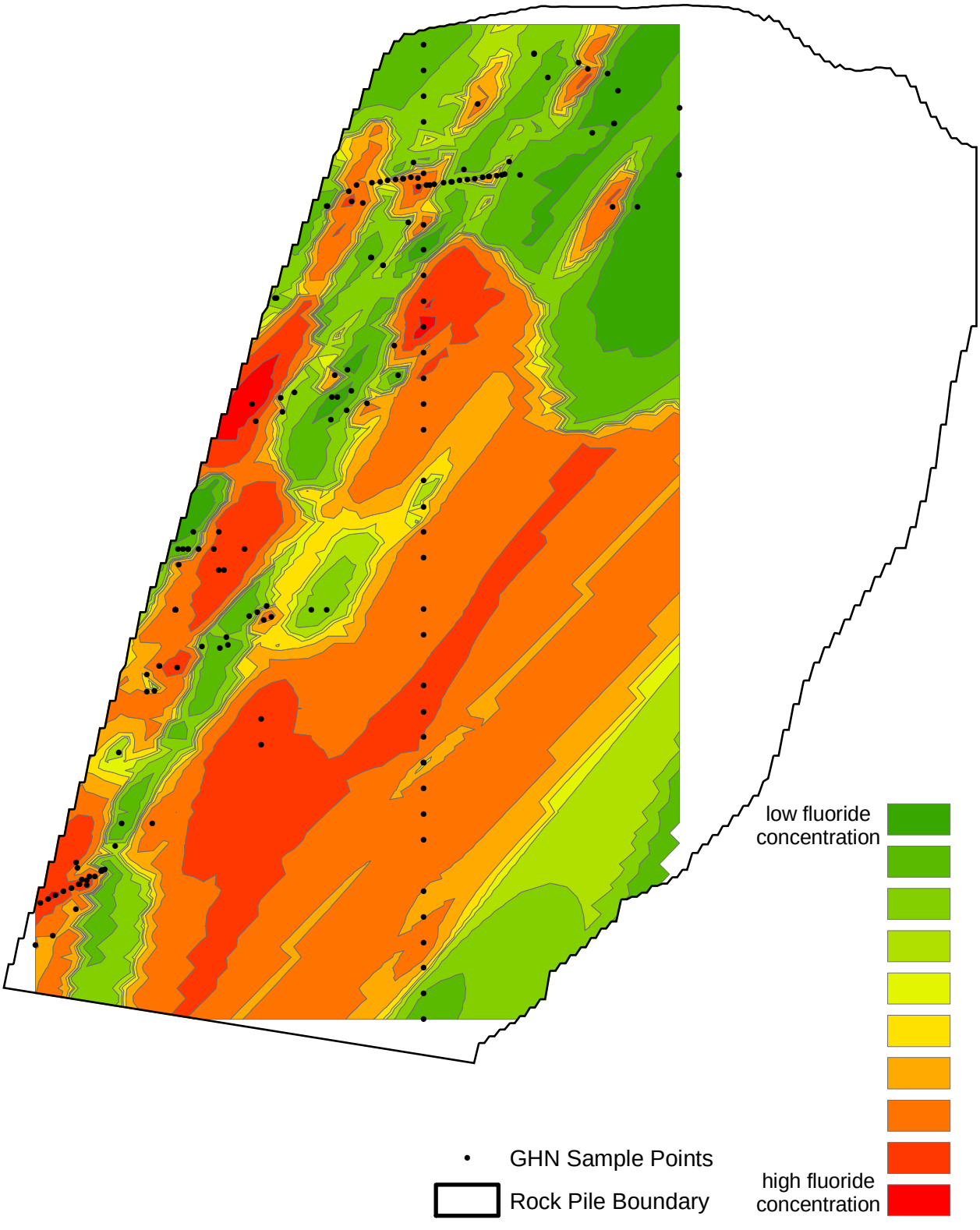

Goathill North Rock Pile Modeling

Inverse Distance Weighting #5

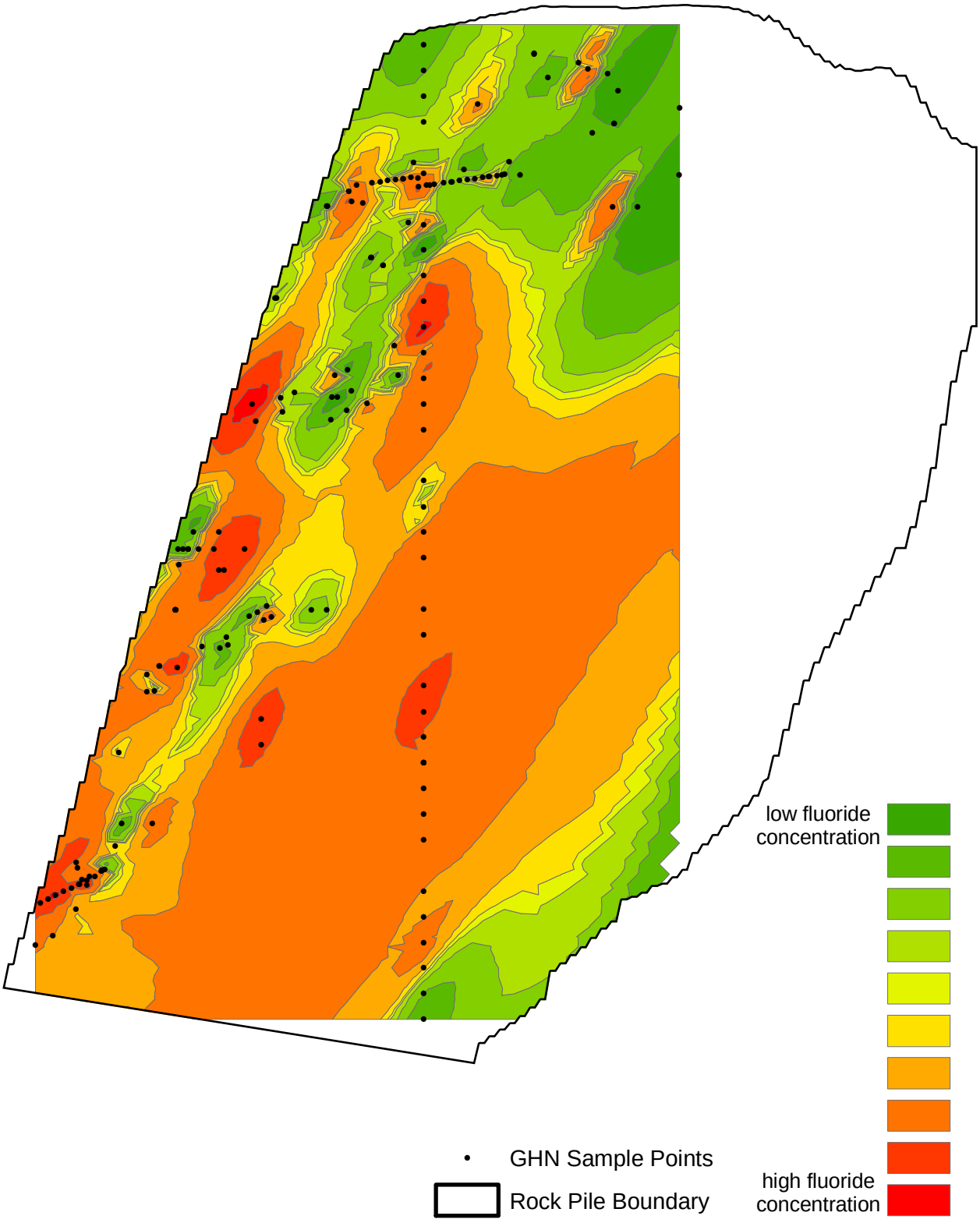

Goathill North Rock Pile Modeling

Inverse Distance Weighting #6

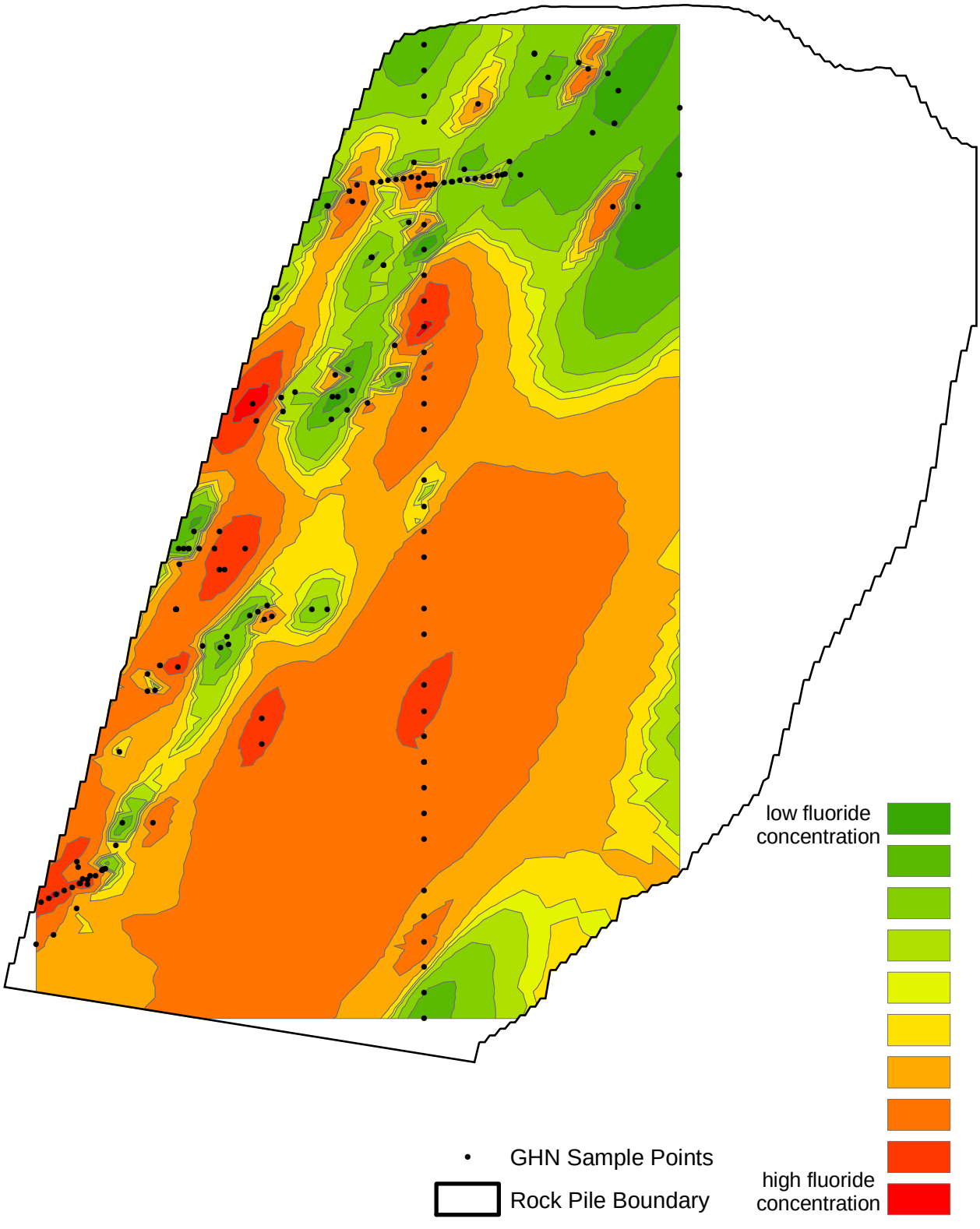

Goathill North Rock Pile Modeling

Inverse Distance Weighting #7

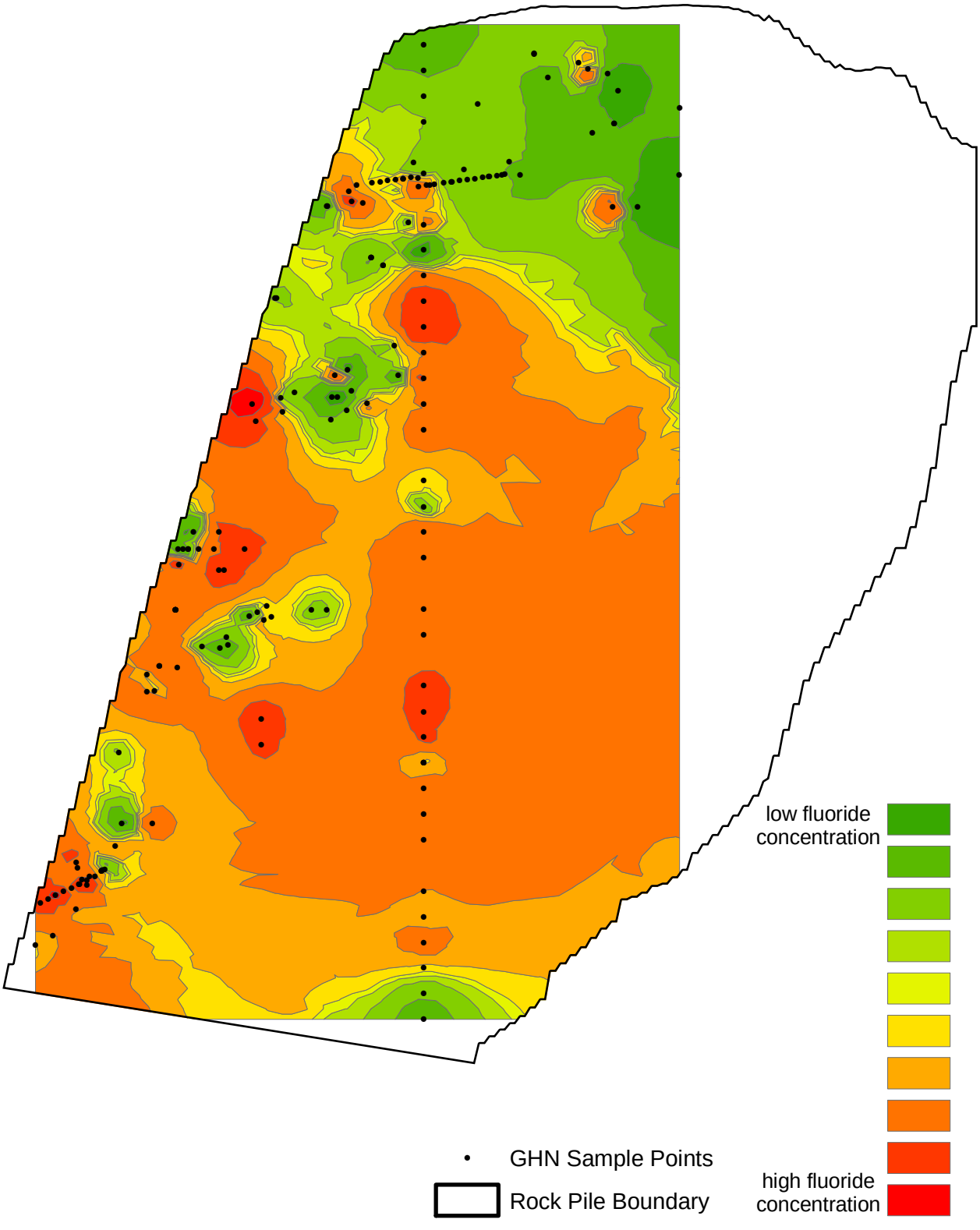

Goathill North Rock Pile Modeling

Inverse Distance Weighting #8

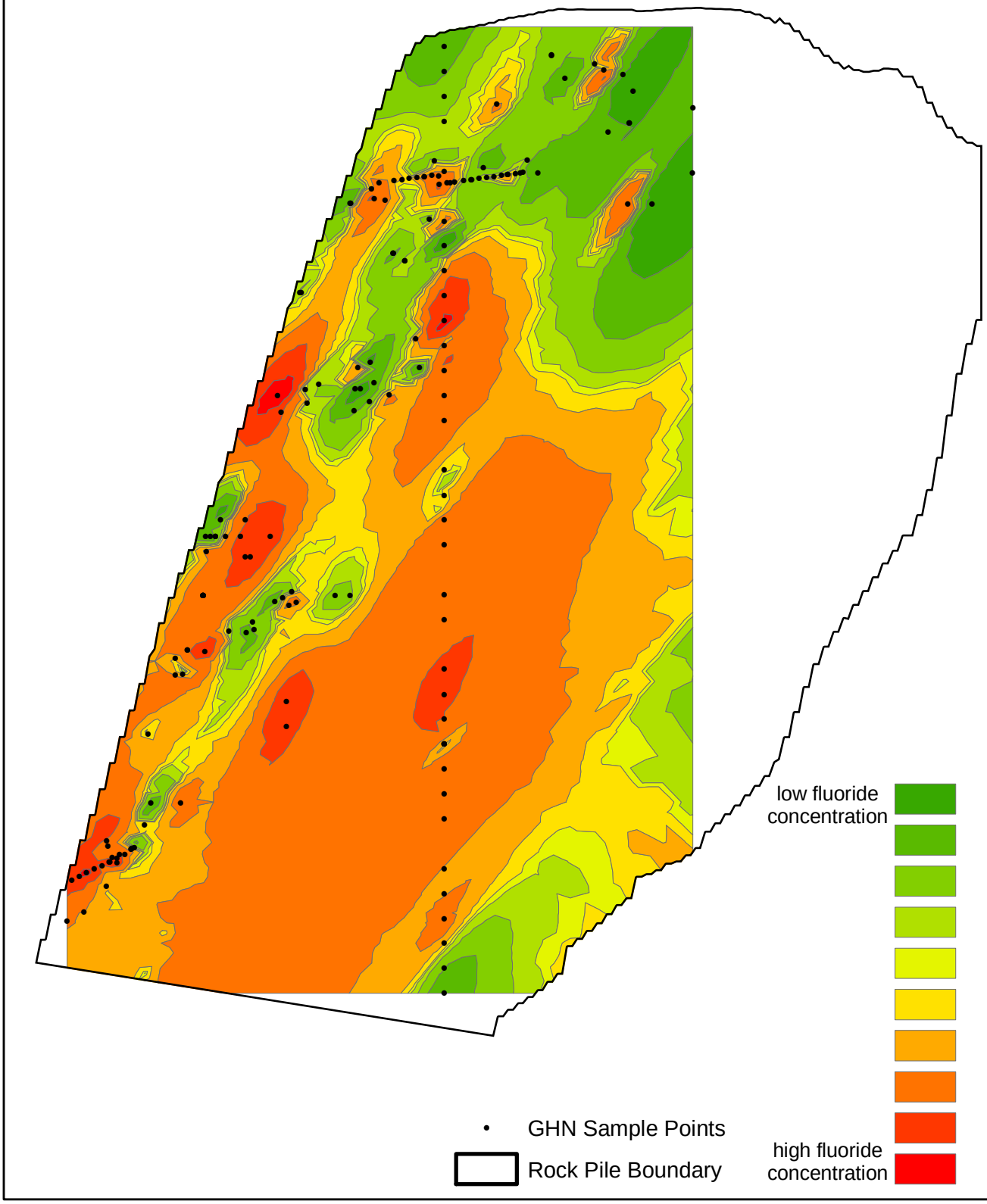

Goathill North Rock Pile Modeling

Radial Basis Function #1

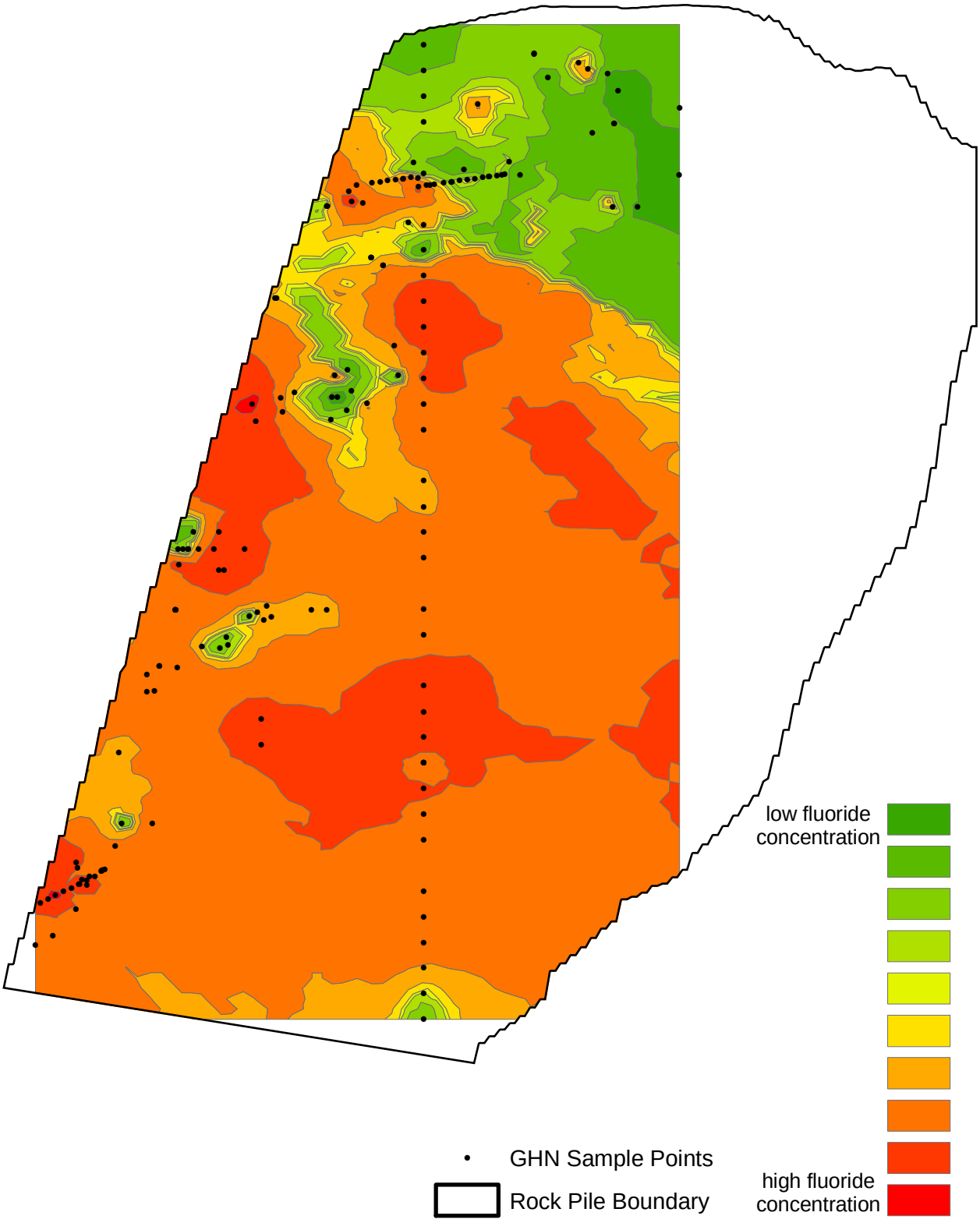

Goathill North Rock Pile Modeling

Radial Basis Function #2

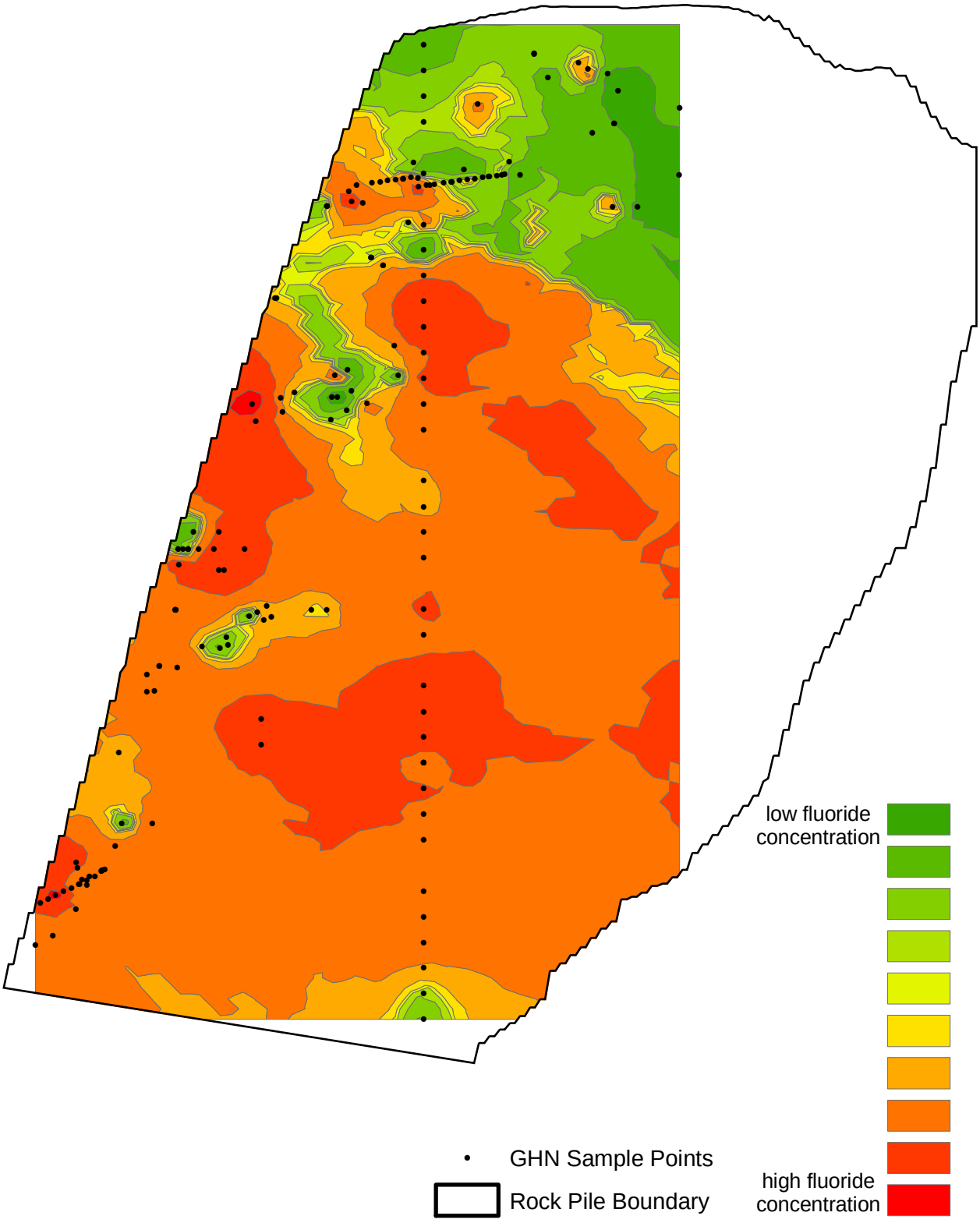

Goathill North Rock Pile Modeling

Radial Basis Function #3

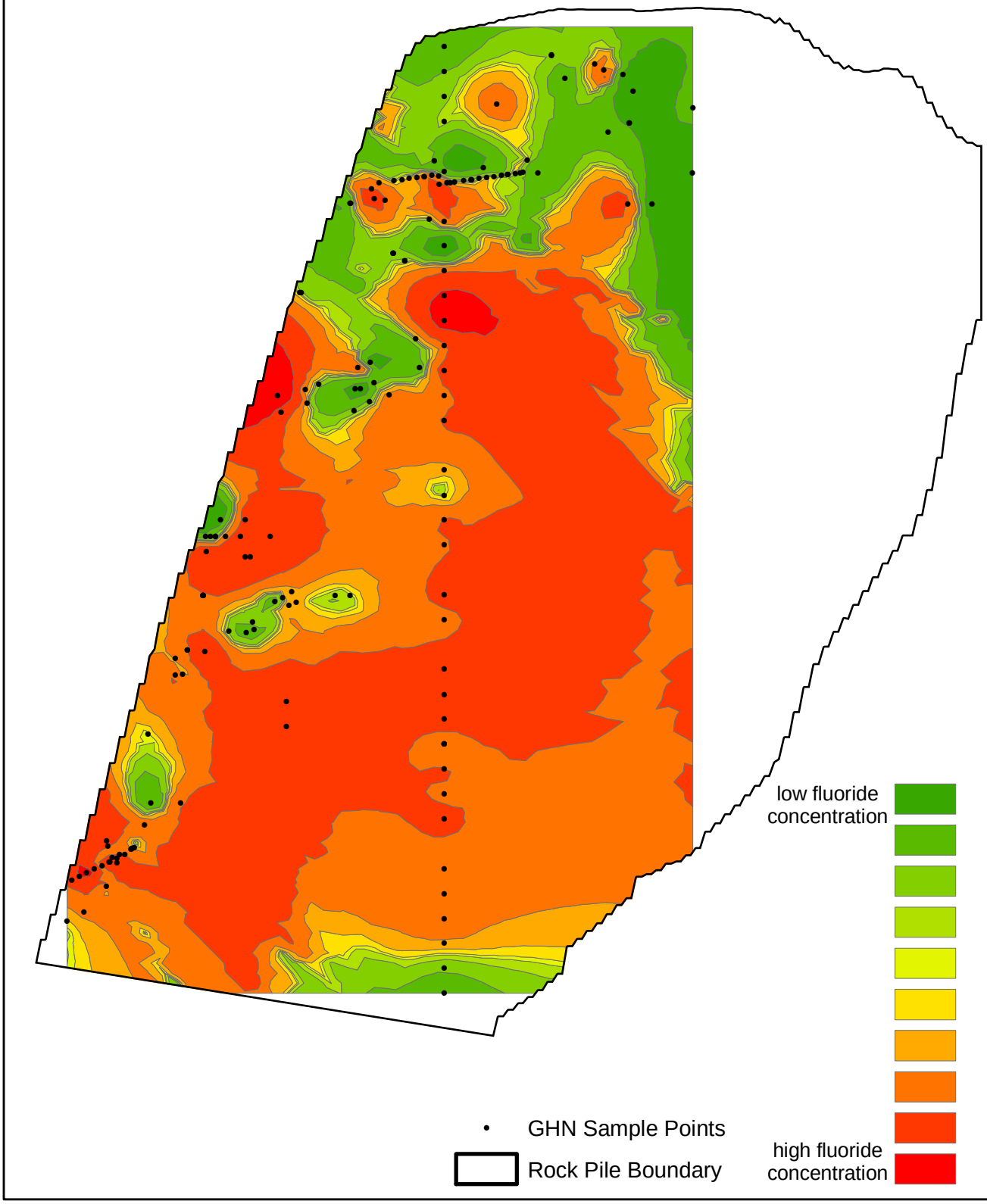

Goathill North Rock Pile Modeling

Radial Basis Function #4

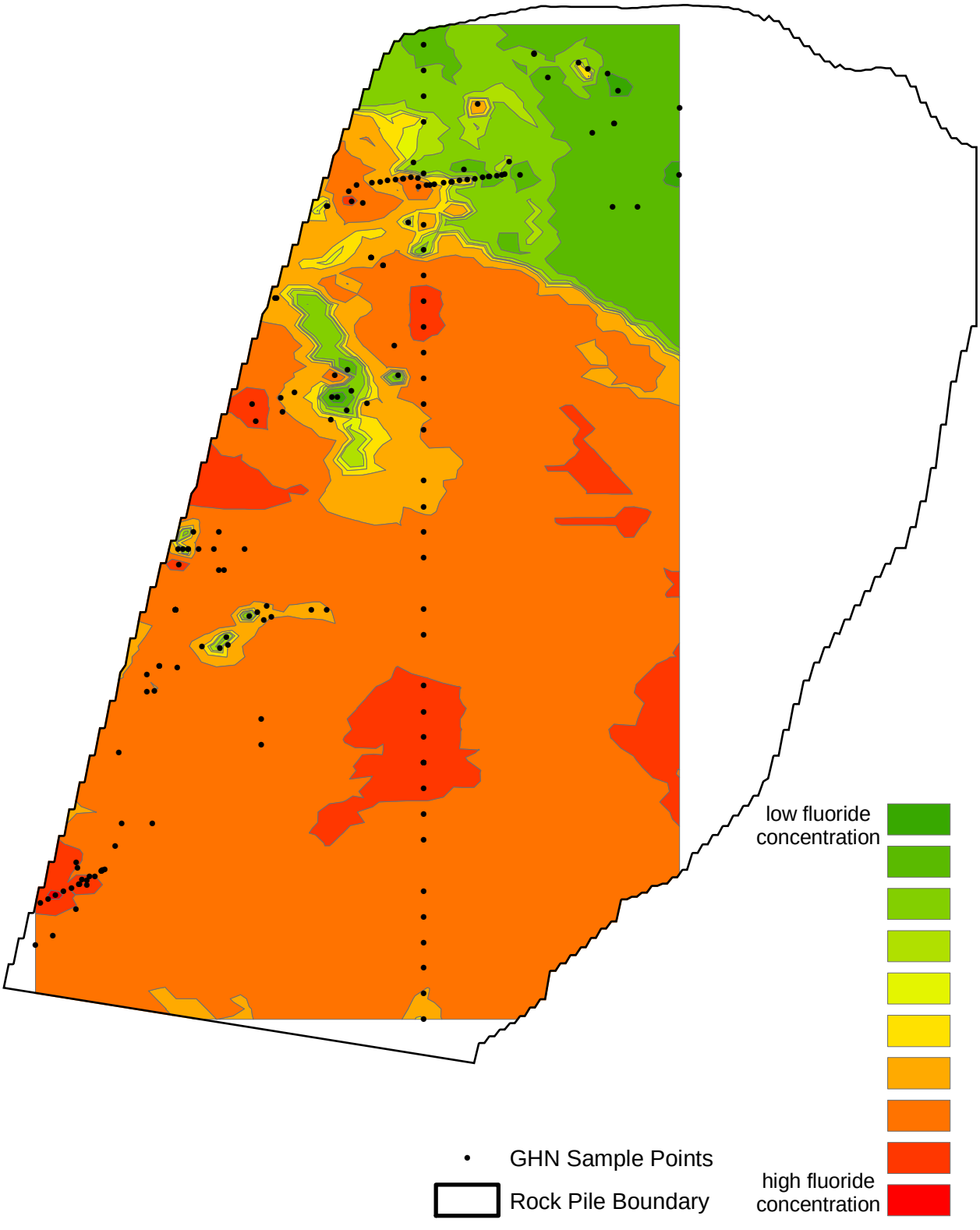

Goathill North Rock Pile Modeling

Radial Basis Function #5

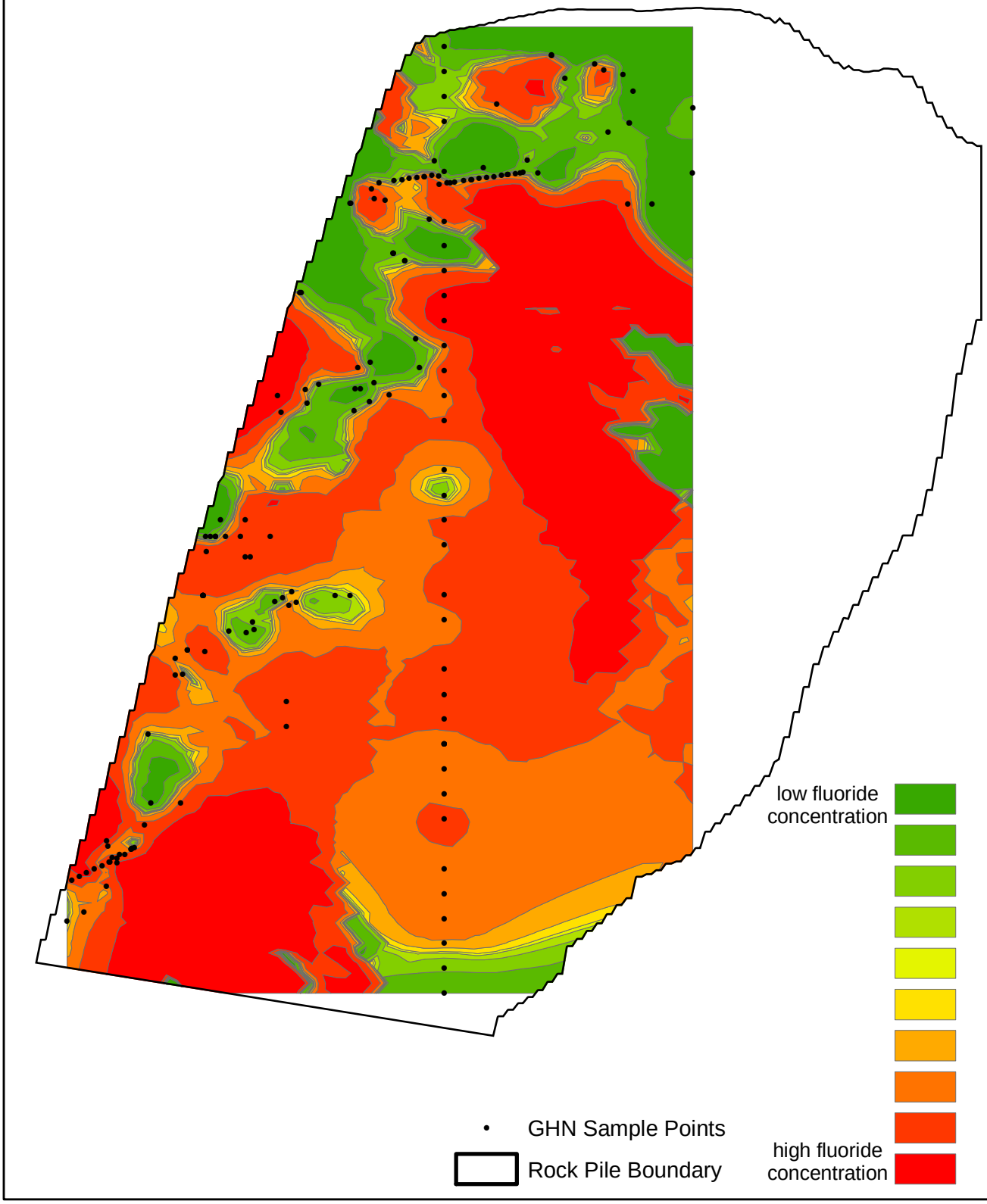

Goathill North Rock Pile Modeling

Radial Basis Function #6

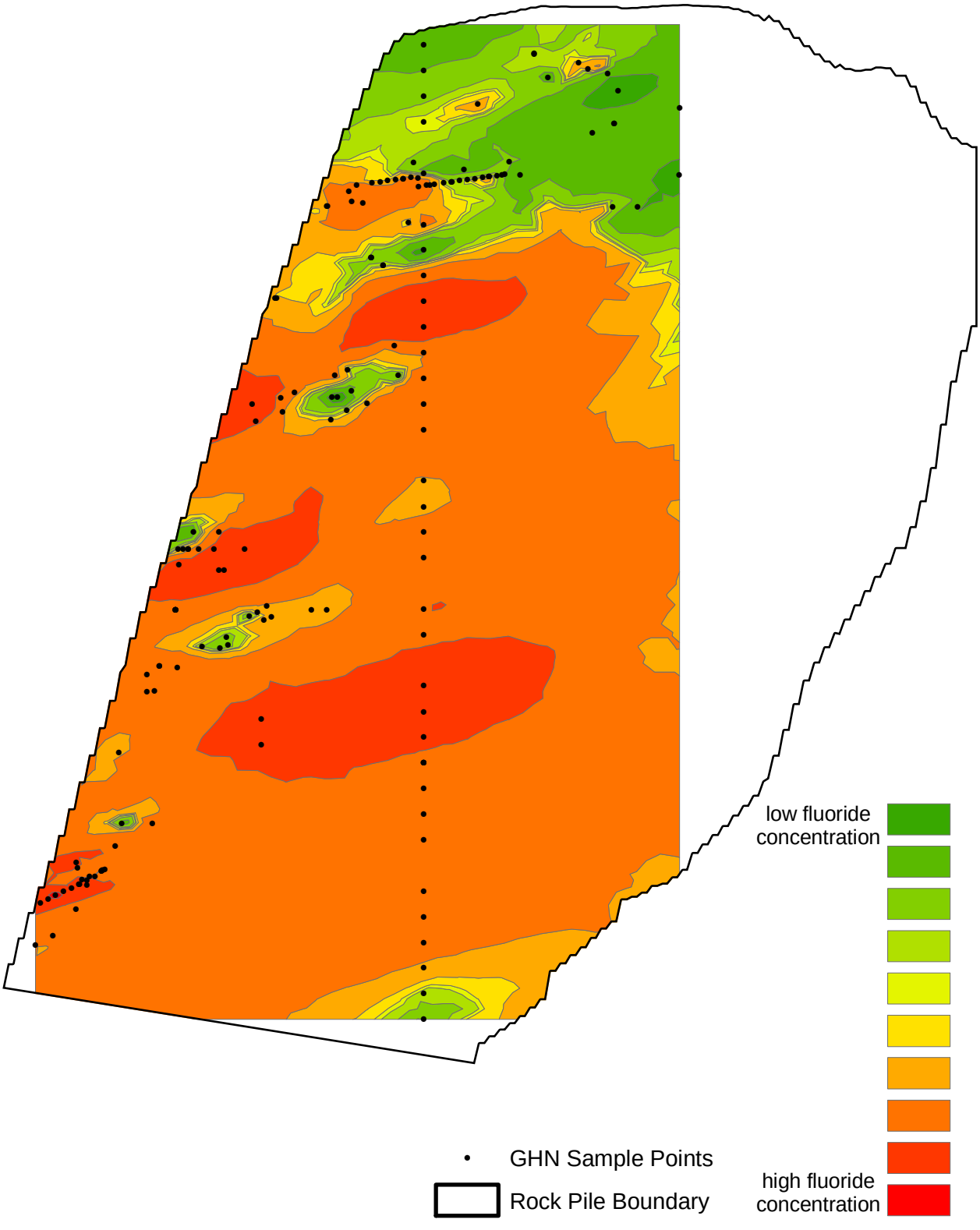

Goathill North Rock Pile Modeling

Radial Basis Function #7

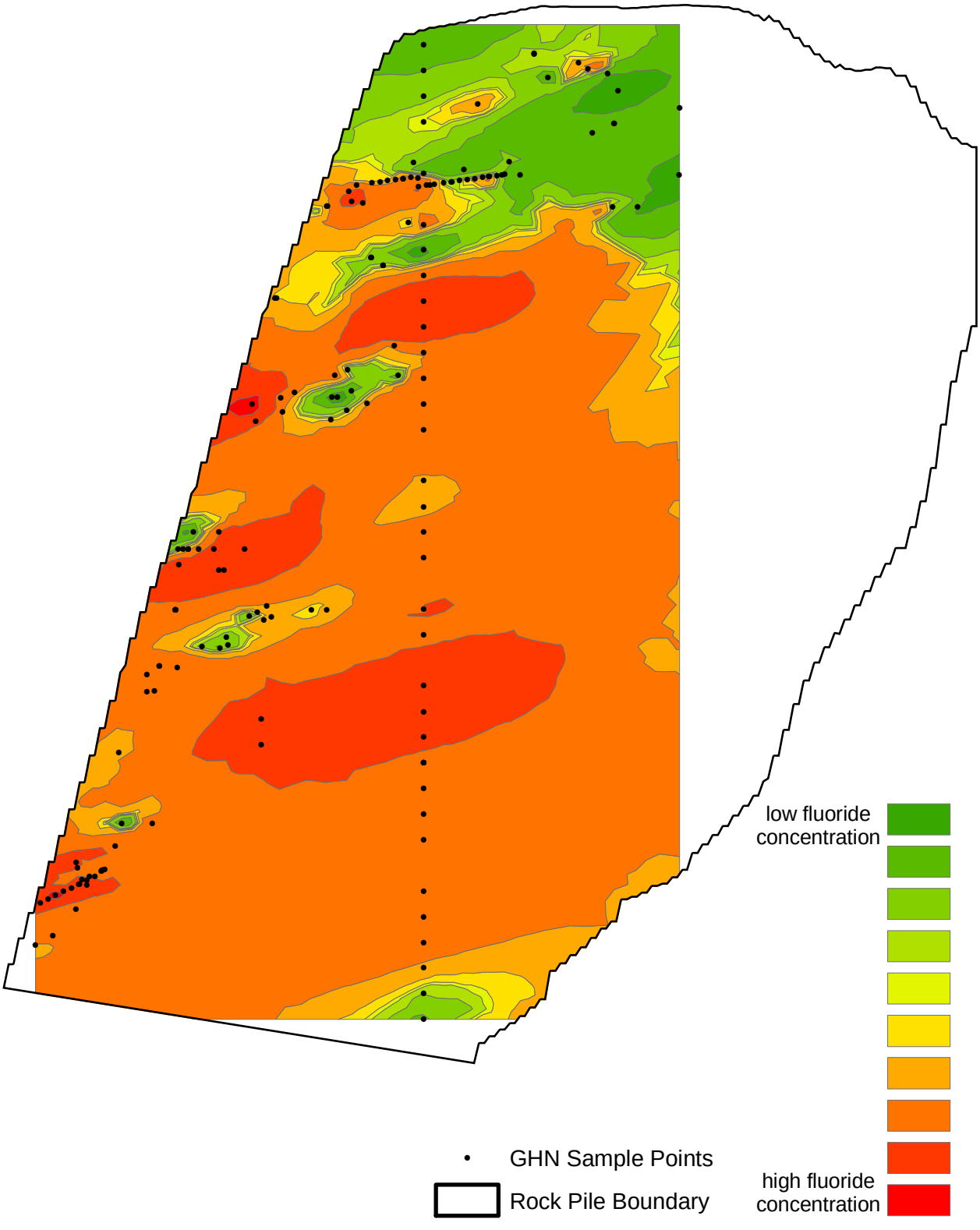

Goathill North Rock Pile Modeling

Radial Basis Function #8

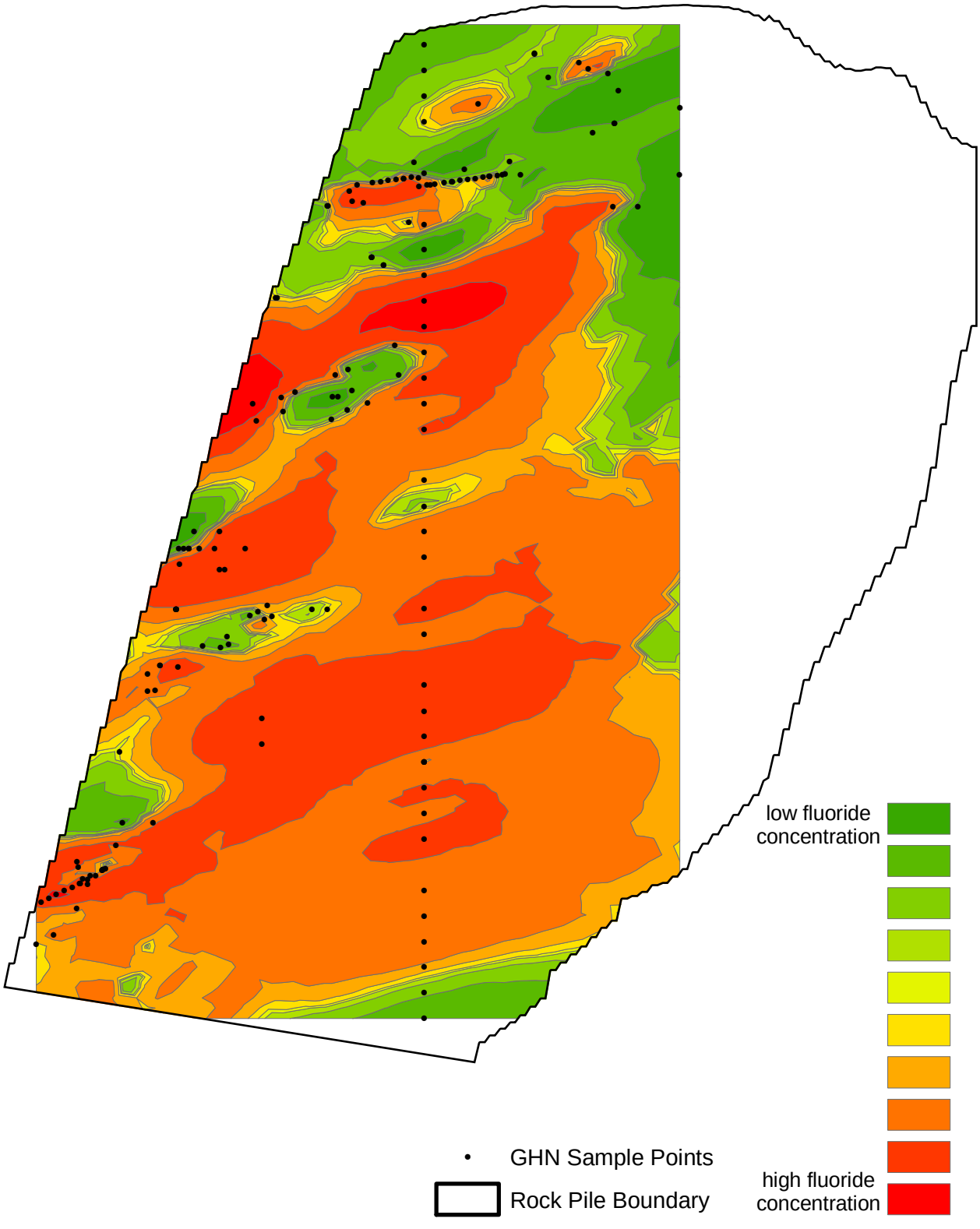

Goathill North Rock Pile Modeling

Radial Basis Function #9

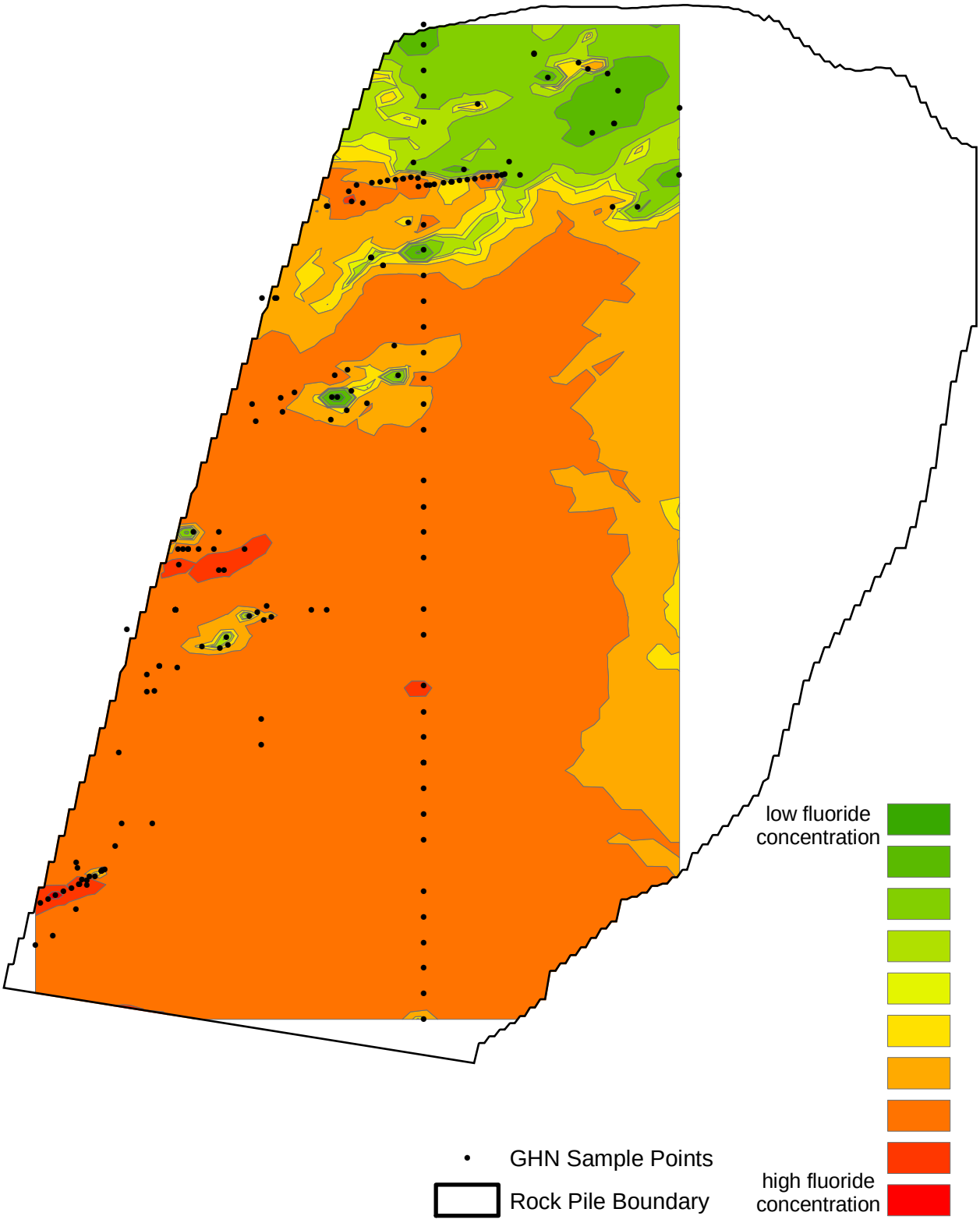

Goathill North Rock Pile Modeling

Radial Basis Function #10

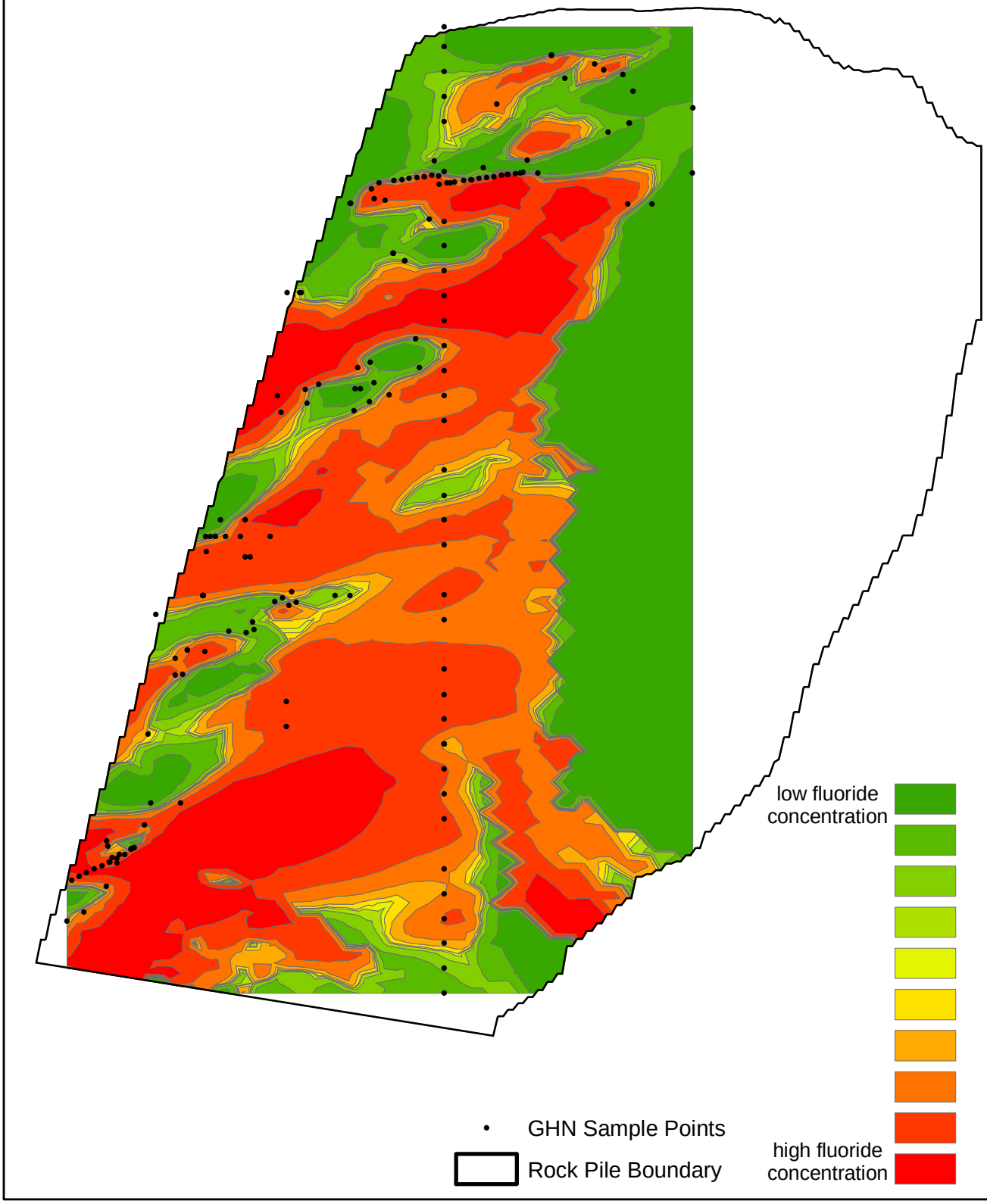

Goathill North Rock Pile Modeling

Global Polynomial Interpolation #1

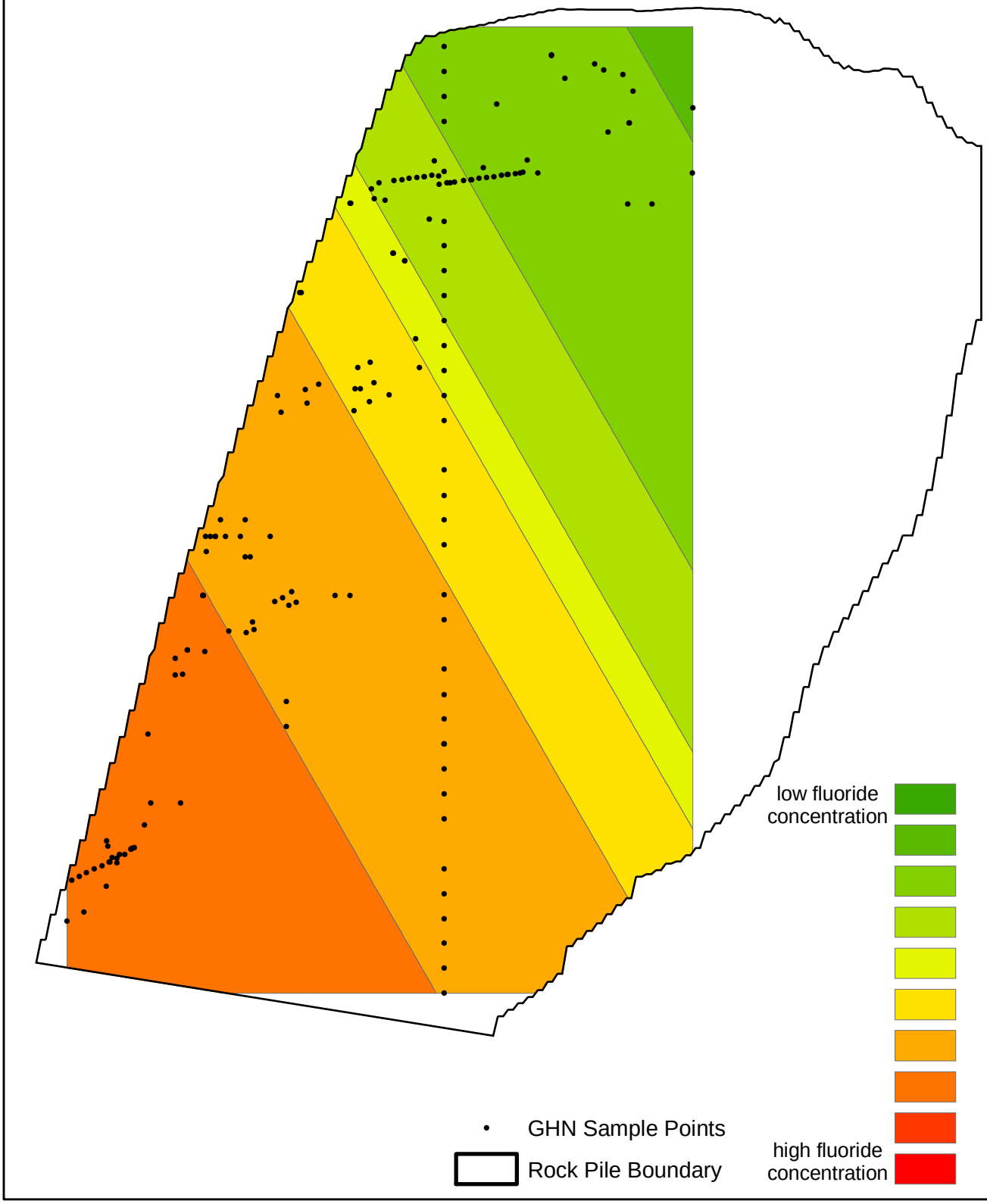

Goathill North Rock Pile Modeling

Global Polynomial Interpolation #2

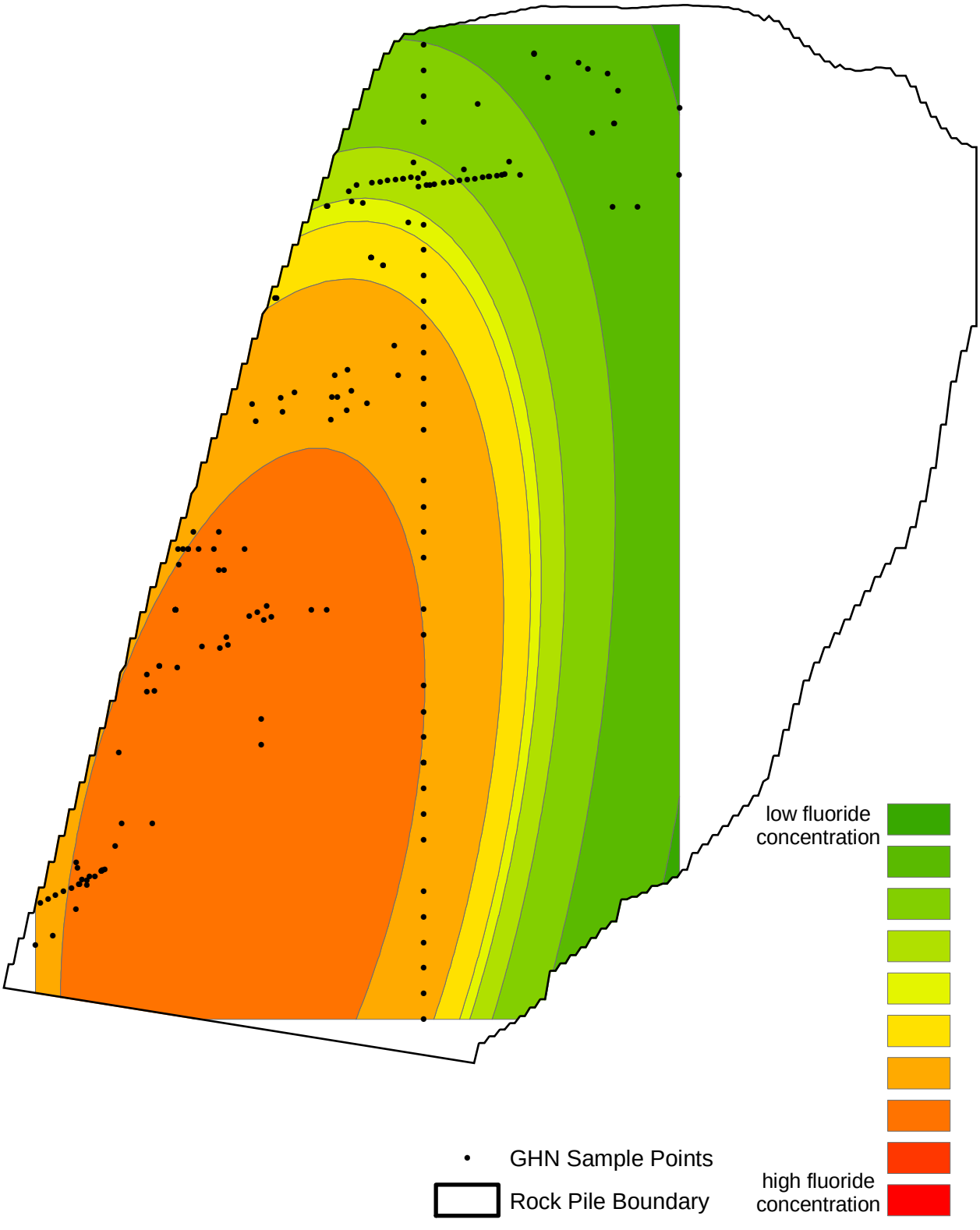

Goathill North Rock Pile Modeling

Global Polynomial Interpolation #3

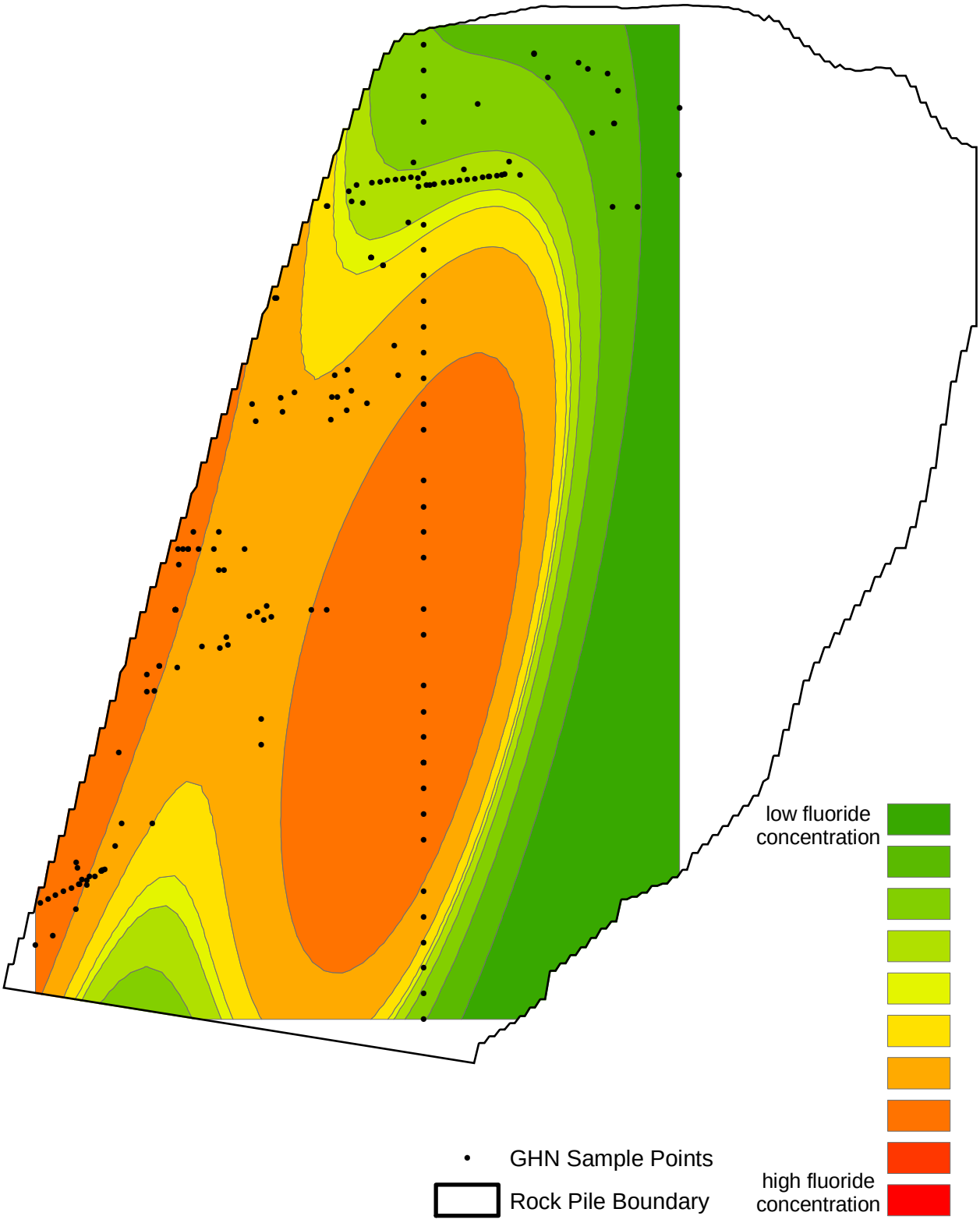

Goathill North Rock Pile Modeling

Global Polynomial Interpolation #4

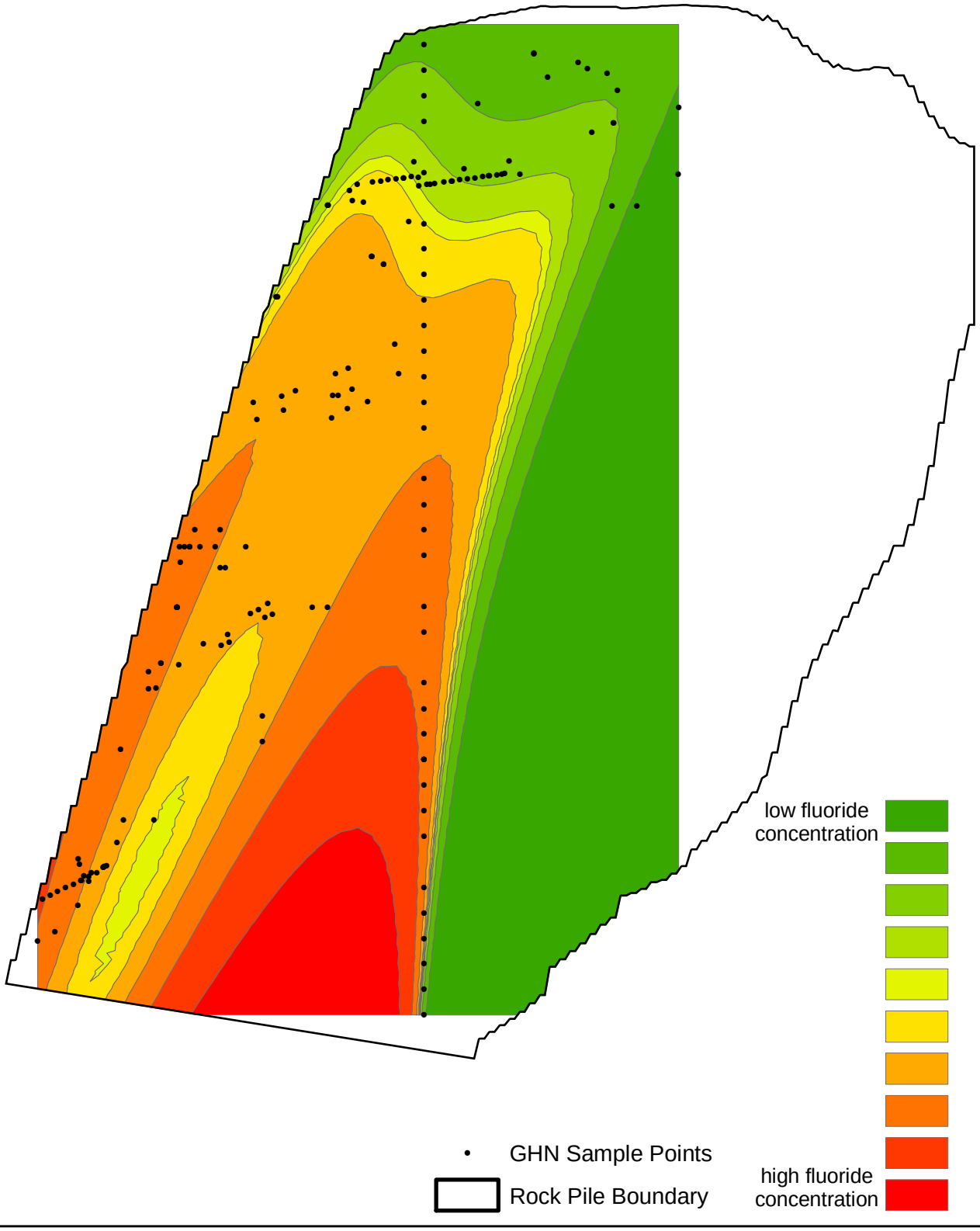

Goathill North Rock Pile Modeling

Global Polynomial Interpolation #5

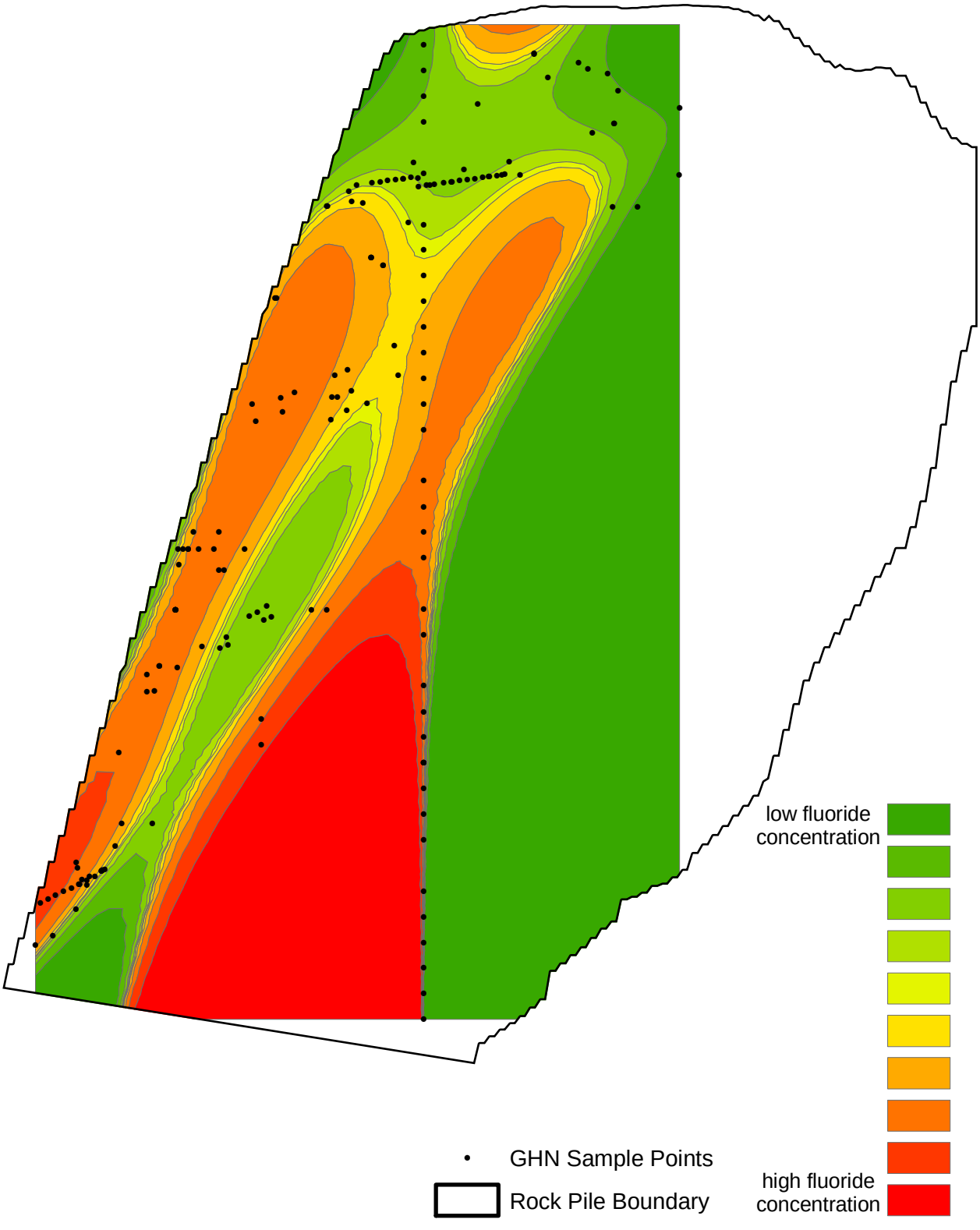

Goathill North Rock Pile Modeling

Global Polynomial Interpolation #6

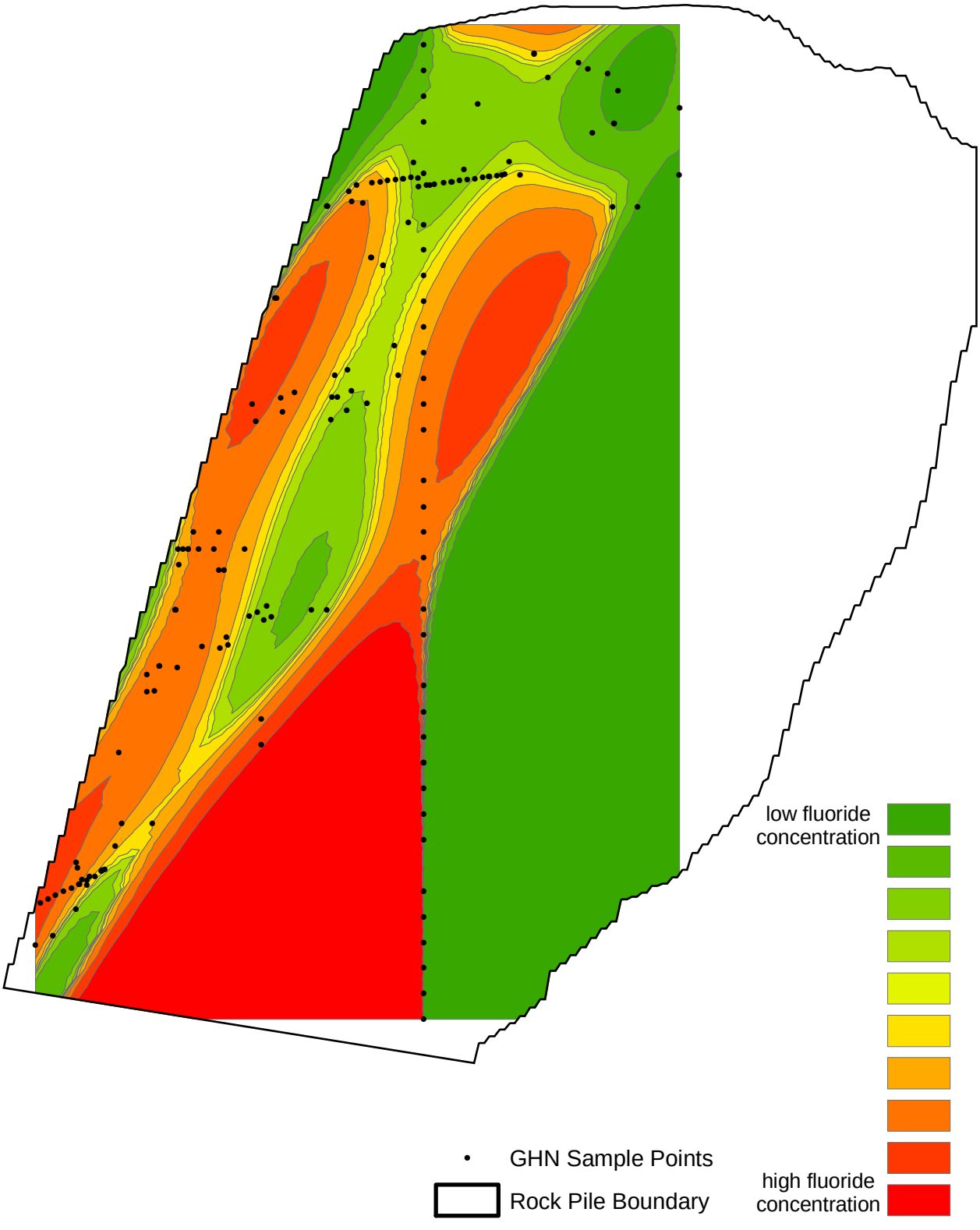

Goathill North Rock Pile Modeling

Global Polynomial Interpolation #7

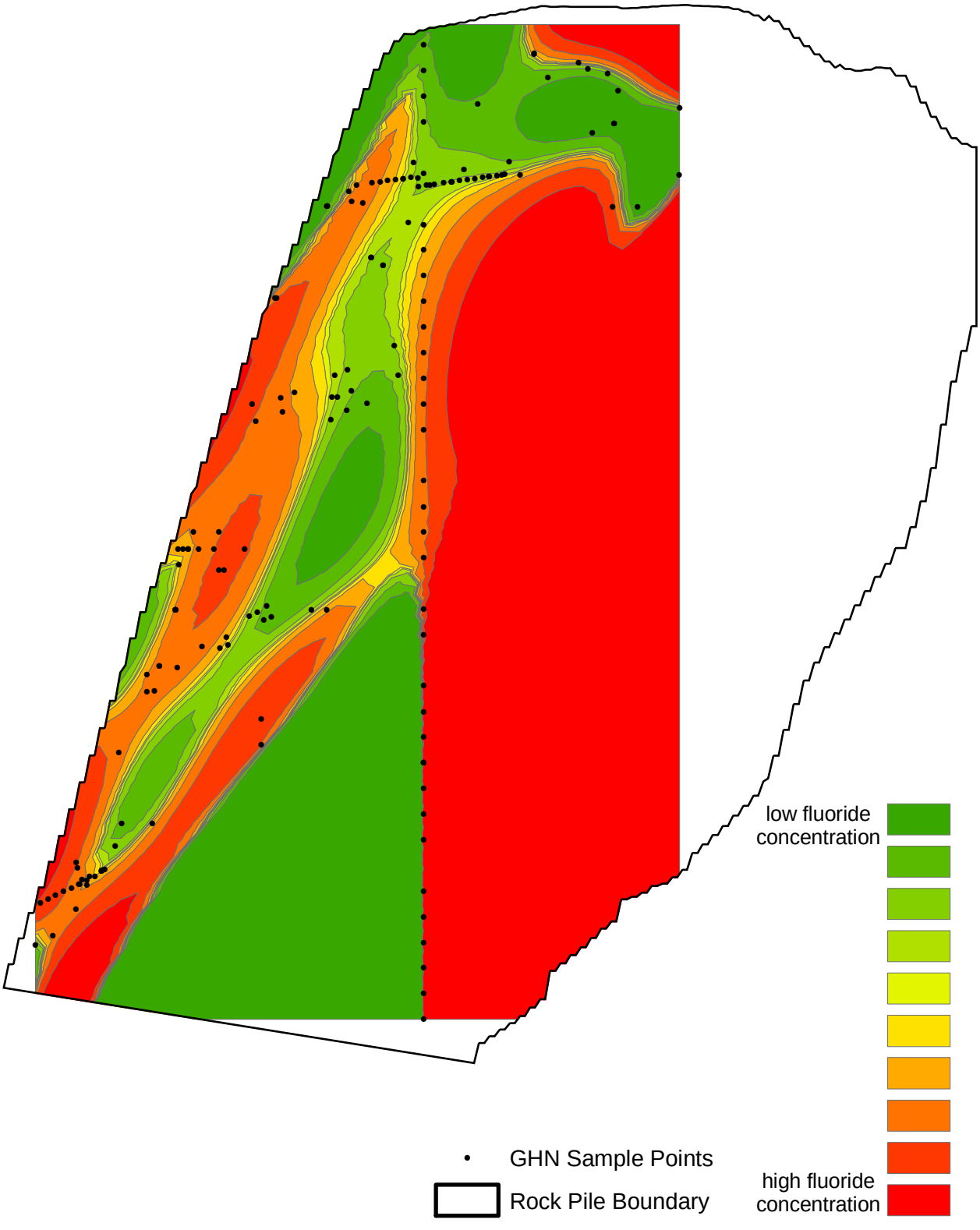

Goathill North Rock Pile Modeling

Global Polynomial Interpolation #8

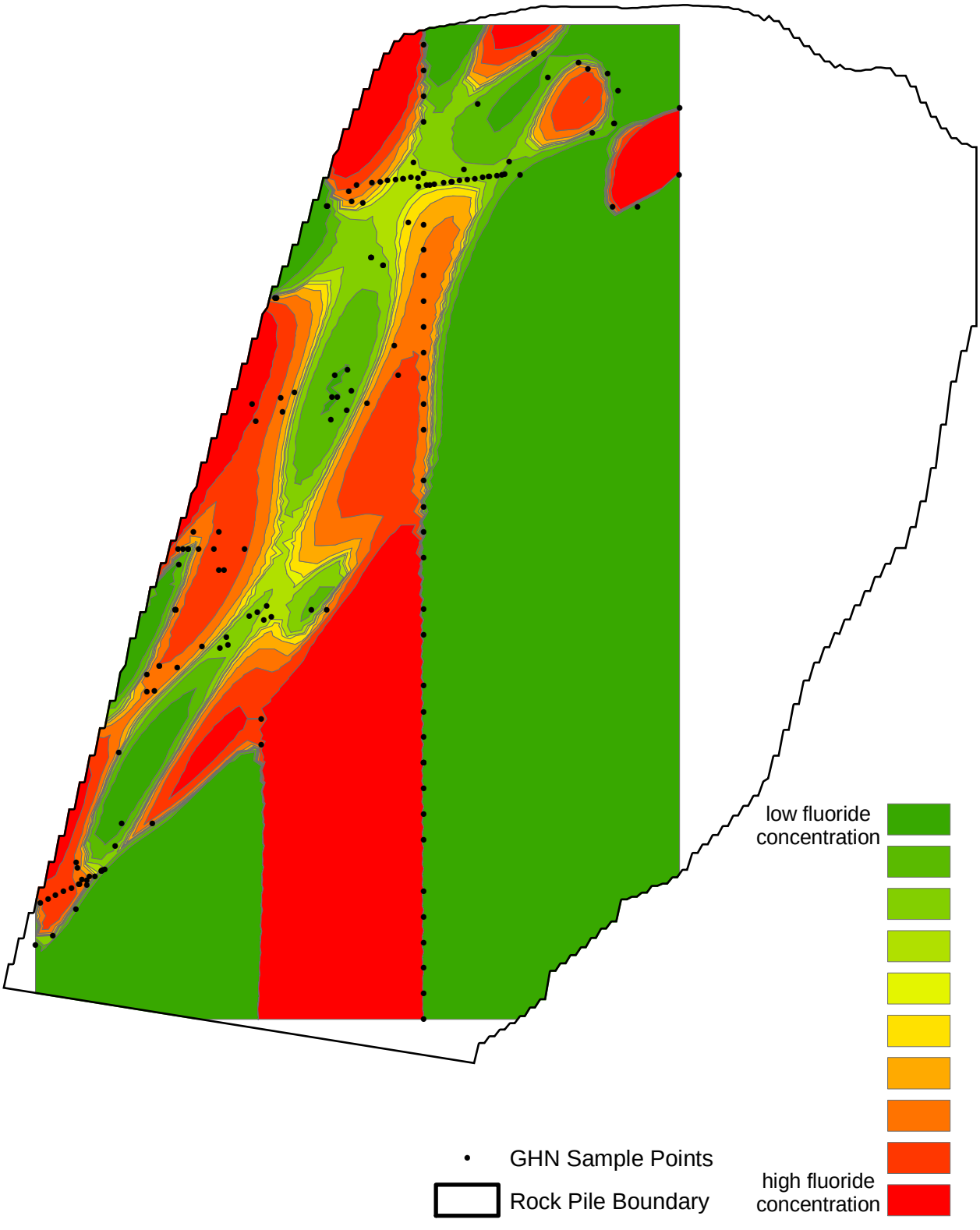

Goathill North Rock Pile Modeling

Global Polynomial Interpolation #9

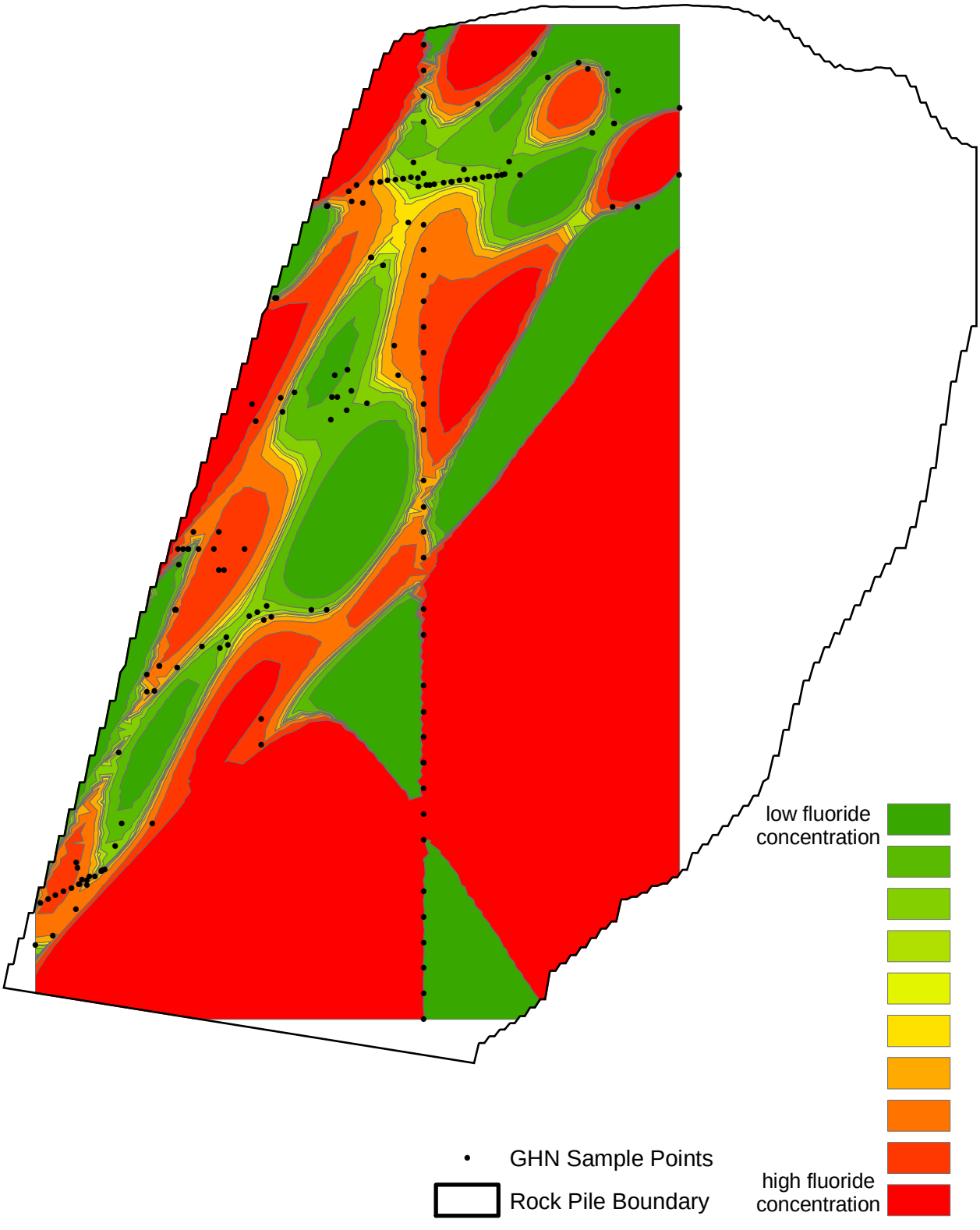

Goathill North Rock Pile Modeling

Global Polynomial Interpolation #10

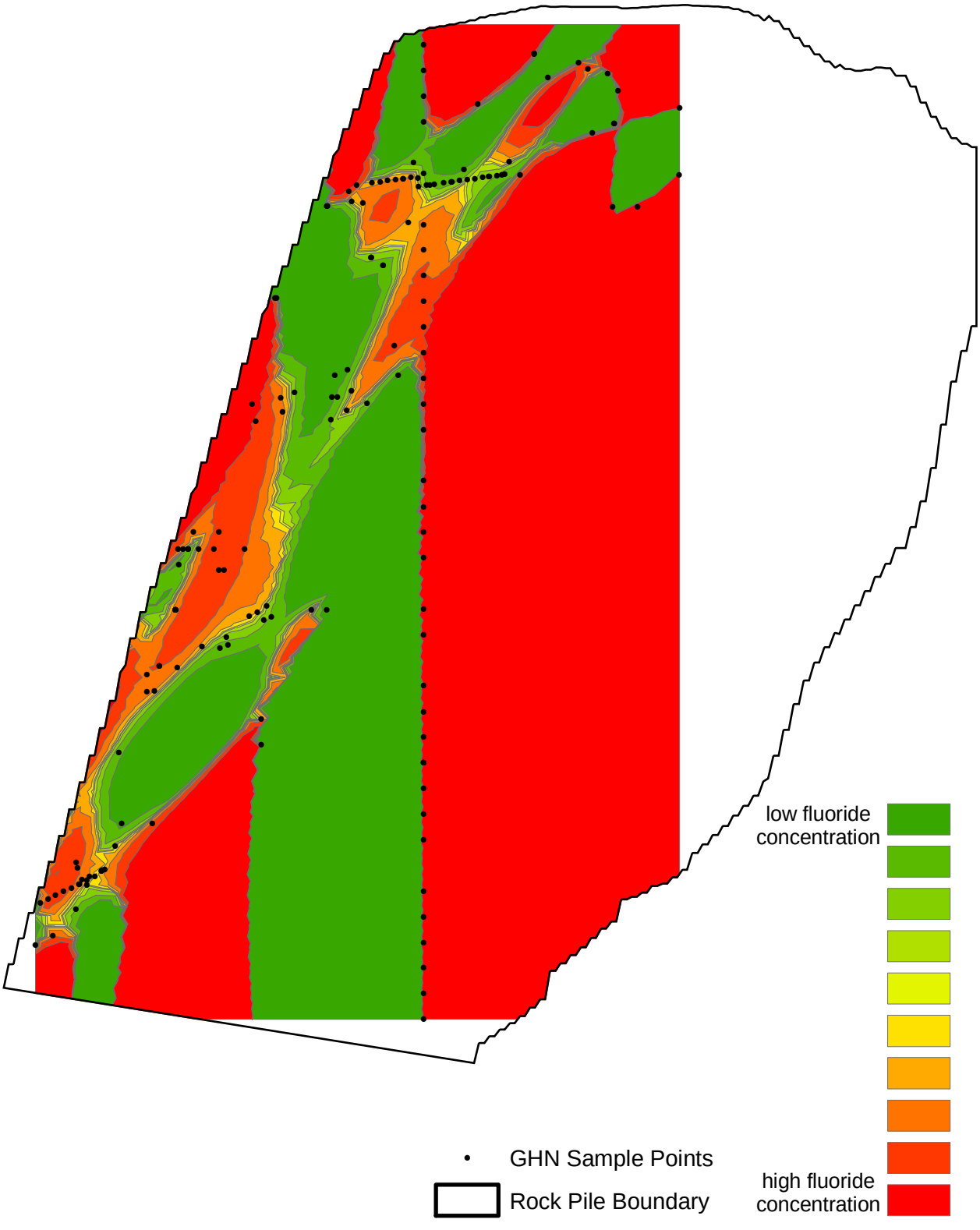

Goathill North Rock Pile Modeling

Local Polynomial Interpolation #1

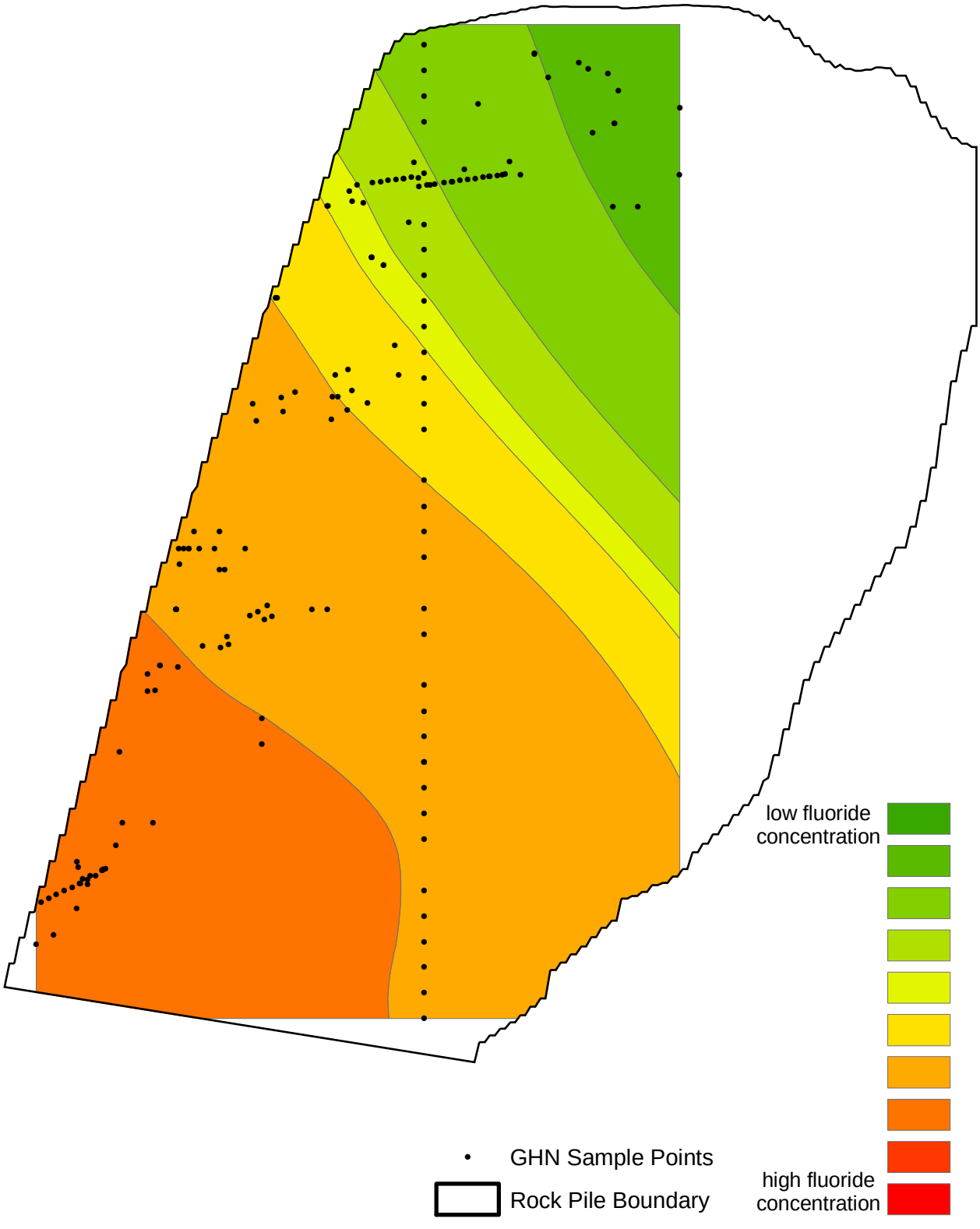

Goathill North Rock Pile Modeling

Local Polynomial Interpolation #2

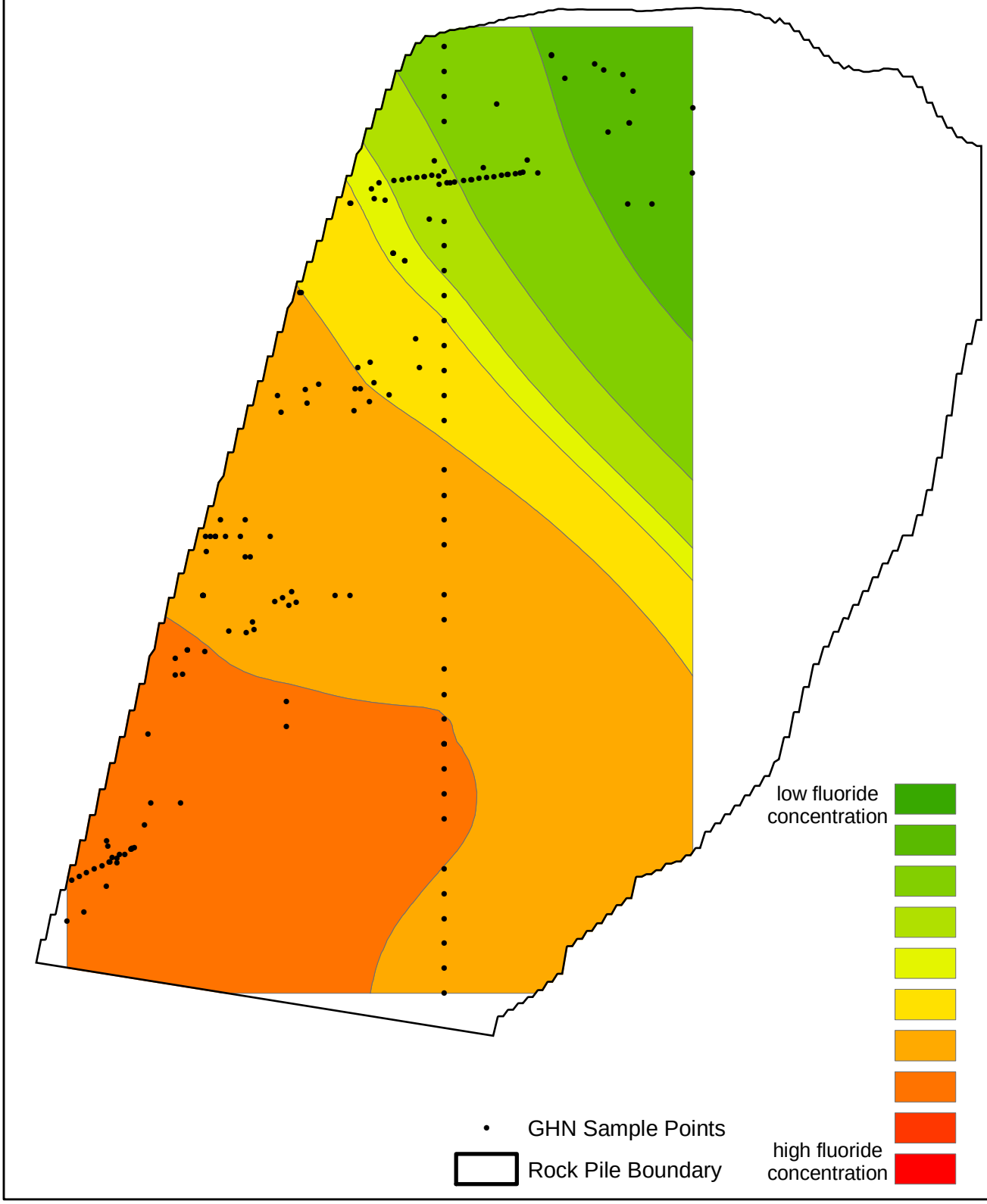

Goathill North Rock Pile Modeling

Local Polynomial Interpolation #3

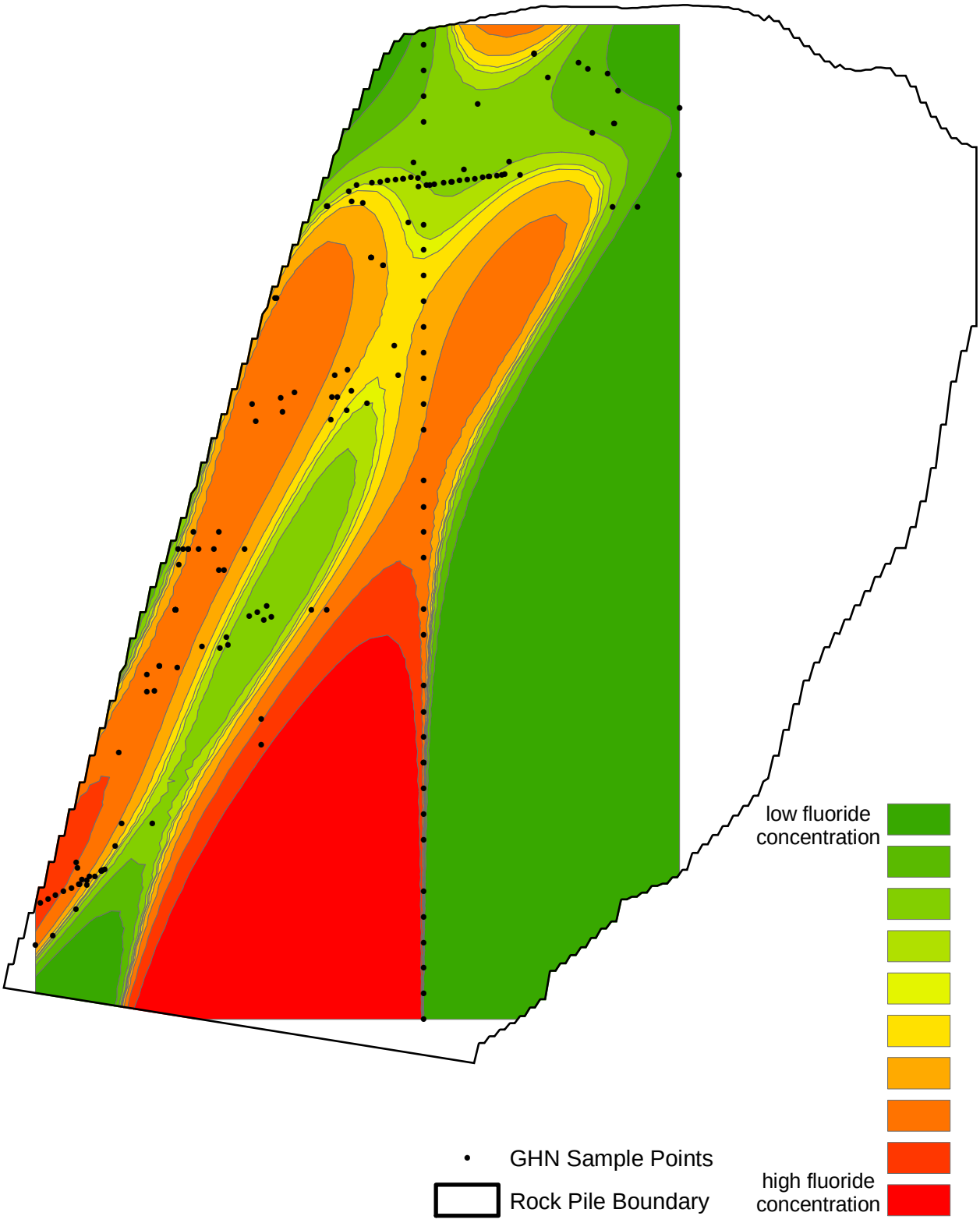

Goathill North Rock Pile Modeling

Local Polynomial Interpolation #4

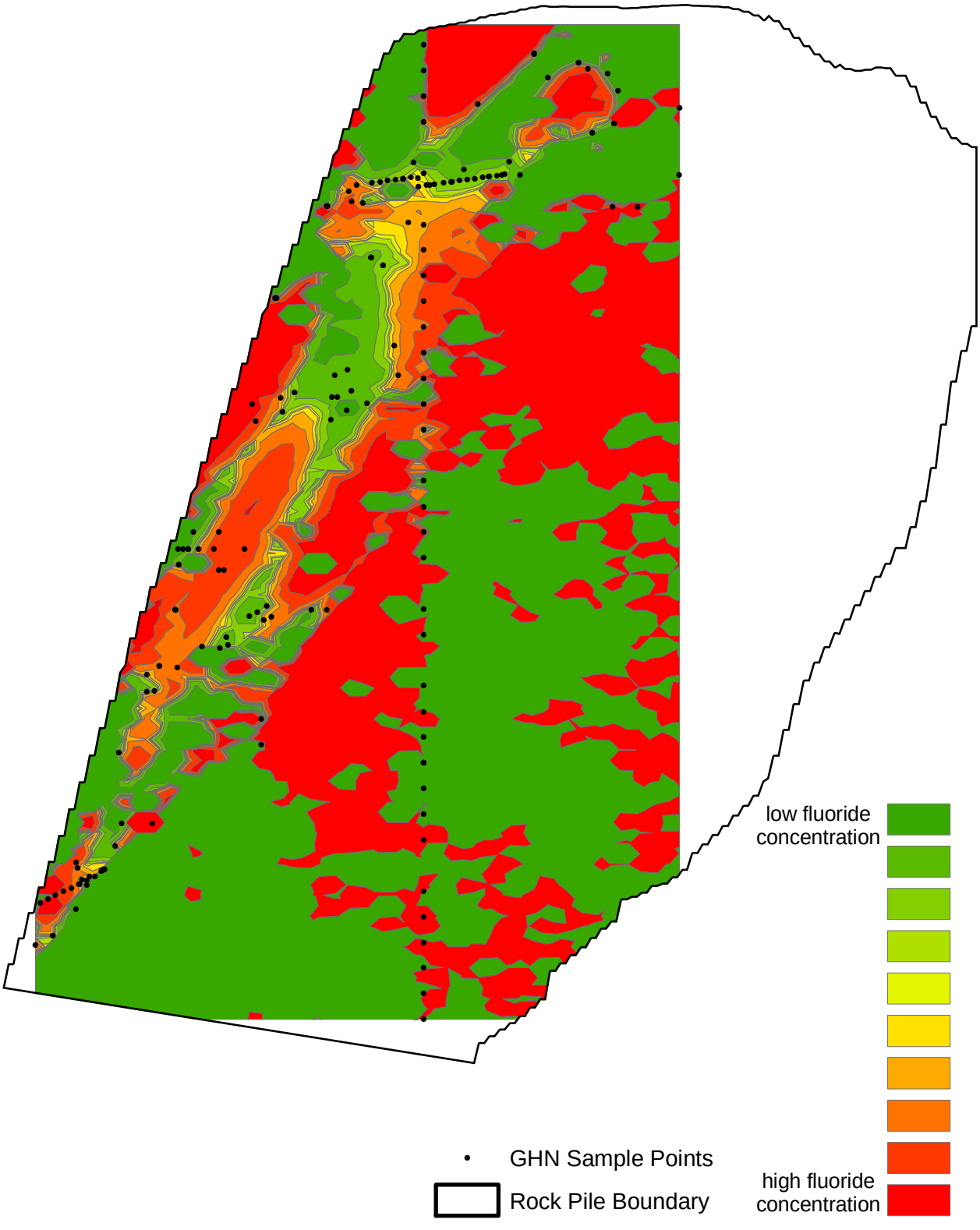

Goathill North Rock Pile Modeling

Local Polynomial Interpolation #5